Impact of peripheral inflammation in the brain:

New roles for the anti-inflammatory molecule Annexin A1

Enrico Cristante

Division of Brain Sciences

Department of Medicine

Imperial College London

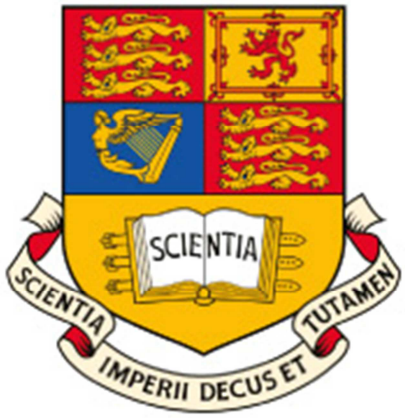

Imperial College London

A thesis submitted to Imperial College London for the degree of

Doctor of Philosophy

February 2013

Abstract

Growing evidence has shown that peripheral inflammation can trigger a central nervous system response, sometimes worsening pre-existing neurological conditions, breaking down the concept of brain as an immune-privileged organ.

Understanding which components contribute to periphery-to-brain communication may help identify molecules exploitable for therapeutic intervention. Usually, inflammation is followed by resolution: one of the main effectors in this process during peripheral inflammation is Annexin A1, while its implications in the CNS are still unclear. This thesis provides evidence for a new face for the molecule: we observed a well-defined expression at blood brain barrier (BBB) at endothelial level and we detected, *in vivo*, significantly higher BBB permeability in the AnxA1 null mice due to disrupted inter-endothelial cell tight junctions, essentially as a consequence to changes in the actin cytoskeleton. Such changes are reminiscent of early MS pathology, a relationship confirmed by detecting a selective loss of ANXA1 in the plasma and cerebrovascular endothelium of MS patients.

Under peripheral inflammatory conditions (*i.p.* lipopolysaccharide, LPS), *in vivo* data suggested an inherent sex difference in BBB response, while i*n vitro* studies confirmed the protective action of sex hormone 17β-Estradiol on the endothelium through ANXA1 modulation.

Within the CNS, we detected a constitutively higher microglial density and pro-inflammatory environment in the Anxa1 null mouse, which worsened upon peripheral inflammation. In a neurodegeneration model (6-hydroxydopamine), genotype-related differences in microglial invasion occurred, while subsequent peripheral inflammatory challenges synergised and caused worse dopaminergic neuronal loss only in the knock-out model.

These original data unveil a novel functional paradigm for ANXA1 as a “translator” between peripheral immune system and CNS through novel pathways compared to its well-characterized peripheral role. In addition, this study opens up a novel path to find therapeutic applications against disorders characterized by central and peripheral inflammation.

Table of contents

Table of figures

Table of tables

Declaration of originality

I, Enrico Cristante, hereby declare that the work presented in this thesis is my own and to the best of my knowledge is original. Any content derived from other sources including figures, data and material has been appropriately indicated, acknowledged and referenced within the text.

Signed: 

Date: 28 February 2013

List of abbreviations

17βE	17 β-Estradiol
6-OHDA	6-hyroxydopamine
ABC	Avidin–biotin complex
ABP	Actin binding protein
AD	Alzheimer's disease
AJ	Adherens junction
ALS	Amyotrophic lateral sclerosis
ANXA1	Annexin A1 (human gene)
ANXA1	Annexin A1 (human protein)
Anxa1	Annexin A1 (murine gene)
Anxa1	Annexin A1 (murine protein)
$Anxa1^{-/-}$	Anxa1 null mouse
APC	Antigen-presenting cell
APS	Ammonium persulfate
AS	Antisense clone
BBB	Blood-brain barrier
BCA	Bicinchoninic Acid Assay
BCSFB	Blood-cerebrovascular fluid barrier
BM	Basal membrane
BMEC	Brain microvascular endothelial cell
BRB	Blood-retina barrier
BSA	Bovine serum albumin
CD11b	Cluster of differentiation molecule 11 b
CD14	Cluster of differentiation molecule 14
cDNA	complementary DNA
CMV	Cytomegalovirus
CMV	Cytomegalovirus
CNS	Central nervous system
COX	Cyclo-oxygenase
Ct	Threshold cycle
CVO	Circumventricular organ
DA	Dopamine
DAB	Diaminobenzidine
DAMP	Damage-associated molecular pattern
DAPI	4',6-diamidino-2-phenylindole
Dk	Donkey
DMEM	Dulbecco's modified Eagle medium
DMSO	Dimethylsulfoxide
DNA	Deoxyribonucleic acid
DPBS	Dulbecco's modified phosphate buffered saline
DPN	Diarylpropionitrile
DPX	Di-N-Butylephthalate in xylene

DW	Dry weight
e.g.	exempla gratia
EAE	Experimental allergic encephalomyelitis
EAE	Experimental autoimmune encephalomyelitis
EB	Evans blue
ECL	Enhanced chemiluminescence
EGF	Epidermal growth factor
ELISA	Enzyme-linked immunosorbent assay
eNOS	Endothelial nitric oxide synthase
EPC	Embryonic precursor cells
ERE	Estrogen-responsive element
ERK	Extracellular signal-regulated kinase
ERα	Estrogen receptor α
ERβ	Estrogen receptor β
ESAM	Endothelial cell-selective adhesion molecule
FCS	Fetal calf serum
FITC	Fluorescein isothiocyanate
FL	Full length clone
FPR	Formyl peptide receptor
FPRL	Formyl peptide receptor-like
G-1	Bromo-benzodioxol-tetrahydro-cyclopenta-quinolin-ethanone
G-15	Bromo-benzodioxol-cyclopenta-quinoline
GAP	GTPase-activating protein
GAPDH	Glyceraldehyde 3-phosphate dehydrogenase
GDP	Guanosine diphosphate
GEF	Guanine nucleotide exchange factor
GPCR	G-protein coupled receptor
GPR30	G-protein coupled receptor 30
GRE	Glucocorticoid responsive element
GTP	Guanosine triphosphate
HBSS	Hank's buffered saline solution
hCMEC/D3	Human cerebrovascular endothelial cell line/clone D3
HIV	Human immunodeficiency virus
hrANXA1	Human recombinant ANXA1
HRP	Horseradish peroxidase
HRT	Hormonal replacement therapy
HUVEC	Human umbilical endothelial cells
i.e.	id est
i.p.	Intraperitoneal
i.v.	Intravenous
Iba-1	Ionized calcium binding adaptor molecule 1
ICAM	Intercellular adhesion molecule
IF	Immunofluorescence
IFN	Interferon
Ig	Immunoglobulin
IHC	Immunohystochemistry
IL	Interleukin

iNOS	Inducible nitric oxide synthase
iNOS	Inducible nitric oxide synthase
ITR	Inverted terminal repeats
IκB	Nuclear factor of kappa light polypeptide gene enhancer in B-cells inhibitor
LB	Luria Bertani
LBP	LPS-binding protein
LPA	Lysophosphatidic acid
LPS	Lipopolysaccharide
LXA4	Lipoxin A4
MAPK	Mitogen-activated kinase
MCS	Multiple cloning site
MLC	Myosin light chain
MLCP	Myosin light chain phosphatase
MMP	Metalloprotease
MPP^+	1-methyl-4-phenylpiridinium
MPTP	1-methyl-4-phenyl-1,2,3,6-tetrahydropyridine
MRI	Magnetic resonance imaging
Ms	Mouse
MS	Multiple sclerosis
MTA	Material transfer agreement
NAWM	Normal appearing white-matter
NF-kB	Nuclear factor kappa-light-chain-enhancer of activated B cells
NGF	Neuronal growth factor
NGS	Normal goat serum
NMDA	N-methyl-D-aspartate
NO	Nitric oxide
NPF	Nucleation promoting factor
NS	Non-significant
NSAIDs	Non-steroidal anti-inflammatory drugs
NSDA	Nigro-striatal dopaminergic
NVU	Neurovascular unit
OVX	Ovariectomized
PAGE	Polyacrilamide gel electrophoresis
PAMP	Pathogen-associated molecular pattern
PBS	Phosphate buffered saline
PCR	Polymerase chain reaction
PD	Parkinson's disease
PFA	Paraformaldehyde
P-gp	P-glycoprotein
PHTPP	Phenyl-trifluoro-methyl-pyrazolo-pyrimidin-phenol
PKC	Protein kinase C
PLA	Proximity ligation assay
PLA2	Phospholipase A2
PMN	Polymorphonuclear leukocyte
PPT	Propylpryazole-triol
PVM	Perivascular macrophage
qPCR	Quantitative real-time PCR

Rb	Rabbit
RIPA	Radioimmunoprecipitation assay
RNA	Ribonucleic acid
RNS	Reactive nitrogen species
ROCK	Rho-associated protein kinase
ROS	Reactive oxygen species
Rt	Rat
RT	Room-temperature
RT-PCR	Reverse-transcription PCR
SAA	Serum Amyloid A
SAPK/JNK	Stress-activated protein kinase/c-Jun N-terminal kinase
SDS	Sodium dodecyl sulphate
SEM	Standard error of means
shRNA	Short-hairpin RNA
SNpc	Substantia nigra pars compacta
SNpr	Substantia nigra pars reticulata
TAE	Tris-acetate-EDTA
TBI	Traumatic brain injury
TBS	Tris-buffered saline
TE	Tris-EDTA
TEER	Trans-endothelial electrical resistance
TEMED	Tetramethylethylenediamine
TGF	Transforming growth factor
TH	Tyrosine hydroxylase
TH-IR	Tyroxine Hydroxilase immuno-reactive
Thr	Thrombin
TJ	Tight junction
TLR	Toll-like receptor
TMB	3,3',5,5' Tetramethylbenzidine
TMB	3,3',5,5'-tetramethylbenzidine
TNF	Tumor necrosis factor
VCAM	Vascular cell adhesion molecule
VEGF	Vascular endothelial growth factor
VTA	Ventral tegmental area
WML	White-matter lesion
WPRE	Woodchuck Hepatitis Post-Transcriptional Regulatory Element
WT	Wild-type
WW	Wet weight
ZO-1	Zonula occludens-1
β-gal	β-galactosidase

Acknowledgements

Someone said that doing a successful PhD truly ranks among the most complicated challenges one can face, but also amongst the most educative ones. I now realise how much I have grown up during the last 4 years and this is entirely thanks to the luck of having met extraordinary people, whom now I would like to acknowledge.

First, I would like to express my deep and sincere gratitude to my supervisor and friend, Dr. Egle Solito, for the opportunity to work on this project. Her constant supervision, mentoring, 24/7 availability, unconditional support and especially her infinite patience have truly impacted on my education and strong dedication as scientist. Her knowledge of the subject and the valuable discussions have been of great value to me and to the overall success of the project. Her pragmatic experience, along with her way of treating me not as a student, but as a friend and colleague, has accompanied me through the first steps in the fascinating, and complicated, scientific world. Silently, I have learnt a lot from her during these 4 years and I will benefit from these precepts not only in my career but in my whole life.

Special thanks go to my co-supervisor, Prof. Glenda Gillies, as well for the chance to work on this project and for being always available to discuss project advances and issues. In addition, I am extremely thankful to Dr. Simon McArthur for teaching me so much, for assistance during many experiments and for his numerous contributions to this thesis, fully acknowledged in the text.

I am extremely grateful to Wellcome Trust, for supporting economically the project and the position, helping me with international meetings attendance and living expenses.

A special mention goes to my MSc supervisor, Prof. Dominic Wells, as he has always been available and full of thoughtful suggestions during the whole tortuous path of the PhD.

I am grateful to Prof. Rod Flower and Prof. Mauro Perretti and their group for the possibility to perform several experiments at William Harvey Research Institute, as well as to Prof.

Magdi Yaqoob for the constant support after the moving. A special thank-you goes to the Renal TMT group for their help in settling down in the new laboratories.

Further to this, I must thank those numerous people that supplied samples or intellectual expertise exploited in my research, including Prof. Babette Weksler, Dr. Ignacio Romero and Prof. Pierre-Olivier Coureaud for providing hCMEC/D3 cell line and useful trouble-shooting discussions, Dr. Rachel Brown for showing primary culture isolation, Mr. Julius Kieswich for help and assistance during many *in vivo* experiments.

A huge acknowledgement goes to Dr. Alejandro Lopez-Ramirez, which resulted to be an invaluable source of help and discussion about *in vitro* permeability assays as well as a very good person and friend. At the same level, I should thank three special and valuable people, with whom I shared joy and sorrow of being a PhD student. First, my great friend and previous flatmate Dr. Evangelos Pazarentzos, not only for the help provided with lentiviral particles production, but especially for his genuine and truthful friendship during the last 4 years, making me feel welcome and loved in any situation; I wish you all the best luck for your new life in San Francisco. Second, my other previous flatmate and great friend Dr. Chris P Watson, for the serious and semi-serious discussion on the blood-brain barrier and in general on what life in science means; your positive and happy way of living has been a great example for me to improve. Third, Dr. Callum Parr, because by working closely with you I discovered a very nice person and genuine friend, discrete, polite and helpful, similar to me in many aspects; most of all, the perfect buddy for our amazing California road trip.

A special mention goes to Dr. Lorenzo D'episcopo, another great person and friend met during my years at Imperial College London.

Many thanks to those students (Mr. Jakob Mathiszig-Lee, Mr. Samuel Chee, Ms. Yoko Nakamura, Ms. Samantha Price, Ms. Vanessa Di Lorenzo, Ms. Elisa Maggioli) I had the chance to help throughout their projects, for their experimental contributions.

A big thank-you to all the people of the 4th and 5th floor at Hammersmith, in particular to Camilla, Loukia, Miriam, Sofia, Ioanna, Justina, Antonio, Charlotte, Tarin, Christoph, Ghada, Anne-Laure, Ryota, Bevan, Praveen, Alex, Daniele, Christopher, Daniel, Katrin.

A special mention also to the people met during my last year at William Harvey, because they made me feel very welcome and comfortable.

I am extremely grateful to my friends in London (Maurizio, Mose, Kristie, Laura, Paolo, Lydia, Thomas, Zeta, Elina, Eleni, Damien, Andrea, Giulia, Elia) and in Italy (Fede, Stefano, Deb, Marco, Elene, Ale, Marco, Boz, Flavio, PaoloG, Ross), because if I managed to keep a bit of balance to enjoy my out-of-work life is truly thanks to them.

I should also thank those artists that supported me during the long days and nights of my lab work and write-up with their great melodies: so thank you Benjamin Francis Leftwich, Banner Pilot, Latterman, Lawrence Arms, Isbells, Mazzy Star, Trespasser Williams, Casey Shea, Album Leaf, Lana del Rey, Verdena, and many others.

Last, but by no means least, I want to deeply thank my family, mum, dad and my brother Giacomo; exactly 5 years have passed since my moving to London, which was possible exclusively thanks to their belief and help. During this time, I have felt sometimes a bit “home-sick” and melancholic, but I have always been aware of the great opportunity I was experiencing as well as of their invaluable, continuous, optimistic support and advice.

Finally, words would not be enough to thank my beloved Stephanie, my guardian angel: without her discrete and patient presence, emotional support, smiles and positivity, I certainly would have not achieved all this. The dedication I put on this thesis and the results I have achieved during this course are also yours.

‘Life is not easy for any of us. But what of that? We must have perseverance and above all confidence in ourselves. We must believe that we are gifted for something and that this thing must be attained’

(Marie-Curie)

‘…and I know when you're living under sheets of snow
it can look like the world’s gone black
but remember that the sun comes back.
At least they say it does’

(Alchemy - Banner Pilot)

Chapter 1 – General introduction

1.1 General aspects of inflammation

Inflammation is a primordial, highly evolutionary-conserved active response mounted by the innate immune system in response to injury, xenobiotics exposure and infections in order to promote recovery. The final goal of inflammation is not only to clear the environment from harmful agents but mainly to restore tissue homeostasis and to stimulate healing processes where necessary (Janeway and Medzhitov, 2002). In its absence, injuries and infections would never be tackled, with unrelenting deterioration of the affected tissue and consequent risks for the entire organism. The typical signs of inflammation were first described by the roman doctor Celsus in the 1st century AD as: *rubor, tumor, calor, dolor* (redness, swelling, heat and pain, respectively) while *function lesa* (loss of function) was added more recently; remarkably, they do not always appear together and simultaneously during an inflammatory event.

There are several possible triggers for an inflammatory reaction, usually classified as *physical*, *chemical* and *biological causes*. The latter are by far the most common ones, including microbial infections (bacteria, fungi, viruses, protozoa, parasites).

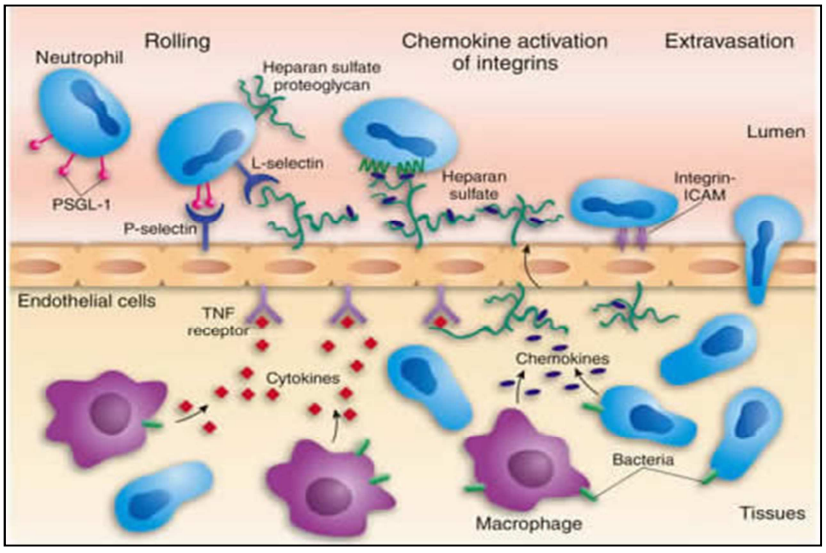

Figure 1.1 Inflammation cascade. Overview of typical sequential vascular and cellular events occurring during an inflammatory reaction (Janeway and Medzhitov, 2002)

Inflammation can be classified in *acute* and *chronic*.

Acute inflammation is the initial intense response that the organism activates to remove the harmful problem, which can originate from the outside or from inside the host. In the case of an acute reaction not being able to restore the homeostasis of the injured site in a limited amount of time due to the persistence of the harmful stimulus or to inefficiencies of the defensive process itself, inflammation undergoes a strategic change becoming *chronic*.

Chronic inflammation is characterized by a progressive shift in the type of cells which are recruited to the site of the reaction (mainly monocytes, lymphocytes and plasma cells) and is characterized by simultaneous active inflammatory events, tissue destruction and inefficient repairing by fibrotic tissue deposition. An inflammatory response is a highly harmonized process where several phenomena happen in a defined schedule, prompted to rapidly and effectively overcome the harmful agent in a multi-tasking fashion. Auto-immune diseases, aging and prolonged exposure to toxic compounds are the main causes that trigger a shift towards chronicity (Johnson, 2006). When such a response is not maintained, as in the case of insufficient, excessively sustained or inappropriate inflammation, the final outcome is undoubtedly different, indeed causing pathological disorders like allergies, atherosclerosis, autoimmune diseases, and participating in many others like cancer and cardio-vascular pathologies. It is not surprising that the inflammatory response, normally protective, has been nicknamed “the silent killer”.

1.1.1 Cellular and molecular mediators of inflammation

Inflammation often generates a wide sequence of events, known as the acute phase response; this represents a potent host defensive process aimed at limiting proliferation and diffusion of the insulting agent. It includes generalised processes like activation of the sympathetic nervous system, changes in cardiovascular functions, in the neuroendocrine balance (*i.e.* activation of the hypothalamic pituitary adrenal axis) and behavioural changes (Lucas *et al.*, 2006). Triggering all these systemic processes requires a highly organised cascade of molecular and cellular events. If we have to describe a typical inflammatory reaction, numerous components participating in this complex process should be mentioned, which contribute to promptly trigger a quick and highly hierarchical signalling cascade, as depicted in Figure 1.1.

In terms of cellular participants, the major ones are the granulocytes, mainly the neutrophils, the mast cells and the mononuclear phagocytes, monocytes and macrophages.

A typical acute inflammatory reaction is started by the prompt activation of the resident defensive cells, the macrophages (although others should also be included, like mast cells

and dendritic cells), which sense a dangerous stimulus (microbial agents, necrotic tissue, toxic substances, *etc.*) through their numerous membrane receptors and start battling against it, while requiring for more support from other compartments. As a consequence of these rapid events, a quick (in the range of minutes) and progressive recruitment of the granulocyte neutrophils occurs; this cell type possesses important phagocytic properties towards bacteria and external physical insults. Their activation through several mediators inside the inflamed tissue is followed by an intense release of proteolytic enzymes and toxic mediators aimed at tackling the insult. Usually, a typical acute reaction is characterised by the progressive substitution in the type of cells recruited: the neutrophils are short-lived cells (around 1 day), so after 4 hours from the inflammatory initiation, monocytes are recruited instead by switching the type of mediators released from the injured site. Inside the tissue, monocytes differentiate into macrophages, which present longer life span and a dedicated defensive plethora of functions (chemotaxis, enzymes and toxic products release, phagocytosis).

During inflammation, a great number of chemical mediators is involved, a condition necessary to sustain the recruitment and the activation of the correct type of leukocytes only in the injured tissue. The release of inflammatory signals like histamine, serotonin and prostaglandins (derivatives of the arachidonic acid metabolism) is in charge to trigger dramatic vascular alterations (vascular tone, expression of adhesion molecules, changes in paracellular permeability) which result in the invasion of the target tissue by blood-derived proteins as those of the complement system, responsible for the lysis and opsonisation of microbial and exogenous agents, and the coagulation system, which contributes to further increase the vascular permeability. The contemporary release of chemotactic molecules like chemokines, the lipoxygenase products like leukotriene B_4, and some complement proteins themselves, along with pro-inflammatory activating signals like cytokines (TNF-α, IL-1 and in part IL-6) is required for the intense blood-born cells recruitment by acting on the endothelium or directly on the cells to be recruited; in this way, the cells are able to be directed towards the source of the insult and thanks to their activated state they will fight against it. Lysosomial enzymes (proteases, nucleases, lipases, *etc.*), production of reactive oxygen species (ROS) and reactive nitrogen species (RNS) are the major candidates for the elimination of the insulting agent, along with the damaged surrounding tissue.

Since the inflammatory response is tightly linked with the resolution/repair phase, anti-inflammatory mediators (mainly cytokines like TGF-β and IL-10, arachidonic acid anti-inflammatory metabolites as some lipoxins, and other peptides) and signals aimed to stimulate the regeneration of the injured parenchyma (by cell substitutes recruitment/regeneration or fibrotic tissue deposition by fibroblasts) are normally released when the original cause of the reaction is close to be eliminated (Norling and Serhan, 2010; Norling *et al.*, 2012).

Cooperation between the innate and adaptive immune responses is critical to enable the correct tackling of the trigger. Distinct types of effector T lymphocytes are involved in bridging the innate inflammatory response towards the development of a more injury-specific adaptive reaction. For example, certain sub-types of T cells, once entered in the injured site, play important roles in the control of intracellular pathogens by activating macrophages, cytotoxic T lymphocytes and by producing IFN-γ. As an example, T_H17 cells are fundamental to potentiate the inflammatory response mediated by neutrophils and monocytes. In this concerted action, the innate immunity should be able to limit the problem until antigen-specific adaptive immune responses are established (Koyasu and Moro, 2012).

Inflammation is substantially a protective response, aimed to be positive for the host, therefore it should not be regarded as a form of disease, but as a powerful non-specific reaction against the initial cause of the insult and its consequences. When control of one or more of the phases is lost, detrimental consequences can definitely occur, as noticed in several pathologies with a chronic inflammatory component, where the destructive power of inflammation overtakes the positive outcomes of the reaction.

1.2 Inflammation in the central nervous system

All the structural and functional districts of human body can be injured by inflammation, including the central nervous system (CNS). The healthy brain was once regarded as an "immune privileged" organ, protected from immune responses (Lucas *et al.*, 2006; Ransohoff and Brown, 2012): this concept arose due to the protection offered by the blood

brain barrier (BBB) but also because of the almost complete absence of the classical antigen presenting cells, the dendritic cells, therefore stating the apparent inability to sustain the maturation of an adaptive immune reaction *de novo*. Moreover, the fact that some of the most evident features of a typical inflammatory reaction (like oedema formation, or leukocyte recruitment) seemed to be absent or limited, reinforced this simplistic concept. The brain can definitely be subjected to immune reactions like inflammation but the concept of "neuro-inflammation" should not be taken *sensu stricto* as inflammatory reactions in the nervous system do not show all the 5 typical hallmarks, but they do resemble the molecular and cellular features of a typical inflammatory event of peripheral tissues, despite not showing evident changes. In the CNS are evident prompt increase in expression of typical inflammatory markers, production of cytokines (such as TNF-α, IFN-γ or IL-17) and acute inflammatory messengers and other key features of all inflammatory reactions as well as the characteristic intensity and efficacy, which all guarantee an effective tackling of the injurious stimulus. More in detail, activation of all the glial resident population is the hallmark of CNS inflammatory reactions; astrocytes and oligodendrocytes are able to respond and to release inflammatory mediators like cytokines and reactive oxygen species (Allan and Rothwell, 2001; Lucas *et al.*, 2006; Mena and Garcia de Yebenes, 2008; Allen and Barres, 2009; Glass *et al.*, 2010), supporting the development of an inflammatory reaction. More importantly, the quick activation of the resident population of myeloid-lineage immune cells (as in the peripheral system with macrophages) plays an essential role in starting and orchestrating the innate response and, eventually, directing the following adaptive immunity. Pericytes, the perivascular macrophages (both involved in the complex functional composition of the microvasculature), the mast cells (Ransohoff and Brown, 2012) and, above all, the microglia (Guillemin and Brew, 2004) are the main protagonists of the CNS innate immune response.

1.2.1 Microglia: the good and the bad of central inflammatory responses

Microglia are by far the most studied and preeminent type of specialised macrophages adapted to the neural environment (Garden and Moller, 2006; Ransohoff and Perry, 2009). Described for the first time by Pio del Rio Hortega in 1919 (McGeer and McGeer, 2011), these spidery small cells were found to constitute around 5-15% of the total cell CNS population and to be the principal CNS resident cell type in charge of recognizing harmful stimuli and mounting a consequent reaction (Czeh *et al.*, 2011).

Their developmental origin has been source of a huge debate in the scientific community: recent studies have dismissed the hypothesis that these cells have a neuro-ectodermal origin like astrocytes and oligodendrocytes (Ransohoff and Perry, 2009), supporting instead the derivation from mesodermal progenitors distinct from the ones that generate future peripheral macrophages and circulating monocytes (Chan *et al.*, 2007; Ginhoux *et al.*, 2010). More in detail, microglia progenitors appear to populate the nervous system during two very short and defined temporal windows of the fetal and postnatal development: first, mesodermal progenitors (sometimes called amoeboid microglia) from the yolk sac or another hematopoietic organ of the developing embryo enter and seed the forming nervous system mainly through meninges, ventricles and choroid plexus; later in the second phase, this happens through the blood vessel walls (Czeh *et al.*, 2011).

Once CNS has been populated, microglia progenitors adapt to the neural environment and take part directly in the development of the nervous system, by removing apoptotic cells, regulating axon formation and length, stimulating angiogenesis and releasing neurotrophic factors. So formed resident microglia represent the life-long population, which is able to sustain its self-renewal through slow local cell division (Perry *et al.*, 2010) and only in small part (perivascular microglia and few specific parenchymal regions) by peripheral circulating cells contribution (Chan *et al.*, 2007; von Bernhardi *et al.*, 2010). On the other hand, a more intense turnover from circulating monocytes occurs under pathological conditions (Hanisch and Kettenmann, 2007; D'Mello *et al.*, 2009; Ajami *et al.*, 2011; Mizutani *et al.*, 2012), with infiltrating cells differentiating into microglia with a stronger expression of functional molecules and better phagocytic functions and antigen presenting-cell properties (Czeh *et al.*, 2011).

Exploring microglial activity and biology has not been an easy task indeed, due to absence of specific microglial markers able to discriminate microglia from those peripheral monocytes assuming microglia-like features during disease (Gao and Hong, 2008).

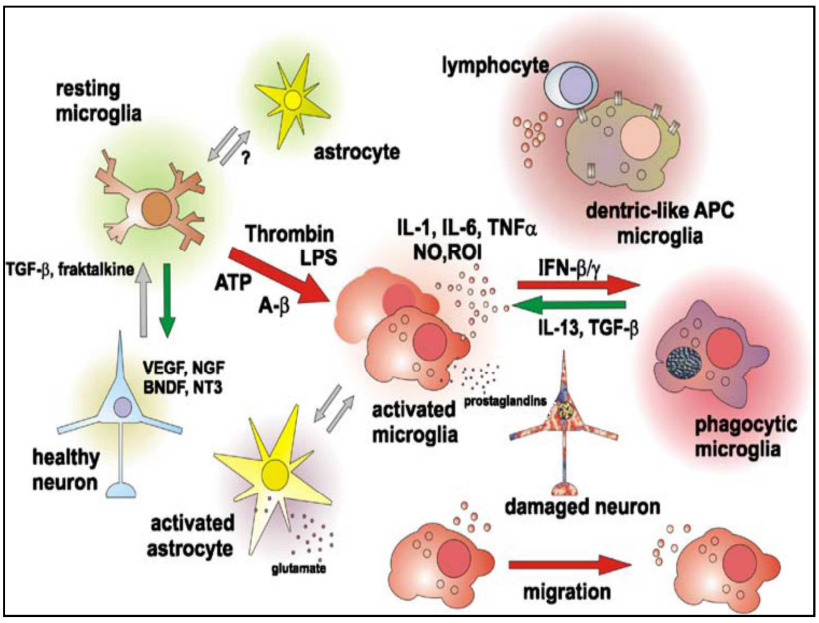

Figure 1.2 Microglia activity phenotypes: Reactive-activated microglia can be divided in numerous sub-phenotypes. From Garden and Moller 2006.

Initially, it was believed that microglia exist in only two functional and morphological forms, the resting and the activated.

This view has proved to be highly limited (Garden and Moller, 2006; Hanisch and Kettenmann, 2007) to describe the complex and variable physiology of this multifaceted cell type. The present knowledge about microglial activation lays on the existence of three distinct phenotypes known as amoeboid, ramified-resting/surveying and reactive-activated microglia which may exploit different functions. As previously described, the amoeboid microglia are associated with development of CNS, synaptic remodelling and plasticity (Chan *et al.*, 2007; Hanisch and Kettenmann, 2007). The ramified-resting/surveying form represents the type of microglia associated with a healthy CNS: it exhibits a branched morphology and low expression of surface antigens. This is not a real resting phenotype but more correctly an activity state, since cells are constantly monitoring the brain parenchyma through their highly motile processes (Nimmerjahn *et al.*, 2005), sensing any change in physiological conditions and cleansing the extracellular fluid in order to maintain central homeostasis. Disturbance of brain homeostasis causes a prompt shift towards the reactive-activated form: the complexity of this phenotype depends on the fact that we can distinguish between an "alerted" subtype, characterized by a local, transient and subtle activation (often not recognizable) of specific functions, and a "reactive" subtype, represented by more evident

functional and morphological changes (Hanisch and Kettenmann, 2007; Perry *et al.*, 2010). As a general description, fully activated microglia exhibit changes in morphology, up-regulation and synthesis *de novo* of specific membrane molecules, like the Toll-like receptors (TLR) family [able to recognise pathogen-associated molecular patterns or PAMPs and danger-associated molecular patterns, or DAMPs (Rivest, 2009; Ransohoff and Brown, 2012)], chemotaxis and consequent migration to the site of interest, phagocytic properties, antigen presentation, rapid proliferation and secretion of numerous inflammation mediators like cytokines, chemokines, eicosanoids, reactive oxygen species (ROS) (Aloisi, 2001; Lucas *et al.*, 2006; Gao and Hong, 2008).

It is important to emphasise that changes in morphology, expression of certain molecules or fulfilment of certain functions are not simple guides to define the reactivity of these cells. What defines which level of activation will be generated is not clear, but it seems that most hinges on the intensity, on the nature and on the sequence of the triggering stimulus/i, as happens for peripheral macrophages and the supposed M1 (classically activated phenotype) and M2 (alternatively activated) dichotomy (Hanisch and Kettenmann, 2007; Perry *et al.*, 2010). On this behalf, some scientists (Hanisch and Kettenmann, 2007; Ransohoff and Perry, 2009; Perry *et al.*, 2010) sub-divide the reactive-fully activated form in two main further classes, the phagocytic one [amoeboid-shaped, able to invade inflamed lesions and to phagocytize foreign materials and dying cells, therefore with a potentially anti-inflammatory/pro-resolving role as we and others have already demonstrated (McArthur *et al.*, 2010; Czeh *et al.*, 2011)] and the non-phagocytic one (highly proliferative and secreting pro-inflammatory cytokines, truly the intermediary between the phagocytic and the ramified-resting forms); more phenotypes could actually exist, making a real strict classification rather limiting and not representative of the multi-faceted ability to sense the precise nature of the stimuli, resulting in different activation patterns, as seen in Figure 1.2.

Importantly, microglia acts in concert with astrocytes and oligodendrocytes, either when in a “surveying” state or when activated and committed to quickly restore brain welfare: during neuroinflammation, these cells collaborate to promote clearance of any insulting factor to favour regeneration of the affected tissue, also through release of neurotrophic factors (Perry, 2004; Gao and Hong, 2008).

1.2.1.1 Contributions of microglia in neurological disorders

Inflammation has always to be considered a protective response aimed at removing the harmful stimuli and to initiate a healing/repairing process, which should rebalance the homeostasis as close as it was before the insult occurred. The same stands for CNS: without neuroinflammation, restoring the normal functionality and structural harmony of the tissue, such an essential working unit, would be practically impossible. Microglia should always be considered first as a beneficial cell type if we consider the numerous positive actions that can exert, like scavenging toxic compounds, phagocytising and inactivating infectious organisms, releasing trophic factors promoting neuronal survival like the nerve growth factor (NGF), stimulating astrocytes to promote axonal growth, *etc.* However, due to the high susceptibility of the nervous system to stress factors and strength of the defensive responses and to the contained nature of this compartment, excessive microglial activation could become destructive with consequent damage in healthy regions, explaining why microglial reactions are more tightly regulated in time and space when compared to macrophages of other tissues (Gao and Hong, 2008; Lucin and Wyss-Coray, 2009). As an example of potential damaging role of this potent reaction, it is important to note how strikingly neuroinflammation is related with many diseases affecting the CNS, like stroke (Lucas *et al.*, 2006) and aging-related neurodegenerative disorders as Alzheimer's disease (von Bernhardi *et al.*, 2010), Parkinson's disease (Frank-Cannon *et al.*, 2009), amyotrophic lateral sclerosis, prion disease (Cunningham *et al.*, 2005) and multiple sclerosis (Stolp and Dziegielewska, 2009). Microglial reactions are normally self-limiting, resolving once eradication of the initial insult has occurred. However, functional impairment and loss of regulation can occur in response to non-successfully eradicated persistent trigger/s (that may or may not be the initial cause of the degenerative event, or may have been accumulated during the cells life-span) as demonstrated in the aforementioned disorders (Perry, 2004; Tansey *et al.*, 2007; Frank-Cannon *et al.*, 2008; Gao and Hong, 2008; Rivest, 2009). Over time, such conditions may lead to the switch from the protective role of microglia to detrimental effects of its actions on the CNS environment and cellular components, worsening the actual pathological state, creating a vicious self-propagating loop (over-activated microglia causing neuronal death, which in turn triggers subsequent microglial activation; as depicted in Figure 1.3) negatively contributing to the outcome of

the disease. In the case of Parkinson's disease, for example, microglia could be activated by infectious events, traumatic brain injury or extracellular α-synuclein (Glass *et al.*, 2010), resulting in *microgliosis* (accumulation of activated microglial cells) with subsequent increase in inflammatory (release of cytokines, prostaglandins, lytic enzymes) and oxidative stress inside the challenged area (Knott *et al.*, 2000). This can play a very harmful effect towards the delicate and vulnerable dopaminergic neuronal networks lost in Parkinsonian patients, as thoroughly reviewed by Tansey *et al.* (Tansey *et al.*, 2007). In the case of Alzheimer's disease, instead, a decreased ability by microglia to clear toxic β-amyloid, and an immoderate pro-inflammatory/cytotoxic behaviour by microglia, are shown to play an essential role in the pathophysiology of the disease (Rivest, 2009).

Microglia show, therefore, a double-sword role: on one hand they definitely exert a neuroprotective role, supporting the development of the neuronal tissue and forming the first line of defence in the CNS, readily committed to respond to any insulting stimulus and promoting a prompt resolution; from the other side, it can result in neurodegenerative consequences, when its power becomes excessive for the goal that must be achieved. Understanding these two opposite roles of microglia behaviour will allow minimizing the harmful and capitalizing the beneficial effects.

1.3 Effect of peripheral inflammation

Increasing experimental and clinical evidence indicates that CNS not only is characterised by the ability to develop inflammatory reactions within the nervous tissues, but also can be strongly affected by peripheral inflammation (Perry, 2004; Cunningham *et al.*, 2005; Perry *et al.*, 2007; Perry, 2010). We all are aware that peripheral/systemic inflammatory reactions communicate with the brain as it can be easily seen in normal life by the appearance of a clearly brain-driven response, the so called "sickness behaviour", characterised by general malaise, including lethargy, fever, reduced activity, energy saving mechanisms, and so on (Dantzer, 2004). Interestingly, the events triggered by a peripheral inflammatory reaction within the central nervous system are quick and can have a high impact on the homeostasis of the tissue, involving molecular (cytokines) and cellular components similar to those activated contemporarily in the periphery (Qin *et al.*, 2007).

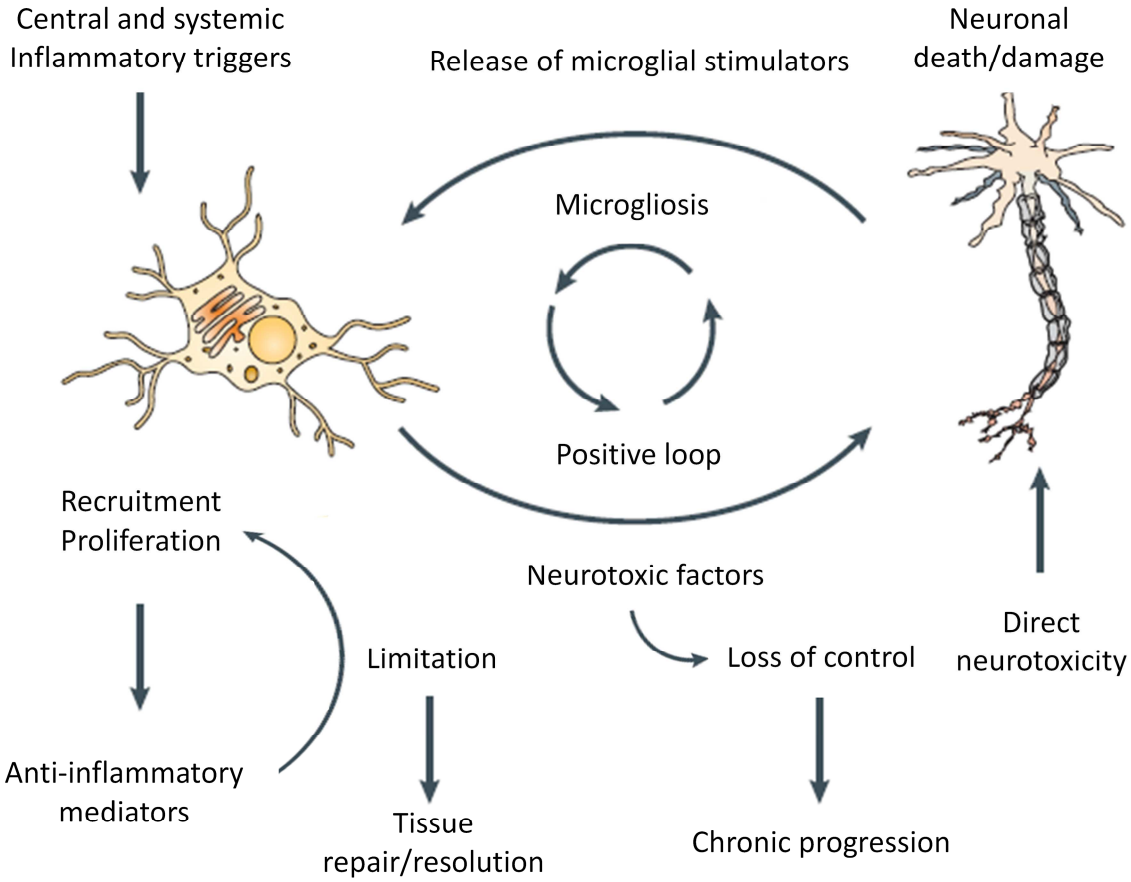

Figure 1.3 Inflammation determines the progression and outcome of neurodegenerative diseases. Insults to the CNS driving to neuronal death cause activation of surrounding microglia, which promptly start to release an array of inflammatory mediators aimed at eradicating the initial insult. Normally, self-controlling innate immune mechanisms maintain tight control of neuro-inflammatory events, restoring the CNS homeostasis as soon as the traumatic event has been solved. However, a self-perpetuating vicious cycle between neuronal damage and inflammatory response could lead to an escape from the regulatory system, therefore the immune response becoming chronically destructive. Adapted from Block *et al.*, 2007.

Consequences of these peripheral events could play a role in worsening, or even triggering, neuroinflammation correlated with neurological diseases by causing microglial chronic over-activation and the consequent onset of detrimental effects overcoming the beneficial ones in the pathology (Aloisi, 2001; Gao and Hong, 2008). However, it should be emphasised that in healthy young individuals, symptoms and consequences of systemic inflammation are usually transient, short-lived and leave no long-term consequences, thanks to the tight regulatory system (Perry, 2010).

The major impact seems to occur in aged individuals or those with on-going neurodegeneration, seemingly mediated by microglia and by their long-lived nature, which attributes them an intrinsic innate immunity memory. Hugh Perry's group in the University of Southampton proposed that existing chronic neuroinflammation and aging are able to induce microglia to acquire a particular form of activated phenotype, that has been called "primed"; chronic exposure to the same stimulus over time could be the primary cause of this state, which is characterized by morphological changes (typical of an activated state), high levels of transcription of inflammatory cytokines (like TNF-α and IL-1β) with minimal translation and a consequent inefficient response, resulting in the failure to completely effect clearance and induce restoration of homeostasis. Intriguingly, they also suggest the possibility that aging of the brain could be another factor leading to "microglial priming", with all the changes and stimuli received by the CNS during the course of life (Perry, 2010; von Bernhardi *et al.*, 2010). As Perry and his collaborators, as well as others groups, recently demonstrated in a number of neurodegenerative models (Cunningham *et al.*, 2005; Godbout *et al.*, 2005; Pott Godoy *et al.*, 2008), the concomitant occurrence of a peripheral insult in an already injured brain is able to induce a more rapid and intense over-activation of microglia, whose beneficial roles get completely overtaken by the strong pro-inflammatory cytokines and reactive (Pott Godoy *et al.*, 2008) mediators release, accelerating neural death and cognitive alterations.

From a physiopathological point of view, multiple sclerosis represents a good example of multi-factorial disease with a strong participation of inflammation in the CNS. Many of the relapses experienced by patients are tightly linked with infection and inflammatory events (Perry, 2004), which confirms the impact of peripheral inflammation in a injured brain, most likely populated by "primed" microglia. Also, it is well known that systemic infections in aged people may also result in cognitive disturbances like delirium, while several Alzheimer's disease patients die as a consequence of systemic infections impacting on the injured brain.

1.3.1 How peripheral events communicate into the brain

Understanding the routes of communication between peripheral immune responses and the brain has not been an easy challenge (Dantzer, 2004; Perry *et al.*, 2007). There are several potential routes by which systemic events are passed to the brain, which can be divided in neural, humoral and cellular pathways (Ferrari and Tarelli, 2011). First, on-going peripheral reactions occurring in the thoracic-peritoneal cavity can be sensed and transmitted to specific brain regions via neural afferent pathways, mainly through the vagus nerve (Dantzer, 2004). Also those events occurring in the oral cavity (for example during periodontal diseases) can be signalled into the CNS. On the other hand, peripherally-arising signals (mainly pro-inflammatory cytokines like IL-1β, TNF-α and IL-6) and even PAMPs (for example the lipopolysaccharide (LPS), the main cell-wall component of gram-negative bacteria) can access the nervous system through brain sites that lack a proper blood brain barrier, known as circumventricular organs, through fenestrated capillaries or through vascular regions with a damaged or more permeable BBB due to pre-existing pathological conditions (Perry *et al.*, 2007; Machado *et al.*, 2011). The BBB itself, through its numerous cellular components like endothelial cells (Singh and Jiang, 2004; Murray *et al.*, 2011), perivascular macrophages (Garden and Moller, 2006) and astrocytic feet can sense and or actively transport circulating signals and respond to them, affecting the behaviour of neurons, astrocytes but especially of resident microglia population (Dantzer, 2004; Perry, 2004). The peripheral signals can also increase the BBB permeability or even temporarily damage its peculiar tightness, therefore allowing an easier access of molecules and immune cells into the brain parenchyma. Recently, growing evidence has shown the longer-term entry of activated peripheral immune cells during systemic inflammatory diseases (mainly monocytes, bone marrow derived microglia-like cells and lymphocytes) from the inflamed periphery into the brain (D'Mello *et al.*, 2009), where these cells can directly release pro-inflammatory cytokines. Interestingly, the communication between the brain and the periphery is not a one-way road, but it is actually characterised by a more complex relationship, where signals not only go from the periphery to the brain, but also they can travel in the opposite direction, as happens, for instance, during acute brain injuries, which induce early hepatic expression of chemokines and cytokines able to trigger mobilisation of leukocytes and recruitment in the injured tissue (Ferrari and Tarelli, 2011).

With all this in mind, it's clear that understanding the routes and especially the mechanisms of the communication "periphery-to-central" is extremely important to limit the phenotypic switch seen in microglia cells of neurodegenerating or aged brains, counteracting the consequences of systemic inflammation on the brain of a population which is living longer (Perry *et al.*, 2007).

1.4 Resolution of inflammation

As it has been described previously, the power of inflammation is given by potent signals which regulate the quick amplification and events cascade; their control is of paramount importance, in order to maximize the benefit of the response, minimize unwanted side effects that lead to chronicity and are on the basis of all the chronic inflammatory disorders. Limitation and suppression of inflammation have been one of the leading therapeutic approaches studies in pre-clinical and clinical research, with non-steroidal anti-inflammatory drugs (NSAIDs) being an excellent example. However, it should not be forgotten that the initiation of an inflammatory response also triggers a set of resolution pathways, the so called "resolution phase", which is an *active* phenomenon brought about by endogenous anti-inflammatory agonists triggering a series of events aimed to restore tissue homeostasis, integrity and functionality (Serhan, 2007; Serhan *et al.*, 2007; Perretti and Dalli, 2009). Resolution is something more than anti-inflammation: the latter, represented by certain cytokines like IL-4, IL-6, IL-10, TGF-β, cytokines inhibitors and soluble receptors (Opal and DePalo, 2000), is mainly based on suppressing the release and the action of the various pro-inflammatory mediators which maintain the whole process "switched-on"; resolution, instead, goes beyond, directly down-regulating the recruitment of inflammatory cells like PMNs, restoring vascular component homeostasis, contributing to clear death cells left on the battle-field, therefore releasing factors aimed at supporting not only the extinguishing of the reaction but especially the restoration of tissue structural and functional homeostasis as close to normality as possible.

This complex phase of inflammatory reactions is characteristic of every tissue, therefore also of the brain, where the typical mechanisms and mediators of resolution have been also detected (Knott *et al.*, 2000; Lukiw *et al.*, 2005; Biber *et al.*, 2007; Serhan, 2007; Gao and Hong, 2008).

Recently, limitation of inflammation along with homeostasis and integrity restoration through exploitation of endogenously produced molecules have been regarded as a smarter move compared to the simplistic blockage of the reaction (and of its beneficial consequences) and it has become a principal therapeutic target against the side effects of the defensive response (Perretti and Dalli, 2009): interventions aimed at regulating the expression and efficacy of pro-resolution factors or mimicking their effects are promising, but a complete knowledge of these factors and of their biology is needed before their therapeutic potential can be addressed. Several local endogenous resolution autacoids are involved, their synthesis being mediated directly by the initial pro-inflammatory stimuli that triggers the reaction itself. In particular, lipidic mediators such as lipoxins, resolvins and protectins have acquired lately great importance and interest due to their potent resolutive action and to the fact that they derive from the "pro-inflammation to resolution" class switch of the same synthetic pathways of pro-inflammatory lipidic mediators like leukotrienes and prostaglandins (Serhan, 2007; Serhan *et al.*, 2007), which is based on the essential polyunsaturated fatty acids (PUFAs) pathways such as the eicosapentaenoic acid (EPA) and the docosahexaenoic acid (DHA).

Glucocorticoids (GCs) are another important class of molecular mediators of the resolution: these cholesterol-derived hormones have a wide range of actions (see below), which are exerted both through genomic and non-genomic mechanisms. The anti-inflammatory protein Annexin A1 (ANXA1 for the human form; Anxa1 for the rodent form) has been discovered as the main "second messenger" of the mechanisms of actions of the glucocorticoids (Flower and Blackwell, 1979; Blackwell *et al.*, 1980), therefore it represents an important endogenous contributor to resolution of inflammation.

1.4.1 The Annexin protein family: generalities

Previously known as macrocortin or lipocortin-1, ANXA1 belongs to the Annexins super-family (Parente and Solito, 2004; Solito *et al.*, 2008). More than 100 proteins of annexins in more than 45 eukaryotic species are known, which all conserved a high homology throughout evolution. In humans, the Annexins super-family consist of 12 members, which are thought to have evolved and differentiated from an ancestral *Anxa13* gene (Iglesias *et al.*, 2002). Each protein contains a highly conserved C-terminal core formed by several (usually four) repeat sequences (60-70 amino acids each) that are involved in binding negatively charged (acidic) phospholipids in a Ca^{2+}- dependent manner, and a more variable (and unique for each member of the family) N-terminal region that gives the functional peculiarity to each member of this family (Gerke *et al.*, 2005). The name Annexins was chosen due to the ability of the first identified members to "annex" or hold together calcium and negatively charged phospholipids. Annexins are mainly localized in the cytosol whether in a soluble form or associated with other cellular components (proteins or lipids), but can also be identified associated to the cell surface or released in the surrounding micro-environment (Solito *et al.*, 2006). Changes in cellular localisation occur promptly in presence of specific stimuli, along with changes in tissue expression (Perretti and Dalli, 2009). Although no known disease has been linked so far with a direct dysfunction of a particular annexin (for example, no genetic disorders involving annexin genes are known), the term *annexinopathies* has been coined to refer to those diseases where a strong correlation between the condition and the Annexin expression dysregulation has been identified. These proteins have been defined as disease modifiers (Fatimathas and Moss, 2010) in conditions such as cancer, diabetes and disorders of circulatory system.

1.4.1.1 Annexin A1

1.4.1.1.1 Annexin A1: molecular properties

Annexin A1 is a monomeric amphipathic protein composed of 346 amino acids weighting 38714 Da. The gene encoding for this protein is 18637 bp long and it is located on the human chromosome 9, region 9q11-9q22, showing a high degree of homology between

different mammalian and avian species. Annexin A1 is characterised by an N-terminal unique domain (amino acids 1-40) which contains the entire biological activity; several post-translational (phosphorylation, myristoilation, trans-glutamination, glycosylation) modifications sites are also present and may affect functionality and localisation of the molecule. Also, proteolysis can occur at specific sites and profoundly affect the potency of the biological responses (Vong *et al.*, 2007). The C-terminal domain, consists in 4 homologous repeats each one formed by five α-helices, as shown in Figure 1.4.

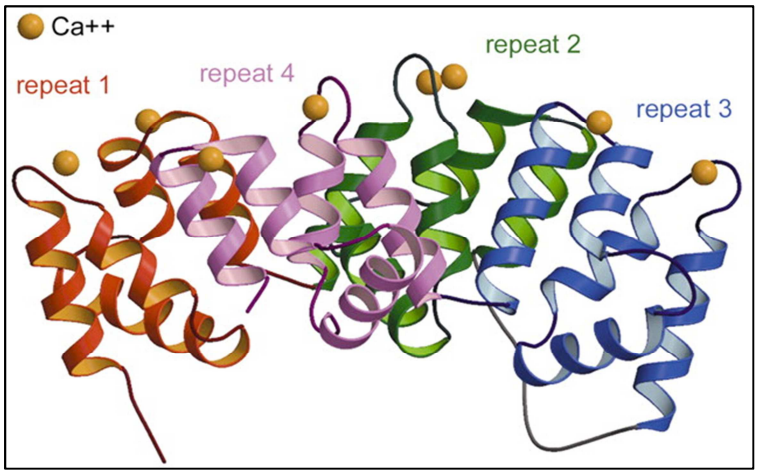

Figure 1.4 Molecular structure of Annexin A1. Ribbon presentation of the three-dimensional structure of AnxA1. Adapted from Rescher and Gerke, 2004.

The molecule presents a concave shape, with two calcium binding sites expressed on the outer side. The N-terminal domain integrates into repeat 3 of the folded core domain in the Ca^{2+}-free protein. Upon Ca^{2+} binding, the N-terminal α helix is expelled from the protein core and becomes accessible for other interactions (Rosengarth and Luecke, 2003). In the Ca^{2+}-bound conformation, the annexins can attach to membranes through the core domain, with the Ca^{2+} ions serving a bridging function.

1.4.1.1.2 Distribution of Annexin A1 in the periphery

ANXA1 location varies between tissue and cell types and it is often found in discrete populations of differentiated cells. This mediator is widely distributed in the body: in fact, it is found in white blood cells, stromal cells of the lung, bone marrow, intestine and biological fluids (Perretti and Dalli, 2009). In circulation, granulocytes like neutrophils and mast cells present a great cellular amount of ANXA1, predominantly at the level of intracellular granules; also monocytes express a lot of it in the cytoplasm or associated to the membrane depending on the level of activation, and macrophages show a huge increase due to full cell differentiation/specialisation [up to 4% of the total protein content (Lim and Pervaiz, 2007)].

Lymphocytes show a modest expression of it, while B cells and platelets interestingly show undetectable levels of ANXA1 expression.

Past and recent studies have shown the ability of this protein to respond promptly to certain anti-inflammatory stimuli like glucocorticoids or pro-inflammatory stimuli as LPS (Solito *et al.*, 2003; Solito *et al.*, 2006; Skrahina *et al.*, 2008), by undergoing post-translational modifications (Solito *et al.*, 2006; McArthur *et al.*, 2009; Yazid *et al.*, 2009) which lead to translocation from inside the cell body to the cell surface where it is readily available for its functions. So far, the mode of secretion of the protein has been an unsolved topic: since ANXA1 lacks a signal peptide for externalisation, it cannot be secreted through a classical pathway. Granule extrusion upon activation is the main explanation but it is valid only for certain type of cells (granulocytes and mast-cells mainly); in other cell types, non-classical pathway have been proposed, like through the ABC-A1 transporter system (Omer *et al.*, 2006) or via microparticle release (Dalli *et al.*, 2008).

1.4.1.1.3 The Annexin A1 receptors: a complex topic

Once on the cell surface or in the surrounding of the cell, Annexin A1 can act through an autocrine or paracrine fashion and exert its vast plethora of potent functions. The possibility for AnxA1 to play certain roles intracellularly has been confirmed in recent studies (Solito *et al.*, 2006) but since initial studies demonstrated the presence of ANXA1 saturable binding sites on the cell surface of human and rodent peripheral blood leukocytes (Perretti *et al.*, 1993; Goulding *et al.*, 1996), the autocrine/paracrine pathways has been the main research direction taken to understand the molecular mechanisms triggered by this mediator. Recent studies, although not always conclusive and extensively reviewed elsewhere (Walther *et al.*, 2000; Le *et al.*, 2002; Perretti, 2003; Migeotte *et al.*, 2006; Perretti and Dalli, 2009), have suggested that this protein interacts with receptors of the seven transmembrane G-protein coupled formyl peptide receptor (FPR) family (Figure 1.5).

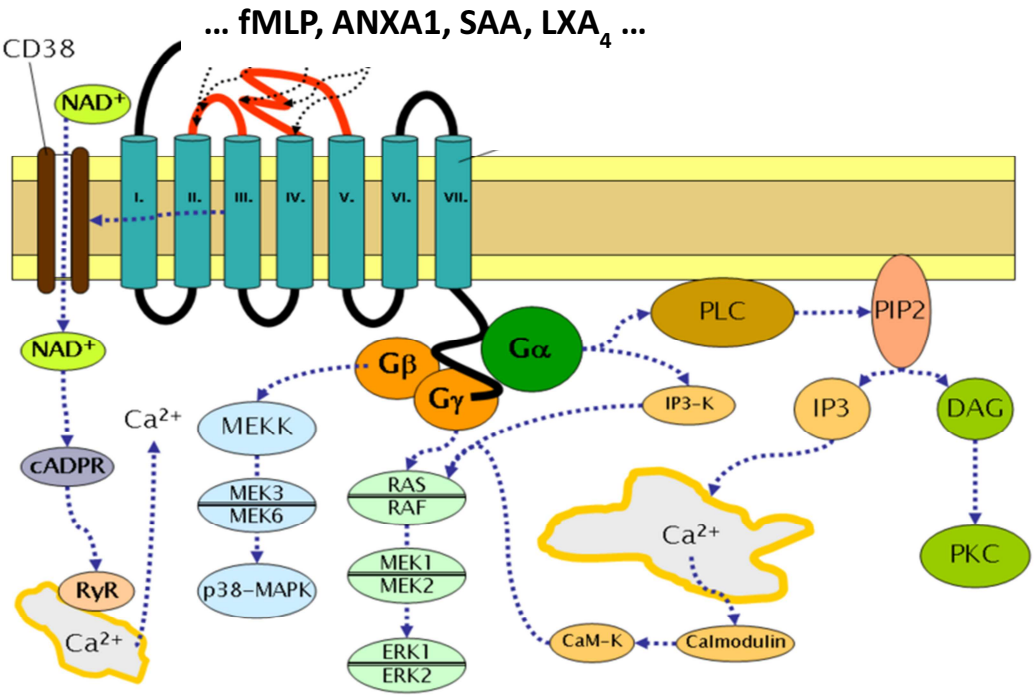

Figure 1.5 Structure and intracellular signalling pathways activated on agonist binding of FPRs. It is evident that increase in Ca2+ is the main signal triggered to induce cellular responses. Modified from Le, Murphy et al. 2002.

Initially identified on the surface of the neutrophils as the receptors for the strong chemoattractant N-formylated peptides (arising from bacterial and host cell-derived mitochondrial protein degradation), these receptors have a wide range of ligands, including endogenous acute phase response molecules like serum Amyloid A (SAA), endogenous (Resolvin D_1, Lipoxin A_4) and synthetic (Humanin) anti-inflammatory molecules and pathological peptides like β-Amyloid (Le *et al.*, 2002; Perretti, 2003). So far, 3 subtypes have been identified in humans: FPR1, FPR2 (also known as FPR Like 1 or FPRL-1, recently renamed as the Lipoxin A4 (LXA4) receptor, ALXR) and FPR3 (FPRL-2), all of them with a wide variety of endogenous and exogenous ligands, which bind the three receptors with very different affinities (Perretti, 2003; Migeotte *et al.*, 2006). These molecules are expressed in a very wide range of cell types, which include mainly immunity-related cells like, besides neutrophils, monocytes/macrophages, dendritic cells, endothelial cells, fibroblasts and stromal cells. In the central nervous system, the situation is still not clear (Solito *et al.*, 2008) but all the three members have been detected either in microglia or astrocytes or in both (FPR1 and FPR2), while some recent evidence has been reported for expression at the level of microvascular endothelium (Mou *et al.*, 2012).

1.4.1.2 Annexin A1 functions in acute inflammation and beyond

Annexin A1 shows involvement in a wide array of functions, like cell-growth regulation (Ang *et al.*, 2009), tumorigenesis (de Coupade *et al.*, 2000), cell differentiation, neuroendocrine activity regulation (McArthur *et al.*, 2009). However, the most prominent studies have been focusing on the anti-inflammatory role of ANXA1 in the periphery, especially thanks to the exploitation of the Anxa1 null mouse (Roviezzo *et al.*, 2002; Hannon *et al.*, 2003), which interestingly exhibits exaggerated responses in many of the inflammatory pathways. In particular, as mentioned before, Annexin A1 has been deeply studied for its mediating role in the anti-inflammatory action of glucocorticoids; in fact, it has been observed its high ability to independently mimic many if not all the effects brought about by GCs (Blackwell *et al.*, 1980; Goulding *et al.*, 1996) in several inflammatory models as well as its GC-inducible nature (Solito *et al.*, 1994).

During inflammatory reactions, this effector, along with its proteolysis-derived peptides such as the N-terminal fraction named Ac_{2-26} (Perretti and Dalli, 2009), is up-regulated and translocated from the cytosol to the cell membrane and the surrounding environment. Here, it primarily prevents the phosphorylation/activation of phospholipase A_2 (PLA_2), which is the enzyme responsible for the release of arachidonic acid from cell membrane phospholipids, the consequence of which is the suppression of eicosanoid synthesis (Flower and Blackwell, 1979; Parente and Solito, 2004). These findings were produced *in vitro* and confirmed *in vivo*, thanks to the useful Annexin A1 null mouse, which showed exacerbated inflammation, increased PLA_2 expression and activity and a consequent resistance to GCs treatment (Hannon *et al.*, 2003). Past experiments have shown other enzymes to be targets of Annexin A1 action in controlling inflammation, like inducible cyclo-oxygenase-2 (COX-2; another important enzyme for conversion of arachidonic acid into pro-inflammatory mediators like prostaglandins) and inducible nitric oxide synthase (iNOS; involved in the production of nitric oxide, which is a free radical involved in tackling pathogenic infections) (Parente and Solito, 2004). Production and release of other potent inflammatory mediators, like pro-inflammatory cytokines, histamine (on mast-cells) and ROS, are also negatively affected, both directly and indirectly by ANXA1, at the level of innate immune cells (Parente and Solito, 2004; Perretti and D'Acquisto, 2009).

The most important action of Annexin A1, though, remains the halting effect on leukocyte migration and invasion of the inflamed tissue as well as their viability; this links perfectly if we consider that this is also one of the major anti-inflammatory properties of glucocorticoids. Circulating neutrophils first, and monocytes later on, extravasate into an inflamed area through a multistep process in which the endothelium activated by cytokines derived from the injured site sustains rolling of the white blood cells, their firm adhesion through interactions between a class of proteins on the leukocytes (called selectins and integrins) and their endothelial cognate partners (adhesion molecules), and final migration through the endothelium (Janeway and Medzhitov, 2002). The whole process is Annexin A1 sensitive. In fact, this protein has been shown to be mobilized upon leukocyte-endothelium adhesion and then to inhibit neutrophil inflammatory function as well as monocytes recruitment (Parente and Solito, 2004). The mechanism is not fully clear yet, but it seems to involve L-selectin shedding from leukocyte membranes, influence of cytoskeletal organisation of the attached cells, blockage of firm-adhesion binding sites on the endothelium [$\alpha_4\beta_1$ integrin; (Solito *et al.*, 2000)] and probably by down-regulation of chemoattractant receptors (Walther *et al.*, 2000; Perretti, 2003). This role explains the anti-inflammatory impact of the protein in several ischemia-reperfusion injury models, both at the level of the myocardium (La *et al.*, 2001) and of the brain (Gavins *et al.*, 2007).

Interestingly, much evidence suggest Annexin A1 to be involved also in apoptosis, by activating caspase-3 signalling pathway (Solito *et al.*, 2001). Since controlled cell death is one of the mechanisms in place to maintain a tight regulation of inflammatory cells present on the battle field, this ANXA1 function could be easily explained as part of the anti-inflammatory/resolution machinery. On this regard, we should also mention its ability to serve as a “eat-me” or “find-me” signal on apoptotic cells, which are rich in negatively charged phospholipids like phosphatidylserine on the outer membrane (Parente and Solito, 2004; McArthur *et al.*, 2010), promoting chemotaxis of macrophages and clearance of the injured site from potential signals able to perpetrate the inflammatory reaction over time. Stimulation of anti-inflammatory cytokines like IL-10 and TGF-β1 (Ferlazzo *et al.*, 2003), along with the whole array of resolutive functions described above, well represents how ANXA1 plays a central role in dampening inflammatory responses and contributing to restoration.

Recently, roles of ANXA1 in the adaptive immunity have been proposed according to first experimental evidences of T lymphocytes expression (D'Acquisto, 2009; Perretti and D'Acquisto, 2009): interestingly, it seems that ANXA1 shows a pro-adaptive immunity phenotype (shifting the balance towards T_H1 and cell-mediated responses, strengthening T cell receptor signalling) and a completely opposite responsiveness to glucocorticoids.

Most, if not all, of the studies cited in this paragraph justify ANXA1 functions through its ability to bind and activate one or more of the three members of the FPR receptor family. Full length AnxA1 protein is able to bind either FPR1 or FPR2, while N-terminal peptides seem to be able to bind and activate only FPR2 (Hayhoe *et al.*, 2006; Migeotte *et al.*, 2006). The current view supports the concept of FPR2 being a conveyer of proper anti-inflammatory signals (Perretti, 2003; Perretti and Dalli, 2009), while FPR1 seems to have a more heterogeneous nature probably due to its ability to bind either pro-inflammatory or anti-inflammatory/pro-resolution mediators, as previously described.

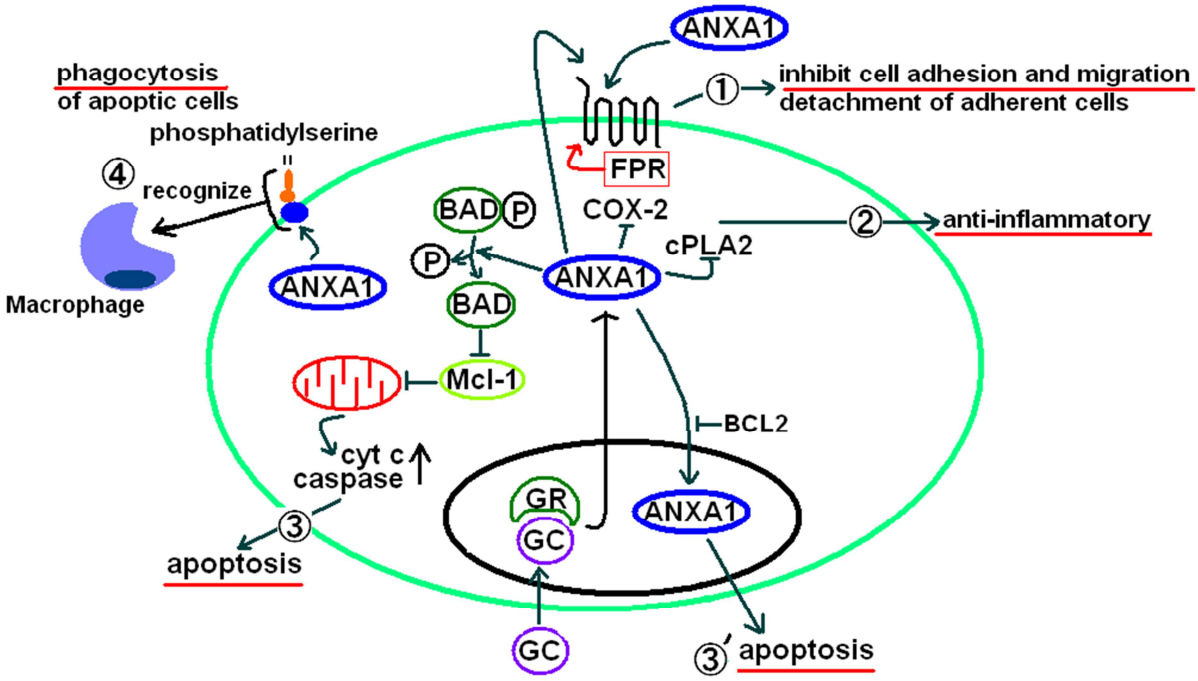

Figure 1.6 The principal biological actions of Annexin A1. The anti-inflammatory/pro-resolution mediator Annexin A1 has been found to be involved in 1) negatively regulating leukocytes extravasation 2) inhibiting cytosolic PLA_2 3) and 3') inducing apoptosis in certain cell-types, at certain doses and through multiple pathways 4) representing an "eat-me" signal for apoptotic cells and consequently mediating phagocytosis of these by professional phagocytes. Adapted from Lim and Pervaiz, 2007.

Being a constitutive protein, there have been several suggestions about ANXA1 being involved in several human disorders, primarily with an inflammatory component, even though it has been never reported to be the primary cause of a disease. For example, Annexin A1 undergoes an abnormal metabolism in cystic fibrosis and other lung disorders (Smith *et al.*, 1995), while auto-antibodies were detected in a number of conditions, maybe explaining the glucocorticoid resistance observed (Podgorski *et al.*, 1992). Also, it has been proposed as a marker for autoimmune diseases like systemic lupus erythematosus and Crohn's disease or for certain tumours (Goulding *et al.*, 1989; Stevens *et al.*, 1993).

1.4.1.3 Annexin A1 role in the brain

In contrast to the extensive knowledge of the peripheral activation of Annexin A1, no clear understanding exists about the mechanism of action in the brain, where it has also been identified (Knott *et al.*, 2000; Solito *et al.*, 2008). Extensive studies have also shown the strong involvement of ANXA1 in HPA axis regulation (Woods *et al.*, 1990; Buckingham *et al.*, 2006), where it plays a significant role in mediating the negative feedback actions of glucocorticoids on various steroid-releasing hormones: since this neuro-endocrine system is the principal source of stimulation and production of glucocorticoids, it is interesting to note how tightly these molecules are functionally bound to the anti-inflammatory mediator. As for the rest of the brain, protein expression has been detected in several central cellular components, such as the ependymal cells, glial cells such as microglia and astrocytes (McKanna, 1993), large and small gauge blood vessels and restricted neuronal populations, as extensively reviewed by Solito *et al.* (Solito *et al.*, 2008). Interestingly, ANXA1 is expressed in the cells of the innate immune system of the brain, posing the question whether its role is the same as in the peripheral immune system or if there are special peculiarities. To that extent, growing evidence suggests that this protein does take part into the resolution of inflammation: in fact, Annexin A1 has been shown to prevent *in vitro* COX-2 and iNOS activation in microglia, and to mediate other glucocorticoids-linked actions that limit stressing conditions for the delicate cerebral environment (Minghetti *et al.*, 1999). Annexin A1 expression was seen to directly correlate with neurodegenerative disorders like multiple sclerosis [MS; (Elderfield *et al.*, 1992)], in particular at the level of active lesions and sclerotic

plaques; also, severity of the symptoms in a rodent model of MS, the experimental autoimmune encephalomyelitis [EAE; (Huitinga *et al.*, 1998)], was seen to be reduced by ANXA1 N-terminal intracerebral administration, while the same model set on the Anxa1 null mouse developed a less severe pathology, indicating an apparent contradiction which may be explained with the multi-faceted roles of ANXA1 between innate and adaptive immunity (Paschalidis *et al.*, 2009). Other positive effects by the protein were detected in neurodegenerative models cause by cerebral ischemia or N-methyl-D-aspartate (NMDA) excitotoxicity (Relton *et al.*, 1991; Black *et al.*, 1992). Also, evidence for an increase in ANXA1 expression was reported (Knott *et al.*, 2000) on activated microglia cells present in the degenerating substantia nigra pars compacta (SNpc) of *post-mortem* tissue of PD patients. In recent years, several mechanisms of actions have been proposed for its supposed neuroprotective action, spanning from being an endogenous controller of microglia over-activation or a direct fail-safe signal acting on neurons, determining their fate on the basis of the level of damage undergone (Solito *et al.*, 2008). We recently demonstrated ANXA1 to be important for microglia-driven clearance of apoptotic neurons (McArthur *et al.*, 2010), which is an essential requirement to avoid secondary necrosis and perpetuation of central inflammation (Tansey *et al.*, 2007). Neuroprotective roles of ANXA1 were also shown in acute neurodegenerative events like the middle cerebral artery occlusion and reperfusion model of stroke (Rothwell and Relton, 1993; Gavins *et al.*, 2007): infarct volume, along with neurological damage/clinical score, leukocyte adhesion and inflammatory markers, were negatively altered in the Anxa1 null mouse but could be improved by intravenous administration of recombinant ANXA1.

Anti-inflammatory/pro-resolution therapies have been proposed as a potential approach in chronic neurodegenerative diseases. Long term treatment with non-steroidal anti-inflammatory drugs (NSAIDs) seems to offer some protection in AD and PD, likely by targeting the inflammatory arsenal of the innate immune cells of the brain (Minghetti *et al.*, 1999) and it is interesting to parallel the role of some of the mediators released upon NSAIDs stimulation [like aspirin-triggered lipoxins; (Perretti *et al.*, 2002)] with ANXA1 functions.

Also, treatment with glucocorticoids, that are the main triggers for ANXA1 expression, have been tested as potential therapy for diseases with neuroinflammatory participation (Lucas *et al.*, 2006). All these evidences and considerations clearly elevate Annexin A1 as a "hot" potential therapeutic molecule, whose role seem to be key, although yet far to be clear, also in the central nervous system.

Chapter 2 – Aims and objectives

2.1 Hypothesis and aims

Exaggerated central inflammatory responses appear to exacerbate neuronal loss in existing degenerative conditions (Block *et al.*, 2007) and systemic inflammation has arisen to be one of the primary factors that clinically lead to worsening existing neuroinflammation (Perry, 2004; Perry *et al.*, 2007).

A means to control the communication of peripheral inflammatory events into the damaged CNS would certainly represent a powerful tool to ameliorate the overall outcome of the disease. Studying endogenously produced mediators of anti-inflammation and inflammatory resolution and adapting them to specific clinical conditions could generate novel insights for the discovery of new therapeutic tools able to tackle more "naturally" the problem (Dufton and Perretti, 2010). In the peripheral system, Annexin A1 has represented for years a candidate for resolution: for instance, it is up-regulated in peripheral inflammatory cells and in the liver in response to pro-inflammatory stimuli, promoting a shift towards a more anti-inflammatory phenotype and resolution by driving to inflammatory cell apoptosis and phagocytosis by professional macrophages (Parente and Solito, 2004; Perretti and Solito, 2004).

Overall, this broad study aimed at improving the understanding of communication occurring between peripheral immune events and CNS and about how an important biological component as annexin A1 takes part in this process.

Preliminary unpublished data, reviewed in Figure 2.1 and Figure 2.2, showed the presence of a specific temporal and spatial pattern of Anxa1 expression in critical anatomical and functional regions both under basal conditions or peripheral inflammatory challenge; in particular, a periphery/central interface as the microvascular bed was Anxa1 positive as well as the substantia nigra pars compacta (SNpc), the area of the brain undergoing neurodegeneration in PD.

We **hypothesized** that ANXA1 may be a key molecule regulating the transfer of systemic inflammatory reactions into an intact or injured brain, controlling the consequent response mounted by the brain, ultimately limiting neurotoxicity. Therefore, it may represent an endogenous anti-inflammatory effector not only in the periphery, but also in the CNS.

In particular, we **proposed** Annexin A1 to play a neuroprotective role at various levels, regulating the behaviour of BBB as well as limiting microglial hyper-activation in response to **a)** peripheral inflammation, **b)** on-going degenerative conditions or **c)** both, thereby beneficially controlling neuroinflammation, pre-existing neurodegeneration and pathological outcomes.

Using an integrative *in vivo/in vitro* approach, our aims included:

- **understanding** if and how **ANXA1** participates in regulating **BBB integrity** and **responsiveness** in basal conditions and under systemic inflammatory events;
- a comprehensive **characterisation** of the **temporal and spatial pattern of ANXA1 expression** in the normal brain in response to peripheral inflammation, in order to define a functional link for the protein in regulating cerebral immune homeostasis;
- the **evaluation** of the effects brought by **peripheral inflammation** in worsening the neuronal damage under **neurodegenerative conditions**, using experimental PD model based on 6-hydroxydopamine-induced lesion [6-OHDA; (Gillies and McArthur, 2010)] of the nigro-striatal dopaminergic pathway (NSDA), depicting microglia involvement and the impact of ANXA1 on the neurodegenerative outcome.

The overall goal of this thesis was thus to investigate the relevance of central ANXA1 as an essential “communication bridge”, able to sense, decode and translate events occurring in the rest of the organism into the CNS, with the ultimate aim to maintain the general homeostasis, without limiting the physiological periphery-to-brain communication, but instead regulating it in case of excesses.

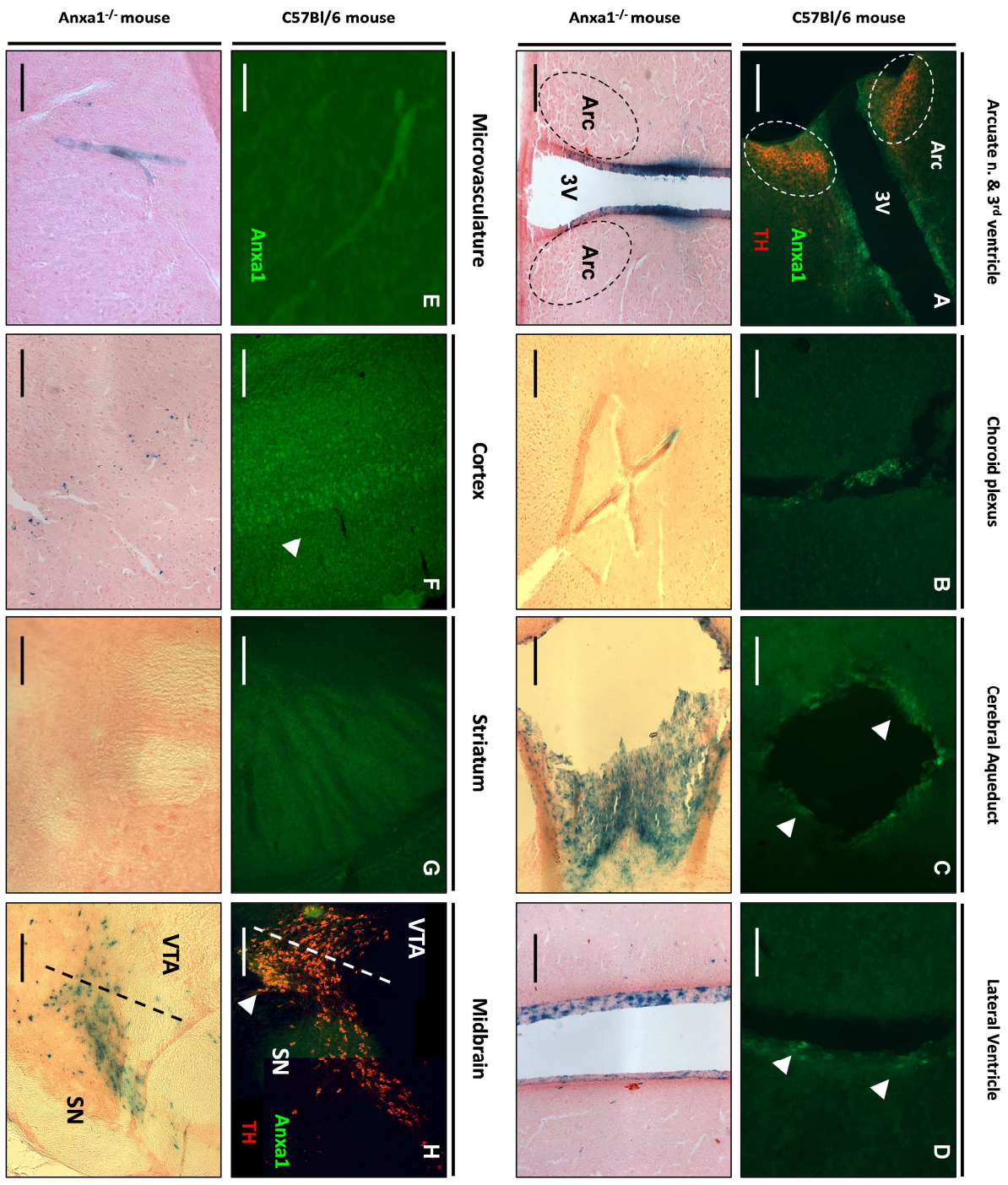

Figure 2.1 Anxa1 basal expression in various brain regions. Sections are from healthy untreated animals and suggest the presence of basal Anxa1 in numerous cell types and functionally relevant brain regions. Sections from wild-type C57Bl/6 mice were stained by immunofluorescence for Anxa1, while those from Anxa1 null mice were probed for β-galactosidase activity through *X-gal* staining; this was possible because exons 2-4 of the *Anxa1* murine gene were replaced with β-galactosidase coding sequence (*LacZ*) as reviewed (Hannon *et al.*, 2003). For technical details please refer to General methods. Scale bars: 800 µm. TH: tyrosine hydroxylase positive neurons; Anxa1: Annexin A1.

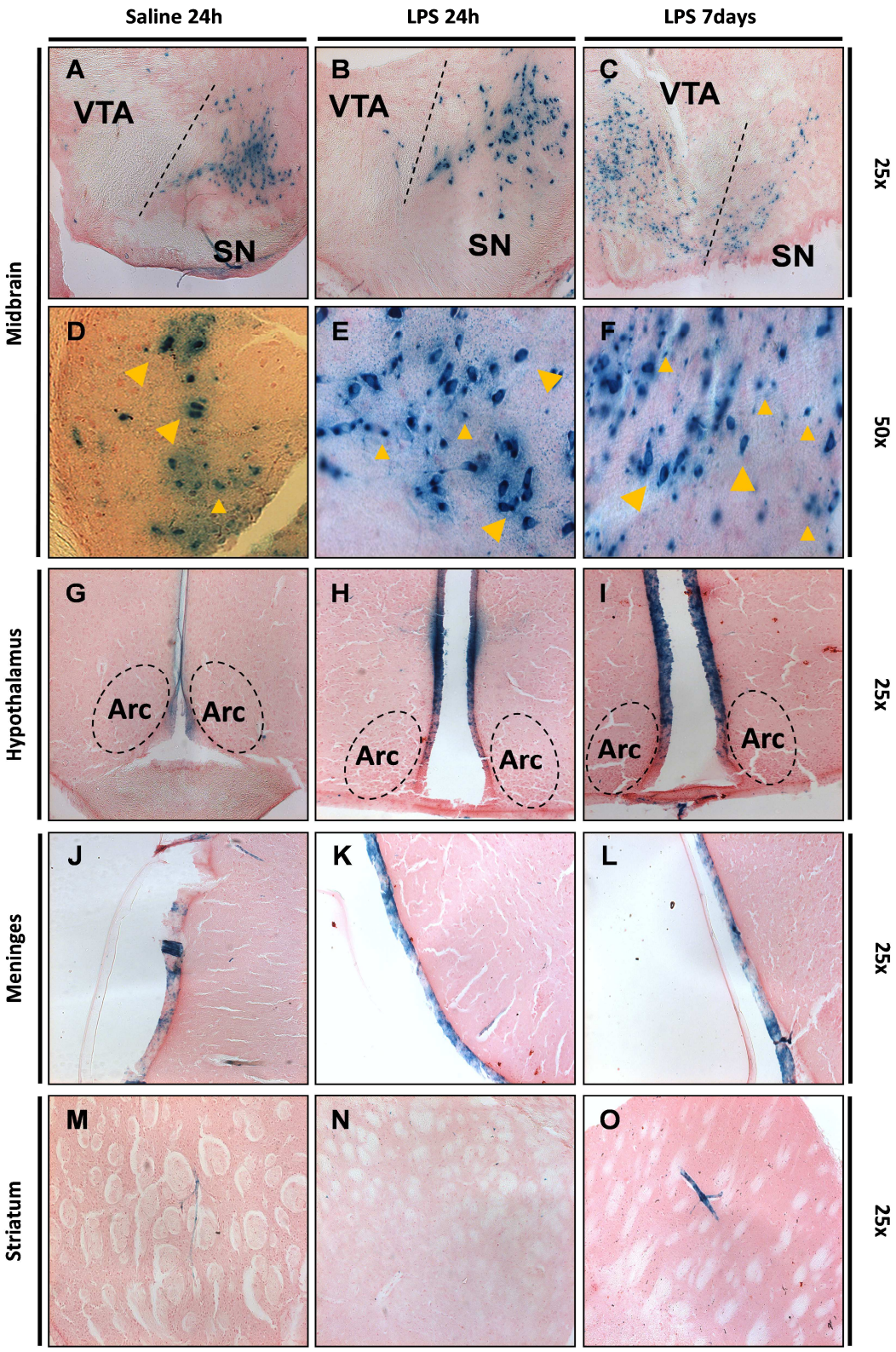

Figure 2.2 Activation of Anxa1 promoter under LPS challenge in midbrain, hypothalamus, striatum and meninges. *X-gal* staining in Anxa1 null mice brain slices was performed according to an established method. Big-headed arrows in **D|**, **E|** and **F|** indicate neuron-like cells while small-headed arrows point to small glia-like cells. Results for 2 hours LPS administration are not presented since very similar to 24 hours. Pictures produced by Dr. S. McArthur and used for grant application.

Chapter 3 – General methods

3.1 Materials

Reagent description and composition of solutions used in the various methods described below can be found in Chapter 10, the Appendix, Section 10.1. For antibodies and primer details refer to sections 10.2 and 10.3, respectively.

3.2 Methods

In this section, methods that have been used extensively throughout the project are described. For methods relevant for only one specific part of the thesis, please refer to the specific result chapter.

3.2.1 *In vivo* methods

All animal experiments were performed in accordance with the UK Animals Scientific Procedures) Act 1986, under project licence (PPL 70/7082), and personal licence (PIL 70/21936). *In vivo* experiments were carried out on 2-4 month-old male or female mice as stipulated. All mice were group-housed in the facilities at the Hammersmith Campus of Imperial College London with sawdust and paper-wool nesting material provided. A 12:12 hour light/dark cycle at 22°C was used. Food pellets and water were available *ad libitum*. Wild-type animals were from the C57BL/6 strain and were purchased from Charles-River (UK). After arrival, animals were allowed to acclimatize to their new surroundings for at least a week. Annexin A1 null mice ($Anxa1^{-/-}$) were bred in-house (Hannon *et al.*, 2003). All $Anxa1^{-/-}$ mice used for experiments were genotyped by polymerase chain reaction (PCR) according to standard procedures [as described in (Hannon *et al.*, 2003)] prior to use, using plasmids bearing the murine coding sequence for Anxa1 or β-galactosidase as controls.

3.2.1.1 LPS time-response in wild-type and Anxa1 null mice

Wild-type and Anxa1 null male mice (2/3 months old; *n*=4/group) were weighed before treatment and then received a single intraperitoneal (*i.p.*) dose of 3 mg/kg LPS in 100 µl saline or 100 µl 0.9% saline for control animals (2 hours, 24 hours and 7 days as time points).

Group of animals were sacrificed at the scheduled time points (2 hours, 24 hours and 7 days after LPS injection), perfused, fixed and brain tissues collected as explained in the following paragraph.

3.2.1.2 Perfusion, fixation and collection of brain tissue

Animals were deeply anesthetised by *i.p.* injection of 100 µl sodium pentobarbitone (60 mg/ml). Once fully anesthetised, an incision was made through the peritoneal cavity, revealing the diaphragm. The heart was then revealed by cutting through both sides of the rib cage and the diaphragm. Blood samples were collected by cardiac puncture of the right ventricle and the right atrium was cut to allow release of blood. Blood was washed out of the body by perfusion through the left ventricle with approximately 15 ml of filtered saline at 4°C, followed by fixation by perfusion with approximately 20 ml of filtered 2% PFA (paraformaldehyde) in PBS (Phosphate buffered saline) 0.01 M at 4°C. Brains were rapidly removed and post-fixed in 2% PFA overnight at 4°C, cryoprotected in 30% sucrose solution for 2 days at 4°C and frozen on dry ice, for long-term storage at -80°C. In some cases, samples were not exposed to formaldehyde, but were snap-frozen in isopentane cooled on dry ice and subsequently frozen at -80°C.

3.2.1.3 *In vivo* administration of Evans Blue

Evans blue dye extravasation was chosen to detect changes in permeability *in vivo*. This technique is based on the small molecule Evans blue; once in the blood stream, most of it binds to albumin and serum proteins, while a small portion remains uncoupled. In normal conditions, non-significant amounts are able to cross the blood brain barrier and leak into the brain parenchyma, while under certain stimuli the leakage increases mainly via the non-specific vesicular-mediated or the paracellular pathways (Pardridge *et al.*, 1985; Greenwood *et al.*, 1988). Male and female animals (2 months old) were purchased from Charles-River or obtained from our running colony of Anxa1$^{-/-}$ mice and divided in treatment groups (n=4-5/group). Before the LPS/saline administration, animals were weighed in order to work out the LPS dosage.

Those belonging to different time point groups (4 hours, 24 hours and 7 days) were injected *i.p.* with a single dose of 3 mg/kg LPS in 100 µl 0.9% saline solution or 100 µl 0.9% saline solution for the control animals (24 hours as unique time point). Animals were placed under warming lamp for 5 minutes to facilitate tail vein visualization and 100 µl of filtered 2% Evans blue solution were injected intravenously. After allowing 1 hour for the dye to diffuse from the circulation into the tissues, a sample of blood was collected and mice were perfused with 15 ml cold saline to remove Evans Blue from the circulatory system. Brains were rapidly removed and sliced in the two hemisphere by cutting through the midline using a scalpel; one half was post-fixed (in 4% PFA) overnight at 4°C and then cryoprotected in sucrose, while the other half was used for the spectrophotometric assay described in the next section.

3.2.1.4 Evans Blue detection in brain homogenates and serum samples

The following protocol was adapted from published methods (Morrey *et al.*, 2008; Manaenko *et al.*, 2011). Brain tissue was collected as described in section 3.2.1.2 and dissected along the cerebral midline. One half was placed in 4% PFA in PBS 0.01 M and the other half in 3 ml PBS 0.01 M and placed on ice. The hemisphere was mechanically homogenised and 2.5 ml of 60% trichloroacetic acid (TCA) was added; samples were mixed for 10 seconds and left on ice for 30 minutes. Tubes were then centrifuged at 1000x*g* for 30 minutes and 200 µl of the supernatant were spectrophotometrically assayed at 620 nm alongside a standard curve ranging from 20 µg/ml to 2 ng/ml of Evans Blue dye.

Blood samples obtained by cardiac puncture were allowed to clot at 37°C for 10 minutes and then centrifuged at 1200x*g* RPM for 30 minutes at 4°C; the resulting supernatant (serum) was collected in a fresh tube. Serum samples were analysed 1:40 in a final 200 µl volume. Final values were normalized to tissue weight and expressed as percentage of serum dye content, as reported (Morrey *et al.*, 2008):

$$\frac{(\mu g \text{ of dye in brain}) \,/\, (\text{mg of tissue})}{(\mu g \text{ of dye in serum})} \times 100$$

3.2.2 *In vitro* methods

3.2.2.1 Cell culture

3.2.2.1.1 Origin of hCMEC/D3 cell line

The hCMEC/D3 (human cerebrovascular endothelial cell line/clone D3) cell line was obtained by Dr I. Romero, Professor O. Couraud and Professor B. Weksler (Cornell University, NY, USA) under a signed material transfer agreement (MTA). This cell line was originally established as described in Weksler *et al.*, 2005 (Weksler *et al.*, 2005). Briefly, isolation of primary endothelial cells was undergone on a surgical excision of cerebral tissue from an epilepsy female patient (surgery performed at Kings College Hospital), following the protocol established at King's College London for rat brain endothelial cells isolation and reported in the literature (Abbott *et al.*, 1992). Purified endothelial cells were immortalized by sequential lentiviral transduction of human telomerase reverse transcriptase (hTERT), a ribonucleoprotein which maintains the telomere ends of chromosome, therefore preserving the genetic information present in the genome and the ability to replicate safely, and of Simian virus 40 (SV40) large T antigen, which is a viral proto-oncogene driving the host cell cycle towards the S phase (DNA replication) and G2 phase (cell division).

Clonal selection was performed according to several parameters, like morphology, proliferating capacity, and stable expression of typical endothelial phenotype markers (Weksler *et al.*, 2005).

3.2.2.1.2 Routine cell culture of hCMEC/D3 cell line

hCMEC/D3 cell line was maintained in EGM-2 MV (Lonza, CH) provided with all the growth factors (see Appendix, section 10.1.3) as indicated by the authors (Weksler *et al.*, 2005) and in the original datasheet. Cells have been used until passage 35, since this has been defined as the limit after which cells start losing their microvascular endothelial phenotype. T-75 growth flasks (VWR, UK) were routinely used to expand the number, while 10-cm dishes, 6-, 12-, 24-well plates (Corning Inc., Sigma, UK), labtek devices and transwells (see below) were used to run the functional experiments.

Before plating, growth surface was coated with rat tail collagen (BD Biosciences, UK) for 1h, 37°C or overnight at room temperature (RT). Working volumes were chosen to be between 0.2 and 0.5 ml/cm^2. Cells were passaged during their log-phase of division (approximately when they reached 70-80% of confluence). First, they were washed twice with DPBS (Dulbecco-modified phosphate buffered saline) without Ca^{2+}/Mg^{2+}, then incubated with enough volume of Trypsin-EDTA (Lonza, CH) at 37°C; enzymatic activity was stopped with fresh growth medium and cells were counted by using a disposable haemocytometer (Kova Glasstic slide 10; Hycor biomedical Inc., US); the required number of cells (calculated knowing that the optimal plating concentration should be 25000 cells/cm^2) were subsequently harvested at 1200 x *g* (centrifuge model: Harrier 15/80; MSE, UK) at RT for 5 minutes and the pellet was resuspended in fresh medium and transferred into the plate.

3.2.2.1.3 Cryopreservation of hCMEC/D3 cell line

Frozen stocks were regularly produced by detaching the cells through trypsinisation, resuspending around $4 \cdot 10^6$ of them in freezing medium (see Appendix 10.1.3) and storing them in cryovials (containing 1 ml of the cell suspension; cryovials from Nalgene, Sybron Int., US), which were then frozen down at approximately 1°C per minute in a -80°C freezer using a freezing device filled with isopropanol (as specified in the datasheet; Nalgene, Sybron Int., US). After 24 hours, samples were transferred to the -196°C liquid nitrogen general stock.

3.2.2.1.4 Thawing hCMEC/D3 cell line

A frozen stock vial was removed from the liquid nitrogen tank and placed immediately inside the incubator (37°C). Once the cell suspension had completely thawed (within 2 minutes maximum), cells were transferred into a 15 ml Falcon tube and 5-10 ml of pre-warmed EGM-2 MV medium was added drop-by-drop to dilute the toxic effect of DMSO. Cells were then sedimented by centrifugation, supernatant was aspirated and fresh medium was added to resuspend the pellet. The volume was finally transferred into a new T-75 flask and fresh medium was replaced 24 hours after thawing.

3.2.2.1.5 Cell transfection of hCMEC/D3 cell line

Following the manufacturer's instructions, HiFect (Lonza, CH) was employed to transfect hCMEC/D3 cells. Cells were seeded in 10 cm dishes or 12-well plates and transfected when they reached 60/80% of confluence after replacing the medium with fresh 2/3 hours before the transfection, to induce cell division and consequent higher accessibility of the transfected DNA into the cell nuclei.

24 hours later, cells were washed with DPBS without Ca^{2+}/Mg^{2+} and medium changed with fresh one. Cells were harvested or put under selective agent (Geneticin G418®; for stable transfected clones selection) after further 24 hours of growth.

3.2.2.1.6 Paracellular permeability assessment

The permeability of hCMEC/D3 cell monolayers to molecules of different sizes was measured, as described [(Dehouck *et al.*, 1992; Weksler *et al.*, 2005; Forster *et al.*, 2008)] and represented in Figure 3.1, on 12-well plate transwell polycarbonate inserts (surface: 1.1 cm^2; pore size: 0.4 µm; Sigma-Aldrich, UK) coated as following: 1h RT with 1:20 calf-skin collagen solution in HBSS without Ca^{2+}/Mg^{2+}; 1h RT with 1:100 fibronectin solution in HBSS without Ca^{2+}/Mg^{2+}. $1.8x10^5$ cells were seeded on the filters in complete EGM-2 MV medium. When cells reached 100% confluence, they were quickly washed in HBSS without Ca^{2+}/Mg^{2+} and medium was switched to EGM-2MV provided with all the growth factors but VEGF for 96 hours, to limit over-growth and support the formation of a tight monolayer. Certain stimuli were added during the incubation without VEGF (long incubation with 17-β Estradiol; see experimental plans) while others (TNFα and IFNγ) were added in the last 24 hours. At the end of the stimulation, the experiments were performed using FITC-labelled dextran (molecular weight 70 kDa; Sigma-Aldrich, UK) dissolved to 3 mg/ml in transport buffer (2% Fetal calf serum (FCS) DMEM without phenol-red) and added (500 µl) carefully on top (the upper chamber) of the cells. One insert (empty filter) was treated exactly as described above but no cells were plated; this served to measure the resistance of the plastic surface itself. The various transwell filters were carefully moved to the first row of wells of 12-well plates where 1.5 ml of transport buffer was added for each well. At 10 minute intervals, insert were moved to the next row of wells, for a total of 60 minutes.

The fluorescent content of the wells was sampled for fluorescence emission using a fluorescence multiwell plate reader (VersaMax, Molecular Probes) with the following parameters: excitation wavelength: 485 nm; emission wavelength: 520 nm. To define a concentration-dependent transport parameter, the clearance principle was used. Cleared volume for each time interval was calculated following this equation:

$$[V]cl = \frac{[C]l \times [V]l}{[C]u}$$

$[C]_u$ represents the fluorophore concentration on the upper chamber, while $[V]_l$ and $[C]_l$ the volume and the fluorophore concentration in the lower chamber, respectively. Concentration values of the lower chamber were calculated by plotting a standard curve of known amounts of FITC-dextran. An increment of cleared volumes was plotted against time of measurement (60 minutes); the slope of the linear curve proportionally represents the permeability properties of the monolayer and defines PS, the permeability surface area, which indicates the resistance opposed to the clearance:

$$\text{PS TOT} = \text{slope}$$

The total resistance opposed to the passage of the dye is the sum of the resistance offered by the monolayer and the one offered by the filter itself; so:

$$\text{PS TOT} = \text{PS endo} + \text{PS filter}$$

Therefore, Ps endo can be calculated by subtracting PS filter from PS TOT.

Since the permeability coefficient (in physics also called conductance) is defined as the inverse of the resistance, the permeability coefficient of the endothelium (P_e) can be calculated as follows:

$$\text{Pe} = \text{P TOT - P filter} = \frac{1}{\text{PS TOT}} - \frac{1}{\text{PS filter}}$$

Endothelial permeability coefficient (Pe) was calculated in unitary value ($^{cm}/_{min}$) as described (Dehouck *et al.*, 1992). Each single experimental repeat was performed in duplicate and at least 3 independent repeats were performed for each set of treatments. Values usually are reported as relative percentage of the control. Average control/untreated Pe value is: $5x10^{-5}$ cm/min.

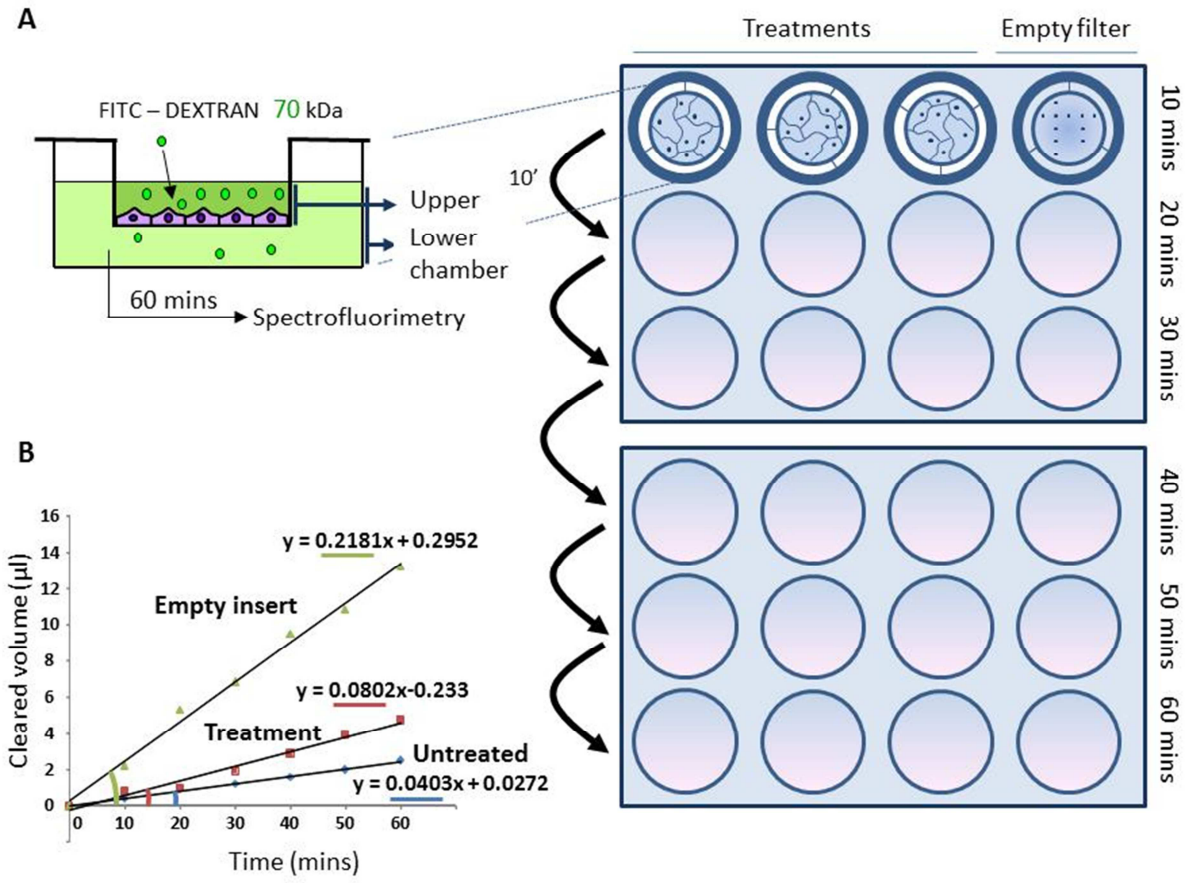

Figure 3.1 Procedure and principles of the in vitro paracellular permeability assay. A) Visual description of the transwell system and temporal procedure used to measure paracellular permeability on hCMEC/D3 monolayers. B) Principle of the cleared volume by which permeability coefficient is calculated; slopes of the lines are indicated in the equation and in the x/y graph (as the angular coefficient). See section above for detailed description.

3.2.2.1.7 Electrical resistance measurement

Another way of assessing the tightness of cellular monolayers was by calculating the resistance offered by the monolayer to ions passage/electric currents, defined transendothelial electrical resistance (TEER). 100% confluent cultures underwent TEER measurements using a two-electrodes Millicell-ERS apparatus (Millipore, UK). TEER were expressed as Ohms·cm^2 (Ω·cm^2) and values obtained from collagen-coated cell-free inserts were subtracted from the resistance values of the cultures to yield the resistance values due to the cells only. In some cases, after empty filter subtraction, values have been reported as relative percentage of the untreated control. Average control value obtained for cell cultures was 44.88 ± 1.44 Ω·cm^2 while for primary cultures was 100 ± 4.15 Ω·cm^2.

3.2.3 Immunoassays: Enzyme-linked immunosorbent assay (ELISA)

3.2.3.1 Principles

Enzyme-linked immunosorbent assay (ELISA) is an immunoassay used to detect and quantify analytes by using antibodies specific for that antigen. The most widely used type of ELISA for antigen quantification is the sandwich ELISA, so called because the molecule of interest is bound between two antibodies (Lequin, 2005). First, a primary antibody (called capture antibody) is incubated in a 96 well plate in order to tightly bind to the plastic, which is specifically treated for this application. After occupying the free sites with a blocking solution, to avoid unspecific further binding, samples containing the analyte are incubated and this step is then followed by several washes, to remove unbound molecules. The second antibody, called detecting antibody, is then added to each well. Therefore, this technique is possible only if two antibodies specific for two different epitopes of the antigen of interest and from different species origin exist. The final step involves the use of a conjugated tertiary antibody produced against the isotype and species, which the detecting antibody belongs to. Conjugation of the tertiary antibody with an enzyme like horseradish peroxydase (HRP) or alkaline phosphatase (AP) and incubation with a substrate like 3,3',5,5' Tetramethylbenzidine (TMB), which can be converted to a coloured product, allows the amplification of the signal and detection of even small quantities of antigen. Absorbance at specific wavelength will be directly proportional to the amount of antigen captured into the wells.

3.2.3.2 Quantification of Annexin A1 protein by ELISA

Total human Annexin A1 in cell cultures samples was measured by ELISA, following a protocol developed at William Harvey Research Institute, Queen Mary University London (Goulding *et al.*, 1990).

At each step, 100 µl of the different solutions was the volume chosen per well. Mouse monoclonal antibody (called m1B, produced in-house through hybridoma formation) was used as capture antibody at 10 µg/ml concentration in bicarbonate buffer and absorbed on ELISA-treated plates (Nunc MaxiSorp, ThermoScientific, UK) overnight at 4°C.

Plates were then washed 3 times with bicarbonate buffer and blocked with PBS without Ca^{2+}/Mg^{2+} 1% bovine serum albumin (BSA) for 1 hour at 37°C. During the incubation, ANXA1 standards were prepared (500, 250, 125, 62.5, 31.25, 15.62, 7.8, 3.9, 1.95, 0.98, 0.49 and 0 ng/ml) in assay diluent (PBS without Ca^{2+}/Mg^{2+} 1% Triton-X-100). Unknown samples were treated as follows: cell medium samples were loaded neat, cells lysate samples were diluted 1:5; human and rodent serum samples were loaded neat. Samples were loaded and incubated for 1 hour at 37°C. Plates were washed 5 times with 0.9% NaCl 1% Triton-X-100 and incubated with 1 µg/ml of detecting antibody (Rabbit polyclonal anti-ANXA1; Invitrogen, UK) for 1 hour at 37°C. After 5 washes, immune-complexes were detected by adding the tertiary goat-anti-rabbit IgG antibody, which is conjugated to alkaline phosphatase. After 5 final washes, reaction was triggered by incubation with a solution of p-Nitrophenyl phosphate (tablets from Sigma, UK) in bicarbonate buffer and plates were left in the dark for 10-20 minutes, until a clear yellow colour was formed, paying attention to avoid saturation of highest standard points and of more concentrated samples. Plate wells were finally measured for their absorbance at 405 nm and corrected at 540 nm as reference wavelength, using a spectrofluorimeter (Tecan Infinite M200 Pro, Tecan, Austria).

3.2.4 Protein isolation and analysis: immunoblotting

3.2.4.1 Protein extraction from tissue

For tissue protein analysis, two protocols were adopted, the first one for total protein extraction, the second one for soluble and insoluble protein fractionation. Animals were transcardially perfused with filter-sterilized saline (0.9% NaCl) and brains were excised and subsequently snap-frozen in isopentane cooled in liquid nitrogen and stored at -80°C. A portion of the frontal cortex was obtained by using a scalpel, weighted and homogenised in radioimmunoprecipitation assay (RIPA) lysis buffer (5 µl/mg tissue) through a homogenizer (Omni Int., US) at 4°C for total protein extraction. The homogenate was left at 4°C for 30 minutes under agitation and subsequently centrifuged (bench centrifuge model: Biofuge Fresco, Heraeus, Thermo Scientific, UK) at 14000x*g* for 30 minutes at 4°C. Supernatant was kept while pellet was discarded.

For soluble/insoluble extraction, the tissue portion was homogenised in Triton X-100 extraction buffer (5 µl/mg tissue), left at 4°C for 30 minutes under agitation and subsequently centrifugated at 14000x*g* for 30 minutes at 4°C. Supernatant was then transferred to a separate tube and labelled as the soluble fraction. 150 µl of the same lysis buffer supplemented with 1% sodium dodecyl sulfate (SDS) was added to the pellet, subsequently disrupted with an ultrasonic crusher (Ultrasonic processor; Jencons, US with the following parameters: 30% duty cycle, output control 2; 3 strokes/10 sec each with 15 seconds on ice between each stroke), left under agitation at 4°C for 15 minutes and centrifugated at 14000x*g* for 20 minutes at 4°C. The supernatant was collected and labelled as the insoluble fraction.

3.2.4.2 Protein extraction from cells

For cell-line analysis, cells were trypsinised, collected and the pellet frozen at -80°C. RIPA lysis buffer (100 µl/0.5x10^6 cells) was added and cells were homogenised through 3 cycles of freeze and thawing. If the lysate was too viscous, it was passed through a syringe needle (30G) to shear DNA and make it easier to handle. Samples were then centrifuged at 14000x*g* for 30 minutes at 4°C and the supernatant transferred in a separate tube.

In the case of soluble and insoluble fraction isolation, 1% Triton X-100 DPBS with Ca^{2+}/Mg^{2+} solution was first used to extract all the soluble proteins for 5 minutes on cell monolayers; this was saved as the soluble fraction. Subsequently, after 2 quick washes in DPBS without Ca^{2+} and Mg^{2+}, a new buffer was added (Insoluble β-actin extraction buffer) and cells were scraped, passed through a fine 30G needle, sonicated as described above in case the viscosity of the material (mainly due to sheared DNA) remained too high (Cramer *et al.*, 2002). Both fractions were centrifuged at 14000x*g* for 20 minutes at 4°C, and supernatants transferred to fresh tubes (soluble and insoluble fractions). Please refer to Chapter 4 for more details.

3.2.4.3 Protein content estimation

Protein concentration of the samples was calculated through Bicinchoninic Acid Assay (BCA; Thermo Fisher Scientific, UK). Briefly, this assay is based on two reactions: first, the reduction of copper cations (Cu^{2+}) derived from the component cupric sulphate to Cu^{+} by peptide bonds, a reaction proportional to the amount of proteins present; second, the chelation of the Cu^{2+} ions by bicinchoninic acid molecules, which results in the formation of a purple product with high light absorbance at 562 nm wavelength (Smith, Krohn *et al.* 1985). 96 well plates were used and each sample was analysed in triplicate. Dilutions of the samples were prepared using the lysis buffer as diluent; a standard curve was produced using BSA as the standard (0; 0.2 mg/ml; 0.4 mg/ml; 0.6 mg/ml; 0.8 mg/ml; 1 mg/ml; 1.5 mg/ml; 2 mg/ml points). All wells received 200 µl of a solution formed by mixing 50 parts of solution A (which contains bicinchoninic acid and sodium tartrate in an alkaline - pH 11.2 - buffer) and 1 part of solution B (4% cupric sulphate pentahydrate solution) as described in the manufacturer's protocol. Plates were incubated at 37°C for 30 minutes and then read at 562 nm with a spectrophotometer. Interpolation of absorbance and standard known concentration was used to calculate the sample protein content.

3.2.4.4 Electrophoresis and immunoblotting

Equal amounts (10-50 µg of tissue lysates; 5-15 µg of cell lysates) of extracted proteins were separated by SDS-polyacrylamide gel electrophoresis, based on the principles described by Laemmli in his pioneering work (Laemmli, 1970); reducing conditions and usage of SDS as anionic detergent determine the separation of the different protein entities according only to their molecular weight. For tight- and adherence junctions detection, pre-casted 4-20% gradient poly-acrylamide gels (Tris-Glycine Novex; Invitrogen, USA) were used, while for the other molecules studied gels were cast in house. To accomplish that, glasses for gel electrophoresis were mounted by using 1.5 mm spacers and the relative support (Biorad, UK); resolving gels were prepared at 10 or 12% of poly-acrylamide content, pH 8.8, poured into the gap between the outer and the inner glass and left to polymerise for 15-20 minutes at RT. A thin layer of water or absolute alcohol was added right after layering the solution to avoid any reaction between air and the solidifying gel.

The resolving gel acrylamide concentration was chosen according to the size of the proteins to be studied. After polymerisation occurred, the liquid added on top was discarded and the resolving gel was overlaid with 4% polyacrylamide stacking gels, pH 6.8.

Samples were prepared in loading buffer (see Appendix; section 10.1.8) and subsequently boiled at 95°C for 5 minutes to denature the proteins. After loading the samples and pre-stained standards (Page Ruler Plus; Thermo Scientific, UK) into the wells, gels were mounted into the running apparatus (Biorad, UK) and run at 30 mA/gel for stacking, then 50 mA/gel for resolution in running buffer. Resolved proteins were transferred to nitrocellulose membrane (Hybond®, Amersham Biosciences, UK): a gel sandwich was prepared in a cassette (Bio-Rad, UK) by layering fibre pad, filter paper, gel, membrane, filter paper and fibre pad. The cassette was placed in the appropriate module and tank, filled with chilled transfer buffer and connected to the power pack for 1 h at 400 mA, 100 V. Membranes were then blocked in 3% BSA in Tris-buffered saline 0.1% Tween-20 (TBS-T) for 45 minutes-1 hour to block non-specific antibodies binding. Membranes were then washed briefly in TBS-T before incubation with primary antibody at the desired dilution (prepared in 3% BSA TBS-T) overnight at 4°C. Membranes were then washed in TBS-T once for 30 minutes and twice for 15 minutes to ensure removal of unbound antibody, incubated with the host-specific HRP-conjugated secondary antibody for 1-2 hours at RT and washed again as above.

Immune-reactive bands were visualised by enhanced chemiluminescence (ECL) reaction: this is based on the hydrogen peroxide-dependent oxidative activity of HRP on luminol, which results in the subsequent emission of light; the intensity is proportional to the quantity of the enzyme (so to the quantity of the bound protein of interest) and can be captured on an autoradiographic film. The ECL commercial kit by Thermo Scientific, UK was chosen and consisted in preparing a working solution by mixing equal volumes of reagents A and B. Membranes were submerged in this mix for 1 minute; the excess of liquid was then removed, immunoblots were wrapped in plastic film prior to exposure to X-ray films (GE Healthcare; Amersham Biosciences, UK and Santa Cruz Biotech; US), which occurred for 10 seconds – 10 minutes under dark conditions. Films were developed by using an automatic developer and fixer machine.

To re-probe the membranes with different antibodies, these were stripped in stripping buffer (Restore Western Blot; ThermoScientific, UK) under gentle agitation for 15 minutes at RT, then washed in TBS-T and re-blotted for β-actin or GAPDH as internal controls that ensured similar loading for all the samples/wells.

X-Ray films were scanned at high resolution and band intensities were detected through Image J software densitometry application, normalising the values against the internal loading controls of each sample. Results of the repeats of the same condition were averaged as well as results from different independent blotting repetitions.

3.2.5 Molecular biology

3.2.5.1 RNA extraction

Total RNA was extracted from cell pellets according to the manufactures instruction, using the RNAeasy Qiagen kit (Qiagen Ltd, UK). All steps were performed quickly at room temperature using RNAse-free filtered-pipette tips to avoid contamination. Briefly, lysis buffer RLT (provided with the kit) was added to the cell pellet previously collected (350 µl is recommended as enough for 10^6 cells). The mixture was quickly mixed by pipetting up and down and transferred into QIAshredder columns (Qiagen Ltd., UK) and centrifuged for 2 minutes at 12000x*g* to shear genomic DNA. An equal volume of 70% (v/v) ethanol was added to the eluate and mixed by pipetting. Samples were then transferred to an RNAeasy mini spin column which was centrifuged for 1 minute at 10000x*g*. Buffer RPE was then added into the column and centrifugation (1 minute, 10000x*g*) was repeated; this washing step was repeated twice. 40 µl RNAse-free water was added on the silica-membrane of the column, which was left to stand for around 1 minute, after which columns were centrifuged at maximum speed for 1 minute. Samples were analysed for RNA concentration and nucleic acid purity by spectrophotometry, using a NanoDrop (Thermo Scientific, UK) and following manufacturer instructions. Samples were kept at -20°C until further use.

3.2.5.2 Reverse transcription polymerase chain reaction (RT-PCR)

For the first strand cDNA synthesis, 3 µg of total extracted RNA were used. These were denatured with 3 µl oligo $(dT)_{15}$ (Promega, UK) for 5 minutes at 65°C, followed by reverse transcription at 42°C for 2 hours using 0.6 mM dNTP solution (Invitrogen, UK) 1 U/ml RNAsine® ribonucleases inhibitor (Promega, UK), 50 U/reaction of Moloney murine leukaemia virus reverse transcriptase (M-MLV RT; Promega, UK).

10 µl of the reverse transcription reaction were used for PCR reactions, together with 1.5 mM $MgCl_2$ final concentration, 0.5 mM dNTP, 1 µl Taq polymerase and PCR buffer mix, all from Invitrogen, UK. The cycling parameters consisted of a denaturing step for 5 minutes at 95°C, followed by 40 cycles of denaturation for 1 minute at 95°C, primer specific annealing for 1 minute (see Appendix; section 10.3), extension step for 1 minute at 72°C. A final extension stage was also included for 15 minutes at 72°C.

3.2.5.3 Scale-up amplification of plasmids through QIAGEN MAXI prep Kit

Plasmids were amplified in order to obtain large quantities of them for further applications (lentiviral particle production and transfections). Maxi-prep plasmid DNA purification kit (Qiagen, UK) was chosen as it gives endotoxin-free purified DNA, an important aspect considering future cell culture use. Starter cultures (5 ml Luria Bertani (LB) broth supplemented with 100 µg/ml ampicillin) were prepared from colonies bearing the correct plasmids or from glycerol stocks. These were allowed to grow with vigorous shaking (~300 rpm) at 37°C for 8 hours. Subsequently, 200 ml of LB broth (supplemented with ampicillin) in a capable flask were inoculated with 400 µl of the starter culture (1:500 dilution) and incubated at 37°C with vigorous shaking for 12-16 hours. Afterwards, bacteria were collected through centrifugation (4000x*g* for 20 minutes, 4°C) and pellet was frozen; a sample from the suspension was taken and DNA was extracted to assess the identity of the plasmid. Pellets were allowed thawing and treated exactly as indicated in the provided protocol. The DNA obtained was finally diluted in a suitable volume of Tris-EDTA (TE) buffer (provided with the Qiagen kit) in order to achieve a final concentration of around 1 µg/µl, as measured using NanoDrop 1000 spectrophotometer (Thermo Scientific, UK).

3.2.5.4 Checking the identity of the constructs through restriction enzymes

Identity and possible recombination in original vectors and ligation products was checked through at least 3 different restriction enzymes and via sequencing with specific primers to check the correct insertion, frame and identity of the insert. Restriction pattern identification was performed using Webcutter 2.0 (Yale University, USA), Vector NTI 10.30 (Invitrogen, UK) and by using the plasmid sequences provided by the manufacturer or the authors of the original vectors. Every restriction reaction was performed on DNA samples from colonies picked-up from selective agar plates and purified by MINI prep plasmid DNA purification Kit (Qiagen, UK) according to the supplier's instructions. When correct colonies were identified, stocks were prepared (15% glycerol; 75% bacterial suspension) and stored at -80°C.

3.2.5.5 Agarose gel electrophoresis

10 µl samples of PCR reactions or restriction reactions were mixed with 10X gel loading buffer to reach a final concentration of 1X, loaded and run, each of them in separate wells, along with 6 µl of 1 Kb ladder (Invitrogen, UK) in agarose gels, prepared using 1X Tris-Acetate-EDTA (TAE) buffer as solvent, stained with Ethidium Bromide (0.02% v/v) or the safer GelRed® (Invitrogen, UK; 1:10000 (v/v) as recommended by the manufacturer) and run at 80-100V (if regular-sized gels) or 70-90V (if mini-gels) in order to assure 5-8V/cm max. Gels were soaked into 1X TAE running buffer. Concentration of the gels was decided according to the band pattern expected (briefly: 0.7% to separate species with length around or longer than 3 Kb; 0.8% to separate species with length around 1 Kb; 1% to separate species less than 1 Kb long; 1.5% to separate species shorter than 500 bp long; 2% to separate species shorter than 200 bp long). Gels were observed under UV rays through Gene Genius luminometer (Syngen, USA) and images were acquired and modified to avoid saturated signals using the provided software (Syngen, USA).

3.2.5.5.1 Agarose gel densitometric analysis

Analysis of the RT-PCR products were performed under ultraviolet light using a specific gel-docking system (MultiGenius; Syngene, UK). The provided software was used to adjust exposition and background in order to clearly visualise the bands.

3.2.6 Immunophenotyping of tissue and cells

3.2.6.1 Immunofluorescence on tissue slices

Frozen mouse brains, fixed for 24 h in 4% PFA in 0.01 M PBS at 4°C, were sliced into 15 µm-thick sections on a freezing microtome (Bright Instruments Ltd, UK) and stored at -20°C in anti-freeze solution. Sections were washed 2 times (5 minutes/wash; RT) with TBS 1X and permeabilized for 10 minutes in 0.5% Triton X-100 in TBS 1X under agitation, at RT. To limit auto-fluorescence, sections were incubated for 5 minutes in Sudan Black solution, washed twice in tap water under agitation (3 minutes/wash; RT), blocked for 30 minutes at RT in blocking solution to limit non-specific secondary antibody binding. Primary antibodies (diluted as detailed in Appendix, Section 10.2) incubation was performed overnight at room temperature (unless otherwise stated in the Results) in antibody buffer. The following day, sections were rinsed 3 times in antibody buffer and then incubated for 1-2 h at RT with specific secondary antibodies in antibody buffer. Finally, sections were rinsed 3 times in TBS 1X and manually mounted on gelatine-coated slides, allowed to air-dry and cover-slipped under mounting solution with or without 4',6-diamidino-2-phenylindole (DAPI) (Prolong Gold Antifade mountant with DAPI; Invitrogen, UK).

Digital images of the immunostained tissue sections were captured using a system consisting of a Hamamatsu C4742-95 CCD camera (Hamamatsu Photonics UK Ltd, UK) attached to a Nikon TE2000U inverted microscope (Nikon UK Ltd, UK).

3.2.6.2 Immunofluorescence on cells

Cells were cultured on Labtek multiwell glass slides (Invitrogen, UK) or on glass coverslips treated with specific agents to increase attachment of the cells (rat tail type I collagen for hCMEC/D3), growth up to 100% confluent and treated with the different stimuli. After a quick wash in warm DPBS without Ca^{2+}/Mg^{2+}, cells were fixed in different ways according to the past experience and literature: with 4% PFA for 10 minutes at RT (ANXA1 (McArthur, Cristante *et al.* 2010); Zonula Occludens-1; VE-Cadherin), with 100% methanol at 4°C followed by cold absolute acetone for 3 minutes at RT (Furuse *et al.*, 1994) and personal communication from Dr AM Lopez-Ramirez [Open University, UK; (Lopez-Ramirez *et al.*, 2012) for Occludin, Claudin 5], with 4% PFA in cytoskeleton preserving buffer for 30 minutes at RT for Fibrillar Actin (Cramer *et al.*, 2002). After fixation, cells were washed twice in DPBS with Ca^{2+}/Mg^{2+} (~ 1 min/wash, RT), permeabilized for 5 minutes, then blocked in blocking buffer for 30 minutes at RT. Primary antibodies were diluted at the desired concentration (see Appendix; section 10.2) in antibody buffer and enough volume was layered onto the cells, which were incubated overnight (tight- and adherence-junctions) under agitation at RT, or for 1 hour at RT (ANXA1). Rhodamine-conjugated or Alexa-488-conjugated phalloidin was incubated at room temperature for 15-20 minutes under agitation. After washing 3 times in DPBS with Ca^{2+}/Mg^{2+} 1% FCS, 0.1% BSA (10 minutes/wash at RT, to ensure major removal of unbound primary antibody), fluorophore-conjugated secondary antibodies were diluted in antibody buffer and applied for 1 h in the dark at RT. Finally, samples have been washed 3 times in DPBS with Ca^{2+}/Mg^{2+} (10 minutes/wash, RT) and once in DPBS with Ca^{2+}/Mg^{2+} 0.1% Triton X-100 (10 minutes, RT) air-dried and mounted using Mowiol or Prolong Gold Antifade with DAPI.

Digital images of the immunostained tissue sections were captured using the same system described for tissue samples. Alternatively, confocal microscopy [TCS SP5 (Leica, UK) equipped with: Argon-UV (351 nm) laser, Diode 405 (405 nm) laser, Argon (488 nm) laser, Helium-Neon (543 nm) laser, DPSS 561 (561 nm) laser; 10X (HCX PL APO CS dry; 0.4 numerical aperture), 20X (HCX PL APO CS dry; 0.7 numerical aperture), 40X (HCX PL APO dry; 0.85 numerical aperture), 63X (HCX PL APO water-immersion; 1.2 numerical aperture) objectives) was conducted along with Z-stack analysis to increase detail depiction, using Leica Application Suite software provided.

3.2.6.3 β-galactosidase staining on tissue slices

Blood was washed out of the body by perfusion through the left ventricle with approximately 15 ml of filtered saline at 4°C. Brains were rapidly removed and divided coronally in 2 mm slices; these were fixed in fresh 4% PFA for 1 hour at 4°C. After rinsing them 3 times (30 minutes each) in rinse buffer, brain chunks were incubated overnight at room temperature with staining buffer. The following day, they were rinsed three times in PBS 0.01M, post-fixed in 4% PFA for 2 hours at room temperature or overnight at 4°C. 15-µm sections were produced by cryostat cutting. After having let them dry, sections were counterstained with eosin Y (0.1% w/v) for 15 seconds, rinsed once in tap water (5 minutes), dehydrated in 95% ethanol for 2 minutes, cleared in xylene for 10 seconds and mounted with Di-N-Butylephthalate in xylene (DPX; VWR, UK).

3.2.6.4 Flow cytometry

Cells were washed once with DPBS without Ca^{2+}/Mg^{2+} and quickly trypsinised before fixation in 2% PFA for 15 minutes at RT. Cells were then pelleted and washed with DPBS with Ca^{2+}/Mg^{2+} twice and incubated for half hour at room temperature in blocking buffer with or without permeabilisation (represented by 0.025-0.1% (v/v) saponin).

Cells were then washed twice with wash buffer with or without saponin and then incubated with primary antibodies diluted in antibody buffer for 1 hour at room temperature. Next, cells were washed twice before incubation for 1 h at RT in the dark with fluorophore-conjugated secondary antibodies, washed twice and finally re-suspended in 300 µl of DPBS with Ca^{2+}/Mg^{2+}.

Analysis by flow cytometry was performed within 1 h using a FACScan II analyzer (Becton Dickinson, UK), with 15 mW argon ion laser (488 nm) and Consort 32 computer running CellQuest software (Becton Dickinson, UK). Log_{10}(mean intensity of fluorescence) histograms (256-channels) were obtained from approximately 10000 cells from a gate set-up according to Forward Scatter (FSC) and Side Scatter (SSC) parameters (representing cellular dimensions and granularity). FlowJo (Tree Star, USA) was used to assess differences in fluorescence intensity.

3.2.7 Statistical analysis

Number of repeats and experiments is reported in the figure legends. Normally distributed data are presented as mean ± standard error of means (SEM) of *n* samples per group.

Data have been analysed using Excel, GraphPad Prism 5 or SPSS; two-tailed Student's *t*-test has been chosen for comparisons between two previously assessed normally distributed populations while one-, two- or three-way ANOVA and Bonferroni's, Tukey's or Dunnett's (comparison to a reference control group) multiple comparison *post-hoc* test for more than two groups, depending on the number of variables of the study. A *p* value lower than 0.05 was considered statistically significant.

Chapter 4 – Annexin A1 physiological role at BBB level

4.1 Overview and aim of the chapter

In this chapter, I will present the most significant data obtained about the mechanistic involvement of ANXA1 at the level of the endothelium forming the BBB. Using a comprehensive approach, which included a comparative *in vivo* permeability assessment between the Anxa1 null mouse and the wild-type counterpart, primary isolation of microvascular endothelial cells and *in vitro* extensive exploitation of a human cell line, we were able to pinpoint ANXA1 to be a critical component for the barrier integrity of BMECs.

4.2 Protection of the central nervous system: the need for barriers

Undoubtedly, the brain is the most complex organ of the body. Evolution has provided the CNS tissues with protective bony formations, connective ensheathing membranous structures (the meninges) and a fluid cushion (the cerebrospinal fluid). These properties define a physically confined and protected environment, though unable to undergo major changes in response to external stimuli. Brain energy requirements are very intense [around 20% of the total oxygen consumption (Clark & Sokoloff, 1999) and 25% of glucose utilization (Attwell and Laughlin, 2001)] due to the high number of operations that it has to constantly process, while tight ionic homeostasis at synaptic levels appear to be fundamental for the correct CNS activity (Abbott, 2005); therefore, the brain strongly depends on the constant maintenance of a controlled internal environment. Every tissue of the body is able to adapt to small fluctuations in the concentration of hormones, ions and nutrients, which occur typically after eating or exercising; the central nervous system cannot sustain this type of sharp changes, since these would result in uncontrolled neuronal activity (some ions and amino-acids are involved in neurotransmission) and in irreversible damage of the circuitry and delicate brain parenchyma. The evolutionary pressure for structures able to control the CNS homeostasis has brought the development of specialised barriers able to separate the central tissues from the periphery and to regulate the molecular traffic between the two compartments. These structures can also control pathogenic agents and microorganism invasion, as well as uncontrolled cellular invasion from the blood stream, which would all result in serious consequences for this delicate environment.

Thus, a great variety of highly specialised barriers have evolved in different areas of the CNS-blood interfaces (Neuwelt *et al.*, 2011): the blood-cerebrospinal fluid barrier (BCSFB), the blood-retinal barrier (BRB), the blood-nerve barrier, the blood-labyrinth barrier, the ventricular ependyma (although there is no complete agreement in including this structure among the specialised barriers array) and the blood-brain barrier (BBB), which is the focus of this and of the following two chapters.

4.3 Peculiarities and commonalities of the different barriers

Brain barriers exert similar functions but each one shows particular properties. Structural isolation is permitted thanks to specific features of each barrier, but all of them have an important point in common: the presence of a specialised endothelium or epithelium as an essential component. The characteristics of this vary in the different barriers. In the case of the blood-retina barrier, a highly restricted layer of epithelial cells (the retinal pigment epithelium) and a tight vascular endothelium contribute to its characteristic limited permeability; a similarly tight endothelium is also peculiar to the blood brain barrier.

In the brain, there are, however, structures that lack an endothelial BBB and are characterised instead by fenestrated leaky capillaries: these are known as circumventricular organs (CVOs), which are present at the level of specific regions containing neurons specialised in neurosecretory and chemosensitive functions; thanks to the permissive barrier structure (glial coverage offers only a partial hindrance), these areas of the brain are able to sense signals from the periphery (Engelhardt and Sorokin, 2009). Similarly, BCSFB is formed by a dense tangle of leaky capillaries, the choroid plexuses (which are present at the level of the lateral, third and fourth ventricles), surrounded by tightly organised epithelial cells: here, the nourishing and protecting cerebrospinal fluid is produced and distributed through the CNS.

Bearing in mind these examples, we now know that the properties of the barriers cannot be reduced simplistically to the status of tightness of its endothelium.

4.4 The blood-brain barrier (BBB) in physiological conditions

Among all the specialised brain barriers, the blood brain barrier (BBB) covers the largest surface area, therefore representing the site where most of the peripheral stimuli impact, inducing central responses. The BBB has the fundamental role of tightly checking the movement of molecules and inflammatory cells from the circulating blood, protecting the CNS from potentially harmful compounds (microorganisms, toxins and, in physiological conditions, certain immune cells) and regulating the passage of nutrients, signals waste and other molecules to the brain tissue (Abbott *et al.*, 2006; Abbott *et al.*, 2012).

4.4.1 Historical background

The existence of brain barriers, and more specifically of a BBB, was firstly investigated by the German physiologist and Nobel laureate Paul Ehrlich in the late XIX century. He observed that the administration of intravenous or sub-cutaneous dyes in experimental animals resulted in heavy staining of all the organs except the brain and the spinal cord. Initially, the conclusions drawn were wrongly attributed to supposed tissue- and organ-specific affinities of the dyes (Engelhardt and Sorokin, 2009). Further work from Ehrlich's student, Edwin Goldman, shed more light on these observations: by directly injecting brains with the same dyes, clear staining of the nervous system was observed, while peripheral tissue remained unstained. The explanation was the existence of a physiological barrier between the CNS and the rest of the body, able to hold back and control the movement of certain molecules. Due to light microscopy limitations, a definite anatomical and functional demonstration of the existence of the BBB came only in the 1950s (Dempsey & Wislocki, 1955), thanks to the exploitation of the newly developed transmission electron microscopy. Through these techniques, it was possible to correlate the localisation of the BBB with the microvascular endothelial cells. The existence of a complex arrangement of different cell types and molecular structures became clear; since then, this has been the basis of the peculiar barrier properties of the microvasculature of the brain parenchyma when compared to their peripheral equivalents.

4.4.2 Development of the blood-brain barrier

The CNS vasculature develops similarly to the peripheral one: embryonic precursors cells (EPCs; also known as angioblasts) are formed in the yolk-sac mesoderm and invade the head region tissues in early phases of embryogenesis, differentiating into endothelial cells and defining a vascular plexus that runs around the entire surface of the neural tube (Mehta and Malik, 2006; Abbott *et al.*, 2010; Neuwelt *et al.*, 2011). From here, further vascularisation processes occur in the developing brain: capillaries can sprout from the plexus by stimuli linked to the metabolic demands of the expanding neuroectoderm and invade the forming parenchyma. While forming, the brain vasculature is further stabilized by the recruitment of other supporting cells and by the deposition of the extracellular matrix, which represents a strong signal towards maturation and against further proliferation/migration (Abbott, 2005); these steps are all finely tuned by the surrounding environment with its important cues coming from neighbouring cells. In this way, the complexity of the brain barriers can be sequentially achieved, along with their full functionality.

Since a certain degree of isolation of the CNS from the rest of the forming organism is required also during development, functionally effective barrier molecular structures, like tight junctions complexes between endothelial cells and specific transporters, are present shortly after the microvasculature starts to invade the CNS tissue (in the mouse this occurs between E11 and E17), although BBB maturation (like astrocytes generation and end-feet extension) continues in later stages as well as during the first post-natal days (Liebner *et al.*, 2008; Abbott *et al.*, 2010; Daneman *et al.*, 2010).

Interestingly, the ependyma lining the cerebral ventricles of the developing brain (called neuroependyma) constitutes a proper tight barrier during embryogenesis but not at later times, when the adult ependyma is a more permeable interface (Neuwelt *et al.*, 2011).

4.4.3 The neurovascular unit

The definition of the anatomy and localisation of the BBB are constantly receiving novel inputs from the discovery of new interactions and participations (Neuwelt *et al.*, 2011). While initially neurobiology research was mainly driven by a unique interest in the neurons,

in recent years scientists have discovered that a neuro-centric focus is not sufficient but instead simplistic, therefore emphasizing the fact that all cell types in the brain including neuronal, glial and vascular components, must be examined in an integrated context both under physiological and the pathological conditions. Not only the neurons but also the BBB strongly depends on the inputs received from the microenvironment (Lok *et al.*, 2007) and the current tendency is to cluster the BBB cellular and molecular components into the wider concept of the neurovascular unit (NVU), which also includes microglia, neurons and oligodendrocytes (Neuwelt *et al.*, 2011). Nerve terminals sheathe brain capillaries, potentially providing a source of molecules (neurotransmitters) able to modulate microvascular permeability (Abbott, 2002). Circulating blood cells (in particular the polymorphonuclear cells, the lymphocytes and the monocytes) and their inflammatory mediators (cytokines) should also be included into an "extended" concept of NVU (Neuwelt *et al.*, 2011), because they have been shown to be important mediators of CNS pathophysiology and directly interact with the BBB vasculature. Initial evidence has been produced in support of this novel concept (Joice *et al.*, 2009; Cowan and Easton, 2010).

Increasing evidence is showing that the interactions occurring between these cellular components are essential to maintain homeostasis of the entire CNS, as well as to respond to inflammation and disease. Since the definition of the existence of a NVU, novel concepts have arisen: the hemodynamic neurovascular coupling between blood flow and brain activity; the importance of cellular inputs derived from neuronal cells that contribute to evoke the BBB phenotype; the parallelism underling both neurogenesis and angiogenesis in the CNS; the potential exchange of trophic factors that may link neuronal, glial and vascular homeostasis. These and other phenomena appear to rely on the existence of a tripartite synapse (Perea *et al.* 2009), established between endothelium, astrocytes and neurons. It is therefore essential to understand and expand the knowledge of the regulatory mechanisms not only in each NVU component, but also between different players; only in this way it will be possible to fully explain how the structural integrity of the barrier is achieved and modulated (and could eventually be restored under pathological conditions).

4.4.4 Composition of the blood-brain barrier

Historically, BBB has been recognised to be formed mainly by the highly specialised microvascular endothelial cells, the glial/supportive cells astrocytes, the pericytes, the perivascular macrophages/antigen-presenting cells and the cellular basal membrane (Abbott *et al.*, 2006; Engelhardt and Sorokin, 2009). The major components are represented in Figure 4.1.

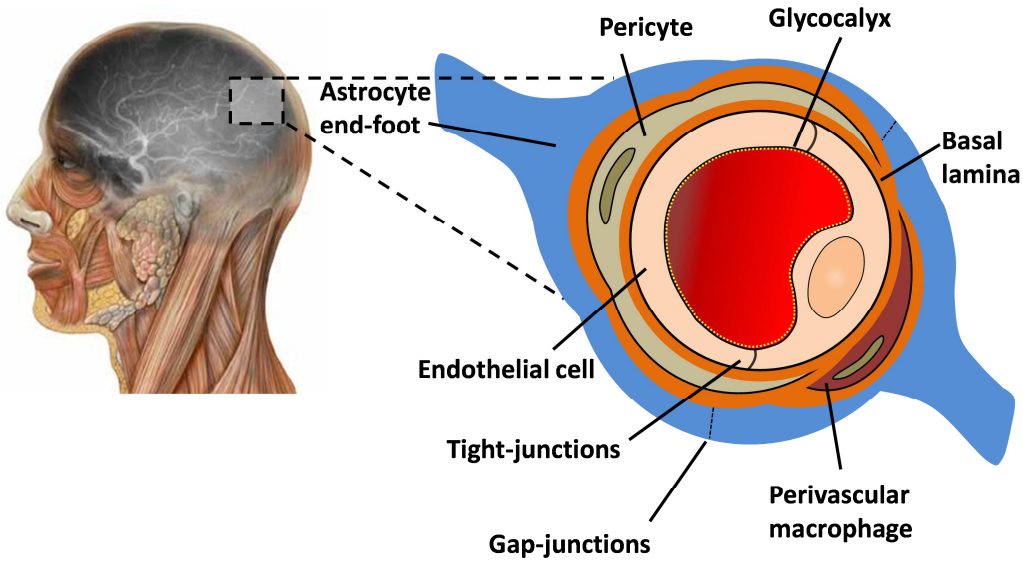

Figure 4.1 Principal components of the blood brain barrier. The main components of the blood-brain barrier are depicted. Neurons, microglia and other components have not been represented for clarity purposes but their role in the neurovascular unit has been extensively described in the text. Figure modified with permission of Dr CP Watson; original picture based on Cecchelli, Berezowski *et al.* 2007.

4.4.4.1 The BBB endothelium

The main component of the BBB, and the one that provides the core of this complex structure, is the brain microvascular endothelial cells (BMECs). Compared to peripheral capillary endothelial cells, BMECs show a tightly sealed phenotype: blood cells and substances cannot cross the endothelium layer easily as no fenestrations are present.

A reduced constitutive non-specific transcytosis (pinocytosis) means that hydrophilic molecules can only cross the BBB and enter the brain parenchyma from the blood stream only almost exclusively through specific transporters and receptor mediated transcytosis.

Such specialised tightness is allowed by the presence of complex cell-cell junction complexes (described more in detail in Figure 4.4), which show a higher degree of complexity compared to those of peripheral capillaries (Engelhardt and Sorokin, 2009) and this is reflected in the differential expression patterns of cell junctions genes (Wolburg and Lippoldt, 2002). Thus, cerebral endothelial cells are much less permeable even to small ions like Na^+ and Cl^- than their peripheral counterparts, as represented by the much higher transendothelial electrical resistance (TEER) measurable in the brain capillaries [in the magnitude of 1500 $\Omega \cdot cm^2$ as reported (Deli *et al.*, 2005; Abbott *et al.*, 2006)].

The BBB endothelium shows other special properties, such as a higher number of mitochondria, necessary to produce the energy (*i.e.* ATP) required by the highly numerous and specialised influx and efflux pumps (Wolburg and Lippoldt, 2002). In addition, these cells show a very low basal expression of leukocyte-adhesion molecules like ICAM-1, VCAM-1, and leukocyte-rolling molecules like P- and E-selectins, but they can be promptly up-regulated by specific inflammatory signals (Whalen *et al.*, 1998; Dobbie *et al.*, 1999).

4.4.4.1.1 Annexin A1 in the endothelium

While several reports concerning other annexins and their endothelial localisation and involvement exist, the role of Annexin A1 in the endothelium is practically an unexplored area. Only a few scattered studies have investigated why this protein is present at this level and how it affects endothelial functions. In particular, two early reports (Patte and Blanquet, 1992a, b) observed ANXA1 to be associated with the membrane of HUVEC cells (the most widely used model of peripheral endothelial cells) and to affect the cell cycle. In inflammation, a cleaved form of ANXA1 produced and released by activated neutrophils has been shown to re-organize adhesion molecules on the same cell line, inducing a more intense leukocyte extravasation (Williams *et al.*, 2010). No reports so far have investigated the role of ANXA1 at the level of the microvascular endothelium and of the BBB. As it occurred for the peripheral system, the attention has been focused exclusively on the blood cells, since ANXA1 is historically recognised for its anti-inflammatory role played at this level.

4.4.4.2 The astrocytes and the astrocytic end-feet

Astrocytes are a type of glial cell and one of the most numerous cell types in the CNS. They play several roles in tissue homeostasis (glia comes from the Greek word for "glue", which semantically indicates their supportive role), which span from regulation of metabolism (as glycogen and lactate reserve), regulation of ionic concentrations and pH in neuron-rich regions, buffering and release of neurotransmitters, immunity regulation (as potential antigen-presenting cells) and players in nervous system repair (Abbott *et al.*, 2006; Allen and Barres, 2009). Importantly for the purpose of our interest, astrocytes are able to extend their end-feet so that they stay in close contact with the vascular unit (98% of the cerebral micro-vascular tree is ensheathed by astrocytic end-feet lamellae), defining the so-called *glia limitans perivascularis* (Engelhardt and Coisne, 2011), which not only represents a physical barrier for molecules and cell passage but also shows several specialized features such as up-regulation of specific transporters and receptors on the endothelial cells, modulation of vascular tone and blood flow (Abbott *et al.*, 2006; Engelhardt and Sorokin, 2009; Neuwelt *et al.*, 2011), contributing to the BBB-specific features. The *glia limitans* and the vasculature also define a perivascular space important for antigen presentation and immune-surveillance (Engelhardt and Coisne, 2011).

Astrocytes are very important for the correct development of the blood-brain barrier: temporal and spatial characterisation has shown their regulatory role (Liebner *et al.*, 2008; Alvarez *et al.*, 2011). In particular, soluble factors released by astrocytes (for example transforming growth factor-β (TGF-β), glial derived neurotrophic factor (GDNF) and steroids such as hydrocortisone) as well as direct contact with BMECs are essential aspects for the correct induction of their peculiar BBB properties (Abbott, 2002). Also, astrocytes have proved to be very important for the definition of quick changes in BMECs tightness, for example when a higher metabolic support is required by the neurons (Abbott, 2002).

4.4.4.3 The basement membranes

Generally, the basement membranes (BMs, also known as basal lamina) are considered as part of the extracellular matrix and are composed of several structural molecules such as collagen type IV isoforms, nidogens, fibronectin, laminin, perlecan and other proteoglycans (Mehta and Malik, 2006; Engelhardt and Sorokin, 2009). Endothelial cells are able to synthesize and secrete these constituents on the abluminal/parenchymal surface during angiogenesis and vasculogenesis, which represent a supportive/anchoring structure for their correct functioning. More in detail, two distinct BBB basement membranes can be distinguished: one originating from the endothelium and one from the astrocytes, which underlie the endothelium and cover the astrocytic end feet, respectively (Engelhardt and Sorokin, 2009). Interestingly, these two distinct structures are clearly distinguishable at the level of post-capillaries venules, while they are fused to form one single basement membrane at the level of brain capillaries.

The BM of the capillaries play an essential role in modulating and remodelling the endothelium; not only it serves as an anchoring support for the endothelium, which expresses several BM receptors [the integrins; (Engelhardt and Sorokin, 2009)], but it also has been observed that inflammatory stimuli can stimulate BM-disruptive enzymes which denude regions of the endothelial lining. Cell adhesion can also be modulated at the level of the BM, therefore indicating an overall role in barrier function and integrity (Mehta and Malik, 2006; Engelhardt and Sorokin, 2009).

4.4.4.4 The glycocalyx

The glycocalyx is a negatively charged surface made of proteoglycans, glycosaminoglycans and plasma proteins, which is secreted on the luminal (blood-stream) side of the endothelial monolayer. At the level of the BBB, its role is still not fully clarified (Neuhaus *et al.*, 2009) but initial evidence supports similar roles as those served in the peripheral vascular system, where this structure limits leukocyte attachment to the endothelial surface and potentially the passage of macromolecules (Mehta and Malik, 2006).

4.4.4.5 The pericytes

Pericytes represent a "hot-topic" in terms of identification of their role as BBB components. Previously known as adventitial cells, pericapillary cells, intramural cells or Rouget's cells, these are small contractile and phagocytic cells that surround the endothelial cells monolayer with secondary cellular branches and are also enclosed by the endothelial BM. Embryonically, they have a mesodermal origin: they migrate as general macrophages into the tissue during the late stages of vascularization, developing the specialised pericyte phenotype thanks to stimuli from the vascular microenvironment (Guillemin and Brew, 2004). They are ubiquitously present in every microvascular bed of most tissues but especially at the level of the BBB and of the BRB. Originally, they were thought to structurally support the vascular endothelium and to regulate local blood flow of small-calibre vessels devoid of smooth muscle cells (Thomas, 1999), since they were found to express receptors for vasoactive mediators (Healy and Wilk, 1993). While a role in coagulation pathway has been also proposed, pericytes are now included among the central players of the immune response of the brain (Thomas, 1999): in fact, pericytes are not only able to increase paracellular permeability during inflammatory reactions by contraction, but are also to act as antigen-presenting cells (APCs) and since the perivascular space of microvessels is now regarded as an important site for the development of adaptive immune reactions, these cells have been gaining even more interest and importance. Recently, two important reports (Armulik *et al.*, 2010; Daneman *et al.*, 2010) shed more light on the topic: by using pericyte-deficient murine models, both works indicated a direct involvement of this cell-type during BBB embryological development, as well as in the regulation of the BBB permeability to low- and high-molecular-mass tracers by affecting transcytosis. Such effects seem to be mediated by maintaining the correct astrocytic end-feet polarity along the cerebral microvasculature and by regulating the correct BBB-specific gene expression in the endothelial cells (Armulik *et al.*, 2010).

The direct involvement of these cells in several neurological disorders like Alzheimer's disease, diabetic retinopathy and those with an inflammatory component indicate how crucial this cell type appears to be at the interface between the peripheral system and CNS.

4.4.4.6 The perivascular macrophages

Perivascular macrophages (PVMs) are considered a subset of brain-resident macrophages, whose role has just started to become clearer. This cell type resides in the perivascular space created between the BBB endothelium and the *glia limitans perivascularis*, where they act as sentinels for peripheral harmful stimuli plus they convey information about the CNS health status to the peripheral cells that enter this space. It has been difficult to distinguish them from pericytes (Guillemin and Brew, 2004): based on their morphology and on developmental studies, PVMs were shown to be derived from migration of bone marrow precursors that populate the brain in early postnatal life and turn over slowly during life (Serrats *et al.*, 2010), therefore they are different from resident histiocytes present in peripheral capillaries already during vasculature development (Guillemin and Brew, 2004). PVMs do not show proliferative ability (differently from microglia and pericytes) but together with pericytes they can serve as APCs, representing important implications since the CNS lacks proper professional antigen-presenting cells (therefore proposing a potential role of PVMs in pathologies like multiple sclerosis). In this way, immune surveillance of the nervous brain parenchyma as well as of the peripheral system [by monitoring the blood stream composition (Serrats *et al.*, 2010)] appear possible.

4.4.5 Vascular localisation of the blood-brain barrier

One of the most important questions lately posed by scientists is which parts of the microvascular tree possess the real and fully-developed BBB phenotype. Every organ possesses a microvasculature network composed of arterioles, capillaries and venules to meet the local energy requirements of the underlying tissue. As every organ has defined specialisations, so does the endothelium, which shows structural and functional differences among different organs (fenestrated kidney glomerular capillaries compared to brain microvasculature are good examples) but also within the same microvascular tree. Recent (Macdonald *et al.*, 2010) and less recent (Ge *et al.*, 2005) reviews indicate the existence of important heterogeneity in endothelial cells of the cerebral microvasculature. By analysing gene expression differences, Macdonald *et al.* (Macdonald *et al.*, 2010) observed that both capillaries and venules presented a basal expression of basic BBB-associated genes, like

those involved in formation of cell-cell junctions, transporters and metabolic enzymes, but capillaries showed a higher enrichment and specialisation towards a full blood-brain barrier phenotype. These findings are confirmed by protein expression (Ge *et al.*, 2005), which included also arterioles in their analysis. A potential explanation for this heterogeneity is that special vascular functions can be divided in this way along the length of the microvasculature tree, with the capillaries being the most specialised in finely tuning the passage of small molecules, while the larger arterioles and especially venules are involved in the passage of bigger molecules and peripheral cells into the CNS. The reason for these differential properties could reside on the effect that shear stress can have at different levels of the vascular tree, as well as on the influence of neighbouring cellular components like pericytes and astrocytes; however, a proper explanation is still lacking (Ge *et al.*, 2005; Macdonald *et al.*, 2010).

These findings have important consequences for BBB endothelium *in vitro* models, since venular endothelial cells showed less complex cell-cell junctions formation and transporters presence, which is paralleled by a less tight phenotype.

Interestingly, some evidence is beginning to arise on regional heterogeneity, *i.e.* differences between the same portions of the microvasculature (*e.g.* capillaries) present in different regions of the same organ; in fact, BBB properties of different brain lobes at various ages (for example the hippocampus), or between white and grey matter, show a certain degree of difference (Pelegri *et al.*, 2007; Zeevi *et al.*, 2010).

4.5 Functions of the blood-brain barrier

Since the BBB represents the largest CNS-blood/periphery interface in humans (it represents an area of 12 to 18 m^2 per adult human brain on average), it shows a predominant role in regulating the cerebral environment (Abbott *et al.*, 2010).

As already mentioned, the BBB protects the brain from fluctuations in ionic concentration that could play a detrimental role on synaptic and axonal action potentials. Also, it physically limits neurotoxic interferences that could occur if peripheral neuroactive molecules (for example excitatory amino acids like glutamate) could freely penetrate into the CNS.

In addition, the BBB controls the passage of many plasma proteins as those involved in the coagulation cascade (fibrinogen, thrombin, *etc.*) or the complement components which have a high index of neurotoxicity, along with some endogenous metabolites, xenobiotics from the diet or certain nutrients at high concentrations. Overall, the blood-brain barrier functions as a physical, a metabolic and a transport highly specialized barrier, as described in Figure 4.2.

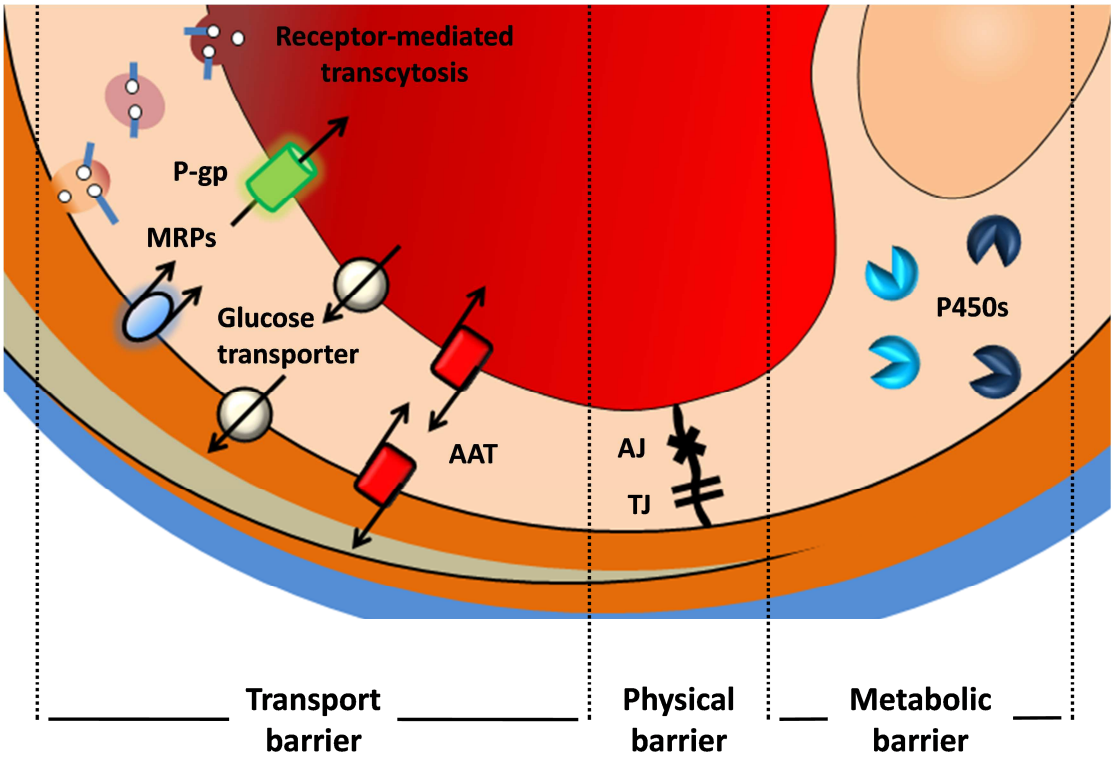

Figure 4.2 The three main BBB functions. BBB presents a distinctive phenotype which is characterized by three types of barrier function. These are: a physical barrier, formed by tight- (TJ) and adherens-junctions (AJ) components, that hampers the paracellular flow of molecules; a transport barrier, which is able to regulate the traffic of hydrophilic substances between peripheral blood and CNS through transmembrane proteins as the P-glycoprotein (P-gp), the multi-drug resistance associated proteins (MRPs), the amino acid transporters (AATs), glucose transporters; a metabolic barrier, which consists in drug catabolic enzymes like cytochrome P450s (P450s) ones. Some bigger molecules can cross the BBB by receptor specific and non-specific transcytosis. Figure based on Cecchelli *et al.*, 2007.

4.5.1 The transport barrier

Lipophilic molecules are theoretically able to cross the BBB simply by passive diffusion through the cellular membranes. Small non-polar gaseous molecules like O_2 are able to freely diffuse through the lipid membranes, in a similar way to other small lipophilic molecules such as ethanol (Abbott *et al.*, 2006; Abbott *et al.*, 2010).

On the other hand, the passage of water-soluble molecules is severely restricted by the physical tight properties of the endothelium, as explained in Section 4.5.3. This phenomenon virtually isolates the brain from essential nutrients like sugars and amino acids; since the level of non-specific/non-receptor mediated endocytosis is extremely low when compared to other tissue endothelial cells, evolution has led to a complex system of highly substrate-specific transporters that are a peculiarity of the BBB. Some of these selective transporters are expressed only at the luminal side (facing the blood stream) of the endothelium, some others only at the abluminal side (towards the brain parenchyma), others on both sides. Therefore, the localisation of these transporters determines also the preferred directionality of the specific molecules - *i.e.* towards the CNS (absorption), or towards the blood stream (excretion).

Several reviews have extensively described the BBB transporters system (Abbott *et al.*, 2010) and the main classes have been depicted in Figure 4.3. We should remember the important transport system of glucose and amino acids, present on the BBB endothelium, where tightly regulates the amount of energetic molecules and potential neurotransmitter entering the brain; another important example is the ATP-binding cassette (ABC) transporter family (P-glycoprotein, also known as MDR-1, is one of the most relevant members), which mainly contribute to the efflux of potentially toxic catabolites (Abbott *et al.*, 2010; Neuwelt *et al.*, 2011). To transport molecules with a considerable molecular weight as cytokines, immunoglobulins and other proteins, receptor-mediated transcytosis is the only feasible pathway that can be used at BBB level. This is mediated mainly by caveolae-based vesicle formation which promptly forms upon receptor(s) engagement. The transcellular pathway is also the main one used by certain leukocytes when entering the CNS for patrolling and pathological implications, as it will be described more extensively. Figure 4.3 reviews the main transporter pathways at the level of the BBB.

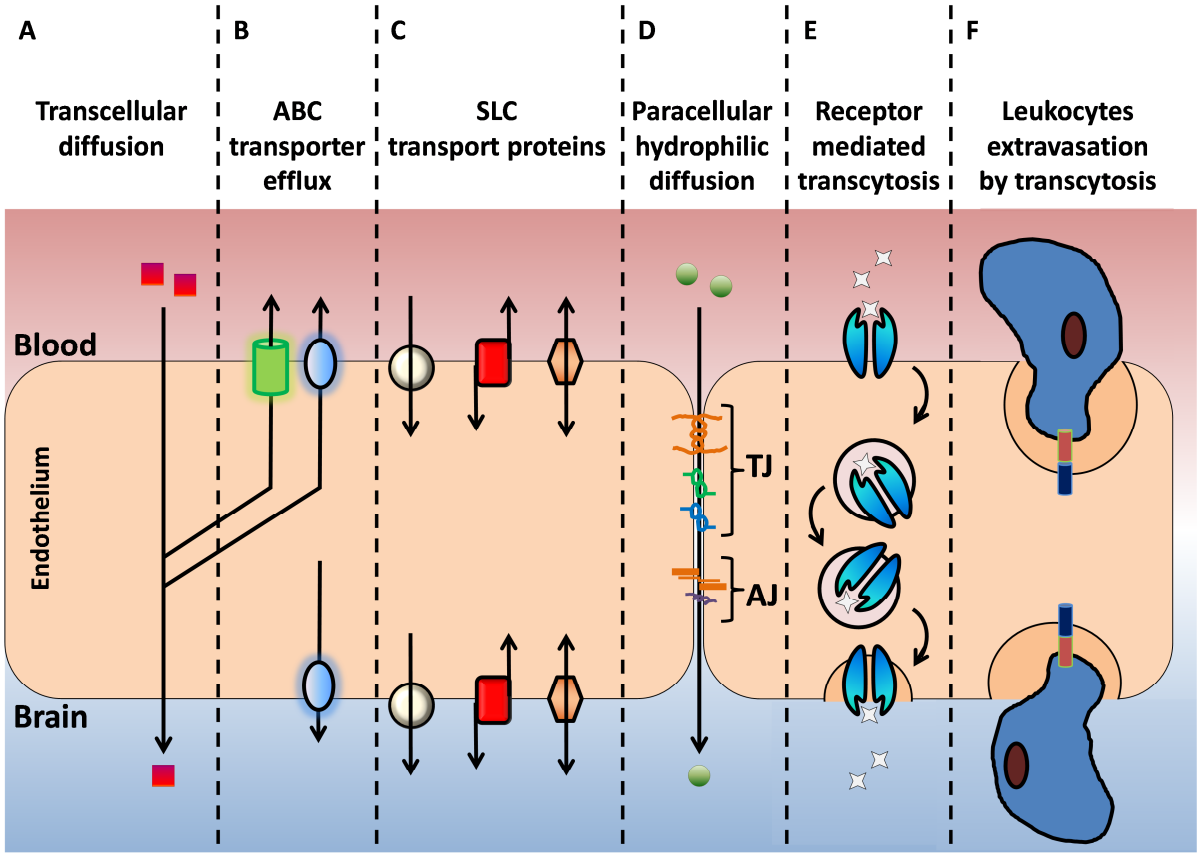

Figure 4.3 Transport systems at the level of the BBB. A| Lipophilic molecules are able to passively diffuse through the cell membrane and to cross the endothelium. For water-soluble molecules, highly specialised transports play a key role in the whole process. **B|** Active efflux carriers (ABC transporters) are able to pump out of the CNS all those molecules with intrinsic toxicity. **C|** Solute carriers (SLCs) are another form of specialized transporters, which actively transport small essential nutrients as glucose, amino acids and nucleotides. The direction of net transport is fundamental and depends on the cellular (luminal *vs.* abluminal) localisation of the transporters. **D|** The paracellular diffusion of water-soluble small molecules is strongly limited by the presence of healthy cell-cell junctions and it only involves ions and water, while **E|** receptor-mediated transcytosis is acquiring more and more evidence and consideration across the BBB endothelium. Non-receptor mediated transcytosis is very limited at this level. **F|** Leukocytes cross the BBB either by a process of diapedesis through the endothelial cells (penetrating close to the tight junctional regions), or via modifications of the tight junctions. Figure based on Abbott *et al.*, 2010 (Abbott *et al.*, 2010).

4.5.2 The metabolic barrier

Drug metabolism is exerted mostly by the liver, highly specialised in modifying a vast array of molecules. Since the nervous tissue is so extremely vulnerable to toxic molecules, either endogenous products or exogenously derived through the diet, the BBB offers a long list of metabolizing enzymes that promptly act to inactivate potential toxicity or to modify their bioavailability. This is mostly true for molecules such as drugs, which may have wanted and

unwanted effects at the level of the CNS. Phase I enzymes (like cytochrome P450s) and phase II enzymes (UDP-glucuronosyltransferase, glutathione S-transferase, *etc.*) have been identified at the level of the human BBB endothelium, strongly affecting the impact and the duration of action for numerous pharmacological molecules (Strazielle and Ghersi-Egea, 2005).

4.5.3 The physical barrier

The primary and fundamental extreme tightness of the blood-brain barrier is given by the fact that BMECs are sealed together in a way that is only present at this anatomical level. Consequently, endothelial paracellular (*i.e.* between the cells) permeability to small solutes is dramatically limited compared to most types of endothelia and has to occur through the transporter system; also, the filtration coefficient for water is extremely low. This peculiar feature can be achieved thanks to specialized junctional complexes, the adherens junctions (AJs) and the tight junctions (TJs), as described in Figure 4.4, Panel A. Gap junctions (GJs) represent structures connecting the cytoplasm of neighbouring cells, therefore promoting molecular exchanges and perpetuation of signalling waves along the vascular tree; however, these structures are almost absent from most of the brain microvasculature and do little towards the maintenance of the structural integrity, therefore they won't be further described (Sato *et al.*, 2002).

4.5.3.1 The adherens junctions

AJs play a fundamental role in the development and further maintenance of the endothelial sealed phenotype. These membrane-associated molecular complexes are mainly present at the basolateral level of the endothelial cells. The main component of this family is VE-cadherin, a Ca^{2+}-regulated protein that mediates cell-cell adhesion via interactions of the extracellular domains of proteins expressed in adjacent cells (Brown and Davis, 2002). The cytoplasmic portion of VE-cadherin is directly or indirectly linked to the actin cytoskeleton (see below) by the scaffolding proteins α-, β-, γ-catenin (also included in the family) and members of the p120 family, like plakoglobin (Engelhardt and Sorokin, 2009; Abbott *et al.*,

2010; Komarova and Malik, 2010). In this way, the cytoskeleton of neighbouring cells is tightly connected in order to allow mechanical cell-cell communication. VE-cadherin, and other members of the family, has been shown to be benefit from phosphorylation, since its interaction with β-catenin is potentiated (Komarova and Malik, 2010).

VE-cadherin has been shown to be fundamental for the correct close apposition of cell membranes and overall the formation of the zipper-like structures that characterise BMECs and capillary beds in general. Deletion of this protein, in fact, is embryonically lethal due to immature vascular development and exaggerated leakage in the forming CNS (Carmeliet *et al.*, 1999). In some old studies this class of proteins has been considered as less relevant for the regulation of the BBB permeability (Breier *et al.*, 1996), but more recent findings have confirmed that a proper establishment of adherens junctions is required for the expression and correct placement of the major tight-junction components such as claudin-5 (Taddei *et al.*, 2008) while disruption of AJs leads to barrier disruption (Wolburg and Lippoldt, 2002). Recently, the new concept of discontinuous adherens junctions has been coined, which involves the direct physical connection of VE-cadherin and other AJs components to some actin cytoskeleton filaments (*e.g.* the stress fibres) mediating the response of the endothelium to certain stimuli, such as pro-inflammatory cytokines (Millan *et al.*, 2010).

4.5.3.2 The tight junctions

Tight junctions (TJs) were found in the 1960s by electron microscopy as points where the outer leaflets of the membranes between adjacent endothelial cells were fused in the so-called “kissing” points (Farquhar and Palade, 1963; Brightman and Reese, 1969; Wolburg and Lippoldt, 2002), as illustrated in Figure 4.4, Panel B. Their composition varies greatly depending on the location and the role of the endothelium. As already mentioned, post-capillary venules are characterised by not-complex and poor tight-junctions, to allow rapid blood-tissue exchanges in these compartments. On the other side, BMECs show the most complex and restrictive composition of tight junctions of the entire body, which results in the effective limitation in the passage of small polar solutes and even ions (Liebner *et al.*, 2008). This results in a high *in vivo* electrical resistance of around 2000 $\Omega \cdot cm^2$ (Abbott *et al.*, 2010). The inter-endothelial tight junctions are formed by an array of transmembrane

(claudins, occludin, junctional adhesion molecules) and cytoplasmic (zonula occludens, cingulin) molecules ultimately linked to the actin cytoskeleton (Wolburg and Lippoldt, 2002).

Occludin was the first transmembrane junctional molecule to be studied at the cerebral endothelial cell level (Mehta and Malik, 2006). With a molecular weight of 65 kDa, it is found at the level of every branch of the vascular bed throughout the body, but it is expressed at the highest levels in endothelial cells of the CNS (Furuse *et al.*, 1993). It consists in four transmembrane domains and two extracellular loops, the latter being able to form homotypic bonds with counterparts present on adjacent cells. In the cytosol, occludin binds indirectly to the actin cytoskeleton through another tight junction component, zonula occludens-1 (ZO-1; see below), which is important to structurally stabilize the tight junctions. Interestingly, mice carrying a null mutation on the occludin gene are viable, do not show gross changes in tight junction morphology or relevant alterations in paracellular permeability, indicating, therefore, that this component is not essential for cell-cell junction formation but it is more an accessory molecule that maintains and regulates the tight endothelium; this role is achieved by modulation of the phosphorylated and ubiquitinated state of the protein (Papadopoulos *et al.*, 2004), which normally is linked to dissociation from the membrane, internalization and consequent increased paracellular permeability. Stress factors like small GTPases (see below), oxidative stress and angiogenic inducers (*e.g.* VEGF) have an effect on barrier permeability by promoting the regulatory modifications that show a negative effect on the protein functionality (Coisne and Engelhardt, 2011).

Claudins are a family of proteins crucial for the formation of barrier properties (Wolburg and Lippoldt, 2002). More than 24 members are known in humans, some of which are also expressed in non-endothelial cells; all are formed by four transmembrane domains and two extracellular domains, similarly to occludin, although not showing sequence homology. In BMECs, only claudin-1, -3, -5 and -12 are present (although this presents some controversy due to cross-reactivity of antibodies and high sequence homology), with claudin-5 being highly endothelial cell-specific (Engelhardt and Sorokin, 2009). Claudins have been shown to be sufficient to form fully functional tight junctions and to be fundamental for the correct establishment of the BBB properties (actually, they are considered the major contributors of

barrier functionality); in fact, claudin 5 knock-out (KO) mice die shortly after birth due to excessive leakage at the BBB level (Gavard and Gutkind, 2008).

The **immunoglobulin supergene family members** (JAMs; 3 members have been discovered so far, JAM-1, -2 and -3) are single-pass membrane proteins with a long extracellular domain (Nasdala *et al.*, 2002), while **endothelial cell-selective adhesion molecule** (ESAM)-1 has just become object of study. Both classes of protein have been shown to be part of the tight junctions of the blood-brain barrier: their role in paracellular permeability regulation is still disputed but its known that JAMs, besides their roles in cell adhesion and leukocyte transmigration, can increase cellular resistance by forming homodimers between neighbouring membranes in cells that do not normally form tight junctions (Williams *et al.*, 1999), plus it is able to drive occludin localisation at the intercellular junctions level (Del Maschio *et al.*, 1999). Finally, the Ig-superfamily member **platelet endothelial cell adhesion molecule-1** (PECAM-1) was found to be localized at the basolateral level and to be involved in cell-cell junctions, including at the BBB level (Graesser *et al.*, 2002).

All these integral TJ membrane proteins, along with some AJs, are linked inside the cells through an important class of cytoplasmic peripheral membrane proteins, members of the membrane-associated guanylate kinases (MAGUKs), namely the zonula occludens (ZO) proteins, (ZO-1, ZO-2 and ZO-3), which anchor the transmembrane structure to the cellular actin cytoskeleton and give overall stability to the entire structure (Mehta and Malik, 2006). Also, some old evidence (Fanning *et al.*, 1998) supports a potential role of ZOs in serving as chaperones for the correct maturation and localisation of the other TJs components.

4.5.3.2.1 Tight junctions and cell polarity

It is worth mentioning that another important role of TJs (and indirectly of AJs, for their influence on correct TJs formation) is to contribute to the definition of the molecular polarity of the cells, defining specialised luminal and abluminal membrane compartments (Dejana 2004). By acting as limiting factors towards the free diffusion of transmembrane molecules and lipid rafts on the lateral cell membranes, the TJs maintain a specific polarized organization in terms of transporters, channels, enzymatic proteins, *etc.* which determines

the differential functionality of different regions of the cellular membrane. The establishment of cell polarity also requires cell growth and motility inhibition, which are strongly affected by TJs and AJs, important mediators of growth factors and signals as vascular endothelial growth factor (VEGF) and others (Dejana 2004; Shin, Fogg *et al.* 2006).

4.5.3.3 Endothelial cell-basal lamina interactions

Endothelial cells express transmembrane molecules called integrins, which are heteromeric molecules involved in anchoring the cellular structure on the sub-endothelial basal lamina/extracellular matrix (Mehta and Malik, 2006). Integrins localize in specific abluminal cellular sites called “focal adhesions” or “focal contacts” (see Figure 4.4), which are tightly connected to the actin cytoskeleton and together with TJs and AJs are very important for paracellular permeability definition. In fact, blocking integrins and focal adhesions with neutralizing antibodies resulted in increased passage of molecules through the endothelium (Dejana *et al.*, 1993).

4.5.4 The importance of maintaining low paracellular permeability

The contribution of the CNS barriers in controlling the exchanges from the peripheral compartments is essentially dual, involving both a passive role in limiting vascular leakage of blood-derived molecules and an active role in guiding inflammatory cell migration.

Maintenance of extremely low paracellular permeability at the level of the BBB depends on several factors. Tight junction formation between endothelial cells is strongly affected by astrocytes and astrocyte-derived soluble factors, as demonstrated by several studies where *in vitro* BBB models have been improved by using astrocyte-conditioned medium (Abbott *et al.*, 2006; Abbott *et al.*, 2012). Also, the pericytes are increasingly considered as important modulators for the proper definition of low permeability coefficients; overall, all the NVU components may influence the homeostasis of the cell-cell endothelial junctions (Neuwelt *et al.*, 2011). Generally, maintaining a healthy tight BBB is of fundamental importance for the homeostasis of the entire CNS. While normal passage of small and big solutes is carefully regulated by the BBB transporter system, in the case of paracellular permeability this tight

control can be partially or totally lost: blood-derived ions, proteins, nutrients, circulating signalling molecules and even cells can more easily access the brain in high concentrations through newly-formed gaps, immediately starting to cause damage (Abbott *et al.*, 2006; Abbott *et al.*, 2010; Simpson *et al.*, 2010).

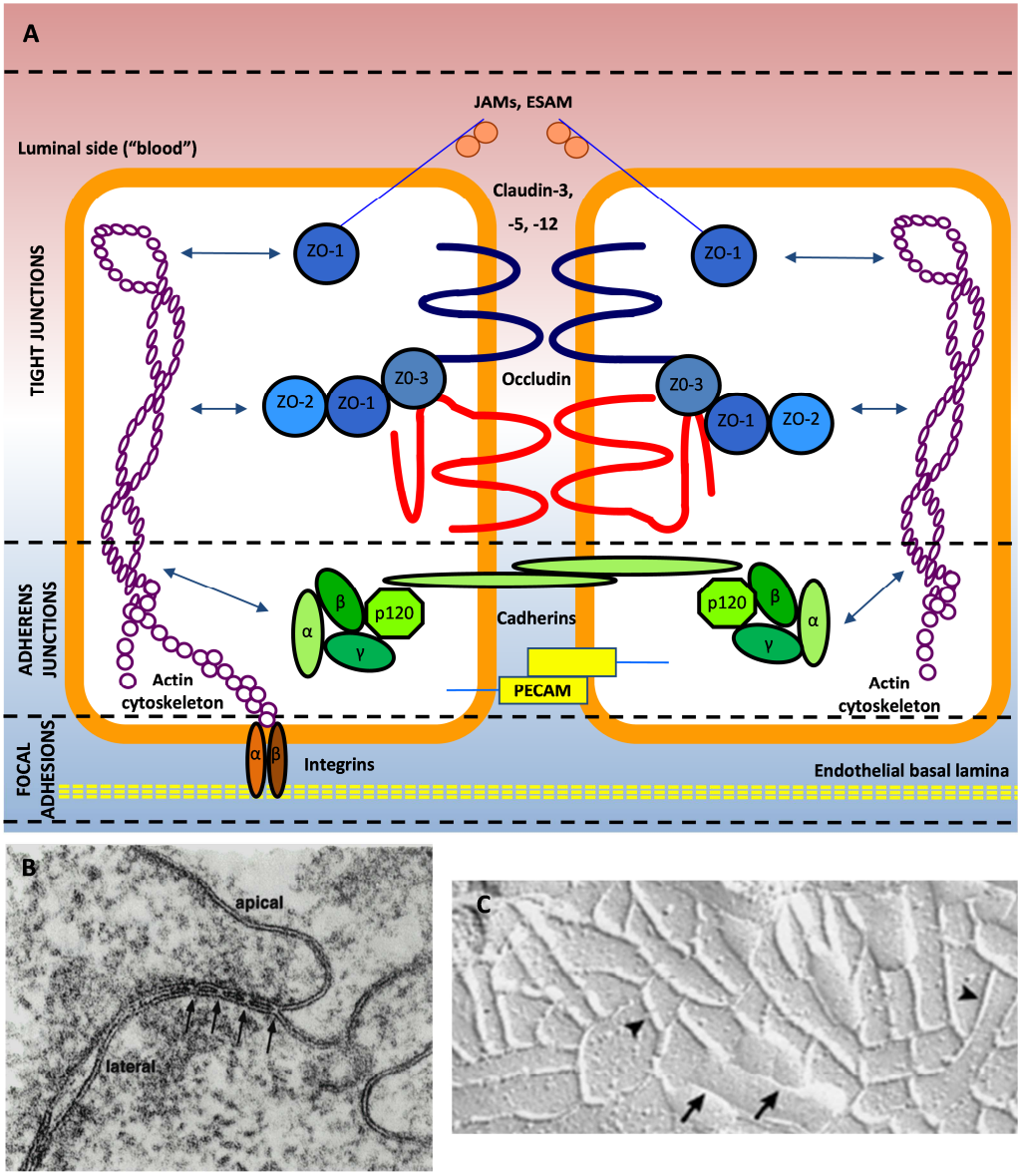

Figure 4.4 Cell-cell junction composition. A| At tight junctions level, cell adhesion is maintained by claudins, occludin, JAMs and ESAM-1. **B|** Transmission-electron microscopy image of "kiss" cell-cell fusion between adjacent cells. **C|** Freeze-fracture electron microscopy, showing the continuous and complex morphology of the tight junctions at the level of BMECs. Figure A adapted from Abbott *et al.*, 2010. Electron microscopy images taken from Stevenson and Keon, 1998 & Tsukita *et al.*, 2001.

It is now clear that many permeability-increasing agents have an action on the paracellular permeability. Most of these factors, like platelet-activating factor (PAF), VEGF, histamine, inflammatory cytokines, cytochalasin B and D, *etc.* trigger a series of molecular events that are reflected in changes in cell shape, like cell-rounding, therefore on the cellular cytoskeleton, which result in gap formation between endothelial cells due to loss of the highly organized inter-cellular junctions. To understand this, we should analyse the importance of the cytoskeleton, and its strong relationship with all the molecular components of the physical barrier.

4.5.4.1 The actin cytoskeleton in the endothelium

The cytoskeleton is the cellular skeleton, contributing to an enormous array of events like cell locomotion, definition of cellular shape and polarity, emission of cell protrusions (philopodia, lamellipodia, *etc.*), intracellular trafficking, structural cell support, cell-cell contact definition, basal lamina anchorage and focal adhesion formation (Hall, 1998; Lai *et al.*, 2005; Prasain and Stevens, 2009). All these functions are the net result of centrifugal and centripetal tensions generated by the various cytoskeletal components (Mehta and Malik, 2006). This shows how important is the cytoskeleton in defining properties of the various cell types, constituting the base for others to form, such as endothelial cell junctions.

4.5.4.1.1 Generalities

The cytoskeleton is essentially formed by microfilaments, microtubules and intermediate filaments. Microtubules represent thick (diameter around 23 nm) polymers of α- and β-tubulin, that could be coarsely defined as supportive beams of the cells due to their property of resisting compression; they do not appear to be directly involved in the regulation of paracellular permeability (Mehta and Malik, 2006) but their disruption has been shown to impair endothelial barrier (Prasain and Stevens, 2009). Intermediate filaments and microfilaments are instead the “cables” of the structure, being thinner (diameter between 6 and 10 nm) and involved in generating tension. Intermediate filaments are relatively stable structures that primarily maintain cell shape and structure; they are

formed by several molecules such vimentins, lamin, keratin, and others depending on the location. Microfilaments are thin, long filaments formed by polymerized monomers of actin, which is one of the most highly conserved and abundant proteins in eukaryotes (Firat-Karalar and Welch, 2011). Several studies have confirmed the primary role played by these three cytoskeletal components, in constant and intimate communication with each other to maintain numerous cell functions (Prasain and Stevens, 2009). In particular, actin microfilaments appear to be the most dynamic structures, therefore most studies have focused their attention on these.

4.5.4.1.1.1 Actin organisation

The polymerisation of actin is a phenomenon involved in almost every aspect of cell physiology, including membrane structure and function maintenance, cytokinesis, migration, endocytosis, exocytosis.

Actin is a globular ATP-binding protein normally present in two conformations: globular (G-) actin, which indicates monomers of the molecule, and fibrillar (F-) actin, which indicates polarized filaments of many actin molecules upon ATP binding. At the level of the endothelium, actin constitutes around the 10% of the entire protein content (Prasain and Stevens, 2009); therefore, the actin cytoskeleton is by far the most important modulator, representing a quickly responding structure.

The dynamics of the entire actin cytoskeleton are reflected in the transition between G- and F-actin, a phenomenon directly linked to ATP binding and hydrolysis (Prasain and Stevens, 2009; Lee and Dominguez, 2010). Through two complex processes called nucleation and elongation, F-actin quickly forms and grows unidirectionally (the so called “actin treadmilling”, depicted in Figure 4.5, Panel D). The balance between polymerisation and depolymerisation is defined by several modulators, whose mechanisms started to be elucidated only recently.

These are mainly involved in providing or sequestering G-actin monomers from the growing filaments (actin-binding proteins (ABP) such as cofilin and profilin), or in forming the pro-nucleation complexes that direct formation of a stable multimer of G-actin monomer, chemically unstable, thus representing the true rate-limiting step in F-actin formation. A more detailed molecular explanation of the polymerisation of actin can be found in some recent reviews (Prasain and Stevens, 2009; Lee and Dominguez, 2010).

4.5.4.1.1.1.1 Annexin A1 and actin

Several reports support the role of ANXA1 as an actin-binding protein, or at least as an inner regulator of the actin cytoskeleton. Due to their calcium-binding nature, annexins are regarded as important factors mediating responses to changes in this ion levels, for example membrane structure and function regulation (Gerke *et al.*, 2005). They have been observed to interact with G- and F-actin in cell-free *in vitro* models, while this has been difficult to prove *in vivo* and in cell models. In particular, Annexin A2 was the first one shown to bind actin filaments in a Ca^{2+}-dependent manner (Hayes *et al.*, 2004). Annexin A1 was also shown to co-localise with F-actin during phagosome formation (Patel *et al.*, 2011) and to directly impact on actin polymerisation by interacting with profilin, which is an important actin-binding protein able to catalyse ADP-ATP conversion of actin and to stimulate F-actin formation (Alvarez-Martinez *et al.*, 1996; Alvarez-Martinez *et al.*, 1997). Some evidence also supports the participation of ANXA1 and ANXA2 in complexes which are involved in the actin cytoskeleton formation, like Arp2/3 complex (Ghitescu *et al.*, 2001; Hayes *et al.*, 2004; Prasain and Stevens, 2009).

Actin and annexins show concomitant re-distribution in response to certain stimuli, which may suggest close parallelisms between these molecules. Notably, all these findings have been only demonstrated *in vitro*; they suggest the relevance of this class of proteins in actin physiology and dynamics, but they should be confirmed in cell models and *in vivo* before definite conclusions can be drafted.

4.5.4.1.1.2 Cytoskeletal structures

In general, F-actin organizes mainly into three distinct cytoskeletal structures (Prasain and Stevens, 2009). The first is the membrane skeleton, which is formed by short F-actin filaments (yellow structures, Figure 4.5, Panel A) that are distributed right underneath the cell membrane, where it acts as a scaffolding structure for the membrane itself, affecting its ability to distend, affecting the overall cell shape.

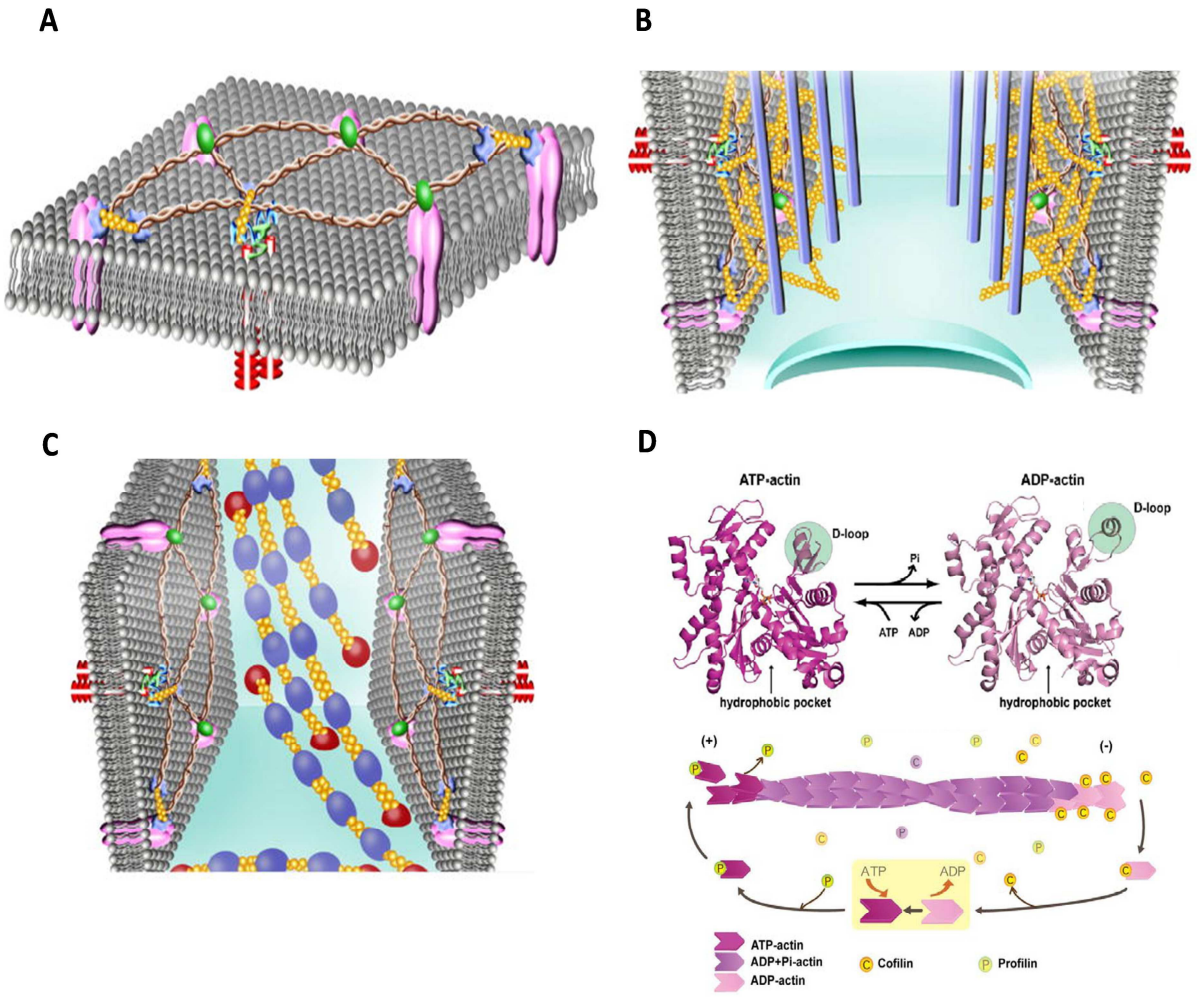

Figure 4.5 Actin cytoskeleton structures and F-actin formation. A| The membrane skeleton determines membrane architecture and enables for membrane distensibility. It is formed by short F-actin filaments (yellow structures), interconnected by spectrin molecules (brown structures). **B|** The cortical actin rim is intimately associated with cell-cell and cell-matrix adhesion complexes. **C|** Stress fibres run through the cytosol and interact with focal adhesion complexes. **D|** Structural differences between ATP-bound and ADP-bound actin monomers and schematic definition of the actin thread-milling model determining F-actin unilateral formation. Panels A, B and C have been modified from Prasain and Stevens, 2009, while panel D was taken from Lee and Dominguez, 2010.

The second one is the cortical actin rim (Figure 4.5, Panel B), which is a fundamental structure, running along the cell membrane and lying underneath the membrane skeleton with which it is intimately interacting. The cortical actin is formed by a dense tangle of long F-actin fibres, linked to the endothelial junctional components as ZO-1, α- and β-catenin, and a large plethora of accessory proteins, which have the role to maintain the correct location and actin state of this structural formation, limiting the generation of excessive F-actin, which would result in the stress fibres. The latter is the third actin formation present in cells (Figure 4.5, Panel C): stress fibres are bundles running throughout the cytosol, which are able to generate intense contraction within the cell body. They are formed by short polymerised actin fibres, myosin filaments, some actin-binding proteins and are anchored to the membrane; specific contractile molecules (myosin motor proteins) run along the F-actin fibres generating centripetal (inward) tension, which counteracts the centrifugal (outward) tension established by the cortical actin rim. Stress fibres are also very important for focal adhesion formation, since they directly interact with the cytoplasmic tail of the integrins.

4.5.4.1.2 Modulation of actin polymerisation and effect on intercellular junctions

Early studies by Madara *et al.* (Madara *et al.*, 1986; Madara *et al.*, 1987), although not in the brain vascular endothelium, produced the first evidence for an association of tight junctions with actin cytoskeleton; moreover, they observed a strong correlation between the perturbation of intercellular junctions, structural disorganisation of the cytoskeleton and concurrent alteration of the barrier function.

A precise mechanism by which actin exerts its influence on TJs is currently not clear (Lai *et al.*, 2005): structurally, the cortical actin rim is essential to anchor all the intercellular junctions and to sustain the molecular connection with adjacent cells, therefore, it is clear that stress fibres show a negative effect on the formation and on the maintenance of the cellular junctions, since they generate forces that are opposite to the one contributing to junctional complexes maintenance. However, the precise relationship between these opposing forces is not completely understood yet and new mechanisms have also been proposed, linking actin remodelling to secondary messengers like Ca^{2+}, which can mediate

the activity of certain enzymes that have been shown to modify and negatively modulate the expression and the distribution of TJs and AJs. Nevertheless, it is clear that one of the primary roles of the contractile apparatus is to regulate endothelial barrier properties: while stress fibres constitute a negative factor towards paracellular permeability, the thickening of the cortical actin rim coincided with reduction of the permeability (Crawford *et al.*, 1996), therefore the whole process should be tightly controlled. The cytoskeleton can be modulated by an enormous variety of intracellular mechanisms, which all converge on affecting the degree of actin polymerisation, the F-actin intracellular localisation and the contractility that is subsequently generated (Mehta and Malik, 2006). Among these mechanisms we should mention the serine-threonine phosphatases (regulation of the activity state of some contractile molecules), the Ca^{2+} channels (a molecular cascade can be triggered by high concentrations of the cation, with consequent effects at the level of the contractile apparatus), the actin-binding proteins and their action towards F-actin formation, the adenylyl cyclases and the small guanosine triphosphate (GTP) binding proteins (Prasain and Stevens, 2009). This last class of modulators is definitely the most important, responsive and tightly controlled system existing to control actin cytoskeleton dynamics, therefore it deserves a detailed description.

4.5.4.1.2.1 The role of small GTP binding proteins

The Rho family of monomeric small GTPases has been shown to play an important role in the regulation and modulation of the endothelial barrier function by directly affecting the actin cytoskeleton. Being GTPases, they cycle between an active, GTP-bound state and an inactive, GDP-bound state (Beckers *et al.*, 2010). Guanine nucleotide exchange factors (GEFs) catalyse the exchange of GDP for GTP, therefore mediating the activation of the molecule; GTPase-activating proteins (GAP) instead catalyse the inactivation of the enzymes by promoting the hydrolysis of GTP. The first member of the family was identified in 1985 (Wojciak-Stothard and Ridley, 2003) and was RhoA; so far, 21 members have been identified, with Rho (A, B, C, D, G), Rac (1, 2, 3), Cdc42 (Hs/G25K, TC10, Tc1) being the most prominent sub-classes. In particular, RhoA, Rac1 and Cdc42 are the best characterized ones.

RhoA has been reported to stimulate formation of stress fibres and focal adhesions; therefore it has always been regarded as effector acting against endothelial tightness and towards increase of permeability. Through its downstream mediator, Rho-associated protein kinase (ROCK), active RhoA inhibit, by phosphorylation, the activity of the myosin light chain phosphatase (MLCP). Such event causes a net increase in myosin light chain (MLC) phosphorylated form, which is the one that interacts with actin and slide along actin filaments causing contraction (Wojciak-Stothard and Ridley, 2003; Mehta and Malik, 2006; Beckers *et al.*, 2010). Active RhoA induces actin polymerization and stress fibre formation by inhibiting (through phosphorylation) the actin-binding protein cofilin, which has a role in depolymerising F-actin and moving the balance towards G-actin (Maciver and Hussey, 2002). Several vasoactive mediators like thrombin, LPS, lysophosphatidic acid (LPA), histamine and VEGF induce quick activation of RhoA, subsequently resulting in the generation of cytoskeletal tension and hyper-permeability. Since attachment and extravasation of leukocytes through endothelium have been shown to cause stress fibre formation and endothelial contractility, there is evidence that this is at least partially RhoA-mediated, which can be activated by signals triggered from adhesion molecules as VCAM-1 and E-selectin (Wojciak-Stothard *et al.*, 1999). In addition, RhoA is also able to negatively influence permeability through an actin-independent mechanism: being a protein kinase, it has the ability to phosphorylate occludin and claudins, reducing their membrane association and overall the strength of cell-cell junctions (Persidsky *et al.*, 2006). Therefore, RhoA is usually regarded as a tightness-disruptive molecule and not as a mediator involved in junctional maintenance (Beckers *et al.*, 2010). In fact, it has been observed that in resting conditions RhoA is usually inactivated by other small GTPases. However, one recent work (van Nieuw Amerongen *et al.*, 2007) reported complete opposite results, indicating that basal RhoA activity in resting conditions was fundamental to generate a higher affinity between cortical actin and junction proteins (VE-cadherin), adding more complexity to the topic (Wojciak-Stothard *et al.*, 2001).

Stress fibre formation and actin polymerisation are not always followed by an increase in paracellular permeability. As explained in section 4.5.4.1.1.2, the cortical actin rim is a fundamental scaffolding structure to support and mechanically sustain the cell-cell junctions, therefore its potentiation brings definitely an improvement in terms of tightness

(Crawford *et al.*, 1996). **Rac1** appears to be the Rho family member in charge of enhancing the endothelial barrier function: in the absence of vasoactive stimuli, this molecule tends to show always a basal level of activity, reinforcing its importance in maintaining cell-cell junctions. On the other hand, Rac1 is down-regulated upon stimulation with permeability-enhancing factors, like thrombin (Wojciak-Stothard *et al.*, 2001), indicating its opposing effects to RhoA. Noteworthy, Rac1 may also show barrier disturbing functions, in particular under oxidative stress conditions (Beckers *et al.*, 2010). **Cdc42** plays a more limited role in the maintenance of basal paracellular permeability and tightness properties, while being more active during cell mobility and migration [generation of filopodia (Ridley, 1999)], which governs angiogenesis events.

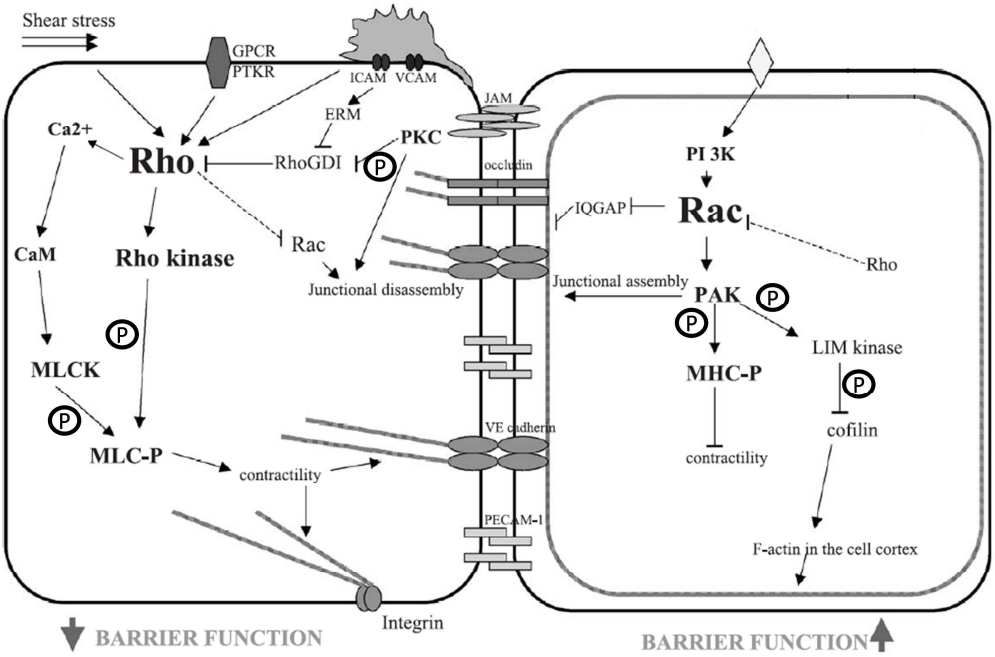

Figure 4.6 Overall view of the signalling mechanisms regulating endothelial permeability. This image describes the main signalling pathways triggered by RhoA and Rac1. Please note that some pathways have not been depicted for space constraints reasons. RhoA tends to cause a phenotype towards increase of barrier permeability; Rac1 instead shows an overall influence towards the reinforcement of the barrier properties. Exceptions to these concepts exist; please refer to the text for further details. Image taken and modified from Wojciak-Stothard *et al.*, 2001.

However, it is induced in a delayed fashion upon stimulation with certain vasoactive stimulants like thrombin, possibly paralleling the endothelial barrier recovering after the initial, prompt RhoA-mediated effects (Wojciak-Stothard and Ridley, 2003; Mehta and Malik, 2006; Beckers *et al.*, 2010) and it may represent a negative-feedback mechanism towards AJs-reassembly after an insult, therefore rescuing the permeability. Overall, the main members of the Rho GTPases family are deeply involved in the regulation of the actin cytoskeleton and consequently into the modulation of cell-cell junctions: very complex signalling pathways can be triggered both in basal/resting conditions and upon stimulation by a vast plethora of vasoactive agents, as illustrated in Figure 4.6.

4.5.5 Modelling the blood brain barrier

Increased interest in deciphering the physiological and pathological mechanisms of the BBB has led to the development of numerous ways of investigation (Chen *et al.*, 2003; Wee Yong, 2010). In the clinic, brain imaging (*e.g.* MRI), biomarker identification and histology are the current techniques of choice to detect alterations and BBB-related damage; for *in vivo* animal models, intravital microscopy represents the technique of choice to study leukocyte-endothelium interactions, but it can only reach superficial blood vessels, which tend to lack a fully developed BBB phenotype. Moreover, these techniques do not reach a degree of detail sufficient to describe the various cellular and molecular mechanisms. These and other limitations have pushed the development of numerous *in vitro* models, each characterised by its own advantages and disadvantages. Modelling such a complex structure *ex-situ* has proved to be a difficult task, in particular reproducing the characteristic low paracellular permeability, the complex transport system and the peculiar apical-basolateral polarisation. Since most of these properties are centred on the BBB endothelium, the greatest interest has been focused on that. Initially, epithelial cells with similar features to brain endothelial cells (*i.e.* Madin-Darby canine kidney cells; MDCK) were used as BBB model, as well as human umbilical endothelial cells (HUVECs), which bore the advantage of being human. An ambiguous model used for several years has been the ECV304, initially claimed to derive from transformed endothelial cells but recently found to be closer to epithelial than endothelial cells (Cabrita *et al.*, 2006).

Although it may be possible that certain cellular mechanisms can overlap between endothelial and epithelial cells, scientists are in the process of abandoning them for more reliable models. The establishment of successful and reproducible protocols for brain capillary isolation (Hatherell *et al.*, 2011), along with the ability of selectively culturing the endothelial cells without causing loss of the cellular phenotype, represented an essential step forward in modelling the BBB in a more reliable fashion. The most widely used primary cultures have always been those from rodent, due to the high availability of transgenic animals and pathological models, as well as reagents necessary for the studies, like antibodies and expression vectors. The small size limits the yield, plus some properties typical of higher mammalians cannot be reproduced faithfully; therefore, some efforts has been dedicated at optimising brain capillary extraction from bovine and porcine specimens sometimes with optimal results (Patabendige *et al.*, 2012), as well as from human surgical material, which cannot be considered healthy and physiological though. The establishment and optimisation of static endothelial cell monocultures on transwell filter devices allowed to mimic more closely the bipartite *in vivo* environment and to induce the peculiar membrane polarisation (Grant *et al.*, 1998).

The necessity to develop high throughput assays to test drugs and specific conditions does not find in primary cultures a sufficient means to meet the high requirements of cells, leading to the development of immortalized cell lines, easy to culture and possibly able to retain their differentiating properties even after repetitive passages, reducing labour and costs usually linked with primary isolation. One of the best characterised brain endothelial cell lines is RBE4, obtained from rat brain microvascular endothelial cells (Lippmann *et al.*, 2012) as well as GP8, also of rat origin (Galati and Di Giovanni, 2010). Amongst the most widely used, the murine cell lines bEND.3 (Cavegn and d'Ydewalle, 1996) and bEND.5 (Hamberger *et al.*, 2009) represent a good means to study molecular signalling pathways and permeability regulation. Some bovine immortalized cell lines also exist, although much less characterised and used.

One of the main limitations of primary cultures and cell lines of non-human origin has always been the inability to reproduce the same degree of expression and complexity of the human BBB and BMECs. Therefore, in the last decade most of the efforts has been thrown

into the development of cell lines of human origin. To date, the best characterised human cell line is the hCMEC/D3, which was obtained from a surgical excision from the temporal lobe of an adult female with epilepsy (Weksler *et al.*, 2005). This cell line has now been used in more than 60 publications, especially for drug transport/efflux studies and to investigate permeability regulation. Recently, a new conditionally immortalized human microvascular endothelial cell line called TY08 was established (Sano *et al.*, 2010), but it did not reach equal levels of reliability compared to hCMEC/D3. Currently, smart approaches are being developed to develop new BMEC lines from pluripotent stem cells (Lippmann *et al.*, 2012), with promising results.

All these monoculture models of endothelial cells represent easy and reproducible ways to study a number of aspects in the BMECs physiology, but they lack a number of critical features necessary for the correct full development of true BBB properties; absence of typical stimuli from the surrounding environment can also cause de-differentiation of the endothelial cells and loss of BBB-specific features. Nowadays, technical efforts are focused on co-cultures models with astrocytes and/or pericytes, which are fundamental to induce and maintain a properly formed BBB *in vivo* (Abbott *et al.*, 2006; Armulik *et al.*, 2010; Daneman *et al.*, 2010). Considerably higher TEER and lower paracellular permeability values have been obtained with several co-cultures models (Descamps *et al.*, 2003; Coisne *et al.*, 2005; Abbott *et al.*, 2012), both growing endothelial cells in contact or not with the accessory cells, as well as by using conditioned medium. Triple co-culture models including endothelial cells, astrocytes and pericytes are currently being investigated (Hatherell *et al.*, 2011), while interest has been generated by the BBB phenotype-inductive role of neurons in cultured BMECs, as well as from the role of microglia cells and macrophage-related cells (Garden & Moller, 2006; Banerjee & Bhat, 2007). Finally, the role of shear-stress in inducing BBB-specific phenotype has received increasing evidence and has led to the development of dynamic *in vitro* flow models mimicking physiological conditions of brain capillaries (Cucullo *et al.*, 2011; Naik & Cucullo, 2012). Shear-stress was able to improve the TEER values (Wilhelm *et al.*, 2011) and to induce a resting a-mitotic phenotype more resembling the conditions found *in vivo*. Further investigation on this field is currently undertaken and will hopefully generate more information.

Some acellular and *in silico* models, aimed to study drug membrane penetration and CNS distribution, have been recently developed and have started to be used by pharmaceutical companies, although their applicability and reliability still have to be proved and improved (Naik & Cucullo, 2012). Overall, the constant need to pre-screen and validate novel CNS therapeutics, as well as certain pathological toxins and disease conditions, is pushing to develop continuously new *in vitro* models, possibly able to reproduce a reliable BBB. The large number of different *in vitro* models suggests the absence of the perfect model and rather the necessity to find and use those more advantageous for the studied question, complementing them with the still informative *in vivo* and human studies.

4.5.6 The blood brain barrier as a therapeutic target

Since BBB damage appears to be present in several neurological disorders, it is not surprising to see many efforts thrown towards the development of potential therapies for these diseases that target the impairment of the barrier. Since BBB dysfunction can either be a causative phenomenon or a propagative/exacerbating event in the course of the disease, limiting its impairment would potentially reduce the severity of the pathology and facilitate recovery (Abbott *et al.*, 2006; Vastag, 2010). As inflammation and inflammatory mediators are the primary cause for the negative effects at the barrier level, most of the attempts have been focused on halting the inflammatory reaction: glucocorticoids like dexamethasone have shown to improve (Romero *et al.*, 2003; Cucullo *et al.*, 2004; Bauer *et al.*, 2005) the physical and transport barrier properties of the blood brain barrier, but their usefulness in MS patients decrease with time (Plumb *et al.*, 2002).

Therefore, other approaches are currently being tested, which mainly target either the strength of the intercellular junctions or the expression of adhesion molecules on the endothelial cells. For example, the potential use of flavonoids has generate interest; normally used with success as a treatment of some venous insufficiency pathologies, these molecules have given promising results in the EAE model of MS (Simka, 2009).

Equal interest has generated the possibility to deliberately increase basal permeability to improve administration of therapeutic molecules into the brain. This is a topic still at its

infancy and brings a lot of complications: in fact, the therapeutic opening needs to be tightly controlled and as brief as possible, to limit the impact of oedema and extravasation of peripheral molecules into the tissue. Some novel studies, mainly targeting tight junction expression, have started to provide some promising results (Farkas *et al.*, 2005; Campbell *et al.*, 2011). Noteworthy is the "Trojan horse-like approach" which has been developed by William Pardridge to deliver therapeutic molecules into the brain by coupling them to molecular portions that allow to cross the barrier by exploiting a natural occurring transcytosis mechanism (Vastag, 2010).

4.6 Methods

Please refer to Chapter 3 (General methods) for general *in vivo* and *in vitro* procedures. Here I will provide more details about certain technical aspects and describe those procedures specifically used for the purpose of only this chapter. Please refer to the Appendix (Chapter 10) for solutions composition.

4.6.1 Magnetic resonance imaging (MRI)

MR imaging of anaesthetised wild-type and Anxa1 null mice was performed using a 9.4T Varian Direct Drive system and quadrature volume head RF coil. The MRI protocol consisted of dynamic contrast acquisitions with a multi-slice T1 weighted gradient echo with a fixed 30° flip angle (repetition time 132ms, echo time 2.77ms, field of view 20x20mm, matrix size 128x96, 24 contiguous transverse slices of 0.6mm covering the whole brain). A total of 50 volumes were acquired, with 100µl 0.5mM dimeglumine gadopentetate (Magnevist, Schering Health Care Ltd, UK) administered intravenously after the 14th volume at a rate of 3.3µl/s (average of 0.02 mmol/kg of body weight, resulting in a total dose of 0.5 mmol per animal). TOPPCAT software (Barboriak *et al.*, 2004; Barboriak *et al.*, 2008) was used to create quantitative maps of fractional volume. Kind help and support for the technical procedure and data interpretation was provided by Dr. J. Lopez-Tremoleda and Dr. M. Wylezinska-Arridge (Biological Imaging Centre (BIC); Imperial College London, UK).

4.6.2 Brain water content determination by wet-to-dry weight ratio

The procedure followed published methods (Xiao *et al.*, 2004; Yan *et al.*, 2011). Animals were deeply anesthetised by *i.p.* injection of 100 µl sodium pentobarbitone (60 mg/ml). Once fully anesthetised, the heart was revealed by cutting through both sides of the rib cage and the diaphragm. Blood samples were collected by cardiac puncture of the right ventricle while the right atrium was cut to allow release of blood. Blood was washed out of the body by perfusion through the left ventricle with approximately 15 ml of filtered saline solution. Brains were rapidly removed, placed on microscope glass slides, weighed (WW, wet weight) and then placed in a laboratory oven (set at 100°C) for 24 h.

Samples were weighted again (DW, dry weight) and results were expressed as percentage of water content towards total wet weight, according to the following equation:

$$\frac{(\text{WW-DW}) \times 100}{\text{WW}}$$

4.6.3 Electron microscopy

Processing and analysis of transmission electron microscopy (TEM) images were performed by Dr. Helen Christian (Oxford University, UK). Cells monolayers were grown in transwell inserts at the described conditions. Preparation occurred as described (McArthur *et al.*, 2009). Briefly, cells were fixed in 0.05% (w/v) glutaraldehyde in PBS 0.01M pH 7.4 for 20 minutes at 4°C, washed briefly in PBS 0.01M, and transferred to a solution of 2.3 M sucrose in PBS at 4°C overnight.

Cryoprotected cells were snap-frozen, freeze-substituted at −80°C in methanol for 48 h, and embedded at −20°C in LRGold acrylic resin (London Resin, Reading, UK) in a Reichert freeze-substitution system (Reichert MM80E; Leica, UK). Ultrathin sections (50–80 nm) were stained for ANXA1 by immunogold labeling using a rabbit polyclonal anti-ANXA1 (Invitrogen, UK) for 2 hours at RT followed by 1 hour incubation with anti-rabbit IgG linked to 15 nm gold particles (British Biocell, Cardiff, UK). Sections were then mounted and examined morphologically with a JEOL 1010 transmission electron microscope (JEOL, Peabody, MA).

4.6.4 hCMEC/D3 cell culture and stable transfection

Human cell line hCMEC/D3 was maintained as described in Section 3.2.2.1.2. Transfection was performed as described in Section 3.2.2.1.5, using plasmids produced by Dr. Solito (Solito *et al.*, 1998b) bearing either an antisense sequence directed against messenger RNA products of the ANXA1 gene or the full length coding sequence (coding DNA) of ANXA1 itself, or an empty plasmid as control for transfection effects (pRc/CMV; Invitrogen, UK). Both plasmids contain the gene for the antibiotic Geneticin® resistance, which allowed selection of cells that stably incorporated the plasmid into their genome (initial 7 days: 400 µg/ml; subsequently 200 µg/ml). Resistant clones were cultured until they achieved a good

size; then passaged by using replica disks into 24-well plates and expanded into more capacious culturing devices. When enough cells were obtained, they were grown until confluent and immunophenotyped for ANXA1 and for the major tight- and adherens-junction components expression by flow-cytometry. For certain studies, only the best stable clones were used, which were "pRc/CMV-empty 3" (E3), "Antisense 4" (AS4) and "Full-length 11" (FL11).

4.6.5 Lentiviral vector production

In order to achieve a more definite regulation of ANXA1 on hCMEC/D3 cell line, replication-deficient lentiviral particles bearing either full length cDNA of ANXA1 or specific silencing sequences were produced, since this approach allowed for quicker, more efficient and more stable integration as reported (Vigna and Naldini, 2000).

Production of lentiviral particles for stable expression of transgenes was conducted in collaboration with Dr. E. Pazarentzos (Imperial College London, UK), whose help and advice are fully acknowledged. For details on the production, refer to Appendix, section 10.4.

4.6.5.1 Infection and selection of infected cells

hCMEC/D3 cells were seeded on 12-well plates at low density. When 30-50% confluent, cells were transduced with 500 µl of virulent medium supplemented with 1 µg/ml of Polybrene® (Sigma-Aldrich, UK) for 6 hours. Fresh EGM-2 MV medium was added to the infection, diluting the existing infectious medium at least 3 fold. The next day, medium was changed to fresh one and cells were left to recover for 8 hours. Medium was again replaced with fresh EGM-2 MV supplemented with puromycin (16 µg/ml for pLKO.5-based viral infections; 5 µg/ml for modified pLenti7.3-based viral infections) and selection occurred for 3-4 days before switching the medium to a reduced selection (5 µg/ml and 2 µg/ml respectively).

Resistant cells were cultured until confluent and a fraction of them was assessed for expression of the transgene or shRNA-dependent down-regulation of the gene of interest by flow cytometry or western blotting.

4.6.6 Co-immunoprecipitation of proteins

hCMEC/D3 cells were seeded and grown on 10-cm plates until confluent and left 24 hours in medium without VEGF to improve the formation of a full and tight monolayer. Cells were scraped and lysed in 1 ml/plate of RIPA buffer. More than 250 µg of total protein were resuspended in 1 ml of RIPA buffer and pre-cleared (removing any unspecific binding occuring between proteins and mouse or rabbit IgG) using 5 µl of naive mouse or rabbit serum (according to the source of the antibody used for the immunoprecipitation) and 30 µl of protein G sepharose-coated beads (Sigma, UK; in resuspension buffer) under rotation for 1 hour, at 4°C. Samples were centrifuged at 13000 RPM for 1 minute and supernatant retained; this was incubated overnight at 4°C with the immunoprecipitation-specific dose of the antibody raised against the desired protein to pull-down. Specifically, 2 µg of an anti-ANXA1 antibody raised in rabbit [called "Hortense", home-raised by Dr. Solito (Solito *et al.*, 1998a)], 3 µg of monoclonal anti-β actin and 3 µg of the anti-tight and adherens-junctional proteins antibodies were incubated with 250 µg of total proteins. Negative controls were also included, consisting in incubating the total protein lysate with mouse or rabbit control IgG isotype. 80 µl of protein G sepharose-coated beads were added and rotated at 4°C for 4 hours.

Samples were centrifuged at 13000 RPM for 1 minute and supernatant was discarded. Pellet (*i.e.* beads and pulled-down proteins and complexes) was washed three times in low buffer and then twice in high buffer to remove any unspecific or weak interactions. Beads were then resuspended in 40 µl Tris.HCl, pH 7.4 with protease inhibitors. Reducing sample buffer was added, samples were boiled for 5 minutes at 95°C to denature proteins, separate them from each other and from the beads. After a final centrifugation the supernatant was separated by SDS-PAGE using 10% gels and immunoblotted using antibodies directed towards the molecule which had been pulled down and potential interacting targets.

4.6.7 Small GTPases pull-down assay

hCMEC/D3 cells were grown on 6-cm Petri dishes until confluence and then incubated overnight in complete EGM-2 MV medium without VEGF before exposure to recombinant human ANXA1 (in-house stock (Lim *et al.*, 1998) used at 20 µg/ml final concentration for 3 hours) or thrombin (from Sigma, UK; used at 1 IU/ml final concentration for 8 minutes as a positive up-regulator of RhoA activity). Cells were then lysed and scraped off the plates in Cell Biolabs specific lysis buffer (5X lysis buffer, Cell Biolabs Inc, USA). The GTP-bound active form of RhoA was isolated as previously reported (Wojciak-Stothard *et al.*, 2001): the whole lysate was incubated with 200 µl of GST-tagged recombinant Rhotekin bound to glutathione beads (a kind gift from Dr. B. Wojciak-Stothard), while the activity of Rac1 was measured by isolating the GTP-bound active form through GST-tagged p21-activated kinase binding domain (PAK1-PBD) bound to glutathione beads (Cell Biolabs Inc, USA). A control plate was also grown and lysate prepared as described above and loaded with guanosine-5'-O-γ-thio-triphosphate (GTPγS) or GDP respectively to have a positive or negative internal control, as suggested (Cell Biolabs Inc, USA).

Lysates and beads mixtures were rotated for 1 hour at 4°C and washed three times in lysis buffer. Affinity-precipitated active forms of RhoA and Rac1 proteins were resolved by SDS-PAGE and detected by Western blotting. 10 µg of the total lysate were run in parallel to measure the total quantity of the small GTP-ases of interest along with loading control (GAPDH).

4.6.8 Soluble and insoluble β-actin extraction

Soluble *vs.* Insoluble β-actin extraction was conducted as described (Cramer *et al.*, 2002) with slight modifications. Latrunculin treatment, a potent cytoskeletal actin depolimerizing agent (20 µM final concentration; Cayman Chemical, US) for 10-30 minutes was included as a positive control. hCMEC/D3 cells were seeded on 10-cm dishes and grown until confluent in complete EGM-2 MV medium. Medium was then changed to EGM-2 MV without VEGF for 24 hours. Globular monomeric actin (G-actin) was extracted by washing cells briefly with DPBS without Ca^{2+}/Mg^{2+} followed by 5 minutes incubation at RT with 1 ml of soluble actin extraction buffer, which contained 1 µg/ml unlabelled phalloidin (Sigma, UK) to stabilize the

cytoskeletal actin. The volume was removed and centrifuged at 1000x*g* for 5 minutes at 4°C to remove any detached cell; the supernatant was saved and stored at -80°C**.** Cells were washed quickly three times with DPBS without Ca^{2+}/Mg^{2+}; after that, fibrillar polymeric cytoskeletal actin (F-actin) was extracted by incubating with 1 ml of insoluble actin extraction buffer and by scraping cells off the plate through a sterile tissue culture scraper. The lysate was sonicated for 10 seconds (30% duty cycle, output control 2; Ultrasonic processor, Jencons) and centrifuged at maximum speed at 4°C for 10 minutes. Supernatant was saved for further analysis. In parallel, total β-actin samples were prepared by growing and treating cells in the same way and by extracting the whole protein content by using 1 ml RIPA buffer, scraping off cells from the dish and briefly sonicating the lysate to ease the viscosity. Samples were quantified for their protein content and the following quantities were loaded and resolved on a SDS-PAGE: 3 µg for the total extraction, 6 µg for the soluble extraction, 2 µg for the insoluble extraction. These quantities were optimised so that the intensity of the bands obtained on the blots were not saturated, therefore allowing for detection of changes between treatments.

4.6.9 Proximity ligation assay

In order to detect points of interaction between ANXA1 and β-actin within hCMEC/D3 monolayers, a proximity ligation assay (PLA; Duolink, Olink Bioscience) was used, able to detect points of close (40 nm) vicinity. The principle of this relatively new technology is based on two unique probes (provided with the commercial kit), which consist of a secondary antibody attached to a unique synthetic oligonucleotide. The proximity of the probes allows DNA ligation at the exact location where these probes are localised. The distance of the oligonucleotides permitting DNA hybridization and ligation is small (<40nm) so only proteins that interact can allow ligation. The ligated DNA can then be amplified by DNA polymerase and detected through labelled oligonucleotides complementary to the amplified sequence. This technique provides very high sensitivity as the ligated DNA is amplified several fold, resulting in enhancement of the initial ligation event.

As the spots can be counted, the PLA signal provides not only the exact spatial information (the location of the interaction events) but also an objective way of quantifying these events.

Optimised protocols and technical support were kindly provided by Dr. E. Thymiakou and Prof. V. Episkopou (Imperial College London, UK) (Thymiakou and Episkopou, 2011), while procedure was performed together with Dr. S. McArthur. Briefly, wild-type hCMEC/D3 were grown on transwell filters until confluent as described; after fixation in 2% (w/v) PFA for 10 minutes at RT and subsequent washes in DPBS with Ca^{2+}/Mg^{2+}, monolayers were permeabilized in 0.5% Triton X-100 in DPBS with Ca^{2+}/Mg^{2+} for 5 minutes at RT and blocked for 1 hour at 37^{o}C using Duolink II Blocking Solution (1X). Primary antibodies anti-ANXA1 and anti-β-actin were then diluted to the desired concentration (see Appendix; Section 10.2) in Duolink II Antibody Diluent (1X) and incubated for 1 hour at RT, under slow agitation. Meanwhile, the two PLA probes (Duolink II anti-Mouse MINUS and Duolink II anti-Rabbit PLUS) were prepared by 1:5 dilution in Antibody Diluent (1X). Filters were washed twice (5 minutes/wash) with 1X Duolink II Wash Buffer A under agitation and at RT. After this step, PLA probes were added and samples were incubated in a pre-heated humidity chamber for 1 h at 37°C. The Duolink II Ligation stock was prepared following the datasheet and the provided ligase was added (1:40) just before incubation with the samples, which were washed once (5 minutes/wash) before the ligation which lasted 30 minutes at 37°C in a pre-heated humidity chamber. Then, Duolink II Amplification stock was prepared in and the provided DNA-polymerase was added (1:80) just before incubation with the samples, which were washed twice (2 minutes/wash) in Wash Buffer A before incubation for 2 h in a pre-heated humidity chamber at 37°C. Finally, samples were incubated 2 times (10 mins/incubation) in 1X Duolink II Wash Buffer B (containing fluorescently-labelled probes), then washed briefly in 0.1X Duolink II Wash Buffer B. To visualise F-actin, filters were incubated for further 20 minutes in Alexa 488-conjugated phalloidin (Invitrogen, UK) diluted 1:40 in DPBS with Ca^{2+}/Mg^{2+}. Filter were mounted with Prolong anti-fade mounting medium (Invitrogen, UK) and visualized by confocal microscopy.

4.6.10 Murine primary microvascular endothelial cell isolation

The following isolation protocol was kindly provided and explained by Dr. R. Brown (King's College London); it is based on those developed by Coisne *et al.* (Coisne *et al.*, 2005) and on that used in the Professor NJ Abbott laboratory at King's College London (Abbott *et al.*, 1992). Volumes and concentrations are optimised to be effective for 12 mouse brains. Solution composition is described in the Appendix, Section 10.1.

Animals were quickly sacrificed by deep anaesthesia, decapitated and brains were extracted from the skull and placed into a 50 ml falcon filled with ice-cold DPBS with Ca^{2+}/Mg^{2+}.

When all the animals had been culled and operated, brains were deprived of the cerebellum, sliced into hemispheres and transferred into ice-cold wash buffer and left to chill for 15 minutes. The following steps were all performed under a tissue culture laminar flow hood to guarantee sterile conditions and avoid contamination of the preparation.

Each half brain was rolled on dry Kimberly tissue to remove meninges and surface blood vessels; after moving it to a Petri-dish, a sterile Q tip was used to remove remaining blood vessels identified under a dissecting microscope (Meiji, Japan). Striatum, choroid plexus and white matter were removed using sterile fine forceps. After these operations, cleaned halves were placed into a 50 ml falcon tube containing 25% BSA solution. When all the brains underwent the cleaning procedure, they were homogenised with 15 strokes in a Dounce glass homogenizer with a large (0.06-0.08 mm) clearance pestle. Small volumes were processed to guarantee a complete homogenisation. Homogenate was repeatedly triturated until smooth with a 10 ml plastic pipette. Tubes were centrifuged at 3000x*g* for 25 minutes at 4^{o}C. After the first spin, tubes were carefully turned on themselves to loosen the plug formed on the top of the volume (containing mainly myelin, astrocytes and other cell types not necessary for the preparation); volume and plug were quickly poured into a new sterile 50 ml Falcon tube and underwent trituration by repeated pipetting and a following centrifugation at 3000x*g* for 25 minutes at 4^{o}C. The first tube was capped and left on ice upside down to remove any remaining myelin from the capillary pellet. Clean pellets from the two tubes were resuspended in wash buffer, joined together and applied to a 70 μm filter, meant to trap big vessels. The filter was washed with 10-15 ml of wash buffer.

The capillary-enriched filtrate was centrifuged at 1200x*g* for 7 minutes at 4^{o}C and pellet was resuspended in enzyme cocktail solution (10 ml/preparation) and incubated at 37^{o}C in shaking water bath.

Tubes were centrifuged for 5 minutes at 1500x*g* at 4^{o}C and pellets washed more than 3 times with wash buffer. Capillaries were seeded in a small volume of primary endothelial cell medium (2 ml) in T25 flask (pre-coated for at least 3 hours with home-made rat tail type I collagen, kindly provided by Dr. Rachel Brown).

Puromycin (4 μg/ml) was used for the first 3 days of culturing for maximal removal of contamination from non-resistant cell types. Primary cultures resulted in > 95% pure microvascular endothelial cells as assessed by endothelial markers phenotyping (tight and adherens junctions). Medium was changed every 4 days; when cultures were 70-80% confluent, cells were trypsinised and seeded on transwell inserts (Corning, Sigma-Aldrich, UK) coated in rat tail type I collagen at a density of 80000 cells/cm^2. When cells reached confluence, medium only in the lower chamber was replaced to complete medium devoid of fetal bovine serum and cultures were left for 3 days to increase their tightness, as reported (Coisne *et al.*, 2005).

4.7 Results

The major aim of the thesis is to unravel the involvement of ANXA1 in the mechanisms of communication between peripheral immune system and CNS; therefore, we first focused on the potential role of this protein at BBB level, which represents the real and definite interface between the two compartments and an important check-point. Initial findings (Figure 2.1) led us to hypothesise for a physiological role of Annexin A1 at the level of the BMECs, where the fully-developed BBB is formed and functions (Macdonald *et al.*, 2010).

4.7.1 Anxa1 null mice show increased basal paracellular permeability

Figure 4.7 clearly shows Annexin A1 to be well expressed at the level of the endothelium of the microvasculature, both in human (non-neurologic control *post-mortem* cortical excision; see Section 5.3.3 for tissue processing and staining methods) and murine tissues (Figure 4.7; panels A, B, C). Lack of Anxa1 caused increased basal Evans Blue intracerebral leakage (Figure 4.7; panel D), which was paralleled by an augmented serum IgG extravasation (Figure 4.7; panel F) in the brain parenchyma (see white arrows). In order to confirm the constitutive higher BBB endothelium-related permeability *in vivo*, we compared magnetic resonance imaging (MRI) signals from adult male C57Bl/6 wild-type and Anxa1 null mice following the dimeglumine gadopentetate administration. Considerable leakage of contrast medium was detected into the brain parenchyma of Anxa1 null mice, especially at the level of the midbrain, while no changes were detected in wild-type counterparts, as expected (Figure 4.7; Panel G). Interestingly, these results were not paralleled by changes in water content between the genotypes (Figure 4.7; panel E), indicating that the increased diffusion of substances is not accompanied by cerebral oedema formation.

4.7.2 The expression and distribution of tight and adherens junctions components are disrupted in Anxa1 null mice

Such a strong evidence for an increased permeability in Anxa1 null animals led us to investigate further how Annexin A1 is mechanistically involved in the correct BBB functionality. As shown in Figure 4.8 (Panels A and B), we did not detect evident changes in major components of the BBB such as pericyte organisation, astrocytic end feet positioning and basal lamina formation, or the expression of the efflux pump *p*-glycoprotein (MDR-1), that could have suggested an alternative explanation to the changes observed. We then investigated the major components of TJs, namely claudin-5, ZO-1 and occludin, and the major AJ component VE-cadherin, responsible for the establishment of full BBB tightness. Interestingly, we observed, by confocal microscopy, a significant organizational disruption in Anxa1 null mice (Figure 4.8; Panel C) mainly for occludin and VE-cadherin. Further analysis by western blot revealed also a significant reduction in these components' content in the insoluble/membrane associated fraction of cortical homogenates in Anxa1 null mice (Figure 4.10). These observations were confirmed by confocal analysis of primary cerebral microvascular capillaries (Figure 4.8; Panel D). Notably, histological analysis of kidney cortex (Figure 4.9; Panel A), a tissue rich in tight junctions but functionally and anatomically unrelated to BBB, revealed no evident occludin disorganization in null mice compared to wild-type, supporting the high anatomical specificity for this phenotype. ANXA1 is a member of the large family of Annexins (see Chapter 1, Introduction) and compensatory effects have been detected in several tissues of the Anxa1 null mouse (Hannon *et al.*, 2003). Therefore, we looked for differences in the expression of Anxa2, which has been reported to play a tight-junction protein-like role in the epithelial cells of the kidney (Lee *et al.*, 2004) and of Anxa5, which has unrelated roles (van Engeland *et al.*, 1998).

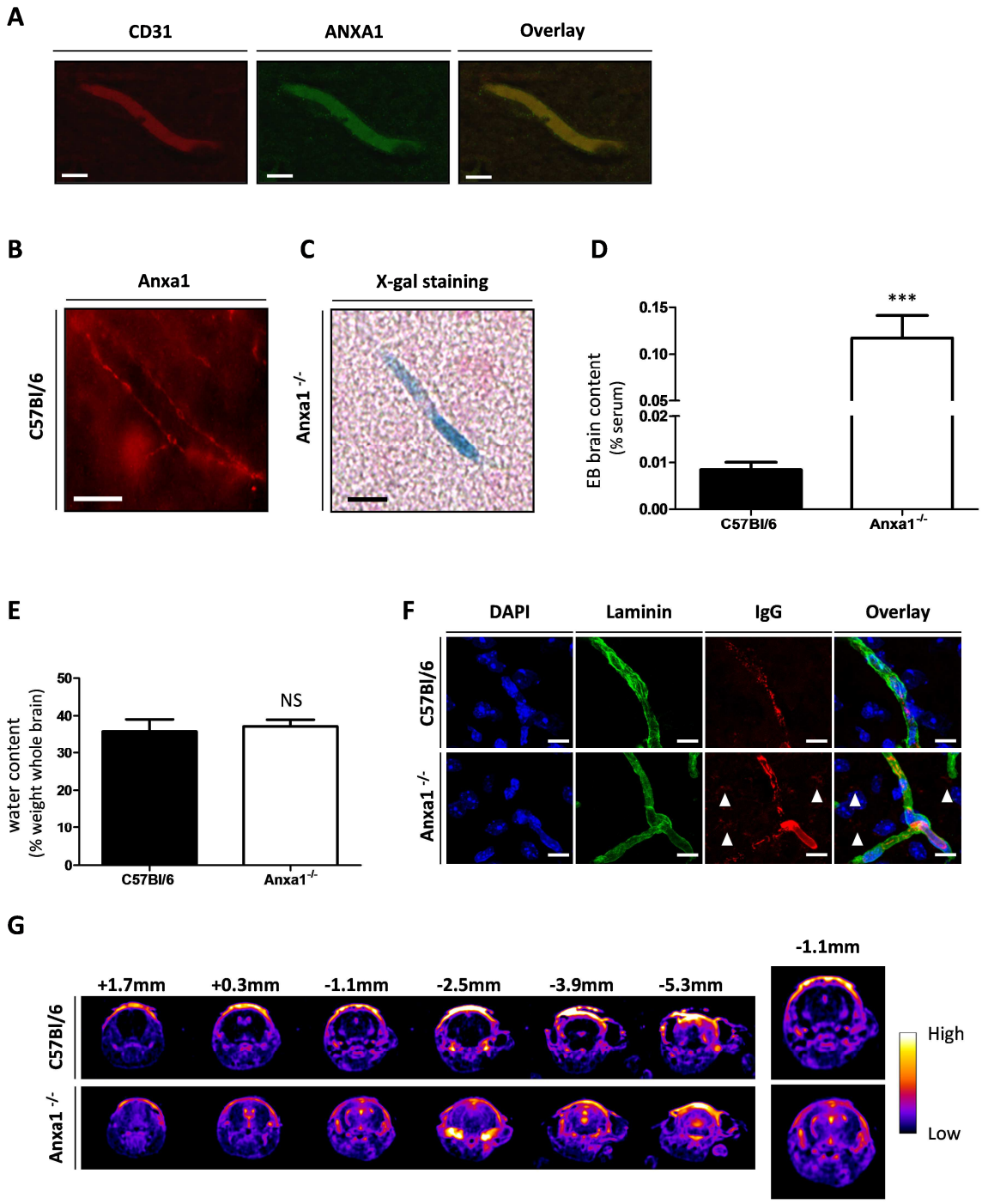

Figure 4.7 Annexin A1 is expressed in brain microvascular endothelium and Anxa1$^{-/-}$ mice show constitutively elevated BBB permeability. A| Confocal microscopic analysis of ANXA1 expression on the endothelium of a human cortical capillary, immunofluorescently labelled for endothelial marker CD31 (green) and ANXA1 (red); scale bar is 10 µm. **B|** Confocal microscopic analysis of Anxa1 expression on mouse capillary, immunofluorescently labelled for Anxa1 (red); scale bar is 20 µm. **C|** Microscopic analysis of Anxa1 null mouse capillary, histochemically stained for β-galactosidase activity and counterstained with eosin Y; scale bar is 20 µm. **D|** Basal permeability was assessed in untreated young adult animals (2-3 months old). Results are presented as means ± SEM (*n*=4) of the percentage of the serum dye content compared to the amoung (ng) of Evans Blue (EB) extravasated into the brain parenchyma/mg of total tissue. *t*-test between the two independent groups was

performed and $p<0.05$ was considered significant. *** $p<0.001$. **E|** Percentage of brain water content/total wet brain weight in male C57Bl/6 mice and Anxa1 null mice; results are presented as means ± SEM (n=4/genotype). Student's t-test between the two independent groups was performed. **F|** Extravasation of IgG (red) into brain parenchyma in wild-type and Anxa1 null mice, tissue nuclei stained with DAPI (blue), laminin (green) to delineate basement membrane of capillaries; arrows indicate clear points of mouse IgG extravasation into brain parenchyma; scale bar is 10 µm. **G|** T_1-weighted dynamic contrast MRI series of coronal cranial sections taken at various distances from bregma of wild-type and Anxa1 null mice. Brighter areas show increased dimeglumine gadopentetate leakage. Typical profile of n=5 mice/genotype are shown. Panels A, C, D & F produced with help from Dr. S McArthur.

Although we did not detect any change in total expression in the whole cortical tissue extracts (data not shown), in contrast we detected an increase in Anxa2 expression in total homogenates from isolated Anxa1 null mouse brain capillaries (Section 3.2.4.1) compared to the wild-type counterpart (Figure 4.9; Panel B), which may suggest the presence of partial compensatory mechanisms in place of the cognate molecule.

4.7.3 Annexin A1 regulates paracellular permeability in an *in vitro* model of BMECs

Since the above described *in vivo* and *ex vivo* experiments indicated that Annexin A1 exerts its role on BBB permeability at the level of the cerebro-vascular endothelium, we looked at primary isolated and culture of microvascular capillaries from wild-type and AnxA1 null mice. Pure endothelial cell cultures were grown until 100% confluent. *In vitro* paracellular permeability indicated two-fold increase in leakiness of the barrier properties of the cellular Anxa1$^{-/-}$ monolayers (Figure 4.11; Panel A). In order to understand the mechanisms by which Annexin A1 affects the BBB permeability, we moved to an established *in vitro* model based on the line called hCMEC/D3 (Weksler *et al.*, 2005). Firstly, we stably modified ANXA1 expression of these cells and characterised their properties as depicted in Chapter 9, Section 10.5.

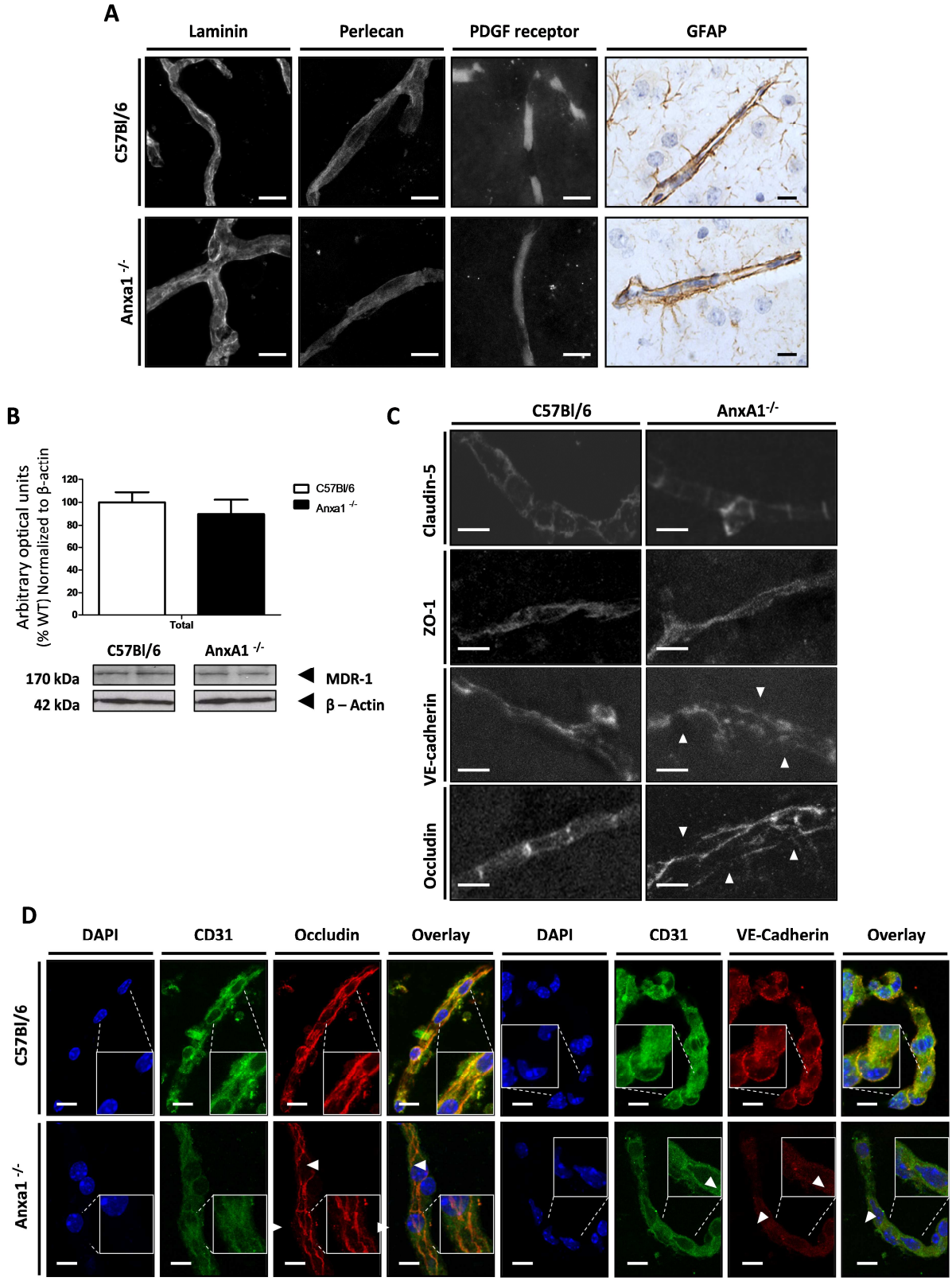
A
Laminin
Perlecan
PDGF receptor
GFAP
C57Bl/6
Anxa1 -/-
B
Arbitrary optical units
(% WT) Normalized to β-actin
120
100
80
60
40
20
0
Total
C57Bl/6
Anxa1 -/-
C57Bl/6
AnxA1 -/-
170 kDa
42 kDa
MDR-1
β – Actin
C
C57Bl/6
AnxA1-/-
Claudin-5
ZO-1
VE-cadherin
Occludin
D
DAPI
CD31
Occludin
Overlay
DAPI
CD31
VE-Cadherin
Overlay
C57Bl/6
Anxa1 -/-

Figure 4.8 Lack of Anxa1 results in disruption of tight- and adherens junctions. A| Confocal microscopic analysis of the typical BBB basement membrane proteins laminin and perlecan, the pericyte marker PDGF receptor, and bright field microscopic analysis of the astrocyte marker GFAP in wild-type and Anxa1$^{-/-}$ mice; typical examples from *n*=3 mice per genotype, scale bars are 10 µm. **B|** Total expression of *p*-glycoprotein transporter MDR-1α was assessed on total cortical lysates from wild-type and Anxa1 null mice. Histograms indicate densitometric analysis of blots normalized to β-actin loading control and expressed as percentage of wild-type control (mean ± SEM; *n*=3 independent experiments, each with *n*=4 male samples/genotype). Student's *t*-test was performed showing no significant difference. **C|** Immunofluorescent analysis of claudin-5, ZO-1, occludin and VE-cadherin in cortex sections from wild-type and Anxa1 null mice reveal disordered localization of occludin and VE-cadherin but not evident disruption of Claudin-5 and ZO-1; typical images from *n*=6 mice per genotype, scale bar is 10 µm. **D|** Confocal microscopic analysis of occludin and VE-cadherin expression in isolated cortical capillaries from wild-type and AnxA1$^{-/-}$ mice *in vitro*. Arrows indicated points of altered or absence expression of the correspondent junctional protein. Nuclei are labeled with DAPI, endothelial cells were identified by immunofluorescent detection of CD31 (green), occludin and VE-cadherin are immunofluorescently labelled in red; typical images from *n*=3 independent preparations; scale bar is 10 µm. Panels A & D produced with help from Dr S. McArthur.

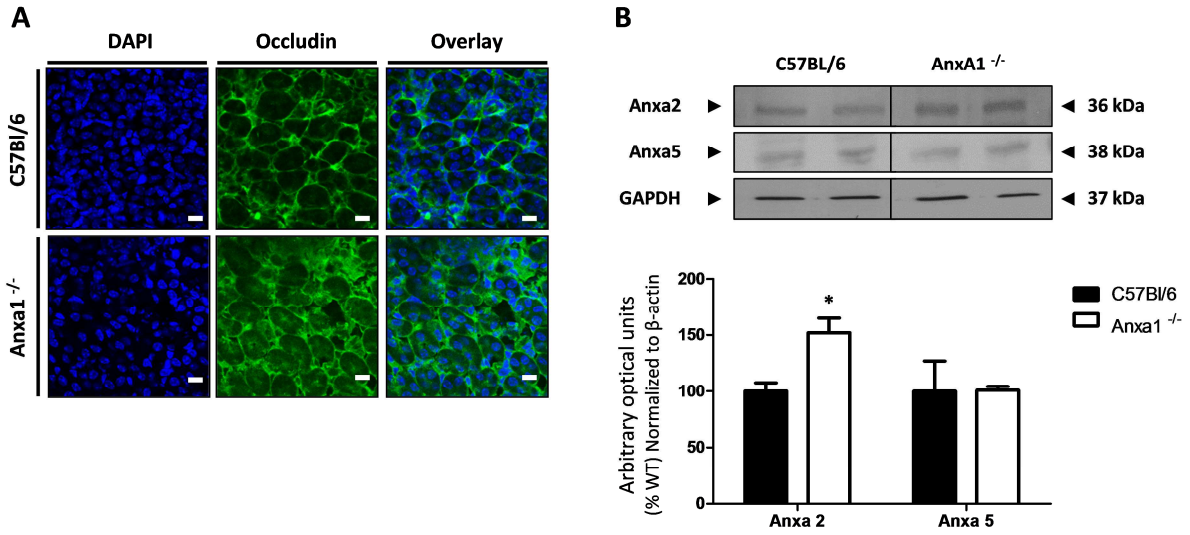

Figure 4.9 Occludin expression in cortical kidney and compensatory over-expression of Anxa2. A| Confocal microscopic analysis of occludin expression in the kidney from wild-type (C57Bl/6) and Anxa1 null mice; typical examples from *n*=3 mice per genotype. Scale bar: 20 µm. **B|** Typical western blot analysis of annexin A2 (Anxa2; A) and annexin A5 (Anxa5; B) expression in extracts from isolated cerebral capillaries of wild-type and AnxA1 null mice, alongside GAPDH loading controls; *n*=3 independent experiments, each with *n*=4 male samples/genotype. Histograms show densitometric analysis of 4 animals per genotype, expressed as mean ± SEM. Student's *t*-test between the two independent groups was performed. * $p<0.05$ *vs.* C57Bl/6.

Using paracellular permeability in vitro assay, we showed (Figure 4.11; Panel B) that cells bearing an antisense sequence against ANXA1 had significantly greater trans-endothelial permeability than untransfected or pRc/CMV empty plasmid-transfected hCMEC/D3 cells, while cells stably expressing increased levels of the protein showed a lower transcellular permeability, indicating the formation of a tighter cellular monolayer. Furthermore, no significant endocytosis of the fluorescent dextran was detected, indicating that differences in the permeability coefficients were mainly due to changes in the paracellular passage of substances (See Chapter 10, Section 10.7) as in part it has been already indicated by others (Plateel *et al.*, 1997).

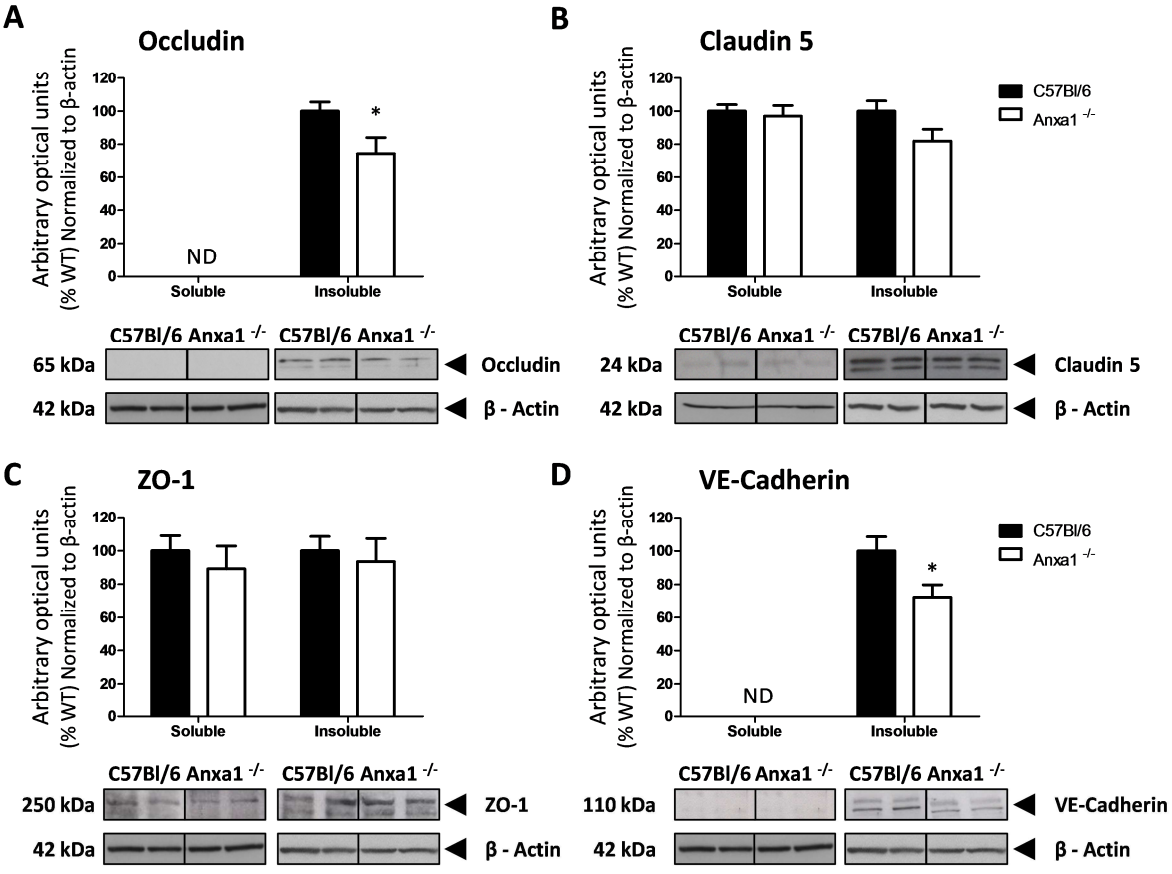

Figure 4.10 Lack of Anxa1 results in decreased expression of insoluble occludin and VE-cadherin. Typical western blot analysis of soluble and insoluble protein fractions from cortical extracts from wild-type and Anxa1 null mice. Analysis of the major tight-junctions components: **A|** occludin **B|** claudin-5 **C|** ZO-1 and one of the main adherens junctions **D|** VE-cadherin. Histograms indicate densitometric analysis of blots normalized to β-actin loading control and expressed as percentage of wild-type control (mean ± SEM; *n*=3 independent experiments, each with *n*=4 male samples/genotype). Student's *t*-test between the two independent groups was performed. * $p<0.05$ *vs.* wild-type control.

These findings were supported by studies showing a direct correlation between ANXA1 expression and TEER (Figure 4.11; Panel C): antisense cells showed a significantly reduced TEER compared to the other cell lines analysed.

To confirm the direct contribution of ANXA1 towards endothelial tightness, wild-type untransfected cells were incubated with a neutralizing monoclonal antibody against the protein (Pepinsky *et al.*, 1990), which significantly enhanced paracellular permeability (Figure 4.11; Panel D) of the monolayers.

Since paracellular permeability across the cerebral microvascular endothelium is affected by the correct arrangement and regulation of tight and adherens junction complexes, which we proved already to be disrupted in Anxa1 null mouse (Figure 4.9 and Figure 4.10), we first examined ANXA1 distribution on hCMEC/D3 cells polarized monolayers by electron microscopy. As evident from Figure 4.11, Panel F and also confirmed in Figure 4.12, ANXA1 is mainly localized in proximity of cell membrane, mostly at points of close cell-cell contact [electron-rich "kiss-points"; (Stevenson and Keon, 1998)]. Since this is where the junctional complexes contribute to the extremely low paracellular permeability of BMECs, we examined the distribution of occludin and VE-cadherin (the two proteins which showed major disruption in the murine brain sections) on hCMEC/D3 cell monolayers. A clear loss in normal peripheral organisation of occludin and VE-cadherin was evident in the antisense cells when compared with either mock-transfected or full-length ANXA1 stable cells (Figure 4.11; Panel E). Lower levels of expression for occludin, claudin-5 and VE-cadherin were also detected, as depicted by flow-cytometric analysis in Section 10.5 (Appendix), when stable clones were immunophenotyped. FL cells showed a stronger and more continuous staining, paralleled by increased levels of expression of the major adhesion molecules (Figure 10.2).

Direct interactions between ANXA1 and the major two junctional components, whose expression and organisation were found to be altered, was assessed by co-immunoprecipitation (Figure 4.11; Panel G). We could not detect direct interaction between ANXA1 and occludin, while we could detect some limited interaction with VE-cadherin, although the efficiency of the technique was not exceptional. This indicates that ANXA1 may affect junctional complexes by directly interacting with the most important component of the adherens junctions family (Wolburg and Lippoldt, 2002).

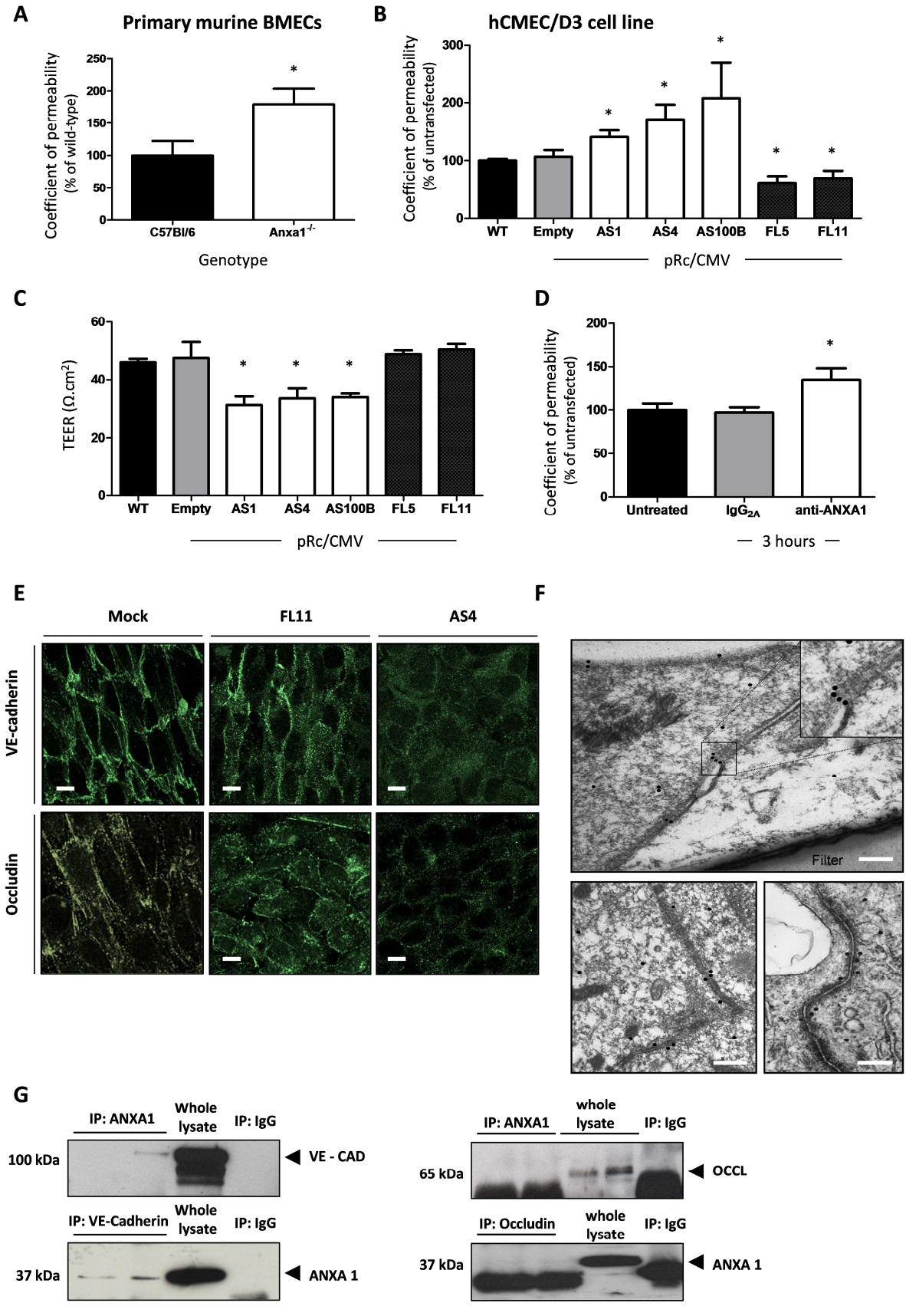
A
Primary murine BMECs
Coefficient of permeability (% of wild-type)
250
200
150
100
50
0
*
C57Bl/6
Anxa1-/-
Genotype
B
hCMEC/D3 cell line
Coefficient of permeability (% of untransfected)
300
200
100
0
*
WT
Empty
AS1
AS4
AS100B
FL5
FL11
pRc/CMV
C
TEER (Ω.cm2)
60
40
20
0
WT
Empty
AS1
AS4
AS100B
FL5
FL11
pRc/CMV
D
Coefficient of permeability (% of untransfected)
200
150
100
50
0
Untreated
IgG2A
anti-ANXA1
3 hours
E
Mock
FL11
AS4
VE-cadherin
Occludin
F
Filter
G
IP: ANXA1
Whole lysate
IP: IgG
100 kDa
VE - CAD
IP: VE-Cadherin
Whole lysate
IP: IgG
37 kDa
ANXA 1
IP: ANXA1
whole lysate
IP: IgG
65 kDa
OCCL
IP: Occludin
whole lysate
IP: IgG
37 kDa
ANXA 1

Figure 4.11 Annexin A1 modulates paracellular permeability *ex vivo* and *in vitro*. A| Paracellular permeability was conducted with 70 kDa FITC-dextran on primary cerebrovascular endothelial cells isolated from wild-type (C57Bl/6) and Anxa1 null mice (*n*=12/preparation) grown on transwells. Values are representative of four independent experiments, performed in duplicate, expressed as percentages of the wild-type control and represented as mean ± SEM. Student's *t*-test was conducted between the two independent groups. * $p<0.05$ *vs.* wild-type control. **B|** Relative paracellular permeability coefficients and **C|** TEER measured in wild-type hCMEC/D3 human brain microvascular endothelial cells WT or stable hCMEC/D3 clones transfected with a pRc/CMV plasmid alone (Empty) or containing an antisense ANXA1 sequence (AS1, AS4, AS100B) or full-length ANXA1 (FL5, FL11); data are representative of at least three independent experiments, performed in triplicate, expressed as mean ± SEM, * $p<0.05$ *vs.* WT clones. **D|** Paracellular permeability of wild-type hCMEC/D3 monolayers following exposure to a neutralizing anti-ANXA1 antibody at 20 µg/ml for 3 hours, compared to exposure to an irrelevant mouse IgG isotype control (30 µg/ml); data are representative of at least three independent experiments, performed in triplicate, expressed as mean ± SEM, * $p<0.05$. **E|** Confocal microscopic analysis of VE-cadherin and occludin in polarized monolayers of WT, FL11 and AS4 hCMEC/D3 clones reveals marked disturbances in both proteins in AS clones; typical example from *n*=3 independent preparations, scale bar is 10 µm. **F|** Electron microscopic analysis of immunogold labelling for ANXA1 in wild-type hCMEC/D3 cells grown as a polarized monolayer on a transwell polycarbonate filter reveals a striking localization of the protein at points of cell-cell contact. Top panel is a transverse image through the cell monolayer, bottom panels are vertical images of cell contacts; scale bar is 200 nm. Images were produced and provided by collaborator Dr. H. Christian (Oxford University). **G|** Co-immunoprecipitation analysis of ANXA1 and TJ and AJ interactions. Upper panel: 250 µg of total hCMEC/D3 cell extracts were immune-precipitated with 3 µg of a polyclonal anti-VE cadherin or 5 µg of monoclonal anti-ANXA1 and western blot was performed with either anti-ANXA1 antibody or anti-VE cadherin antibody, respectively; bottom panel: 3 µg monoclonal anti-occludin antibody or 5 µg monoclonal anti-ANXA1 was used to immune-precipitate complexes and western blot was performed with either anti-ANXA1 or anti-occludin antibody, respectively.

4.7.4 Annexin A1 profoundly affects the actin cytoskeleton

The stability of both tight and adherens junctions within the intercellular connections is determined to a large extent by the actin cytoskeleton, and in particular by interactions between the actin cytoskeleton and the cell membrane (Wittchen *et al.*, 1999). Since we have already shown that ANXA1 plays an important regulative role for hormone exocytosis at cytoskeletal level (McArthur *et al.*, 2009), we looked for differences within capillaries isolated from wild-type and Anxa1 null mice (Figure 4.12; Panel A).

Rhodamine-conjugated phalloidin staining revealed significant differences, as wild-type vessels were shown to possess dense bundles of longitudinally aligned actin fibres, in marked contrast to AnxA1$^{-/-}$ vessels, in which only sparse discontinuous actin fibres were evident. Moving to the *in vitro* model, we compared the phenotype of actin microfilaments within WT, FL and AS hCMEC/D3 cells.

Whilst wild-type and FL cells showed strong cortical actin staining, AS cells exhibited a distorted actin cytoskeleton, with a marked alteration in cell shape and an apparent loss in polarity (Figure 4.12; Panel B). Consequently, we concluded that ANXA1 must have a profound effect on the correct formation and organisation of the actin cytoskeleton.

To investigate how this can be accomplished, we investigated the association between ANXA1 and the actin cytoskeleton. Initial co-immunoprecipitation experiments identified a clear biochemical interaction between ANXA1 and β-actin (Figure 4.12; Panel C); this evidence was supported by confocal microscopic analysis of points of ANXA1/β-actin interaction in wild-type hCMEC/D3 cells, using a proximity ligation assay (PLA) as shown in Figure 4.12; Panel D. Clear co-localization of ANXA1 and β-actin was shown through this technique, mostly in proximity of cortical F-actin fibres, supporting once again the idea that ANXA1 may play an important role in formation/stabilisation of the actin cytoskeleton fibres.

In order to get a more definite up-regulation in ANXA1 expression, we produced lentiviral particles bearing the human ANXA1 coding sequence under the transcriptional control of the cytomegalovirus (CMV) promoter. These particles were used to infect exponentially growing hCMEC/D3 cells, which were further selected for puromycin resistance and for expression of ANXA1 by western blotting and flow cytometry analysis.

Figure 4.12, Panel E shows the major differences in terms of F actin between mock-infected and full length ANXA1-infected cells (IgG2A isotype control treated): thicker cortical actin cytoskeleton was evident in the ANXA1-infected cells, along with a more elongated conformation and close association between neighbouring cells, indicating that a higher constitutive expression of the protein contributes significantly to the formation of a more continuous and stable cortical cytoskeleton as well as positively affecting the polarity of the cellular monolayer. The higher level of F-actin at the cortical level was paralleled by an increased F/G β-actin ratio which was detected biochemically, as represented in Figure 4.12, Panel E. Differently from mock-transfected cells, full length ANXA1-treated cells were able to show a detectable level of ANXA1 in the insoluble fraction, likely to be directly interacting with insoluble F-actin fibres.

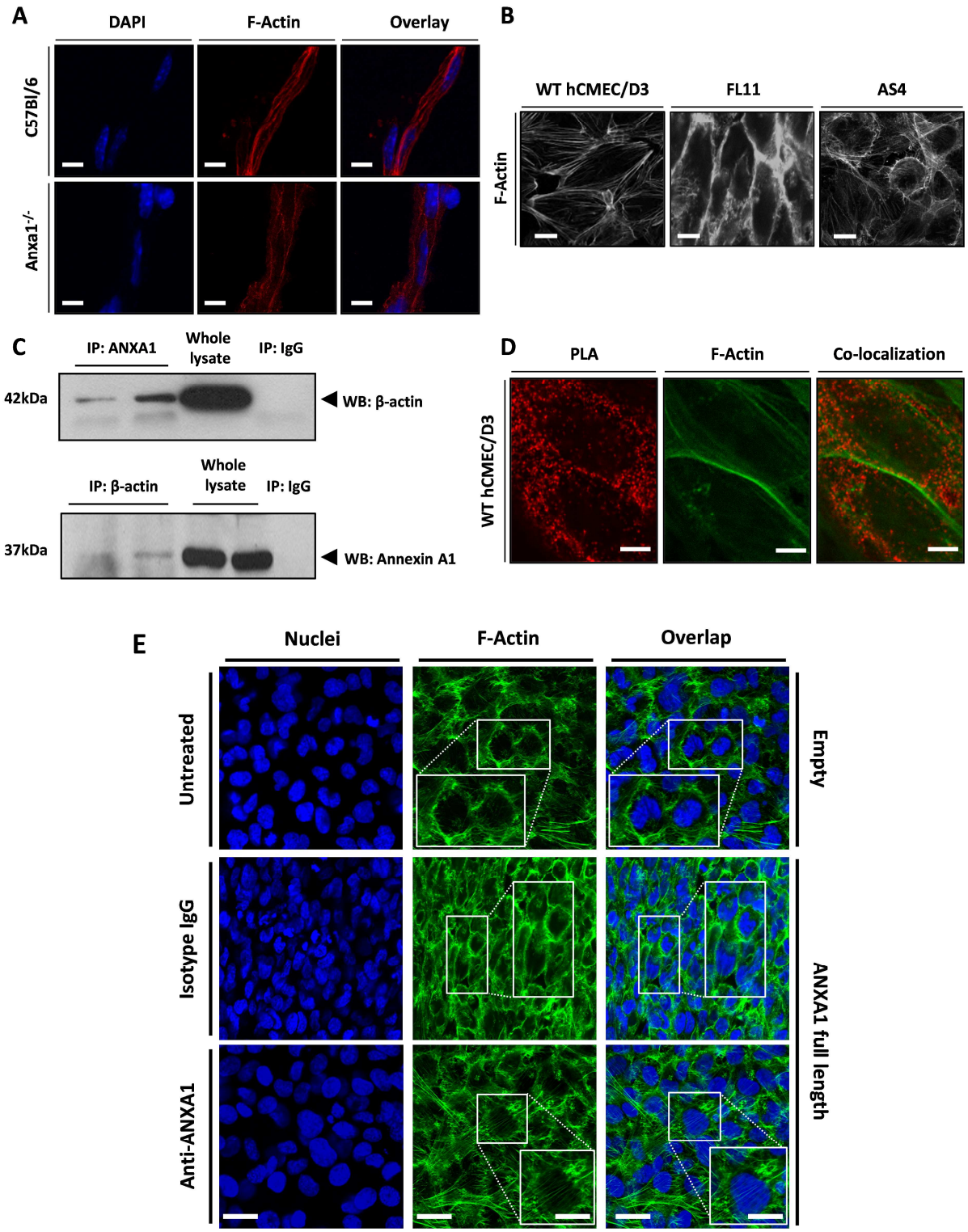
A
DAPI
F-Actin
Overlay
C57Bl/6
Anxa1-/-
B
WT hCMEC/D3
FL11
AS4
F-Actin
C
IP: ANXA1
Whole lysate
IP: IgG
42kDa
WB: β-actin
IP: β-actin
Whole lysate
IP: IgG
37kDa
WB: Annexin A1
D
PLA
F-Actin
Co-localization
WT hCMEC/D3
E
Nuclei
F-Actin
Overlap
Untreated
Isotype IgG
Anti-ANXA1
Empty
ANXA1 full length

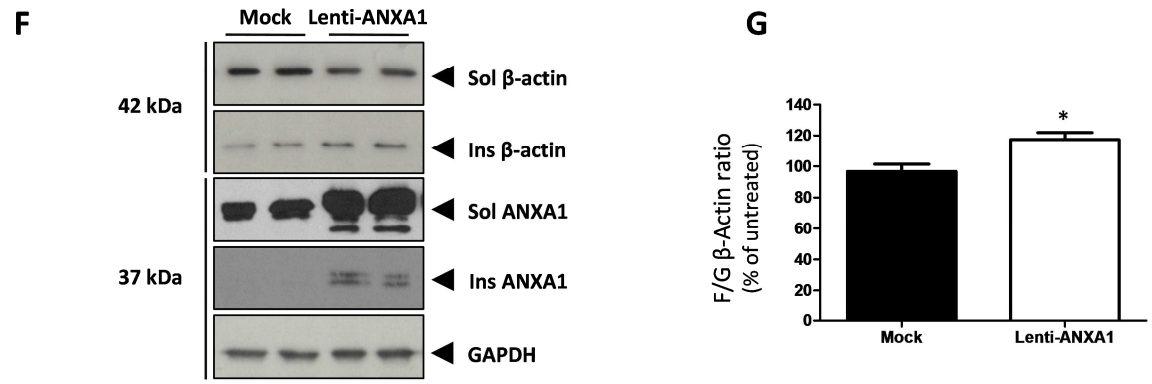

Figure 4.12 ANXA1 directly affects the formation and location of cytoskeletal actin microfilaments. **A|** Rhodamine-phalloidin staining of F-actin in isolated brain capillaries from WT and AnxA1$^{-/-}$ mice, identified by staining nuclei with DAPI (blue) and F-actin with rhodamine-phalloidin (red); typical images from *n*=3 independent preparations, scale bar is 10 µm. **B|** Rhodamine-phalloidin staining was performed on WT, FL11 and AS4 hCMEC/D3 clones monolayers, revealing a disorganized cytoskeletal structure in AS4 cells; scale bar is 10 µm. **C|** Co-immunoprecipitation analysis of ANXA1 and β-actin interaction. Top panel: 250 µg of total cell extracts were immuno-precipitated with 2 µg of an anti-ANXA1 antibody and western blot was performed with an anti-β-actin antibody. Bottom panel: 250 µg of total cell extracts were immune-precipitated with 5 µg of a monoclonal anti-β-actin antibody and western blot was performed with anti-ANXA1 antibody. **D|** Confocal microscopic analysis of ANXA1 and β-actin co-localization in WT hCMEC/D3 cell monolayers determined by use of the proximity ligation assay (PLA, red), and F-actin identified by Alexa 488-conjugated phalloidin staining (green) in WT hCMEC/D3 cells. Images are from a 400 nm optical section; scale bar is 5 µm. **E|** Confocal microscopic analysis of F-actin in mock transfected and full length ANXA1 infected hCMEC/D3 cell monolayers following exposure to a neutralizing anti-ANXA1 antibody at 20 µg/ml for 3 hours, or to an irrelevant mouse IgG isotype control (30 µg/ml); data are representative of at least three independent experiments. Scale bars 5 µm, while inset scale bars 7.5 µm. **F|** Biochemical analysis of G (soluble) and F (insoluble) β-actin in hCMEC/D3 cells mock- or full length ANXA1-infected. Histograms represent analysis of three different experiments, performed in triplicate; data are presented as mean ± SEM. Student's t-test between the two independent groups was performed with * indicating $p<0.05$ *vs.* untreated. Panels A, B and D were produced together with Dr. S McArthur.

Treating these cells with a monoclonal antibody anti-ANXA1 (the same one used in Figure 4.11; Panel D) resulted in a loss of thickness at the cortical level, with the appearance of more disorganized stress fibres throughout the cytosol.

Overall, these findings confirmed that ANXA1 may provide its role both through an endogenous and an exogenous role, as already suggested on Figure 4.11, Panel A-D by overexpressing total ANXA1 or blocking the action of the released molecule.

4.7.5 *In vivo* and *in vitro* BBB integrity restoration by recombinant ANXA1

In previous reports we have shown the potential of recombinant human ANXA1 (rANXA1) in significantly rescuing aberrant phenotypes when given exogenously (Solito *et al.*, 2000; McArthur *et al.*, 2009). Therefore, we investigated whether a similar action of ANXA1 could be identified in the restoration of BBB function both *in vivo* and *in vitro*. Intravenous administration of rANXA1 (0.67 μg/kg body weight) to Anxa1 null mice was chosen on the basis of previous studies (de Coupade *et al.*, 2001); we observed that 24 hours after the *i.v.* administration of ANXA1 and of Evans blue dye (1 hour prior assessment) significantly reduced the degree of tracer extravasation into the brain, effectively rescuing the enhanced BBB leakage (Figure 4.13; Panel A). This phenomenon was also reproduced by the treatment of AnxA1$^{-/-}$ mouse brain microvascular endothelial primary cultures and AS hCMEC/D3 clones with human recombinant ANXA1 at 20 μg/ml, where the protein was able to significantly reduce paracellular permeability towards that of untransfected cells (Figure 4.13; Panel B and C), closely correlating with our *in vivo* data. Interestingly, treatment of wild-type hCMEC/D3 cells with ANXA1 also produced a decrease in the basal permeability (Figure 4.13; Panel C), indicating that a potentiation of basal tightness is also possible.

To further investigate the mechanism whereby rANXA1 could rescue the permeability deficit seen in AnxA1$^{-/-}$ mice or in AS clones when given exogenously, we analysed the role of the main formyl peptide receptor (FPR) family member, FPR2, which we, and others, have previously shown to mediate the actions of ANXA1 in different cellular contexts (Solito *et al.*, 2000; Perretti, 2003). First we confirmed that hCMEC/D3 cells expressed FPR2 (and FPR1) by using flow cytometry, although their expression at the endothelial levels has been already reported in different species (Mou *et al.*, 2012); the results are shown in Figure 4.13, Panel E. To test FPR2 involvement we used WRW4 (used at 5 μM concentration), a very specific FPR2 antagonist. WRW4 had an effect when administered before ANXA1; two-way ANOVA identified significant (p<0.05) interaction between WRW4 and ANXA1. Overall, this may indicate that FPR2 is occupied by exogenously administered ANXA1, but also may be interested in the action brought by ANXA1 molecules constantly released by the cells, which therefore is able to mediate a basal autocrine/paracrine action and in this way to contribute to the basal paracellular permeability.

Considering that the levels of ANXA1 released by wild-type, AS and FL cell monolayers follow the intracellular relative expression (*i.e.* AS clones released less ANXA1 while FL more compared to WT; see Table 4.1), this may give another potential mechanism to explain the differences in terms of paracellular permeability that were observed between clones.

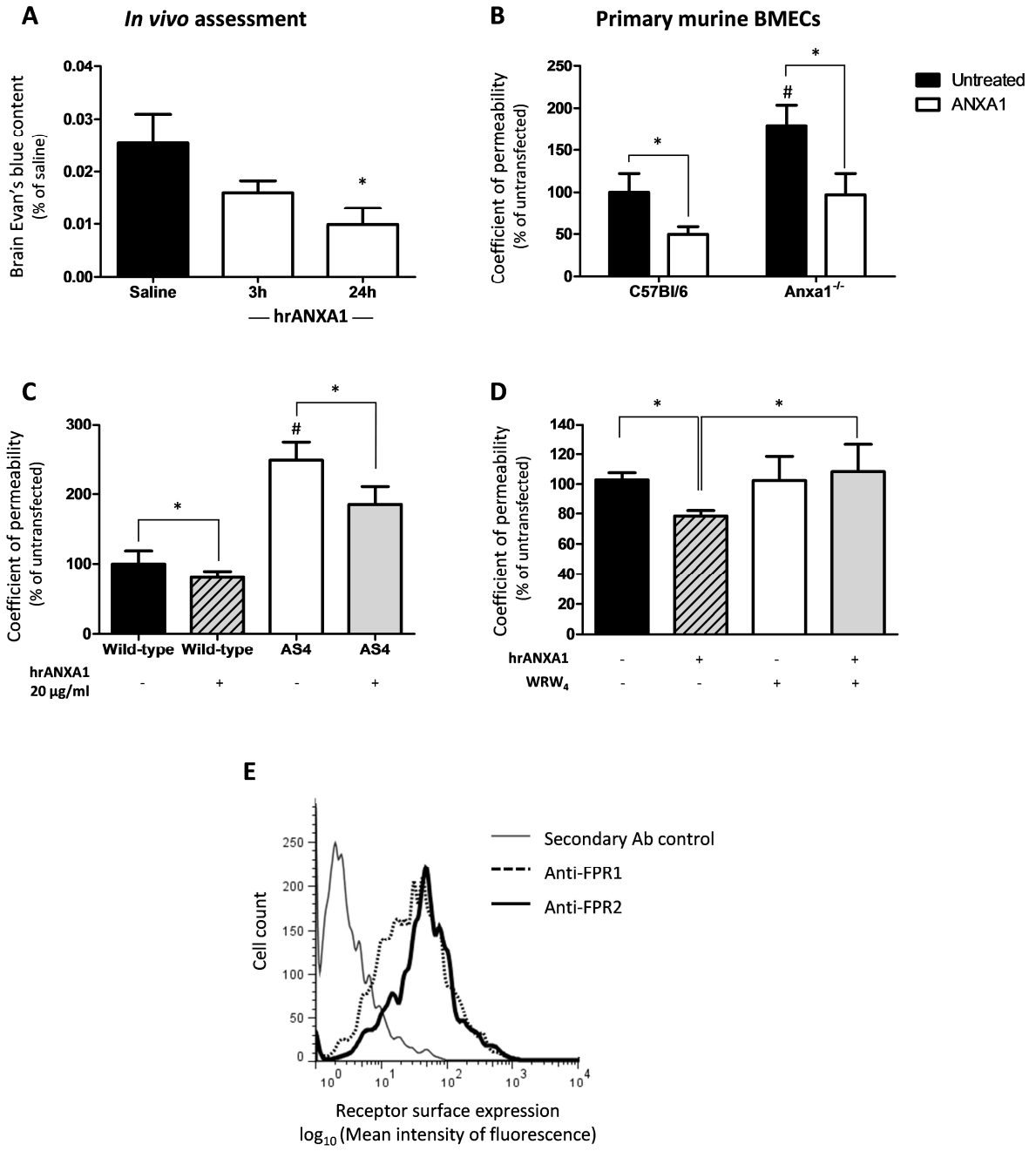

Figure 4.13 Exogenous ANXA1 restores BBB integrity *in vivo* and *in vitro*. A| Anxa1$^{-/-}$ mice (*n*=6) were pre-treated intravenously with 0.67 µg/kg body weight of rANXA1 in saline and after 3 or 24 hours were further injected with 100 µl 2% Evans blue in saline. Data are expressed as mean ± SEM. One-way ANOVA was conducted and followed by Tukey's range *post-hoc* test; * indicates $p<0.05$ *vs.* saline control and it was considered as significant. **B|** Administration of 20 µg/ml rANXA1 3 hours prior to analysis of significantly reduced permeability in primary brain endothelial cells isolated from Anxa1 null mice and littermate controls. One-way ANOVA was conducted and followed by Tukey's range *post-hoc* test. Data are representative of at least three independent experiments, performed in triplicate, expressed as mean ± SEM. * $p<0.05$; # $p<0.05$ *vs.* untreated wild-type. **C|** Administration of 20 µg/ml human recombinant ANXA1 3 hours prior to analysis significantly reduced paracellular permeability in WT hCMEC/D3 cells, and significantly improved the permeability in AS clones towards WT; data are representative of at least three independent experiments, performed in triplicate, expressed as mean ± SEM. One-way ANOVA was conducted and followed by Tukey's range *post-hoc* test. * $p<0.05$ *vs.* untreated wild-type and was considered as significant. **D|** Administration of the FPR2 antagonist WRW_4 at 5 µM 10 minutes prior to treatment with 20 µg/ml ANXA1 for 3 hours blocked the effect of ANXA1 on paracellular permeability. Data are representative of at least three independent experiments, performed in duplicate, expressed as mean ± SEM. Two-way ANOVA was performed and followed by Bonferroni *post-hoc* test, in which * indicates $p<0.05$ and was considered as significant. **E|** Expression of FPR1 and FPR2 in untransfected hCMEC/D3 cells. Representative example of flow cytometric analysis of FPR1 and FPR2 expression in untransfected hCMEC/D3 cells; at least 10000 events were analysed after proper gating; histograms represent one of 6 independent experiments.

	Untreated	**CMV-empty**	**Antisense AS4**	**Full length ANXA1 FL11**
ANXA1 in the medium (ng/ml)	4.422 ± 0.087	4.563 ± 0.095	3.33 ± 0.186 *	5.82 ± 0.427 *

Table 4.1 hCMEC/D3 clones release different amounts of ANXA1 into the cell culture medium. Secreted ANXA1 was measured by ELISA on medium collected from 100% confluent monolayers incubated for 24 hours with fresh medium but without incubation with stimuli. One-way ANOVA was conducted and followed by Tukey's range *post-hoc* test. Data are representative of at least three independent experiments, performed in triplicate, expressed as mean ± SEM. One-way ANOVA was performed and followed by Dunnett *post-hoc* test against a reference group (Untreated), in which * indicates $p<0.05$ and was considered as significant.

Following the identification of endogenous ANXA1 as a stabilizer for both fibrillar actin and consequently cell polarity, we assessed the effects of exogenous hrANXA1 (20 µg/ml; 3 or 24 hours treatment) on the actin cytoskeleton on wild-type hCMEC/D3 monolayers (Figure 4.14). Interestingly, the cortical actin cytoskeleton showed increased thickness and number of fibrillar actin fibres, while the few stress fibres present throughout the cell body showed high polarity, following the longitudinal cell axis. Endogenous ANXA1 staining was identified throughout the entire cytosol, but particularly it defined a continuous sub-membranous ring that strongly co-localized with the cortical actin fibres (white arrows, Figure 4.14; Panel A).

Interestingly, the microscopic results were paralleled by biochemical analysis of the F/G actin ratio in the hCMEC/D3 cells treated with hrANXA1 (Figure 4.14; Panel B): actin polymerization appeared to be improved by the exogenous stimulus, replicating findings that we have already reported in a different system (McArthur *et al.*, 2009).

Since exogenous hrANXA1 showed a direct effect on cortical actin fibres, we assessed the consequent effect on cell junction component expression after stimulation of wild-type hCMEC/D3. All the major tight- and adherens-junction proteins analysed (occludin, claudin-5, ZO-1 and VE-cadherin) showed increased expression at membrane-associated level (insoluble fraction) as evident from , Panel C, which could be closely linked structurally to improved cortical F-actin driven by the treatment and functionally to the increased tightness observed in terms of paracellular permeability (Figure 4.12; Panel C).

Taking into account the profound effects that exogenous ANXA1 showed at the level of the actin cytoskeleton, we hypothesised that the rescue effect shown on the Anxa1 null mice and on BBB endothelium may be also mediated by targeting actin. Primary wild-type endothelial cells stimulated with hrANXA1 for 3 hours (20 µg/ml) showed an improved cortical actin cytoskeleton, closely resembling the results obtained with the human cell line hCMEC/D3 (Figure 4.15; Panel A). Anxa1 null mice primary endothelial cells showed a disrupted actin cytoskeleton, rich in disorganised stress-fibres and devoid of continuous membrane-associated actin fibres. Treatment with hrANXA1 for 3 hours improved the disrupted phenotype, strongly reducing the presence of stress-fibres in favour of cortical F-actin filaments.

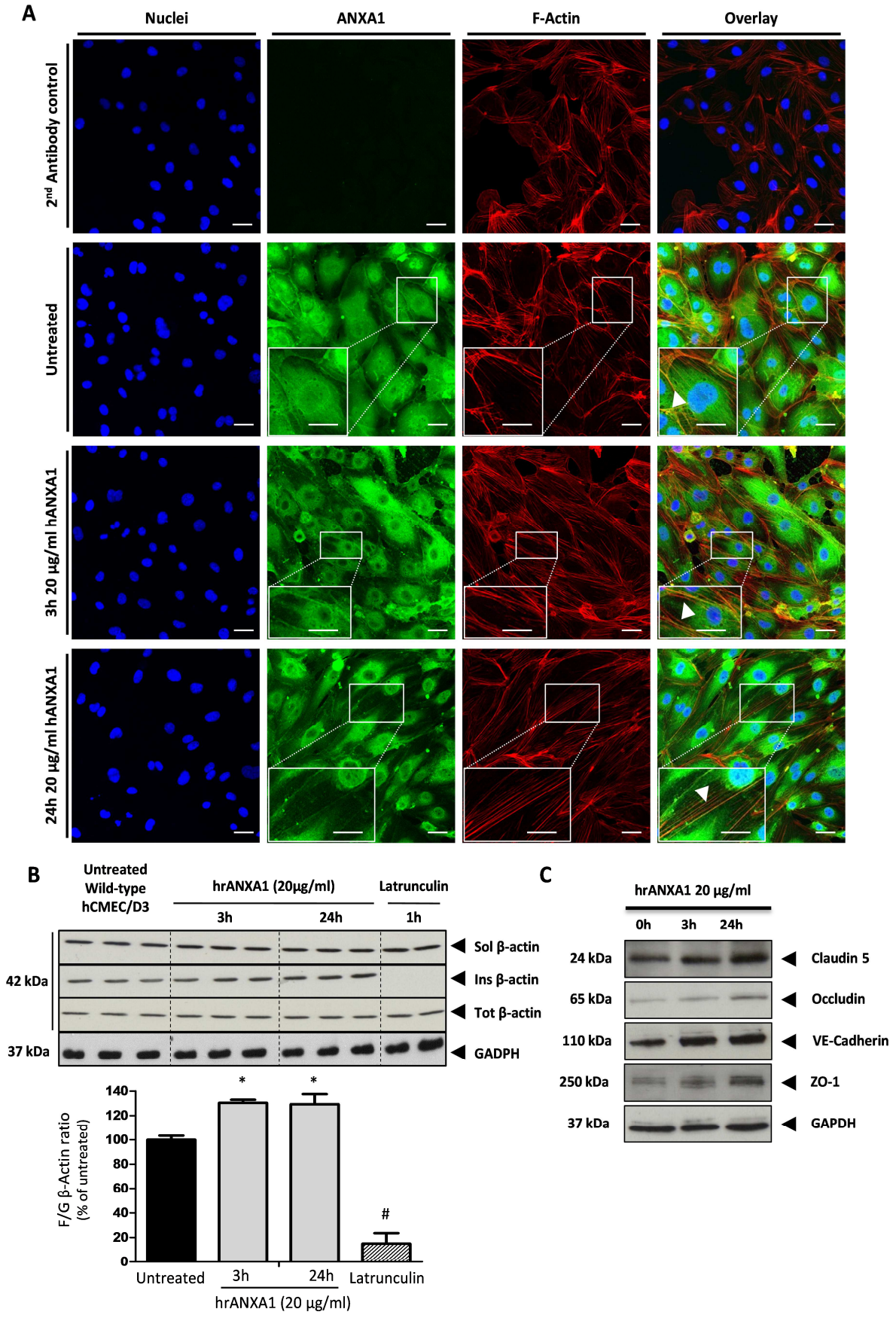
A
Nuclei
ANXA1
F-Actin
Overlay
2nd Antibody control
Untreated
3h 20 µg/ml hANXA1
24h 20 µg/ml hANXA1
B
Untreated Wild-type hCMEC/D3
hrANXA1 (20µg/ml)
Latrunculin
3h
24h
1h
42 kDa
37 kDa
Sol β-actin
Ins β-actin
Tot β-actin
GADPH
F/G β-Actin ratio (% of untreated)
Untreated
3h
24h
Latrunculin
hrANXA1 (20 µg/ml)
C
hrANXA1 20 µg/ml
0h
3h
24h
24 kDa
65 kDa
110 kDa
250 kDa
37 kDa
Claudin 5
Occludin
VE-Cadherin
ZO-1
GAPDH

Figure 4.14 Effects of ANXA1 on wild-type hCMEC/D3 on actin cytoskeleton polymerization and cell-cell junctions. A| Confocal microscopic analysis of ANXA1 and F-actin co-localization in WT hCMEC/D3 cell monolayers stimulated with human recombinant ANXA1 (20 μg/ml) for 3 hours and 24 hours. ANXA1 was detected by incubation with a rabbit-polyclonal antibody and with Alexa 488-conjugated anti-rabbit IgG secondary antibody, while F-actin was detected by rhodamine-phalloidin staining. White arrows indicate regions of clear co-localization. Scale bars are 5 μm. **B|** Biochemical analysis of G (soluble) and F (insoluble) β-actin in hCMEC/D3 cells treated with 20 μg/ml hrANXA1 for 3 or 24 hours, or with 10 μM of the actin-depolymerizing agent latrunculin (as positive control for low F/G β-actin ratio) for 1 hour. Histograms represent analysis of three different experiments, performed in triplicate; data are presented as mean ± SEM. One-way ANOVA was performed and followed by Bonferroni *post-hoc* test, in which * indicates $p<0.05$ and was considered as significant. Student's *t*-test between the two independent groups (untreated and latrunculin) was performed with # indicating $p<0.05$ *vs.* untreated. **C|** Administration of 20 μg/ml rANXA1 to wild-type hCMEC/D3 cells induces an upregulation of membrane associated (insoluble) occludin and VE-cadherin expression as measured by western blot. Results are representative of three independent experiments.

The direct effect of exogenous hrANXA1 on the actin cytoskeleton organisation was also confirmed on hCMEC/D3 cells with a constitutive lower expression of ANXA1. In order to obtain more definite reduction in the protein expression compared to what was achieved by stable transfection (Figure 4.11), we opted for shRNA technology, by producing lentiviral particles bearing a specific shRNA sequence directed towards a portion of the ANXA1 mRNA. We had the chance to test 5 different human ANXA1-specific shRNA (named 1257, 1258, 1259, 1260 and 1261). We concluded that shRNA 1258 and 1259 did not produce a significant reduction in ANXA1 expression (data not shown), while the others did produce a considerable reduction, with the simultaneous infection with two different shRNA lentiviral particles producing the best results (Figure 4.15; Panel B). We then focused on hCMEC/D3 cells infected stably with 1257+1261 and observed the effect of exogenous hrANXA1 on actin cytoskeleton (3 and 24 hours treatment; 20 μg/ml ANXA1). Similarly to what we observed in AS stably transfected cells (Figure 4.12), actin cytoskeleton is heavily disrupted along with cell polarity and correct juxtaposition with the neighbouring cells (Figure 4.15, Panel C). Treatment with hrANXA1 partially improves the phenotype in a time-dependent fashion, by increasing the amount of F-actin at the cortical level, reducing the amount of unorganised stress fibres present throughout the cytosol.

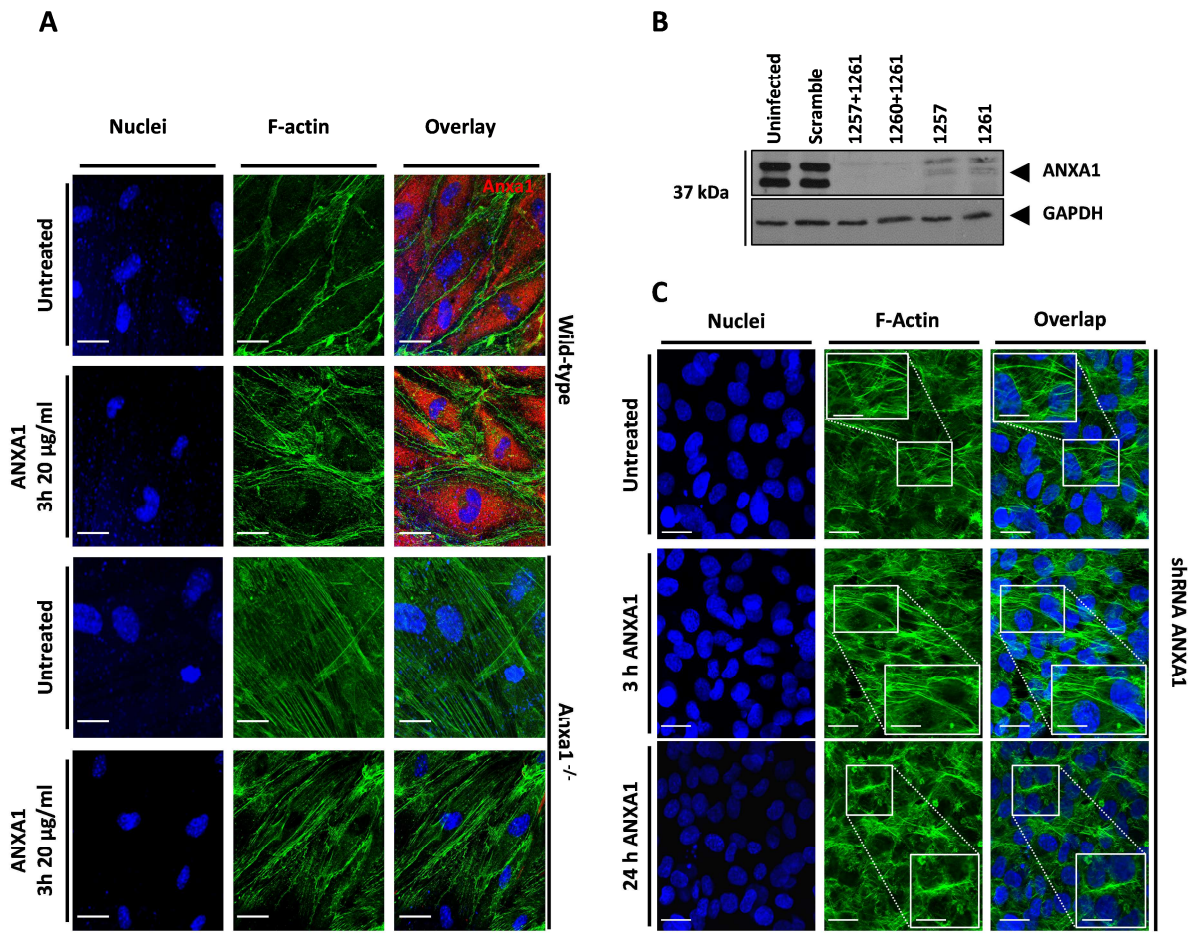

Figure 4.15 Effects of hrANXA1 on wild-type and Anxa1 null primary endothelial cultures and shRNA infected cells. A| Confocal microscopic analysis of ANXA1 and F-actin co-localization in primary endothelial monolayers derived from wild-type and Anxa1 null mice. The monolayers were stimulated with hrANXA1 (20 µg/ml) for 3 hours. ANXA1 was detected by incubation with a rabbit-polyclonal antibody (Zymed; Invitrogen, UK) and with Alexa 594-conjugated anti-rabbit IgG secondary antibody, while F-actin was detected by Alexa 488-conjugated phalloidin staining. Scale bars are 5 µm. **B|** Evaluation of ANXA1 expression on hCMEC/D3 cells infected with different types and combinations of shRNA-bearing lentiviral particles and selected for stable genomic integration by culturing under puromycin selective agent. ANXA1 expression was evaluated by Western blotting. 10 µg of total lysate extraction were loaded/lane and run as described in the general methods. Nitrocellulose membranes were probed for ANXA1 (in-house rabbit polyclonal anti-ANXA1) and subsequently stripped and re-probed for GAPDH as internal loading control. **C|** Confocal microscopic analysis of F-actin localization in hCMEC/D3 stably expressing 1257+1261 shRNA sequences directed towards ANXA1 messenger RNA. The cell monolayers were stimulated with human recombinant ANXA1 (20 µg/ml) for 3 and 24 hours. F-actin was detected by Alexa488-conjugated phalloidin staining. Scale bars are 5 µm and 7.5 µm (inset).

4.7.6 Mechanistic involvement of ANXA1 in regulating the actin cytoskeleton

So far we have described the direct involvement of ANXA1 as a fundamental regulator of paracellular permeability. This role appears to be exerted both via an endogenous (direct interaction of the protein with β-actin and the cortical actin cytoskeleton) and an autocrine/paracrine mechanism (constitutive release of ANXA1 which signals through FPR2 receptors, ultimately affecting the organisation of the actin microfilaments and overall their shape, polarity and location in regards to the neighbouring cells). At this stage, we sought to identify the molecular mechanism(s) whereby the two pathways could be reconciled. Firstly, we observed that treating wild-type hCMEC/D3 monolayers for 24 hours with 20 μg/ml hrANXA1 induced a marked increase in intracellular ANXA1 (Figure 4.16; Panel A), a result supported by previous studies identifying a similar effect of the bioactive N-terminal peptide towards total intracellular ANXA1 (Rescher *et al.*, 2002). This self-potentiating action of ANXA1 is important but not sufficient to explain the rescuing effect of exogenous hrANXA1 seen *in vivo* and *in vitro* (Figure 4.13). Therefore, we investigated which signalling pathways could have been triggered by ANXA1 upon binding and activation of its main receptor FPR2. As extensively described (Section 4.5.4.1.2), small GTPases have an essential role in the control and regulation of the actin cytoskeleton, of the tight junctions formation and overall of the paracellular permeability; moreover, we have already shown that ANXA1 is able to regulate RhoA-dependent pathway in endocrine cells (McArthur *et al.*, 2009). Therefore, we measured the activity of the major small GTPases proteins in the wild-type hCMEC/D3 cells and in ANXA1 antisense clones (Figure 4.16; Panels B and C). Interestingly, whilst levels of active RhoA were low in wild-type cells, activity was markedly increased in antisense clones. Importantly, this activity was significantly reduced by treatment with hrANXA1 (20 μg/ml, 3 hours), indicating that the absence of endogenous ANXA1 permits excessive activity of RhoA, a factor known to trigger enhanced paracellular permeability via increased actin cytoskeleton instability (*i.e.* stress fibres formation and destabilization of the cortical F-actin ring). Moreover, we could also detect an increased level of basal Rac1 activity in WT hCMEC/D3 compared to AS cells, partially restored by ANXA1 treatment. Basal activity levels of Rac1 are well known to have a positive effect on paracellular permeability through an effect directed towards the cortical actin cytoskeleton, which sustains cell-cell junctions maintenance (Wojciak-Stothard *et al.*, 2001; Komarova and Malik, 2010).

The third GTPase analysed, namely Cdc42, also showed a different level of activity in cells with lower endogenous ANXA1 levels; since its involvement in terms of BBB paracellular permeability definition and maintenance is less understood and most probably not as important as it is known for RhoA and Rac1, we did not investigate further. Therefore, the treatment of either AnxA1 null mice or ANXA1 antisense hCMEC/D3 clones with hrANXA1 limits RhoA and improves Rac1 activities, stabilizing the actin cytoskeleton towards the formation of healthy tight junctions, which ensure appropriate BBB integrity.

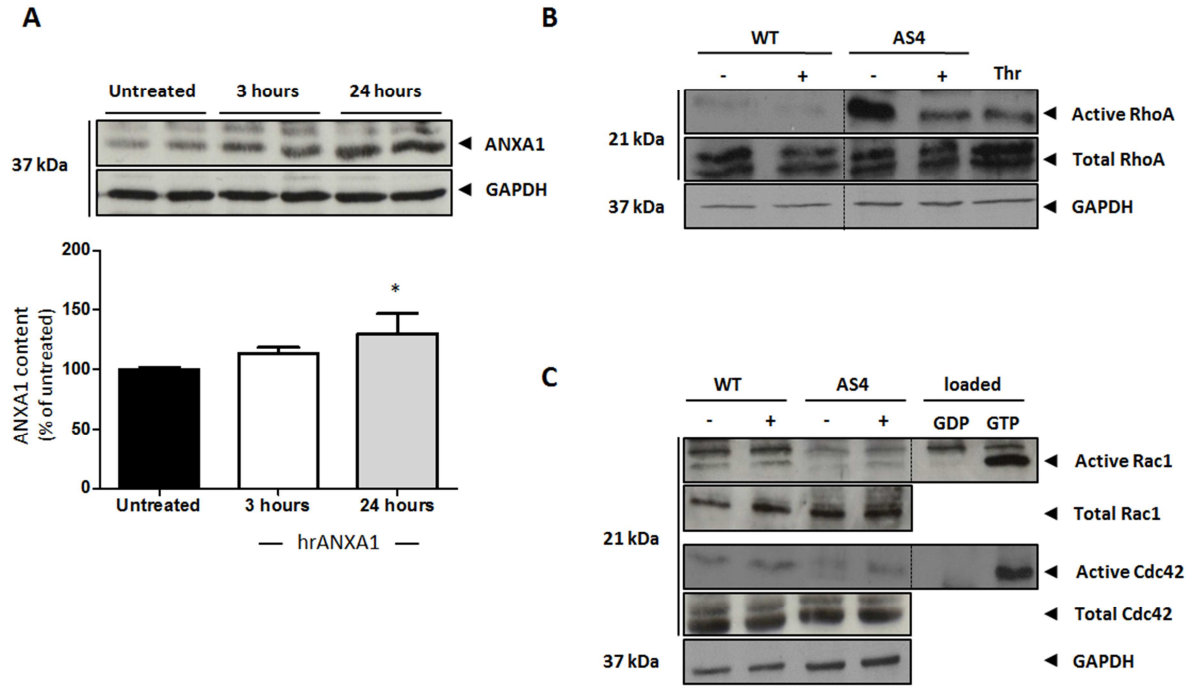

Figure 4.16 Exogenous ANXA1 both enhances endogenous ANXA1 and inhibits activity of the RhoA small GTPase in hCMEC/D3 cells. A| Treatment of wild-type hCMEC/D3 cells with 20 µg/ml hrANXA1 for 3 or 24 hours induces upregulation in endogenous ANXA1 expression, as indicated in the representative Western blot (upper panel) and in the densitometric analysis (lower panel); data are representative of at least three different experiments, performed in duplicate, and are presented as mean ± SEM. One-way ANOVA was performed and followed by Bonferroni *post-hoc* test, in which * indicates $p<0.05$ *vs.* untreated. **B|** hCMEC/D3 cells transfected with an antisense sequence to ANXA1 exhibit constitutively raised activity of the small GTPase RhoA, an effect that can be reversed by treatment with 20 µg/ml hrANXA1 for 3 hours. Thrombin (Thr; used 1 IU/ml in serum-free medium for 8 minutes) was used as positive control. Data are representative of $n=3$ independent experiments. **C|** hCMEC/D3 cells transfected with antisense sequence to ANXA1 exhibit constitutively decreased activity of Rac1 and Cdc42, an effect that can be reversed by the treatment with hrANXA1 for 3 hours. Separate cell lysates were loaded for 30 minutes at 37°C with either GTPγS or GDP (provided with the assay kit) in order to have positive and negative internal controls. These were run in parallel with the unknown samples for the isolation and detection steps and finally visualised to confirm successful procedure. GAPDH was chosen as loading internal control. Data for Rac1 are representative of at least three independent experiments, while Cdc42 has been studied only once, therefore these data should be defined as only preliminary.

4.8 Discussion

The BBB plays a vital role in at the interface between the periphery and the CNS, acting as a physical barrier, interpreting and decoding the stimuli that travel through the blood, which indicate the overall state of the entire body. The physiological mechanisms regulating the BBB permeability are not fully clear yet; that is why there is increasing interest in defining and mechanistically explaining how the peculiar physiological properties of the BBB are maintained, so that the main protagonists in this process can be possibly exploited as therapeutic targets under pathological conditions (Komarova and Malik, 2010).

4.8.1 Annexin A1 as a new player in the definition of BBB properties

Our *in vivo* data showed that BBB permeability is significantly greater in Anxa1$^{-/-}$ mice than in wild-type controls; this defect in basal paracellular permeability could be reversed by 24 hours intravenous treatment with human recombinant ANXA1. Interestingly, the 10-fold increase in paracellular permeability did not result in oedema formation (Figure 4.7, Panel D) or in any symptomatic manifestation, indicating that the mechanisms dedicated to drain the CSF back into the blood stream [like the arachnoid villi in the sagittal sinus of the dura mater (Yamashima 1986) or the aquaporins in the astrocytic end-feet (Filippidis et al., 2011)] are able to compensate the augmented fluid passage, protecting the entire brain from building noxious pressure. Importantly, the defect caused by the lack of Anxa1 seemed to affect only the endothelium of the BBB, without causing any morphological defect on the main other components of this complex structure (Figure 4.8).

Complementary evidence obtained from the human cell line hCMEC/D3 showed ANXA1 to be distributed distinctively at the sub-membranous level (Figure 4.11, Panel F; Figure 4.14, Panel A). ANXA1 expression was shown to inversely correlate with paracellular permeability to 70 kDa fluorescent dextran, since ANXA1 positively correlated with cell-to-cell junction proteins (Figure 4.11), in particular occludin and VE-cadherin, as already shown in our animal model. Having confirmed a strong ANXA1 expression in the choroid plexus epithelial cells (see Chapter 2 and Chapter 5) may contribute to support this novel idea, since they also exhibit highly organised tight junctions and may benefit from this novel ANXA1 role.

Overall, these novel findings propose ANXA1 as a new fundamental endogenous component of the system that regulates and maintains BBB permeability, and highlights its role in the physiology of cerebral microvasculature. Moreover, the ability to restore an altered phenotype shown by hrANXA1 both *in vivo* and *in vitro* intriguingly gives this protein high potential to be therapeutically exploited.

The experiments performed to unravel this new role for ANXA1 at the BBB endothelium level all revealed the important effects on the stability of the actin cytoskeleton, which affects consequently the cellular polarity and tight and adherens junction formation/maintenance. We have identified a number of pathways through which ANXA1 is able to regulate the conformation of the cytoskeleton: endogenous ANXA1 is able to directly interact with β-actin, while released/exogenous ANXA1 influences the complex small GTPases signalling pathways involved in the cytoskeleton dynamics.

4.8.1.1 Endogenous Annexin A1 targets the actin cytoskeleton

The results presented in this chapter have stressed the importance of ANXA1-actin interaction to maintain BMECs peculiar tightness. The idea of ANXA1 directly interacting with actin and the cytoskeleton has been proposed for several years to explain many of the functions that ANXA1 mediates (Schlaepfer and Haigler, 1987; Alvarez-Martinez *et al.*, 1996; Patel *et al.*, 2011). However, evidence for ANXA1 and F- or G-actin interaction was almost exclusively obtained from cell-free *in vitro* biochemical assays, a factor that reduced the applicability and reliability of these findings.

In this chapter, we were able to detect direct binding of ANXA1 and β-actin (Figure 4.12) in a human cell line model. Although Annexin A1 has been indicated as strong F-actin binding protein (Cote *et al.*, 2010), in our model this interaction appeared mainly, but not exclusively, to involve cytosolic rather than fibrillar actin as demonstrated by several biochemical approaches and by microscopy. In fact, only a percentage of the points of co-localisation visualised by the proximity ligation assay were also co-localising with actin microfilaments forming the cytoskeleton, while the majority seemed to be scattered throughout the cytosol, always in the vicinity of regions where the F-actin fibres were

abundant. Moreover, we were able to detect ANXA1 only in the soluble fraction of total protein extracts (Figure 4.12; Panel F), therefore indicating that the interaction with insoluble actin fibres was not normally detectable or it was not enough stable under physiological conditions. We could only detect ANXA1 in the insoluble fraction in hCMEC/D3 overexpressing ANXA1 (Figure 4.12; Panel F), letting us speculate that only a considerable increase in protein expression can result in the protein being able to stably interact with the actin microfilaments, as already shown elsewhere *in vitro*. Given that ANXA1 appeared to bind predominantly to soluble G-actin, it was tempting to speculate on a potential role as an endogenous effector specialised in stabilizing actin monomers and oligomers prior to addition to the growing cytoskeleton (Lee and Dominguez, 2010). Currently, we know that the assembly of stable actin dimers or trimers is the rate limiting step in the formation of actin fibres, so to overcome the kinetic hurdle, cells are provided with a broad set of actin-nucleating protein complexes called actin nucleators, which are formed by various components (nucleation promoting factors; NPFs) and present enzymatic and chaperone-like activity favouring actin filaments formation (Firat-Karalar and Welch, 2011). Interestingly, ANXA2 has been shown to be an important nucleating protein for endosomal transport and trafficking (Morel *et al.*, 2009); this may certainly reinforce the possibility that also ANXA1 may play a similar role at the level of the BBB endothelium. In support of the involvement of ANXA1 in the regulation of actin filaments formation, previous work showed this protein to directly interact with profilin, another member of the huge family of ABPs (Alvarez-Martinez *et al.*, 1996; Alvarez-Martinez *et al.*, 1997).

Additionally, we should also remember that ANXA1 is a strong Ca^{2+}-dependent binding protein of negatively charged phospholipids, which are abundant in the inner membrane leaflet of live cells and in the external one of apoptotic cells. Patel *et al.* (Patel *et al.*, 2011) demonstrated that sub-membrane ANXA1 is able to link actin microfilaments to the plasma membrane in order to generate enough support and strength for membrane protrusions and phagocytic cup formation. We did identify ANXA1 to be present most prominently at the same sub-cellular level (Figure 4.11; Panel D), therefore it is highly possible that the endogenous population of the protein could also act as an anchor for the cytoskeleton, so that it can be linked and maintained at the sub-membranous level, where it serves as an important scaffolding structure for the cell-cell junctional components.

This statement is strongly supported by several findings here reported (in particular by Figure 4.11, Panel F and Figure 4.12, Panel D), in which the correlation between sub-membranous ANXA1 and cortical F-actin is clearly evident.

Finally, we also detected biochemical interaction between a limited quantity of VE-cadherin and ANXA1, as presented in Figure 4.11, Panel G. Considering the position of ANXA1 close to cell-cell junctions levels and cortical actin microfilaments, it is possible that the protein is part of a complex at the cell junctional level. We cannot exclude a potential role of ANXA1 as linking factor between VE-cadherin and cortical F-actin, which represents an important interaction for junctional correct assembly and overall for tight junction assembly. However, the strong evidence obtained on ANXA1 role on actin cytoskeleton, along with the limited co-immunoprecipitation with VE-Cadherin, led us to conclude that this interaction, if real, could represent close proximity between the two proteins and a similar positioning inside the cells, more than a real physical interaction.

In our model, we did observe a positive effect of ANXA1 in terms of cortical actin ring formation and towards cell polarity definition; we did also identify a limited number of stress fibres, which ran parallel to longitudinal cellular axis (Figure 4.12; Panel B). Considering this and the possible link between ANXA1 and VE-cadherin (both structural and functional), it is possible that this protein also influences the formation of discontinuous adherens junctions, suggested to occur in confluent endothelial monolayers and to be involved in regulation of junction formation and paracellular permeability, making the entire monolayer readily responding to certain stimuli (Millan *et al.*, 2010).

Although the scope of this part of the project was not to describe in detail the molecular involvement of endogenous ANXA1 in actin cytoskeleton dynamics, we could gather a strong evidence, along with other published work (Patel *et al.*, 2011), placing ANXA1 as an endogenous regulator of actin microfilaments behaviour by taking part directly into the filaments formation and cytoskeleton localisation.

4.8.1.2 Annexin A1 also functions in an autocrine/paracrine fashion

In a previous report (McArthur *et al.*, 2009), we showed Annexin A1 to be linked with inhibition of hormone exocytosis through actin polymerization triggered via FPR receptor-dependent stimulation of RhoA kinase (ROCK) activation. Here, in addition to the endogenous role of ANXA1, we observed a similar autocrine/paracrine action of ANXA1 (Figure 4.12 and Figure 4.16), which resulted in increased F/G actin ratio, confirming previous evidence (Ikebuchi and Waisman, 1990), as well as in the potentiation of cortical actin ring. ANXA1 is constantly released by microvascular endothelial cells and we have observed that considerable levels of exogenous protein are able to trigger new synthesis of the protein itself, therefore reinforcing its endogenous role. Moreover, we showed that basal ANXA1 also serves to constitutively inhibit the small GTPase RhoA [as it normally happens at cell confluence (Beckers *et al.*, 2010)] while guaranteeing a certain degree of Rac1 activity. RhoA is known to initiate a signalling pathway resulting in the formation of disorganised stress actin fibres generating centripetal forces, which destabilize cell junctions and paracellular permeability (Wojciak-Stothard *et al.*, 2001; Zlokovic, 2005). Instead, Rac1 has been shown to stabilize the endothelial junctions, favouring the formation of cortical fibrillar actin ring and reducing itself RhoA (Wojciak-Stothard and Ridley, 2003). Improvement of the endothelial barrier function can therefore be achieved by increasing the Rac1/Rho activity ratio by either inactivating Rho or activating Rac1, with exogenous ANXA1 seemingly involved in both pathways.

We did not investigate post-translational modifications of tight and adherens junctions, which can be linked to small GTPases action (Wojciak-Stothard *et al.*, 2001; Wolburg and Lippoldt, 2002; Wojciak-Stothard and Ridley, 2003), mainly because of the lack of specific antibodies for phosphorylated tight- and adherens-junctions components; therefore, we cannot exclude that the inhibitory ANXA1 action on RhoA does also involve blocking negative effects directly exerted on tight-junctions [occludin and claudins mainly (Wojciak-Stothard and Ridley, 2002)], besides blocking those played on the cytoskeleton; moreover, we cannot exclude that augmented Rac1 directly phosphorylates VE-cadherin, which has a positive effect in terms of junctions formation, as reported (Seebach *et al.*, 2007).

We did not make use of any specific antagonist or inhibitory molecule directed towards one of the members of this numerous family since they would have caused changes in terms of BBB permeability in the conditions in which we work (confluent monolayers, supposed quiescent state of the cells).

As for the autocrine/paracrine action of ANXA1, significant reports have indicated FPR2 to be the major ANXA1 putative receptors (Perretti, 2003; Migeotte *et al.*, 2006; Perretti and D'Acquisto, 2009). Interestingly, several reports have linked FPRs with activation of signalling pathways based on small GTPases, like Rac1 (Belisle and Abo, 2000), Cdc42 (Glogauer *et al.*, 2000) and Rho-based signalling (Simoes and Fierro, 2005). These works based their investigation on different models, while none has so far linked FPRs with RhoA/Rac1 in endothelium; however, they may indicate that the complex role of ANXA1 in reducing RhoA activity while guaranteeing basal Rac1 activity may be exerted through different receptors of the same family. The strong downstream implication of Protein Kinase C (PKC) in several FPRs ligands responses (Le *et al.*, 2002) as well as in the activation of RhoA - by phosphorylation and inactivation of the inhibitory protein RhoGDI (Wojciak-Stothard *et al.*, 2001; Wojciak-Stothard and Ridley, 2002) - definitely supports our idea.

The autocrine/paracrine role produced by ANXA1 may be particularly important from a pharmacological point of view, as not only it supports the importance of the continuous release of protein outside the cell to contribute to the maintenance of BBB structure and function, but also it propose ANXA1 to be amenable for future therapeutic targeting in conditions associated with an impaired BBB. This point is further reinforced by our experiments with the Anxa1 null mouse, where, even in the absence of intracellular AnxA1, we could induce a significant phenotypic rescue through treatment with hrANXA1, again highlighting the central role of FPR2 and its potential for therapeutic exploitation.

4.9 Limitations of the study

Every model presents limitations; for example, we could consider limited the *in vivo* mouse model, since it presents BBB permeability values different if compared to humans. On the other side, *in vitro* cell line models are based on simplified conditions, which may limit the

impact of the findings. We tried to adopt a multi-targeting approach to complement our findings. Results derived from human samples represent a plus, not only because they offer more reliable mechanistic explanation, but also because they offer the possibility to test new potential treatments. Consequently, we chose the immortalised cell line hCMEC/D3 as *in vitro* model for brain cerebrovascular endothelium, since it proved to be easy to use and reliable in its phenotype, as many recent published studies certainly testify. When possible, we tried to rely on primary murine BMECs to confirm the major findings obtained *in vivo* and in the cell line; however, cost, time and handling constraints limited their extensive use.

As with any *in vitro* cell line models, we had to face several constraints. In general, the isolation of primary cells from their natural environment causes the loss of some of their features and this is particularly true for CNS-derived endothelial cells. Immortalization with viral oncogenes (SV40 large T antigen, used with hCMEC/D3, is one of these) has possibly contributed to the alteration of the phenotype. A way to compensate for the lack of endogenous stimuli is to grow hCMEC/D3 in co-culture with those important components of the BBB known to be extremely important to induce the peculiar properties of BMECs, namely astrocytes (Abbott, 2002; Abbott *et al.*, 2006; Wilhelm *et al.*, 2011) and pericytes (Armulik *et al.*, 2010). Soluble released factors (Alvarez *et al.*, 2011) as well as direct contact between endothelial cells (Wilhelm *et al.*, 2011) and other cells are fundamental to promote immune quiescence and limit the basal active phenotype usually visualized in cell lines. Some initial attempts have been described but have failed to show significant improvements (Hatherell *et al.*, 2011), therefore further optimisation will be required to obtain reproducible and satisfying results. We did not test co-cultures for several reasons: first, we decided to simplify the model conditions and to focus on endothelial cells biology; second, we could not have access, at the time, to a good line of astrocytes or pericytes, possibly non tumorigenic; third, funds limitations placed these experiments beyond the primary scope of the study. This may seem a limitation, since all our studies have focused on permeability regulation, which depends on the correct expression and formation of junctional proteins and on the proper cellular and molecular polarisation. This is a likely reason for why hCMEC/D3 monolayers showed low TEER values compared to *in vivo* values (Crone and Olesen, 1982) or other mammalian primary cells, like rodent, porcine and bovine models (Deli *et al.*, 2005; Abbott *et al.*, 2012; Patabendige *et al.*, 2012) or cell lines

(Silwedel and Forster, 2006). However, the values we were able to obtain - around 50 $\Omega \cdot cm^2$ - are among the best ones for this line. Despite these considerations, we were able to detect clear-cut differences linked to changes in Annexin A1 expression levels, as well as to give proof of concept for the putative mechanisms of action. Since we wanted to justify the pioneering results obtained in the Anxa1 null mouse through albumin-bound Evans Blue, we decided to use tracers with a significant molecular weight (FITC-conjugated dextran 70 kDa), likely not affected by the leakiness shown by hCMEC/D3 with ions (low TEER) and small tracers [FITC-conjugated dextran 4 kDa; (Wilhelm *et al.*, 2011)].

Shear-stress is another important and often not mentioned physiological stimulus that contributes to the peculiar specialisation of BMECs (Cucullo *et al.*, 2011). The microvascular cerebral blood flow creates intense forces values that seem to contribute to the differentiation of the endothelium into the highly specialised BBB phenotype and to intervene in every functions of the barrier (paracellular permeability regulation, leukocyte migration, *etc.*). The reasons for the improvement offered by shear-stress are not fully clear, but seem to be linked to aerobic metabolism changes (Cucullo *et al.*, 2011).

Several other aspects of the complex structure of the NVU have not been taken directly into account; for example, the glycocalyx, *i.e.* the luminal layer of extracellular polymers, was not taken into consideration during the study despite its presence on vascular endothelial cells (Ebong *et al.*, 2011) because we looked at the passage of molecular tracers from the luminal side to the abluminal, not at the uptake of these by endothelial cells. Also, growing evidence is currently supporting the importance of basal lamina (Engelhardt and Sorokin, 2009; Engelhardt and Coisne, 2011) and perivascular space in defining the barrier in its entirety but it seems to be more relevant for cellular transmigration than for the diffusion/passage of molecules. We cannot exclude a role of ANXA1 in other cellular components, like the astrocytes, which were shown to express the protein (Young *et al.*, 1999; Knott *et al.*, 2000; Probst-Cousin *et al.*, 2002).

Knowing the fundamental role played by these cells in determining the correct maturation of blood-brain barrier, such investigation will deserve future attention.

Gross ANXA1-linked changes in receptor-mediated or non-specific transcytosis have not been detected during our paracellular permeability studies (Appendix; Figure 10.3); these observations were only drawn from microscopic analysis of hCMEC/D3 monolayers without investigating for changes in the molecular pathways involved in this process, like caveolae formation (Nag *et al.*, 2011). However, no reports linked ANXA1 to caveolae regulation.

Finally, we did not consider the role of phosphorylated forms of tight junctions; first, because there is a shortage of specific antibodies able to recognized these post-translationally modified forms; second, the relevance of these modification still needs to be confirmed, with some supporting a negative effect on the overall stability of the cellular junctional complex (Murakami *et al.*, 2009) and others indicating a correlation with functional membrane localisation (Sakakibara *et al.*, 1997; Wong, 1997).

4.10 Future work

Before moving on to investigate the therapeutic exploitability of this protein, the molecular pathways involved in ANXA1 exogenous pool mechanism should be elucidated in detail starting from the evidence we have already collected (FPR2 involvement; small GTPases).

With this work, we have detailed the physiological ANXA1 implications in paracellular permeability, whose impact on the brain parenchyma should also be clarified. The interest now moves to the impact of the protein in terms of endothelium-leukocyte interactions, since this has great clinical implications. Indeed, recently we started to investigate the role of ANXA1 in the interactions between leukocytes and vasculature from the endothelium point of view, since all the previous studies have instead only considered its effects played on circulating cells (Perretti *et al.*, 2002; Roviezzo *et al.*, 2002; Yazid *et al.*, 2010).

Regulation of the adhesion molecules by different levels of ANXA1 expression, together with the implications on endothelium extravasation by patrolling circulating cells are aspects undergoing already deep investigation.

4.11 Summary and conclusions

This chapter described the latest evidence for a direct implication of ANXA1 in contributing to the correct formation and assembly of the actin cytoskeleton, directly influencing the entire process of cell-cell junctions formation. This represents indeed a novel role, different from the classic immunological participation, which the protein has been historically linked to. We added more information to the scattered reports present in literature about the structural involvement of ANXA1 into cytoskeleton dynamics, by focusing our attention within the BBB endothelium, which was until now an unexplored field in terms of ANXA1 functions. Interestingly, there seem to be two ways by which ANXA1 produces its physiological role, one by the endogenous pool and the other one by the released population of ANXA1 molecules. We propose that these two pathways act in concert to maintain tight junction formation, and through this they preserve efficient BBB function, as described in Figure 4.17.

Our results showing that a reduction in ANXA1 expression in BMECs leads to a decrease in the formation of junctions and a loss of cellular polarity, with a consequent increase in paracellular permeability, may definitely provide important clinical implications for conditions where ANXA1 is reduced at this level; please refer to Chapter 5 for more details. In parallel, the enhanced junction formation obtained through increased ANXA1 expression and exogenous recombinant protein may also be therapeutically useful.

Overall, it is not too speculative to propose Annexin A1 as a new endogenous mediator participating in endothelial barrier maintenance and limiting the response to permeability-increasing mediators as it will be discussed more in detail in Chapter 6. This class of endogenous factors are normally present in blood plasma, enriched within the endothelium and are also concentrated in certain spots of the tissue interstitium to continuously provide support for the vascular integrity. Among these factors, we should mention fibroblast growth factor (FGF), which mediates the integrity of TJs and AJs or cyclic adenosine-monophosphospate, which shows stabilization of microvascular barrier properties by positively regulating Rac1 activity and protecting against disruptive stimuli, like thrombin or bacterial inflammogens (Baumer *et al.*, 2008). Annexin A1 could definitely be listed as one of these factors, specific for the blood brain barrier endothelium.

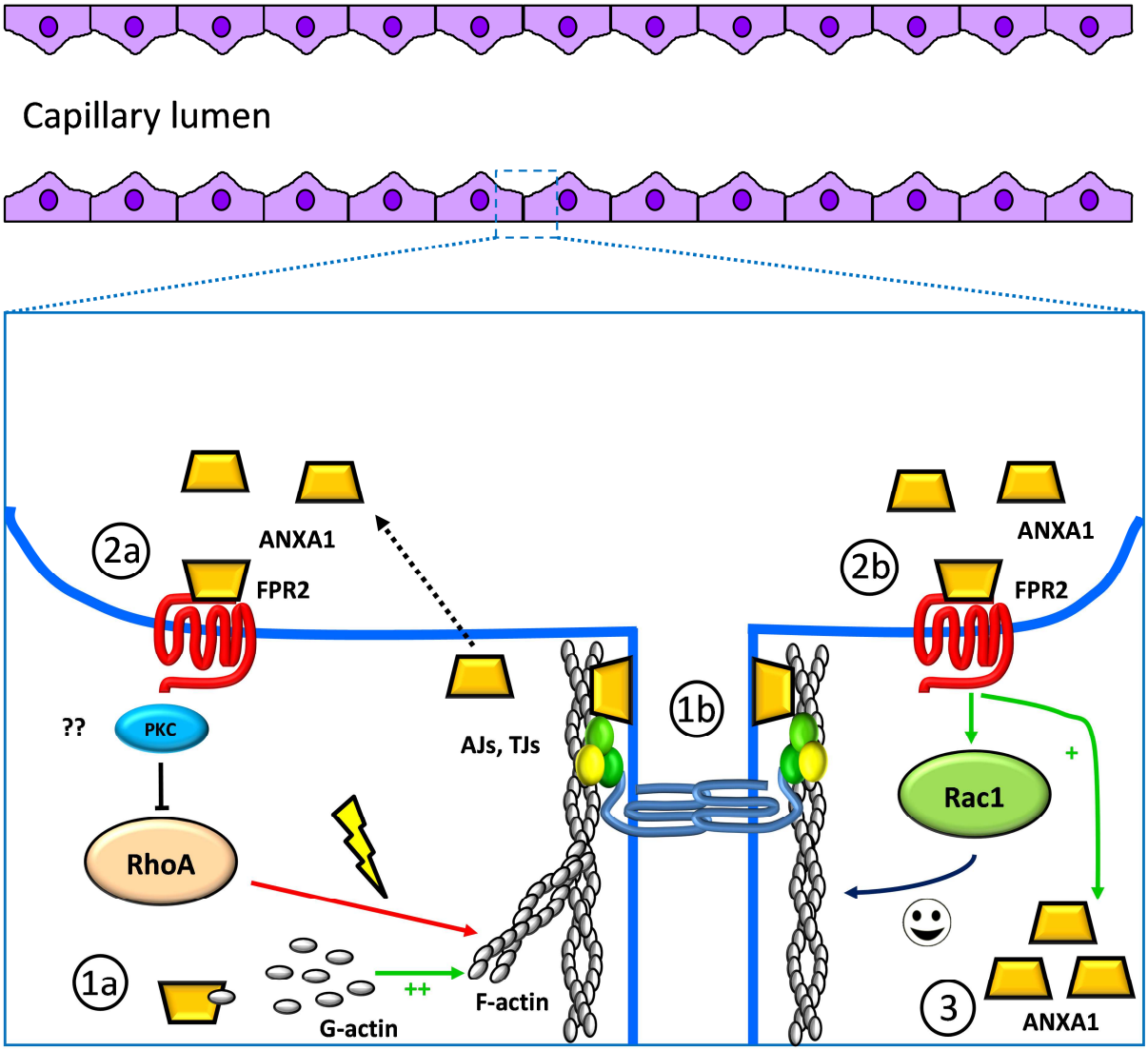

Figure 4.17 Schematic representation of potential mechanisms of action of ANXA1 in BBB integrity maintenance. Our experimental evidence demonstrated the existence of at least two mechanisms mediating the effects of ANXA1 on paracellular permeability. **1a|** Endogenous ANXA1 binds to β-actin, promoting cytoskeleton formation, and **1b|** serving as an anchor linking it to the plasma membrane facilitating the establishment of tight junctions between endothelial cells. Released ANXA1 acting via FPR receptors **2a|** inhibits the activity of RhoA and **2b|** promotes the activity of Rac1, which can limit RhoA-dependent stress fibre formation as well as activating MLCP, therefore preventing the contraction of actin-myosin filaments; overall, this promotes cytoskeletal stability and enhances tight junction formation, hence contributing to BBB integrity. **3|** Exogenous ANXA1 appeared also to have a positive effect on the total ANXA1 content, therefore potentiating the endogenous mechanism of action.

Chapter 5 – Annexin A1 implications on the BBB under pathological conditions

5.1 Overview and aim of the chapter

In this chapter, I will present some still-in-progress data on ANXA1 expression in the BBB under pathological conditions such as multiple sclerosis. The introductive section is not completely exhaustive of all the literature published; this is merely for the purpose of thesis scope and length. Therefore, I often refer to literature for more detailed information.

These data offer novel clinical perception on ANXA1 role in disease and they correlate well with our previous findings (presented in Chapter 4) on the Anxa1$^{-/-}$ mouse, which defined the *benchside* of the project, underlining once more the central role played by the protein and the implications that a lack of it could mean in the pathophysiology of diseases like multiple sclerosis, as well as proposing a novel therapeutical target.

5.2 Involvement of the BBB in pathology and aging

The blood brain barrier is often regarded as a static, passive structure that merely serves as an impediment to molecular access (*i.e.* drug delivery) into the CNS (Carvey *et al.*, 2009). The neuron-centred vision of central diseases often precluded consideration of a potential role of the vasculature in the disease pathogenesis, despite knowing how highly vascularized is the brain [400 miles of capillaries run within the human brain parenchyma; (Grammas *et al.*, 2011)]. The reality is, instead, that in a number (if not in all) of CNS pathologies, BBB physiology is altered, negatively contributing to the outcome of the disease. It is not clear if changes in BBB physiology should be considered more as one of the causes of the disease, as part of the pathophysiological process, as a consequence of the disease or both (Carvey *et al.*, 2009). Nonetheless, recent evidence supports the hypothesis of endothelial dysfunction as a link between neurological impairment and vascular disease and as a crucial sensitizing/worsening factor in the development of CNS disorders (see Figure 5.1).

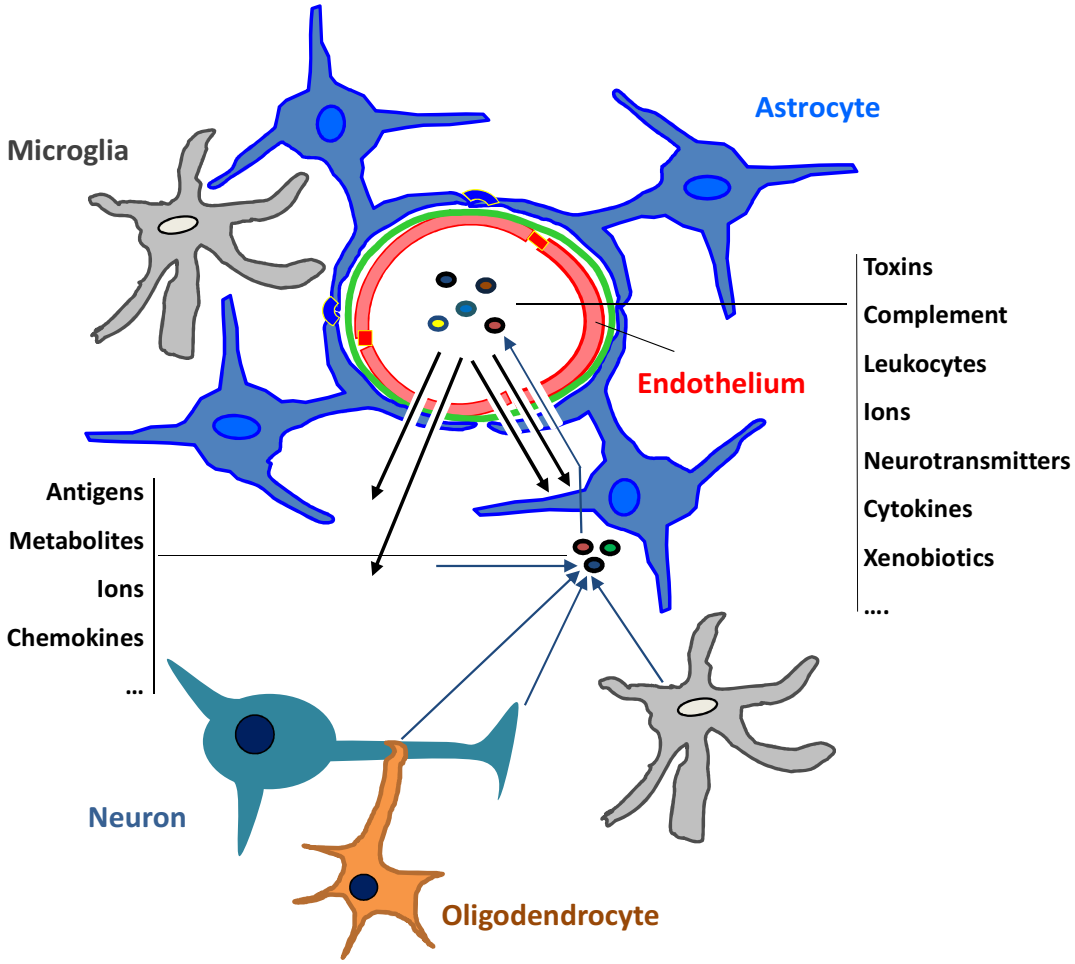

Figure 5.1 Dysfunction of the blood-brain barrier during neurological diseases. Impairment of the barrier mediated by neuroinflammation leads to disruption of the physiological boundaries between the peripheral blood stream and the brain parenchyma. As a result, circulating factors as toxins, complement, ions and in certain cases even leukocytes can enter the brain and be sensed by the various components of the neurovascular unit. Chemokines, metabolites, neurotransmitters *etc.* may then leave the brain parenchyma and enter the blood stream. The uncontrolled mixing that can occur between compartments that are usually separated strongly contributes to determine a self-sustaining process participating in the disease process. Adapted from Carvey *et al.*, 2009.

The concept of the BBB as a static structure is now old-fashioned and starts to be replaced with the idea of BBB being a dynamic interface not only responsive to signals coming from the periphery through the blood stream, but also derived from the brain parenchyma. Stroke and ischemic brain oedema, traumatic brain injury (TBI), multiple sclerosis (MS), human immunodeficiency virus (HIV) and other pathogenic infections, Alzheimer's disease (AD), Parkinson's disease (PD), amyotrophic lateral sclerosis (ALS), inflammatory pain, epilepsy and brain tumours are only a small number of CNS disorders, with involvement of

the BBB (Engelhardt and Sorokin, 2009; Grammas *et al.*, 2011; Neuwelt *et al.*, 2011). The impairment in the regulation of exchange occurring towards the brain could allow many molecules, agents and even uncontrolled immune cells to access the nervous parenchyma (Coisne *et al.*, 2005; Stolp and Dziegielewska, 2009; Zlokovic, 2005). The initial opening of the BBB can be seen as a potential attempt to recruit more defensive tools and to try to resolve the harmful insult, but in presence of an excessive phenomenon, it would seem that the inflammation becomes uncontrolled and detrimental, ultimately contributing to the neuronal death. Factors that are produced during neuroinflammation, like pro-inflammatory cytokines (mainly TNF-α, IL-1 and IL-6), reactive oxygen species (ROS), bradykinin and prostaglandins, lead to BBB opening (Deli *et al.*, 2005). In support of this, much interest is now focused on anti-oxidant and anti-inflammatory therapies as modulatory approaches to treat inflammatory-mediated diseases and to limit the implications on the microvasculature (Coisne and Engelhardt, 2011).

The level of BBB injury can be very different, but normally changes can be of two types: complete breakdown of barrier function (for example in stroke or in brain tumours) and subtle functional and structural barrier impairment without massive initial damage (for example in AD and PD) as reviewed (Wolburg and Lippoldt, 2002). Pathological conditions can, therefore, affect various features of the barrier. To cite only some recent evidence, it is becoming clearer the involvement of pericytes in certain metabolic-related pathologies of the BRB (Diffley *et al.*, 2009), while astrocytic regulatory role can also be altered, with numerous molecules (aquaporins, TGF-β, proteolytic enzymes like metalloproteases that can affect basal lamina, *etc.*) showing altered expression (Abbott *et al.*, 2006; Carvey *et al.*, 2009). Within the endothelium, oxidative stress and the generation of ROS has been detected as a consequence of initiating pathological factors like amyloid-beta in AD, mutated scavengers in ALS and certain products expressed by HIV. BMECs possess a great number of mitochondria, therefore being highly susceptible to oxidative challenges (de Castro *et al.*, 2010; Grammas *et al.*, 2011). Overall, all these alterations were shown to be mediated by inflammatory mediators released during the pathogenesis events (Abbott *et al.*, 2006), which ultimately caused changes at the level of correct tight- and adherens-junctions formation and functionality, as well as in the activation of the endothelium, which responds by increasing the expression of leukocyte adhesion molecules.

Therefore, the ultimate effect is the alteration of the controlled permeability to solutes and cells (Carvey *et al.*, 2009; Coisne and Engelhardt, 2011; Grammas *et al.*, 2011). These changes can either be intense and clearly evident, as during the manifestation of the disease, or more subtle (at the level of the signalling pathways regulating the barrier properties), detected during neurological disorder asymptomatic phases. Those changes might therefore be an early step on the way to develop further barrier damage, ultimately contributing to the disease appearance.

In conclusion, the endothelium of the blood brain barrier is primarily involved in CNS disorders due to its high responsive nature and ability to sense even small alterations both within CNS and in the periphery. Inflammatory signals represent the link between the pathology and the vascular impairment, in both directions, as it is becoming clear for multiple sclerosis, which represents a good example of the complex signals and events occurring in neurological diseases with disruption of the BBB.

5.2.1 BBB and multiple sclerosis

5.2.1.1 Multiple sclerosis: generalities

Multiple sclerosis is a heterogeneous and complex diseases characterised by inflammation, demyelination, scarring and axonal degeneration in the CNS, first described in 1868 by JM Charcot (Clanet 2008;Compston and Coles, 2008). MS represents truly a good example of multi-factorial disorder, since it arises after exposure to various, and mostly unknown, environmental trigger(s). The development of MS is thought to require a combination of factors acting on susceptible genetic traits, leading to a response targeting the myelin sheaths surrounding the nerves (Glass *et al.*, 2010).

The pathological mechanisms of the disease have lately become clearer: MS has an irregular temporal and spatial development throughout the neuraxis, with a predilection for optic nerves, periventricular white matter, brain stem and spinal cord. What characterise the disease is the classical MS lesion called plaque or scar (scleroses), an area where myelin degenerates and gets removed by macrophages and microglial cells, while axons remain relatively preserved in their morphology but functionally are deeply impaired. MS lesions

are also characterised by pronounced astrocytic gliosis and formation of glia scars, aiming to constrain the problem (Compston and Coles, 2008).

The most common theory of MS pathogenesis is that it is an autoimmune inflammatory condition and it involves the role of activated leukocytes, mainly $CD4^+$ lymphocytes, antibody-producing plasma cells and macrophages, penetrating the brain parenchyma and causing damage to the nervous tissue by attacking the myelin sheaths around axons of the brain and spinal cord. However, the aetiology of the disease is complex, not yet fully understood and controversial (Behan and Chaudhuri, 2010): in general, myelin shows metabolic abnormalities that may be caused by a combination of genetic predisposition, environmental factors, infectious factors and others listed as potential cumulative cues leading to the development of the disease (Marrie 2004). Viral and bacterial infections are thought to be strong candidates as factors able to initiate the disease, since they may activate the immune system against auto-antigens such as myelin, potentially through mechanisms as molecular mimicry (Sospedra and Martin, 2005; Ascherio and Munger, 2007). Genetic factors are thought to play a role, since the risk of acquiring MS is higher in relatives of people diagnosed with the disease and various polymorphisms in T and B cells loci are reported to influence susceptibility to MS (Fugger *et al.*, 2009), but the strength of familial influence is still a huge matter of debate (Compston and Coles, 2008). Both innate and adaptive immunity are involved in the pathology, with the former showing a prominent role in the initiation of the disease, in particular through the role of cells such as dendritic cells, macrophages and microglia (Bailey *et al.*, 2007; Glass *et al.*, 2010). Various environmental factors have received past and current attention as susceptibility triggers [the example of the role of sun and vitamin D being extremely significant (Ascherio *et al.*, 2010)]; however, their actual role and importance is still debated (Compston and Coles, 2008).

The huge debate on MS currently occurring testifies how unclear the definition of the pathological mechanisms is and how important this is to develop preventive and curative approaches. At present, there is no known cure for MS: current treatments attempt to return function after an attack, prevent new relapses and prevent permanent disability. One of the factors negatively affecting the success of therapies is the chronic presence of

inflammation, which is the basis for the vicious perpetuation and exacerbation of the disease. Moreover, pre-existing central inflammation has been proposed as one of the potential causes for the disease: in fact, one of the hypotheses is that neuroinflammation could lead to generation of ROS and other toxic reactive species, which attack the normal brain antigens, forming neo-antigens (Minagar and Alexander, 2003). These can either leave the brain for lymphoid tissues (Weller *et al.* 2009), inducing a classically-activated adaptive immune response or may be presented directly *in situ* to naïve lymphocytes by antigen-presenting-like cells such as microglia, perivascular macrophages, pericytes, BMECs and astrocytes (Hemmer *et al.*, 2004; Minagar and Alexander, 2003).

5.2.1.2 Brain barrier alterations in MS pathology

Despite the aetiology of the disease still remaining unclear, it is widely accepted that BBB and BCSFB alterations are among the earliest abnormalities seen in MS, as testified by the clear vascular leakage of fibrinogen and other serum proteins described in *post-mortem* MS brains (Coisne and Engelhardt 2011), which plays an important role in the development and progression of the disease. While the BCSFB alterations in TJs have only been poorly characterised, despite the choroid plexus being one of the principal entry paths for immune cells into the inflamed CNS (Engelhardt and Wolburg 2004; Engelhardt and Sorokin 2009; Coisne and Engelhardt 2011), interest has mainly focused on alterations at the BBB level. In the interesting study by Plumb *et al.* (Plumb *et al.* 2002), around 40% of all the microvessels analysed in MS patients (either with a relapsing-remitting or chronic progressive disease) showed alterations (ZO-1 and occludin discontinuous staining, focal leakage of serum proteins, leukocyte capping), indicating how diffuse the implication of the vasculature can be.

The fact that some vessels of the normal appearing white matter (NAWM) also showed some degree of alteration supports the idea of vascular changes occurring much earlier than the pathological events and symptoms, therefore lesion activity not being a prerequisite for barrier alterations. Moreover, this evidence led some scientists to propose this as a primary initiating event in the pathology of the disease (Stolp and Dziegielewska, 2009).

Two types of BBB disruption are known to occur in MS patients: first, phases of intense acute focal loss of barrier, characteristic of acute and chronic MS lesions; second, diffuse dysregulated BBB is seen in patients with a long-term, low-intensity pathology (Bennett *et al.* 2010).

The mechanisms for the breakdown of the barriers are incompletely understood, but some recent evidence indicates inflammation and inflammatory mediators as the key cause in triggering all the vascular-related events seen during the course of the disease (Minagar and Alexander 2003). Activation of the endothelium (changes in paracellular permeability and adhesion molecules) alters the BBB properties and contributes to the progression of the pathology (Carvey *et al.* 2009; Coisne and Engelhardt 2011; Holman *et al.* 2011) through the recruitment of activated T-lymphocytes, which tend to focally accumulate in the perivascular space of the capillaries and post-capillary venules (between the endothelium, the basal lamina and the astrocytic end-feet), a phenomenon that has been named "perivascular cuffing" (Minagar and Alexander 2003; Engelhardt and Coisne, 2011). Here, leukocytes undergo a certain number of phases resulting in the invasion of the CNS and their detrimental action. Linked to these aspects, recent studies have also shown the relevant role played by meningeal barrier and subarachnoid space for inflammatory cell recruitment and pathology outcome (Howell *et al.*, 2011; Choi *et al.*, 2012).

The experimental allergic encephalomyelitis (EAE) murine model shares several commonalities with the human disease, plus gives many indications about barriers disruption and how activated lymphocytes enter the intact CNS (Bennett *et al.* 2010; Grammas *et al.* 2011), since this model is not driven from central triggers (Engelhardt and Coisne, 2011; Huitinga *et al.*, 1998). IFN-γ and TNF-α, among the cytokines elevated in MS, and free radicals have been shown to disrupt certain tight junctions and to reduce VE-cadherin (Jy *et al.* 2004).

Gross focal disruption of the BBB has been consistently demonstrated *in vivo* in acute relapsing and chronic progressive events; in parallel, subtle increase in vascular permeability has also be shown in early stages and during remission of the disease (Plumb *et al.* 2002), causing a consequent confined leakage of serum proteins into the brain parenchyma which may represent a sensitizing event (Simpson *et al.* 2010). Mouse models with impaired

junction molecules and subsequent enhanced paracellular permeability demonstrated that the disruption of the endothelial tightness favour the entry via the paracellular pathway of activated leukocytes (Engelhardt and Coisne, 2011). Not only lymphocyte extravasation is important for the pathogenesis of the MS, but also the invasion by neutrophils and monocytes has been shown to stand a role in this pathology (Bolton *et al.* 1998; Allport *et al.* 2000); these other leukocytes are well known to cross the endothelium by provoking a direct disruption of the junctional complexes, and the rate of migration increased in presence of already damaged junctions. The same considerations stand also for the BCSFB, which has a central role in lymphocytes invasion during multiple sclerosis (Engelhardt and Sorokin 2009).

Nowadays, it is still unclear if the disassembly of the barriers is secondary to the characteristic inflammation of the disease, or alternatively if the weakening of the barriers actually precedes the inflammatory process, therefore supporting the theory of MS being also a hemodynamic vascular disorder, as a party of researchers, led by Zamboni and his colleagues, has been trying to propose (Zamboni *et al.* 2007; Simka 2009). Despite these recent innovative hypothesises have been strongly reshaped and debased by strong patient studies (Comi *et al.*, 2013), this new enthusiasm around the question has posed the vasculature topic under the spotlight of the MS community. Today, subtle BBB leakage can be detected via perfusion magnetic resonance imaging (MRI), which has become an important diagnostic instrument (Abbott *et al.*, 1999; Plumb *et al.* 2002) to detect new inflammatory lesions in relapsing-remitting or chronic progressive MS patients.

5.2.2 BBB alterations with ageing

Ageing has an important impact on the integrity of all tissues, including the blood-brain barrier. Constant daily stimulation, adaptation, reorganisation, *etc.* have a cumulative effect on this complex structure and compromise the fundamental role of the BBB. Several age-related changes are evident in the BBB properties, both at an anatomical and a physiological level. For example, aged microvessels show a smaller diameter and an increased tortuosity, which can have consequences in terms of shear-stress (Cucullo *et al.* 2011); endothelial cells show fewer mitochondria, indicating therefore impairment from the transporters point of

view (Zeevi *et al.* 2010). Defects in transport of glucose, amino acids, hormones and other important molecules has also been shown giving higher risk of nutrient-deficient syndromes and cognitive decline. The specialized efflux pump system of the BBB also showed decreased activity (in particular P-gp), which could clearly explain some neurological conditions of the elderly like delirium and the adverse effect of certain medications (Toornvliet *et al.* 2006). No known aging-effects on tight-, adherens-junctions or surface adhesion molecules have been reported, although they seem to respond much more quickly and intensely after an insult. Interestingly, vascular regional heterogeneity has also been proposed for the ageing of the BBB: in fact, greater vascular impairment appears in certain brain regions of the old mouse (Pelegri *et al.* 2007). All these changes seem to occur gradually during life-time, and do not normally (Carvey *et al.* 2009) result in evident changes in the overall integrity [at least in human; some animal models showed controversial results (Campbell *et al.* 2007; DiNapoli *et al.* 2008)]; however, it is clear that the aged BBB is more prone to react to certain conditions, by responding with a more intense increase in paracellular permeability and loss of its main properties (Zeevi *et al.* 2010). Old individuals are often characterised by white-matter lesions (WML), which are a strong indication of the impairment in the microvasculature: in fact, local low serum protein extravasation has been indicated as a major factor in determining the activation of surrounding glial cells with the consequent damage of circumscribed areas of white matter (Simpson *et al.* 2010; Zeevi *et al.* 2010).

The role of aging at the level of other components of the NVU (*e.g.* pericytes, astrocytes, basal lamina) has not been sufficiently investigated; however, it is becoming clearer why aging represents the most important risk factor for neurological disorders, and yet another important factor to take into account when investigating the central role of the BBB in neurological disorders.

5.3 Methods

Please refer to Chapter 3 for the description of general *in vitro* procedures. More details about certain technical aspects of procedures specifically used for the purpose of only this chapter and about clinical details of the cases analysed will be here provided. Please refer to the Appendix (Chapter 10) for solution composition.

5.3.1 Ethical approval

Human tissue samples were provided by the UK Multiple Sclerosis Tissue Bank and the UK Parkinson's Disease Society Tissue Bank at Imperial College London. Patients' blood samples were provided by Dr A. Malaspina (North-East London and Essex MND Care and Research Centre. Ethics Committee: 09/H0703/27). Informed consent was obtained from all the individuals recruited. Blood samples and clinical information were collected following consent. The study has followed established standard of practice (SOPs) and the experiments were conformed to the principles set out in the World Medical Association Declaration of Helsinki.

5.3.2 Selection of human *post-mortem* tissue

Human post mortem samples were obtained from brains of cases of neuropathologically confirmed MS, PD and non-neurologic controls. Brains were selected according to the following criteria: 1) availability of full clinical history 2) no evidence of cancer at post-mortem 3) negligible atherosclerosis of cerebral vasculature. Demographic data for the samples used are described in the Appendix (Table 10.4 and 10.5).

5.3.3 Staining of human *post-mortem* tissue

After collection, tissue was divided in specific regional and sub-regional areas, fixed in 10% PBS-buffered formalin and embedded in paraffin. From each paraffin block, 8 µm sections were cut and used for immunohistochemistry. Sections were deparaffinised in xylene and rehydrated in decreasing alcohols. Endogenous peroxidase activity was inhibited by

incubation in peroxidase inhibiting buffer for 30 minutes at room temperature. Sections were rinsed twice in TBS 1X and incubated for 1 h at room temperature in blocking solution to saturate non-specific binding. Then, sections were incubated overnight at 4°C with anti-human ANXA1 primary antibody (Invitrogen, UK), rinsed twice in washing solution, incubated in biotinylated goat-anti rabbit secondary antibody (Vector Laboratories, UK) at the dilution of 1:100 for 2 hours at room temperature, rinsed twice with TBS 1X and incubated for 45 min in the avidin–biotin complex (ABC) conjugated with HRP in TBS (Vector Laboratories, UK). Following two washings in TBS 1X, the reaction was developed in developing solution for 5 minutes. Sections were rinsed twice in TBS 1X, counterstained with Ehrlich's haematoxylin for 2 minutes, rinsed in tap water for 5 minutes, fast dip in acid alcohol and again rinsed in tap water twice (1 minute/wash). Sections needed to be dehydrated in 95% ethanol for 2 minutes, cleared in xylene for 10 seconds and mounted with DPX mountant for bright-field microscopic analysis. The staining was performed by Dr. S. McArthur.

5.3.4 Light microscopy

Brightfield photomicrographs were captured at room temperature using a Nikon Eclipse E800 microscope fitted with a 60X oil immersion objective lens (NA 1.4mm, WD 0.21mm), a CoolSNAP-Procf camera (Roper Scientific, UK) and Image ProPlus 4.5.1 software (Perkin-Elmer, UK). Pictures were acquired by Dr. S. McArthur.

5.3.5 Plasma anti-ANXA1 autoantibodies measurement via ELISA

Human plasma samples from MS and healthy donors were used to measure ANXA1 content by ELISA as reported in the General methods (Chapter 3).

Detection of serum autoantibodies directed towards human ANXA1 was performed by Dr. S. McArthur according to a published protocol (Goulding *et al.*, 1989). Plastic ELISA 96-well plates (Nunc MaxiSorp, ThermoScientific, UK) were coated with 100 µl/well bicarbonate buffer, containing 10 µg/ml hrANXA1 at 4°C overnight; two wells were coated with only bicarbonate buffer and used as negative controls.

After 3 washes with bicarbonate buffer, wells were blocked with 100 µl/well 0.01M PBS (pH 7.2) containing 1% FCS at 37°C for 1 hour. Control and patient serum samples were diluted 1:20 in 0.01M PBS containing 1% FCS, loaded into the plate (100 µl/well) and incubated for 1 hour at 37°C. Two wells were incubated without human serum to account for further unspecific secondary antibody binding. Plates were washed 7 times with wash buffer, and then incubated with HRP-conjugated goat-anti human IgG/IgM (1:1000; Sigma, UK) in antibody buffer for 1 hour at 37°C. After 7 washes with wash buffer, plates were incubated with 100 µl/well of commercial (eBioscience, UK) 3,3',5,5'tetramethylbenzidine (TMB) HRP substrate and incubate at room temperature for 10 minutes until clear colour was developed. The reaction was finally stopped with 100 µl/well of stop reaction. Plates were read at 450 nm, with background correction at 570 nm.

Results were expressed in ELISA units, which are defined as follows:

$$\text{ELISA unit} = \frac{\text{Absorbance (450 nm-570 nm)} \times \text{dilution factor}}{\text{reaction volume}}$$

5.3.6 Testing plasma from MS patients effects on paracellular permeability

On the basis of previous reports (Alexander *et al.*, 2007; Minagar *et al.*, 2003; Proia *et al.*, 2009), we decided to test the effects of plasma derived from patients affected by MS, in order to obtain more information about some of the findings described in this chapter. In particular, the investigation conducted by Alexander *et al.* (Alexander *et al.*, 2007) was of special relevance, since they observed down-regulation of Annexin A1 of human brain endothelial cells after incubation with 10% serum from relapsing-remitting MS patients.

hCMEC/D3 wild-type cells were cultured on transwell filters as described in the General methods chapters. When confluent, cell monolayers were incubated with EGM-2 MV medium complete with all the growth factors except for VEGF. After 3 days, fresh medium with all the growth factors (except for VEGF) and 20% plasma from a MS patient or a control patient was replaced for 24 hours. Paracellular permeability of 70kDa FITC-dextran was assessed over 60 minutes (Section 3.2.2.1.6).

After the experiment, cells were washed in DPBS without Ca^{2+} and Mg^{2+}, quickly trypsinised and lysed in RIPA buffer as described in section 3.2.4.2.

Total ANXA1 quantity was then measured via ELISA and normalized against total protein content, which was measured by BCA assay.

Permeability coefficients (expressed as percentages of the permeability coefficients obtained in cells incubated with healthy control plasma samples) were then plotted against the normalized quantity of ANXA1 and correlation was defined through GraphPad Prism 5.

5.4 Results

5.4.1 Expression of ANXA1 is selectively lost from the cerebral capillaries of MS *post-mortem* cases, but not with other neurodegenerative conditions

Whilst examination of samples from PD cases revealed that expression of ANXA1 was maintained within the cerebral capillaries, ANXA1 was not detectable in those of *post-mortem* subjects who had died with multiple sclerosis (Figure 5.2, Panel A). The loss of ANXA1 was moreover highly cell-specific, being limited to capillary endothelial cells of the BBB brain parenchyma, as both leukocytes and other vascular sites with strong ANXA1 expression, such as the ependyma, choroid plexus and meningeal vessels, remained highly immunoreactive (Figure 5.2, Panel B).

Since an old report linked the development of autoantibodies directed towards ANXA1 in patients with auto-immune disorders like systemic lupus erythematous (SLE), independently of the treatment the patients were receiving (Goulding *et al.*, 1989), we decided to look for differences in autoantibodies in 10 healthy subjects and in 10 patients with MS, as this, if true, could have proved to be a potential explanation for the great differences in microvascular ANXA1 observed.

The level of auto-antibodies was very low in controls and in MS patients (Figure 5.2, Panel C) and we did not observe any difference in terms of type of disease (relapsing/remitting compared to secondary progressive MS) or treatment received by the patients (data not shown). Therefore, this was not a plausible reason for the selective loss.

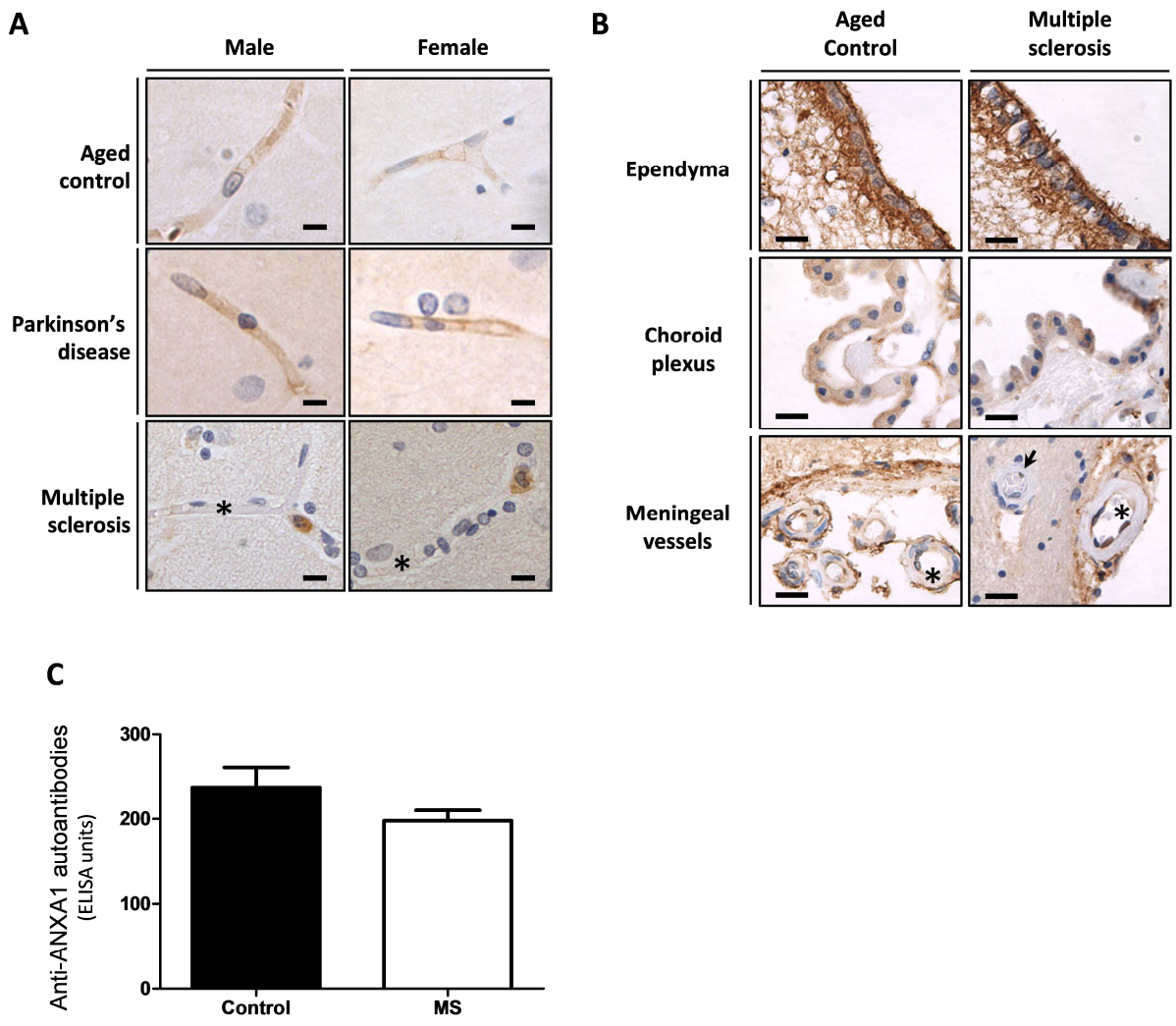

Figure 5.2 Expression of ANXA1 is selectively lost from the cerebral capillaries of subjects with multiple sclerosis, but not with other neurodegenerative conditions. A| Immunohistochemical analysis of ANXA1 expression within cortical capillaries of human male and female *post mortem* brains. Note in particular the strong expression of ANXA1 in circulating leukocytes of multiple sclerosis cases, but the absence of endothelial ANXA1 positivity (marked by asterisks). Typical images from cases described in Table 8.1, sections are 8µm thick, while scale bar is 10 µm. **B|** Immunohistochemical analysis of ANXA1 expression within the ependyma of the lateral ventricles, the choroid plexus and the meningeal blood vessels of aged controls and MS cases. Black arrow indicates the lack of expression of ANXA1 in parenchymal microvessel endothelial cells of MS cases, compared with the meningeal vessel endothelial cells (marked by asterisks); sections are 8 µm thick, scale bar is 20 µm. **C|** Detection of auto-antibodies in the plasma samples of MS patients (*n*=10) and healthy age- and sex-matched controls (*n*=10). Results are indicated in ELISA units, calculated as specified in the methods; data are presented as mean ± SEM. No statistical differences have been detected after Student *t*-test. Panels A, B and C were produced by Dr. S. McArthur.

5.4.2 Effect of MS plasma on endothelial ANXA1 content and permeability

Having shown that the expression of auto-antibodies against ANXA1 is not responsible for the peculiar decrease in ANXA1 in BBB endothelium, we decided to investigate further by testing if plasma from patients affected with MS presented some factors that could negatively influence the expression of ANXA1 and consequently the paracellular permeability endothelial monolayers. Interestingly, MS patients showed a significant reduction in circulating ANXA1 in the plasma (Figure 5.3; Panel A), which could definitely have an important effect on paracellular permeability, aware of the exogenous ANXA1 role. Using the *in vitro* hCMEC/D3 model, we observed (Figure 5.3; Panel B) that exposure to MS patient plasma induced a significant increase in paracellular permeability, which closely correlated with a plasma-induced reduction in endothelial ANXA1 expression; this effect was not seen in cells exposed to plasma from healthy donors.

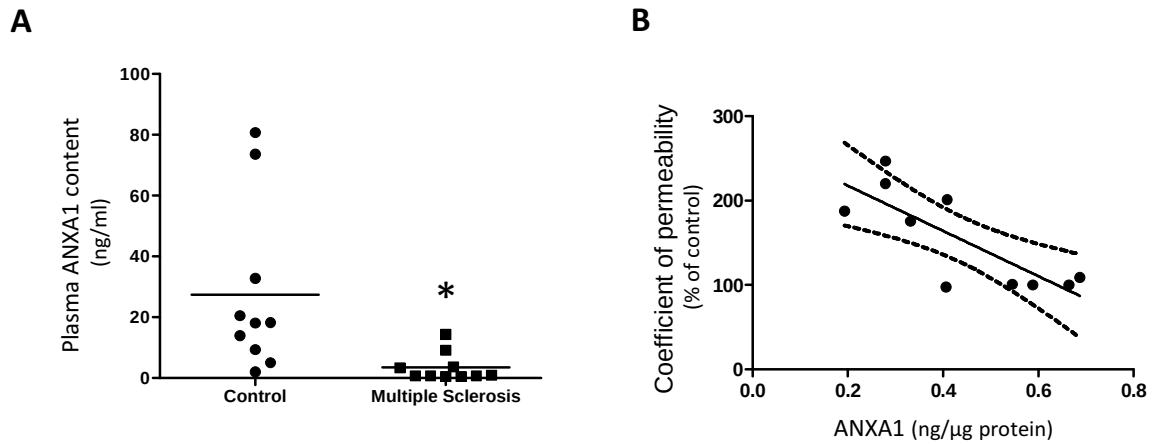

Figure 5.3 Plasma from MS patients contains less ANXA1 and reduces ANXA1 content and paracellular permeability of endothelial cells. A| Plasma ANXA1 content from MS patients and healthy age- and sex-matched controls was calculated by ELISA; lines indicate mean values. Student *t*-test was performed between the two independent groups, with * indicating significant $p < 0.05$ *vs.* control group. **B|** Paracellular permeability coefficient (expressed as percentage of the untreated control) of monolayers of human hCMEC/D3 cells following exposure for 24h to medium containing 20% plasma from MS patients, correlated with total levels of ANXA1 in the same hCMEC/D3 cells following exposure; linear regression line and 95% confidence intervals are marked, coefficient of correlation is 0.38, $p < 0.05$.

5.5 Discussion

These results strongly support for a role of ANXA1 as a main player in the maintenance of BBB integrity, following and complementing the mechanistic evidence that has been described in Chapter 4.

5.5.1 ANXA1 expression changes in MS: which implications?

Our finding of a selective loss of ANXA1 expression in the cerebral capillary endothelium of MS subjects is particularly important. As mentioned in the introduction, tight junctions like occludin have been reported to be impaired in their expression and distribution within the microvascular endothelium of MS patients, clearly paralleling our findings in AnxA1$^{-/-}$ mice. One fundamental detail that should be mentioned is that the endothelial ANXA1 down-regulation occurs also in normal appearing white matter (NAWM); several reports stated the presence of aberrant vascular properties in areas not (yet) affected by active lesions, therefore our findings may definitely confirm that and contribute to the debate concerning if changes in BBB permeability precede leukocyte extravasation, or represent a consequence of immune cell accumulation (Engelhardt and Coisne, 2011; Larochelle *et al.*, 2011). In particular, our finding on ANXA1 down-regulation at sites distant from active lesions strongly suggests a pre-existing weakening of BBB integrity to the development of active demyelination. Despite increasing evidence strongly supports the fact that T lymphocytes normally enter the healthy and diseased brain by crossing the endothelium via transcytosis (Engelhardt and Sorokin 2009) leaving the tight junctions intact (Engelhardt and Wolburg 2004), alterations at the level of the paracellular permeability are equally important and influent since they may lead to an even more intense cellular invasion or, if the impairment is considerable, it may represent a further way of invasion (Minagar and Alexander 2003; Grammas *et al.* 2011).

Previous reports have suggested both beneficial (Huitinga *et al.*, 1998) and detrimental (Paschalidis *et al.*, 2009) roles for ANXA1 in the widely-used animal model EAE; another work reported the evidence for ANXA1 expression in various cell types populating disease plaques, without adding more about the implications that this protein could have in the course of the disorder (Probst-Cousin *et al.*, 2002).

The discrepancy with some of our findings from human disease may be justified by the use of a controversial animal model (Friese *et al.*, 2006), which however has given important information especially concerning the vasculature implications (Bennett *et al.*, 2010; Engelhardt and Coisne, 2011). In support to our findings and hypothesis, we should note that our studies on the role of ANXA1 were undergone in a defined cell/tissue type by studying changes in paracellular permeability, rather than examining the multiple complex interacting systems that may be involved in a whole animal model of disease. Moreover, we have been the first ones to focus on the endothelium: this is an important source of externalized ANXA1, which can ideally target other cell types, like circulating leukocytes. To this regard, we have previously shown ANXA1 to limit leukocyte extravasation through binding of the $\alpha_4\beta_1$ integrin VLA4, blocking leukocyte adhesion to the endothelium (Solito *et al.*, 2000). It is important to remember that one of the most widely used treatments to limit MS symptoms is currently the monoclonal antibody *Natalizumab* (commercialized as Tysabri by Biogen Idec and Élan), which targets the same integrin as ANXA1. It is therefore easy to speculate that the down-regulation of ANXA1, occurring in the cerebral microvascular endothelium as well as in the blood of MS subjects, may represent the loss of an endogenous break aimed at limiting excessive leukocyte adhesion.

Glucocorticoids are strong inducers of ANXA1 and are widely used as therapeutic agents in the treatment of MS thanks to their anti-inflammatory properties, a fact that suggest again the importance that ANXA1 may play in the disease. Although we don't have experimental proof of an effect of glucocorticoids-triggered ANXA1 in restoring BBB integrity in MS patients, we can strongly suppose it, especially if considering that glucocorticoids like dexamethasone can induce ANXA1 expression in hCMEC/D3 cell line (data not shown).

5.5.2 Why ANXA1 expression is selectively lost from BBB endothelium in MS?

The most intriguing, and complex, question that remains to be elucidated is to understand how and why ANXA1 expression decreases so massively and in such a selective way at the level of the microvasculature of MS cases. Other conditions like PD and AD (data not shown, very similar to PD and aged controls), also characterised with a degree of BBB breakdown and persistent neuroinflammation, do not show such a phenotype.

At present the reasons for these differences are unclear. Possibly, one of the determinants could be in the different nature of these neurological disorders: PD and AD have their source of degeneration and inflammation within the CNS, while MS seem to be determined more by the impact of inappropriate activation of the peripheral immune system (Hemmer *et al.*, 2004). Growing evidence is confirming this last concept, indirectly supporting the fact that peripheral stimuli are extremely important, especially for MS; in literature, we can find evidence indicating that blood samples from MS patients can decrease TEER *in vitro* (Proia *et al.*, 2009) and that can also induce a down-regulation in ANXA1 amongst other proteins within endothelial cells (Alexander *et al.*, 2007). The typical elevation in cytokines (mainly TNF-α) and/or other soluble unknown molecules observed in MS patients, in particular those in relapsing/remitting phase where the disease is highly active (Alexander *et al.*, 2007; Carrieri *et al.*, 1998) may represent a possible explanation, especially in light of what happens to microvascular endothelial-specific ANXA1 under acute pro-inflammatory conditions (please refer to Chapter 6). Chronic contact with these pro-inflammatory cytokines are known to produce significant effects on brain barrier components, in particular on tight-junctions (Engelhardt and Sorokin, 2009), so it is very likely that this action may also be mediated by affecting modulating molecules like ANXA1. Our data confirms and extends these two studies (Alexander *et al.*, 2007; Proia *et al.*, 2009), plus it provides a clear rationale for a correlation between ANXA1 expression and changes in BBB permeability in MS, potentially opening a new avenue in the investigation of this disease.

5.6 Limitations of the study and future work

Clearly, these findings represent only initial observations which should be confirmed by a larger cohort of samples. In particular, it would be extremely interesting to differentiate MS patients according to disease classification (relapsing/remitting, secondary progressive, primary progressive, progressive relapsing), since some recent studies (Komori *et al.*, 2012; Teunissen *et al.*, 2011) have evidenced marked differences in certain pathophysiological factors. Nonetheless, the body of evidence strongly supports the histological results showing loss in specific ANXA1 expression as they were distinctly reproduced in every MS-related tissue analysed (10 cases, regardless the MS subtype).

At present, we are liaising with clinicians to significantly extend the screening of MS plasma samples for ANXA1 concentration and the latest results are confirming the finding of a constitutively lower protein concentration linked to the disease. A new focus will be to analyse longitudinal samples, so that we could possibly understand if this specific decrease in the protein is linked to a peculiar phase of the disease or if it is present throughout the pathology. Several factors have been reported to be informative markers linked to new relapse phases or even potential predictors (Gurevich *et al.*, 2009; Kalinowska-Lyszczarz *et al.*, 2011) so it would be interesting to understand if ANXA1 may play a similar role.

The disruptive effects shown by MS plasma on BMECs tightness and total protein content have to be confirmed with a larger cohort of samples, from which correlation studies would certainly benefit. It would be extremely interesting to identify the molecular culprit(s) for this effect, investigating first the most logical candidates (for example pro-inflammatory cytokines raised in the plasma, reactive species, endogenous toxins) and then eventually move to alternative ones. We may benefit from high-throughput tools like proteomics, which are able to assess numerous samples and to identify major differences, on which then we may want to focus more in details.

5.7 Summary and conclusions

Our results undoubtedly confirmed a role for ANXA1 in the vasculature; the specific drop in the microvessels represents a novel finding, while the drop in plasma certainly opens new avenues for exploitation as a biomarker, if we can further confirm the absence at early phase of disease. The interest in decoding the complex mechanism that regulates barrier properties is very high at the moment, in particular for the identification of endogenous molecules that can dynamically regulate and support the communication between periphery and brain, affecting the overall homeostasis of the CNS. Considering how common alterations in BBB for MS patients are, how highly specific is the loss of ANXA1 from MS capillaries and how strong is the relevance in terms of BBB physiology, we can definitely say that annexin A1 is one of the molecules, with great therapeutic potential and it may also constitute a novel highly specific biomarker for early disease detection (Alexander *et al.*, 2007).

Chapter 6 – Annexin A1 and peripheral inflammation at the BBB: sex-dependent differences

6.1 Overview and aim of the chapter

Chapter 4 and 5 have described the important role of ANXA1 at BMECs level, maintaining physiological tight barrier properties as well as being implicated in conditions such as MS. Bearing in mind the ultimate aim of the project, *i.e.* to elucidate ANXA1 role in periphery-to-brain communication, we complemented these findings by investigating the protein involvement at BBB level during peripheral inflammatory conditions. Since MS patients usually show a peculiar high pro-inflammatory profile in their blood, known to be responsible for the perpetuation of the disease, the findings presented have also strong clinical implications. Furthermore, since many central and peripheral inflammatory diseases are strongly biased by the sex of the patient, while ANXA1 is regulated by steroids (Solito *et al.*, 1998; Solito *et al.*, 2003b) and a steroid messenger at the same time, we expanded our experimental plan to investigate sex differences.

6.2 The blood brain barrier as a signalling interface

Until recently, the BBB was considered to be a passive, impermeable barrier to immune cells and diffusible factors produced in the periphery. However, the BBB dynamically senses and responds to what happens elsewhere in the body. Due to its peculiar location, the endothelium represents a common and accessible target for all the molecules circulating in the blood, such as physiological hormones, nutrients, signalling molecules, or pathological cardiovascular risk factors, mediators of oxidative stress happening somewhere else, molecular signals indicating tissue disorders. The endothelium of the BBB is at the forefront of the defensive system of the CNS and it is deeply affected by peripherally-originated factors and actively responds to them (Carvey *et al.*, 2009). The polarized transporter and receptor system of the BBB is seen as the conveyer of a directional signalling on the BMECs: upon ligand binding, signals are generated and are transferred into brain parenchyma and *vice versa*.

One of the main features modulated by systemic signals is barrier integrity, whose implications in physiology and pathology have been extensively described in the previous chapters.

In addition, directional release of substances is also another way to respond to certain stimuli; therefore, BMECs are not passive mediators in this type of communication, instead they actively participate in decoding what happens in the periphery and how the CNS should respond to that.

6.2.1 How peripheral inflammation impacts at the BBB level

In the previous chapter, I have described how factors produced in the CNS during neurological disorders impact on the homeostasis of the BBB, determining the implication in diseases like AD and PD (Coisne and Engelhardt, 2011). Similarly, there is now clear evidence that the CNS mounts a complex response to systemic inflammatory processes, through different pathways. One of these involves the BBB, either by impacting directly on BMECs or on astrocytes, pericytes and perivascular macrophages (Abbott, 2002; Guillemin and Brew, 2004). Overall, BBB responds via regulation of endothelial cells tightness and specific gene transcription regulation (Nadeau and Rivest, 1999), which ultimately convey the signal to the CNS. Subtle changes in BBB function and basal permeability may certainly have long lasting effects on the overall CNS homeostasis or at least increase the susceptibility of the CNS to develop neurodegenerative conditions. For instance, increasing evidence describes the impact of developmental peripheral inflammatory events on the initiation of neurological conditions through a direct “imprinting” effect at the level of the brain vasculature (Stolp and Dziegielewska, 2009). Indeed, it is not scientifically accepted that peripheral signals are able to enter into the depth of the brain parenchyma to stimulate neurons and other resident cells. Other relevant findings report the impact of infection and related inflammation on the brain through the BBB: activation of microglial cells by peripheral stimuli has been shown to be dependent on specific receptors present at the BMECs level (Gosselin and Rivest, 2008), while the upregulation of adhesion molecules on endothelial cells triggered by inflammatory stimuli (both central and peripheral) is now widely accepted (Carvey *et al.*, 2009).

6.2.1.1 The role of pathogen-associated molecules (PAMs)

The main protagonists in defining the impact of inflammation on the BBB are inflammogens and pro-inflammatory mediators. Pathogen-related molecules such as LPS, a cell wall component of Gram-negative bacteria, are well known to modulate effects at the BBB level, not only when released in the brain parenchyma during CNS-related infections but especially when circulating in the blood, following systemic infections (McAllister and van de Water, 2009; Nagyoszi *et al.*, 2010). Apparently, this happens either directly through an action on endothelial cells (Descamps *et al.*, 2003) or indirectly through other BBB components, such as astrocytes (Abbott *et al.*, 2006). There is no evidence for direct entry of PAMs in the brain parenchyma (Singh and Jiang, 2004; Banks and Robinson, 2010). Instead, these molecules signal through specific receptors, called Toll-like receptors (TLRs), a huge family of transmembrane proteins (in human there are 10 members) some of them abundantly expressed at the BMEC level (Nagyoszi *et al.*, 2010). These receptors are able to recognize a great number of molecules sharing specific molecular patterns conserved among pathogens (the PAMPs). Also, there are some specialised TLRs, able to recognize molecules linked to the damaged tissue (the already mentioned DAMPs). These receptors are highly dynamic and respond quickly to the immunological state of the host; for example, in presence of infection, inflammation and oxidative stress are well known to up-regulate the expression of specific TLRs, augmenting their responsiveness.

When circulating, LPS is bound to a soluble acute protein called LPS-binding protein (LBP); in this form they can bind to the receptorial complex for LPS on cells surface, which is formed by CD14, TLR-4 and the accessory protein MD-2 (Singh and Jiang, 2004), triggering complex intracellular signalling pathways, as depicted in Figure 6.1. The ultimate effects triggered by LPS on BBB are: increased paracellular permeability, by alteration of the junctional components, increased adsorptive endocytosis of substances, increased diapedesis of peripheral cells, both by augmented adhesion molecules and efficiency of the trans-cellular route of barrier crossing, alterations at the level of the transport system, secretion of several molecules (mainly pro- and anti-inflammatory cytokines, chemokines, reactive oxygen species) in a polarized fashion (Banks, 2006; Verma *et al.*, 2006; Nagyoszi *et al.*, 2010).

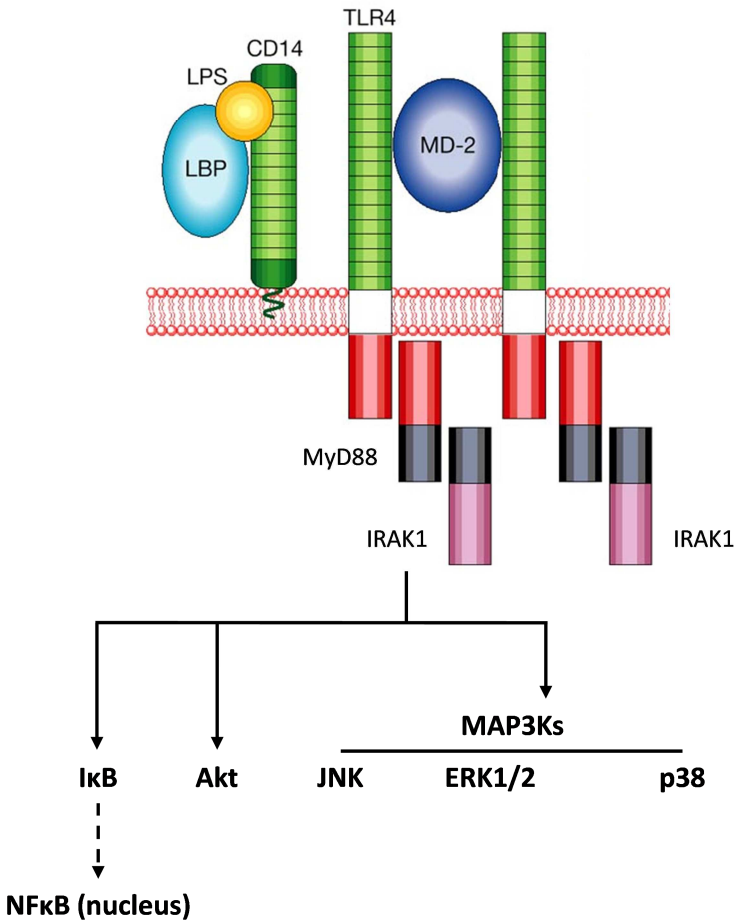

Figure 6.1 Signalling triggered upon LPS binding. LPS is bound by LBP, and the complex is recognized by CD14, which is weakly associated to the cell membrane. This complex is able to activate TLR4, in turn signalling through the adaptor protein MyD88 and the serine kinase IRAK, responsible for the major molecular signalling pathways triggered downstream. The mechanism by which TLR4 is activated is not known and could be either direct or indirect. From Aderem and Ulevitch, 2000.

6.2.1.2 The role of inflammatory mediators and cytokines

It should be noted that, unless septicaemic conditions are reached, it is very difficult to obtain blood concentrations of pathogen-related molecules sufficient to be able to significantly affect the cerebral endothelium. More likely, the effects on BBB due to infections are triggered by the subsequent exponential release of inflammatory mediators. Interestingly, in areas of focal inflammation, infiltrating cells from the circulation, as well as activated resident cells like microglia, may create a *milieu* where the concentration of the cytokines reach much higher values than reported in the periphery and in circulation; such condition may therefore be enough to trigger substantial effects on the local

microvasculature (Wong *et al.*, 1999). In addition, oxidative stress represents an important factor determining the direct damage to the BBB, affecting tight-junctions structure and homeostasis, with consequent disruption of BBB tightness (Lehner *et al.*, 2011). Excitatory neurotransmitters (like glutamate and serotonin), histamine, arachidonic acid, endothelin-1, *etc.* also contribute to negatively affect the barrier functionality (Abbott, 2002). Enzymes like metalloproteases (MMPs) released by circulating or activated brain resident myeloid cells also play a primary role in disrupting cell junctions, basal lamina and overall the well-being of the barrier (McColl *et al.*, 2008; Stolp and Dziegielewska, 2009). However, the principal inflammatory messengers to readily affect the BBB are the pro-inflammatory cytokines, in particular TNF-α, IL-1β, IL-6 and interferons (IFNs), typically released during inflammatory reaction in response to infections or other insults; they show a strong influence on the BBB behaviour (Nadeau and Rivest, 1999; McAllister and van de Water, 2009; Stolp and Dziegielewska, 2009), on BMECs (Lopez-Ramirez *et al.*, 2012) and direct and indirect effects within the CNS, as reviewed in Figure 6.2.

Most of the studies have focused on TNF-α, since it is considered to be the one most readily released during inflammation, initiating the so called acute phase reaction. It is clinically relevant, since it is implicated in several neurological disorders, mainly AD, PD and depression. Moreover, TNF-α is believed to play a key role within the pathological process of multiple sclerosis and its animal model of experimental autoimmune encephalomyelitis (EAE). In particular, not only it is produced by T lymphocytes invading the brain parenchyma, but it is also up-regulated in the serum of several patients before a relapse of active disease and it negatively affects the BBB and its peculiar tightness, while positively regulating the expression of adhesion molecules like ICAM-1 and VCAM-1, which represents a strong activation of the cerebrovascular endothelium (Minagar and Alexander, 2003; Silwedel and Forster, 2006).

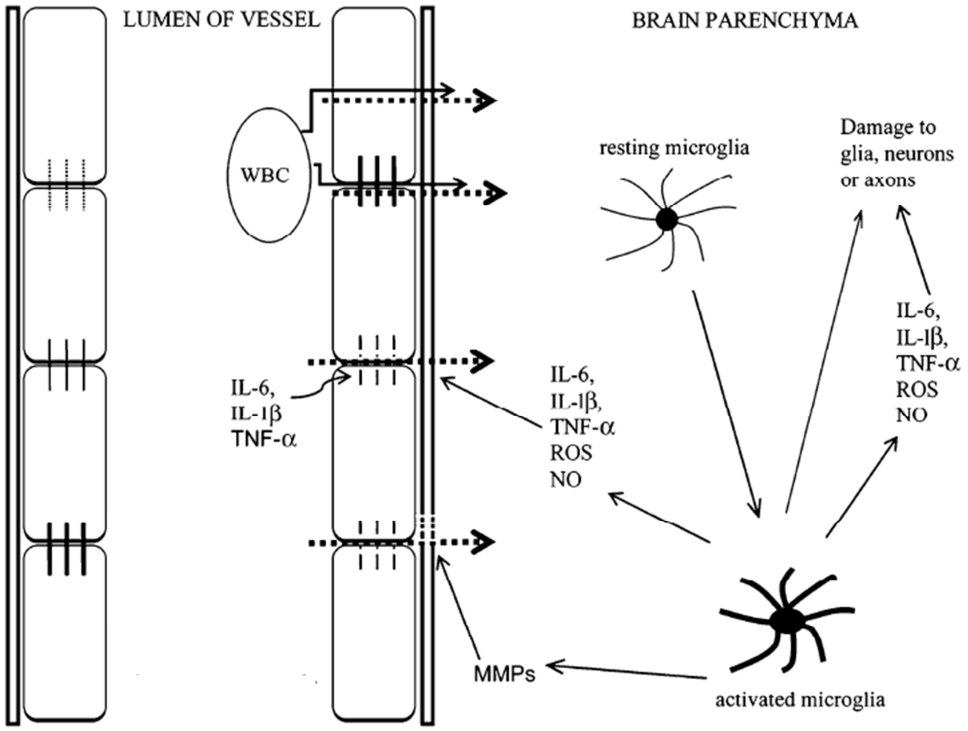

Figure 6.2 The impact of pro-inflammatory cytokines on the endothelium of the BBB. Systemic inflammatory mediators can signal through the endothelium of the BBB and cause alterations of the tight junctions with a consequent increased permeability, increased expression of adhesion molecules, release of cytokines in the brain parenchyma and subsequent activation of the resting microglia, which can become over-activated and cause neuronal damage. As a consequence of these events, white blood cells may be able to move through BBB. Adapted from Stolp and Dziegielewska, 2009.

TNF-α is believed to stimulate the production of soluble mediators, such as prostaglandins and nitric oxide in the endothelium of brain capillaries as well as in the more accessible CVOs, which would represent the molecules to carry the signal into the brain parenchyma (Nadeau and Rivest, 1999). The BMECs highly express receptors for all the major inflammatory cytokines. In particular, TNF-α shows the ability to bind two receptors, respectively called TNF receptor type-1 (TNF-R1 or p55) and TNF receptor type-2 (TNF-R2 or p75), both of which present a death-domain in their cytosolic C-terminal portion. TNF-R1 and TNF-R2 (in fewer amounts) are both expressed on BBB (Nadeau and Rivest, 1999; Pan and Kastin, 2002). They both bind soluble trimeric forms of TNF-α as well as membrane-bound trimeric forms. Moreover, since the cytosolic domains are particularly different between the two receptors, it is believed that this may be linked to differential signalling triggers (Nadeau and Rivest, 1999).

In fact, p55 TNF-R1 is implicated in the upregulation of iNOS, COX enzymes, the adhesion molecules, the apoptotic pathway and the activation of NF-κB, while p75 TNF-R2 is more involved in cytokine production and integrin up-regulation.

Several cytokines have been studied for their ability to cross the BBB and TNF-α is among these; interestingly, for TNF-α this occurs through the same TNF-α receptors, in a saturable and highly specific fashion, as shown by Pan & Kastin (Pan and Kastin, 2002). In pathological conditions, modelled by EAE, the transport of this relevant cytokine appears to be highly up-regulated, with important clinical implications (Pan *et al.*, 1996).

6.2.1.2.1 Signalling pathways triggered by TNF-α and disruption of BBB

We are now aware that cytokines can be actively transported through the barrier, so they are able to directly target CNS-resident cells (Nadeau and Rivest, 1999). However, being messenger molecules, TNF-α and other molecules main role is to take part in a signalling cascade involving a specific order of cells to be targeted and consequent amplification of the signal at each step to be achieved, in order to generate the appropriate response. Targeting BMECs is an essential step in the communication brought by pro-inflammatory cytokines. The signalling cascades triggered by cytokines are extremely complicated and ramified, as evident from the simplified cartoon on Figure 6.3, which exemplifies the TNF-α-triggered signalling. Not all of these pathways are activated upon binding of the ligand, since extensive cross-talk between them exists and usually one dominates over the others. For example, the nuclear factor-κB (NF-κB) negatively affects apoptosis signalling. Concurrent stimulation of other cytokines in the same cell (as happens during inflammation) can shift the balance towards a specific pathway and a specific functional response. In this way, a restricted number of signalling molecules can simultaneously trigger a vast array of responses on various cells with different roles, defining the appropriate inflammatory response.

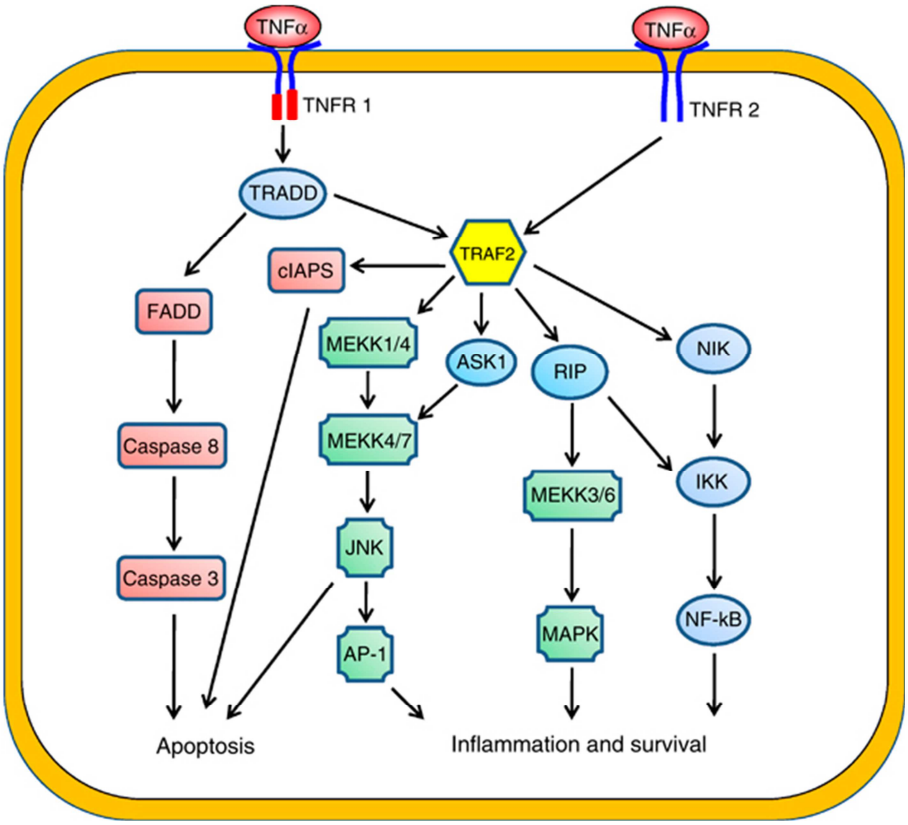

Figure 6.3 Signalling pathways triggered by TNF-α. The cytokine can activate different pathways to induce apoptosis, cell survival or inflammation. In inflammation, TNF-α induces a strong activation of the stress-related JNK group, evokes the activation of p38-MAPK while it is responsible for minimal activation of the classical ERKs. Activation and nuclear translocation of NF-κB is another important pathway occurring in inflammation, which ultimately results in the NF-κB-driven transcription of some important inflammatory genes. Other signalling pathways, not depicted here, include phosphatidylinositol-3-kinase (PI3K)/Akt, which also promotes cell survival. Adapted from (Zhou *et al.*, 2008; Wu and Zhou, 2010).

At the level of BMECs, TNF-α results in increased leakiness and signalling through the BMECs, with the scope to communicate inflammation in the brain parenchyma. In addition, TNF-α can be highly cytotoxic: especially at high concentrations, it triggers the caspase-3/7 pathway and apoptotic cell death program, as recently described in the same *in vitro* cell model we currently use (Lopez-Ramirez *et al.*, 2012): understandably, cell death strongly contributes to the increase in permeability seen in inflammatory conditions. This cytokine is also able to trigger gene transcription through activation of NF-κB: in fact, blockade of this proved to be extremely protective towards the negative effects of inflammation on the endothelium (Zhou *et al.*, 2008). Moreover, quick changes in endothelial cell morphology and permeability are also caused by mechanisms that have been proved to be linked to

activation of RhoA (Wojciak-Stothard *et al.*, 1998; McKenzie and Ridley, 2007) and consequent changes in cortical F-actin, gap formation and negative effects on cell-cell junctions. Although the presence of this signalling pathway has not yet been proved at the level of BMECs, all the mentioned consequences of the cytokine-mediated inflammatory action have been identified by several investigators (Minagar and Alexander, 2003; Deli *et al.*, 2005; Miller *et al.*, 2005; Silwedel and Forster, 2006), confirming the negative impact of pro-inflammatory stimuli and the ultimate disruption of barrier properties. In detail, TNF-α (with or without other accessory cytokines) caused not only paracellular permeability augmentation, by negatively regulating gene transcription, functional localisation and expression of tight-junction proteins such as like occludin (Silwedel and Forster, 2006; Forster *et al.*, 2008; Lopez-Ramirez *et al.*, 2012), claudin-5 (Silwedel and Forster, 2006; Forster *et al.*, 2008; McColl *et al.*, 2008), ZO-1 (Aveleira *et al.*, 2010; Lopez-Ramirez *et al.*, 2012) and JAM-A (Haarmann *et al.*, 2010), and adherens junction proteins such as VE-cadherin (Lopez-Ramirez *et al.*, 2012), but also increased transcytosis (Miller *et al.*, 2005), increased vesicular trafficking, adhesion molecule expression and leukocyte endothelial adhesion and migration (Minagar and Alexander, 2003). All the modifications appear to be triggered through JNK and apoptosis-independent caspase mechanisms, as described (Zehendner *et al.*, 2011; Lopez-Ramirez *et al.*, 2012). In order to perpetuate the inflammatory signal from the periphery into the brain parenchyma, BMECs are also able to synthesise cytokines (Frigerio *et al.*, 1998) and easily-diffusible lipid mediators like prostaglandins (Ek *et al.*, 2001) upon cytokines binding. All these responses strongly impact on the surrounding environment, on neurons but in particular on the highly reactive microglia cells.

In summary, increasing evidence supports the existence of periphery-to-central cross-talk whose primary aim is to generate and assist the resolution of the events; endothelial cells of brain microvasculature are main protagonists in this phenomenon, contributing to the signalling between the two compartments. Inflammation-dependent BBB alterations may therefore result in immediate damage of the brain or in a subtle increase of the brain susceptibility to damage later on during life course, as in the case of developmental inflammation (Stolp and Dziegielewska, 2009).

6.3 Sex dimorphism and role of sex hormones

Several disorders with an immune-inflammatory component present a sex (and age) bias in their presentation and pathophysiology. For example, rheumatic arthritis is more common and severe in women, as well as many other autoimmune diseases. Sex influences strongly characterise the brain, which has been correctly defined as sexually dimorphic: evidence of CNS developmental differences between males and females are becoming clearer and involve changes in synaptogenesis, population of the brain parenchyma by neuroglia and size of nuclei (Bale, 2009). However, the influence of sex hormones does not stop at the developmental level, but lasts throughout life, with different intensity, involving also other aspect of CNS physiology, like neuro-immunity and neuro-inflammation. Across a broad range of human CNS diseases, a significant difference between males and females in incidence, age of onset and severity can be seen. Neurological conditions such as attention deficit/hyperactivity disorder and schizophrenia (more common in males), neurodegenerative disorders like Alzheimer's disease (male:female ratio around 1:3), Parkinson's disease (male:female ratio almost 2:1), stroke, multiple sclerosis (Nilsson, 2007; Vegeto *et al.*, 2008) show different incidence between males and females, at certain ages. Sex hormones are most likely involved, although the mechanisms are not fully clear. Most of them belong to the steroid hormone category, produced by the gonads or the adrenal glands; some other tissues also show the ability to synthesise them by conversion of other sex steroids. In this class of molecules we should mention androgens, like testosterone, estrogens, like estradiol, estriol and estrone, and progestogens, like progesterone.

6.3.1 Estrogen hormones: a short overview

Trying to summarize sex-linked endocrinology is a complex task, since this truly represents one of the widest scientific areas of interest, due to the numerous implications of sex hormones in several life actions: some have attempted this task and I address the interested reader to these authors' work (Brook, 1999; Gillies and McArthur, 2010a). Among all the sex hormones, estrogens (and particularly 17 β-estradiol, the most potent among the three, roughly 10 times more than estrone and 80 times more than estriol) represent the main regulatory female hormones plus offer an advantageous factor, since they provide

protection in diseases prevalent in men; the fact that most of such protection appears rapidly lost after menopause, with the concomitant decrease of these sexual hormones, supports such definition. However, the latest evidence on estrogens shows these hormones have extremely important roles also in men, since many tissues express the enzyme called aromatase, which is able to generate estrogen from circulating male hormone testosterone (Gillies and McArthur, 2010a). This is true particularly in the brain, where enzymatic activity has been detected to be quite strong at the level of different cell types such as astrocytes and neurons.

As for all the steroidal hormones, estrogens derive from cholesterol through a complex series of synthetic reactions which involve several enzymes, most of which (including aromatase) are members of the huge cytochrome P450 superfamily. Stimulation of synthesis of estrogens in the female gonads (the ovaries) is triggered by a specific hormonal cascade which involves the gonadotropin releasing hormone (Gn-RH), followed by the folliculo-stimulating hormone (FSH) and the luteinizing hormone (LH). Interestingly, several non-reproductive tissues, like some brain resident cells, show the capability to synthetize estrogen from male hormones (BMECs, via aromatase) or from cholesterol (astrocytes) in a way independent of the gonadotropins (Krause *et al.*, 2006).

Estrogens can freely diffuse through cell membrane thanks to their amphipathic nature and they exert their functions through estrogen receptors, which are divided in two classes: the classic estrogen receptors, present in two isoforms, estrogen receptor α (ERα) and estrogen receptor β (ERβ) and the more recently discovered estrogen G-protein coupled receptor GPR30 (GPER) (Hazell *et al.*, 2009).

These hormones can mediate their actions through 2 different signalling pathways: the genomic and the non-genomic pathway. Classic ERs belong to the nuclear receptor superfamily and usually work as ligand-activated transcription factors, which are normally present in the cytosol but can dimerize and migrate into the nucleus upon ligand binding, where they can recognize and bind on estrogen responsive elements (EREs) present in the regulatory sequences of genes (Gillies and McArthur, 2010a). In this way, transcription of estrogen-responsive genes can be triggered or repressed (according to the mechanism adopted by the receptor and the type of co-activators or co-repressors that are recruited in

the site) and expression of the gene product modulated. It is possible that classic ERs can also work independently from ligand binding (*ligand independent pathway*), for example through phosphorylation triggered by other stimuli (Cenni and Picard, 1999). Moreover, regulation of genes which do not have EREs elements on their promoter, through interference with the binding of other transcription factors, was also shown (*ERE-independent pathway*) (Kurebayashi *et al.*, 1997; Harrington *et al.*, 2003).

The non-genomic pathway was discovered by observing estrogen-dependent effects too rapid to be a consequence of transcription-mediated effects; they usually involve increased intracellular Ca^{2+} by an action on intracellular stores or through an action on calcium channels, regulation of nucleoside (cAMP, cGMP) fluxes, transactivation of membrane receptors, and activation of various kinases involved in intracellular signalling perpetuation such as PKA, PI3K, MAPKs and ERKs. These effects were shown to be mediated either by membrane-associated classic ERs, apparently concentrated at specific cell membrane functional spots (caveolae) or by GPR30. These quick responses can either target specific molecules already existing within the cell by post-translationally modifying their action, or they can ultimately converge with the genomic pathway to affect gene transcription and protein synthesis in a more rapid way. These and other properties of the hormones, extensively reviewed in more comprehensive articles (Arnal *et al.*, 2007), make estrogens an extremely interesting target of study.

6.3.1.1 Regulation of ANXA1 by estrogens

ANXA1 expression and action is intimately regulated by steroids like glucocorticoids (Solito *et al.*, 2003b; Parente and Solito, 2004; Perretti and D'Acquisto, 2009; Perretti and Dalli, 2009); this triggered growing interest to see if and how the molecule was affected by estrogens and in particular by the most potent 17β-estradiol. An early report indicated up-regulation in synthesis and secretion of ANXA1 by 17β-estradiol (Castro-Caldas *et al.*, 2001) in a human lymphoblast leukaemia cell line. Our group was the first to prove a direct transcriptional effect of estrogen at the level of ANXA1 human and mouse promoter (Solito *et al.*, 2003a): as reviewed in Figure 6.4, we investigated the presence of putative ERE consensus sequences, according to the optimal binding sequence described by others

(Driscoll *et al.*, 1998; Gruber *et al.*, 2004) both in mouse and human promoters through a server for the prediction of known regulatory transcription elements (Farre *et al.*, 2003). Overall, we were unable to detect palindromic ERE sequences in either promoters, but only regions with a reasonable similarity (within 85% similarity) to half of the consensus ERE for ERα and ERβ, while the mouse *AnxA1* gene promoter showed also some other less similar putative elements upstream, indicating therefore a higher potential responsiveness. Other works confirmed our findings, for example by showing that ANXA1 was transcriptionally induced by estradiol in a model of breast cancer, mediating the anti-proliferative effect of the hormone (Ang *et al.*, 2009), while Davies *et al.* (Davies *et al.*, 2007) showed that ovariectomy in rodents negatively affected the expression of ANXA1 in the pituitary gland, while estradiol replacement restored it.

More recently, estradiol was shown to swiftly modulate ANXA1 location on the membrane of human polymorphonuclear (PMN) leukocytes in a non-genomic fashion and to confer an anti-inflammatory profile upon inflammatory stimuli (Nadkarni *et al.*, 2011) while in the brain microvasculature, ANXA1 has been shown to be mediator of the protective action of estradiol under inflammatory conditions, limiting the excessive adhesion of leukocytes on post-capillary venules (Hughes *et al.*, 2012).

Overall, despite the mechanisms of regulation being still not fully clear, increasing evidence is supporting the direct influence of estrogen on the expression and functional modulation of our molecule of interest.

6.3.1.2 Impact of 17 β-estradiol in the CNS and brain microvasculature

Several experimental and clinical studies have shown the influence of estradiol in the CNS, where it was proved to be involved in learning and memory mechanisms, mood definition and neurological development [for an extensive review refer to (Gillies and McArthur, 2010b)]. On the clinical side, epidemiological studies comparing reproductive or senescent female and male patients have triggered great interest in estrogen-based treatments as a possible therapy for neurodegenerative and neuro-inflammatory disease, leading to the initiation of several clinical trials (Nilsson, 2007; Vegeto *et al.*, 2008).

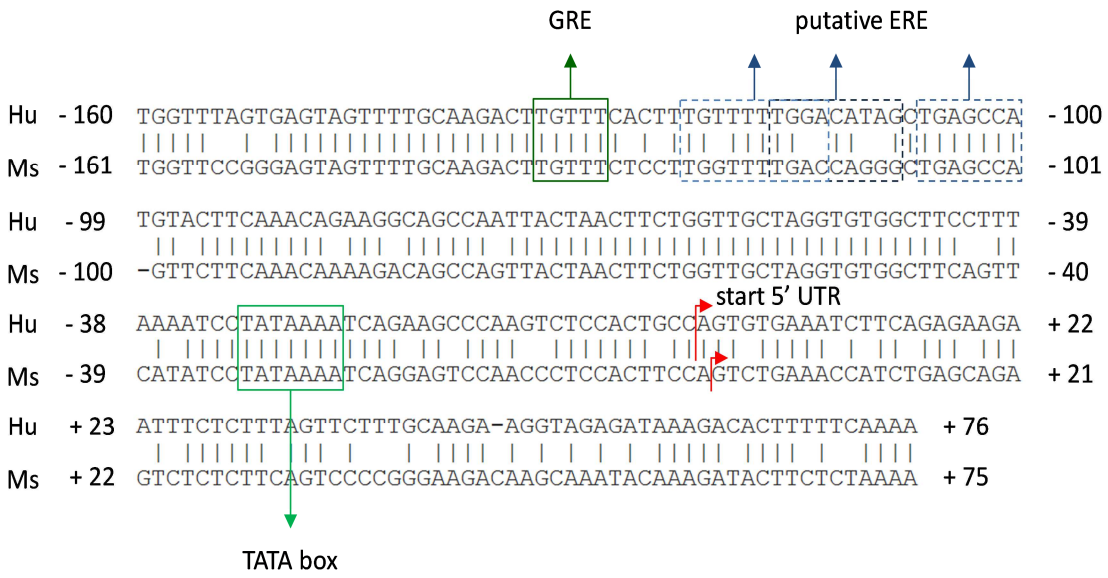

Figure 6.4 Comparative analysis of human and murine Annexin A1 promoter sequences. The figure reviews the finding reported in (Solito *et al.*, 2003a). The human (Hu) and murine (Ms) promoter sequence comprised in the first 1000 bp upstream the beginning of the first region, the 5' UTR, including the TATA box, were selected for human and murine *Annexin A1* genes through UCSD Genome Browser and compared by BLAST® algorithm, identifying a stretch of around 200 bp with overall 82% identity. Through the PROMO ALGGEN server (Farre *et al.*, 2003), a software for prediction of known transcription regulatory elements on DNA sequences, GRE and ERE putative sequences were identified within the sequence of interest, allowing for maximum 15% matrix dissimilarity between the query and the consensus.

Initial studies have shown their protective action towards neurological disorders when presented in physiological concentrations/doses, in particular by triggering molecules with a neuro-trophic action, or with anti-apoptotic properties (Gillies *et al.*, 2004), or stimulating the proliferation of stem cells helping regeneration (Maggi *et al.*, 2004; Vegeto *et al.*, 2008). Above these effects directly impacting on the affected neurons, estradiol is believed to possess strong immune-modulatory properties, which are exerted on the inflammatory reactions triggered in the CNS during neurodegenerative conditions. In particular, Vegeto's group and others (Maggi *et al.*, 2004; Krause *et al.*, 2006; Vegeto *et al.*, 2008) have elegantly shown the modulatory role on activated microglial cells, reducing pro-inflammatory cytokines and mediators release, their phagocytic phenotype, the production of ROS and nitric oxide via inducible NO synthase (iNOS), the activity of cyclo-oxigenases (COXs) which are all factors involved in the perpetuation of the disease.

Some evidence is arising concerning the ability of estradiol to reduce the expression of adhesion molecules on brain microvasculature, hampering the recruitment of more inflammatory molecules into the CNS. This has been observed in the case of AD and MS, offering new possibilities for therapeutic amelioration (Maggi *et al.*, 2004; Vegeto *et al.*, 2008). Nitric oxide by endothelial NO synthase (eNOS) was also shown to be regulated in the endothelium (Nilsson, 2007), along with mitochondria functions [important for energy purposes, highly required in endothelium (Yang *et al.*, 2005; Herson *et al.*, 2009)]. Also, estradiol showed clinical impact on the outcome of vascular-related diseases such as stroke and consequent vasogenic oedema (Nilsson, 2007; Herson *et al.*, 2009), indicating therefore direct implications on the brain vasculature. This also extends the discussion to the regulation of the integrity of the BBB and of barrier permeability, which is strongly affected by inflammation as explained earlier. Estradiol was shown to ameliorate the permeability of the BBB *in vivo*, since female mice appeared to possess a significantly less permeable barrier while experiments involving ovariectomy or animals in reproductive senescence showed that this advantage over males was eliminated (Bake and Sohrabji, 2004; Sohrabji and Bake, 2006; Bake *et al.*, 2009). Cell junctions like occludin were shown to be negatively modulated in absence of sex hormones, such a phenomenon being reversed by estradiol replacement (Kang *et al.*, 2006). Also claudin-5 expression showed a similar phenotype in aged or ovariectomised animals (Bake and Sohrabji, 2004; Burek *et al.*, 2010). These results justify aging-related BBB weakness and have been taken as partial explanation for the fact that several neurological disorders shown amelioration during pregnancy (when levels of estradiol are very high) and exacerbation in post-menopause or in the post-pregnancy period (Vegeto *et al.*, 2008; Wilson *et al.*, 2008). Supposedly, these actions are mediated via ERα at BMECs level, limiting the NFκB-mediated effects of inflammation (Galea *et al.*, 2002; Krause *et al.*, 2006; Nilsson, 2007; Vegeto *et al.*, 2008). Only few scattered reports to our knowledge have attempted to investigate the protection offered by the steroid from the BBB integrity point of view. One (Galea *et al.*, 2002) showed that pre-incubation with estradiol was able to limit the upregulation of adhesion molecules on endothelial membrane by blocking the inflammation-induced DNA binding by the transcriptional factor NFκB.

The most closely related study (Forster *et al.*, 2008) indicates a protective effect on hCMEC/D3 cell line under TNF-α offered by the glucocorticoid hydrocortisone, which parallel the inductive effects shown by the synthetic glucocorticoid dexamethasone under non-inflammatory conditions (Romero *et al.*, 2003). Therefore, knowing the impact that estradiol are believed to have on tightness properties of the brain barrier and with the evidence produced on estrogen modulation of ANXA1 promoter (Solito *et al.*, 2003a), we **hypothesised** a protective role under inflammatory insults by this hormone, through the modulation of the molecule Annexin A1.

6.3.1.3 Therapeutical exploitation of estradiol

Many studies approaching the "bench-side" have been disappointing so far, partly due to a lack of knowledge about the molecular mechanisms and about the timing of action of estradiol, therefore triggering the need to clarify how and when this hormone becomes beneficial. Past and more recent evidence clearly supports a beneficial effect of estradiol but what years of studies on estrogen dosing for hormonal replacement therapies (HRTs) have taught, is that supplementation of hormones (estradiol and progesterone) needs to occur in a very controlled and tight fashion; in fact, the Women's health initiative memory study (WHIMS) indicated an increased risk for dementia and cognitive impairment for women choosing HRT when already in menopause (Sohrabji and Bake, 2006). Also, recent evidence has demonstrated clearly that combinations of endogenous gonadal hormones, more than single ones, truly regulate the immunological status of the CNS (Sohrabji and Bake, 2006). This evidence was followed by findings of high hormonal doses resulting in detrimental effects like in the case of vascular-related diseases as stroke (Herson *et al.*, 2009) or in the modulation of important molecules like occludin (Ye *et al.*, 2003), while replacement after a long period of low hypoestrogenicity did not produce protection in a model of aged animals (Bake and Sohrabji, 2004).

The neuro- and vascular-related protection tightly depends on the clinical situation and experimental procedure. Beneficial effects of estrogen have been pre-clinically achieved only when given before the inflammatory burst, while it proved ineffective or even detrimental when provided after the initiation of the reaction (Vegeto *et al.*, 2008).

It is clear, therefore, that timing of hormonal replacement in relation to the target, the stage of menopause and the initiation of the inflammatory challenge has a huge importance. Interestingly, some studies on murine models have evidenced how hormones normally not released by male gonads, like estradiol, could play a detrimental role in neurodegenerative conditions when administered in the male individuals (Gillies *et al.*, 2004). This is one of the reasons why novel research has been looking for endogenous mediators of these hormones, which may modulate the mechanism of action in a less invasive fashion compared to that offered by exogenously given hormones and may suggest novel exploitable applications.

6.4 Methods

Please refer to Chapter 3 for the description of general *in vivo* and *in vitro* procedures. Here I will provide details about certain technical aspects of procedures specifically used for the purpose of only this chapter. Please refer to the Appendix (Chapter 10) for solutions composition.

6.4.1 *In vivo* techniques

6.4.1.1 *In vivo* experimental plan

In order to evaluate sex dimorphic responses to peripheral inflammation in terms of barrier permeability changes, we compared males and females C57Bl/6 mice over the time after challenging them *i.p.* with a single dose (3 mg/kg) of LPS, followed by *i.v.* Evans Blue circulation for 1 hour and subsequent evaluation of extravasation in the brain parenchyma as described (Section 3.2.1.3). LPS exposure time points analysed were: 4 hours (3 hours + 1 hour Evans Blue circulation); 24 hours (23 hours + 1 hour Evans Blue circulation) and 7 days (7 days + 1 hour Evans Blue circulation). Section 10.9 (Figure 10.4; Panel A) in the Appendix describes the experimental plan.

Since we detected significant differences between males and females after 4 hours LPS exposure (Figure 6.5), we decided to use this as end-point for the following experiment involving ovariectomy of female C57Bl/6 animals.

6.4.1.2 Surgical rodent ovariectomy

This procedure was performed by expert veterinary surgeons at Charles River Laboratories, according to the published guidelines (Burek *et al.*, 2010). Comprehensive description is reported in the Appendix, Section 10.8.

6.4.2 *In vitro* techniques

6.4.2.1 *In vitro* experimental plan

For permeability studies, hCMEC/D3 were grown on transwell filters; when cells reached 100% confluence, medium was changed to complete EGM-2MV without VEGF for 4 days (tightness incubation period) and stimuli were provided during this period of time. In detail, long incubation with 17β-estradiol (100 nM) or with the monoclonal antibody (or with the isotype control) occurred for 4 days, providing a repeated dose every 24 hours. Short incubations with the hormone occurred within the last 24 hours of the tightness incubation period. TNF-α and IFN-γ were both provided together at 10 ng/ml in the last 8 or 24 hours of the incubation period. For all the expression studies, cells were grown on tissue culture-treated 24- or 12-well plates at a density that allowed becoming fully confluent and tight after 4 days of growth. This allowed us to perform long incubations with the stimuli (up to 4 days). This choice was made to obtain conditions resulting in healthy growth and reproducible results in a setting close to what observed in functional permeability studies. In fact, we observed that non-polarized monolayers grown on surfaces other than transwell tend to overgrow and suffer once they reach 100% confluence, preventing us from keeping them in culture for long (4 days) incubations in such conditions. Figure 10.4, Panel B in the Appendix describes the experimental plan for *in vitro* experiments.

6.4.2.2 Estrogen receptors agonists and antagonists

In order to investigate which estrogen receptor(s) is involved in the modulation of ANXA1, we made use of highly specific agonising and antagonising molecules. The agonists chosen were: propylpryazole-triol (PPT) for ERα (used at EC_{50}=200 pM); Diarylpropionitrile (DPN) for ERβ (used at EC_{50}=850 pM); bromo-benzodioxol-tetrahydro-cyclopenta-quinolin-ethanone (G-1) for GPR30 (used at 20 nM). The antagonists were: Phenyl-trifluoro-methyl-pyrazolo-pyrimidin-phenol (PHTPP) for ERβ (200 nM pre-incubation for 10 minutes, followed by 100 nM β-estradiol); bromo-benzodioxol-cyclopenta-quinoline (G-15) for GPR30 (200 nM pre-incubation for 10 minutes, followed by 100 nM β-estradiol). Total incubation time was 8 hours (β-E peak of ANXA1 induction of either intracellular or extracellular ANXA1).

6.4.2.3 Quantitative reverse transcription (RT) PCR

RNA from untreated and treated cells was extracted using Qiagen RNeasy Mini Kit (Qiagen, UK). 1 µg of RNA was reverse-transcribed for 2 h at 42°C using 30 International units (IU) of AMV retrotranscriptase (Promega Ltd, UK) according to manufacturer instructions, with oligo$(dT)_{15}$ (Promega, UK) and RNAsin Ribonuclease inhibitor (Promega, UK). Negative controls were also included (a reaction without RNA). 5 µl of RNA solution were taken from each sample and used to create a mix solution. 100, 10 and 1 ng of reverse-transcribed RNA were analysed in triplicates by quantitative PCR according to manufacturer instructions (Quantitect SYBR green PCR kit; Qiagen, UK) and the following thermal cycle: initial denaturation - 15 mins, 95°C; 40 cycles comprising denaturation – 15 sec, 94°C, annealing – 30 sec, 60°C, extension – 30 sec, 72°C. Data acquisition was performed during each extension cycle and melting curves were produced during the final ramping step up to 95°C.

Each set of primers (specific for SYBR green quantitative PCR and purchased from Qiagen, UK; the sequence is undisclosed) was tested for optimal efficiency first.

A linear standard curve was generated:

$$\text{threshold cycle } (C_t) \textit{ vs. } \log_{10}(\text{reverse-transcribed RNA loaded quantity})$$

From this curve, the quantity of reverse-transcribed RNA giving a C_t around 22-26 (in the middle of the exponential phase of the reaction) was calculated and the slope of the curve was used to calculate the efficiency of the reaction as:

$$E = 10^{-1/\text{slope}}$$

Efficiency values around 1.8/2.2 (representative of reactions where the number of products double at every cycle) were considered satisfying (Pfaffl, 2001; Bustin, 2010).

Since we decided to use a highly expressed housekeeping gene, the ribosomal RNA 18S (rRNA18S), we chose to use $C_t = 15$ to calculate the quantity of reverse-transcribed RNA that needed to be analysed, because this value was in the middle of the exponential phase, therefore in the quantitative part of the whole reaction; moreover, the quantity of reverse-transcribed RNA was, in this way, more similar to the ones that needed to be loaded for the other primers, therefore the role of normalization through the housekeeping gene was

more reliable. After all these considerations, a second reaction was set up: the amounts of reverse-transcribed RNA calculated for each set of primers were loaded in triplicates for all the samples to be assayed. The new mathematical model presented (Pfaffl, 2001) was applied in order to obtain a relative quantification of the target genes, normalized towards the reference housekeeping gene.

The ratio "treated sample *vs.* control" was calculated as:

$$\text{Ratio} = \frac{(\text{E target gene})^{\Delta\text{Ct (control – sample)}}}{(\text{E reference gene})^{\Delta\text{Ct (control – sample)}}}$$

This mathematical model has been considered as the most precise one among those available so far, because it results in precisely describing if and how treated cells differ compared to the untreated controls, exploiting one (or more) reference genes as normalization means, in order to limit the effect of intra-assay variability; moreover, it does not assume a perfect reaction efficiency of 2 as other models do but it includes the efficiency value inside the final equation, so that these have their own weight.

6.4.3 Immunofluorescent detection of FPR2 on hCMEC/D3 surface

To evaluate the level of surface expression of FPR2, hCMEC/D3 cells were plated in collagen-coated labtek chambers at low density to allow a more detailed microscopy analysis. Cells were treated or not with β-estradiol, TNF-α and IFNγ and at the end of the stimulation they were pre-labelled with anti-FPR2 monoclonal antibody diluted in DPBS with Ca^{2+}/Mg^{2+} for 1 h at 4°C, under agitation. Under these conditions, only receptors present on the cell surface bind the antibody, without internalizing. Cells were then washed and fixed for 10 minutes with 4% PFA. Fluorescent staining was performed by Alexa488-conjugated anti-Ms IgG and mounting with Prolong® anti-fade mountant (Invitrogen, UK) followed by confocal microscopy (Maderna *et al.*, 2010).

6.4.4 Surface-bound ANXA1 retrieval

In order to obtain ANXA1 molecules non-covalently bound on cell surface in a Ca^{2+} dependent manner, stimulated hCMEC/D3 were washed briefly with DPBS with Ca^{2+}/Mg^{2+} and incubated for 20 minutes at 4°C under slow agitation with a small volume of 1 mM EDTA, 1 mM EGTA in DPBS without Ca^{2+}/Mg^{2+}. Subsequently the liquid was retrieved, briefly spun down to remove any detached cells and frozen for further assessment.

6.5 Results

6.5.1 BBB-related sex differences towards peripheral inflammation

Figure 6.5, Panel A shows a clear sex-dependent response of the BBB permeability to a single peripheral dose of LPS (3 mg/kg) in wild-type young adult (2 months old) mice: male animals responded with an increased Evans Blue extravasation after 4 hours from LPS *i.p.* administration, while female animals did not show such change. Basal tightness was restored in the following time points (24 hours and 7 days). In contrast, the same analysis in Anxa1 null mice (2 months) presented higher (10-fold) permeability values but loss of sex-related response.

To observe if such behaviour was linked to circulating sex hormones, we performed an *in vivo* barrier permeability assessment using reproductively senescent (15 months old) female wild-type animals, which were compared to young adult female counterparts and challenged *i.p.* with LPS for 24 hours. Interestingly, we detected (Figure 6.5; Panel B) a significant increase in dye extravasation in the aged-animals, supporting the growing evidence for the involvement of a female sex-hormone in the BBB. Interestingly, we did not detect basal differences in terms of dye extravasation between young and old female animals, which closely match other reports in literature (Sandoval and Witt, 2011).

In order to investigate if 17 β-estradiol (17 βE) participates in protecting the brain barrier from opening under peripheral inflammatory insult, we performed ovariectomy on a set of young adult female wild-type animals, which were implanted with osmotic mini-pumps constantly releasing either 17 β-estradiol or the vehicle cyclic oligosaccharide β-cyclodextrin (Burek *et al.*, 2010). As illustrated in Figure 6.5, Panel C, ovariectomy did not cause increase in the basal dye extravasation rate, while vehicle replacement impaired the female-dependent protection towards peripheral inflammation (4 hours post LPS *i.p.* administration, the time point where sex differences where initially observed; Figure 6.5; Panel A) which was provided in intact young females. Replacement of 17 βE as the only sex hormone allowed restoration of the protective phenotype, indicating that at least partial involvement of the steroid.

Since we were ultimately interested in the role of ANXA1 as a BBB-specific modulator in the cross-talk between peripheral inflammatory events and CNS responses, we went to investigate Anxa1 expression at the level of brain microvessels, isolated as described in Chapter 4. To our surprise, we could detect basal differences in Anxa1 content in whole lysates between young adult females, old females and males, with the former showing the highest intensity of expression (Figure 6.5; Panel D). Under acute inflammatory challenge, Anxa1 expression increased in the young females, while the other two groups did not show any change, supporting our hypothesis of a direct female-related modulation of the Anxa1 expression at the level of the brain barrier in presence of inflammation.

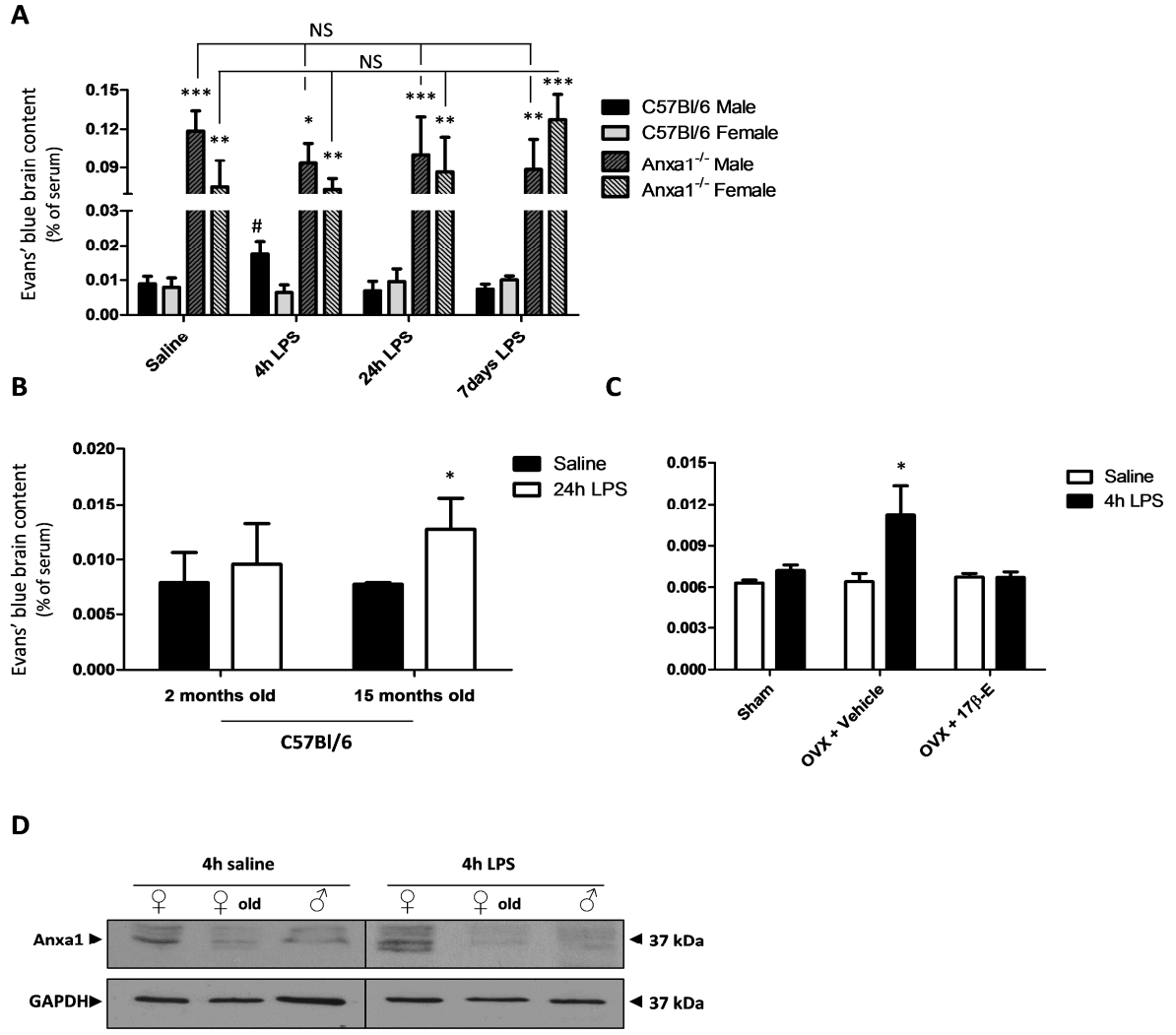

Figure 6.5 Sex influences barrier responses to peripheral inflammation. A| Young adult (2 months old) wild-type (C57Bl/6) and Anxa1$^{-/-}$ mice (*n*=5) were pre-treated intraperitoneally with 3 mg/kg body weight of LPS (strain O111:B4) in saline for 3 hours, 23 hours and 7 days or with 100 µl saline (24 hours) as negative control. After the end of incubation time, they were intravenously injected with 100 µl 2% Evans blue in saline. Dye was allowed to circulate for 1 hour, before brain dye

content was assessed spectrophotometrically and normalized to plasma levels. Data are expressed as mean ± SEM. One-way ANOVAs were conducted to compare genotype- and sex-related differences. Tests were followed by Tukey's range *post-hoc* test; *, ** and *** respectively indicate $p<0.05$, $p<0.01$ and $p<0.001$ *vs.* sex-related saline control. # indicates $p<0.05$ *vs.* sex-related saline control. **B|** Wild-type (C57Bl/6) young adult (2 months old) or reproductive senescent (15 months old) females were *i.p.* treated with either 3 mg/kg body weight of LPS (strain O111:B4) in saline for 23 hours or with 100 µl saline and subsequently assessed for Evans blue extravasation as described for Panel A. Two-way ANOVA was performed (age and LPS administration as variables), followed by Tukey's range *post-hoc* test. Interaction between age and treatment was detected. # indicates $p<0.05$ *vs.* age-related saline control and it was considered significant. **C|** Ovariectomised animals were implanted with minipumps constantly releasing either 17 β-estradiol (2 µg/kg/day) or vehicle for 14 days and then assessed by Evans Blue. Two-way ANOVA was performed (hormone replacement and LPS administration as variables), followed by Tukey's range *post-hoc* test. Interaction between hormone replacement and treatment was detected. * indicates $p<0.05$ *vs.* saline-treated groups and the other LPS-treated groups. **D|** Total expression of Anxa1 was assessed on brain microvessels lysates from wild-type C57Bl/6 young, old females and young males by western blotting. Typical examples from $n=3$ mice per preparation are shown here. Panel A was produced with the help provided by Dr. S. McArthur.

6.5.2 ANXA1 expression and release is regulated by 17 β-estradiol

In vivo experiments proposed two important facts: β-estradiol was directly involved in sex-dependent differences shown by the BBB in response to peripheral inflammation and annexin A1 showed a differential behaviour between genders, dependently on hormonal influence.

Without excluding the involvement of other sex hormones towards ANXA1 expression, we decided to simplify our investigation by focusing primarily on ANXA1 modulation by the potent female sex hormone. To do that, we moved back to the *in vitro* model of human BMECs of choice, the hCMEC/D3 cell line.

Figure 6.6 clearly shows the impact of 17 β-estradiol on ANXA1: Panels A and B indicate a dose-dependent effect for both ANXA1 release in cell medium and for ANXA1 cellular content. 100 nM was chosen as optimal dose for further experiments. Interestingly, released ANXA1 showed a fluctuating time-dependent behaviour over the period analysed, indicating a non-linear hormonal modulation; in parallel, we detected a positive effect of estradiol on cellular ANXA1 and a partial time-dependent fluctuating effect, more narrow and limited compared to Panel A.

This finding represents an important aspect to be considered with regard to the physiological oestrous cycle, where release of estradiol in the blood varies over time, with consequent changes from low to high concentrations, achieved by summation of different doses.

In Panel E we studied the effect of β-estradiol from transcription point of view; we identified a quick and strong response on *ANXA1* gene, *FPR1* gene expression appeared to be inhibited by the hormone, while *FPR2* gene transcription peaked at 4 hours and then decreased quickly under basal levels.

Such findings, in particular those depicted in Figure 6.6 Panel E, are in accordance with previous evidence on the ANXA1 promoter responsiveness to hormonal challenges, as described in Figure 6.4. A quick prediction analysis of *FPR1* and *FPR2* human promoters identified (data not shown) in *FPR1* promoter one ERE-like sequence close to the TATA box, while in *FPR2* promoter we identified several ERE-like sequences scattered in the promoter sequence, indicating that also these genes, similarly to *ANXA1*, are directly modulated (as we have seen from the quantitative mRNA studies; Figure 6.6, Panel E) by the hormone. Therefore, ANXA1 behaviour appeared to be intensively modulated by estradiol in all its aspects, from gene transcription, to protein formation and externalisation.

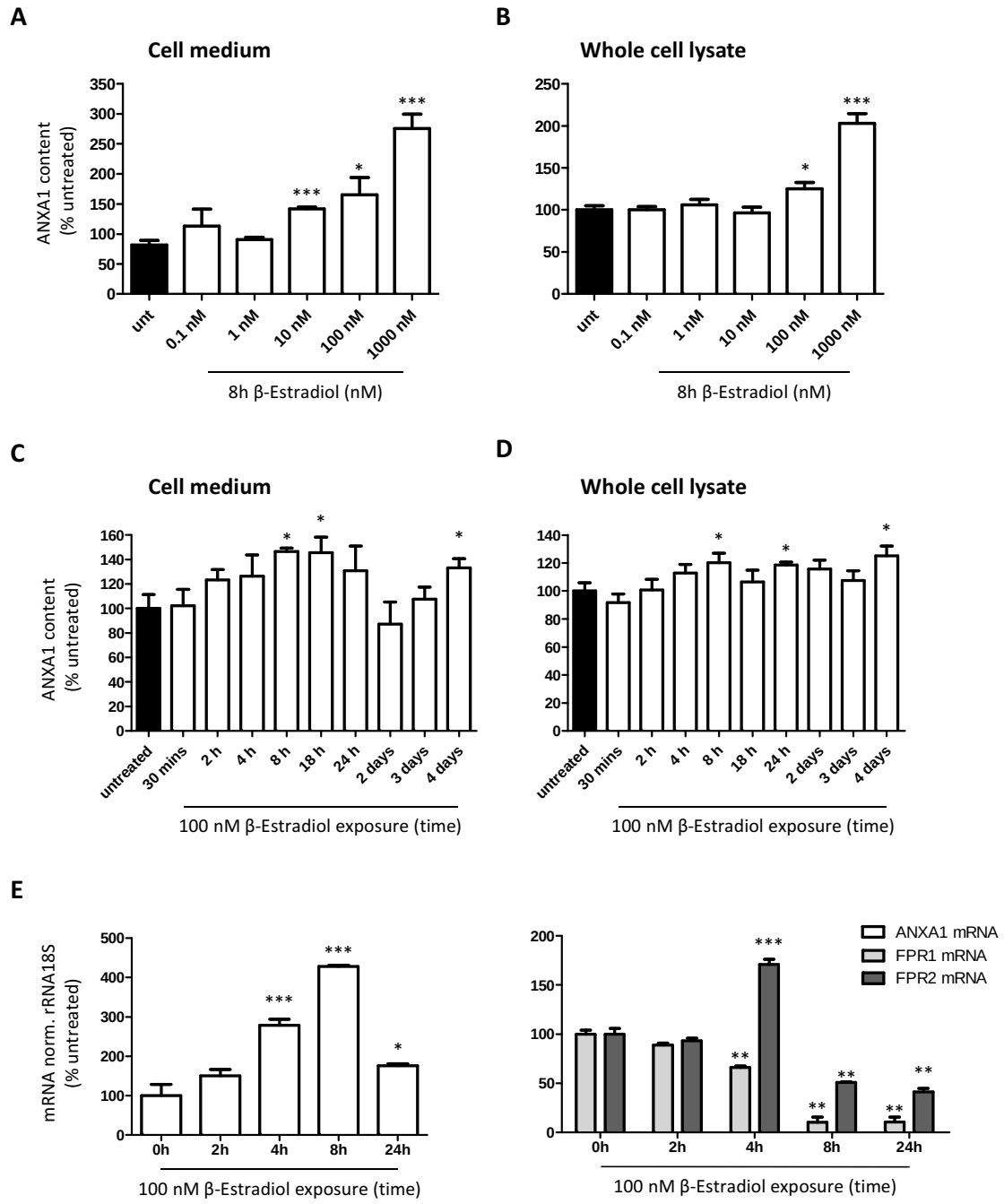

Figure 6.6 17 β-estradiol regulates release and expression of ANXA1 in hCMEC/D3. Dose-response study of ANXA1 **A|** release in cell medium and **B|** quantity in whole cell lysate, assessed by sandwich-ELISA. Exposure to different doses was performed for 8 hours. Data are representative of at least three independent experiments, performed in quadruplicate, expressed as mean ± SEM. One-way ANOVA was performed, followed by Tukey's range *post-hoc* test; * and *** indicate $p<0.05$ and $p<0.001$, respectively. Time-course study of ANXA1 **C|** release in cell medium and **D|** in whole cell lysate. Long-term administration (2, 3 and 4 days) was performed by repeating the dosing every 24 hours. Chosen dose was 100 nM according to the dose-response study. Data are representative of at least three independent experiments, performed in quadruplicate, expressed as mean ± SEM. One-way ANOVA was performed, followed by Tukey's range *post-hoc* test; * and *** indicate p<0.05 and p<0.001 *vs.* untreated, respectively. **E|** Evaluation of transcription regulation of *ANXA1*, *FPR1* and *FPR2* genes by effect of 17 β-estradiol. Quantitative PCR was performed on whole RNA cells

extracts after stimulation with the hormone for different time points, using highly specific qPCR primers as indicated in the methods. Data are representative of three independent experiments, performed in triplicate, expressed as mean ± SEM. One-way ANOVA was performed, followed by Tukey's range *post-hoc* test; *, ** and *** indicate $p<0.05$, $p<0.01$ and $p<0.001$ *vs.* 0 hours, respectively.

6.5.2.1 Estradiol differentially modulates ANXA1 synthesis and release

In order to understand which estrogen receptor(s) is(are) involved in modulating ANXA1, we used specific agonists and antagonists directed towards the two classic ERs, ERα and ERβ, and the more recently discovered G-protein coupled receptor called GPR30. Doses were based on published findings (Harrington *et al.*, 2003) while timing was preliminarily assessed through a time course study (not shown).

Interestingly, hCMEC/D3 cell line possesses all the three forms of estrogen receptors, as illustrated in Figure 6.7, Panel A. Using a GPR30-selective agonist (G-1; 8 hours), we were able to reproduce the same effect of β-estradiol in terms of ANXA1 release in the cell medium, while using a GPR30-selective antagonist blocked the effect of estradiol. In terms of ANXA1 content in whole cell lysate, ERα-specific agonist PPT (8 hours) was able to mimic the effect of β-estradiol ($p<0.07$ *vs.* untreated), while ERβ-specific agonist DPN inhibited ANXA1 expression. Unfortunately, we cannot count on specific ERα antagonists, but only on ERβ ones, which blocked β-estradiol (Figure 6.7; Panel B).

Overall, these data should indicate a complex interaction between the two classic estrogen receptors: if either one or the other is activated by specific agonists, the response is different if compared to what happens by concomitant activation by the pan-ligand 17β-estradiol. Therefore, two distinct mechanisms seem to exist to achieve estradiol-dependent regulation of ANXA1: release into medium, which is a non-genomic phenomenon, is directly mediated by the action of the transmembrane receptor GPR30, while ANXA1 synthesis, most likely through transcription regulation, is affected by ERα and ERβ.

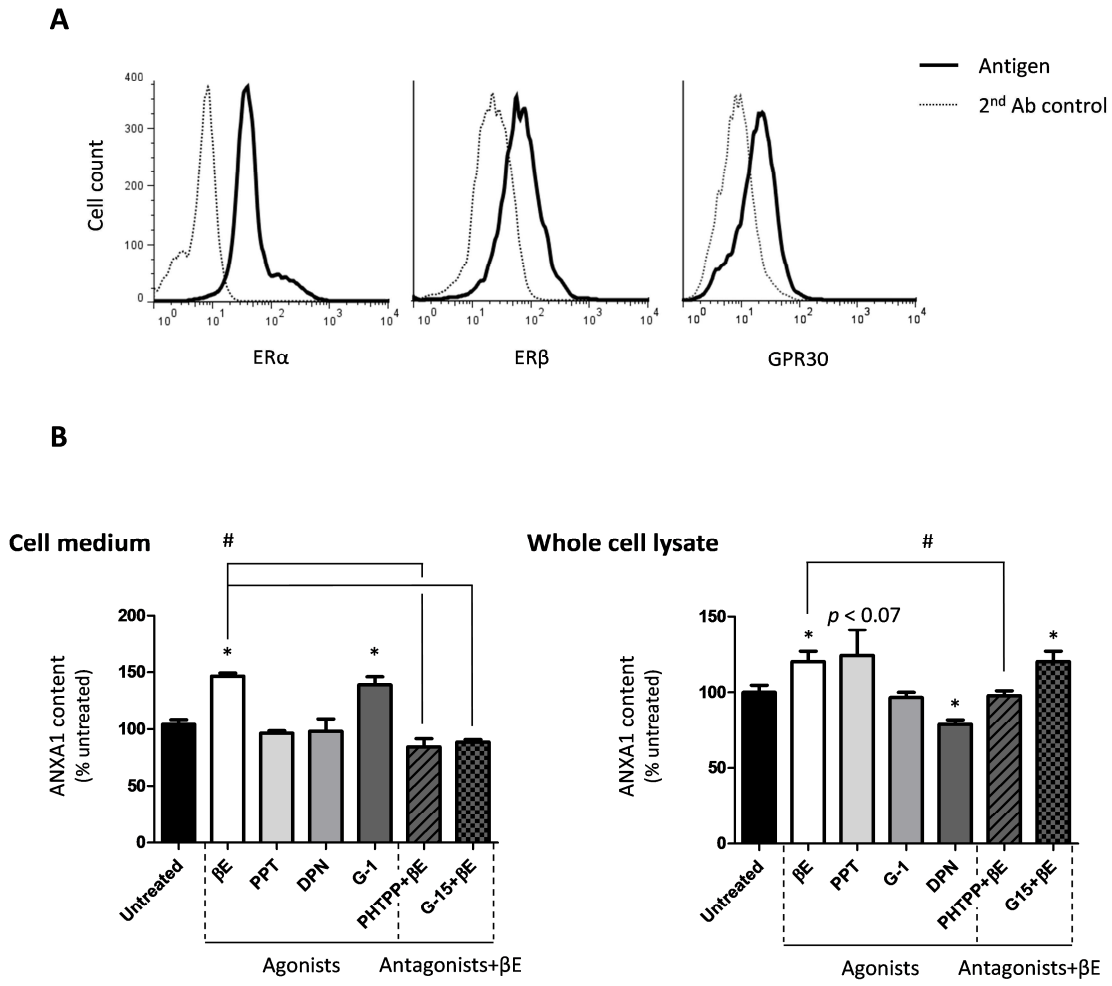

Figure 6.7 Estrogen receptors involvement in ANXA1 regulation. A| Representative flow cytometry profiles showing the expression of all three major β-estradiol receptors in untransfected hCMEC/D3 cells. At least 10000 events were analysed after gating; histograms represent one of 3 independent experiments. **B|** Experiment looking at the effect of selective agonists of different estrogen receptors for ANXA1 release and ANXA1 expression regulation in whole cell lysate. Incubations with the different stimuli were performed for 8 hours. β-estradiol: 100 nM; PPT (ERα): 200 pM; DPN (ERβ): 850 pM; G-1 (GPR30): 20 nM; PHTPP (ERβ): 200 nM; G-15 (GPR30): 200 nM. Data are representative of at least three independent experiments, performed in triplicate, expressed as mean ± SEM. Two-ways ANOVAs were performed, followed by Tukey's range *post-hoc* test; * indicate $p<0.05$ *vs.* untreated. Not all the groups are here presented ("antagonists alone" groups omitted, as they didn't show any significant effect).

6.5.3 Estradiol protects the BMECs under inflammatory conditions

Several reports indicated a protective effect of pre-incubation with steroid hormones as hydrocortisone or dexamethasone on BMECs, potentiating their tightness and limiting the effects caused by inflammation (Romero *et al.*, 2003; Forster *et al.*, 2008).

We have proved that β-estradiol has important modulatory functions towards ANXA1, which is now known as an essential component of barrier integrity (Chapter 4 and 5). So, we moved to test possible links between the steroid and the anti-inflammatory molecule on cell monolayers challenged with inflammatory conditions. As representative pro-inflammatory molecules, we used TNF-α and IFNγ (10 ng/ml), which were exposed for 24 hours on the luminal side (*i.e.* blood side) of tight and confluent monolayers grown on transwell filters (Forster *et al.*, 2008; Haarmann *et al.*, 2010). Recently published evidence (Lopez-Ramirez *et al.*, 2012) confirmed the expression of both TNF-α receptors (TNFR-1 and TNFR-2) and IFN-γ receptor on this human cell line, as it was already known for mammalian cerebrovascular endothelial cells (Okuda *et al.*, 1999). Pre-exposure for 8 hours was able to produce a tighter monolayer (Figure 6.8; Panel A) and it was able to block the TNF-α/IFN-γ permeability increase (around 20%) compared to not hormone pre-treated cells.

Similar results were obtained for long pre-exposure with β-estradiol: TEER measurements (Figure 6.8; Panel B) highlighted the decreasing effect of inflammation on the overall tightness. Similar results were also obtained by evaluating changes in paracellular permeability (Figure 6.8; Panel C).

We believe this type of stimulation every 24 hours for 4 days resembles more closely what happens within the female organism, where the oestrous cycle is responsible for the constant presence of the hormone, present at high concentrations for most of the duration. Also, it has been shown that periodic repeated administration of β-estradiol helped reduce the effective amount of hormone necessary to obtain biological responses *in vitro* (Caulin-Glaser *et al.*, 1996). Since our ultimate aim was to mechanistically describe why young females showed protection towards peripheral inflammation, we focused only on long estrogenic pre-incubations for the following experiments.

Overall, these set of experiments highlighted the protective effect offered by estradiol, which was able to improve endothelium properties and to limit the inflammatory derived leakage.

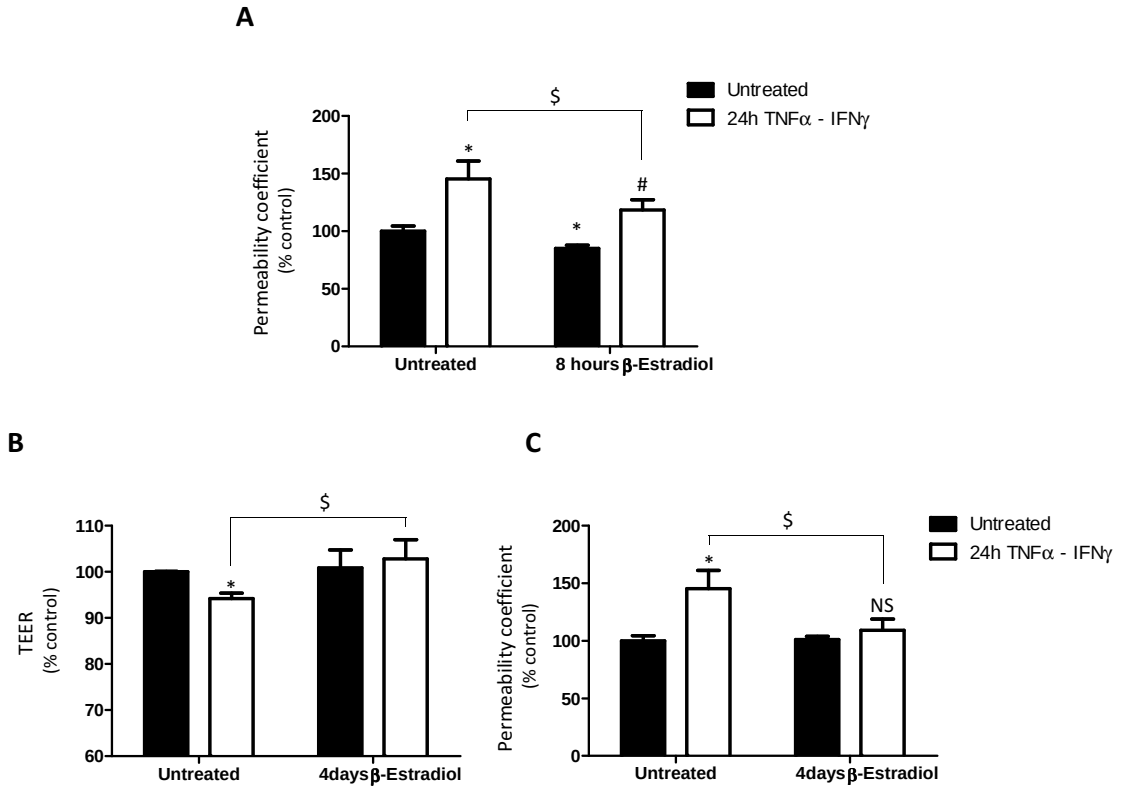

Figure 6.8 Short or long pre-incubation with 100 nM β-estradiol prevent inflammatory alterations of the barrier. A| Pre-incubation with 100 nM β-estradiol for 8 hours (short pre-incubation) contributes to a tighter endothelium and limits the expected permeability increase caused by pro-inflammatory cytokines. Long-pre-incubation (4 days) with β-estradiol limits **B|** the decrease in TEER caused by pro-inflammatory cytokines and **C|** the increase in paracellular permeability. Data are representative of at least three independent experiments, performed in duplicate, expressed as mean ± SEM. Two-ways ANOVAs were performed, followed by Tukey's range *post-hoc* test which indicated (in A| and B|) an overall effect of pre-incubation with estradiol. * indicates $p<0.05$ *vs.* untreated, # indicates $p<0.05$ *vs.* basal estradiol-treated, while $ indicates $p<0.05$ *vs.* estradiol-untreated TNF-α/IFN-γ treated. NS indicates non-significant differences *vs.* untreated.

6.5.4 ANXA1 mediates the protective effect offered by β-estradiol

Since β-estradiol showed a strong positive regulation of ANXA1 synthesis and release, both after a short time incubation (8 hours) and a long one (4 days), we investigated if this protein is somehow a mediator of estrogen anti-inflammatory effects on BMECs.

First, we tested whether cells with a constitutive higher ANXA1 expression could present a similar protection. Full length (FL11) hCMEC/D3s showed tighter permeability in untreated conditions as already shown in Chapter 4.

Incubation with pro-inflammatory cytokines TNF-α and IFN-γ caused, as expected, a great increase in permeability in wild-type cells. Interestingly, the effect was significantly limited in FL cells with higher expression of ANXA1 (Figure 6.9; Panel A), tightly resembling what happened in those monolayers pre-incubated with estradiol (Figure 6.8; Panel A).

Subsequently, since estradiol showed great ability to up-regulate ANXA1 release, we investigated the role played by the externalised pool. To do that, we pre-incubated hCMEC/D3 monolayers with a daily dose of human recombinant ANXA1 for 4 days before cytokines challenge (during the last 24 hours). Interestingly, ANXA1 pre-exposure was able (Figure 6.9; Panel B) to stop the cytokine-induced increase in permeability, similarly to the protection offered by β-estradiol pre-exposure and by ANXA1 over-expression in FL hCMEC/D3 cells.

To further test our hypothesis of ANXA1 as a mediator of estradiol action, we first used cells with a constitutive reduced expression of ANXA1 (AS hCMEC/D3). These cells showed a constitutively higher permeability due to lower ANXA1 (extensively described in Chapter 4) as described in Figure 6.9, Panel C; also, they did not show increased leakiness under inflammatory stimulation, which closely matched the results obtained in Anxa1 null mice challenged with LPS (Figure 6.5; Panel A). More importantly, while pre-exposure with β-estradiol resulted in the abolishment of the cytokines-driven permeability increase in wild-type cells, it failed to produce any effect on AS cells, as sex failed to impact on AnxA1 null mice.

Panels A, B and C of Figure 6.9 indicate the important role played by ANXA1 in presence of inflammatory mediators and suggests, along with the *in vivo* data, the requirement for this protein to obtain the β-estradiol-specific protection. To confirm this, further paracellular permeability assays were performed by stimulating cells with β-estradiol along with a neutralizing anti-ANXA1 antibody (introduced in Chapter 4). Both stimuli were added together every 24 hours, for 4 days, while mouse $IgG2_A$ isotype was used as negative control. Figure 6.9, Panel D shoes that by blocking the action of ANXA1 released in the cell medium, the overall protection offered by estradiol in presence of pro-inflammatory stimuli was completely lost, while no change was produced in presence of an unrelated mouse isotype antibody.

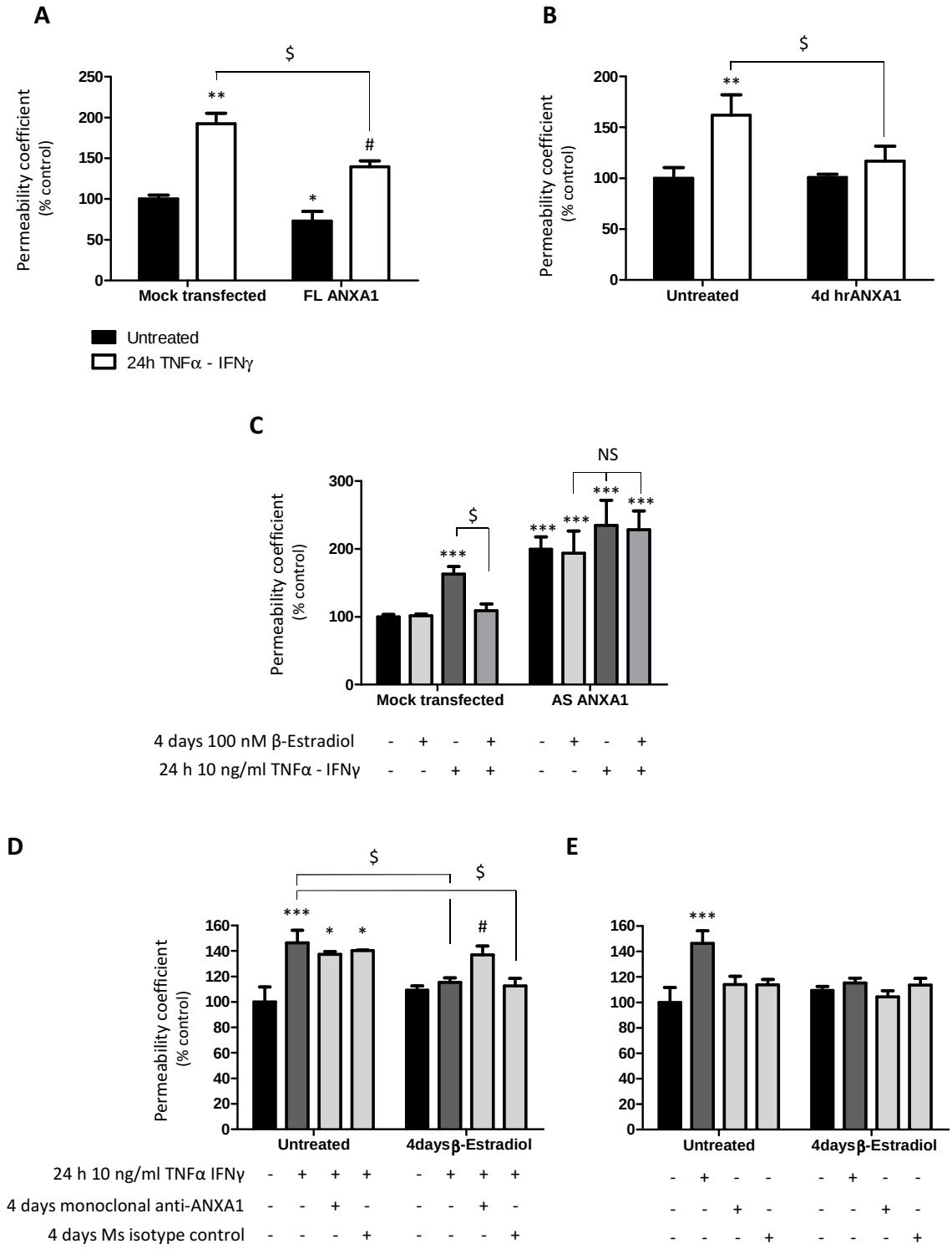

Figure 6.9 ANXA1 modulates the protective effect offered by estradiol. A| WT or FL11 hCMEC/D3 cells were incubated with inflammatory stimuli for 24 hours and permeability was then assessed. **B|** WT hCMEC/D3 cells were pre-incubated with hrANXA1 for 4 days (repeating the dose every 24 hours) and then with inflammatory stimuli for the last 24 hours, then assessing the permeability. **C|** WT or AS4 hCMEC/D3 cells were pre-incubated or not with β-estradiol (4 days, repeating the dose every 24 hours) and then with inflammatory stimuli for the last 24 hours and permeability was then assessed. Data are representative of at least three independent experiments, performed in duplicate, expressed as mean ± SEM. Two-ways ANOVAs were performed, followed by Tukey's range

post-hoc test. In A| * indicates $p<0.05$ *vs.* untreated mock, $ $p<0.05$ *vs.* mock cytokines treated, while # indicates $p<0.05$ *vs.* FL ANXA1-untreated. In B| *** indicates $p<0.001$ *vs.* untreated mock-transfected; $ $p<0.05$ *vs.* mock TNF-α/IFN-γ treated. **D|**and **E|** Testing the involvement of ANXA1 in β-estradiol protection by co-incubating cells with neutralizing monoclonal anti-ANXA1 (20 μg/ml) or mouse IgG_{2A} isotype control (30 μg/ml) for 4 days (repeating the dose every 24 hours) along with 100 nM β-estradiol and pro-inflammatory cytokines. Data are representative of at least three independent experiments, performed in duplicate, expressed as mean ± SEM. Three-ways ANOVA was performed (β-estradiol exposure, incubation with monoclonal anti-ANXA1, pro-inflammatory cytokines exposure as variables), followed by Tukey's range *post-hoc* test, which identified interaction between the three conditions and between estradiol pre-exposure and pro-inflammatory cytokines ($p<0.05$). * and *** indicates $p<0.05$ and $p<0.001$ *vs.* untreated, respectively; $ $p<0.05$ *vs.* untreated TNF-α/IFN-γ treated; # indicates $p<0.05$ *vs.* β-estradiol treated TNF-α/IFN-γ.

6.5.5 β-estradiol reverses cytokine-dependent negative effect on ANXA1 release and FPR2 surface exposure

Having demonstrated the direct involvement of ANXA1 in short and long estradiol pre-exposure before pro-inflammatory cytokines challenge, we investigated how protein synthesis and release were modulated by either one of the two stimuli or by both, in order to gain more evidence for the interconnected relationship between ANXA1 and the hormone. Therefore, we exploited sandwich ANXA1 ELISA to measure differences in protein release as well as protein content in whole cell lysate, as depicted in Figure 6.10, Panel A and B. Interestingly, cytokines exposure produced a significant reduction in ANXA1 release, which could be directly taken as partial explanation of the effect caused by the two cytokines in terms of paracellular permeability. Pre-exposure with β-estradiol (100 nM; 4 days, repeated every 24 hours) produced incremental release and most importantly was able to reverse the effect produced by cytokines, resulting in an increased release in ANXA1. As a consequence, by flow cytometric analysis we detected (Figure 6.10; Panel D) less ANXA1 bound on cells surface after cytokine stimulation, but again this could be prevented and actually reversed by β-estradiol exposure for 4 days. ANXA1 content in whole cell lysate was also found to be up-regulated in presence of one or both stimuli, indicating therefore that cells are prepared by estradiol as well as by cytokines to respond to the inflammatory event through increased synthesis of our protein of interest.

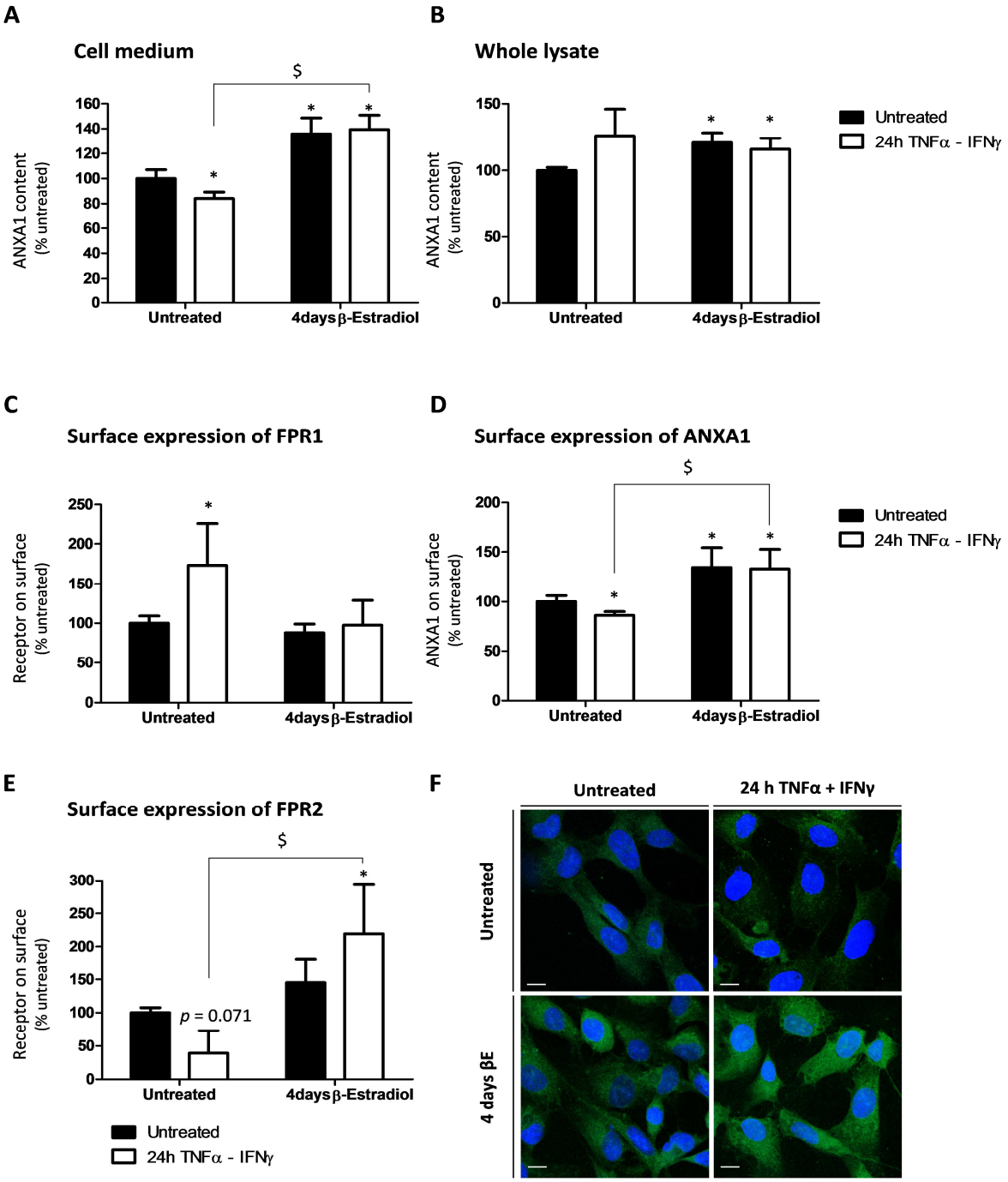

Figure 6.10 ANXA1 release and expression is altered by pro-inflammatory stimuli but rescued by β-estradiol pre-exposure. A| and **B|** show ANXA1 content in cell medium and whole cell lysate, respectively, analysed by ANXA1 sandwich ELISA. Data are representative of 4 independent experiments, performed in quadruplicate, expressed as mean ± SEM. **C|**, **D|** and **E|** indicate surface expression of FPR1, ANXA1 and FPR2 on confluent monolayers under different conditions, analysed by flow cytometry. Data are representative of 4 independent experiments, performed in quadruplicate, expressed as mean ± SEM. **F|** shows FPR2 surface expression on untreated and treated hCMEC/D3 cells. Nuclei are stained with DAPI (blue). Two-ways ANOVAs were performed followed by Tukey's range *post-hoc* test, which identified an interaction between pro-inflammatory cytokines and estradiol pre-exposure in A| C|, D| and E| ($p<0.05$). * indicates $p<0.05$ *vs.* untreated, while p=0.071 is also *vs.* untreated; $ indicates $p<0.05$ *vs.* untreated TNF-α/IFN-γ treated.

As discussed in Chapter 1 and 4, the FPR receptors are important regulators for ANXA1 action, their presence on cell surface being able to modulate how intense the action produced by the protein is going to be. We saw that the two main FPRs, FPR1 and FPR2, are transcriptionally regulated by β-estradiol (Figure 6.6; Panel E); in parallel, we detected a swift upregulation in FPR1 surface expression under cytokines stimulation, which was limited significantly in presence of estradiol pre-exposure; FPR2 surface expression, instead, was negatively regulated by TNF-α and IFN-γ, while a long pre-exposure with the sex hormones could produce an exactly opposite effect under the same inflammatory conditions, rendering BMECs more responsive to ANXA1. Figure 6.10, Panel F shows how receptor expression on cell surface decreased after 24 hours exposure to inflammatory challenge, while it strongly increased if cells were pre-exposed to estradiol before being challenged with cytokines.

Overall, peripheral inflammatory stimuli appear to strongly limit the anti-inflammatory arsenal of BMECs by limiting ANXA1 release and reducing FPR2 expression on cell surface, therefore strongly reducing the potential of the autocrine/paracrine circuitry defined by these molecules. Chronic exposure to β-estradiol was able to prevent such phenomenon.

6.5.5.1 β-estradiol and TNF-α regulate ANXA1 phosphorylation status

To delineate a mechanism of action by which β-estradiol is able to counteract the negative effect on ANXA1 release by inflammatory stimuli, we looked at the phosphorylation state of released and membrane-bound ANXA1 under various combinations of stimuli. The N-terminal of ANXA1 has potential sites for phosphorylation: it has been shown to be the substrate of a number of kinases, like the epidermal growth factor (EGF) receptor for tyrosine phosphorylation (de Coupade *et al.*, 2000) or the protein kinase C (PKC), responsible for serine and threonine phosphorylation (Solito *et al.*, 2006). Phosphorylation of the protein affects its structure and consequently its physiology.

Strong evidence supports the observation that phosphorylation on the serine 27 residue is important for translocation from the cytosol to the cell surface (Solito *et al.*, 2006) in a model of neuroendocrine cells, where ANXA1 plays an important role in controlling

hormonal release. Mutations of this or of other residues (serine 45) completely blocked ANXA1 externalisation. Similar results were also obtained in another cell model with strong exocytosis properties (McArthur *et al.*, 2009).

Following these studies, we decided to check for differences in ANXA1 phosphorylation rate. Since these were non-genomic modifications, happening very quickly (in the order of minutes) and lasting for a short time, but triggering a series of downstream events resulting in gross changes after several hours (*i.e.* significant increase in permeability), we chose to maintain the long pre-exposure with β-estradiol but to use a short incubation (20 minutes) with only TNF-α (to avoid overlapping between different cytokines' signalling pathways). Since Figure 6.9 and Figure 6.10 showed β-estradiol, as well as pro-inflammatory stimuli, to modulate specifically the externalised ANXA1 pool, which then quickly binds cell targets in the vicinity, we first investigated differences in ANXA1 phosphorylation at the level of membrane-bound protein, detached through extensive EDTA/EGTA wash (see Section 6.4.4). Figure 6.11, Panel A shows differences in terms of total ANXA1 (reproducing even more clearly the results described in Figure 6.10, Panel D); our assay did not detect Tyr21-phosphorylated ANXA1 (both on the EDTA/EGTA wash and in the cell medium; data not shown), supporting the solely intracellular existence of this ANXA1 species. Interestingly, changes in total ANXA1 were also reflected in terms of Ser27-phosphorylated ANXA1: estradiol pre-exposure caused more ANXA1 to be membrane-associated but it also increased the percentage of the serine-phosphorylated species. Interestingly, a short incubation with TNF-α limited significantly the amount of total ANXA1 on cells surface, even reducing the one present on basal-untreated conditions; serine 27-phosphorylated form was also dramatically reduced compared to the control. The pre-incubation with β-estradiol rescued such phenotype, allowing a high quantity of total and ser27-phosphorylated protein to remain at the membrane, where it may be able to signal through the target cells.

Therefore, β-estradiol was able to increase the amount of Ser27-phosphorylated ANXA1, which is thought to have a direct impact on the externalization of the protein and its consequent autocrine/paracrine action; also, this status seems important to tackle the effect that TNF-α showed towards ANXA1 release either in short or long exposure.

To get a preliminary confirmation of such a conclusion, we incubated cells with β-estradiol (4 days; 1 dose every 24 hours) after a short pre-incubation with the GPR30 specific antagonist called G-15 (exactly following the same posology), since this receptor seems to be the one able to generate prompt non-genomic responses. Through a modified version of ANXA1 sandwich ELISA, we observed (Figure 6.11, Panel B) that long-incubation with β-estradiol was able to increase the Ser27-phoshorylated ANXA1 on the cell medium but this effect was blocked by pre-incubation with the GPR30 receptor-specific antagonist (G-15), suggesting the strong possibility of its involvement in this complex mechanism. Since phosphorylation is an event classically starting from within the cell, we extracted total cell lysate and probed for Serine27-phosphorylated ANXA1 in presence or absence of the different stimuli, including a short pre-incubation with G-15 before each dose of β-estradiol. We could detect a small increase in ANXA1 site specific phosphorylation under long estradiol incubation, which could be blocked by pre-incubation with G-15. Under other combinations of stimuli we could not detect significant differences at least at the intracellular level, indicating therefore that the action of TNF-α may affect other aspects on this pool, which will deserve more attention in the near future.

Overall, here we detected phosphorylation on Serine27 residue of ANXA1 most likely (directly or indirectly) mediated by GPR30; this event appeared to be important for its externalisation and functional membrane association both under basal and inflammatory conditions, as confirmed by recent work (McArthur *et al.*, 2009; Nadkarni *et al.*, 2011). TNF-α blocked phosphorylation at this precise residue, directly affecting the overall protein externalisation. Nonetheless, Serine27 seems to be essential for the estradiol-specific action on counteracting inflammation effects, rescuing ANXA1 correct release.

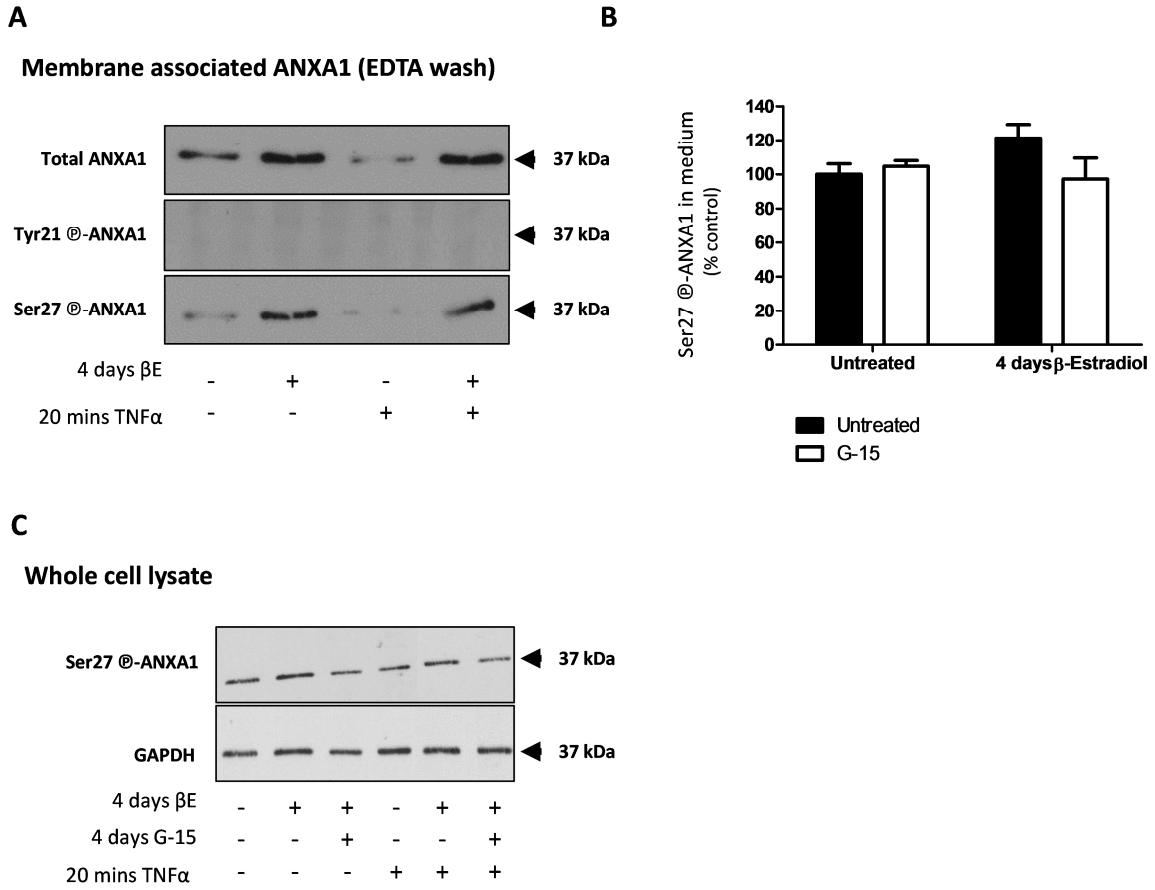

Figure 6.11 Phosphorylation of ANXA1 on Serine27 is mediated by the transmembrane estrogen receptor GPR30. A| EDTA/EGTA washes were analysed via immuno-blotting for ANXA1 phosphorylation at different functionally relevant residues, namely Tyrosine21 and Serine27. Short TNF-α incubation was used to identify a quick post-translational modification. **B|** Since the concentration of phosphorylated-ANXA1 in cell medium may be too low for detection with immuno-blotting, we adapted the ANXA1-specific ELISA to detect the Serine27-phosphorylated form. G-15 was added 30 minutes before each daily dose of β-estradiol. **C|** Immuno-blot showing Serine27-phosphorylated ANXA1 under various conditions. β-estradiol was administered every 24 hours for 4 days; G-15 was also given every 24 hours for 4 days, 30 minutes before estradiol. TNF-α stimulation was performed for 20 minutes only, instead. Data are representative of 2 independent experiments; blots show representative results, while in B| data are expressed as mean ± SEM (*n*=2; statistics not performed).

6.5.6 Pro-inflammatory stimulation disrupts the actin cytoskeleton, which is protected by chronic pre-exposure with β-estradiol

So far, we understood that pro-inflammatory stimuli (mainly conveyed by TNF-α) disrupted endothelial barrier tightness, with a significant increase in paracellular permeability; ANXA1 significantly was affected by these conditions, its release from BMECs being significantly reduced.

However, both events were prevented in cells pre-incubated with β-estradiol. To understand how the chronic pre-exposure to the sex hormone can block the effect of inflammation on the endothelium, we investigated one of the major target of the disruptive action produced by pro-inflammatory cytokines, as well as the major target of ANXA1 in these cells, *i.e.* the actin cytoskeleton. TNF-α and IFN-γ caused a significantly greater insoluble/soluble β-actin ratio (F/G actin; Figure 6.12, Panel A), which mirrors the increased formation of disorganised non-polarized stress fibres throughout the cytosol, as evidenced in Figure 6.12, Panel C. Chronic β-estradiol exposure was able to reinforce the cortical F-actin ring under basal conditions; under inflammatory challenge, it also avoided the increase in impaired actin polymerisation, maintaining the correct cortical location of actin fibres and functional polarity of the cells forming the monolayer. Interestingly, these findings were also paralleled in primary capillaries extracted from young adult females, males or old females treated with peripheral inflammatory stimuli. In particular, old females showed a completely disorganised actin cytoskeleton (Figure 6.12, Panel C), in high contrast to what shown by young female capillaries, which maintained a continuous and more functional morphology closely similar to non-inflammatory conditions.

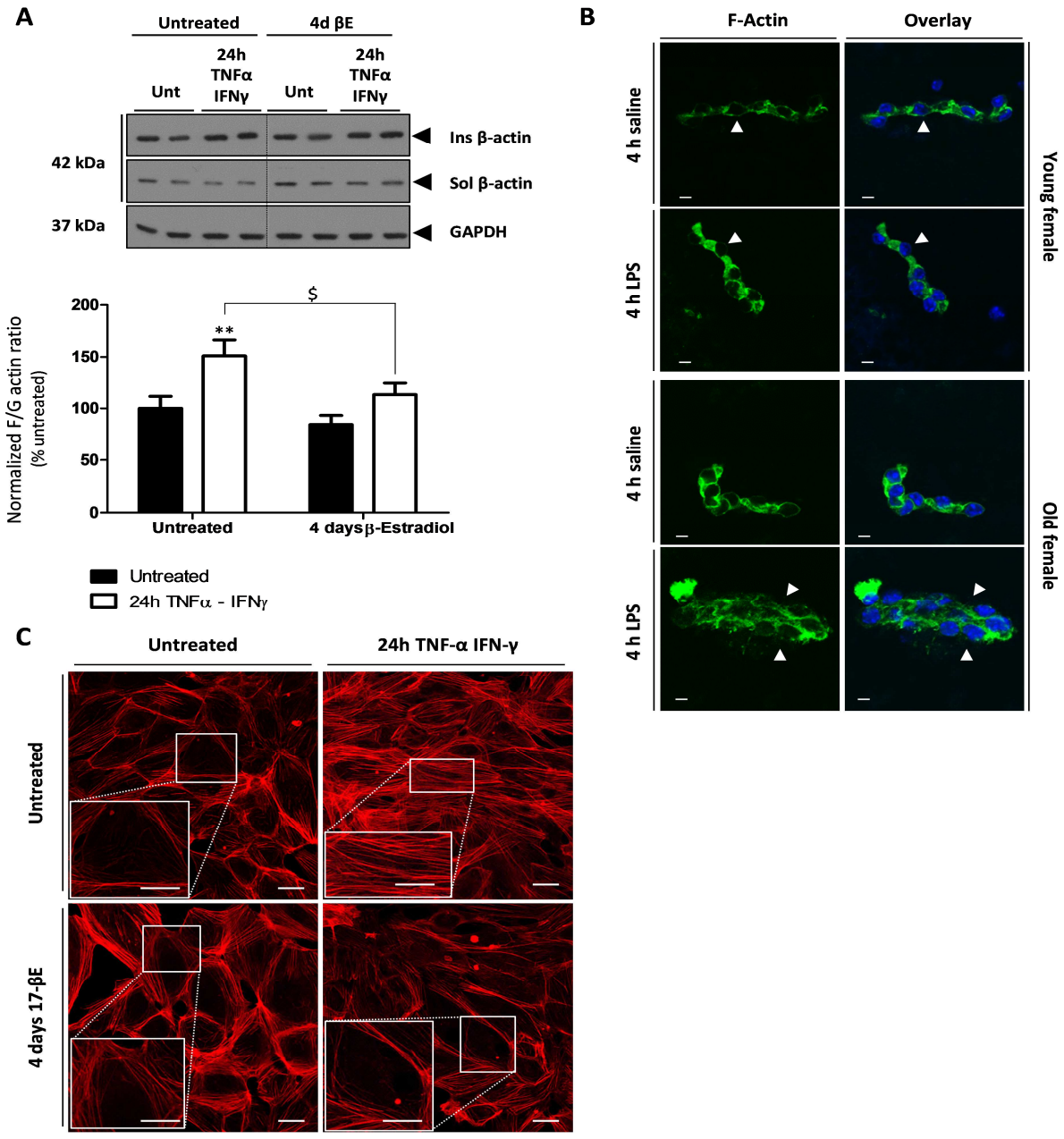

Figure 6.12 Pre-incubation with β-estradiol prevents the disruptive effect of pro-inflammatory cytokines on the actin cytoskeleton. A| Biochemical analysis of G (soluble) and F (insoluble) β-actin in hCMEC/D3 cells treated or not with TNF-α and IFN-γ after pre-exposure with β-estradiol. Histograms represent three independent experiments, performed in duplicate; data are presented as mean ± SEM. Two-ways ANOVA was performed, followed by Tukey's range *post-hoc* test, which identified an effect of β-estradiol ($p<0.05$); ** indicates $p<0.05$ *vs.* untreated; $ indicates $p<0.05$. **B|** Primary capillaries were extracted from young adult females, male and old females, treated *i.p.* with saline or LPS, quickly fixed and stained with Alexa488-conjugated phalloidin and mounted in Prolong anti-fade mountant with DAPI (Blue; Invitrogen, UK). White arrows point to regions of particularly important actin cytoskeleton integrity or disruption. Scale bar: 10 µm. **C|** Confluent hCMEC/D3 cells pre-treated or not with β-estradiol for 4 days were treated (or not) with TNF-α and IFN-γ for 24 hours. Subsequently, cells were fixed and permeabilized before staining with rhodamine-conjugated phalloidin. Images are representative of at least 3 different preparations. Scale bars: 30 µm (main image) and 10 µm (inset). Panel B was produced thanks to help provided by Dr. S. McArthur.

6.5.7 Cell-cell junction components are protected by β-estradiol

Estrogens have shown to have multiple effects on junctional proteins physiology, especially under non-inflammatory conditions (Nilsson, 2007; Burek *et al.*, 2010), in which hormonal stimulation appears to be important to trigger the expression of some of these components (Kang *et al.*, 2006). Having investigated the implications of 17 β-estradiol in rescuing the correct cytoskeleton structure and functional organisation, we checked if these events resulted also in protection of the major components of tight and adherens junctions. Pro-inflammatory cytokines like TNF-α present a well-known disruptive action on these structures by affecting both their expression and their functional localisation, ultimately causing an increased permeability (Silwedel and Forster, 2006; McKenzie and Ridley, 2007; Aveleira *et al.*, 2010). These findings were also confirmed in our model: 24 hours treatment of confluent cell monolayers with TNF-α and IFN-γ caused cell elongation/contraction and a significant decrease in the total expression levels of occludin and ZO-1 Figure 6.13; Panel A and D), which were paralleled by an almost complete loss of membrane-associated staining of these proteins (Figure 6.13; Panel B and E). These results were clearly paralleled on extracted brain capillaries: occludin staining of old female mice resulted deeply altered (Figure 6.13; Panel C) as a consequence of peripheral inflammatory stimulation. However, β-estradiol pre-exposure was able to prevent such strong disruption, contributing to the maintenance of continuous staining over large areas of the treated monolayers.

Another essential tight junction component, claudin-5, did not show alterations in total expression after inflammatory challenge (Figure 6.13; Panel F) but we did detect upregulation following chronic β-estradiol exposure, as already reported by others (Burek *et al.*, 2010). Despite expression being unaltered, membranous functional expression of claudin-5 was disrupted (Figure 6.13; Panel G), with only few short punctuated cell-cell contact areas still positive for the protein.

Also in this case, β-estradiol pre-treatment gave some sort of protection against the following inflammatory stimulation, with more contact areas presenting continuous staining.

Finally, VE-cadherin, the main adherens junction component, appeared unaltered in terms of total expression (Figure 6.13; Panel H) as already shown in peripheral vasculature

(Hofmann *et al.*, 2002), but resulted lost from cell membrane (Figure 6.13; Panel I) and almost completely internalized under inflammatory conditions. Pre-exposure with estradiol did not alter its basal localisation but it was able to prevent, at least in part, the disruptive effect shown under cytokines stimulation.

To our knowledge, this evidence represents novel findings and well explains how the protective role of a long hormonal pre-exposure can potentiate the response given by BMECs against the disruptive role produced by inflammatory mediators. Taking into account β-estradiol modulatory effect on the actin cytoskeleton helps to understand the whole protective mechanism.

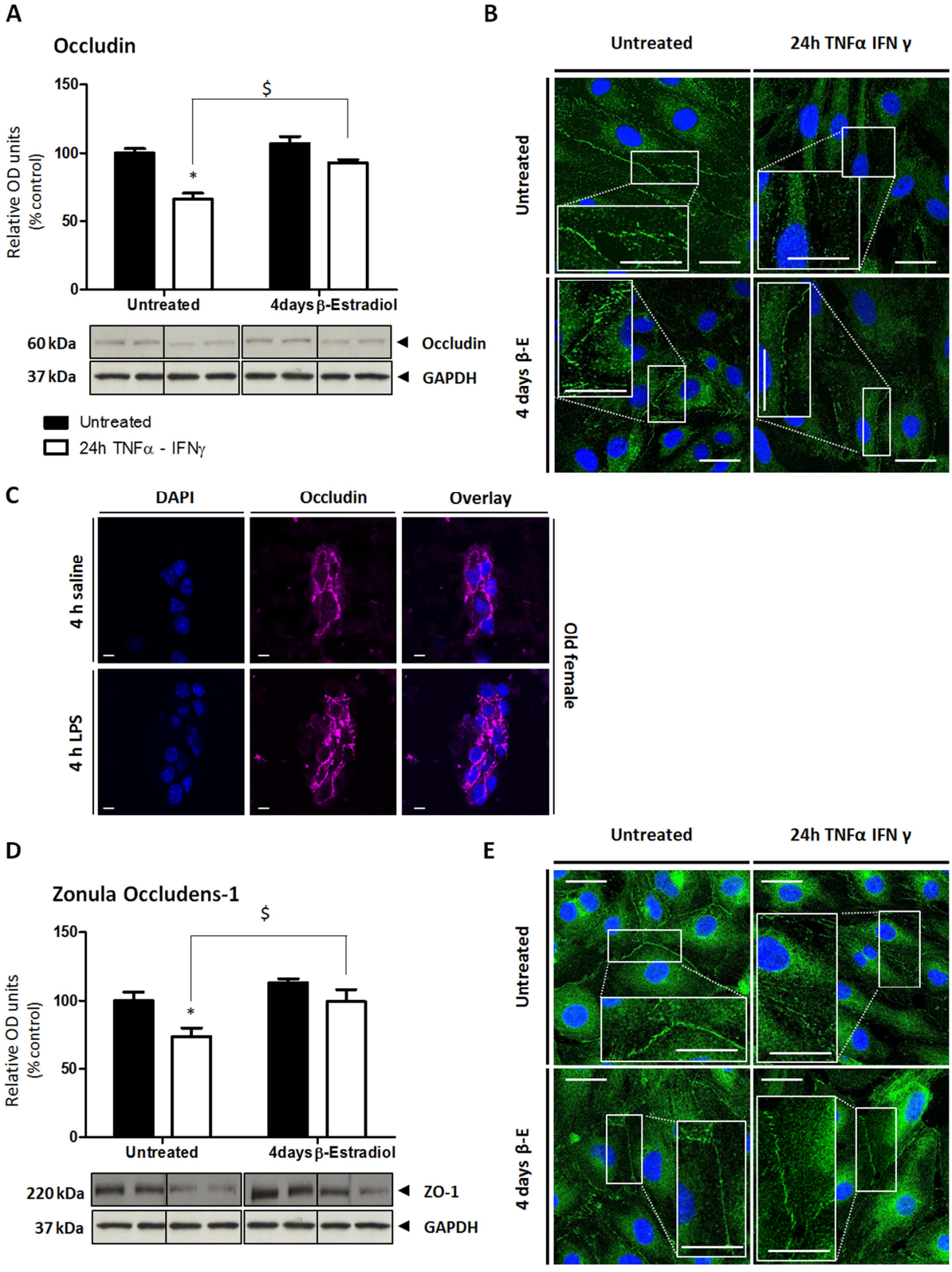
A
Occludin
Relative OD units (% control)
150
100
50
0
$
*
Untreated
4days β-Estradiol
60 kDa
37 kDa
Occludin
GAPDH
Untreated
24h TNFα - IFNγ
B
Untreated
24h TNFα IFN γ
Untreated
4 days β-E
C
DAPI
Occludin
Overlay
4 h saline
4 h LPS
Old female
D
Zonula Occludens-1
Relative OD units (% control)
150
100
50
0
$
*
Untreated
4days β-Estradiol
220 kDa
37 kDa
ZO-1
GAPDH
E
Untreated
24h TNFα IFN γ
Untreated
4 days β-E

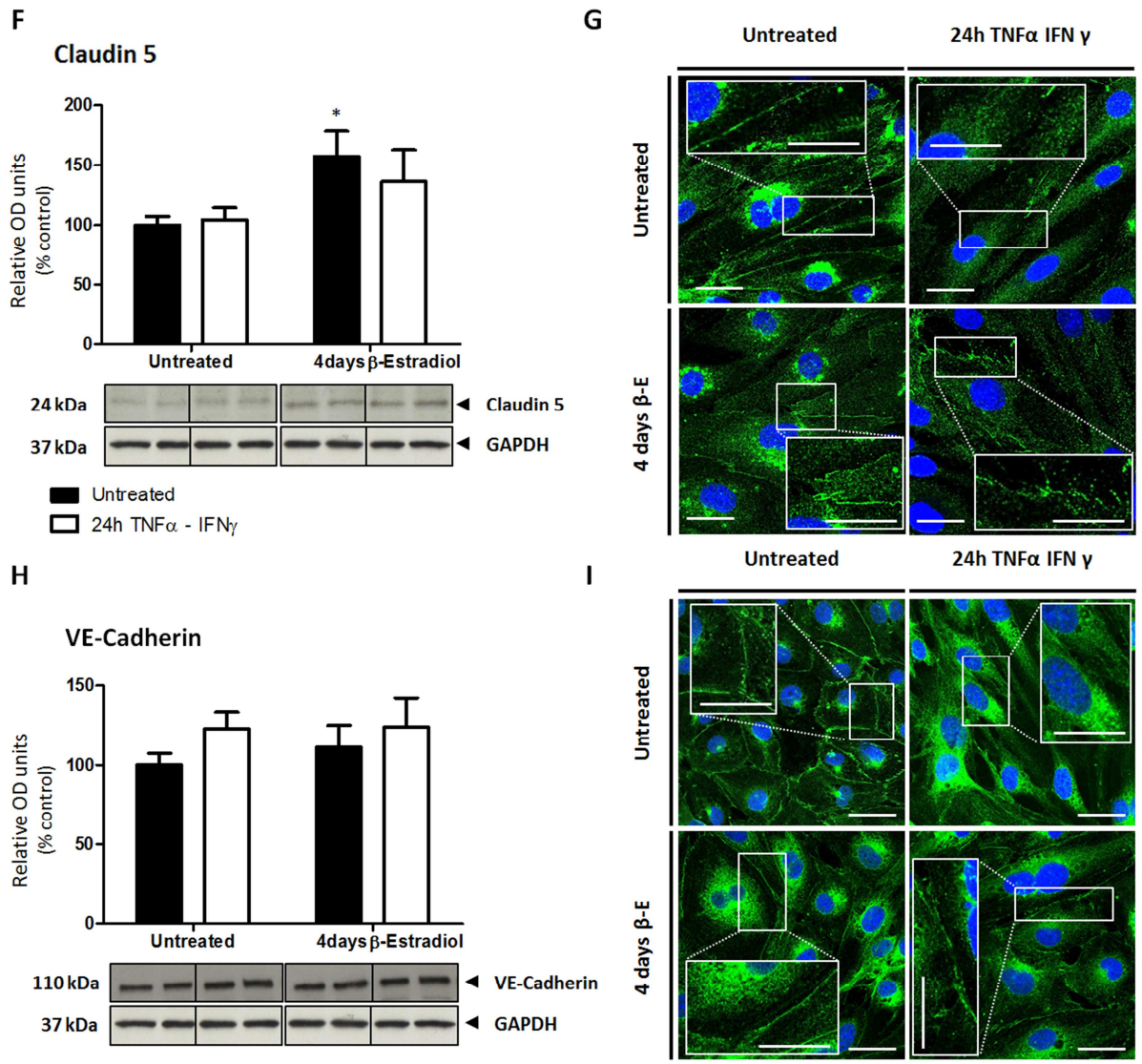

Figure 6.13 Estradiol pre-exposure prevents cytokine-dependent alterations in expression and functional localisation of cell junctions component. A|, **D|**, **F|** and **H|** show typical western blots of total content of occludin, zonula occludens-1 (ZO-1), claudin-5 and VE-cadherin alongside GAPDH loading controls in extracts from wild-type hCMEC/D3 treated in the specified conditions. *n*=3 independent experiments, each performed in duplicate. Histograms show joined densitometric analysis of all the experiments, expressed as mean ± SEM. Two-ways ANOVA followed by Tukey's *post-hoc* test was performed, * indicating $p<0.05$ *vs.* untreated, while $ indicates $p<0.05$ *vs.* untreated TNF-α/IFN-γ treated. **B|**, **E|**, **G|** and **I|** present confocal microscopy analysis of occludin, ZO-1, caludin-5 and VE-cadherin expression in confluent monolayers of hCMEC/D3 cells. Typical examples from *n*=3 experiments. Scale bar: 30 µm and 10 µm (inset). **C|** shows confocal analysis of occludin staining in primary vessels extracted from reproductively senescent female mice treated *i.p.* with either saline or 3 mg/kg LPS for 4 hours. Typical examples from *n*=3 experiments. Scale bar: 10 µm. Panel C produced thanks to the help provided by Dr. S. McArthur.

6.6 Discussion

This chapter described the latest findings on the involvement of ANXA1 in the response mounted by BMECs under peripheral inflammatory challenges, as well as a novel ANXA1-dependent mechanism contributing to sex dimorphic responses at BBB level. These results support once more the new role of ANXA1 as one of the main protagonists of the regulatory system controlling paracellular permeability, but they also propose further functional implications in the protective mechanism triggered by circulating sex hormones. We believe to have provided convincing proof of concept as well as clearer details, compared to similar studies (Burek *et al.*, 2010).

6.6.1 ANXA1: a principal player in sex-dependent BBB response to peripheral inflammation

Interestingly, young adult male mice showed a significant increase in Evans Blue brain content 4 hours after peripheral LPS administration, which subsided to basal levels 24 hours after. Females did not show any quantitative change, suggesting the presence of a protective mechanism.

Our attention was drawn immediately by the potential effects that sex hormones may show on endothelial cells; in particular, 17 β-estradiol represented a strong candidate due to its prominent role both in physiology and in pathology. We confirmed its involvement by employing senescent animals; although murine senescence does not closely match what happens during human female menopause (Sohrabji and Bake, 2006; Vegeto *et al.*, 2008), the circulating levels of female hormones decrease significantly (Parkening *et al.*, 1978) limiting sex-dependent influences, which is what happened also in our model (Figure 6.5; Panel B). In addition, rescuing ovariectomised animals with β-estradiol provided a stronger confirmation of the involvement of the steroid (Figure 6.5; Panel C). Indeed, numerous reviews and articles reported the enormous effects of this steroid in the brain (Maggi *et al.*, 2004; Vegeto *et al.*, 2008), with many stressing the impact shown on vasculature and endothelial cells (Sohrabji and Bake, 2006; Nilsson, 2007; Burek *et al.*, 2010).

Recent investigations clearly showed that circulating estrogen does offer vascular protection [nicely reviewed by Nilsson, 2007 (Nilsson, 2007)]. In particular, the great interest on these vascular-related protective opportunities offered by estradiol and sex hormones is to attribute to several experimental and population-based studies, indicating that women are protected from stroke, many neurodegenerative disorders and cardiovascular diseases, an advantage which fades away with menopause. Our study started from this evidence and we believe it has contributed to add more mechanistic details, focusing specifically on the brain microvascular district. In particular, our findings have set Annexin A1 among the main effectors involved in protecting the BBB and the CNS itself from those signals produced by inflammatory events happening elsewhere in the body, as well as an important character in defining sex dimorphism. In fact, Anxa1 null mice failed to show sex-related differences (Figure 6.5): on one hand, this confirmed the important role of the protein; on the other, it opened several questions about why null mice failed to show both sex-dependent differences and significant increase under inflammatory conditions. Among possible explanations, one should account that the basal increased barrier permeability of knock-out mice (more than 10 times higher than wild-type) is so high that either a further increase is not permitted by some sort of compensatory mechanism [for example through up-regulation of other permeability regulators; we hypothesised Anxa2 (Hannon *et al.*, 2003)] or it is technically not detectable by the sensitivity limits of the assay chosen (Evans blue extravasation in the brain parenchyma). However, it is also possible that the lack of Anxa1 prevents the expected barrier leakiness: in fact, we have shown that pro-inflammatory cytokines significantly block the release of the protein from BMECs, which we believe could represent a way to lead the expected response.

6.6.2 ANXA1 physiology is regulated by β-estradiol

6.6.2.1 Genomic pathways

Figure 6.6 and Figure 6.10 show very clearly how the β-estradiol is able to modulate both transcription and release of the ANXA1, both through the classic estrogen receptors ERα and ERβ, as well as the new membrane-associated GPR30. Others already have shown β-estradiol influence of ANXA1 expression (Davies *et al.*, 2007; Ang *et al.*, 2009). The steroid

was shown to activate cAMP-responsive element binding proteins (CREBs) and to induce transcriptional activity also through these factors (Wade and Dorsa, 2003); interestingly, Antonicelli *et al.* (Antonicelli *et al.*, 2001) demonstrated the presence of a CRE element on ANXA1 promoter, while Ang *et al.* (Ang *et al.*, 2009) showed the direct involvement of β-estradiol-dependent action on ANXA1 transcriptional regulation, which was confirmed by us in a previous unpublished study (Solito *et al.*, 2003a). Our group was the first to describe the ANXA1 promoter from estradiol point of view (Solito *et al.*, 2003a), as seen in Figure 6.4. Putative ERE-like sequences were identified both on the human and murine sequences and we also showed the direct implications and impact of classical and non-classical estrogen receptors on ANXA1 behaviour. Aware of the results generated by using specific agonists and antagonists (Figure 6.7), we concluded that the genomic action of estradiol is mediated by both classical ERs: activation of ERβ resulted in a negative effect on ANXA1 basal expression, possibly through an ERE-independent action on other transcription factors (Gruber *et al.*, 2004), while selective ERα activation with PPT resulted in ANXA1 up-regulation. Blockade of ERβ and consequent stimulation with estradiol did not result in ANXA1 induction, indicating therefore that estradiol may need both receptors to be active. Receptor-specific agonists are highly specific molecules which bind exclusively to only one receptor and are able to trigger specific conformational changes that determine its activation at very low concentrations (850 pM for PPT, for example). Molecules like estradiol are able to bind several targets and therefore they may not be as good in activating a specific receptor as its specific agonist is; so this may be why we did not detect a raised ANXA1 expression in presence of the ERβ specific antagonist PHTPP.

Importantly, ANXA1 receptor family also showed tight transcriptional regulation by β-estradiol, reinforcing the strong impact of this hormone on this signalling platform. Apparently, these results clashed with a recent publication (Mou *et al.*, 2012), which showed inflammogens up-regulating murine FPR2 transcription in a different BBB-like (bEND.3) *in vitro* model.

The stimulus used is different from the ones we chose, plus only transcription of the receptor was quantified, which is not anymore considered a reliable way to understand how the functional expression of a protein is affected by certain stimuli.

Nonetheless, our results indicated a different regulation between the two FPR members under inflammation, which well fits with the latest theories indicating FPR1 to be a pro-inflammatory effector, swiftly up-regulated during acute inflammation and able to interact with acute-phase protein like serum amyloid A (SAA), while FPR2 being more an anti-inflammatory modulator, the principal mediator and conveyor of ANXA1 action (Perretti and Dalli, 2009; Dufton and Perretti, 2010).

6.6.2.2 Non-genomic pathway

Regulation of *ANXA1* gene transcription was an important effect shown by estradiol; however, the most prominent action was the GPR30-induced ANXA1 release, which also held important implications under inflammatory conditions. The mechanism(s) by which ANXA1 is externalised of the cytoplasm is poorly understood, although it appeared to be independent from the classical endoplasmic reticulum/Golgi pathway of exocytosis (Philip *et al.*, 1998). However, it seems to require the activation of kinases as PKC, which ultimately lead to ANXA1 serine-phosphorylation (Solito *et al.*, 2003b; Yazid *et al.*, 2009). Other limited studies also proposed the involvement of the ATP-binding cassette (ABC) transporter proteins (Parente and Solito, 2004; Solito *et al.*, 2006), which are in some cases involved in physiological molecules release. In our model, we did identify an estradiol-dependent increase in Serine27-specific phosphorylation, which was prevented by blocking GPR30 with its specific antagonist G-15 (Figure 6.11). This effect was detected both in the intracellular pool of ANXA1 and in the one released in the cell medium, directly affecting, we believe, the total amount of ANXA1 that is released under estrogenic stimulation and that is able to bind to the cell surface. Although the definition of the signalling pathways triggered by this relatively novel receptor is still far from complete as well as the novel evidence concerning the classical ERs being membrane associated and triggering non-genomic effects, we now know that GPR30 is able to stimulate the activation of PKC, at least in a sub-population of neurons injured in a model of hyperalgesia (Kuhn *et al.*, 2008).

Moreover, the estradiol-specific GPCR is also able to trigger the activation of the phosphatidylinositol 3-kinase (PI3K) (Prossnitz *et al.*, 2007), which we have shown to play a key role in activating PKC in the neuroendocrine system (Solito *et al.*, 2003b). Taking this into account, it seems plausible to hypothesize GPR30 as receptors able to trigger ANXA1 phosphorylation for ANXA1 release and surface translocation.

We did not investigate estradiol-related effects on the shedding of microparticles bearing ANXA1. Such response is gaining increasing interest in the scientific community, since these submicrometre-sized vesicles represent an alternative way of releasing factors as well as a suitable potential bio-markers (Angelillo-Scherrer, 2012). One study linked the level of circulating estradiol with the amount of pro-inflammatory and pro-coagulant microparticles in the blood (Jayachandran *et al.*, 2009). More recently, another report indicated the quick non-genomic effect of estrogenic pre-incubation of PMN cells before a pro-inflammatory stimulus in limiting the release of pro-inflammatory microparticles presenting ANXA1 on their surface (Nadkarni *et al.*, 2011). Although this study analysed a different experiment asset, it indicated the potential involvement of sex hormones like estradiol in novel pathways, which should be definitely investigated considering the importance of endothelial-derived microparticles (Grammas *et al.*, 2011).

6.6.2.3 Circulating versus central estrogen

Knowing that β-estradiol is able to modulate ANXA1 expression, which is linked with the endothelium integrity, it may be argued that male individuals should present higher physiological levels of permeability (Figure 6.5) but this is not the case. As already mentioned in the Section 6.3, gonads are the primary but not the only source of sex steroids: both males and females present many non-reproductive tissues expressing aromatase P450, the enzyme able to convert testosterone (and other steroids) to 17 β-estradiol. Astrocytes are among those cells with high enzymatic activity, suggesting that cerebrovascular concentration of estrogen may be different from circulating levels.

Therefore, estrogenic influences on basal expression of ANXA1 among male and female individuals could be similar, contributing to the comparable levels of basal permeability. Under inflammatory conditions, what really seems to make a difference is the circulating estrogen, absent from male and reproductively senescent female animals, those unable to counteract the barrier leakage (Figure 6.5).

6.6.3 ANXA1 as a principal mediator of estradiol protective action

In the present chapter, we identified a close relationship between BBB-specific estradiol action and ANXA1 under peripheral challenges. We modelled these conditions through the potent inflammatory cytokine TNF-α, which takes part to the initial stages of amplification of the inflammatory reaction, induces a strong activation of two main pathways, the first one represented by the mitogen-activated protein kinases (MAPK), which activate specific transcription factors, while the other one represented by activation and nuclear translocation of NF-κB, usually through degradation of its inhibitory proteins (*i.e.* IκB), ultimately resulting in inflammatory genes transcription (Maggi *et al.*, 2004). In the present report, we did not detect any difference in terms of classically activated signalling pathways (as reviewed in Figure 10.5; Appendix). 30 minutes exposure to TNF-α [as well as 24 hours (not shown; comparable to 30 minutes)] caused augmented p65 nuclear translocation, not prevented by estradiol pre-exposure. Similarly, TNF-α exposure triggered intensive phosphorylation of several MAPK (p38; ERKs; SAPK-JNK) and IκB and estradiol did not prevent/limit the activation of these pathways. Another signalling pathway analysed was phosphatidylinositol-3-kinase (PI3K)/Akt, which seemed to be only minimally activated; as expected by its limited involvement.

Although these findings apparently confute earlier reports (Galea *et al.*, 2002; Sumanasekera *et al.*, 2007), we should take into account the possibility that differences in NFκB nuclear action occurred in a different time frame than the one we used (10-30 minutes) or perhaps the monomer p65 was not the one to investigate (since NFκB is formed by combinations of different monomers, among which p50, p52, p65, p100, *etc.*). Notably, we did not investigate the c-*fos*-mediated transcription pathway, which is another mechanism by which TNF-α controls genes expression.

On the other hand, these findings support and strengthen the presence of a novel *non*-conventional anti-inflammatory mechanism of estradiol based on ANXA1. In our model, estradiol directly counteracted the effects caused by inflammation by blocking the cytokines-dependent negative impact on ANXA1 release and FPR2 surface exposure (Figure 6.10), restoring and potentiating this pathway. We currently ignore the full mechanism through which the normal protein release is limited by pro-inflammatory cytokines, although we obtained clear evidence for the involvement of post-translational phosphorylation at crucial sites of the protein [see Figure 6.11 and (Solito *et al.*, 2003b)]. This does certainly represent a strong base for future investigation. Overall, the fact that estradiol was shown to play its role towards peripheral inflammation principally by rescuing the ANXA1-FPR2 circuitry gives a huge importance and add a novel central role to it not only considering the implications played on a healthy endothelium (as detailed in Chapter 4) but especially those here described under phlogistic conditions.

6.6.4 ANXA1 anti-inflammatory action on the BBB: possible implications

In this chapter, we identified a new negative action of pro-inflammatory stimuli on ANXA1 release, which certainly contributes to cause increased permeability, but we also observed how estradiol was able to block this effect and actually to increase the amount of protein externalized; this certainly strengthened ANXA1 action and counteracted the effects provoked by inflammation. To this regard, we should not forget that certain ways, through which pro-inflammatory cytokines like TNF-α and IFN-γ produce disruptive consequences on endothelium, include the activation of highly disruptive pathways like the RhoA- (Wojciak-Stothard *et al.*, 1998) and the PLA_2-dependent ones (Heller and Kronke, 1994). We (Chapter 4) and others (Hannon *et al.*, 2003; Parente and Solito, 2004) have clearly shown both of these mechanisms to be strongly targeted by ANXA1. Long-term effects on tightness-related proteins, like occludin and adherens-junctions, were also described for TNF-α (McKenzie and Ridley, 2007); it is not too speculative to propose ANXA1 to counteract and rescue these events, as we have been able to observe in highly disrupted endothelial monolayers (Chapter 4). In a recent report, TNF-α and IFN-γ were shown to trigger caspases dependent pathways in the same *in vitro* model (hCMEC/D3 line); dependently on the concentration

used, these were either leading to cell death or to specific disruption of cell-cell junctions and loss of barrier tightness (Lopez-Ramirez *et al.*, 2012). Interestingly, Annexin A1 is known to regulate caspase 3 activity (Solito *et al.*, 2001) and in a model of spinal cord injury it was shown to play a neuroprotective role by limiting the activation of this intracellular signalling pathway (Liu *et al.*, 2007). This evidence, although not tested in our model, may provide a novel explanation for ANXA1 central protection and anti-inflammatory role.

6.7 Limitations of the study

In this section of the study, we tried to combine *in vivo* evidence with *in vitro* mechanistic investigation to support the strong implications of annexin A1 in inflammatory pathways mediated by cytokines like TNF-α; also, we showed the involvement of the protein in the protection offered by chronic exposure to a female sex-hormone like β-estradiol. To model peripheral inflammation, we did not use LPS to test permeability changes *in vitro*, despite this has been widely used (Descamps *et al.*, 2003; Mou *et al.*, 2012). Despite these cells do express (Figure 10.6; Appendix) the receptors (TLR-2 and TLR-4) and the accessory proteins (MD2 and CD14) necessary to respond to the inflammogen, the LPS binding protein (LBP), whose role appears to be essential to trigger an effect, is absent from the medium. Also, permeability increase caused by the inflammogen was much less pronounced than the one provoked by TNF-α and IFN-γ, which could have limited the definition of a sensitive assay where treatment-specific effects could be detected. Most importantly, LPS would have represented a model of septicaemia, not a proper way to mimic peripheral inflammation: pro-inflammatory cytokines circulating in the blood are the real mediators of peripheral immune events and those truly impacting on the brain interfaces.

Estradiol is a potent gonadal female hormone, which has several implications in numerous cellular functions; specifically for the brain microvasculature, it was shown (Krause *et al.*, 2006) to affect not only paracellular permeability, but also other functions, some of which have been reported to be affected by ANXA1 action, for example mitochondrial efficiency, blocking free radicals production and COXs activity, cytokines-related apoptosis as well as cytokines-triggered increase in adhesion molecules (Nilsson, 2007).

Since we were particularly interested in the role of ANXA1 on paracellular permeability and cytoskeleton regulation, we left out these additional areas of interest, but we believe they may conceal other mechanisms of action helpful to explain the results.

Notably, gonadal estradiol represents only a piece of that complex puzzle that is the sex-related endocrine system. Several other players are released, defining a complex network of molecules, whose concentration varies during the oestrous cycle and at different combinations of hormones and doses correspond different actions on the cerebrovascular system (Kang *et al.*, 2006; Krause *et al.*, 2006). Although we have shown *in vivo* that 17 β-estradiol is directly involved in protecting females (ovariectomy experiment; Figure 6.4), we should take into account possible synergistic effects with other sex hormones like progesterone, which has been proposed to have joint effects with estradiol on ANXA1 modulation as introduced by Nadkarni *et al.* (Nadkarni *et al.*, 2011), and testosterone, which can be converted in estradiol (Krause *et al.*, 2006).

Although it is absolutely relevant to consider that cerebral concentrations of estradiol are very similar between male and female individuals thanks to the aromatase-specific activity, we decided to focus on stimulations that mimic the effect of circulating estradiol synthetized in female gonads, since we initially detected a specific female protection, which was absent in male mice.

In terms of peripheral inflammatory model, apparently we could not find any difference in the numerous signalling steps triggered by a short incubation with pro-inflammatory cytokine; confirmation of these results will be extremely important and will have to focus on longer incubation times. In this way, we hopefully will be able to increase the strength of these findings and will support the central role of ANXA1. In our experiments, we focused on the incubation with two pro-inflammatory cytokines, TNF-α and IFN-γ, with important clinical implications [in MS; (Carrieri *et al.*, 1998; Proia *et al.*, 2009)] recently validated as an optimal model for barrier increases in permeability (Lopez-Ramirez *et al.*, 2012). Despite that, these cytokines have also been shown to be directly transported within the brain (Nagyoszi *et al.*, 2010) or to undergo non-specific diffusion within the brain parenchyma after augmented permeability, which is an aspect we did not have the chance to investigate. More interestingly, peripheral signals are widely sensed by endothelial cells, triggering

numerous molecular responses, like further unidirectional release of cytokines and mediators (arachidonic acid, prostaglandins, nucleotides, *etc.*) in the brain parenchyma (Banks, 2006). Although we failed to detect, in our *in vitro* model, any significant change in cytokines release under the various stimuli (not shown), whose nature is still debated, future attention will be required on these aspects.

6.8 Future work

With all this in mind, future research should be focused on the molecular dynamics involved in ANXA1 release, both in presence of pro-inflammatory stimuli and estradiol. Our initial results (Figure 6.11) seem to have paved the way towards the right direction: future studies of other known sites of post-translational modifications are required, though; for example, investigating if Tyrosine21-phosphorylation could offer direct explanation for the retaining effects caused by pro-inflammatory cytokines.

We feel it will be important to generate a better understanding of routes of periphery-brain communication through the BBB, keeping a special eye on the new dynamic role of annexin A1. In particular, we should not forget the fundamental role played by other important sensors forming the BBB, *i.e.* the perivascular macrophages, pericytes and astrocytes (Thomas, 1999; Serrats *et al.*, 2010), which latest evidence depicted as extremely valuable in generating a response.

Brain barriers age as the rest of the organism and respond less well to certain treatments like the hormonal ones (Sohrabji and Bake, 2006); since these studies will be mostly relevant for applications dedicated for aged people with neurological conditions, it will be important to consider the differences that characterised the aged BBB. Unfortunately, literature leaves big gaps in this area, which need to be filled soon.

6.9 Summary and conclusions

In this chapter, we gained strong confirmation for a protective role of estradiol on cerebral endothelium; to this, we added novel evidence for ANXA1 involvement in this mechanism. Estradiol pre-exposure resulted in actions that closely resembled those played physiologically by ANXA1 on the BBB: regulation of actin cytoskeleton, stabilization of cell-cell junctions between adjacent cells and protection of the barrier tightness; we think that these events are able to tackle the disruptive role brought by uncontrolled inflammation. Therefore, estradiol pre-exposure may be able to "prime" the endothelium to respond to possible disruptive stimuli by modulating the readily available pool of ANXA1.

Overall, these findings lead us to define a new potential mechanism (described in Figure 6.14) of action for 17 β-estradiol anti-inflammatory/rescuing effect on BMECs, which, if confirmed, may offer novel ideas for further exploitation. Despite some aspects of this complex network still need to be confirmed, such findings could easily be taken into account to justify the strong evidence gathered around the protective role of estradiol on brain microvasculature (Bake and Sohrabji, 2004; Sohrabji and Bake, 2006; Bake *et al.*, 2009) as well as to decipher the numerous contrasting results given by hormonal replacement therapies under inflammatory and neurological conditions (Krause *et al.*, 2006; Li *et al.*, 2011). If translated to the human, these results may therefore suggest ANXA1 as a new endogenous player in the complex action offered by estrogen and represent the basis for a new wave of research on endogenous mediators which may modulate the ultimate hormonal effect in a less invasive fashion.

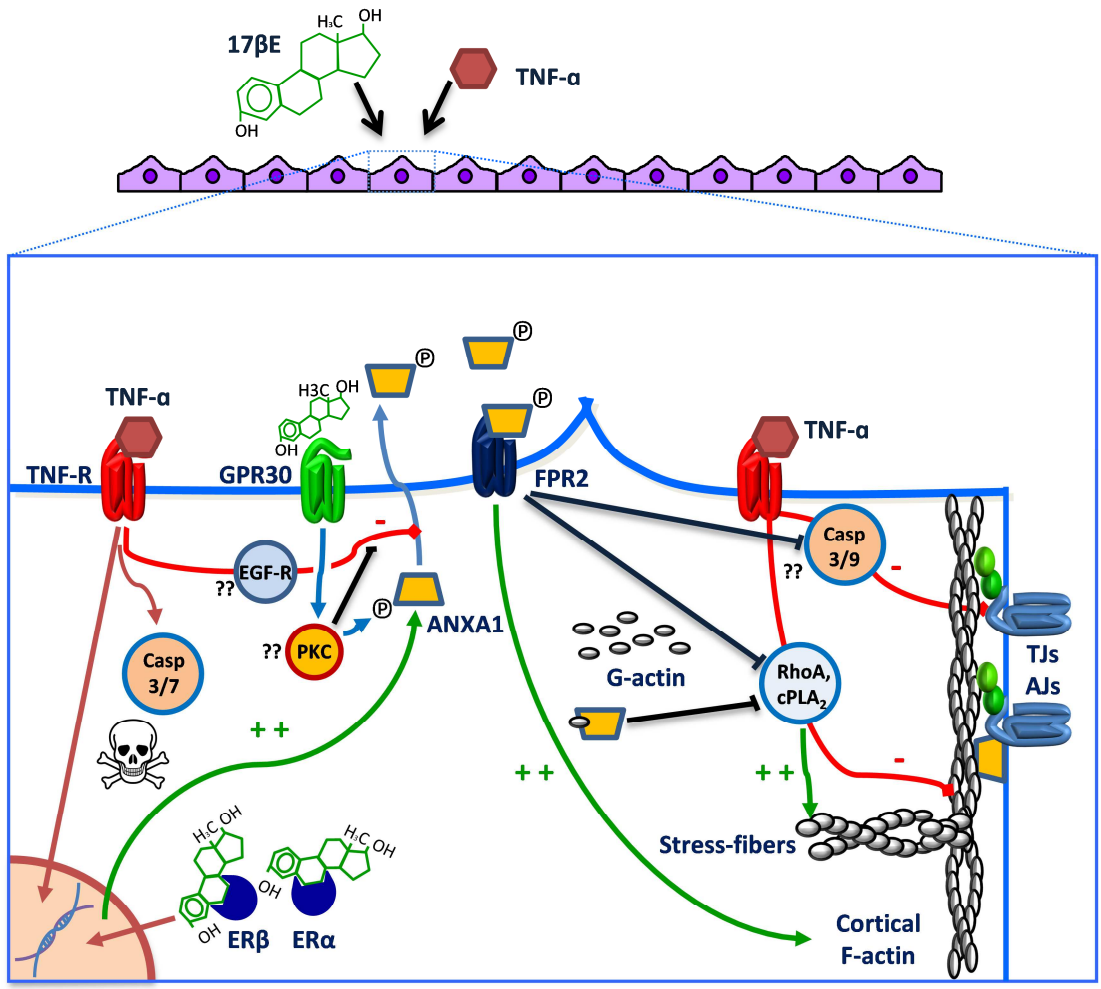

Figure 6.14 Mechanism of action of β-estradiol in BMECs and involvement of ANXA1 as mediator of the steroid. The cartoon illustrates the hypothesized pathways that are triggered by estradiol to limit subsequent increase in brain endothelial permeability under inflammatory conditions. Both genomic and non-genomic actions result in increased ANXA1 expression and release, counteracting the negative influence of pro-inflammatory mediators. ANXA1 exerts its numerous functions both from within the cells (Chapter 4) and from outside, where it is able to trigger a complex autocrine/paracrine mechanism through FPR2. Overall, this counteracts the negative effects that are triggered by pro-inflammatory cytokines like TNFα, which involve activation of RhoA, PLA_2 (both of which are negatively regulated by ANXA1) as well as caspase-3 (regulated by ANXA1), -7 and -9 with consequent apoptosis-dependent or independent actions, direct negative effects on tight junctions (which are rescued, when disrupted, by ANXA1) and induction of other pro-inflammatory mediators with a negative impact on brain endothelium. Through this complex involvement of signalling pathways, triggers and breaks, chronic exposure to estradiol seem to be able to make the cerebrovascular endothelium more resilient to peripheral inflammatory stimuli.

Chapter 7 – Central Annexin A1 under peripheral inflammation and neurodegeneration

7.1 Overview and aim of the chapter

In the previous chapter we have reported the involvement of Annexin A1 at the level of the BMECs, which represents the interface between the peripheral immune system and the CNS. With the knowledge of how inflammatory events happening elsewhere in the body signal and impact the CNS, our subsequent step was to investigate the behaviour of ANXA1 within the brain, both intact and injured. Therefore, we first studied which brain cells normally express the protein and how such expression was modulated by signals coming from outside the brain. As shown in Chapter 2 (Figure 2.1 and Figure 2.2) there is a unique expression pattern of Anxa1 in a distinct region of the midbrain, the substantia nigra pars compacta (SNpc), which is clinically important as containing the dopaminergic neurones that degenerate in Parkinson's disease. In particular, our preliminary study detected both *Anxa1* gene promoter activity (β-galactosidase staining) and protein expression at the level of a sub-population of dopaminergic neurons and at level of microglia-like cells. In addition, a peculiar modulation in *Anxa1* gene promoter activity was evident under systemic inflammatory conditions, indicating that this protein was most likely modulated by peripherally-derived stimuli.

Part of our latest findings on the role of ANXA1 on microglia behaviour have already been published and will only be briefly described for the specific purposes of the chapter. For an exhaustive description, we refer the reader to the relevant publication (McArthur *et al.*, 2010).

7.2 The impact of peripheral inflammation within the brain

As exhaustively considered in the Introduction (Section 1.3), the concept of a brain largely unaffected by peripheral inflammatory events is essentially wrong; CNS is deeply affected by what happens in the rest of the body and responds to it accordingly. *Cellular*, *humoral* or *neural pathways* are in charge of mediating the communication between the two compartments and we demonstrated how Annexin A1 takes part to the regulation of part of this process. Animal and human studies support the primary importance of peripherally-originated inflammatory molecules in mediating sickness-related behaviour.

Once inflammatory messengers have entered the brain, or have been synthesised within the brain (by astrocytes, endothelial cells and perivascular macrophages at the level of the CVOs and neurovascular unit; by other myeloid brain resident cells, as a consequence of the peripherally-triggered signalling), they are able to influence the peculiar nervous system components, primarily the neurons, the ultimate goal being a coordinated response towards the cause of inflammation (Dantzer, 2004). The resident immune cells of the CNS, microglia, are able to promptly sense and respond to the first signs of peripheral signals (Lucas *et al.*, 2006): by releasing pro-inflammatory factors like cytokines, reactive species and lipid metabolites, microglia take part in the amplification of the reaction by sending alert messages throughout the brain, triggering various neuronal structures to mount autonomic and neuro-endocrine defensive actions.

Since the CNS represents a very delicate structure, this series of reactions is supposed to occur in a timely fashion, tightly regulated by specialised anti-inflammatory/resolutive mechanisms, which still need to be fully elucidated (Yong and Marks, 2010). No long-term consequences should be left behind; however, clinical and experimental evidence indicates that inflammatory reactions may not always subside adequately, keeping microglia and other surveillance resident cells persistently in an activated state. Such a situation seems to happen according to the duration and the intensity of the initial inflammatory stimulus, on concurrent or recurrent stimulation and/or on failure of the anti-inflammatory mechanisms. In this scenario, a constant status of stress and damage negatively affects the general homeostasis of the intact brain. Several studies have reported intense and prolonged changes in the brain as a response to peripheral infections and/or inflammation. These include activated microglia phenotype and recruitment of neutrophils and monocytes into the brain (Jeong *et al.*, 2010), leading to long term loss of discrete neuronal populations (Qin *et al.*, 2007) as well as consequent alterations of neurological functions, such as disruptions to psychomotor coordination (Brydon *et al.*, 2008). Understandably, the impact of peripheral inflammatory events may result in the establishment of a constant neuro-inflammatory cycle, which represents one of the most powerful risk factors for many neurological disorders, as well as one of the major mechanisms contributing to the occurrence, recurrence and the persistence of neurodegenerative disorders.

7.2.1 Impact of peripheral inflammation in aging and pathology

Several reports have shown the strong influence of systemic inflammation in patients with on-going neurological conditions, such as AD (Perry, 2010; Murray *et al.*, 2011). In fact, under existing pathological conditions or in the aged brain, the impact of inflammation results in an even more complex set of responses, which are linked to a particular microglia phenotype called "primed": chronic neurodegenerative diseases and aging represent a constant ensemble of subtle, slow, chronic inflammatory stimuli, which bring microglia to adapt into a particular sub-activated status, characterised by proliferation, structural changes towards the activated morphology, increased expression of several cell-surface antigens and transcription of inflammatory genes, but supressed secretion of inflammatory molecules. Microglia represents a group of long-lived cells that retain memory of all the events that occurred in their microenvironment. Therefore, their behaviour is affected in the long term by neurodegeneration, which is characterised by the loss of structure and function of neurons and a constant release of molecules and cellular components into the surrounding environment (Godbout *et al.*, 2005; Tansey *et al.*, 2007). The primed phenotype can be viewed as the result of an adaptation towards subtle constant stimulation, a protective response that avoids over-activation to the same repeated type of trigger. Some have defined it as "alternatively anti-inflammatory" (Perry, 2004) since increasing evidence is reporting low pro-inflammatory cytokines (IL-1, IL-6, TNF-α, IFN-γ) and increased anti-inflammatory ones (TGF-β1) in brains affected from chronic neurodegenerative disorders (Perry, 2010). Some others have defined it as "dystrophic" or partially activated after the observation that diseased or senescent microglia are functionally impaired in their ability to produce neurotrophic factors or to eliminate toxins and dead cells, while showing increased neurotoxicity and reduced anti-oxidant activity (Holmes and Butchart, 2011; L'Episcopo *et al.*, 2011). Regardless of the truth behind its nature, evidence supports that in a neurodegenerating or aged brain different types of stimuli may evoke exaggerated inflammatory responses through this type of microglia, which appear to have a primary impact on disease progression and to contribute towards neuronal loss (Cunningham *et al.*, 2005; Godbout *et al.*, 2005; Couch *et al.*, 2011; Murray *et al.*, 2011).

We should not forget that the primary role of microglia is to contribute to neuroprotection, for example by releasing neurotrophic and survival factors (Gao and Hong, 2008); however, the balance between the positive and negative effects offered by neuroinflammation on its own is very fine: uncontrolled microglial over-activation can become destructive with the consequent damage of healthy or already injured brain regions.

7.2.1.1 Impact of peripheral inflammation in chronic neurodegeneration

We are now aware of the clinical relevance played by neuroinflammation in several neurodegenerative diseases like AD, MS and PD; the fact that BBB is often impaired in these pathologies facilitates the impact of several environmental factors, like infection-driven inflammatory mediators, on creating a vicious self-propagating cycle contributing to the progression of the disease (Perry, 2004, 2010) as depicted in Figure 7.1; in addition, the fact that most of these pathologies (AD and PD) show an increasing risk of developing or exacerbating with age, could be seen as chronic exposure to systemic inflammation. For example, it has been shown that systemic infections of the respiratory tract are tightly associated with one-third of MS relapses, while systemic challenge with bacterial-derived inflammogens or cytokines exacerbated the clinical symptoms of the animal model EAE (Schiffenbauer *et al.*, 1993). Animal and human studies showed increased cognitive decline and exaggerated sickness behaviour in response to systemic inflammation in AD patients and animal models (Holmes and Butchart, 2011); moreover, a strong correlation between elevated peripheral inflammatory indicators and new pathology development or existing pathology exacerbation has been observed, which may be used as prognostic markers.

7.2.1.2 Increase in microglia population under pathological conditions

The parenchymal microglial cells represent a long-lived and stable population derived from the infiltrating phase occurring during gestation. Physiologically, a small number of leukocytes crosses the BBB and enters the CNS; at the same extent, resident microglia is only partially maintained by peripherally circulating cells (*i.e.* monocytes) (Chan *et al.*, 2007; von Bernhardi *et al.*, 2010).

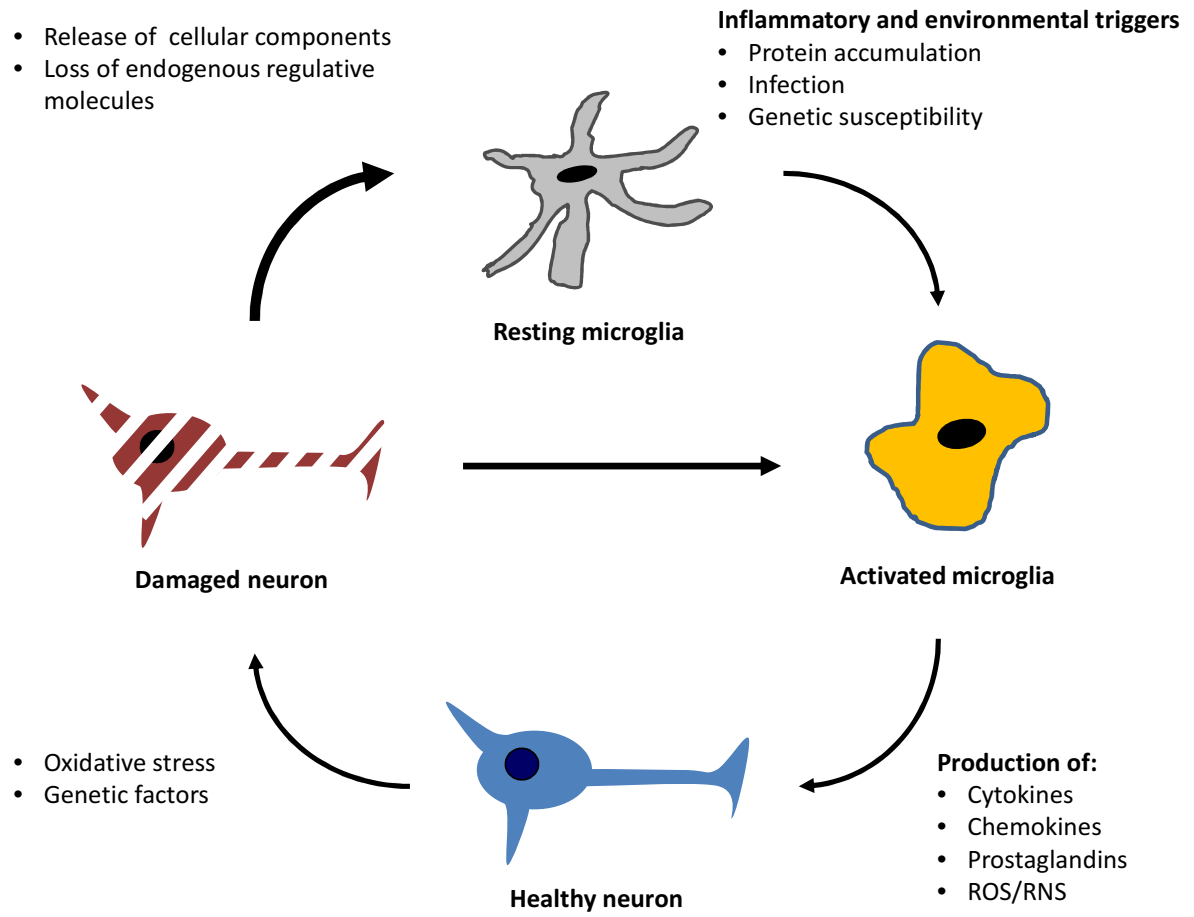

Figure 7.1 Mechanisms and triggers that initiate the vicious cycle of neuroinflammation. Various stimuli can result in activation of microglia, microgliosis and consequent release of toxic substances which negatively target neurons. Alternatively, a healthy neuron may become dysfunctional as a result of built-up oxidative stress or genetic factors, and become a primary stimulus for microglia activation. Adapted from Tansey *et al.*, 2007.

However, the situation changes dramatically under pathological conditions; studies employing chimeric animals or allogenic transplantation clearly showed cells of monocytic nature differentiating into microglia (Djukic *et al.*, 2006; Hanisch and Kettenmann, 2007; D'Mello *et al.*, 2009; Ajami *et al.*, 2011; Mizutani *et al.*, 2012) in support of an on-going inflammatory reaction. Although the molecular mechanism of recruitment is not fully clear, it is evident that haematopoietic cells are an important source for the CNS even when the brain does not show gross signs of acute inflammation but more a subtle chronic inflammatory milieu, characteristic for example of aging (von Bernhardi *et al.*, 2010).

Notably, in a model of meningitis (Djukic *et al.*, 2006), conversion of blood monocytes into microglia did not occur during the acute phase of the disease but during the post-infection period; since this is a crucial phase for the post-infection recovery, the role of these cells is to restore tissue homeostasis. However, the recruitment of monocytes in a non-regulated fashion may become hazardous and potentially exacerbate existing conditions. Interestingly, a recent report (D'Mello *et al.*, 2009) demonstrated how peripheral inflammation is able to indirectly stimulate circulating cell recruitment into the CNS, supporting the huge impact that even low-grade immune reaction may generate. These novel findings opened up new avenues in understanding the pathophysiology of many conditions, as well as offering a new potential delivery strategy of therapeutic molecules (in the form of coding DNA sequences) to the CNS through peripheral haematopoietic cells (Djukic *et al.*, 2006).

7.2.1.2.1 Parkinson's disease: generalities

Although less extensively studied than Alzheimer's disease, today we know that Parkinson's disease can also be profoundly affected by peripheral inflammatory events (Machado *et al.*, 2011). Being the second most common neurodegenerative disorder of aging, and the most common movement disorder, the burden of disability from PD is considerable.

In a nutshell, PD is characterised by degeneration of dopaminergic (DA) neurons mainly at the level of the SNpc; this is a midbrain nucleus included in the basal ganglia system, and the major source of dopamine of the brain. The DA neurons of the SNpc project into the striatum (forming the nigrostriatal dopaminergic pathway, NSDA) and the output signals govern the locomotor behaviour (Brydon *et al.*, 2008). As a consequence of the extensive loss of DA neurons (more than 70% of them have degenerated/died at the time of the first overt pathological signs), clinical signs include motor symptoms such as rigidity, bradykinesia, tremor at rest, gait and balance problems, and non-motor symptoms contributing to deterioration of the life style, including mild cognitive impairment, depression, sleep disorders, olfactory deficits, dementia and increased mortality (Hindle, 2010). Unfortunately there is no yet successful treatment for PD patients to date and this links to the fact that the diagnosis usually occurs when substantial damage has already occurred (Glass *et al.*, 2010).

The aetiology of PD remains still not clear. Once regarded as a purely sporadic disease, nowadays its multifactorial nature is clearly explained by the influence of genetic and environmental factors contributing to the development of the disease along with aging, which still represents the largest single risk factor (Hindle, 2010; Schapira and Jenner, 2011). Environmental risks for PD include exposure to pesticides, heavy metals and solvents, rural environment and some types of jobs with toxins high exposure. Although there are forms of PD that are considered to be purely familial, they account for less than 5% of the total cases (Yang *et al.*, 2009); in many cases, genetic alterations or polymorphisms on certain molecular pathways (mitochondria functions, proteasome and autophagy) represent important susceptibility factors.

In *post-mortem* studies, altered levels of inflammatory cytokines have been detected, along with the typical features of activated microglia. In addition, some recent studies have identified a role for pro-inflammatory CD4+ T helper class-1 (T_H1) lymphocytes, which may contribute to DA neurons toxicity (Glass *et al.*, 2010). These clinical signs stress the impact offered by neuroinflammation in the disease, although we don't know whether this constitutes a primary cause of the DA neurons death or a response triggered towards neuronal loss. Both options may be equally involved in the pathology (Schapira and Jenner, 2011). PD progression strongly depends on a chronic inflammatory *milieu*, with cytokines and nitric oxide being extremely important as amplifiers of the initiating neuro-inflammatory event (McGeer and McGeer, 2004; Glass *et al.*, 2010). Evidence that inflammatory responses are able to trigger loss of dopaminergic neurons is provided by endotoxin-mediated neurotoxicity (Kim *et al.*, 2000).

7.2.1.2.1.1 Impact of systemic inflammation in Parkinson's disease

Being so strongly influenced by neuroinflammation, PD is also intensively affected by peripheral inflammatory events, which can exacerbate the course of the pathology. Today, systemic inflammatory insults are considered risk factors in the PD aetiology and in the exacerbation of existing pathology (Ferrari and Tarelli, 2011). Qin *et al.* (Qin *et al.*, 2007) showed that peripheral administration of the inflammogen LPS is able to cause long lasting subtle neuroinflammation at the level of the SNpc (levels of pro-inflammatory cytokines

elevated for 10 months), which results in delayed loss of DA neurons. Instead, Jeong *et al.* (Jeong *et al.*, 2010) did not report chronic loss of neurons after LPS administration, but focused more on the acute response of the microglia populating this region, which promptly developed an activated morphology and cytokine profile. Recruitment of peripheral monocytes has also been reported and it represents a factor that increases the susceptibility of the SNpc (Jeong *et al.*, 2010). Interestingly, one report (Reale *et al.*, 2009) identified a higher pro-inflammatory profile for peripheral blood mononuclear cells (PBMC; which include monocytes and lymphocytes) in PD patients, which exacerbated in presence of inflammatory stimulation (LPS); this could suggest a cross-talk periphery-brain occurring in both directions as well as the definition of a chronic self-propelling detrimental cycle which contributes to the disease progression.

7.2.1.2.1.2 Peculiar features of the SNpc

PD represents an excellent model to advance the current understanding of neurodegeneration: in fact, the pathological event is well defined and consist in the specific loss of the DA neurons of the SNpc (Schapira and Jenner, 2011), which has been reported to present the highest density of microglia in the whole brain (Kim *et al.*, 2000). Also, DA neurons of the SNpc present a higher intracellular oxidative state due to a high glycolytic regime (Tansey *et al.*, 2007) but mostly because of the synthetic process of dopamine, which requires a series of oxidative reactions and produces high amounts of neuromelanin, known to trigger oxidative reactions. In addition to that, they also show less anti-oxidative defence (Glass *et al.*, 2010). Overall, it is easy to understand how a significant increase in pro-inflammatory reactions involving ROS and RNS, for example in response to systemic inflammation, represent a really serious danger for such a delicate brain area, maximizing the importance of such studies.

7.2.1.2.2 How to model Parkinson's disease

In order to study in detail the pathogenesis of Parkinson's disease, as well as all the factors that may influence the outcome, either positively (potential therapies) or negatively

(environmental triggers, genetic susceptibility, *etc.*), we need to be able to model the pathology accurately; that is why several animal models of the disease are currently chosen and used according to the specific needs of the investigation.

The neurotoxin 6-hydroxydopamine model (**6-OHDA**) in rodents is the traditional model, especially useful for studies investigating the behavioural deficits and motor dysfunctions of the disease. 6-OHDA is a structural analogue of catecholamines (of which dopamine is one of the members) and it is able to exert its toxic effects on catecholaminergic neurons, accessible through the dopamine (DAT) or the noradrenaline (NAT) membrane transporters (Simola *et al.*, 2007). Being unable to cross the BBB, this molecule has to be directly injected in the area of interest through stereotaxic surgery, along with NAT blockers (like desipramine), which impedes targetting noradrenergic neurons. 6-OHDA causes DA neuronal death by triggering an intense oxidative stress (Simola *et al.*, 2007). The toxin can also alter mitochondrial function, by impairing the activity of complex I of the respiratory chain. All these events result in the consequent generation of ROS, which quickly trigger neuronal damage and demise. Importantly, the toxin can be injected on only one side of the animal brain, with the opposite side serving as an intra-animal control. This injection produces DA neuron loss on the injected side while sparing the contralateral DA neurons. There is no evidence of Lewy bodies in this model and the progression of the disease is acute instead of chronic.

The 1-methyl-4-phenyltetrahydropyridine (**MPTP**) model is currently considered the PD model of choice in mice while rats are very insensitive to this toxin. After intraperitoneal injection, the molecule can easily access the brain thanks to its lipid-soluble/amphiphilic nature and it does not show toxicity in the original form but it can be metabolized in the toxic 1-methyl-4-phenylpiridinium (MPP^+) by astrocytic oxidases and in this form it shows preferential toxicity for the DA striatal nerve terminals as well as for DA neurons of the SNpc. The toxin seems to target the mitochondria respiratory chain (complex I), resulting in increased oxidative stress and in a lower energy production. Also, the selectivity of the toxin is not as precise, since the active MPP^+ can target also other neurons and brain cells due to its high penetration and reactivity (Blandini and Armentero, 2012).

More recent models, like the rotenone systemic injection (Blandini and Armentero, 2012) or the intranigral injection of lactacystin (Ahn and Jeon, 2006) target important pathways impaired in the human disease, namely mitochondrial respiratory activity and proteasome, resulting in physiopathological manifestations very similar to those seen in PD (*e.g.* the accumulation and aggregation of α-synuclein and ubiquitin, the progressive oxidative damage, and neuronal apoptosis). The intracerebral injection of inflammogen such LPS has been also explored (Ahn and Jeon, 2006; Liu and Bing, 2011); although it produces selective loss of DA neurons in the SNpc, it does not resemble the main features of PD and it only proves useful to study the impact of inflammation in triggering/progressing the disease.

7.2.1.3 Controlling and limiting the impact of peripheral inflammation

Controlling neuroinflammation is still a major challenge from a therapeutic point of view; therefore, a huge effort has been produced in studying means to control microglia over-activation in all its facets. Several anti-inflammatory and anti-oxidant molecules and therapies have been tested including non-steroidal anti-inflammatory drugs (NSAIDs), iNOS inhibitors, steroids like glucocorticoids (dexamethasone) and immunosuppressants as cyclosporine A (Tansey *et al.*, 2007). The results produced were controversial: while NSAIDs chronic use was reported to reduce the risk of developing PD by about 45% (Chen *et al.*, 2003; McGeer and McGeer, 2004; Tansey *et al.*, 2007) and proved to be useful in animal models of PD (L'Episcopo *et al.*, 2011), most of aforementioned compounds did not show significant improvements during their translation in humans (Allan and Rothwell, 2001), either for their strong side-effects or because the human disease proved to be more complex to treat. Several clinical trials have in fact failed in the past, mainly due to the advanced pathology of the patients enrolled in the studies or because the dosing and timing regimes were wrong. Noteworthy, these drugs are not truly anti-inflammatory, since they do not stimulate the anti-inflammatory/resolution pathway and restoration of the homeostasis, but they rather halt the on-going inflammatory response. For this reason, recent studies are beginning to focus more smartly on endogenous molecules, which could be exploited in a more “natural” way, promoting the resolution of a persistent, dysregulated and detrimental neuroinflammatory reaction. Several counter-regulating mechanisms

(called *Off* signals) have been recently identified as constantly in place. For example, the immunoglobulin family member CD200 (OX-2) normally expressed on neurons binds a ligand on microglia (CD200 receptor) and limits its reactivity; similarly, the chemokine CX3CL1 (more familiarly known as fractalkine) is highly expressed and released constitutively by neurons, binds the microglial receptor CX3CR1 and in its absence neuroinflammatory reactions are exacerbated (Cardona *et al.*, 2006; Biber *et al.*, 2007).

Overall, this evidence indicates that neurons are active regulators of microglia behaviour, and are not simply passive targets of microglial over-activation; neurodegeneration results in a loss of neurons, but also in a considerable loss of endogenous anti-inflammatory mechanisms, which could contribute to the consequent microglia activation (de Haas *et al.*, 2007).

Certain regulatory mechanisms also exist at the level of glia cells, like the nuclear receptor Nurr1 which is able to limit the NF-κB-mediated transcription of pro-inflammatory genes; Nurr1 has been shown to provide protection in animal PD models by reducing the production of neurotoxic mediators by microglia and astrocytes (Saijo *et al.*, 2009; Glass *et al.*, 2010).

7.2.1.3.1 Annexin A1 as a potential counter-regulator of neuroinflammation

Annexin A1 relevance as a modulator of several anti-inflammatory molecules, along with the ability to prevent the activation of reactive enzymes like COXs, iNOS and $cPLA_2$ (Minghetti *et al.*, 1999), to limit the production of cytokines classically shown to be up-regulated in PD (IL-6 and IL-8) (Mogi *et al.*, 1994) and other positive correlations with cerebral ischemia models (Relton *et al.*, 1991; Black *et al.*, 1992; Rothwell and Relton, 1993; Gavins *et al.*, 2007) gave this molecule huge expectations as a neuro-inflammatory modulator. We recently demonstrated ANXA1 to be important for microglia-driven non-inflammatory clearance of apoptotic neurons (McArthur *et al.*, 2010), which is an essential requirement to avoid secondary necrosis and perpetuation of central inflammation.

7.3 Methods

Please refer to Chapter 3 for the description of general *in vivo* and immunostaining procedures and to McArthur *et al.* 2010 (McArthur *et al.*, 2010) for details relative to that publication. Here description about certain technical aspects and the experimental plan specifically used for the purpose of this chapter is provided. Please refer to the Appendix (Chapter 10) for the solution composition.

7.3.1.1 *In vivo* experimental plan

In order to evaluate brain-resident cell responses to peripheral inflammation in terms of dopaminergic neuron survival and specific expression of Anxa1, we compared male wild-type C57Bl/6 or Anxa1 null mice (*n*=4-6/group; 2-3 months old) over the time after challenging them *i.p.* with a single dose (3 mg/kg) of LPS. Animals were culled by anaesthetic overdose, perfused with saline and blood and brains were collected at 2 hours, 24 hours and 7 days after administration of LPS.

To investigate genotype-related differences in DA neurons survival under neurodegenerative conditions, we performed 6-OHDA unilateral intrastriatal infusion (see below) in male wild-type C57Bl/6 or Anxa1 null mice (*n*=4-6/group) and culled them after 24 hours, 1 week, 2 weeks or 4 weeks post-lesioning. Vehicle infusion (1 µl) served as baseline control and was assessed after 24 hours.

To evaluate for a potential synergistic/exacerbating effect of systemic inflammation on on-going neurodegeneration of the SNpc DA neurons, male wild-type C57Bl/6 or Anxa1 null mice (*n*=4-6/group) received 6-OHDA lesions and after 1 week (established as a good time-point where number of dopaminergic neurons was significantly decreased) were challenged *i.p.* with a single dose (3 mg/kg) of LPS. After 1 week mice were placed under terminal anaesthesia for collection of brains. Figure 10.7 visually describes the experimental plan and it has been assigned to the Appendix for space constraints.

7.3.2 Cytokine quantification by ELISA

Blood samples obtained by cardiac puncture were taken from animals that had received *i.p.* administration of LPS for various time frames. The samples were left to clot at 37°C for 10 minutes and then centrifuged at 4000 RPM (~ 1200x*g*) for 20 minutes at 4°C; the supernatant (serum) was collected in a fresh tube, taking care to prevent carry-over of red blood cells. Brain lysates were instead obtained as described in (Puntener *et al.*, 2012). Briefly, half brains were homogenised by sonication (2 cycles; 10 seconds/cycle on ice) in TRIS buffer containing a protease inhibitor cocktail (1ml/100 mg tissue). Samples were centrifuged for 30 minutes at 13000 RPM and supernatants assayed for total protein using the BCA protein assay described in the general Methods.

Serum samples were analysed for TNF-α and IL-6 content while brain lysates were analysed for IL-10 content using ELISA kits (eBioscience, UK) according to manufacturer's instructions. Samples were run in triplicates; serum samples and brain lysates were diluted 1:10 using the provided assay diluent in order to avoid values outside the sensibility range of the kit. Detection of the colorimetric reaction was performed by reading the plates at 450 nm and correcting for unspecific absorbance by subtracting the reading at 570 nm. Brain lysates contents were normalized on total protein content, giving values as ng cytokine/mg protein.

7.3.3 6-Hydroxydopamine (6-OHDA) lesioning of the NSDA pathway

Intracerebral injection of 6-OHDA into the left striatum of mouse brain has previously been shown to induce lesions in the striatum itself (loss of striatal DA) and SNpc [loss of tyrosine hydroxylase immunoreactive, TH-IR, neurons (Callio *et al.*, 2005)]. Dr. S. McArthur provided extensive help and technical advice. Half an hour prior to lesioning, animals were injected *i.p.* with 20 mg/kg of desipramine, an inhibitor of the noradrenalin re-uptake transporter, in order to prevent the access of the toxin to noradrenergic or adrenergic neurons. Animals were then anesthetised by intraperitoneal injection of a mixture of hypnorm/hypnovel (1:1:2; respectively, hypnorm:hypnovel:water). The fur along the snout and on the forehead of the animal was shaved and the area was disinfected by application of 100% ethanol. The animal was then fitted into a stereotactic frame and an incision was made running from midway between the eyes to midway between the ears.

The membranous coating of the skull was then removed to reveal the bregma, which was accentuated by marking with a dissection pin. Using this as starting point, the injection needle was moved 2 mm left and 1 mm towards the tail to sit above the striatum (Callio *et al.*, 2005). This point was marked on the surface of the skull and a hole of approximately 1 mm diameter was drilled using a hand-held dental drill. The meninges were cleared from the surface and the injection needle was lowered 3 mm into the brain. Over a period of 2 minutes 1 µl of 6-OHDA solution or 1 µl of vehicle was injected. The injection needle was then left in place for a further 3 minutes to allow diffusion of the neurotoxin from the lesion site. The animals received 80 µl buprenorphine analgesics (Vetergesic) subcutaneously and were removed from the stereotactic frame. The head incision was sealed with three sutures and the animal was monitored until it had recovered from anaesthesia. Toxin exposure was for 24 hours, 1, 2 and 4 weeks, after which animals were deeply anesthetised, perfused and the brain was collected and fixed. Brains from vehicle-treated animals were collected after 24 hours only, since longer time-points did not show any difference in loss of DA neurons (Jeon *et al.*, 1995).

Previous studies (Gillies *et al.*, 2004) confirmed that placement of 6-OHDA or vehicle injections on the left side had no significant effect on the dopaminergic populations on the right side; therefore, results of DA neurons remaining in the lesioned side were expressed as percentage of DA neurons in the contralateral side, as extensively done in the past (Schwarting and Huston, 1996).

7.3.4 Fluorescence microscopy for quantification

Brain tissue sections prepared as described in the General methods (Chapter 3), were viewed with a Nikon eclipse i50 microscope using Lumen200 fluorescent illumination system (Prior Scientific, USA) with filter sets to detect 488nm (green), 546nm (red) and 310nm (DAPI) excitation wavelength. Images were captured with a QIACAM digital camera (QImaging Inc., Canada) and using Image Pro Plus software 7.0 (Media Cybernetics Inc., UK) to control an OASIS turbo scan system that could create tiled images of whole sections or area of interest. Images were saved with spatial reference information settings for each objective based on calibration images.

7.3.4.1 Quantification of DA neurons and microglia cells on tissue sections

DA neurons were identified as the tyrosine hydroxylase positive (TH^+) cells, which represents one of the rate limiting enzyme in DA synthesis (Kaufman, 1995). To identify microglia, we chose to stain for ionized calcium binding adaptor molecule 1 (Iba1), a cytoplasmic calcium-binding protein thought to play a role in activation of phagocytic myeloid cells. It clearly stains microglia cells, as well as monocytes and resident macrophages in a lesser extent. For double-staining constraints, certain labelling experiments were performed by using integrin-α M (Cd11b), another molecule expressed under basal conditions on cells of a myeloid origin, in particular resident ones. In the brain, these molecules have been shown to be present on resident microglia and to be up-regulated when these cells undergo activation (Ransohoff and Brown, 2012).

TH^+ cells, $Iba1^+$ and Annexin A1 positive ($Anxa1^+$) cells within the SNpc and ventral tegmental area (VTA) were counted using an image analysis software package (Image ProPlus 7.0, Media Cybernetics, UK). Images were projected onto a PC monitor and the sections were analysed by manually single blinded-counting all of the TH^+ cells and $Iba1^+$ located within the two nuclei (whose boundaries were delineated by following the profile described by the TH^+ cells). Definition of the SNpc and VTA boundaries was accomplished along nuclei defined by TH positive cells, following published visual guidelines (Ikemoto, 2007), reviewed in Figure 10.8 (Appendix). In each animal, the total number of positive cells in at least four sections, representative of the whole extent of both nuclei, was counted; sections were labelled as rostral or caudal according to their location relative to the brain area of interest. Average of cell counts per rostral/caudal region was calculated for each group and comparison was made as absolute numbers or percentages of vehicle treated groups to evaluate significant changes in the numbers. This profile-based counting technique for serial reconstruction has proven the most appropriate method when cell numbers are relatively low (Huerta-Ocampo *et al.*, 2005). This two-dimensional method, employed previously (Gillies *et al.*, 2004; Huerta-Ocampo *et al.*, 2005), enables counting of all cells across the whole of the coronal plane of the SNpc and VTA, where TH^+ immunohistochemistry completely delineates nuclear margins. This provides a large sampling window, enabling highly accurate assessment in the (*x, y*) plane, which compares favourably with three dimensional counting methods (Benes and Lange, 2001).

7.3.5 Nitrite content measurement

Nitrite (NO_2^-) levels are good indicators of nitric oxide (NO) production by NO synthase enzymes present in cells or tissues; since NO is a highly reactive molecule, it undergoes a series of reactions with several molecules present in biological fluids and is eventually metabolized to nitrite and nitrate (NO_3^-), the latter being converted to the former almost totally (Rakesh, 2007). Nitrite levels can be measured using the Griess reaction (Green *et al.*, 1982). A total of 50 µl/total brain lysate (generated as described for cytokine extraction) was incubated with 100 µl of Griess reagent (see Appendix) for 15 min. Nitrite production was determined by comparing the absorbance at 540 nm with a standard curve generated by $NaNO_2$, and minimum sensitivity was 3 µM. Nitrite contents were normalized on total protein content.

7.4 Results

7.4.1 Comparison between wild-type and Anxa1 null mice in terms of DA neurons and Iba1$^+$ cells

Immunofluorescence studies on wild-type and on Anxa1 null mouse (Chapter 2; Figure 2.1 and 2.2) showed Anxa1 to be expressed in several regions of the brain and in a wide range of cell types, including putative neurons and microglia. Bright Anxa1 immunoreactivity in wild-type animals and β-gal staining in Anxa1 null mice were present in a small set of cells in the SNpc; double immunofluorescence staining confirmed that these cells were DA neurons, as typified by the positivity to TH specific staining. We characterised these results in more detail, and we observed that a small sub-population of DA neurons (around 15% of total TH$^+$ neurons) were positive for Anxa1 in untreated conditions (Figure 7.2; Panel A) while only a few scattered DA neurons of the neighbouring region VTA (functionally and developmentally distinct) were positive for the protein. We confirmed the intense expression of Anxa1 in the sub-population by confocal microscopy (Figure 7.2; Panel C), which identified the strong presence of the protein within the cell body, although the protein was also present at the level of the axonal fibres as evident from Figure 7.2, Panel A (magnification).

ANXA1 was also expressed in a small portion of TH$^+$ dopaminergic neurons of the human SNpc, paralleling the observations made on the mouse model (Figure 7.2; Panel E). Comparing wild-type and Anxa1 null mice in terms of total number of DA neurons either in the SNpc or in the VTA, we did not detect any significant difference under basal conditions (Figure 7.2: Panel D).

We then characterised genotype-related differences in terms of microglia cells. Interestingly, we detected great differences in the density of microglia cells at the level of the basal mesencephalic basal ganglia: Anxa1 null mice showed a higher values of Iba1$^+$ cells both in the SNpc and in the VTA (Figure 7.3; Panel A and B) compared to the wild-type age- and sex-matched animals. Wild-type animals showed densities comparable with reported values (Kim *et al.*, 2000), which were increased significantly in the KO animals. Interestingly, we were able to detect morphological differences throughout the brain parenchyma, as

depicted in Figure 7.3, Panel F, which shows a representative example taken from the thalamus: wild-type $Iba1^{+}$ microglia cells showed thin, complex ramifications covering large micro-areas of the tissue, while cells stained on sections derived from the Anxa1 null mice appeared with short and limited ramifications. From a functional point of view, $Anxa1^{-/-}$ brain tissue showed increased basal expression of two inflammatory enzymes usually expressed only during immune reactions, iNOS and COX-2. These changes suggested the constitutive presence of an immunologically active state.

We then examined the expression of Anxa1 in resident microglia cells from wild-type animals. Although staining in the Anxa1 null mice for the reporter gene, β-galactosidase, indicated diffuse expression in small microglia-like cells, double immunofluorescence staining for Anxa1 and Cd11b detected only a very low signal, specifically localized in limited regions of the cell body and cell membrane, as evident from Figure 7.3, Panel C. However, we were able to detect a more cell body and ramifications-diffused ANXA1 positivity of several microglia cells in human brain *post-mortem* samples, as represented in Figure 7.3, Panel D (see Section 5.3.3 for tissue processing and staining methods).

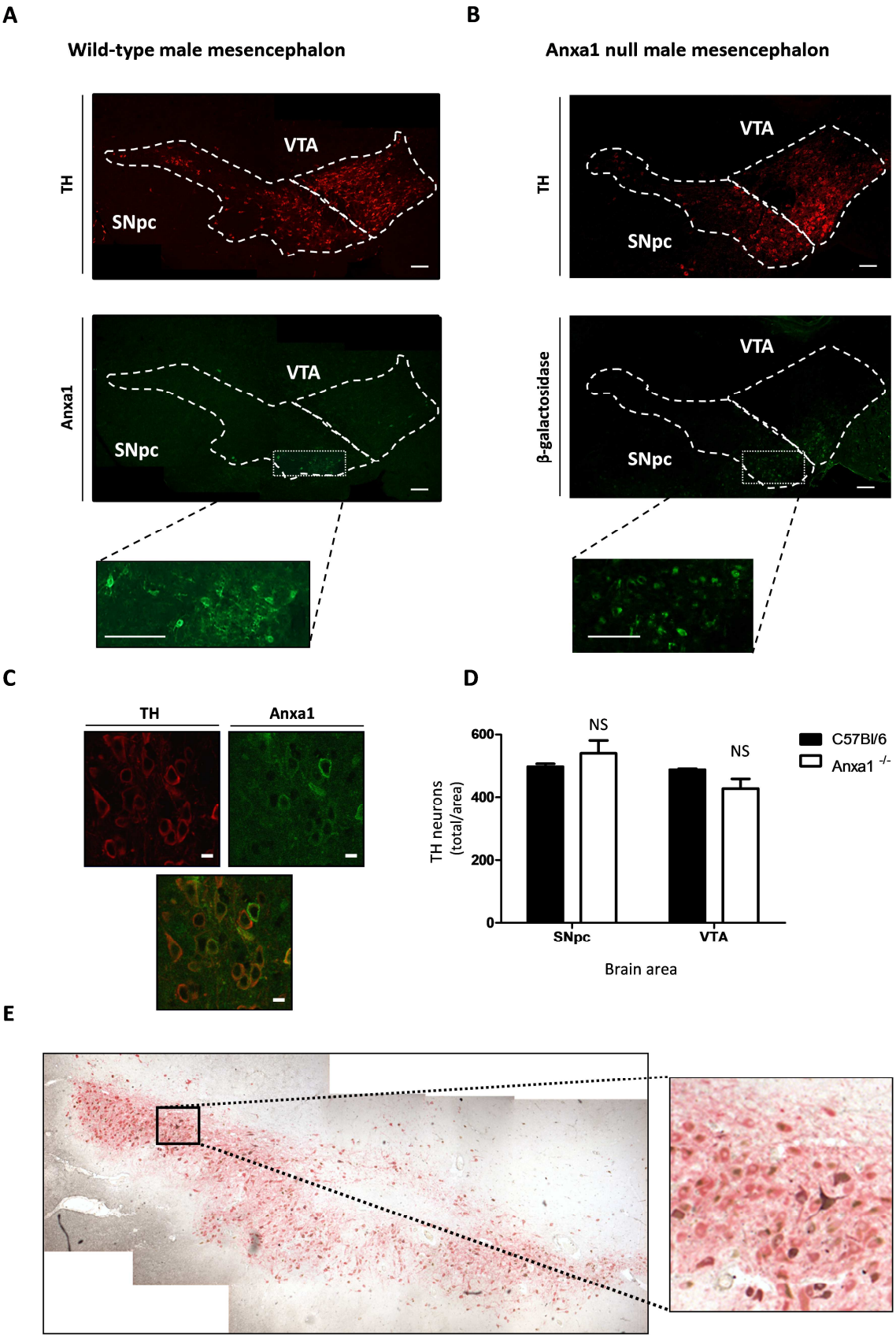
A
Wild-type male mesencephalon
B
Anxa1 null male mesencephalon
TH
VTA
SNpc
Anxa1
β-galactosidase
C
TH
Anxa1
D
TH neurons (total/area)
600
400
200
0
NS
NS
SNpc
VTA
Brain area
C57Bl/6
Anxa1 -/-
E

Figure 7.2 Characterisation of Anxa1 expression and *Anxa1* gene activity in mouse and human mesencephalon. A| Anxa1 (green) and tyrosine-hydroxylase (TH; red) immunofluorescent positivity are visualised in a section representative of the SNpc and VTA in wild-type C57Bl/6 male mice. Typical examples from *n*=3 experiments. Scale bars: 250 µm. **B|** β-galactosidase (green) and tyrosine-hydroxylase (TH; red) immunofluorescent positivity are visualised in a section representative of the SNpc and VTA in wild-type C57Bl/6 male mice. Typical examples from *n*=3 experiments. Scale bars: 250 µm and 125 µm (inset). **C|** presents confocal microscopic analysis of Anxa1 (green) and TH (red) expression in a magnified area of the SNpc. Typical example from *n*=3 experiments. Scale bar: 10 µm. **D|** Quantification of DA TH^+ neurons in the SNpc and VTA of wild-type and $Anxa1^{-/-}$ animals. Histograms show results from *n*=6 animals/genotype and are expressed as mean ± SEM (total n° cells/region of interest). Student *t*-test between the genotypes showed non-significant (NS) differences. **E|** Immunohistochemistry analysis of human substantia nigra from a patient affected by a non-relevant pathology. TH^+ neurons were stained in pink, while ANXA1 in brown using horseradish peroxidase- and alkaline phosphatase-conjugated antibody and Vector kits (Vector Laboratories, UK) to develop colorimetric reactions. Panels C and E were produced by Dr. S McArthur.

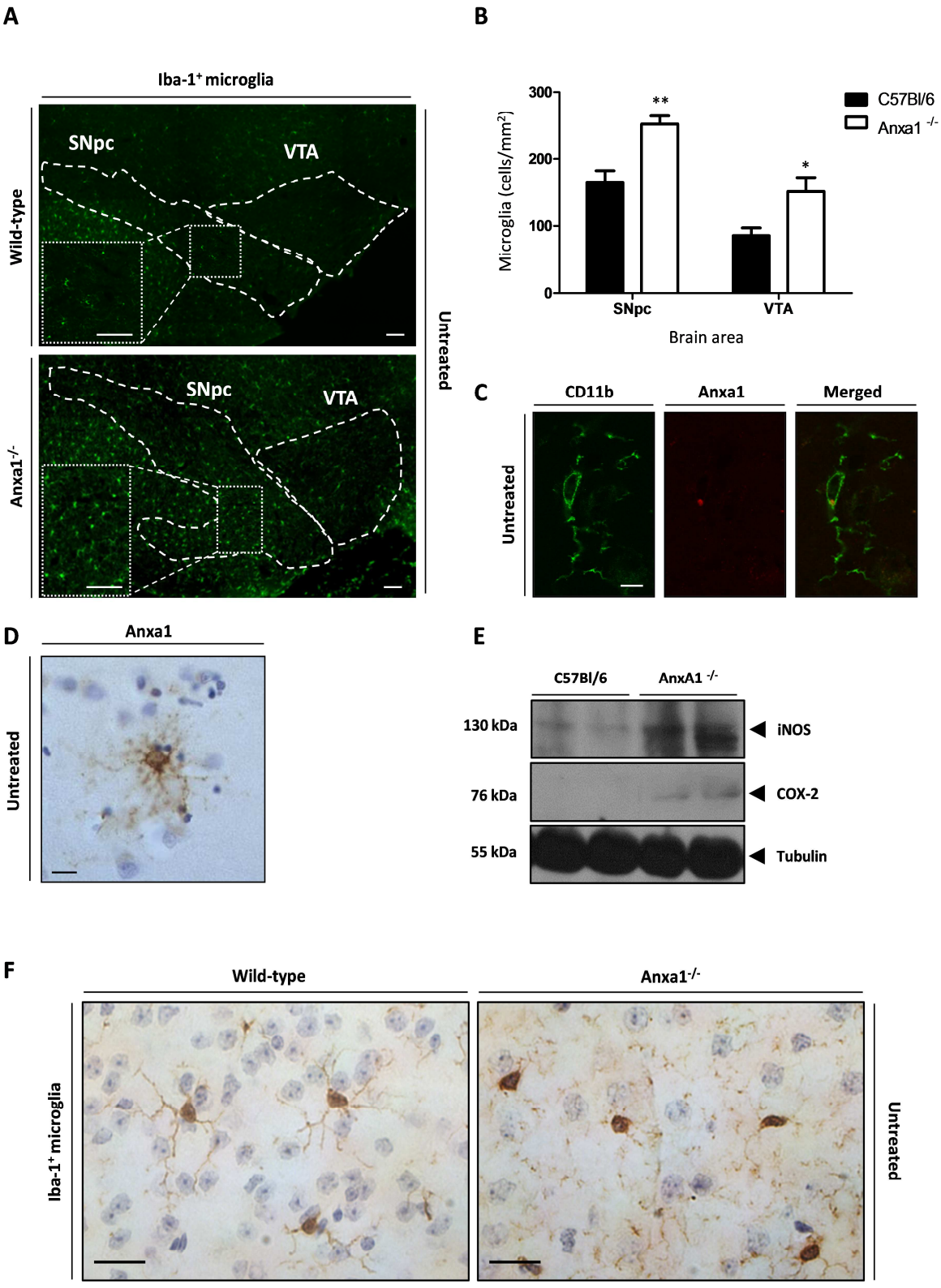
A
Iba-1+ microglia
Wild-type
SNpc
VTA
Anxa1-/-
SNpc
VTA
Untreated
B
Microglia (cells/mm2)
300
200
100
0
**
*
C57Bl/6
Anxa1 -/-
SNpc
VTA
Brain area
C
CD11b
Anxa1
Merged
Untreated
D
Anxa1
Untreated
E
C57Bl/6
AnxA1 -/-
130 kDa
iNOS
76 kDa
COX-2
55 kDa
Tubulin
F
Wild-type
Anxa1-/-
Iba-1+ microglia
Untreated

Figure 7.3 Genotype-related differences in the number and morphology of Iba1$^+$ cells populating the SNpc and the VTA. A| Iba1$^+$ (green) immunofluorescent positivity is visualised in a section representative of the SNpc and VTA in wild-type and Anxa1 null male mice (2-3 months old). Anatomical regions boundaries were defined through double-staining for TH (not shown). Typical examples from *n*=3 animals. Scale bars: 250 µm. **B|** Quantification of Iba$^+$ cells density in the SNpc and VTA of wild-type and Anxa1$^{-/-}$ animals. Histograms show results from *n*=6 animals/genotype and are expressed as mean ± SEM (*n* cells/mm^2). Student *t*-test between the genotypes was performed, with * and ** indicating $p<0.05$ and $p<0.01$ *vs.* wild-type, respectively. **C|** Confocal microscopic analysis of Cd11b (green), used as a marker for resident microglia and Anxa1 (red) in a magnified area of the SNpc of wild-type male mice (2-3 months old). Typical example from *n*=3 experiments. Scale bar: 10 µm. **D|** Representative immunohistochemistry analysis of ANXA1 expression in microglia resident in the cortex derived from a human healthy donor. ANXA1 was stained in brown using HRP-avidin-biotin complex (ABC) Vector kit (Vector Laboratories, UK) and DAB to develop based colorimetric reaction. Scale bar: 10 µm. **E|** Representative Immuno-blots show differences in expression of iNOS and COX-2 between genotypes in whole brain extracts; α-tubulin was used as loading control. 50 µg of total protein were loaded per lane. **F|** Representative immunohistochemistry analysis of Iba1$^+$ expression chosen as marker for microglia resident; images shown were taken from the thalamus of either untreated wild-type or Anxa1 null male mice (2-3 months old). Iba1 was stained in brown using HRP-avidin-biotin complex (ABC) Vector kit (Vector Laboratories, UK) and DAB to develop the colorimetric reaction; sections were counterstained with hematoxylin (see Section 5.3.3. for tissue processing and staining methods). Scale bar: 20 µm. Panel D and F were produced by Dr. S McArthur.

7.4.2 Impact of peripheral inflammation upon the midbrain

7.4.2.1 Specific temporal pattern of Anxa1 expression in the SNpc under peripheral inflammatory challenge

The finding that only a small percentage of the DA neurons of the murine and human SNpc express Annexin A1 raised interest on the modulation of the protein under inflammatory and neurodegenerative conditions. Due to the peculiar localisation of Anxa1 in such an important region, we decided to focus on this area, using the neighbouring VTA, rich in dopaminergic neurones functionally distinct, as an internal control to compare the specificity of the possible changes. Only few studies have looked, to our knowledge (Qin *et al.*, 2007; Jeong *et al.*, 2010), beyond the acute phase of the impact of peripheral LPS in the brain (24 hours), when pro-inflammatory cytokines production seems to peak; our initial data (Figure 2.2) demonstrated the importance of looking beyond this phase.

Interestingly, a single dose of LPS (3 mg/kg) administered *i.p.* was able to induce an increase in the number of Anxa1 positive DA neurons, which started after 24 hours and became statistically significant after 7 days, as shown in Figure 7.4, Panel A and B.

No significant changes occurred in the percentage of $Anxa1^{+}$ DA neurons of the VTA, which remained particularly low. This dose of LPS has been widely used to define a moderate non-lethal peripheral immune reaction, which normally resolves within 24-36 hours (Figure 7.6; Panel A and B) from administration; despite their increased endotoxin-related vulnerability (Damazo *et al.*, 2005), Anxa1 null mice have been extensively tested to be able to undergo such a challenge (Roviezzo *et al.*, 2002).

More in detail, we observed an increase in the number of neurons present along a well-defined strip of DA neurons. Importantly, this phenomenon occurred with a different time-course when compared to the expression of peripheral inflammatory markers (Figure 7.6; Panel A and B). As already reported in other studies (Roviezzo *et al.*, 2002; Damazo *et al.*, 2005), Anxa1 null mice show a basal level of pro-inflammatory cytokines higher than wild-type, which was also reproduced during peripheral inflammatory challenges with a more intense and prolonged pro-inflammatory status as testified by TNF-α (Panel A) and partially by IL-6 (Figure 7.6; Panel B).

Interestingly, while we did not detect any significant difference in terms of numbers of TH-immunoreactive (TH-IR) cells of the SNpc in the wild-type during the peripheral inflammatory challenge, we observed a significant decrease in the number of TH-IR neurons of the Anxa1 null mice after 24 hours from LPS *i.p.* administration, which was restored after 7 days (Figure 7.4; Panel C). This may strongly indicate more the transient loss of dopaminergic phenotype than the actual loss of the neurons, since both loss and restoration appeared to occur swiftly and may well suggest the establishment of particularly challenging conditions within the midbrain microenvironment. The number of TH-IR neurons in the VTA did not show any significant change for both genotypes.

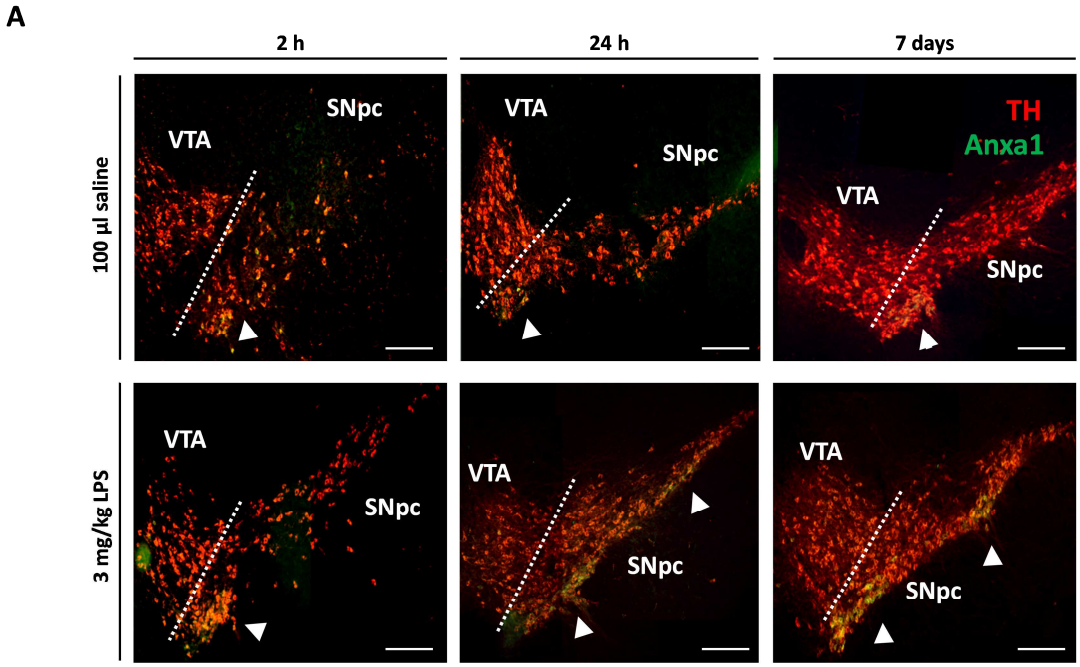
A
2 h
24 h
7 days
100 µl saline
3 mg/kg LPS
VTA
SNpc
TH
Anxa1

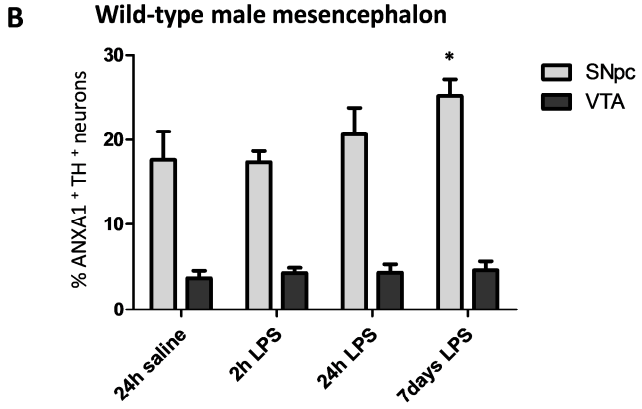
B
Wild-type male mesencephalon
% ANXA1 + TH + neurons
SNpc
VTA
24h saline
2h LPS
24h LPS
7days LPS

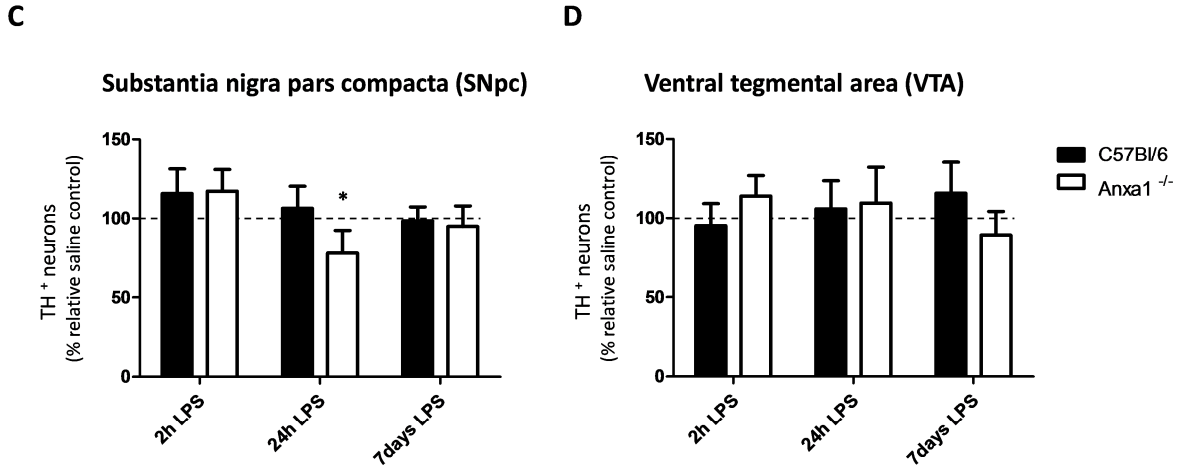
C
Substantia nigra pars compacta (SNpc)
D
Ventral tegmental area (VTA)
TH + neurons
(% relative saline control)
C57Bl/6
Anxa1 -/-
2h LPS
24h LPS
7days LPS

Figure 7.4 Effects of systemic LPS challenge on Anxa1 expression on SNpc DA neurons of wild-type and Anxa1$^{-/-}$ brains. A| Anxa1 expression was monitored by immunofluorescence (Anxa1: green; TH: red) in the midbrain regions SNpc and VTA after challenging the animals with one *i.p.* dose 3 mg/kg of LPS or 100 µl saline (as a negative control) for 2 hours, 24 hours or 7 days. Images are representative examples of one half of the midbrain. Each treatment group included 4-6 animals. Scar bar: 500µm **B|** Quantification of the percentage of Anxa1^{+} TH^{+} cells out of the total of TH^{+} neurons of either SNpc or VTA under the different challenging conditions. 24 hours saline is shown as negative control, omitting the other time points studied since they did not show any significant difference among themselves or towards the untreated control. Data are presented as mean ± SEM (*n*=4-6 animals/group). One-way ANOVA was performed for each genotype study, followed by Bonferroni *post-hoc* test between the different data sets. * indicates $p<0.05$ compared to the correspondent saline and untreated control. **C|** and **D|** show the quantification of TH^{+} neurons either in SNpc or in VTA, respectively. Results are expressed as relative percentage of total TH^{+} neurons compared to the time-related saline control and are presented as mean ± SEM. For each genotype, one-way ANOVA was performed, followed by Bonferroni *post-hoc* test between the different data sets. * indicates $p<0.05$ compared to the correspondent saline control.

7.4.2.2 Microglia recruitment under peripheral inflammatory conditions

Microglia cells are extremely sensitive to what happens in the periphery (Czeh *et al.*, 2011), so we investigated the effect of peripheral LPS on Iba1^{+} cell density in both genotypes. We detected an increase in Anxa1 null mice already after 24 hours, accompanied by increased intensity of staining and a less ramified morphology (Figure 7.5; Panel A and D); the number of recruited microglia cells remained increased after 7 days. WT animals showed slower kinetics, with a significant increase in microglia density only after 7 days (Figure 7.5; Panel A and C), despite the peripheral inflammatory reaction being already resolved (Figure 7.6; Panel A and B). The number of cells/mm^2 of Anxa1 null animals remained higher than the wild-type at every time point studied. The VTA showed no significant change in cell density at any of the points studied (Figure 7.5; Panel B). In both genotypes, a substantial part of the newly recruited microglia appeared to come from the neighbouring area, the SNpr, as we detected in another set of experiments (see below).

In the AnxA1 null mouse, the morphology of β-galactosidase positive cells changed in the SN over the course of a week following LPS administration, and notably the VTA began to present cells positive for β-galactosidase activity (Chapter 2; Figure 2.2). We checked this in wild-type animals: peripheral inflammation was neither able to induce an increase in Anxa1 expression in VTA resident microglia nor a general visible change in protein localisation (Figure 7.5; Panel B and E).

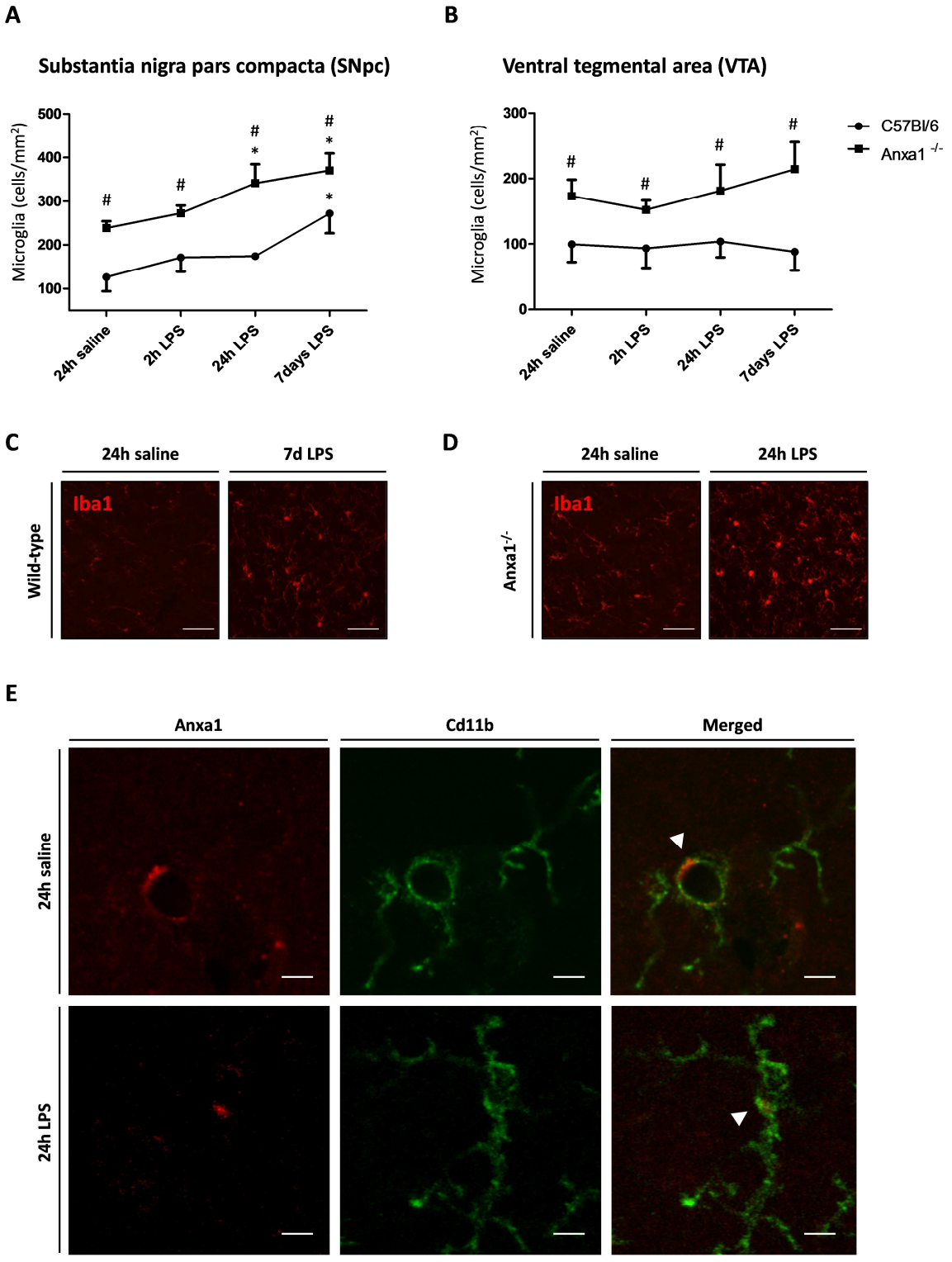
A
Substantia nigra pars compacta (SNpc)
Microglia (cells/mm²)
500
400
300
200
100
24h saline
2h LPS
24h LPS
7days LPS
B
Ventral tegmental area (VTA)
Microglia (cells/mm²)
300
200
100
0
C57Bl/6
Anxa1 -/-
C
24h saline
7d LPS
Wild-type
Iba1
D
24h saline
24h LPS
Anxa1-/-
Iba1
E
Anxa1
Cd11b
Merged
24h saline
24h LPS

Figure 7.5 Characterisation of the effect of systemic inflammation on microglia recruitment in the SNpc and VTA and changes in expression of microglia-associated Anxa1. A| and **B|** show the results of the quantification of Iba^+ cell density in the SNpc and VTA of wild-type and $Anxa1^{-/-}$ animals challenged with 3 mg/kg dose of LPS *i.p*. The category graphs show results from *n*=6 animals/genotype and are expressed as mean ± SEM (n° cells/mm^2). Two-way ANOVA was performed (time of LPS exposure and genotype as variables) and identified a significant effect of genotype and LPS treatment ($p<0.001$); the analysis was followed by Bonferroni *post-hoc* test. # indicates $p<0.05$ *vs.* wild-type correspondent treatment, while * indicates $p<0.05$ *vs.* 24h saline treated genotype-matched group. **C|** and **D|** show representative magnifications of the SNpc of saline-treated or LPS-treated wild-type and $Anxa1^{-/-}$ animals stained for Iba1. Scale bar: 100 µm. **E|** Representative images from confocal microscopy performed on SNpc sections from saline- or LPS-treated wild-type animals. Anxa1 (red) and Cd11b (green) co-localisation is visualized. 2 hours LPS, 7 days LPS and other saline-treated controls have been omitted because comparable to the 24h saline treated sample here shown. Arrows indicate points of Anxa1 staining within $Cd11b^+$ cells. Scale bar: 5 µm. Panel E produced together with Dr. S McArthur.

Annexin A1 has been reported to be positively linked to IL-10 release in a macrophage cell line (Ferlazzo *et al.*, 2003). Interestingly, we detected a significant genotype-related difference, both basally and under peripheral inflammatory challenge, in terms of brain IL-10 content: while wild-type animals showed a basal level of around 0.6 ng/mg protein, which increased as a direct consequence of the peripheral inflammatory challenge 24 hours after LPS administration, Anxa1 null mice showed a very low concentration of the cytokine, which did not change significantly under inflammatory challenges.

Annexin A1-induced IL-10 release has also been described to be an iNOS (an enzyme mainly expressed in the brain by microglia and astrocytes, especially after injury) expression modulator (Ferlazzo *et al.*, 2003). Since we detected basal expression of iNOS in the Anxa1 null mouse compared to the wild-type counterpart, we measured the content of nitrite in brain lysates, as an indication of the gaseous product NO: basally, null mice showed an overall higher content, which significantly increased under peripheral challenge (Figure 7.6; Panel D).

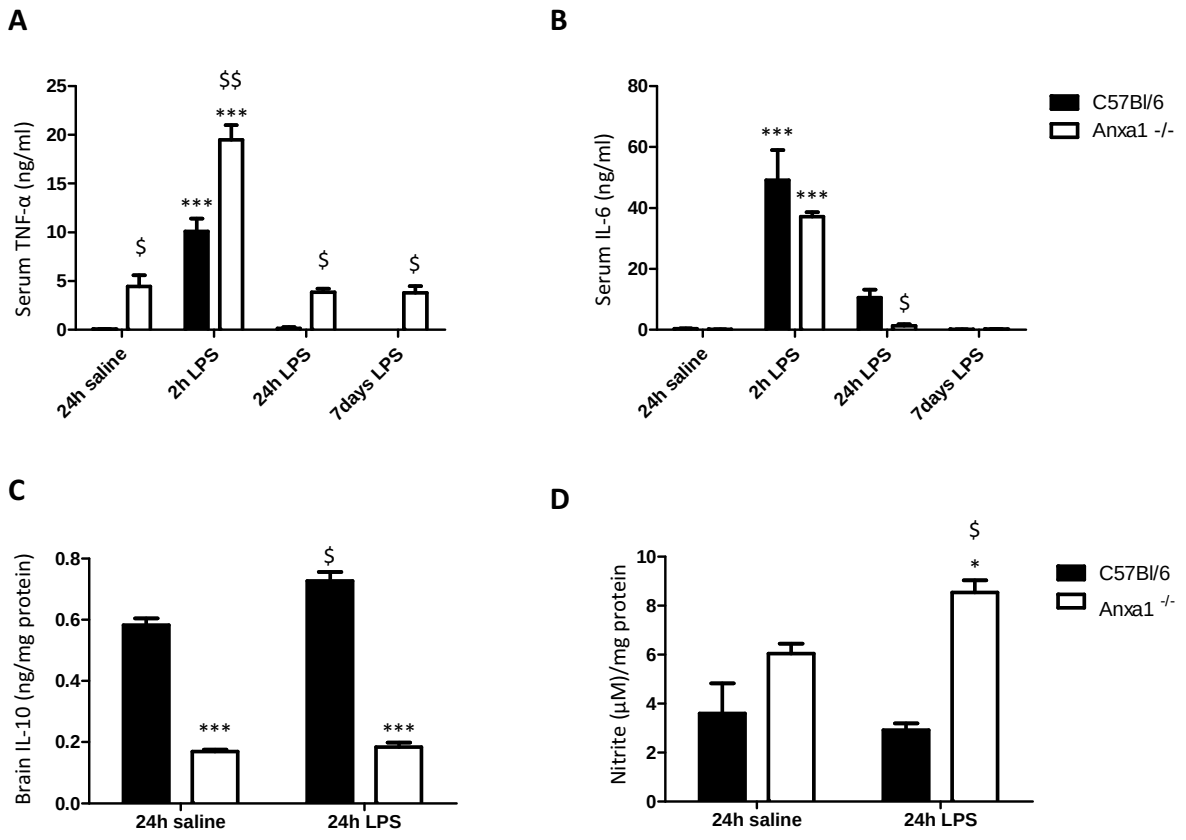

Figure 7.6 Temporal profile of pro-inflammatory cytokines in the serum and brain homogenates and of nitrite brain content from treated wild-type and Anxa1 null mice challenged with *i.p.* LPS. A| and **B|** Serum samples from LPS treated and saline treated controls were obtained and analysed for cytokines levels (TNF-α and IL-6) using ELISA commercial kits and following manufacturer's instructions. Results are from *n*=4-6 animals and were normalized to the saline-treated counterpart to remove any effect due to saline treatment; data are presented as mean ± SEM (ng/ml). Two-way ANOVA was performed (time of LPS exposure and genotype), which indicated a significant effect of genotype and time of LPS treatment ($p<0.001$) as well as an interaction between the two ($p<0.01$) for TNF-α; the analysis was followed by Bonferroni *post-hoc* test, $ and $$ indicating $p<0.05$ and $p<0.01$ *vs.* wild-type correspondent treatment, while *** indicates $p<0.001$ *vs.* 24h saline treated genotype-matched group. **C|** shows differences in IL-10 whole brain concent between wild-type and Anxa1 null mice, either saline or LPS-treated for 24 hours. Two-way ANOVA was performed (type of stimulation and genotype), which indicated a significant effect of genotype and type of treatment ($p<0.001$) as well as an interaction between the two ($p<0.01$); the analysis was followed by Bonferroni *post-hoc* test, $ indicating $p<0.05$ *vs.* wild-type saline-treated group, while *** indicates $p<0.001$ *vs.* genotype-matched group. Results are from *n*=3-5 animals and are presented as mean ± SEM (ng/mg protein). **D|** shows normalized nitrite whole brain content between wild-type and Anxa1 null mice, either saline or LPS-treated for 24 hours. Results are from *n*=3-5 animals and are presented as mean ± SEM (μM/mg protein). Two-way ANOVA was performed (type of stimulation and genotype), indicating a significant effect of genotype ($p<0.01$).

7.4.3 Impact of neurodegeneration in the midbrain

7.4.3.1 Genotype-related differences in TH positive neuronal loss in the SNpc

The expression of Annexin A1 in DA neurons of the SNpc raised further questions, linked to the potential role as an anti-inflammatory protein under physiological conditions as well as under neurodegenerative conditions (Parkinson's disease). Therefore, we used our well-established model of experimental PD, the intrastriatal administration of 6-OHDA, to investigate potential differences in terms of DA neuronal loss between wild-type C57Bl/6 mice and Anxa1 null mice. We chose a sub-maximal dose (2 μg 6-OHDA), shown to cause a gradual loss of DA neurons over the time, plus we treated only the left striatum, in order to have an internal negative control (the contralateral right side) for comparison (Bowenkamp *et al.*, 1996; Schwarting and Huston, 1996).

As evident from Figure 7.7, Panel A, we were able to establish both in wild-type and in Anxa1 null animals a progressive and specific TH^+ neuronal loss in the SNpc, which did not affect significantly the neighbouring region VTA (Figure 7.7; Panel B). In wild-type, loss of TH phenotype started already 24 hours after intrastriatal toxin injection, and progressively continued over the 4 weeks of investigation. By performing TH and Anxa1 double staining on wild-type lesioned animals, we noticed that a considerable percentage of the dopaminergic neurons surviving over the time was Anxa1 positive (Figure 7.7; Panel C): the percentage of Anxa1 positive TH cells increased over the time, which was not due to an increase in the absolute number of Anxa1 expressing neurons (data not shown), but rather to the preferential survival of these cells during the neurodegenerative event. Such phenomenon appeared to be SNpc-specific, since we did not detect any difference in the number of the scattered $Anxa1^+$ TH^+ cells of the VTA (Figure 7.7; Panel D). Interestingly, Anxa1 null mice showed a different phenotype: after an intense loss of TH positivity after 1 day, we were unable to detect further significant changes in the number of remaining neurons; this event caused a significant difference between genotypes at 4 weeks post-toxin administration, therefore indicating slower distinct kinetics in the model when applied to the Anxa1 null animals.

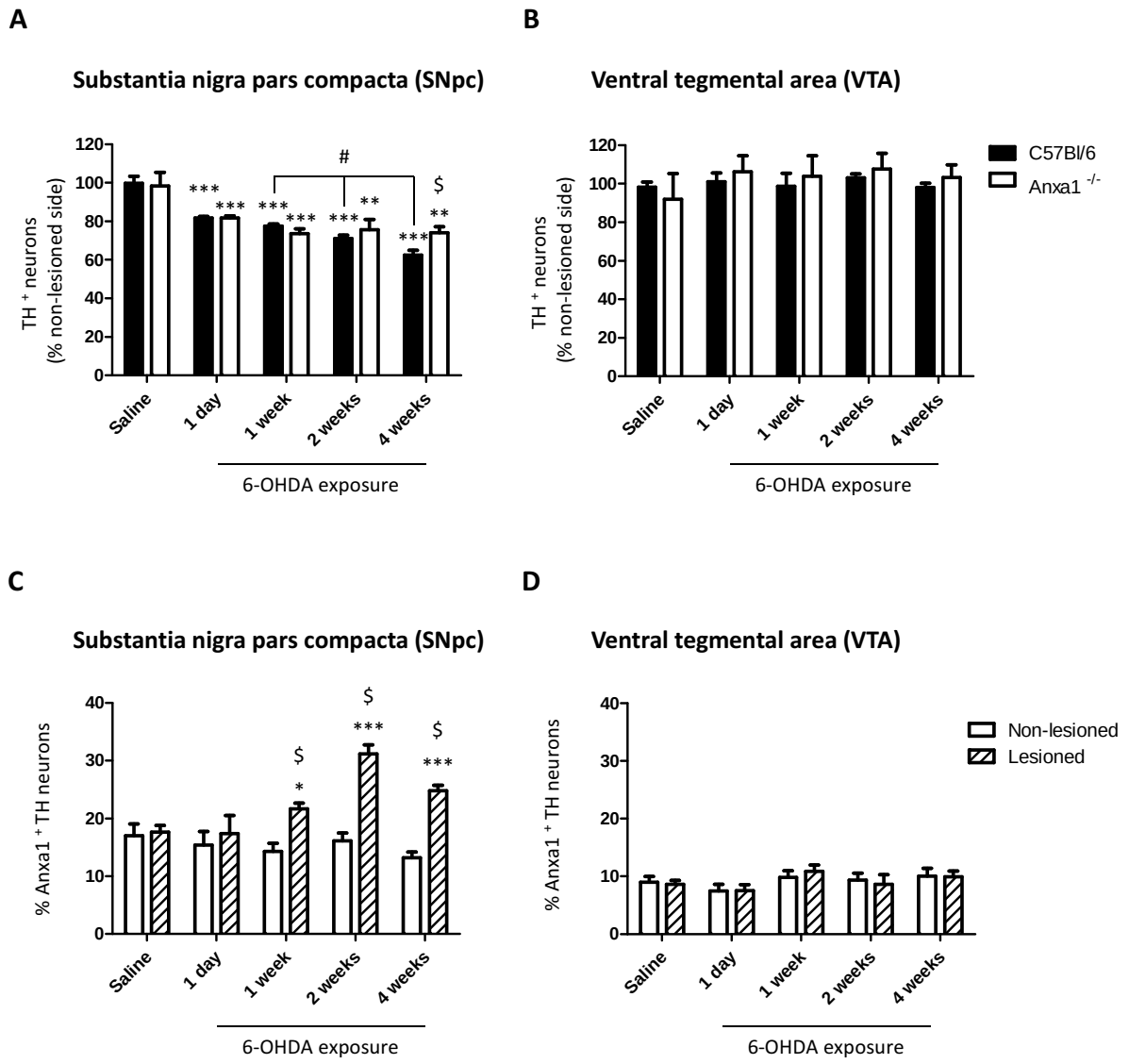

Figure 7.7 Temporal loss of dopaminergic neurons in the midbrain of wild-type and Anxa1 null mice following intrastriatal injection of 6-OHDA. Temporal specific loss of TH positive neurons from the SNpc (**A|**) and VTA (**B|**) of lesioned wild-type and Anxa1 null mice. Each group was formed of *n*=4-6 young males (2-3 months old). Results are presented as mean ± SEM. As negative control we only performed saline intrastriatal injection and exposure for 24 hours. Two-way ANOVA was performed (time of toxin exposure and genotype as variables) and identified a significant effect of toxin exposure and an interaction between the two variables ($p<0.01$ and $p<0.001$, respectively); the analysis was followed by Bonferroni *post-hoc* test. *** and ** indicates $p<0.001$ and $p<0.01$ *vs.* the genotype related saline-treated control, respectively. # indicates $p<0.05$ *vs.* 1 week, 2 weeks and 4 weeks-treated groups. $ indicates $p<0.05$ *vs.* 4 weeks treated wild-type group. **C|** and **D|** quantify the number of Anxa1 positive TH positive neurons of either lesioned or non-lesioned sides of the SNpc and VTA, respectively, in wild-type animals. Values are presented as mean ± SEM (each group included *n*=4-6 animals). Two-way ANOVA (area and time of toxin exposure) was performed and identified a significant effect of toxin exposure ($p<0.01$), of the area analyzed ($p<0.001$) and an interaction between the two ($p<0.001$). The analysis was followed by Bonferroni *post-hoc* test; * and *** indicate $p<0.05$ and $p<0.001$ *vs.* saline-treated correspondent area control, while $ indicates $p<0.05$ *vs.* correspondent time-related non-lesioned area. Panels A-D produced by Dr. S McArthur.

7.4.3.2 Microglia recruitment in the injured site

Intrastriatal injection of 6-OHDA retrogradely targets the SNpc, through the projections that nigral DA neurons send to the striatum. The consequent specific neurodegeneration of the neurons of the SNpc normally triggers the activation of the numerous resident microglia cells and further recruitment from neighbouring regions (Schwarting and Huston, 1996). This phenomenon was also reproduced in our hands (Figure 7.8; Panel A and B) and showed different kinetics and intensity between the analysed genotypes. In the wild-type animals, the number of $Iba1^+$ cells promptly peaked shortly after initiation of the lesion (24 hours post 6-OHDA administration) but steadily and slowly decreased afterwards, returning to the initial density after 4 weeks post-toxin injection. We noticed an increased intensity of microglia-related staining at the level of the SN pars reticulata, as well as the directional migration of cells from this region towards the SNpc, which led us hypothesise that the swift increase in cell number could be at least partially linked to this neighbouring region (Figure 7.8; Panel D). The Anxa1 null mice, on the other hand, showed a slower kinetics; the cell density peaked after 1 week from lesioning onset and remained significantly higher throughout the study, only partially decreasing over time. Absolute density values were constantly higher in the Anxa1 null animals and morphology maintained the characteristic features we found in this genotype, regardless of the treatment (Figure 7.8; Panel C).

No significant differences were noted in the VTA throughout the treatment, either for wild-type or null mice (Figure 7.8; Panel B).

Rapid microglia number increase and activation was not only evident in the SNpc but also in the striatum, which is the area from where the neurodegenerative event started. As evident from Figure 7.9, Panel A, rapid increase in $Iba1^+$ cell number in the lesioned striatum of wild-type animals occurred after 24 hours of toxin exposure, and swiftly subsided thereafter. Similarly to SNpc, the kinetics in the Anxa1 null mice was also slower, while cell density and intensity of Iba1 staining remained persistently high during the time-course (not shown).

Since we wanted to assess if the rapid changes in microglia density were also accompanied by changes in Anxa1 expression or if the protein levels remained unchanged, similarly to what we observed under peripheral inflammatory challenges, we checked (Figure 7.9; Panel B) its expression in CD11b-positive cells in the striatum.

CD11b was chosen both because it allowed us to perform co-staining along with Anxa1 or because it is one of the most extensively-used markers (Larson and Springer, 1990) for cells of myeloid origin (like microglia, resident macrophages, circulating monocytes, natural killer cells). We were able to identify, only in the lesioned striatum of wild-type animals, numerous cells with an intense Anxa1 positivity (pointed by the white arrow in Figure 7.9, Panel B): these cells were positive for Cd11b but showed a completely different morphology compared to the small, ramified cell body of microglia cells, either resting or activated (see previous figures for comparison). These cells showed a globular shape with no apparent ramification. Only a few of these cells were evident in the non-lesioned side of the brain, while many were instead identified in the striatum of the lesioned side, 24 hours after the onset of the neurodegenerative reaction. After that time point, we failed to identify such a huge number of this specific type of cells, which could represent recruited monocytes from circulation.

As specified before, this phenomenon happened in the striatum; myeloid cells in the lesioned SNpc did not show any evident increase in Anxa1 or changes in morphology.

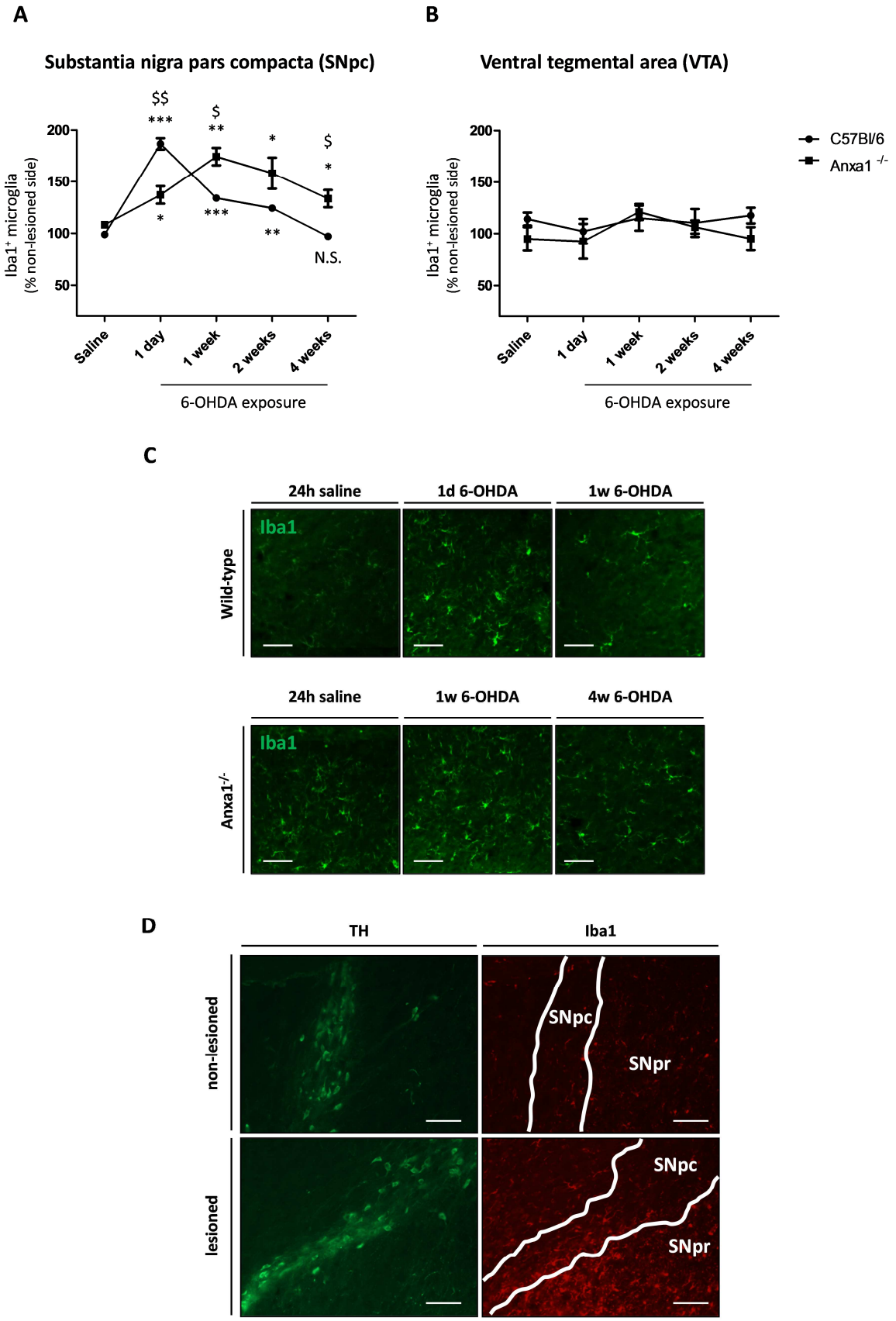
A
Substantia nigra pars compacta (SNpc)
Iba1+ microglia (% non-lesioned side)
200
150
100
50
$$
***
$
**
*
$
*
*
***
**
N.S.
Saline
1 day
1 week
2 weeks
4 weeks
6-OHDA exposure
B
Ventral tegmental area (VTA)
Iba1+ microglia (% non-lesioned side)
C57Bl/6
Anxa1 -/-
Saline
1 day
1 week
2 weeks
4 weeks
6-OHDA exposure
C
24h saline
1d 6-OHDA
1w 6-OHDA
Wild-type
Iba1
24h saline
1w 6-OHDA
4w 6-OHDA
Anxa1-/-
Iba1
D
TH
Iba1
non-lesioned
lesioned
SNpc
SNpr
SNpc
SNpr

Figure 7.8 Temporal microglia recruitment in the lesioned midbrain. A| and **B|** show lesioning-related changes over time in $Iba1^{+}$ cell density from the SNpc and VTA of wild-type and Anxa1 null mice, respectively. Each group was formed of *n*=4-6 young males (2-3 months old). Results are presented as mean ± SEM (percentage of non-lesioned side). As negative control we only performed saline intrastriatal injection and exposure for 24 hours, since longer time points did not result in significant changes. Two-way ANOVA was performed (time of toxin exposure and genotype as variables) and identified a significant effect of toxin exposure ($p<0.001$), of genotype ($p<0.05$) and an interaction between the two variables ($p<0.001$); the analysis was followed by Bonferroni *post-hoc* test. ***, ** and ** indicate $p<0.001$, $p<0.01$ and $p<0.05$ *vs.* the genotype related saline-treated control, respectively. $$ and $ indicate $p<0.01$ and $p<0.05$ *vs.* the correspondent wild-type treated group. **C|** shows representative magnifications of the lesioned SNpc of wild-type and $Anxa1^{-/-}$ treated-animals at different time points, stained for Iba1. Scale bar: 100 µm. **D|** Images are referred to an injured wild-type brain 24 hours after 6-OHDA administration. SNpc was delimited by following the boundaries set by TH positive neurons. SNpr: substantia nigra pars reticulata. Scale bar: 150 µm.

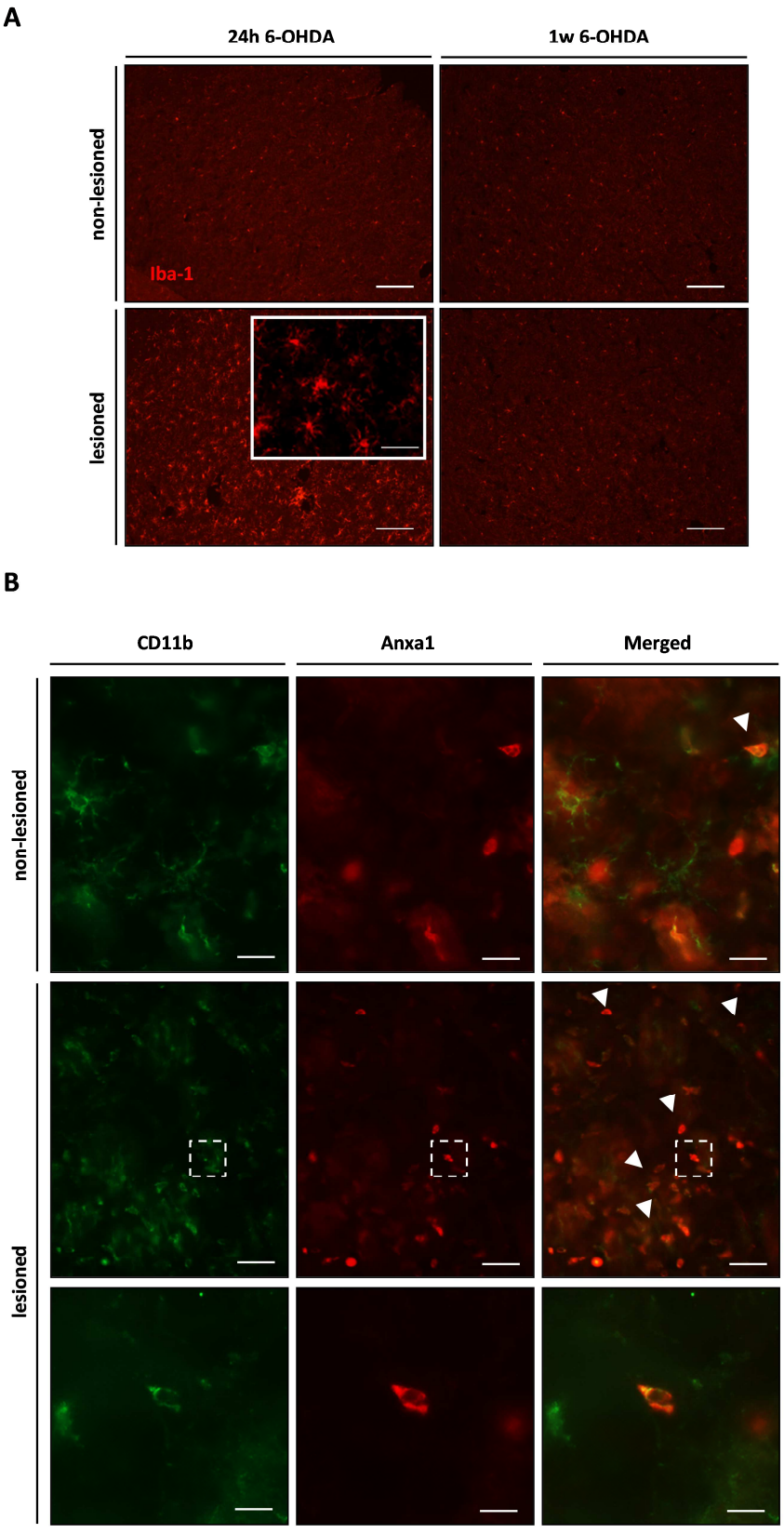
A
24h 6-OHDA
1w 6-OHDA
non-lesioned
lesioned
Iba-1
B
CD11b
Anxa1
Merged
non-lesioned
lesioned

Figure 7.9 Microglia markers-positive cells in the injured striatum. A| shows representative examples of striatal sections from 6-OHDA treated wild-type animals, stained for Iba1. Internal comparison between lesioned and non-lesioned striatum was performed. 2 and 4 weeks treated groups are not reported because results are similar to 1 week-treated group. Inset represents nigral microglia cells magnification. Scale bar 150 µm; inset 75 µm. **B|** Lesioned and non-lesioned striatal regions (24h post-toxin infusion) were compared for Anxa1 expression differences in CD11-stained cells. Arrows indicate cells which showed an intense Anxa1 specific staining, while the squares indicate the region magnified in the pictures in the last row. Images are representative examples. Scale bars: 10 µm (first and second row); 5 µm (last row). Panel A produced by Dr. S McArthur.

7.4.4 How peripheral inflammation impacts the injured substantia nigra

7.4.4.1 Exacerbation in DA neuronal loss

Having characterised the response of the wild-type and Anxa1 null SNpc under separate peripheral inflammatory and neurodegenerative challenges we proceeded to test the most important hypothesis of this section, that is, the impact of systemic inflammatory reactions on on-going neurodegeneration of the NSDA pathway both in the presence and in the absence of Annexin A1. We decided to use 7 days post-6OHDA administration as lesioning end-point because we detected a significant loss of TH^+ cells both in wild-type and in Anxa1 null mice, followed by 7 days of peripheral inflammatory challenge, since we observed significant changes in terms of microglia recruitment (for both genotypes) and Anxa1 expression (in wild-type animals) at the same dose and time frame.

First, we assessed changes in the numbers of DA neurons: both genotypes developed significant loss (around 20% if compared to the contralateral non-injured side) of TH^+ cells after 2 weeks post-toxin intrastriatal injection (Figure 7.10; Panel A), as already seen in the previous experimental set (Figure 7.7; Panel A). Challenging lesioned animals with a peripheral dose of LPS (3 mg/kg) produced a further decrease in the lesion side of only Anxa1 null mice (around 14% in relation to the 6OHDA/saline genotype matched group), which did not reach statistical significance ($p<0.1$). No significant changes were detected in the functionally unrelated VTA region (Figure 7.10; Panel B).

By performing TH and Anxa1 double staining on wild-type lesioned animals, we noticed a significant increase in the number of $Anxa1^+$ TH^+ neurons, while we observed again that a considerable percentage of the dopaminergic neurons surviving over the time were Anxa1

positive (Figure 7.10; Panel C); despite the fact that the treatment caused a considerable loss of TH^+ neurons, the percentage of those Anxa1 increased over the time. Interestingly, we were not able to detect such phenomenon in the Anxa1 null mouse by co-staining β-galactosidase with TH: we detected a decreased number of $\beta\text{-gal}^+$ neurons along with the decrease in the number of TH^+ cells, which underlines the importance of Anxa1 in giving a preferential survival to those cells expressing it within the wild-type lesioned brains.

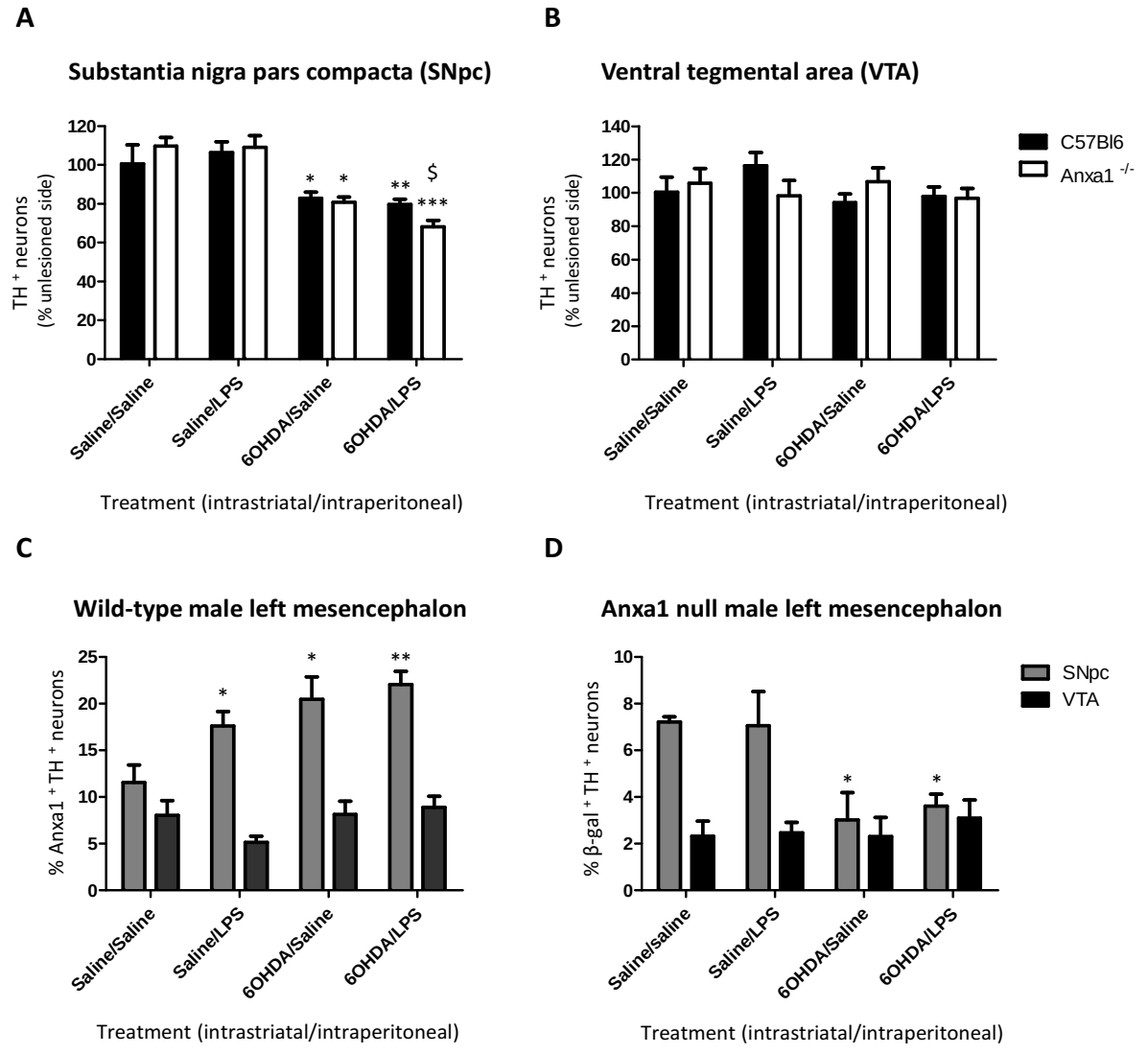

Figure 7.10 Loss of dopaminergic neurons in the midbrain of wild-type and Anxa1 null mice following intrastriatal injection of 6-OHDA and subsequent peripheral inflammatory challenge. A| and **B|** show the temporal specific loss of TH positive neurons from the SNpc and VTA, respectively, from lesioned wild-type and Anxa1 null mice further challenged by single *i.p.* administration of LPS. Results expressed as percentage of the unlesioned side and are mean ± SEM. Three-way ANOVA was performed (genotype, toxin exposure and LPS exposure as variables) and in the lesioned side it identified a significant effect of toxin exposure (p<0.001); the analysis was followed by Tukey's *post-hoc* test. ***, ** and * indicate p<0.001, p<0.01 and p<0.05 *vs.* the genotype related saline/saline-

treated control, respectively. $ indicates p=0.1 *vs.* Anxa1 null-related 6OHDA/saline-treated group and wild-type 6OHDA/LPS-treated group. **C|** quantifies the number of Anxa1 positive TH positive neurons of the intrastriatally injected side of SNpc and VTA, while **D|** quantifies the number of β-gal positive TH positive neurons. Values are expressed as % of double-positive cells among total TH^+ cells and are presented as mean ± SEM (each group included n=4-6 animals). Two-way ANOVA (toxin exposure and LPS exposure) was performed and identified significant effects of toxin and LPS exposure (p<0.05) in the wild-types, and for the toxin exposure (p<0.05) in the Anxa1 null mice. The analysis was followed by Tukey's *post-hoc* test; * and ** indicate p<0.05 and p<0.01 *vs.* saline/saline-treated correspondent area control.

7.4.4.2 Augmented recruitment of microglia in the injured area

The intrastriatal injection of 6-OHDA was able to cause a swift activation of recruitment of microglia (Section 7.4.3.2). Current evidence suggests that in the presence of on-going neurodegenerative processes, these guarding cells are able to enter a primed state where they are not fully activated but they are hyper-responsive to additional stimuli, which in that case can cause exaggerated and prolonged production of neurotoxic inflammatory mediators (Perry, 2010). Such phenomenon strongly indicates that the normal resolution processes may be compromised; therefore we wanted to understand if Anxa1, whose lack was linked to the increased loss of neurons after peripheral inflammatory challenge, could be involved in the mechanisms controlling exaggerated activation, proliferation and recruitment of myeloid cells to the site of injury.

Quantifying $Iba1^+$ cells both in lesioned and non-lesioned sides of wild-type and Anxa1 null LPS-treated mice (Figure 7.11), we observed that Anxa1 null animals (Panel A and D) showed a significantly higher number of microglia (as shown previously in untreated and treated conditions), as well as an intense increase in the number of cells populating the lesioned SNpc: we were able to detect a further significant increase in the lesioned side after further challenge with peripheral LPS (p<0.05). Wild-type animals, on the other hand, responded (Panel A and C) in every condition with an increase in lesioned SNpc microglia density, but did not show any significant increase in presence of both lesioning and peripheral challenge. We did not detect any change in the response of the non-lesioned side, except the higher microglia density in the Anxa1 null mice and the increase induced, in both genotypes, 1 week after peripheral LPS administration. No significant differences were noted in the VTA throughout the treatment, either for wild-type or null mice (Figure 7.8; Panel B).

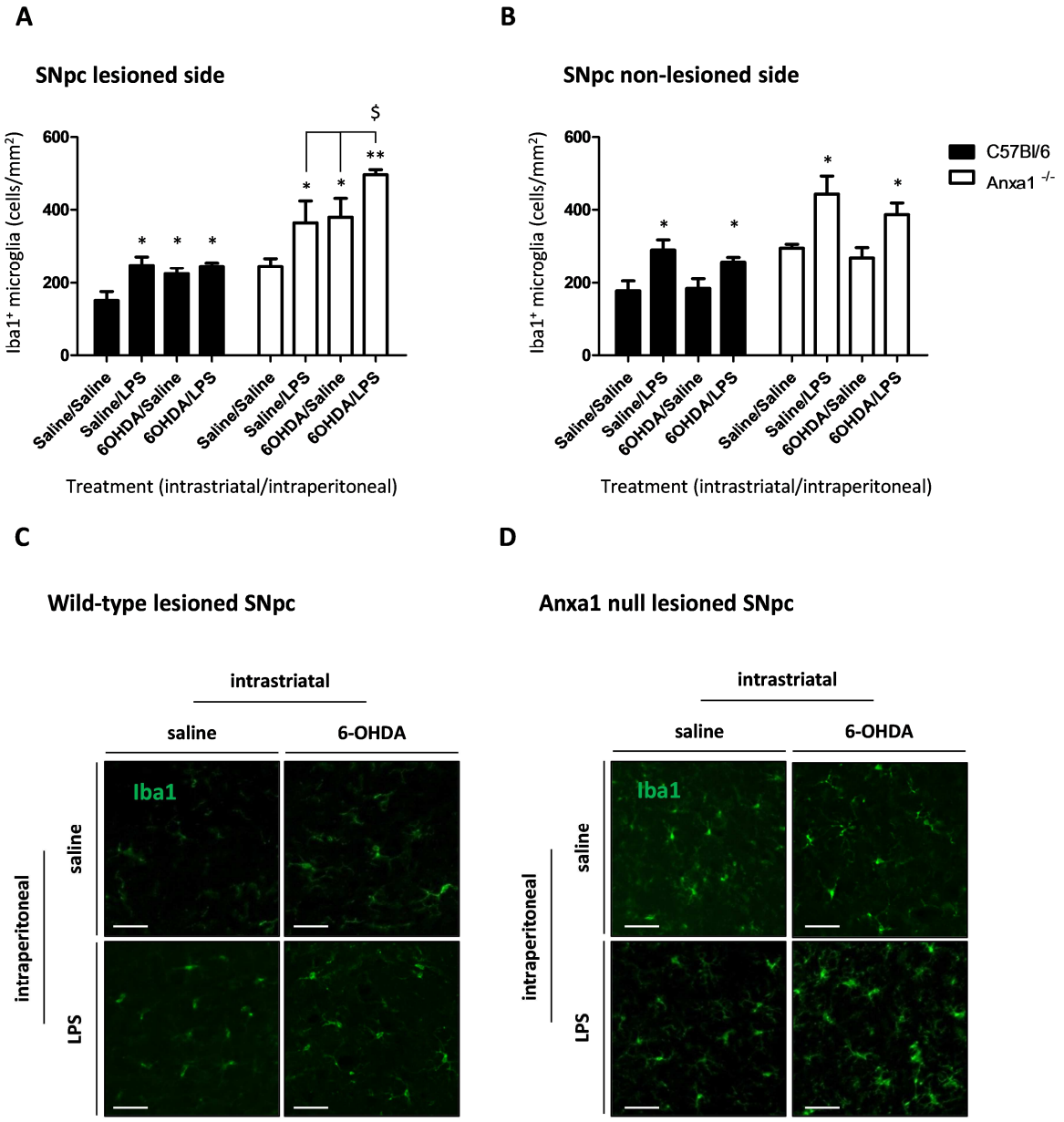

Figure 7.11 Microglia recruitment in the lesioned and peripherally challenged midbrain. A| and **B|** show changes in Iba1^{+} cell density respectively from the lesioned and non-lesioned SNpc of wild-type and Anxa1 null mice. Each group was formed of *n*=4-6 young males (2-3 months old). Results are presented as mean ± SEM (cell density; cells/mm^2). Three-way ANOVA was performed (toxin exposure, LPS exposure, genotype as variables) and in the lesion side it detected a significant effect for toxin exposure, LPS exposure, genotype and interaction between genotype and toxin exposure, as well as between the three variables (p<0.0001). The analysis was followed by Tukey's *post-hoc* test. ** and * indicate p<0.01 and p<0.05 *vs.* the genotype related saline/saline-treated control, respectively. $ indicate p<0.05 *vs.* the Anxa1 null saline/LPS and 6OHDA/saline-treated groups. **C|** and **D|** show representative magnifications of the lesioned SNpc of wild-type and Anxa1$^{-/-}$ treated-animals, respectively, at the different conditions, stained for Iba1. Scale bar: 100 µm.

7.5 Discussion

The main scope of this chapter was to understand if annexin A1 participates in helping the brain to control its inflammatory response under peripheral inflammation and neurodegenerative insults. These data report novel evidence on how annexin A1 expression is modulated by peripheral inflammation specifically at the level of a small sub-population of dopaminergic neurons of the SNpc. Lack of annexin A1 appeared to be crucial in negatively affecting neuronal loss while, most of all, positively affecting microglia density.

7.5.1 The substantia nigra is a peculiar region of annexin A1 expression

Initial findings (Chapter 2) clearly showed that annexin A1 might play a peculiar role in the substantia nigra. In particular, it was evident that Anxa1 was present in two morphologically distinct cellular species, whose behaviour in terms of expression of the protein seemed tightly modulated by peripheral stimuli. We were able to confirm that these cells were a small (less than 20%) population of nigral TH positive dopaminergic neurons (Figure 7.2), along with microglia cells (Figure 7.3), which densely populate this area of the brain (Kim *et al.*, 2000). These findings were not only confined to the rodent brain, but were found to be true also in the human cerebral tissue. In our murine model, both cell types showed to respond differently to injury and inflammation dependent on the presence of Anxa1, suggesting an important intracerebral /protective regulatory role for it.

7.5.1.1 Basal differences in the Anxa1 null mouse

We did not detect any genotype-linked difference in the total number of DA neurons of the areas of interest (SNpc and VTA, as shown in Figure 7.2), indicating that the lack of annexin A1 is not linked with basal changes in the architecture of these neuronal regions. On the other hand, Anxa1 null mice presented a higher microglia cell density under resting conditions (Figure 7.3), along with differences in morphology and intensity of $Iba1^{+}$ marker (reported to increase during cell activation), basal expression of phlogistic enzymes that usually are only expressed under inflammatory conditions (iNOS and COX-2) as reported (Wong *et al.*, 1996).

Overall, the impression is that in the absence of Anxa1, the cerebral *milieu* presents inflammation-prone features, which make it more reactive and vulnerable under certain stimuli. It is unclear why Anxa1 null mice showed higher nigral microglial density under basal conditions but this may be due to various events happening during development and/or adulthood. The basal loss of vascular tightness, which we clearly showed to characterise the Anxa1 null mice (Chapter 4), could have facilitated the access of the brain parenchyma during development, when the barrier is particularly immature and leaky, or after developmental colonisation. In particular, Morgan *et al.* (Morgan *et al.*, 2010) suggested that aberrant infiltration of microglia precursors during development may be triggered by genetic alterations affecting the innate immune system and/or by excessive early neuron generation or the altered development of neuronal connectivity. The lack of *Anxa1* gene may represent a strong genetic influence for the central innate immune system development, as it has been suggested for the peripheral one (Hannon *et al.*, 2003). Notably, some preliminary evidence (data not shown) found no gross permeability differences between wild-type and Anxa1 null mice until post-natal day 17 (P17), most probably indicating that the gross difference noted in adulthood arose only when the barrier reached maturity. Therefore, other events may have contributed to the noted differences; for instance, increased rate of proliferation could also explain why we detected higher cell density in the Anxa1 null mouse, which could be speculatively seen in light of the anti-proliferative and pro-apoptotic role of endogenous Annexin A1 reported in other models (Solito *et al.*, 2001; Lim and Pervaiz, 2007; Ang *et al.*, 2009). Also, peripheral monocytes can access the brain when BBB is opened as a result of cytokines, chemokines and other inflammatory mediators (D'Mello *et al.*, 2009; Ransohoff and Perry, 2009; Morgan *et al.*, 2010): this supports such a possibility under non-pathological conditions for the Anxa1 null mouse, characterised by an altered, higher pro-inflammatory cytokines profile.

We also detected clear alterations on Anxa1 null microglia morphology, especially in terms of reduction of process number and cell soma enlargement (Figure 7.3; Panel A and E). Although morphological analysis of these cells is not a wholly reliable way to determine their activity status (Ransohoff and Perry, 2009; Perry, 2010), these changes are at least indicative of altered microglial activity.

Overall, this may suggest that under unchallenged conditions cells are not in a normal resting state but rather bear a basally-activated behaviour, since they lack Annexin A1, thought to be a potent activity brake.

7.5.1.2 Genotype-related differences on the impact of peripheral inflammation

Under peripheral inflammation, different temporal responses of microglia were detected between the genotypes. Anxa1 null microglia cells seemed to become hyper-sensitive and hyper-responsive despite the absence of real tissue injury and this numerical increase could be attributed to either intense proliferation following extensive activation, or to cell recruitment from close regions (Figure 7.8; Panel D); in addition, the existence of an intense feedback mechanism involving peripherally circulating monocytes has been already shown in wild-type mice by several groups (D'Mello *et al.*, 2009).

In support of the stimulatory action of peripheral inflammation, microglia cells showed clear changes in their morphology (enlargement of the cell body, reduction in cell processes), which have been already reported in the brain of a mouse model of hepatic inflammation (D'Mello *et al.*, 2009) but appeared to be particularly enhanced in the Anxa1 null mice. In both genotypes, this behaviour resulted to be SNpc-specific, which enriches the relevance and the peculiarity of these findings. Moreover, we detected a significant increase in nitrite concentration in the Anxa1 null mouse, both under basal conditions but especially after peripheral challenge, while the presence of anti-inflammatory molecule IL-10 appeared strongly limited, reinforcing the tight link previously shown between ANXA1 and this cytokine (Ferlazzo *et al.*, 2003).

Interestingly, we detected a significant temporary decrease in nigral TH^+ neurons 24 hours after LPS administration, which was restored to saline treated control levels after 7 days (Figure 7.4). The only available evidence showing similar results (in wild-type mice) reported progressive neuronal loss after 7 months after a single administration of LPS (5 mg/kg, a dose very similar to what we used) (Qin *et al.*, 2007).

In our case it is unlikely that after an initial quick cellular loss the brain is able to rapidly regenerate neurons, for two important reasons: first, it is well known that the regenerative potential of the nervous system (Gage, 2003) and in particular of the substantia nigra (Mitsumoto *et al.*, 1998) is limited; second, periphery-brain communication is able to generate a chronic inflammatory environment, which seems to be maintained for a long time despite the systemic reaction being subdued within a short temporal frame (Qin *et al.*, 2007), and probably act against repair and regeneration of the injured tissue. Most likely, we observed a temporary loss of dopaminergic phenotype, characterised by loss in TH positivity (Kaufman, 1995). This event has been reported under conditions of particular stress of nigral neurons (Bowenkamp *et al.*, 1996), which tend to lose their peculiar dopaminergic ability due to the highly inimical environment (oxidative stress, activation of the brain innate immune system). This finding could be the result of a highly challenging *milieu* in the substantia nigra of Anxa1 null mice as a consequence of peripheral inflammation. Indeed, the massive numerical increase in the highly populated microglia pool might represent a source of challenge for the vulnerable TH^+ neurons, possibly through increased levels of NO, as observed in the challenged Anxa1 null mice; this gaseous molecule shows neurotoxicity when produced in high quantities (Rakesh, 2007). This and other factors might have contributed to the pro-inflammatory *milieu* that seems to characterise the nervous tissue of null mice and caused the temporary loss of TH phenotype until rescuing mechanisms, like those offered by astroglia (Lin *et al.*, 1993; Bowenkamp *et al.*, 1996) through neurotrophic/neuroprotective factors, support the endangered cells.

To our knowledge, only one group (Qin *et al.*, 2007) was able to show a direct effect on DA neurons by only peripheral administration of LPS; therefore, our findings of a quick (24 hours) increased vulnerability of DA neurons in presence of peripheral inflammation and in absence of annexin A1 are therefore novel and stress the important role played by this protein in preventing an excessive inflammatory environment building in the brain.

In presence of peripheral inflammation, resident wild-type Cd11b positive cells did not show evident quantitative or qualitative changes in Anxa1 expression, which was maintained in association to the cell membrane at basal levels (Figure 7.5; Panel E), nor we observed a numerical increase in Anxa1 positive microglia cells, as expected from what it was obtained

from the Anxa1 null mouse (X-gal staining; Chapter 2, Figure 2.2). In a related *in vitro* model based on BV2 cells, a murine microglia cell line (McArthur *et al.*, 2010), we observed increased externalisation/release of Anxa1 under inflammatory conditions (Figure 10.9: Panel C). Despite the results here presented, we endorse the theory of microglia being able to respond to a pro-inflammatory environment through modulation of annexin A1 (Solito *et al.*, 2008). The fact that stimulation *in vitro* might generate a different type of response should be taken into account; nonetheless, we strongly believe that the regulation of this protein in myeloid cells occurs in terms of release/mobilisation of the protein (Figure 10.9; Panel C), which only *in vitro*/*ex vivo* studies are able to test.

7.5.1.3 Genotype-related differences on the response to neurodegeneration

The establishment of neurodegeneration represents a direct injurious stimulus within the brain, able to bring direct consequences on the entire surrounding environment, including microglia and their activity (Glass *et al.*, 2010; Ransohoff and Brown, 2012). Choosing to model nigral neuronal loss through 6-OHDA intrastriatal administration, we guaranteed both a direct toxic effect on SNpc TH^+ dopaminergic neurons but also the consequent activation of surrounding microglia, which is particularly abundant in this area (Kim *et al.*, 2000). In our hands, this was observed in lesioned wild-type animals (Figure 7.8; Panel A), which responded to dopaminergic-specific neuronal damage by quick (24 hours) and intense (2-fold) microglial recruitment and density increase, which subsided immediately after, suggesting the existence of a tight control system, able to encourage the beneficial role of microglia (mainly removal of dead neurons to avoid them becoming signals perpetuating inflammation) but to prevent prolonged microglia activity.

Anxa1 null mice showed a different, slower kinetics of microglia recruitment in the lesioned side of the brain, which peaked only after 1 week from toxin injection and remained high without subsiding. This particular behaviour suggests important aspects: first, annexin A1 may be required for microglia activation and recruitment under these conditions, so its absence slowed a prompt reaction; secondly, the absence of Annexin A1 again seem to represent the loss of an important “safety brake”, a signal for homeostasis restoration, since the reaction mounted by microglia in the injured site did not decrease over time.

Although the lesion size did not differ between genotypes, we noticed that many of the surviving dopaminergic neurons expressed Anxa1, which opened a new broad scenario for a potential neuroprotective role. In support of that, Knott *et al.* (Knott *et al.*, 2000) suggested annexin A1 as a rescue signal to damaged neurons in a model of PD.

Anxa1 null mice differed also in this case from wild-types in terms of TH positive neuronal loss: despite the lesioned substantia nigra being more populated by microglia cells, which did not decrease throughout the time window analysed, the typical chronicity of the neuronal loss surprisingly stopped after an initial decreasing phase (Figure 7.7; Panel A). This result could easily refute the hypothetical neuroprotective role for Annexin A1 proposed according to the wild-type results, but alternatively it could be justified by considering the inability of Anxa1$^{-/-}$ microglia to phagocytose apoptotic cells (Figure 10.9; Panel A). We (McArthur *et al.*, 2010) and others (Blume *et al.*, 2009; Blume *et al.*, 2012) have shown Annexin A1 to be an important signal for the removal of apoptotic cells, which are peculiar of neurodegenerative diseases and models, like the 6-OHDA (Gomez-Lazaro *et al.*, 2008). When apoptotic neurons are not efficiently removed by phagocytes, they may occur in secondary necrosis, which still presents the expression of characteristic antigens as it has been observed for TH positive DA neurons (Alavian *et al.*, 2009), so they can ideally be still visualized and counted. Secondary necrotic neurons can eventually become deleterious, since they can trigger an actively pro-inflammatory microglial phenotype, which is neurotoxic (Pais *et al.*, 2008) and annexin A1 is at the forefront in limiting such response to the failure in apoptotic neurons clearance (Blume *et al.*, 2009; Blume *et al.*, 2012). Therefore, we think that the results obtained in the Anxa1 null mouse in terms of DA neurons survival are strongly influenced by the proven inability of Anxa1 null microglia to efficiently remove dead neurons. Moreover, the constantly higher microglia density observed during the lesioning experiment may also depend on the chronic pro-inflammatory environment generated by the inefficient clearance of the apoptotic neurons.

Also, we should not forget that inflammation and its players are originally meant to provide a protective/resolutive/supportive role during injury. This concept is also valid for the brain during neurodegenerative diseases (Ransohoff and Perry, 2009; Wee Yong, 2010; Czeh *et al.*, 2011; Ransohoff and Brown, 2012) and for microglia, which is often referred, too

simplistically, as the bad immune cells (Mena and Garcia de Yebenes, 2008); indeed, microglia is able to release neurotrophic factors against LPS-induced DA neurons damage, at least during its acute response to injury (Sawada *et al.*, 2008). In our case, a longer time course of investigation for the 6-OHDA model of DA neuronal degeneration in Anxa1 null mice would certainly provide more clarity on the real scenario of the model, explaining better the quantitative data obtained.

In an unique way, the lesioned striatum of wild-type animals showed a rapid increase of Anxa1 in Cd11b positive cells (Figure 7.9; Panel B), which could either represent resident microglial cells or derived from adjacent regions, activated by degeneration of surrounding neurons or peripheral monocytes recruited by the injury. The limited specificity of the marker used does not help discriminating between the two hypotheses, although various works support either the first [ANXA1 upregulation in microglia (Knott *et al.*, 2000)] or the second [peripheral recruitment of monocytes (Whitton, 2007; Reale *et al.*, 2009)]. Against the second option, though, it seems that recruitment of monocytes from the periphery may not happen so rapidly (Hanisch and Kettenmann, 2007; Jin *et al.*, 2010) to justify our results. Notably, the analysis of the morphology has never represented a reliable and exhaustive way to define the nature of a cell and its activity status (Aloisi, 2001; Perry *et al.*, 2010), supporting more the use of a combination of cell markers.

Importantly, the rapid increase in Anxa1 expression was not generalized in every striatal Cd11b positive cell and its restoration to basal conditions was very rapid (Figure 7.9), possibly suggesting that this may depend on a tight regulation by specific micro-environmental factors (either inhibitory or stimulatory), as shown in MS patients (Elderfield *et al.*, 1992). We were not able to obtain a similar correlation between Anxa1 expression and Cd11b in the injured SNpc; one possible explanation is that we missed the right time point when these events may have happened.

Overall, these findings described an altered immune-toxic response of Anxa1 null mice to intracerebral 6-OHDA toxin administration, characterised by a delayed but persistent increase in microglia density not followed by chronic loss of dopaminergic neurons.

7.5.1.4 Impact of peripheral inflammation on the injured brain

Under the conditions we employed, we detected no significant effects on the existing lesioning event in wild-type animals (Figure 7.10), while we did find increased loss of TH positive neurons in the challenged Anxa1 null mouse. Along with this, we detected an effect more than either alone but less than additive between lesioning and peripheral inflammatory impact in terms of microglia density within the injured area only in the null mice, while wild-types responded to the two consequent stimuli in a more tightly controlled fashion (Figure 7.11).

It is becoming clear that additional stimuli on a brain already challenged may result in the exacerbation of the symptoms and acceleration of the disease course, the main cause being the hyper-responsiveness of microglia, which during neurodegeneration acquires a peculiar not-fully activated primed phenotype (Perry, 2010). This concept is now receiving great attention because it carries many implications for disease progression and deterioration of quality of life of patients with neurodegenerative disorders; however, still conflicting evidence arise in literature in terms of which phenotype is triggered under neurodegenerative conditions. Typical pro-inflammatory cytokines like TNF-α, IL-1β, IL-6 have been reported to be up-regulated in the 6-OHDA-lesioned SNpc and in striatum (Mogi *et al.*, 1999; Nagatsu and Sawada, 2006) and a fully-activated phenotype of microglia (Gao and Hong, 2008). By contrast, Depino *et al.* (Depino *et al.*, 2003) reported an atypical cytokine response to sub-acute 6-OHDA injection into the striatum, characterised by high cytokines transcription but limited production (the primed phenotype), because 6-OHDA-triggered apoptosis was not sufficient to induce secretion of pro-inflammatory mediators.

The results obtained in our last experiment did not shed more clarity on these open questions, which will require more investigation to be properly answered. These results, together with those from the previous experimental settings, may strongly suggest an important immuno-modulatory role for Annexin A1: in fact, while Anxa1 null microglia suffered the synergistic effects of existing neurodegeneration and the strong impact of peripheral inflammation by further increasing their number, wild-type microglia did not show such influence, therefore presenting a tighter control of exaggerated responses otherwise caused by intense stimuli.

7.5.2 The Anxa1 null mouse provides new details on the central role of Anxa1

Anxa1 null microglia appeared to react excessively to peripheral inflammation, while displaying a peculiar response to 6-OHDA driven neurodegeneration and an exaggerated reactivity when both conditions were present. Overall, all the findings indicate that the lack of Anxa1 may promote a pro-inflammatory/classically activated phenotype, similar to the "M1" status extensively described for resident tissue macrophages, characterised by intense release of toxic effectors and not by efficient tissue clearance, repair and resolution (Czeh *et al.*, 2011). Hyper-responsiveness due to the loss of an endogenous immune-brake may help to explain why Anxa1 null mice suffer the synergistic effect between central and peripheral challenges, resulting in the increased loss of neurons.

Along with the peculiar Anxa1 null microglia basal morphology (Figure 7.3), we could link these observations to aged microglia features: a sensitised phenotype can be produced through all the subtle stimuli received during life-span, characterised by a sensible reduction in all the beneficial actions offered by these cells, for example the clearance of dead cell debris and toxins from the cerebral environment (Czeh *et al.*, 2011). In addition to this, alterations in Annexin A1 functions have been linked to aging (Strijbos *et al.*, 1993), which classically is also characterised by an increased microglia density in unchallenged conditions (Godbout *et al.*, 2005; L'Episcopo *et al.*, 2011).

The hypothesised Anxa1 role in regulating the phenotype of microglia and in negatively limiting the complexity of the response is becoming clearer. We have already described the mechanism contributing to the non-inflammatory/pro-resolutive phagocytosis of apoptotic cells (McArthur *et al.*, 2010) while negatively regulating the aggressive phenotype that microglia can acquire under pro-inflammatory stimuli, characterised by ineffective and detrimental phagocytosis of non-apoptotic/non-injured cells (reviewed in Figure 10.9; Panel B). Our evidence among others (Wu *et al.*, 1995; Minghetti *et al.*, 1999; Knott *et al.*, 2000) that annexin A1 is able to inhibit iNOS and COX enzymes expression along with the production of certain pro-inflammatory precursors and mediators such as arachidonic acid, IL-1β, IL-6 and TNF-α, all found to be up-regulated in certain conditions, clearly supports our (Solito *et al.*, 2008) idea of a mechanism to control innate immunity over-activation lead by Annexin A1, both in the intact or in the challenged-injured brain.

7.5.3 ANXA1 in the neurons: an O*ff* signal for microglia?

One of the most significant results obtained in this section was to describe the modulatory nature of neuronal Anxa1: peripheral inflammation was able to increase the percentage of DA neurons expressing ANXA1 in the SNpc. Under neurodegenerative conditions, instead, these neurons showed the tendency to preferentially survive, while those in the Anxa1 null mouse died regardless of their positivity for the replacing gene reporter β-galactosidase.

The presence of Annexin A1 in neurons has been already reported in literature: Young *et al.* (Young *et al.*, 1999) showed it to be expressed in cerebellar neurons, Knott *et al.* (Knott *et al.*, 2000) detected it in intact and lesioned SNpc DA neurons in PD patients, while others (Strijbos *et al.*, 1991; Eberhard *et al.*, 1994) showed Anxa1 positivity in hippocampal neurons. However, none has reported changes in expression and in the number of Anxa1 positive neurons, which certainly opens up a new scenario for this molecule.

The central response to systemic inflammation is unique and independent when compared to the quick dynamics of the parallel peripheral response, which peaks at 2 hours following LPS injection and subsides back to baseline at 24 hours. Previous reports (Singh and Jiang, 2004; Qin *et al.*, 2007) showed how quickly single LPS injections induced alterations in the brain, especially *de novo* synthesis and release of pro-inflammatory factors (TNF-α, IL-1, NF-κB, NO) by microglia and brain endothelial cells but to our knowledge no information about the effects on neurons exists. Peripheral immune reactions are sensed in the brain as an alarm for potential danger, triggering central responses aimed to help tackling the cause of inflammation. In particular, microglia cells can sense peripheral endotoxins and inflammation (*i.e.* cytokines), by undertaking a pro-inflammatory profile (Cunningham *et al.*, 2005; Perry *et al.*, 2007). The line existing between advantages and disadvantages of such responses is very fine; evolution may have developed a feed-back system centred on specific neurons, able to control the surrounding abundant microglia population from becoming dangerous. Relevantly, it is nowadays clear that neurons are seen not anymore as simple passive targets of the strong potential of microglial cells, but may also control their activity, mainly restricting the intensity of their reactivity under inflammatory conditions (Biber *et al.*, 2007; Zhang *et al.*, 2011).

This is accomplished through a series of physiological molecules, normally expressed and released at the level of neurons [the most indicative examples are CX3CL1 (fractalkine) and CD200-ligand]. Annexin A1 may be certainly included among these *Off* molecules of neuronal origin, especially in light of its innate ability to be secreted and to act in the surrounding environment by targeting neighbouring cells, as seen in other models (Buckingham *et al.*, 2003; McArthur *et al.*, 2009).

Taking into account all these considerations, it appears clearer why neurons expressing Annexin A1 are those surviving longer within the degenerating substantia nigra: the possible scenario indicates the ability to define an anti-inflammatory/modulatory microenvironment around these cells where constant increased release Annexin A1 maintains the surrounding activated microglia less reactive and neurotoxic, therefore halting/delaying their demise. The loss of these neurons, along with these endogenous regulatory molecules, normally coincides with an increased reactivity of microglia, as we have in part seen in the Anxa1 null mouse and others have proved in different models (Biber *et al.*, 2007).

For completion, Annexin A1 may also be considered as an *On* signal, since it is a factor promoting phagocytosis of apoptotic cells, one of the typical actions provided by the beneficial microglia phenotype during neuronal damage, as well as a chemoattractant signal, as recently reported (Blume *et al.*, 2012; Dalli *et al.*, 2012) in other tissue.

7.6 Limitations of the study

The results presented in this chapter do represent an enormous effort to depict cell types, mediators and signals in such a complex physiopathological system. We must not forget that most of the results presented were obtained by manual counting of positive stained cells on brain sections, which required a large amount of time but provided clear quantitative observations. We were able to detect some very informative differences between genotypes, which nicely described a new face for the central role played by this protein and will fuel the ground for future research.

A way to improve this descriptive study would be to perform a parallel staining for a generic neuronal marker (for example nuclear neuronal antigen NeuN) to confirm that the diminution in the TH^+ neurons does actually represent loss of DA neurons and not only the loss of the dopaminergic phenotype. However, the long-standing experience on this model in our laboratory has already confirmed this (Murray *et al.*, 2003; Gillies *et al.*, 2004).

β-galactosidase immunostaining did not replicate quantitatively the results obtained with Anxa1: fewer TH^+ neurons stained positively for this gene reporter, which proved to be a protein quite difficult to visualize with classic immunofluorescence techniques (Figure 7.2; Panel B) at least in brain tissue fixed under these conditions. The limitations faced during the staining and the fact that this protein does not represent a functionally relevant substitute but only an indicator of cells where the Anxa1 promoter is active, brought us to avoid using it as an useful marker for our functional purposes. However, its comparison reinforced the protective role offered by neuronal Anxa1 in wild-type animals under neurodegeneration.

We benefited from the use of Iba1 and Cd11b, among the most used markers for microglia cells, although not fully informative of the activation state of the cells; this represents a very complex topic and recent studies have indicated the need to stain cells with several specific markers in order to discern their particular phenotype. However, this would be complex to do on tissue sections; primary isolation of microglia cells would certainly represent a useful solution. Despite the lack of immune-phenotyping, we detected some clear differences in terms of morphology and cell density, both in untreated and treated conditions.

In terms of annexin A1 expression at microglia level, we confirmed previous results (McKanna, 1993), but we detected only few $Anxa1^+$ microglia in the unchallenged wild-type mouse, and the staining was very localised, as opposed to the results achieved on human tissue. Low immunostaining efficiency may be among the principal causes, as already detected elsewhere (McKanna, 1993; McArthur *et al.*, 2010): annexin A1 is notoriously difficult to identify on brain sections, mainly since the antigen is particularly sensitive to fixation conditions, with several protocols unable to preserve a sufficient immunoreactivity.

7.7 Future work

Overall, in this part of the project we prioritized the description of the complex processes, before focusing on mechanistic details. Simplified *in vitro* experiments with primary microglia from Anxa1 null mice will help understanding more in detail every aspect in which Anxa1 is involved. In particular, it will be extremely useful to detect Anxa1-dependent differences in those pro-inflammatory mediators (cytokines, iNOS, NADPH oxidase and COX enzymes expression) that have been linked to the progression of various disorders (Glass *et al.*, 2010), although some evidence already exists (Wu *et al.*, 1995; Minghetti *et al.*, 1999). These results will certainly clarify the hypothesis of a chronically inflamed brain in absence of Annexin A1, both in presence or absence of various inflammatory stimuli. This will also help to understand if Anxa1 null microglia is a sort of primed microglia or if it becomes fully activated under neurodegenerative conditions. Early studies evidenced marked differences in NO/nitrite between genotypes, as well as in iNOS basal expression, which represent an index of inflammation; it would be interesting to deepen this area as well as investigating other quickly-responding (Czapski *et al.*, 2007; Argaw *et al.*, 2012) NO-producing enzymes as endothelial NOS (eNOS) or neuronal NOS (nNOS).

Since there is growing evidence supporting the existence of a dichotomy of functional phenotypes for microglia as it exists for macrophages [M1 versus M2; see (Czeh *et al.*, 2011)], it will be interesting to investigate if ANXA1 represents a marker for the alternatively activated/beneficial phenotype or if it is a strong inducer of it.

Co-culture experimental settings, using primary mesencephalic mixed neurons and glia cultures from wild-type and Anxa1 null mouse or microglia (BV2) and neuron-like (PC12) cell lines [a model already established by us in previous studies (McArthur *et al.*, 2010)], will immensely contribute to study the role of neuronal Anxa1 as a modulator of microglia activation, as well as the role of microglial Anxa1 as an endogenous immunological brake. Speculatively, we don't think Annexin A1 may represent a direct survival signal for neurons challenged with a specific toxin, although some have proposed a specific transcriptional role for this protein in neurons (Knott *et al.*, 2000); we think instead this protein, when expressed within the neurons, is able to control and limit over-activation of microglia.

A simple experiment with 6-OHDA incubation of midbrain neurons from wild-type or Anxa1 null mouse will certainly help unravelling the question. In parallel, another important aspect to be investigated in the future is the role of peripherally recruited cells within the SNpc (D'Mello *et al.*, 2009). The next experiments will try to shed more light on this topic, giving more indications on the extent of circulating cell recruitment in respect to resident cell proliferation under these stimuli.

7.8 Summary and conclusions

In this chapter, we provided details about the genotype-related differences shown in presence or absence of Annexin A1 in the intact brain, but also in response to peripheral, central challenges or both.

The protein appeared to be strongly modulated in presence of these stimuli, suggesting its direct involvement in the complex regulatory machinery constantly protecting the CNS against excessive detrimental responses. Neurodegeneration in wild-type animals triggered a rapid microglia activation and recruitment in the lesioned site, along with a quick increase in Anxa1 expression, but both events subsided in a relatively short period of time, which could represent, in our opinion, the proof of concept for the regulative role of Anxa1 in central inflammation. On the other hand, the response generated to peripheral inflammatory reactions could be classified by looking at Annexin A1 as one of the key mediators of the central responses to peripheral challenges, with a novel modulatory role play from neurons.

The mechanism of action of annexin A1 is multi-faceted, intervening at different levels as evident in Figure 7.12, sketched according to our latest data and published evidence. Therefore, this molecule may become a new smart target and may represent a novel solution to control detrimental loops and adverse microglia phenotypes (Hanisch and Kettenmann, 2007) especially in the already injured brain, where it has been shown to present a beneficial impact against exaggerated responses.

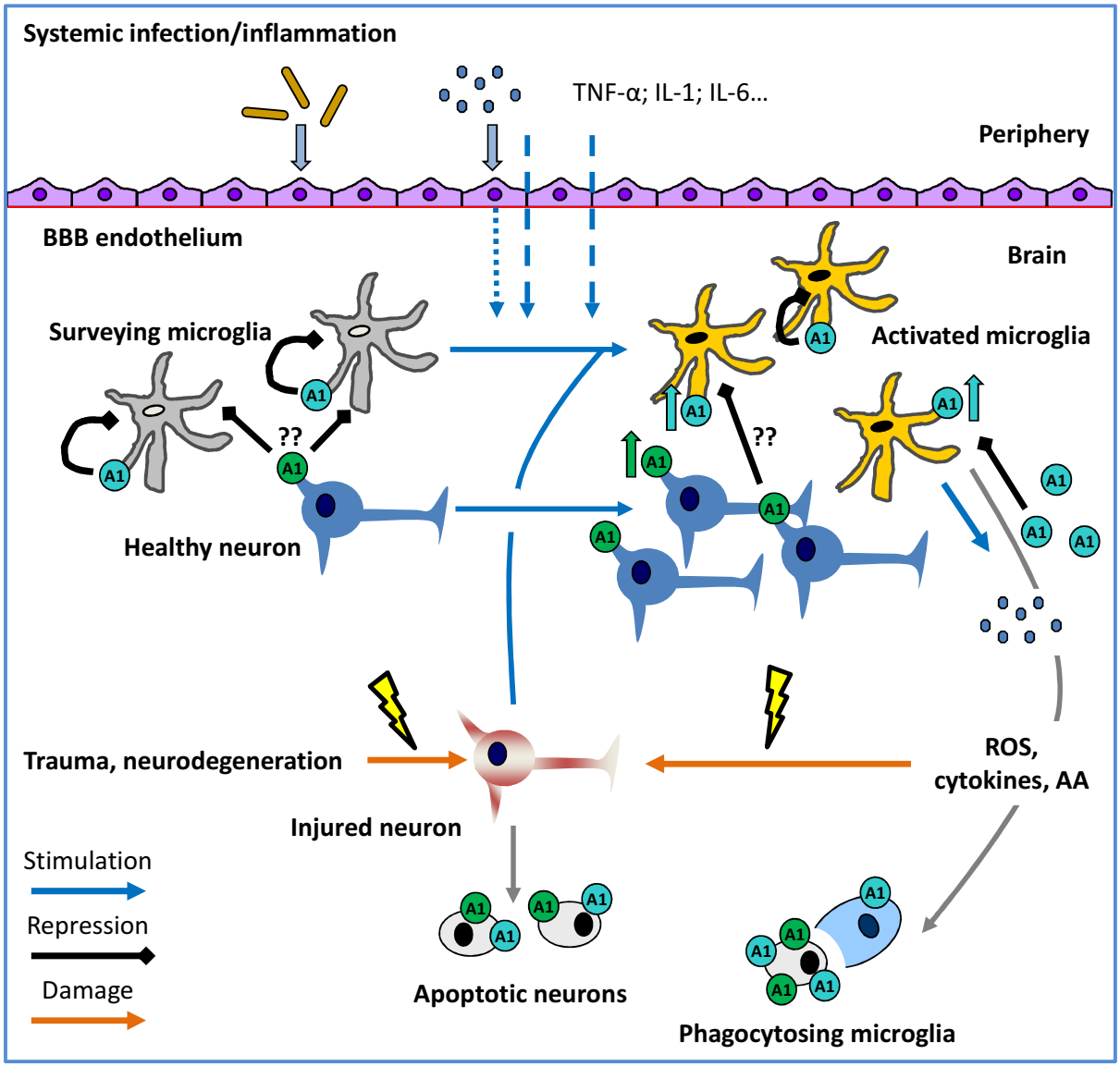

Figure 7.12 Potential mechanisms of Annexin A1 action in presence of peripheral inflammatory conditions, neurodegeneration and the synergistic action of the two. Our recent evidence, along with some previous findings (Young *et al.*, 1999; Knott *et al.*, 2000), has confirmed the expression of annexin A1 on various groups of neurons, like the dopaminergic neurons of the substantia nigra pars compacta. We believe that this molecule acts as an endogenous *off* signal: it is able to keep microglia under tight control in basal conditions, while the upregulation observed during systemic challenges may represent the ability to prevent microglial excessive activation. In addition to that, Annexin A1 is also expressed by microglia itself, where it functions as an immune-modulatory effector towards a pro-resolutive/beneficial phenotype, similarly to its role in the periphery (Parente and Solito, 2004).

Chapter 8 – Summary and future perspectives

8.1 Overview

The findings reported in this thesis identified a new, complex role for ANXA1 in mediating and regulating the intricate interlink between periphery and CNS. By exploiting the highly informative Anxa1 null mouse, along with established cell lines and primary cell cultures, we have been able to unravel new mechanisms of action and new cellular targets for ANXA1 and its physiological and pathological implications. The major findings and conclusions drawn for each part of the study are summarized separately below.

8.2 Annexin A1 physiological role at the blood brain barrier level

In the ideal journey unravelling the role of Annexin A1 in regulating the central impact of peripheral inflammation, we first explored its implications at the level of BBB, in particular the brain microvascular endothelial cells, representing the real interface between the brain and the rest of the body and participating to decode all the signals circulating in the blood.

In order to fully understand the role(s) of Annexin A1 in the impact of inflammation on the BBB, we had to first investigate the physiological implications of the protein at such level. We first detected a characteristic increase in basal leakiness to Evans Blue in Anxa1 null mice. This evidence was further confirmed by immunohistological detection of IgG extravasation, as well as through gadolinium leakage on dynamic contrast MRI (Figure 4.7), while successful rescue of the altered phenotype was also obtained *in vivo* using human recombinant ANXA1 protein. The main gross differences between Anxa1 null mice and wild-type microvasculature were detected at endothelial level, excluding any significant morphological alteration in other important cellular and molecular components of the BBB (Figure 4.8). In particular, major differences at the level of the physical barrier were evident, represented by the disruption in the physiological expression and organisation of occludin and VE-cadherin, extremely important for a functional barrier. As already observed in other tissues (Hannon *et al.*, 2003), Anxa1 null mouse presented a partial compensatory response at the level of the brain microvasculature, offered by another member of the Annexins family, namely Annexin A2, shown to be a junctional peripheral protein (Lee *et al.*, 2004) and cytoskeleton modulatory effector (Morel *et al.*, 2009). In order to investigate the cellular and molecular implications of Annexin A1, we confirmed *in vitro* that Anxa1$^{-/-}$

monolayers of primary murine BMECs presented increased paracellular permeability compared to wild-type ones, supporting the endothelium-specific role of ANXA1. Then, we chose to use a more manageable model, represented by a well-established and intensively used cell line of BMECs, the hCMEC/D3 cell line (Weksler *et al.*, 2005); we successfully modified its endogenous level of ANXA1 expression by antisense technology or stable full length ANXA1 sequence transfection and we were able to show a direct correlation between the degree of protein expression and the level of tightness, as reviewed in Figure 4.11. Annexin A1 was visualized at level of tight cell-cell contacts, in particular in electro-dense areas, where tight junctions usually form; we were only able to detect partial molecular interactions between ANXA1 and VE-cadherin, leaving the question around a role of ANXA1 as a junctional protein still open.

Looking for the true molecular involvement of Annexin A1 in endothelial tightness, we observed major ANXA1-dependent differences in the structural organisation of the actin cytoskeleton and we were able to clearly prove, by multiple approaches, the direct interactions occurring between ANXA1 and the major component of the actin cytoskeleton, *i.e.* β-actin (Figure 4.12). Low levels of ANXA1 produced structural disruption of the cortical F-actin rim, along with the formation of numerous dysfunctional stress-fibres, known to cause loss of tightness in the endothelium (Beckers *et al.*, 2010). Higher levels of ANXA1 were able, instead, to move the shift towards cortical actin cytoskeleton, which truly represents the scaffolding structure necessary for junctions formation and maintenance (Prasain and Stevens, 2009).

Since Annexin A1 was present in cells both in an endogenous and in a released form, we depicted two contributions participating in junctional structure stabilization. The endogenous pool of protein was shown to act as an actin binding protein; the externalised pool, instead, participated in regulating the small Rho GTP-ases pathway, which holds important significance in the regulation of the actin cytoskeleton (Figure 4.13 and 4.17).

With such findings we have been the first to clearly show a new structural role of ANXA1 in contributing to brain microvasculature tightness both *in vivo* and at cellular/molecular level, producing strong implications for the potential utilisation of Annexin A1 as a therapeutic tool.

8.2.1 Future perspectives

In our opinion, the results presented have contributed to advance the knowledge on BBB tightness, cytoskeleton and cellular junctions regulation in the healthy barrier, which certainly presents important implications for non-physiological conditions and aging.

Interestingly, these findings propose several potential applications which may benefit from this novel role of Annexin A1. First, we have demonstrated the possibility to improve basal tightness properties of the BBB endothelium by up-regulating ANXA1 expression or through the treatment with recombinant protein. Several attempts have been made to develop interventions able to support the BBB, not only with the aim to target those pathologies where its peculiar properties tend to fade away, but also to provide a preventative protective treatment before the onset of an insulting stimulus, be it a systemic treatment [for example, the negative effect of chemotherapics (Kannarkat *et al.*, 2007)] or a potent infection, since BBB dysfunction can also be a causative phenomenon, not only a factor propagating an existing condition. Some promising data in the potentiation of BBB have been achieved by using glucocorticoids, able to modulate the cortical actin cytoskeleton and cellular junctions formation (Hoheisel *et al.*, 1998; Romero *et al.*, 2003; Cucullo *et al.*, 2004; Bauer *et al.*, 2005; Forster *et al.*, 2005). Many analogies with the action of ANXA1 can be found, which could possibly explained through the widely-accepted role of this protein as a primary messenger and mediator of glucocorticoid action (Solito *et al.*, 1998); this is true for the classic immune-modulatory action of this class of steroids, but it can easily be true also at this new level of brain microvascular endothelium. In addition, the use of steroids present several side-effects which may undermine the effectiveness of the treatment, therefore the focus of the research has been switched towards endogenous anti-inflammatory mediators able to replicate the effect of these drugs with a lower impact on the whole body; glycerophosphoinositol [GPI; (Cucullo *et al.*, 2004)] is one of these natural compounds and we think ANXA1 will generate novel alternative interest.

Secondly, we were able to reduce tightness either temporarily, by targeting the protein through a neutralizing antibody (Figure 4.13), or constitutively, by down-regulating the expression of the *ANXA1* gene. Increasing interest has been generated by new therapeutic paradigms aiming at transitional barrier opening to improve the administration of

therapeutic molecules into the brain otherwise unable to reach effective concentrations. This new idea requires to be developed very carefully and requires a tight temporal and structural control of the opening to limit noxious side-effects (for instance, the formation of oedema or the extravasation of reactive molecules into the brain). Annexin A1 may represent a potential useful regulator and could guarantee flexibility of action.

Thirdly, rescuing potential is offered by using recombinant human protein, shown to improve the phenotype of the impaired Anxa1 null mouse, as well as of the antisense hCMEC/D3 line (Figure 4.13). Previous reports (Relton *et al.*, 1991) also suggested the therapeutic potential offered by this molecule in reducing the severity of vascular-related pathologies, facilitating the recovery.

Overall, we think to have opened a new pathway in the understanding of the physiological regulation of brain microvasculature extraordinary tightness, offering new options for different applications and a novel *in vivo* platform of constitutive leaky barrier (the Anxa1 null mouse), which may be useful to investigate new mechanisms and test new treatments.

8.3 Annexin A1 implications on the BBB under pathological conditions

With the significant impact of these novel findings in mind, we were intrigued by the observations we obtained from samples derived from MS patients. This disorder is particularly atypical, since it does not seem to have a classical central origin, like AD or PD, but instead it appears to arise from several factors which may start playing their impact from the periphery; also, blood flow and vasculature seem to play an important part. These considerations, along with the results presented, certainly confirm the importance of Annexin A1 at the interface between brain and rest of the body.

Loss of ANXA1 expression was detected in brain capillaries of MS cases (Figure 5.2), a result which appeared extremely tissue-specific as confirmed by the maintenance of expression in other vascular-related sites like the ependyma, the meningeal vessels and the choroid plexus, as well as bigger vessels.

In addition, we were able to detect a significant reduction in plasma ANXA1 content of MS patients as well as a specific permeability-increasing effect on hCMEC/D3 monolayers incubated with the same plasma samples, which was linked to a decreased total level of ANXA1 (Figure 5.3).

8.3.1 Future perspectives

The molecular mechanisms leading to BBB breakdown in MS are not well understood, therefore we think these new findings, together with the new role of Annexin A1, may offer novel hints for future research. It is interesting that one of the most widely and successfully used treatment, namely recombinant interferon β-1-α, is able to indirectly preserve ANXA1 expression in endothelial cells treated with MS patients serum [in an experimental set-up similar to ours; (Alexander *et al.*, 2007)]. This anti-inflammatory cytokine is thought to work by preserving BBB integrity [although this evidence has only be confirmed *in vitro* (Muller *et al.*, 2012; Kraus *et al.*, 2008)]. Annexin A1 could be a mediator of interferon β action and may contribute to explain its efficacy on BBB. Also, interferon β contribute to down-regulate circulating factors (pro-inflammatory cytokines) that have a negative effect (Chapter 5) on the protein expression, in this way limiting the systemic impact of the disease.

The main questions posed by our descriptive study are: why is the expression of Annexin A1 selectively lost from plasma and brain capillaries from multiple sclerosis patients? What factor(s) contribute(s) to that? Ideally, we should start by focusing on alterations in the inflammatory status of MS patients, checking for significant differences in cytokines, chemokines and factors, which are known to negatively affect endothelium. Notably, several reports have already described alterations in fluids towards a pro-inflammatory profile (Carrieri *et al.*, 1998; Minagar *et al.*, 2003). The correlation between peripheral factors and ANXA1 expression will also confirm, once again, the central role played by this protein in the communication between periphery to CNS. The decrease of Annexin A1 from MS brain capillaries and from serum may represent an early phenomenon during the course of the disease, which could therefore be translated into diagnostic exploitation. Possibly, it may reflect an early weakening of the capillaries, with consequent altered exchanges with the brain and the resulting activation of the surrounding areas of the CNS. This event could

also prepare for the augmented entry of circulating leukocytes, which contributes to the progression of the disease. Not randomly, ANXA1 shares the same target (*i.e.* $\alpha_4\beta_1$ integrin) of another widely used treatment for MS, the antibody Natalizumab (Tubridy *et al.*, 1999). Finally, we should not forget that ANXA1 is the key mediator of the peripheral and central action of glucocorticoids, another therapeutic choice for MS. All this represents another confirmation of how this endogenous natural molecule may prove useful therapeutically in future studies. In our opinion, further studies on blood and tissue samples are definitely required to understand if and how lack of protein may alter the leukocytes transmigration across the BBB in MS, which is the major trigger for disease escalation. The current view supports the brain entry of peripheral blood cells mainly through extravasation at the level of post-capillary venules, where the hemodynamic shear forces are more limited. However, there is great focus on the interactions, particularly adhesion, occurring at the level of the capillaries (Steiner *et al.*, 2011); our studies on a human cell line will certainly impact on the current interest.

8.4 Annexin A1 and peripheral inflammation at the BBB: sex-dependent differences

As ANXA1 is an anti-inflammatory protein in the peripheral immune system, the following step was to investigate in details the consequences of peripheral inflammation on BMECs and the involvement of ANXA1. Evans blue *in vivo* brain extravasation under inflammatory conditions (modelled by *i.p.* administration of LPS) showed two important aspects: first, peripheral inflammation caused a transient increase in BBB permeability; second, there is a clear sex-related bias which was lost in Anxa1 null mice (Figure 6.5). By performing similar experiments on aged and ovariectomised animals, we then were able to confirm that this dimorphic response was linked to sex hormones, most likely 17 β-estradiol. Significantly, we observed a sex-dependent modulation of Anxa1 under inflammatory stimulation.

In order to depict the molecular mechanism behind these results, we moved to our established *in vitro* model of BMECs, the hCMEC/D3 cell line. Here, we confirmed modulation of ANXA1 expression by physiological concentrations of 17 β-estradiol, in a time and dose-dependent manner (Figure 6.6) as well as post-translational modifications (Figure

6.12). Interestingly, also ANXA1-specific receptors appeared to be modulated upon exposure to the hormone. More in detail, the effect of the hormone was evident both at the level of the externalised pool of ANXA1, as well as the cellular one, therefore indicating the potential presence of two distinct mechanisms; indeed, we saw that ANXA1 release was mediated through GPR30, the transmembrane receptor for estradiol, while the effect on the whole cell content was probably a combination of both the classic estrogen receptors, ER-α and ER-β action (Figure 6.7).

To shed some light on the sex-dependent results, we decided to focus on long pre-incubations with 17 β-estradiol, so that we could mimic the chronic exposure to hormones occurring *in vivo*. Paralleling the results obtained in the animals, our pre-conditioning protocol was able to protect endothelial monolayers from the disruptive effect caused by pro-inflammatory cytokines (Figure 6.8), both in terms of FITC-dextran paracellular permeability and TEER. Interestingly, we were not able to detect any β-estradiol-dependent alterations in the classical signalling pathways triggered by TNF-α (Appendix; Figure 10.5), as it had been detected in other BBB-related and non-related models (Galea *et al.*, 2002; Ghisletti *et al.*, 2005), instead we saw the important involvement of ANXA1 in mediating the protective effect offered by β-estradiol towards inflammatory stimulation, which indeed could be prevented by blocking estradiol-induced ANXA1 action (Figure 6.10). This phenomenon could be explained in terms of ANXA1 release and autocrine/paracrine pathway, which tended to be limited/blocked by inflammation but protected through chronic estradiol action (Figure 6.11). This result was also accompanied by a similar behaviour for surface-expressed FPR2, which appeared to be negatively modulated by pro-inflammatory cytokines but this effect was completely reverted by pre-incubation with the female hormone. These results may suggest two important novel mechanisms: a new ANXA1-dependent way through which phlogistic mediators disrupt brain barrier properties and a novel explanation for the protective role of 17 β-estradiol on brain microvasculature under inflammatory challenges.

Importantly, these findings were replicated at functional levels: in fact, we were able to see the protective effect conveyed by hormonal pre-incubation being translated into rescuing actin cytoskeleton disruption, tight- and adherens-junctions localisation, which historically

have been known as primary targets of inflammatory mediators as well as ultimate results of the novel role of ANXA1 (Figure 6.13 and Figure 6.14). Overall, these findings confirm ANXA1 as intimately linked to the response generated by microvascular 17 β-estradiol, which has a long standing candidacy as protective effector for the brain vasculature in a number of inflammatory and pathological conditions (Maggi *et al.*, 2004; Vegeto *et al.*, 2008).

8.4.1 Future perspectives

All the results presented in this section confirmed, once more, how central annexin A1 appears to be in many mechanisms and responses. They also provide a good example of potentiation of an endangered barrier, supporting future studies on therapeutic implications on this endogenous mediator. This new avenue could prove valuable to solve many disease-related complications and to avoid the typical side-effects, which unfortunately accompany hormonal treatments (Ye *et al.*, 2003; Sohrabji and Bake, 2006). More importantly, these findings contribute to the on-going debate on some current research focuses: high and persistent levels of pro-inflammatory cytokines both in the CNS and in the peripheral circulatory system play a key role in neurological disorders with vascular components, such as multiple sclerosis (Silwedel and Forster, 2006; Bennett *et al.*, 2010; Coisne and Engelhardt, 2011). Therefore, one may ask if such temporary increase in permeability (as we have detected in male wild-type mice) play a beneficial or detrimental effect. ANXA1-mediated effect of estradiol results to be protective and to limit the course of the inflammatory response, which undoubtedly has advantageous functional roles. Communication between peripheral and central system is undoubtedly necessary and numerous mechanisms exist to ensure prompt signalling and consequently quick central response: endothelial cells are primarily involved in these mechanisms, being able to sense messengers like inflammogens and cytokines and triggering an amplification phase (Banks, 2006; Banks and Robinson, 2010). Therefore, signalling is normally preferred as a way to communicate what it is happening elsewhere in the body; however, in certain conditions, it may be beneficial to induce a modest and reversible barrier opening to permit a quicker and stronger communication and a more rapid and drastic response. Indeed, plasma brings

numerous factors with trophic relevance, which could help normal repair processes in an injured brain; in addition, this may allow "sampling" of the blood by neurons and immune-surveillance brain resident cells (microglia and astrocytes too), in order to remain informed about the peripheral status. Provided that such transient opening events occur in a tightly regulated manner, we should understand that a momentary increase in permeability may be part of the physiological function of cytokines and inflammogens (like LPS) response; the behaviour shown by wild-type male mice in Figure 6.5 represents a good example, since the physiological basal permeability was autonomously restored within 24 hours after LPS administration. Consequences of a prolonged BBB leakage are highly negative and can result in immediate damage of the brain as well as in an increase in brain susceptibility to damage later in life (Stolp and Dziegielewska, 2009): the consequences may be the extravasation of circulating molecules (and potentially cells) that strongly activates the central immune system (Lucas *et al.*, 2006) and exacerbate any existing disease (McColl *et al.*, 2008). Annexin A1, by regulating and limiting permeability changes in presence of harmful stimuli, should therefore be regarded as a protective effector. Losing the ability to regulate its expression and activity could result in exaggerated responses, as shown in the old female animals, whose barrier responded with a prolonged increase in permeability.

8.5 Central Annexin A1 under peripheral inflammation and neurodegeneration

ANXA1 mapping showed a clear SNpc-specific expression on glia-like and a small population of neuron-like cells, which was further modulated by peripheral inflammatory events (Figure 2.2). Such events are responsible for worsening neurodegenerative conditions, so we investigated the protein involvement within the CNS, both under peripheral inflammatory and neurodegenerative conditions. Interestingly, Anxa1 null mouse showed basal microglia density much higher than in wild-type male counterparts (Figure 7.3).

In addition, $Anxa1^{-/-}$ $Iba1^{+}$ cells presented some evident differences in their soma shape and ramifications, possibly suggesting a differential status in absence of the Anxa1, an hypothesis further supported by Anxa1 null whole brain lysates showing increased basal

expression of two inducible enzymes usually expressed by microglia under inflammatory challenge, iNOS and COX-2. This indicated a basal reactivity of the Anxa1 null CNS.

By challenging wild-type and Anxa1 null animals with a single dose of LPS *i.p.*, we generated an exacerbated peripheral inflammatory reaction in the knock-out mouse model [as already reported (Damazo *et al.*, 2005)]. Significant increment in the number of $Anxa1^+$ TH^+ neurons within the SNpc indicated a long-term effect of inflammation in the brain, well after the acute peripheral reaction has subsided; we interpreted this result as a response mounted by delicate neurons to cope with the peripheral challenge. In the Anxa1 null mouse, we observed a temporary (24 hours after *i.p.* LPS administration, restored at normal levels 6 days after) decrease in the total number of nigral TH^+ neurons, which may indicate the establishment of a particularly challenging environment (Figure 7.4). As an explanation, we could consider the exceptionally high increment of Anxa1 null microglia density, accompanied by increased NO production and a reduced efficiency of the anti-inflammatory machinery (IL-10). These results suggest that the absence of Annexin A1 represent the lack of an important immunological brake.

Having verified that peripheral stimulation has a great impact within the SNpc, in particular in the Anxa1 null mouse, we moved to a neurodegeneration model, the 6-OHDA intrastriatal infusion, known to lead to a gradual lesion of the SNpc. Genotype-related differences were detected in terms of microglia recruitment: wild-type animals responded with a quick short-lived increase in cell density in the lesioned SNpc, while the Anxa1 null mice instead displayed a slower kinetics, which peaked at 1 week post-lesioning start and did not seem to resolve completely (Figure 7.8). These findings support for an impaired nature of Anxa1 null microglia cells, which seemed to be less sensitive to neuronal cell damage compared to peripheral inflammation. Surprisingly, we did not detect a negative impact of Anxa1 lack in terms of TH neuronal survival (Figure 7.7); instead, lesioning in null mice showed a different dynamic of cell loss compared to the typically chronic one showed by wild-types. The current knowledge could not fully justify these results, which may be linked to the impaired ability of Anxa1 null microglia to clear apoptotic neurons; however, further investigations will try to shed more light on this topic. Still importantly, those TH^+ neurons expressing Anxa1 (in the wild-type animals) showed a preferential survival rate compared to the

surrounding Anxa1, indirectly supporting the immune-modulatory nature of the protein towards the surrounding reactive microenvironment.

Finally, in order to investigate the impact of peripheral inflammation on on-going neurodegeneration and to understand if the presence of Annexin A1 could play some sort of beneficial/modulatory role, we first induced significant lesioning of the SNpc and then we challenged the animal peripherally with LPS. Wild-type mice did not show differences linked to the subsequent peripheral stimulation, while Anxa1 null mice did show exacerbated loss of TH^+ neurons, which was paralleled by an exaggerated higher microglia cell density in the lesioned side, indicating an additive effect between the two stimuli. Overall, Annexin A1 appeared to be important in controlling the inflammatory impact, possibly helping to limit DA neuronal loss and neurodegenerative progression.

8.5.1 Future perspectives

We believe that these results will stimulate novel interest on the central role of ANXA1 in the periphery-to-brain communication. Malfunctions in the communication pathway may represent a detrimental process common to several neurodegenerative disorders, and ANXA1 may be implicated. In addition, our results contributed to add more information about the peculiar features characterizing the SNpc and to the relevant impact inflammation can have, not only when originated within the brain, but especially when derived from the periphery.

Despite some novel theories sustaining that boosting inflammation and the immune system may represent a new way to obtain beneficial effects on the injured brain (Rivest, 2009; Wee Yong, 2010), medicine has historically reached more successes in inhibiting the immune reaction rather than activating it, the only exception being represented by vaccines (Lucin and Wyss-Coray, 2009).

A clearer knowledge of the mechanisms implicated in immune-central communication and those involved in microglia activation to an aggressive phenotype will certainly indicate a better understanding on how all these events can be controlled. We believe to have started

this contribution by proposing Annexin A1, as well as its small peptides, as a molecule tightly involved in these processes.

Having described the potential role of ANXA1 in limiting the central effects of systemic inflammation opens numerous implications: nowadays, treatments for PD patients are aimed at controlling and limiting symptoms, rather than targeting disease causes and homeostasis restoration, since these are difficult goals to achieve when diagnosis occurs late. In particular, steroidal and non-steroidal anti-inflammatory drugs have been used with mixed success to inhibit excessive microglial activation (in particular the antibiotic minocycline) and the production of pro-inflammatory/toxic cytokines and reactive species (ROS/NOS), which negatively impact on damaged or intact neurons (Chen *et al.*, 2003; Whitton, 2007). These numerous evidences support the potential use of anti-inflammatory drugs to limit the progression of existing neurological disorders, but also to halt the negative impact of reactions transferred from the periphery, which should now be considered strong CNS influencing factors (Chen *et al.*, 2003; Lucin and Wyss-Coray, 2009). However, these drugs bear numerous side effects when given over a long period of time. This is why the attention is now progressively switching into studying endogenous mediators shown to play a role in the anti-inflammatory/pro-resolution action of the drugs, but possibly more gentle in terms of toxic impact on the body. Such approach is now considered a smarter solution by many and will soon produce some new exciting advances in the field, successfully controlling the chronic neuroinflammatory environment, the real perpetuating agent. ANXA1 should be considered one of these endogenous anti-inflammatory molecules (the resolvins) that present a strong candidacy and a valuable potential (Relton *et al.*, 1991; Strijbos *et al.*, 1991; Black *et al.*, 1992; Rothwell and Relton, 1993; Knott *et al.*, 2000). We have been among the first ones to provide some clear mechanistic explanation on some of the beneficial roles of ANXA1 in the brain (McArthur *et al.*, 2010) and this study closely follows by adding novel evidence and broadening the meaning of this molecule.

Our latest observation may produce strong implications for novel ANXA1-based strategies to combat those neurological disorders that show microglia over-activation as a fundamental contributor to the disease, possibly reversing its detrimental state towards a more beneficial one.

8.6 A novel role for ANXA1 in the central impact of peripheral inflammation

There is a growing awareness that systemic inflammation transmits to the brain and, unless the consequent neuroinflammatory response is controlled, it has a huge impact on the CNS. Our work has helped to establish Annexin A1 as a key endogenous molecule involved into periphery-to-brain communication: by limiting the propagation of inflammation, preventing an exaggerated production of inflammatory mediators throughout the body and by triggering the complex resolution process, ANXA1 already contributes to limit the impact that daily inflammatory events can have on the rest of the body and on the CNS. These are already known as the classical array of actions for which ANXA1 has been extensively studied in the last 30 years (Parente and Solito, 2004; Perretti and D'Acquisto, 2009). Here, we showed novel interventions at other fundamental sites along the immune-nervous axis, controlling and regulating the transfer of systemic inflammatory stimuli to the brain, as well as resolving/limiting the central inflammatory responses generated. Annexin A1 plays an important role in maintaining tight and protective the BBB endothelium, a role which is modulated according to the type of stimuli received, so that a correspondent response can be consequently generated. Circulating pro-inflammatory cytokines, which are extremely important messengers, are able to modulate the expression and localisation of ANXA1 with a consequent but transient barrier permeability increase, believed to be beneficial when tightly controlled (Abbott, 2002). In such way, certain informative stimuli may enter the brain and communicate with some of the resident cellular types, like neurons and microglia cells. Within specific brain regions, like SNpc, ANXA1 is expressed according to a peculiar pattern of expression and our evidence strongly supports for a modulatory role both under basal conditions but especially under peripheral stimulation, *i.e.* controlling the neuroinflammatory response generated as a consequence of the signalling cascade triggered through the BBB and limiting excessive activation. We think, therefore, that our recent work greatly support from a molecular, cellular and structural level the working hypothesis of the entire project, depicted in Figure 8.1 and described in (Solito *et al.*, 2008).

Notably, having had the possibility to study a complex phenomenon in an *in vivo* set-up allowed us not only to describe a novel endothelium-specific role for ANXA1, but especially to appreciate the tight relationship existing between the various structures of interest and the responses generated by one when another resulted impaired.

We believe Anxa1 null mouse will still prove to be a useful model to deepen our knowledge on the molecular periphery-to-brain communication, which is still at its infancy. In parallel, *in vitro* experiments between microvascular endothelium, neurons and microglia will confirm molecularly the role of central ANXA1 as a protective communicator.

8.7 Closing comments

Nowadays, we live longer mainly thanks to an improved quality of life and control of diseases but the central impact of infections and of certain diseases (like chronic kidney disease and heart failure) still represents a huge threat. It has been recently reported that a significant part of the next 5 years NHS budget will be spent in treating people with secondary cognitive dysfunction; therefore, future work in this field cannot stop, but should focus on unravelling the mechanisms of interaction between periphery and brain, together with deciphering how we can exploit the novel discoveries therapeutically. Consequently, we will generate new ways able to halt and resolve the detrimental effects brought by inflammation, not simply by temporarily stopping them. Therefore, it is important that research funding into this area does not stop as well as novel approaches and original ideas, which thankfully seems not to lack (Ajami *et al.*, 2011; Hatherell *et al.*, 2011; Abbott *et al.*, 2012; Lippmann *et al.*, 2012; Patabendige *et al.*, 2012).

Our results strongly indicate ANXA1 as a target that should be taken into further research in the next future, so that the novelty of these findings won't wear out too quickly. The multifaceted array of actions shown by this molecule will certainly turn to be an advantage, so that targeting disorders like PD will result practicable and effective and in a novel paradigm of treatments not aiming anymore at limiting the impact of the symptoms but instead at resolving the causes and the aggravating circumstances.

We think that our latest results will generate new enthusiasm around Annexin A1, an old molecule not only since it has been studied for over 30 years, but also because the ancestor gene is around 400 millions years old. The therapeutic potential is in front of everyone's eyes, as well as the possibility to use it as a novel early diagnosis biomarker, which will represent an enormous step forward into more effective therapies and better quality of life.

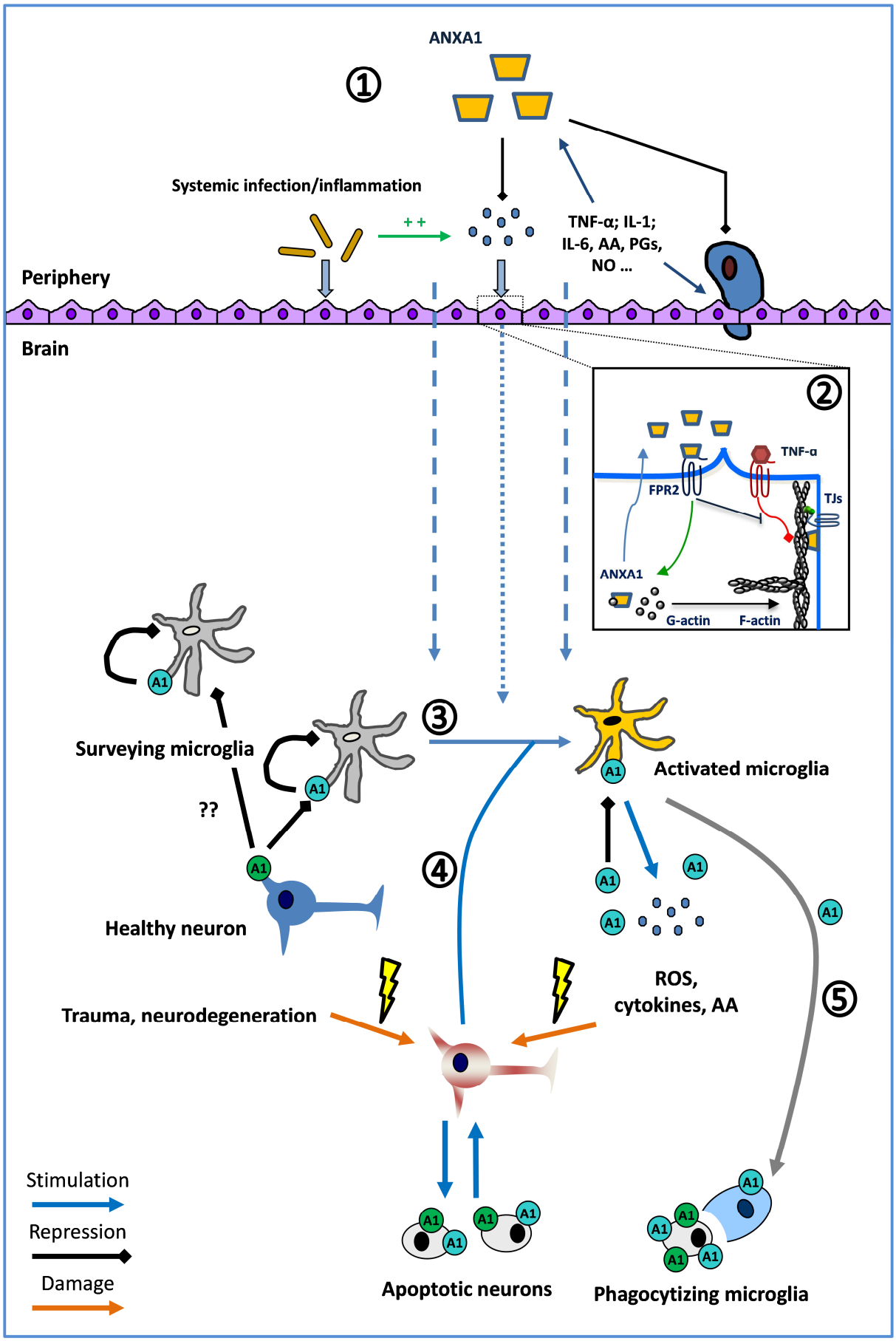
ANXA1
①
Systemic infection/inflammation
++
TNF-α; IL-1;
IL-6, AA, PGs,
NO ...
Periphery
Brain
②
TNF-α
FPR2
TJs
ANXA1
G-actin
F-actin
A1
Surveying microglia
??
③
Activated microglia
④
Healthy neuron
ROS,
cytokines, AA
⑤
Trauma, neurodegeneration
Stimulation
Repression
Damage
Apoptotic neurons
Phagocytizing microglia

Figure 8.1 Working hypothesis modified with evidence produced. This figure represents the working hypothesis, which generated the entire project and was preliminarily presented in Solito *et al*. 2008. **1|** Peripheral infection and inflammation cause the release of pro-inflammatory mediators, including cytokines, arachidonic acid, prostaglandins and nitric oxide. Annexin A1 is triggered as part of the anti-inflammatory/resolution process and it counteracts the action of these mediators, especially in terms of release of the mediators themselves and extravasation of leukocytes through the activated endothelium. **2|** ANXA1 plays a fundamental role in the brain microvascular endothelium, by contributing to maintenance of the peculiar tightness. Under inflammatory stimulation, ANXA1 is modulated and ultimately is able to counteract the effects of the pro-inflammatory stimuli. **3|** The brain also mounts an inflammatory response to systemic inflammation, **4|** as well as to local injury (trauma, stroke, neurodegeneration, *etc.*), which is characterised by microglia cells quickly responding and activating, with consequent release of great amounts of pro-inflammatory mediators. ANXA1 may represent one of the mediators of the tight immune-related control that characterise the brain, supporting beneficial microglia phenotypes, like **5|** the phagocytising one which beneficially clears up apoptotic cell bodies, limiting further damage and amplification of the stimulation (McArthur *et al.*, 2010).

Chapter 9 – References

Abbott, N.J., Chugani, D.C., Zaharchuk, G., Rosen, B.R.*, et al.* (1999). Delivery of Imaging Agents into Brain. Advanced drug delivery reviews *37*, 253-277.

Abbott, N.J. (2002). Astrocyte-endothelial interactions and blood-brain barrier permeability. Journal of anatomy *200*, 629-638.

Abbott, N.J. (2005). Dynamics of CNS barriers: evolution, differentiation, and modulation. Cellular and molecular neurobiology *25*, 5-23.

Abbott, N.J., Dolman, D.E., Drndarski, S., and Fredriksson, S.M. (2012). An improved in vitro blood-brain barrier model: rat brain endothelial cells co-cultured with astrocytes. Methods Mol Biol *814*, 415-430.

Abbott, N.J., Hughes, C.C., Revest, P.A., and Greenwood, J. (1992). Development and characterisation of a rat brain capillary endothelial culture: towards an in vitro blood-brain barrier. Journal of cell science *103 (Pt 1)*, 23-37.

Abbott, N.J., Patabendige, A.A., Dolman, D.E., Yusof, S.R., and Begley, D.J. (2010). Structure and function of the blood-brain barrier. Neurobiology of disease *37*, 13-25.

Abbott, N.J., Ronnback, L., and Hansson, E. (2006). Astrocyte-endothelial interactions at the blood-brain barrier. Nature reviews Neuroscience *7*, 41-53.

Aderem, A., and Ulevitch, R.J. (2000). Toll-like receptors in the induction of the innate immune response. Nature *406*, 782-787.

Ahn, T.B., and Jeon, B.S. (2006). Protective role of heat shock and heat shock protein 70 in lactacystin-induced cell death both in the rat substantia nigra and PC12 cells. Brain research *1087*, 159-167.

Ajami, B., Bennett, J.L., Krieger, C., McNagny, K.M., and Rossi, F.M. (2011). Infiltrating monocytes trigger EAE progression, but do not contribute to the resident microglia pool. Nature neuroscience *14*, 1142-1149.

Alavian, K.N., Sgado, P., Alberi, L., Subramaniam, S., and Simon, H.H. (2009). Elevated P75NTR expression causes death of engrailed-deficient midbrain dopaminergic neurons by Erk1/2 suppression. Neural development *4*, 11.

Alexander, J.S., Minagar, A., Harper, M., Robinson-Jackson, S., Jennings, M., and Smith, S.J. (2007). Proteomic analysis of human cerebral endothelial cells activated by multiple sclerosis serum and IFNbeta-1b. Journal of molecular neuroscience : MN *32*, 169-178.

Allan, S.M., and Rothwell, N.J. (2001). Cytokines and acute neurodegeneration. Nature reviews Neuroscience *2*, 734-744.

Allen, N.J., and Barres, B.A. (2009). Neuroscience: Glia - more than just brain glue. Nature *457*, 675-677.

Allport, J.R., Muller, W.A., and Luscinskas, F.W. (2000). Monocytes Induce Reversible Focal Changes in Vascular Endothelial Cadherin Complex During Transendothelial Migration under Flow. The Journal of cell biology *148*, 203-216.

Aloisi, F. (2001). Immune function of microglia. Glia *36*, 165-179.

Alvarez-Martinez, M.T., Mani, J.C., Porte, F., Faivre-Sarrailh, C., Liautard, J.P., and Sri Widada, J. (1996). Characterization of the interaction between annexin I and profilin. Eur J Biochem *238*, 777-784.

Alvarez-Martinez, M.T., Porte, F., Liautard, J.P., and Sri Widada, J. (1997). Effects of profilin-annexin I association on some properties of both profilin and annexin I: modification of the inhibitory activity of profilin on actin polymerization and inhibition of the self-association of annexin I and its interactions with liposomes. Biochimica et biophysica acta *1339*, 331-340.

Alvarez, J.I., Dodelet-Devillers, A., Kebir, H., Ifergan, I., Fabre, P.J., Terouz, S., Sabbagh, M., Wosik, K., Bourbonniere, L., Bernard, M.*, et al.* (2011). The Hedgehog pathway promotes blood-brain barrier integrity and CNS immune quiescence. Science *334*, 1727-1731.

Andersson, N., Islander, U., Egecioglu, E., Lof, E., Swanson, C., Moverare-Skrtic, S., Sjogren, K., Lindberg, M.K., Carlsten, H., and Ohlsson, C. (2005). Investigation of central versus peripheral effects of estradiol in ovariectomized mice. The Journal of endocrinology *187*, 303-309.

Ang, E.Z., Nguyen, H.T., Sim, H.L., Putti, T.C., and Lim, L.H. (2009). Annexin-1 regulates growth arrest induced by high levels of estrogen in MCF-7 breast cancer cells. Molecular cancer research : MCR *7*, 266-274.

Angelillo-Scherrer, A. (2012). Leukocyte-derived microparticles in vascular homeostasis. Circulation research *110*, 356-369.

Antonicelli, F., De Coupade, C., Russo-Marie, F., and Le Garrec, Y. (2001). CREB is involved in mouse annexin A1 regulation by cAMP and glucocorticoids. Eur J Biochem *268*, 62-69.

Argaw, A.T., Asp, L., Zhang, J., Navrazhina, K., Pham, T., Mariani, J.N., Mahase, S., Dutta, D.J., Seto, J., Kramer, E.G.*, et al.* (2012). Astrocyte-derived VEGF-A drives blood-brain barrier disruption in CNS inflammatory disease. The Journal of clinical investigation *122*, 2454-2468.

Armulik, A., Genove, G., Mae, M., Nisancioglu, M.H., Wallgard, E., Niaudet, C., He, L., Norlin, J., Lindblom, P., Strittmatter, K.*, et al.* (2010). Pericytes regulate the blood-brain barrier. Nature *468*, 557-561.

Arnal, J.F., Scarabin, P.Y., Tremollieres, F., Laurell, H., and Gourdy, P. (2007). Estrogens in vascular biology and disease: where do we stand today? Current opinion in lipidology *18*, 554-560.

Ascherio, A., and Munger, K.L. (2007). Environmental Risk Factors for Multiple Sclerosis. Part Ii: Noninfectious Factors. Annals of neurology *61*, 504-513.

Ascherio, A., Munger, K.L., and Simon, K.C. (2010). Vitamin D and Multiple Sclerosis. Lancet neurology *9*, 599-612.

Attwell, D. and Laughlin S.B. (2001). An energy budget for signalling in the grey matter of the brain. Journal of cerebral blood flow and metabolism *21*, 1133-45.

Aveleira, C.A., Lin, C.M., Abcouwer, S.F., Ambrosio, A.F., and Antonetti, D.A. (2010). TNF-alpha signals through PKCzeta/NF-kappaB to alter the tight junction complex and increase retinal endothelial cell permeability. Diabetes *59*, 2872-2882.

Bailey, S.L., Schreiner, B., McMahon, E.J., and Miller, S.D. (2007). Cns Myeloid Dcs Presenting Endogenous Myelin Peptides 'Preferentially' Polarize Cd4+ T(H)-17 Cells in Relapsing Eae. Nature immunology *8*, 172-180.

Bake, S., Friedman, J.A., and Sohrabji, F. (2009). Reproductive age-related changes in the blood brain barrier: expression of IgG and tight junction proteins. Microvasc Res *78*, 413-424.

Bake, S., and Sohrabji, F. (2004). 17beta-estradiol differentially regulates blood-brain barrier permeability in young and aging female rats. Endocrinology *145*, 5471-5475.

Bale, T.L. (2009). Neuroendocrine and immune influences on the CNS: it's a matter of sex. Neuron *64*, 13-16.

Banks, W.A. (2006). The blood-brain barrier as a regulatory interface in the gut-brain axes. Physiology & behavior *89*, 472-476.

Banks, W.A., and Robinson, S.M. (2010). Minimal penetration of lipopolysaccharide across the murine blood-brain barrier. Brain, behavior, and immunity *24*, 102-109.

Banerjee, S., and Bhat, M.A. (2007). Neuron-Glial Interactions in Blood-Brain Barrier Formation. Annual review of neuroscience *30*, 235-258.

Barboriak, D.P., MacFall, J.R., Padua, A.O., York, G.E., Viglianti, B.L., and, and Dewhirst, M. (2004). Standarized software for calculation of Ktrans and vp from dynamic T1 – weighted MR images. "International Society for Magnetic Resonance in Medicine Workshop on MR in Drug Development: From Discovery to Clinical Therapeutic Trials, McLean VA.

Barboriak, D.P., MacFall, J.R., Viglianti, B.L., and Dewhirst Dvm, M.W. (2008). Comparison of three physiologically-based pharmacokinetic models for the prediction of contrast agent distribution measured by dynamic MR imaging. Journal of magnetic resonance imaging : JMRI *27*, 1388-1398.

Bauer, B., Hartz, A.M., Fricker, G., and Miller, D.S. (2005). Modulation of p-glycoprotein transport function at the blood-brain barrier. Exp Biol Med (Maywood) *230*, 118-127.

Baumer, Y., Drenckhahn, D., and Waschke, J. (2008). cAMP induced Rac 1-mediated cytoskeletal reorganization in microvascular endothelium. Histochemistry and cell biology *129*, 765-778.

Beckers, C.M., van Hinsbergh, V.W., and van Nieuw Amerongen, G.P. (2010). Driving Rho GTPase activity in endothelial cells regulates barrier integrity. Thrombosis and haemostasis *103*, 40-55.

Behan, P.O., and Chaudhuri, A. (2010). The sad plight of multiple sclerosis research (low on fact, high on fiction): critical data to support it being a neurocristopathy. Inflammopharmacology *18*, 265-290.

Belisle, B., and Abo, A. (2000). N-Formyl peptide receptor ligation induces rac-dependent actin reorganization through Gbeta gamma subunits and class Ia phosphoinositide 3-kinases. J Biol Chem *275*, 26225-26232.

Benes, F.M., and Lange, N. (2001). Two-dimensional versus three-dimensional cell counting: a practical perspective. Trends in neurosciences *24*, 11-17.

Bennett, J., Basivireddy, J., Kollar, A., Biron, K.E., Reickmann, P., Jefferies, W.A., and McQuaid, S. (2010). Blood-brain barrier disruption and enhanced vascular permeability in the multiple sclerosis model EAE. Journal of neuroimmunology *229*, 180-191.

Biber, K., Neumann, H., Inoue, K., and Boddeke, H.W. (2007). Neuronal 'On' and 'Off' signals control microglia. Trends in neurosciences *30*, 596-602.

Black, M.D., Carey, F., Crossman, A.R., Relton, J.K., and Rothwell, N.J. (1992). Lipocortin-1 inhibits NMDA receptor-mediated neuronal damage in the striatum of the rat. Brain research *585*, 135-140.

Blackwell, G.J., Carnuccio, R., Di Rosa, M., Flower, R.J., Parente, L., and Persico, P. (1980). Macrocortin: a polypeptide causing the anti-phospholipase effect of glucocorticoids. Nature *287*, 147-149.

Blandini, F., and Armentero, M.T. (2012). Animal models of Parkinson's disease. The FEBS journal *279*, 1156-1166.

Blasi, E., Barluzzi, R., Bocchini, V., Mazzolla, R., and Bistoni, F. (1990). Immortalization of murine microglial cells by a v-raf/v-myc carrying retrovirus. Journal of neuroimmunology *27*, 229-237.

Block, M.L., Zecca, L., and Hong, J.S. (2007). Microglia-mediated neurotoxicity: uncovering the molecular mechanisms. Nature reviews Neuroscience *8*, 57-69.

Blume, K.E., Soeroes, S., Keppeler, H., Stevanovic, S., Kretschmer, D., Rautenberg, M., Wesselborg, S., and Lauber, K. (2012). Cleavage of annexin A1 by ADAM10 during secondary necrosis generates a monocytic "find-me" signal. J Immunol *188*, 135-145.

Blume, K.E., Soeroes, S., Waibel, M., Keppeler, H., Wesselborg, S., Herrmann, M., Schulze-Osthoff, K., and Lauber, K. (2009). Cell surface externalization of annexin A1 as a failsafe mechanism preventing inflammatory responses during secondary necrosis. J Immunol *183*, 8138-8147.

Bolton, S.J., Anthony, D.C., and Perry, V.H. (1998). Loss of the Tight Junction Proteins Occludin and Zonula Occludens-1 from Cerebral Vascular Endothelium During Neutrophil-Induced Blood-Brain Barrier Breakdown in Vivo. Neuroscience *86*, 1245-1257.

Bowenkamp, K.E., David, D., Lapchak, P.L., Henry, M.A., Granholm, A.C., Hoffer, B.J., and Mahalik, T.J. (1996). 6-hydroxydopamine induces the loss of the dopaminergic phenotype in substantia nigra neurons of the rat. A possible mechanism for restoration of the nigrostriatal circuit mediated by glial cell line-derived neurotrophic factor. Experimental brain research Experimentelle Hirnforschung Experimentation cerebrale *111*, 1-7.

Breier, G., Breviario, F., Caveda, L., Berthier, R., Schnurch, H., Gotsch, U., Vestweber, D., Risau, W., and Dejana, E. (1996). Molecular cloning and expression of murine vascular endothelial-cadherin in early stage development of cardiovascular system. Blood *87*, 630-641.

Brightman, M.W., and Reese, T.S. (1969). Junctions between intimately apposed cell membranes in the vertebrate brain. The Journal of cell biology *40*, 648-677.

Brook, C.G. (1999). Mechanism of puberty. Hormone research *51 Suppl 3*, 52-54.

Brown, R.C., and Davis, T.P. (2002). Calcium modulation of adherens and tight junction function: a potential mechanism for blood-brain barrier disruption after stroke. Stroke; a journal of cerebral circulation *33*, 1706-1711.

Brydon, L., Harrison, N.A., Walker, C., Steptoe, A., and Critchley, H.D. (2008). Peripheral inflammation is associated with altered substantia nigra activity and psychomotor slowing in humans. Biological psychiatry *63*, 1022-1029.

Buckingham, J.C., John, C.D., Solito, E., Tierney, T., Flower, R.J., Christian, H., and Morris, J. (2006). Annexin 1, glucocorticoids, and the neuroendocrine-immune interface. Ann N Y Acad Sci *1088*, 396-409.

Buckingham, J.C., Solito, E., John, C., Tierney, T., Taylor, A., Flower, R., Christian, H., and Morris, J. (2003). Annexin 1: a paracrine/juxtacrine mediator of glucorticoid action in the neuroendocrine system. Cell Biochem Funct *21*, 217-221.

Burek, M., Arias-Loza, P.A., Roewer, N., and Forster, C.Y. (2010). Claudin-5 as a novel estrogen target in vascular endothelium. Arterioscler Thromb Vasc Biol *30*, 298-304.

Bustin, S.A. (2010). Why the need for qPCR publication guidelines?--The case for MIQE. Methods *50*, 217-226.

Cabrita, L.D., Dai, W., and Bottomley, S.P. (2006). A family of E. coli expression vectors for laboratory scale and high throughput soluble protein production. BMC biotechnology *6*, 12.

Callio, J., Oury, T.D., and Chu, C.T. (2005). Manganese superoxide dismutase protects against 6-hydroxydopamine injury in mouse brains. J Biol Chem *280*, 18536-18542.

Campbell, S.J., Carare-Nnadi, R.O., Losey, P.H., and Anthony, D.C. (2007). Loss of the Atypical Inflammatory Response in Juvenile and Aged Rats. Neuropathology and applied neurobiology *33*, 108-120.

Campbell, M., Humphries, M.M., Kiang, A.S., Nguyen, A.T*., et al.* (2011). Systemic Low-Molecular Weight Drug Delivery to Pre-Selected Neuronal Regions. EMBO molecular medicine *3*, 235-245

Cardona, A.E., Pioro, E.P., Sasse, M.E., Kostenko, V., Cardona, S.M., Dijkstra, I.M., Huang, D., Kidd, G., Dombrowski, S., Dutta, R*., et al.* (2006). Control of microglial neurotoxicity by the fractalkine receptor. Nature neuroscience *9*, 917-924.

Carmeliet, P., Lampugnani, M.G., Moons, L., Breviario, F., Compernolle, V., Bono, F., Balconi, G., Spagnuolo, R., Oosthuyse, B., Dewerchin, M*., et al.* (1999). Targeted deficiency or cytosolic truncation of the VE-cadherin gene in mice impairs VEGF-mediated endothelial survival and angiogenesis. Cell *98*, 147-157.

Carrieri, P.B., Provitera, V., De Rosa, T., Tartaglia, G., Gorga, F., and Perrella, O. (1998). Profile of cerebrospinal fluid and serum cytokines in patients with relapsing-remitting multiple sclerosis: a correlation with clinical activity. Immunopharmacology and immunotoxicology *20*, 373-382.

Carvey, P.M., Hendey, B., and Monahan, A.J. (2009). The blood-brain barrier in neurodegenerative disease: a rhetorical perspective. Journal of neurochemistry *111*, 291-314.

Castro-Caldas, M., Duarte, C.B., Carvalho, A.R., and Lopes, M.C. (2001). 17beta-estradiol promotes the synthesis and the secretion of annexin I in the CCRF-CEM human cell line. Mediators Inflamm *10*, 245-251.

Caulin-Glaser, T., Watson, C.A., Pardi, R., and Bender, J.R. (1996). Effects of 17beta-estradiol on cytokine-induced endothelial cell adhesion molecule expression. The Journal of clinical investigation *98*, 36-42.

Cavegn, D., and d'Ydewalle, G. (1996). Presaccadic attention allocation and express saccades. Psychological research *59*, 157-175.

Cecchelli, R., Berezowski, V., Lundquist, S., Culot, M., Renftel, M., Dehouck, M.P., and Fenart, L. (2007). Modelling of the blood-brain barrier in drug discovery and development. Nature reviews Drug discovery *6*, 650-661.

Cenni, B., and Picard, D. (1999). Ligand-independent Activation of Steroid Receptors: New Roles for Old Players. Trends Endocrinol Metab *10*, 41-46.

Chan, W.Y., Kohsaka, S., and Rezaie, P. (2007). The origin and cell lineage of microglia: new concepts. Brain research reviews *53*, 344-354.

Chen, H., Zhang, S.M., Hernan, M.A., Schwarzschild, M.A., Willett, W.C., Colditz, G.A., Speizer, F.E., and Ascherio, A. (2003). Nonsteroidal anti-inflammatory drugs and the risk of Parkinson disease. Archives of neurology *60*, 1059-1064.

Choi, S.R., Howell, O.W., Carassiti, D., Magliozzi, R.*, et al.* (2012). Meningeal Inflammation Plays a Role in the Pathology of Primary Progressive Multiple Sclerosis. Brain : a journal of neurology *135*, 2925-2937.

Clanet, M. (2008). Jean-Martin Charcot. 1825 to 1893. International MS journal / MS Forum *15*, 59-61.

Clark D.D. & Sokoloff, L. (1999). Basic Neurochemistry: Molecular, Cellular and Medical Aspects, eds. Siegel, G. J., Agranoff, B. W., Albers, R. W., Fisher, S. K. & Uhler, M. D. (Lippincott, Philadelphia), pp. 637–670

Coisne, C., Dehouck, L., Faveeuw, C., Delplace, Y., Miller, F., Landry, C., Morissette, C., Fenart, L., Cecchelli, R., Tremblay, P.*, et al.* (2005). Mouse syngenic in vitro blood-brain barrier model: a new tool to examine inflammatory events in cerebral endothelium. Laboratory investigation; a journal of technical methods and pathology *85*, 734-746.

Coisne, C., and Engelhardt, B. (2011). Tight junctions in brain barriers during central nervous system inflammation. Antioxidants & redox signaling *15*, 1285-1303.

Comi, G., Battaglia, M.A., Bertolotto, A., Del Sette, M.*, et al.* (2013). Italian Multicentre Observational Study of the Prevalence of Ccsvi in Multiple Sclerosis (Cosmo Study): Rationale, Design, and Methodology. Neurological sciences : official journal of the Italian Neurological Society and of the Italian Society of Clinical Neurophysiology.

Compston, A., and Coles, A. (2008). Multiple Sclerosis. Lancet *372*, 1502-1517.

Cote, M.C., Lavoie, J.R., Houle, F., Poirier, A., Rousseau, S., and Huot, J. (2010). Regulation of vascular endothelial growth factor-induced endothelial cell migration by LIM kinase 1-mediated phosphorylation of annexin 1. J Biol Chem *285*, 8013-8021.

Couch, Y., Alvarez-Erviti, L., Sibson, N.R., Wood, M.J., and Anthony, D.C. (2011). The acute inflammatory response to intranigral alpha-synuclein differs significantly from intranigral lipopolysaccharide and is exacerbated by peripheral inflammation. Journal of neuroinflammation *8*, 166.

Cowan, K.M., and Easton, A.S. (2010). Neutrophils block permeability increases induced by oxygen glucose deprivation in a culture model of the human blood-brain barrier. Brain research *1332*, 20-31.

Cramer, L.P., Briggs, L.J., and Dawe, H.R. (2002). Use of fluorescently labelled deoxyribonuclease I to spatially measure G-actin levels in migrating and non-migrating cells. Cell motility and the cytoskeleton *51*, 27-38.

Crawford, L.E., Milliken, E.E., Irani, K., Zweier, J.L., Becker, L.C., Johnson, T.M., Eissa, N.T., Crystal, R.G., Finkel, T., and Goldschmidt-Clermont, P.J. (1996). Superoxide-mediated actin response in post-hypoxic endothelial cells. J Biol Chem *271*, 26863-26867.

Crone, C., and Olesen, S.P. (1982). Electrical resistance of brain microvascular endothelium. Brain research *241*, 49-55.

Cucullo, L., Hallene, K., Dini, G., Dal Toso, R., and Janigro, D. (2004). Glycerophosphoinositol and dexamethasone improve transendothelial electrical resistance in an in vitro study of the blood-brain barrier. Brain research *997*, 147-151.

Cucullo, L., Hossain, M., Puvenna, V., Marchi, N., and Janigro, D. (2011). The role of shear stress in Blood-Brain Barrier endothelial physiology. BMC neuroscience *12*, 40.

Cunningham, C., Wilcockson, D.C., Campion, S., Lunnon, K., and Perry, V.H. (2005). Central and systemic endotoxin challenges exacerbate the local inflammatory response and increase neuronal death during chronic neurodegeneration. The Journal of neuroscience : the official journal of the Society for Neuroscience *25*, 9275-9284.

Czapski, G.A., Cakala, M., Chalimoniuk, M., Gajkowska, B., and Strosznajder, J.B. (2007). Role of nitric oxide in the brain during lipopolysaccharide-evoked systemic inflammation. Journal of neuroscience research *85*, 1694-1703.

Czeh, M., Gressens, P., and Kaindl, A.M. (2011). The yin and yang of microglia. Developmental neuroscience *33*, 199-209.

D'Acquisto, F. (2009). On the adaptive nature of annexin-A1. Current opinion in pharmacology *9*, 521-528.

D'Mello, C., Le, T., and Swain, M.G. (2009). Cerebral microglia recruit monocytes into the brain in response to tumor necrosis factoralpha signaling during peripheral organ inflammation. The Journal of neuroscience : the official journal of the Society for Neuroscience *29*, 2089-2102.

Dalli, J., Montero-Melendez, T., McArthur, S., and Perretti, M. (2012). Annexin A1 N-terminal derived Peptide ac2-26 exerts chemokinetic effects on human neutrophils. Frontiers in pharmacology *3*, 28.

Dalli, J., Norling, L.V., Renshaw, D., Cooper, D., Leung, K.Y., and Perretti, M. (2008). Annexin 1 mediates the rapid anti-inflammatory effects of neutrophil-derived microparticles. Blood *112*, 2512-2519.

Damazo, A.S., Yona, S., D'Acquisto, F., Flower, R.J., Oliani, S.M., and Perretti, M. (2005). Critical protective role for annexin 1 gene expression in the endotoxemic murine microcirculation. Am J Pathol *166*, 1607-1617.

Daneman, R., Zhou, L., Kebede, A.A., and Barres, B.A. (2010). Pericytes are required for blood-brain barrier integrity during embryogenesis. Nature *468*, 562-566.

Dantzer, R. (2004). Cytokine-induced sickness behaviour: a neuroimmune response to activation of innate immunity. European journal of pharmacology *500*, 399-411.

Davies, E., Omer, S., Morris, J.F., and Christian, H.C. (2007). The influence of 17beta-estradiol on annexin 1 expression in the anterior pituitary of the female rat and in a folliculo-stellate cell line. The Journal of endocrinology *192*, 429-442.

de Castro, I.P., Martins, L.M., and Tufi, R. (2010). Mitochondrial quality control and neurological disease: an emerging connection. Expert reviews in molecular medicine *12*, e12.

de Coupade, C., Ajuebor, M.N., Russo-Marie, F., Perretti, M., and Solito, E. (2001). Cytokine modulation of liver annexin 1 expression during experimental endotoxemia. Am J Pathol *159*, 1435-1443.

de Coupade, C., Gillet, R., Bennoun, M., Briand, P., Russo-Marie, F., and Solito, E. (2000). Annexin 1 expression and phosphorylation are upregulated during liver regeneration and transformation in antithrombin III SV40 T large antigen transgenic mice. Hepatology *31*, 371-380.

de Haas, A.H., Boddeke, H.W., Brouwer, N., and Biber, K. (2007). Optimized isolation enables ex vivo analysis of microglia from various central nervous system regions. Glia *55*, 1374-1384.

Dehouck, M.P., Jolliet-Riant, P., Bree, F., Fruchart, J.C., Cecchelli, R., and Tillement, J.P. (1992). Drug transfer across the blood-brain barrier: correlation between in vitro and in vivo models. Journal of neurochemistry *58*, 1790-1797.

Dejana, E., Raiteri, M., Resnati, M., and Lampugnani, M.G. (1993). Endothelial integrins and their role in maintaining the integrity of the vessel wall. Kidney international *43*, 61-65.

Del Maschio, A., De Luigi, A., Martin-Padura, I., Brockhaus, M., Bartfai, T., Fruscella, P., Adorini, L., Martino, G., Furlan, R., De Simoni, M.G*., et al.* (1999). Leukocyte recruitment in the cerebrospinal fluid of mice with experimental meningitis is inhibited by an antibody to junctional adhesion molecule (JAM). The Journal of experimental medicine *190*, 1351-1356.

Deli, M.A., Abraham, C.S., Kataoka, Y., and Niwa, M. (2005). Permeability studies on in vitro blood-brain barrier models: physiology, pathology, and pharmacology. Cellular and molecular neurobiology *25*, 59-127.

Depino, A.M., Earl, C., Kaczmarczyk, E., Ferrari, C., Besedovsky, H., del Rey, A., Pitossi, F.J., and Oertel, W.H. (2003). Microglial activation with atypical proinflammatory cytokine expression in a rat model of Parkinson's disease. The European journal of neuroscience *18*, 2731-2742.

Descamps, L., Coisne, C., Dehouck, B., Cecchelli, R., and Torpier, G. (2003). Protective effect of glial cells against lipopolysaccharide-mediated blood-brain barrier injury. Glia *42*, 46-58.

Diffley, J.M., Wu, M., Sohn, M., Song, W., Hammad, S.M., and Lyons, T.J. (2009). Apoptosis induction by oxidized glycated LDL in human retinal capillary pericytes is independent of activation of MAPK signaling pathways. Molecular vision *15*, 135-145.

DiNapoli, V.A., Huber, J.D., Houser, K., Li, X*., et al.* (2008). Early Disruptions of the Blood-Brain Barrier May Contribute to Exacerbated Neuronal Damage and Prolonged Functional Recovery Following Stroke in Aged Rats. Neurobiology of aging *29*, 753-764.

Djukic, M., Mildner, A., Schmidt, H., Czesnik, D., Bruck, W., Priller, J., Nau, R., and Prinz, M. (2006). Circulating monocytes engraft in the brain, differentiate into microglia and contribute to the pathology following meningitis in mice. Brain : a journal of neurology *129*, 2394-2403.

Dobbie, M.S., Hurst, R.D., Klein, N.J., and Surtees, R.A. (1999). Upregulation of intercellular adhesion molecule-1 expression on human endothelial cells by tumour necrosis factor-alpha in an in vitro model of the blood-brain barrier. Brain research *830*, 330-336.

Driscoll, M.D., Sathya, G., Muyan, M., Klinge, C.M., Hilf, R., and Bambara, R.A. (1998). Sequence requirements for estrogen receptor binding to estrogen response elements. J Biol Chem *273*, 29321-29330.

Dufton, N., and Perretti, M. (2010). Therapeutic anti-inflammatory potential of formyl-peptide receptor agonists. Pharmacology & therapeutics *127*, 175-188.

Eberhard, D.A., Brown, M.D., and VandenBerg, S.R. (1994). Alterations of annexin expression in pathological neuronal and glial reactions. Immunohistochemical localization of annexins I, II (p36 and p11 subunits), IV, and VI in the human hippocampus. Am J Pathol *145*, 640-649.

Ebong, E.E., Macaluso, F.P., Spray, D.C., and Tarbell, J.M. (2011). Imaging the endothelial glycocalyx in vitro by rapid freezing/freeze substitution transmission electron microscopy. Arterioscler Thromb Vasc Biol *31*, 1908-1915.

Ek, M., Engblom, D., Saha, S., Blomqvist, A., Jakobsson, P.J., and Ericsson-Dahlstrand, A. (2001). Inflammatory response: pathway across the blood-brain barrier. Nature *410*, 430-431.

Elderfield, A.J., Newcombe, J., Bolton, C., and Flower, R.J. (1992b). Lipocortins (annexins) 1, 2, 4 and 5 are increased in the central nervous system in multiple sclerosis. Journal of neuroimmunology *39*, 91-100.

Engelhardt, B., and Coisne, C. (2011). Fluids and barriers of the CNS establish immune privilege by confining immune surveillance to a two-walled castle moat surrounding the CNS castle. Fluids and barriers of the CNS *8*, 4.

Engelhardt, B., and Sorokin, L. (2009). The blood-brain and the blood-cerebrospinal fluid barriers: function and dysfunction. Seminars in immunopathology *31*, 497-511.

Fanning, A.S., Jameson, B.J., Jesaitis, L.A., and Anderson, J.M. (1998). The tight junction protein ZO-1 establishes a link between the transmembrane protein occludin and the actin cytoskeleton. J Biol Chem *273*, 29745-29753.

Farkas, A., Szatmari, E., Orbok, A., Wilhelm, I., Wejksza, K., Nagyoszi, P., Hutamekalin, P., Bauer, H., Bauer, H.C., Traweger, A*., et al.* (2005). Hyperosmotic mannitol induces Src kinase-dependent phosphorylation of beta-catenin in cerebral endothelial cells. Journal of neuroscience research *80*, 855-861.

Farquhar, M.G., and Palade, G.E. (1963). Junctional complexes in various epithelia. The Journal of cell biology *17*, 375-412.

Farre, D., Roset, R., Huerta, M., Adsuara, J.E., Rosello, L., Alba, M.M., and Messeguer, X. (2003). Identification of patterns in biological sequences at the ALGGEN server: PROMO and MALGEN. Nucleic acids research *31*, 3651-3653.

Fatimathas, L., and Moss, S.E. (2010). Annexins as disease modifiers. Histology and histopathology *25*, 527-532.

Ferlazzo, V., D'Agostino, P., Milano, S., Caruso, R., Feo, S., Cillari, E., and Parente, L. (2003). Anti-inflammatory effects of annexin-1: stimulation of IL-10 release and inhibition of nitric oxide synthesis. International immunopharmacology *3*, 1363-1369.

Ferrari, C.C., and Tarelli, R. (2011). Parkinson's disease and systemic inflammation. Parkinson's disease *2011*, 436813.

Filippidis, A.S., Kalani, M.Y., and Rekate, H.L. (2011). Hydrocephalus and aquaporins: lessons learned from the bench. Child's nervous system : ChNS : official journal of the International Society for Pediatric Neurosurgery *27*, 27-33.

Firat-Karalar, E.N., and Welch, M.D. (2011). New mechanisms and functions of actin nucleation. Current opinion in cell biology *23*, 4-13.

Flower, R.J., and Blackwell, G.J. (1979). Anti-inflammatory steroids induce biosynthesis of a phospholipase A2 inhibitor which prevents prostaglandin generation. Nature *278*, 456-459.

Forster, C., Burek, M., Romero, I.A., Weksler, B., Couraud, P.O., and Drenckhahn, D. (2008). Differential effects of hydrocortisone and TNFalpha on tight junction proteins in an in vitro model of the human blood-brain barrier. The Journal of physiology *586*, 1937-1949.

Forster, C., Silwedel, C., Golenhofen, N., Burek, M., Kietz, S., Mankertz, J., and Drenckhahn, D. (2005). Occludin as direct target for glucocorticoid-induced improvement of blood-brain barrier properties in a murine in vitro system. The Journal of physiology *565*, 475-486.

Frank-Cannon, T.C., Alto, L.T., McAlpine, F.E., and Tansey, M.G. (2009). Does neuroinflammation fan the flame in neurodegenerative diseases? Molecular neurodegeneration *4*, 47.

Frank-Cannon, T.C., Tran, T., Ruhn, K.A., Martinez, T.N., Hong, J., Marvin, M., Hartley, M., Trevino, I., O'Brien, D.E., Casey, B*., et al.* (2008). Parkin deficiency increases vulnerability to inflammation-related nigral degeneration. The Journal of neuroscience : the official journal of the Society for Neuroscience *28*, 10825-10834.

Friese, M.A., Montalban, X., Willcox, N., Bell, J.I., Martin, R., and Fugger, L. (2006). The value of animal models for drug development in multiple sclerosis. Brain : a journal of neurology *129*, 1940-1952.

Frigerio, S., Gelati, M., Ciusani, E., Corsini, E., Dufour, A., Massa, G., and Salmaggi, A. (1998). Immunocompetence of human microvascular brain endothelial cells: cytokine regulation of IL-1beta, MCP-1, IL-10, sICAM-1 and sVCAM-1. Journal of neurology *245*, 727-730.

Fugger, L., Friese, M.A., and Bell, J.I. (2009). From Genes to Function: The Next Challenge to Understanding Multiple Sclerosis. Nature reviews Immunology *9*, 408-417.

Furuse, M., Hirase, T., Itoh, M., Nagafuchi, A., Yonemura, S., and Tsukita, S. (1993). Occludin: a novel integral membrane protein localizing at tight junctions. The Journal of cell biology *123*, 1777-1788.

Furuse, M., Itoh, M., Hirase, T., Nagafuchi, A., Yonemura, S., and Tsukita, S. (1994). Direct association of occludin with ZO-1 and its possible involvement in the localization of occludin at tight junctions. The Journal of cell biology *127*, 1617-1626.

Gage, F.H. (2003). Brain, repair yourself. Scientific American *289*, 46-53.

Galati, S., and Di Giovanni, G. (2010). Neuroprotection in Parkinson's disease: a realistic goal? CNS neuroscience & therapeutics *16*, 327-329.

Galea, E., Santizo, R., Feinstein, D.L., Adamsom, P., Greenwood, J., Koenig, H.M., and Pelligrino, D.A. (2002). Estrogen inhibits NF kappa B-dependent inflammation in brain endothelium without interfering with I kappa B degradation. Neuroreport *13*, 1469-1472.

Gao, H.M., and Hong, J.S. (2008). Why neurodegenerative diseases are progressive: uncontrolled inflammation drives disease progression. Trends in immunology *29*, 357-365.

Garden, G.A., and Moller, T. (2006). Microglia biology in health and disease. Journal of neuroimmune pharmacology : the official journal of the Society on NeuroImmune Pharmacology *1*, 127-137.

Gavard, J., and Gutkind, J.S. (2008). VE-cadherin and claudin-5: it takes two to tango. Nature cell biology *10*, 883-885.

Gavins, F.N., Dalli, J., Flower, R.J., Granger, D.N., and Perretti, M. (2007). Activation of the annexin 1 counter-regulatory circuit affords protection in the mouse brain microcirculation. FASEB J *21*, 1751-1758.

Ge, S., Song, L., and Pachter, J.S. (2005). Where is the blood-brain barrier ... really? Journal of neuroscience research *79*, 421-427.

Gerke, V., Creutz, C.E., and Moss, S.E. (2005). Annexins: linking Ca2+ signalling to membrane dynamics. Nature reviews Molecular cell biology *6*, 449-461.

Ghisletti, S., Meda, C., Maggi, A., and Vegeto, E. (2005). 17beta-estradiol inhibits inflammatory gene expression by controlling NF-kappaB intracellular localization. Molecular and cellular biology *25*, 2957-2968.

Ghitescu, L.D., Gugliucci, A., and Dumas, F. (2001). Actin and annexins I and II are among the main endothelial plasmalemma-associated proteins forming early glucose adducts in experimental diabetes. Diabetes *50*, 1666-1674.

Gillies, G.E., and McArthur, S. (2010a). Estrogen actions in the brain and the basis for differential action in men and women: a case for sex-specific medicines. Pharmacological reviews *62*, 155-198.

Gillies, G.E., and McArthur, S. (2010b). Independent influences of sex steroids of systemic and central origin in a rat model of Parkinson's disease: A contribution to sex-specific neuroprotection by estrogens. Hormones and behavior *57*, 23-34.

Gillies, G.E., Murray, H.E., Dexter, D., and McArthur, S. (2004). Sex dimorphisms in the neuroprotective effects of estrogen in an animal model of Parkinson's disease. Pharmacology, biochemistry, and behavior *78*, 513-522.

Ginhoux, F., Greter, M., Leboeuf, M., Nandi, S., See, P., Gokhan, S., Mehler, M.F., Conway, S.J., Ng, L.G., Stanley, E.R*., et al.* (2010). Fate mapping analysis reveals that adult microglia derive from primitive macrophages. Science *330*, 841-845.

Glass, C.K., Saijo, K., Winner, B., Marchetto, M.C., and Gage, F.H. (2010). Mechanisms underlying inflammation in neurodegeneration. Cell *140*, 918-934.

Glogauer, M., Hartwig, J., and Stossel, T. (2000). Two pathways through Cdc42 couple the N-formyl receptor to actin nucleation in permeabilized human neutrophils. The Journal of cell biology *150*, 785-796.

Godbout, J.P., Chen, J., Abraham, J., Richwine, A.F., Berg, B.M., Kelley, K.W., and Johnson, R.W. (2005). Exaggerated neuroinflammation and sickness behavior in aged mice following activation of the peripheral innate immune system. FASEB J *19*, 1329-1331.

Gomez-Lazaro, M., Galindo, M.F., Concannon, C.G., Segura, M.F., Fernandez-Gomez, F.J., Llecha, N., Comella, J.X., Prehn, J.H., and Jordan, J. (2008). 6-Hydroxydopamine activates the mitochondrial apoptosis pathway through p38 MAPK-mediated, p53-independent activation of Bax and PUMA. Journal of neurochemistry *104*, 1599-1612.

Gosselin, D., and Rivest, S. (2008). MyD88 signaling in brain endothelial cells is essential for the neuronal activity and glucocorticoid release during systemic inflammation. Molecular psychiatry *13*, 480-497.

Goulding, N.J., Godolphin, J.L., Sharland, P.R., Peers, S.H., Sampson, M., Maddison, P.J., and Flower, R.J. (1990). Anti-inflammatory lipocortin 1 production by peripheral blood leucocytes in response to hydrocortisone. Lancet *335*, 1416-1418.

Goulding, N.J., Pan, L., Wardwell, K., Guyre, V.C., and Guyre, P.M. (1996). Evidence for specific annexin I-binding proteins on human monocytes. Biochem J *316 (Pt 2)*, 593-597.

Goulding, N.J., Podgorski, M.R., Hall, N.D., Flower, R.J., Browning, J.L., Pepinsky, R.B., and Maddison, P.J. (1989). Autoantibodies to recombinant lipocortin-1 in rheumatoid arthritis and systemic lupus erythematosus. Annals of the rheumatic diseases *48*, 843-850.

Graesser, D., Solowiej, A., Bruckner, M., Osterweil, E., Juedes, A., Davis, S., Ruddle, N.H., Engelhardt, B., and Madri, J.A. (2002). Altered vascular permeability and early onset of experimental autoimmune encephalomyelitis in PECAM-1-deficient mice. The Journal of clinical investigation *109*, 383-392.

Grammas, P., Martinez, J., and Miller, B. (2011). Cerebral microvascular endothelium and the pathogenesis of neurodegenerative diseases. Expert reviews in molecular medicine *13*, e19.

Grant, G.A., Abbott, N.J., and Janigro, D. (1998). Understanding the Physiology of the Blood-Brain Barrier: In Vitro Models. News in physiological sciences : an international journal of physiology produced jointly by the International Union of Physiological Sciences and the American Physiological Society *13*, 287-293.

Green, L.C., Wagner, D.A., Glogowski, J., Skipper, P.L., Wishnok, J.S., and Tannenbaum, S.R. (1982). Analysis of nitrate, nitrite, and [15N]nitrate in biological fluids. Analytical biochemistry *126*, 131-138.

Greenwood, J., Luthert, P.J., Pratt, O.E., and Lantos, P.L. (1988). Hyperosmolar opening of the blood-brain barrier in the energy-depleted rat brain. Part 1. Permeability studies. Journal of cerebral blood flow and metabolism : official journal of the International Society of Cerebral Blood Flow and Metabolism *8*, 9-15.

Gruber, C.J., Gruber, D.M., Gruber, I.M., Wieser, F., and Huber, J.C. (2004). Anatomy of the estrogen response element. Trends Endocrinol Metab *15*, 73-78.

Guillemin, G.J., and Brew, B.J. (2004). Microglia, macrophages, perivascular macrophages, and pericytes: a review of function and identification. J Leukoc Biol *75*, 388-397.

Gurevich, M., Tuller, T., Rubinstein, U., Or-Bach, R., and Achiron, A. (2009). Prediction of acute multiple sclerosis relapses by transcription levels of peripheral blood cells. BMC medical genomics *2*, 46.

Haarmann, A., Deiss, A., Prochaska, J., Foerch, C., Weksler, B., Romero, I., Couraud, P.O., Stoll, G., Rieckmann, P., and Buttmann, M. (2010). Evaluation of soluble junctional adhesion molecule-A as a biomarker of human brain endothelial barrier breakdown. PloS one *5*, e13568.

Hall, A. (1998). Rho GTPases and the actin cytoskeleton. Science *279*, 509-514.

Hamberger, B., Hall, D., Yuen, M., Oddy, C., Keeling, C.I., Ritland, C., Ritland, K., and Bohlmann, J. (2009). Targeted isolation, sequence assembly and characterization of two white spruce (Picea glauca) BAC clones for terpenoid synthase and cytochrome P450 genes involved in conifer defence reveal insights into a conifer genome. BMC plant biology *9*, 106.

Hanisch, U.K., and Kettenmann, H. (2007). Microglia: active sensor and versatile effector cells in the normal and pathologic brain. Nature neuroscience *10*, 1387-1394.

Hannon, R., Croxtall, J.D., Getting, S.J., Roviezzo, F., Yona, S., Paul-Clark, M.J., Gavins, F.N., Perretti, M., Morris, J.F., Buckingham, J.C*., et al.* (2003). Aberrant inflammation and resistance to glucocorticoids in annexin 1-/- mouse. FASEB J *17*, 253-255.

Harrington, W.R., Sheng, S., Barnett, D.H., Petz, L.N., Katzenellenbogen, J.A., and Katzenellenbogen, B.S. (2003). Activities of estrogen receptor alpha- and beta-selective ligands at diverse estrogen responsive gene sites mediating transactivation or transrepression. Molecular and cellular endocrinology *206*, 13-22.

Hatherell, K., Couraud, P.O., Romero, I.A., Weksler, B., and Pilkington, G.J. (2011). Development of a three-dimensional, all-human in vitro model of the blood-brain barrier using mono-, co-, and tri-cultivation Transwell models. Journal of neuroscience methods *199*, 223-229.

Hayes, M.J., Rescher, U., Gerke, V., and Moss, S.E. (2004). Annexin-actin interactions. Traffic *5*, 571-576.

Hayhoe, R.P., Kamal, A.M., Solito, E., Flower, R.J., Cooper, D., and Perretti, M. (2006). Annexin 1 and its bioactive peptide inhibit neutrophil-endothelium interactions under flow: indication of distinct receptor involvement. Blood *107*, 2123-2130.

Hazell, G.G., Yao, S.T., Roper, J.A., Prossnitz, E.R., O'Carroll, A.M., and Lolait, S.J. (2009). Localisation of GPR30, a novel G protein-coupled oestrogen receptor, suggests multiple functions in rodent brain and peripheral tissues. The Journal of endocrinology *202*, 223-236.

Healy, D.P., and Wilk, S. (1993). Localization of immunoreactive glutamyl aminopeptidase in rat brain. II. Distribution and correlation with angiotensin II. Brain research *606*, 295-303.

Heller, R.A., and Kronke, M. (1994). Tumor necrosis factor receptor-mediated signaling pathways. The Journal of cell biology *126*, 5-9.

Hemmer, B., Cepok, S., Zhou, D., and Sommer, N. (2004). Multiple sclerosis -- a coordinated immune attack across the blood brain barrier. Current neurovascular research *1*, 141-150.

Herson, P.S., Koerner, I.P., and Hurn, P.D. (2009). Sex, sex steroids, and brain injury. Seminars in reproductive medicine *27*, 229-239.

Hindle, J.V. (2010). Ageing, neurodegeneration and Parkinson's disease. Age and ageing *39*, 156-161.

Hofmann, S., Grasberger, H., Jung, P., Bidlingmaier, M., Vlotides, J., Janssen, O.E., and Landgraf, R. (2002). The tumour necrosis factor-alpha induced vascular permeability is associated with a reduction of VE-cadherin expression. European journal of medical research *7*, 171-176.

Hoheisel, D., Nitz, T., Franke, H., Wegener, J., Hakvoort, A., Tilling, T., and Galla, H.J. (1998). Hydrocortisone reinforces the blood-brain barrier properties in a serum free cell culture system. Biochem Biophys Res Commun *244*, 312-316.

Holmes, C., and Butchart, J. (2011). Systemic inflammation and Alzheimer's disease. Biochem Soc Trans *39*, 898-901.

Howell, O.W., Reeves, C.A., Nicholas, R., Carassiti, D*., et al.* (2011). Meningeal Inflammation Is Widespread and Linked to Cortical Pathology in Multiple Sclerosis. Brain : a journal of neurology *134*, 2755-2771.

Huerta-Ocampo, I., Christian, H.C., Thompson, N.M., El-Kasti, M.M., and Wells, T. (2005). The Intermediate lactotroph: a morphologically distinct, ghrelin-responsive pituitary cell in the dwarf (dw/dw) rat. Endocrinology *146*, 5012-5023.

Hughes, E.L., Cover, P.O., Buckingham, J.C., and Gavins, F.N. (2012). Role and Interactions of Annexin A1 and Oestrogens in The Manifestation of Sexual Dimorphisms in Cerebral and Systemic Inflammation. Br J Pharmacol.

Huitinga, I., Bauer, J., Strijbos, P.J., Rothwell, N.J., Dijkstra, C.D., and Tilders, F.J. (1998). Effect of annexin-1 on experimental autoimmune encephalomyelitis (EAE) in the rat. Clinical and experimental immunology *111*, 198-204.

Iglesias, J.M., Morgan, R.O., Jenkins, N.A., Copeland, N.G., Gilbert, D.J., and Fernandez, M.P. (2002). Comparative genetics and evolution of annexin A13 as the founder gene of vertebrate annexins. Molecular biology and evolution *19*, 608-618.

Ikebuchi, N.W., and Waisman, D.M. (1990). Calcium-dependent regulation of actin filament bundling by lipocortin-85. J Biol Chem *265*, 3392-3400.

Ikemoto, S. (2007). Dopamine reward circuitry: two projection systems from the ventral midbrain to the nucleus accumbens-olfactory tubercle complex. Brain research reviews *56*, 27-78.

Janeway, C.A., Jr., and Medzhitov, R. (2002). Innate immune recognition. Annual review of immunology *20*, 197-216.

Jayachandran, M., Litwiller, R.D., Owen, W.G., and Miller, V.M. (2009). Circulating microparticles and endogenous estrogen in newly menopausal women. Climacteric : the journal of the International Menopause Society *12*, 177-184.

Jeon, B.S., Jackson-Lewis, V., and Burke, R.E. (1995). 6-Hydroxydopamine lesion of the rat substantia nigra: time course and morphology of cell death. Neurodegeneration *4*, 131-137.

Jeong, H.K., Jou, I., and Joe, E.H. (2010). Systemic LPS administration induces brain inflammation but not dopaminergic neuronal death in the substantia nigra. Experimental & molecular medicine *42*, 823-832.

Jin, R., Yang, G., and Li, G. (2010). Inflammatory mechanisms in ischemic stroke: role of inflammatory cells. J Leukoc Biol *87*, 779-789.

Johnson, T.E. (2006). Recent results: biomarkers of aging. Experimental gerontology *41*, 1243-1246.

Joice, S.L., Mydeen, F., Couraud, P.O., Weksler, B.B., Romero, I.A., Fraser, P.A., and Easton, A.S. (2009). Modulation of blood-brain barrier permeability by neutrophils: in vitro and in vivo studies. Brain research *1298*, 13-23.

Kalinowska-Lyszczarz, A., Szczucinski, A., Pawlak, M.A., and Losy, J. (2011). Clinical study on CXCL13, CCL17, CCL20 and IL-17 as immune cell migration navigators in relapsing-remitting multiple sclerosis patients. Journal of the neurological sciences *300*, 81-85.

Kang, H.S., Ahn, H.S., Kang, H.J., and Gye, M.C. (2006). Effect of estrogen on the expression of occludin in ovariectomized mouse brain. Neuroscience letters *402*, 30-34.

Kannarkat, G., Lasher, E.E., and Schiff, D. (2007). Neurologic complications of chemotherapy agents. Current opinion in neurology *20*, 719-725.

Kaufman, S. (1995). Tyrosine hydroxylase. Advances in enzymology and related areas of molecular biology *70*, 103-220.

Kim, W.G., Mohney, R.P., Wilson, B., Jeohn, G.H., Liu, B., and Hong, J.S. (2000). Regional difference in susceptibility to lipopolysaccharide-induced neurotoxicity in the rat brain: role of microglia. The Journal of neuroscience : the official journal of the Society for Neuroscience *20*, 6309-6316.

Knott, C., Stern, G., and Wilkin, G.P. (2000). Inflammatory regulators in Parkinson's disease: iNOS, lipocortin-1, and cyclooxygenases-1 and -2. Molecular and cellular neurosciences *16*, 724-739.

Komarova, Y., and Malik, A.B. (2010). Regulation of endothelial permeability via paracellular and transcellular transport pathways. Annual review of physiology *72*, 463-493.

Komori, M., Matsuyama, Y., Nirasawa, T., Thiele, H., Becker, M., Alexandrov, T., Saida, T., Tanaka, M., Matsuo, H., Tomimoto, H*., et al.* (2012). Proteomic pattern analysis discriminates among multiple sclerosis-related disorders. Annals of neurology *71*, 614-623.

Koyasu, S., and Moro, K. (2012). Role of Innate Lymphocytes in Infection and Inflammation. Frontiers in immunology *3*, 101.

Kraus, J., Voigt, K., Schuller, A.M., Scholz, M., Kim, K.S., Schilling, M., Schabitz, W.R., Oschmann, P., and Engelhardt, B. (2008). Interferon-beta stabilizes barrier characteristics of the blood-brain barrier in four different species in vitro. Mult Scler *14*, 843-852.

Krause, D.N., Duckles, S.P., and Pelligrino, D.A. (2006). Influence of sex steroid hormones on cerebrovascular function. J Appl Physiol *101*, 1252-1261.

Kuhn, J., Dina, O.A., Goswami, C., Suckow, V., Levine, J.D., and Hucho, T. (2008). GPR30 estrogen receptor agonists induce mechanical hyperalgesia in the rat. The European journal of neuroscience *27*, 1700-1709.

Kurebayashi, S., Miyashita, Y., Hirose, T., Kasayama, S., Akira, S., and Kishimoto, T. (1997). Characterization of mechanisms of interleukin-6 gene repression by estrogen receptor. The Journal of steroid biochemistry and molecular biology *60*, 11-17.

L'Episcopo, F., Tirolo, C., Testa, N., Caniglia, S., Morale, M.C., Impagnatiello, F., and Marchetti, B. (2011). Switching the microglial harmful phenotype promotes lifelong restoration of subtantia nigra dopaminergic neurons from inflammatory neurodegeneration in aged mice. Rejuvenation research *14*, 411-424.

La, M., D'Amico, M., Bandiera, S., Di Filippo, C., Oliani, S.M., Gavins, F.N., Flower, R.J., and Perretti, M. (2001). Annexin 1 peptides protect against experimental myocardial ischemia-reperfusion: analysis of their mechanism of action. FASEB J *15*, 2247-2256.

Laemmli, U.K. (1970). Cleavage of structural proteins during the assembly of the head of bacteriophage T4. Nature *227*, 680-685.

Lai, C.H., Kuo, K.H., and Leo, J.M. (2005). Critical role of actin in modulating BBB permeability. Brain research Brain research reviews *50*, 7-13.

Larochelle, C., Alvarez, J.I., and Prat, A. (2011). How do immune cells overcome the blood-brain barrier in multiple sclerosis? FEBS Lett *585*, 3770-3780.

Larson, R.S., and Springer, T.A. (1990). Structure and function of leukocyte integrins. Immunol Rev *114*, 181-217.

Le, Y., Murphy, P.M., and Wang, J.M. (2002). Formyl-peptide receptors revisited. Trends in immunology *23*, 541-548.

Lee, D.B., Jamgotchian, N., Allen, S.G., Kan, F.W., and Hale, I.L. (2004). Annexin A2 heterotetramer: role in tight junction assembly. American journal of physiology Renal physiology *287*, F481-491.

Lee, S.H., and Dominguez, R. (2010). Regulation of actin cytoskeleton dynamics in cells. Molecules and cells *29*, 311-325.

Lehner, C., Gehwolf, R., Tempfer, H., Krizbai, I., Hennig, B., Bauer, H.C., and Bauer, H. (2011). Oxidative stress and blood-brain barrier dysfunction under particular consideration of matrix metalloproteinases. Antioxidants & redox signaling *15*, 1305-1323.

Lequin, R.M. (2005). Enzyme immunoassay (EIA)/enzyme-linked immunosorbent assay (ELISA). Clinical chemistry *51*, 2415-2418.

Li, M., Zhang, Z., Sun, W., Koehler, R.C., and Huang, J. (2011). 17beta-estradiol attenuates breakdown of blood-brain barrier and hemorrhagic transformation induced by tissue plasminogen activator in cerebral ischemia. Neurobiology of disease *44*, 277-283.

Liebner, S., Corada, M., Bangsow, T., Babbage, J., Taddei, A., Czupalla, C.J., Reis, M., Felici, A., Wolburg, H., Fruttiger, M.*, et al.* (2008). Wnt/beta-catenin signaling controls development of the blood-brain barrier. The Journal of cell biology *183*, 409-417.

Lim, L.H., and Pervaiz, S. (2007). Annexin 1: the new face of an old molecule. FASEB J *21*, 968-975.

Lim, L.H., Solito, E., Russo-Marie, F., Flower, R.J., and Perretti, M. (1998). Promoting detachment of neutrophils adherent to murine postcapillary venules to control inflammation: effect of lipocortin 1. Proc Natl Acad Sci U S A *95*, 14535-14539.

Lin, L.F., Doherty, D.H., Lile, J.D., Bektesh, S., and Collins, F. (1993). GDNF: a glial cell line-derived neurotrophic factor for midbrain dopaminergic neurons. Science *260*, 1130-1132.

Lippmann, E.S., Azarin, S.M., Kay, J.E., Nessler, R.A., Wilson, H.K., Al-Ahmad, A., Palecek, S.P., and Shusta, E.V. (2012). Derivation of blood-brain barrier endothelial cells from human pluripotent stem cells. Nature biotechnology.

Liu, M., and Bing, G. (2011). Lipopolysaccharide animal models for Parkinson's disease. Parkinson's disease *2011*, 327089.

Liu, N.K., Zhang, Y.P., Han, S., Pei, J., Xu, L.Y., Lu, P.H., Shields, C.B., and Xu, X.M. (2007). Annexin A1 reduces inflammatory reaction and tissue damage through inhibition of phospholipase A2 activation in adult rats following spinal cord injury. Journal of neuropathology and experimental neurology *66*, 932-943.

Lok, J., Gupta, P., Guo, S., Kim, W.J., Whalen, M.J., van Leyen, K., and Lo, E.H. (2007). Cell-cell signaling in the neurovascular unit. Neurochemical research *32*, 2032-2045.

Lopez-Ramirez, M.A., Fischer, R., Torres-Badillo, C.C., Davies, H.A., Logan, K., Pfizenmaier, K., Male, D.K., Sharrack, B., and Romero, I.A. (2012). Role of Caspases in Cytokine-Induced Barrier Breakdown in Human Brain Endothelial Cells. J Immunol.

Lucas, S.M., Rothwell, N.J., and Gibson, R.M. (2006). The role of inflammation in CNS injury and disease. Br J Pharmacol *147 Suppl 1*, S232-240.

Lucin, K.M., and Wyss-Coray, T. (2009). Immune activation in brain aging and neurodegeneration: too much or too little? Neuron *64*, 110-122.

Lukiw, W.J., Cui, J.G., Marcheselli, V.L., Bodker, M., Botkjaer, A., Gotlinger, K., Serhan, C.N., and Bazan, N.G. (2005). A role for docosahexaenoic acid-derived neuroprotectin D1 in neural cell survival and Alzheimer disease. The Journal of clinical investigation *115*, 2774-2783.

Macdonald, J.A., Murugesan, N., and Pachter, J.S. (2010). Endothelial cell heterogeneity of blood-brain barrier gene expression along the cerebral microvasculature. Journal of neuroscience research *88*, 1457-1474.

Machado, A., Herrera, A.J., Venero, J.L., Santiago, M., De Pablos, R.M., Villaran, R.F., Espinosa-Oliva, A.M., Arguelles, S., Sarmiento, M., Delgado-Cortes, M.J*., et al.* (2011). Peripheral inflammation increases the damage in animal models of nigrostriatal dopaminergic neurodegeneration: possible implication in Parkinson's disease incidence. Parkinson's disease *2011*, 393769.

Maciver, S.K., and Hussey, P.J. (2002). The ADF/cofilin family: actin-remodeling proteins. Genome biology *3*, reviews3007.

Madara, J.L., Barenberg, D., and Carlson, S. (1986). Effects of cytochalasin D on occluding junctions of intestinal absorptive cells: further evidence that the cytoskeleton may influence paracellular permeability and junctional charge selectivity. The Journal of cell biology *102*, 2125-2136.

Madara, J.L., Moore, R., and Carlson, S. (1987). Alteration of intestinal tight junction structure and permeability by cytoskeletal contraction. The American journal of physiology *253*, C854-861.

Maderna, P., Cottell, D.C., Toivonen, T., Dufton, N., Dalli, J., Perretti, M., and Godson, C. (2010). FPR2/ALX receptor expression and internalization are critical for lipoxin A4 and annexin-derived peptide-stimulated phagocytosis. FASEB J *24*, 4240-4249.

Maggi, A., Ciana, P., Belcredito, S., and Vegeto, E. (2004). Estrogens in the nervous system: mechanisms and nonreproductive functions. Annual review of physiology *66*, 291-313.

Manaenko, A., Chen, H., Kammer, J., Zhang, J.H., and Tang, J. (2011). Comparison Evans Blue injection routes: Intravenous versus intraperitoneal, for measurement of blood-brain barrier in a mice hemorrhage model. Journal of neuroscience methods *195*, 206-210.

Marrie, R.A. (2004). Environmental Risk Factors in Multiple Sclerosis Aetiology. Lancet neurology *3*, 709-718.

McAllister, A.K., and van de Water, J. (2009). Breaking boundaries in neural-immune interactions. Neuron *64*, 9-12.

McArthur, S., Cristante, E., Paterno, M., Christian, H., Roncaroli, F., Gillies, G.E., and Solito, E. (2010). Annexin A1: a central player in the anti-inflammatory and neuroprotective role of microglia. J Immunol *185*, 6317-6328.

McArthur, S., Yazid, S., Christian, H., Sirha, R., Flower, R., Buckingham, J., and Solito, E. (2009). Annexin A1 regulates hormone exocytosis through a mechanism involving actin reorganization. FASEB J *23*, 4000-4010.

McColl, B.W., Rothwell, N.J., and Allan, S.M. (2008). Systemic inflammation alters the kinetics of cerebrovascular tight junction disruption after experimental stroke in mice. The Journal of neuroscience : the official journal of the Society for Neuroscience *28*, 9451-9462.

McGeer, P.L., and McGeer, E.G. (2004). Inflammation and neurodegeneration in Parkinson's disease. Parkinsonism & related disorders *10 Suppl 1*, S3-7.

McGeer, P.L., and McGeer, E.G. (2011). History of innate immunity in neurodegenerative disorders. Frontiers in pharmacology *2*, 77.

McKanna, J.A. (1993). Lipocortin 1 immunoreactivity identifies microglia in adult rat brain. Journal of neuroscience research *36*, 491-500.

McKenzie, J.A., and Ridley, A.J. (2007). Roles of Rho/ROCK and MLCK in TNF-alpha-induced changes in endothelial morphology and permeability. J Cell Physiol *213*, 221-228.

Mehta, D., and Malik, A.B. (2006). Signaling mechanisms regulating endothelial permeability. Physiological reviews *86*, 279-367.

Mena, M.A., and Garcia de Yebenes, J. (2008). Glial cells as players in parkinsonism: the "good," the "bad," and the "mysterious" glia. The Neuroscientist : a review journal bringing neurobiology, neurology and psychiatry *14*, 544-560.

Migeotte, I., Communi, D., and Parmentier, M. (2006). Formyl peptide receptors: a promiscuous subfamily of G protein-coupled receptors controlling immune responses. Cytokine & growth factor reviews *17*, 501-519.

Millan, J., Cain, R.J., Reglero-Real, N., Bigarella, C., Marcos-Ramiro, B., Fernandez-Martin, L., Correas, I., and Ridley, A.J. (2010). Adherens junctions connect stress fibres between adjacent endothelial cells. BMC biology *8*, 11.

Miller, F., Fenart, L., Landry, V., Coisne, C., Cecchelli, R., Dehouck, M.P., and Buee-Scherrer, V. (2005). The MAP kinase pathway mediates transcytosis induced by TNF-alpha in an in vitro blood-brain barrier model. The European journal of neuroscience *22*, 835-844.

Minagar, A., and Alexander, J.S. (2003). Blood-brain barrier disruption in multiple sclerosis. Mult Scler *9*, 540-549.

Minagar, A., Ostanin, D., Long, A.C., Jennings, M., Kelley, R.E., Sasaki, M., and Alexander, J.S. (2003). Serum from patients with multiple sclerosis downregulates occludin and VE-cadherin expression in cultured endothelial cells. Mult Scler *9*, 235-238.

Minghetti, L., Polazzi, E., Nicolini, A., Greco, A., and Levi, G. (1999). Possible role of microglial prostanoids and free radicals in neuroprotection and neurodegeneration. Advances in experimental medicine and biology *468*, 109-119.

Mitsumoto, Y., Watanabe, A., Mori, A., and Koga, N. (1998). Spontaneous regeneration of nigrostriatal dopaminergic neurons in MPTP-treated C57BL/6 mice. Biochem Biophys Res Commun *248*, 660-663.

Mizutani, M., Pino, P.A., Saederup, N., Charo, I.F., Ransohoff, R.M., and Cardona, A.E. (2012). The fractalkine receptor but not CCR2 is present on microglia from embryonic development throughout adulthood. J Immunol *188*, 29-36.

Mogi, M., Harada, M., Kondo, T., Riederer, P., Inagaki, H., Minami, M., and Nagatsu, T. (1994). Interleukin-1 beta, interleukin-6, epidermal growth factor and transforming growth factor-alpha are elevated in the brain from parkinsonian patients. Neuroscience letters *180*, 147-150.

Mogi, M., Togari, A., Tanaka, K., Ogawa, N., Ichinose, H., and Nagatsu, T. (1999). Increase in level of tumor necrosis factor (TNF)-alpha in 6-hydroxydopamine-lesioned striatum in rats without influence of systemic L-DOPA on the TNF-alpha induction. Neuroscience letters *268*, 101-104.

Morel, E., Parton, R.G., and Gruenberg, J. (2009). Annexin A2-dependent polymerization of actin mediates endosome biogenesis. Developmental cell *16*, 445-457.

Morgan, J.T., Chana, G., Pardo, C.A., Achim, C., Semendeferi, K., Buckwalter, J., Courchesne, E., and Everall, I.P. (2010). Microglial activation and increased microglial density observed in the dorsolateral prefrontal cortex in autism. Biological psychiatry *68*, 368-376.

Morrey, J.D., Olsen, A.L., Siddharthan, V., Motter, N.E., Wang, H., Taro, B.S., Chen, D., Ruffner, D., and Hall, J.O. (2008). Increased blood-brain barrier permeability is not a primary determinant for lethality of West Nile virus infection in rodents. The Journal of general virology *89*, 467-473.

Mou, H., Li, Z., Kong, Y., Deng, B., Qian, L., Wang, J.M., and Le, Y. (2012). Proinflammatory stimulants promote the expression of a promiscuous G protein-coupled receptor, mFPR2, in microvascular endothelial cells. Inflammation *35*, 656-664.

Muller, M., Frese, A., Nassenstein, I., Hoppen, M., Marziniak, M., Ringelstein, E.B., Kim, K.S., Schabitz, W.R., and Kraus, J. (2012). Serum from interferon-beta-1b-treated patients with early multiple sclerosis stabilizes the blood-brain barrier in vitro. Mult Scler *18*, 236-239.

Murakami, T., Felinski, E.A., and Antonetti, D.A. (2009). Occludin phosphorylation and ubiquitination regulate tight junction trafficking and vascular endothelial growth factor-induced permeability. J Biol Chem *284*, 21036-21046.

Murray, C.L., Skelly, D.T., and Cunningham, C. (2011). Exacerbation of CNS inflammation and neurodegeneration by systemic LPS treatment is independent of circulating IL-1beta and IL-6. Journal of neuroinflammation *8*, 50.

Murray, H.E., Pillai, A.V., McArthur, S.R., Razvi, N., Datla, K.P., Dexter, D.T., and Gillies, G.E. (2003). Dose- and sex-dependent effects of the neurotoxin 6-hydroxydopamine on the nigrostriatal dopaminergic pathway of adult rats: differential actions of estrogen in males and females. Neuroscience *116*, 213-222.

Nadeau, S., and Rivest, S. (1999). Effects of circulating tumor necrosis factor on the neuronal activity and expression of the genes encoding the tumor necrosis factor receptors (p55 and p75) in the rat brain: a view from the blood-brain barrier. Neuroscience *93*, 1449-1464.

Naik, P., and Cucullo, L. (2012). In Vitro Blood-Brain Barrier Models: Current and Perspective Technologies. Journal of pharmaceutical sciences *101*, 1337-1354

Nadkarni, S., Cooper, D., Brancaleone, V., Bena, S., and Perretti, M. (2011). Activation of the annexin A1 pathway underlies the protective effects exerted by estrogen in polymorphonuclear leukocytes. Arterioscler Thromb Vasc Biol *31*, 2749-2759.

Nag, S., Kapadia, A., and Stewart, D.J. (2011). Review: molecular pathogenesis of blood-brain barrier breakdown in acute brain injury. Neuropathology and applied neurobiology *37*, 3-23.

Nagatsu, T., and Sawada, M. (2006). Cellular and molecular mechanisms of Parkinson's disease: neurotoxins, causative genes, and inflammatory cytokines. Cellular and molecular neurobiology *26*, 781-802.

Nagyoszi, P., Wilhelm, I., Farkas, A.E., Fazakas, C., Dung, N.T., Hasko, J., and Krizbai, I.A. (2010). Expression and regulation of toll-like receptors in cerebral endothelial cells. Neurochemistry international *57*, 556-564.

Nasdala, I., Wolburg-Buchholz, K., Wolburg, H., Kuhn, A., Ebnet, K., Brachtendorf, G., Samulowitz, U., Kuster, B., Engelhardt, B., Vestweber, D*., et al.* (2002). A transmembrane tight junction protein selectively expressed on endothelial cells and platelets. J Biol Chem *277*, 16294-16303.

Neuhaus, W., Germann, B., Plattner, V.E., Gabor, F., Wirth, M., and Noe, C.R. (2009). Alteration of the glycocalyx of two blood-brain barrier mimicking cell lines is inducible by glioma conditioned media. Brain research *1279*, 82-89.

Neuwelt, E.A., Bauer, B., Fahlke, C., Fricker, G., Iadecola, C., Janigro, D., Leybaert, L., Molnar, Z., O'Donnell, M.E., Povlishock, J.T*., et al.* (2011). Engaging neuroscience to advance translational research in brain barrier biology. Nature reviews Neuroscience *12*, 169-182.

Nilsson, B.O. (2007). Modulation of the inflammatory response by estrogens with focus on the endothelium and its interactions with leukocytes. Inflamm Res *56*, 269-273.

Nimmerjahn, A., Kirchhoff, F., and Helmchen, F. (2005). Resting microglial cells are highly dynamic surveillants of brain parenchyma in vivo. Science *308*, 1314-1318.

Norling, L.V., Dalli, J., Flower, R.J., Serhan, C.N., and Perretti, M. (2012). Resolvin D1 Limits Polymorphonuclear Leukocytes Recruitment to Inflammatory Loci: Receptor-Dependent Actions. Arterioscler Thromb Vasc Biol.

Norling, L.V., and Serhan, C.N. (2010). Profiling in resolving inflammatory exudates identifies novel anti-inflammatory and pro-resolving mediators and signals for termination. Journal of internal medicine *268*, 15-24.

Okuda, K., Sakumoto, R., Uenoyama, Y., Berisha, B., Miyamoto, A., and Schams, D. (1999). Tumor necrosis factor alpha receptors in microvascular endothelial cells from bovine corpus luteum. Biology of reproduction *61*, 1017-1022.

Omer, S., Meredith, D., Morris, J.F., and Christian, H.C. (2006). Evidence for the role of adenosine 5'-triphosphate-binding cassette (ABC)-A1 in the externalization of annexin 1 from pituitary folliculostellate cells and ABCA1-transfected cell models. Endocrinology *147*, 3219-3227.

Opal, S.M., and DePalo, V.A. (2000). Anti-inflammatory cytokines. Chest *117*, 1162-1172.

Pais, T.F., Figueiredo, C., Peixoto, R., Braz, M.H., and Chatterjee, S. (2008). Necrotic neurons enhance microglial neurotoxicity through induction of glutaminase by a MyD88-dependent pathway. Journal of neuroinflammation *5*, 43.

Pan, W., Banks, W.A., Kennedy, M.K., Gutierrez, E.G., and Kastin, A.J. (1996). Differential permeability of the BBB in acute EAE: enhanced transport of TNT-alpha. The American journal of physiology *271*, E636-642.

Pan, W., and Kastin, A.J. (2002). TNFalpha transport across the blood-brain barrier is abolished in receptor knockout mice. Experimental neurology *174*, 193-200.

Papadopoulos, M.C., Saadoun, S., Binder, D.K., Manley, G.T., Krishna, S., and Verkman, A.S. (2004). Molecular mechanisms of brain tumor edema. Neuroscience *129*, 1011-1020.

Patabendige, A., Skinner, R.A., and Abbott, N.J. (2012). Establishment of a Simplified in Vitro Porcine Blood-Brain Barrier Model with High Transendothelial Electrical Resistance. Brain research.

Pardridge, W.M., Eisenberg, J., and Cefalu, W.T. (1985). Absence of albumin receptor on brain capillaries in vivo or in vitro. The American journal of physiology *249*, E264-267.

Parente, L., and Solito, E. (2004). Annexin 1: more than an anti-phospholipase protein. Inflamm Res *53*, 125-132.

Parkening, T.A., Lau, I.F., Saksena, S.K., and Chang, M.C. (1978). Circulating plasma levels of pregnenolone, progesterone, estrogen, luteinizing hormone, and follicle stimulating hormone in young and aged C57BL/6 mice during various stages of pregnancy. Journal of gerontology *33*, 191-196.

Paschalidis, N., Iqbal, A.J., Maione, F., Wood, E.G., Perretti, M., Flower, R.J., and D'Acquisto, F. (2009). Modulation of experimental autoimmune encephalomyelitis by endogenous annexin A1. Journal of neuroinflammation *6*, 33.

Patabendige, A., Skinner, R.A., and Abbott, N.J. (2012). Establishment of a simplified in vitro porcine blood-brain barrier model with high transendothelial electrical resistance. Brain research.

Patel, D.M., Ahmad, S.F., Weiss, D.G., Gerke, V., and Kuznetsov, S.A. (2011). Annexin A1 is a new functional linker between actin filaments and phagosomes during phagocytosis. Journal of cell science *124*, 578-588.

Patte, C., and Blanquet, P.R. (1992a). Fibroblast growth factor-stimulated phosphorylation of a lipocortin I-like protein is S-phase cell cycle specific in human vascular endothelial cells. Growth Factors *7*, 107-116.

Patte, C., and Blanquet, P.R. (1992b). [Response of human vascular endothelium to angiogenic fibroblast growth factor: role of 2 lipocortins/annexins]. Bulletin du cancer *79*, 1031-1044.

Pelegri, C., Canudas, A.M., del Valle, J., Casadesus, G., Smith, M.A., Camins, A., Pallas, M., and Vilaplana, J. (2007). Increased permeability of blood-brain barrier on the hippocampus of a murine model of senescence. Mechanisms of ageing and development *128*, 522-528.

Pepinsky, R.B., Sinclair, L.K., Dougas, I., Liang, C.M., Lawton, P., and Browning, J.L. (1990). Monoclonal antibodies to lipocortin-1 as probes for biological function. FEBS Lett *261*, 247-252.

Perea, G., Navarrete, M., and Araque, A. (2009). Tripartite Synapses: Astrocytes Process and Control Synaptic Information. Trends in neurosciences *32*, 421-431.

Perretti, M. (2003). The annexin 1 receptor(s): is the plot unravelling? Trends Pharmacol Sci *24*, 574-579.

Perretti, M., Ahluwalia, A., Harris, J.G., Goulding, N.J., and Flower, R.J. (1993). Lipocortin-1 fragments inhibit neutrophil accumulation and neutrophil-dependent edema in the mouse. A qualitative comparison with an anti-CD11b monoclonal antibody. J Immunol *151*, 4306-4314.

Perretti, M., Chiang, N., La, M., Fierro, I.M., Marullo, S., Getting, S.J., Solito, E., and Serhan, C.N. (2002a). Endogenous lipid- and peptide-derived anti-inflammatory pathways generated with glucocorticoid and aspirin treatment activate the lipoxin A4 receptor. Nat Med *8*, 1296-1302.

Perretti, M., and D'Acquisto, F. (2009). Annexin A1 and glucocorticoids as effectors of the resolution of inflammation. Nature reviews Immunology *9*, 62-70.

Perretti, M., and Dalli, J. (2009). Exploiting the Annexin A1 pathway for the development of novel anti-inflammatory therapeutics. Br J Pharmacol *158*, 936-946.

Perretti, M., Ingegnoli, F., Wheller, S.K., Blades, M.C., Solito, E., and Pitzalis, C. (2002b). Annexin 1 modulates monocyte-endothelial cell interaction in vitro and cell migration in vivo in the human SCID mouse transplantation model. J Immunol *169*, 2085-2092.

Perretti, M., and Solito, E. (2004). Annexin 1 and neutrophil apoptosis. Biochem Soc Trans *32*, 507-510.

Perry, V.H. (2004). The influence of systemic inflammation on inflammation in the brain: implications for chronic neurodegenerative disease. Brain, behavior, and immunity *18*, 407-413.

Perry, V.H. (2010). Contribution of systemic inflammation to chronic neurodegeneration. Acta neuropathologica *120*, 277-286.

Perry, V.H., Cunningham, C., and Holmes, C. (2007). Systemic infections and inflammation affect chronic neurodegeneration. Nature reviews Immunology *7*, 161-167.

Perry, V.H., Nicoll, J.A., and Holmes, C. (2010). Microglia in neurodegenerative disease. Nature reviews Neurology *6*, 193-201.

Persidsky, Y., Heilman, D., Haorah, J., Zelivyanskaya, M., Persidsky, R., Weber, G.A., Shimokawa, H., Kaibuchi, K., and Ikezu, T. (2006). Rho-mediated regulation of tight junctions during monocyte migration across the blood-brain barrier in HIV-1 encephalitis (HIVE). Blood *107*, 4770-4780.

Pfaffl, M.W. (2001). A new mathematical model for relative quantification in real-time RT-PCR. Nucleic acids research *29*, e45.

Philip, J.G., Flower, R.J., and Buckingham, J.C. (1998). Blockade of the classical pathway of protein secretion does not affect the cellular exportation of lipocortin 1. Regulatory peptides *73*, 133-139.

Plateel, M., Teissier, E., and Cecchelli, R. (1997). Hypoxia dramatically increases the nonspecific transport of blood-borne proteins to the brain. Journal of neurochemistry *68*, 874-877.

Plumb, J., McQuaid, S., Mirakhur, M., and Kirk, J. (2002). Abnormal endothelial tight junctions in active lesions and normal-appearing white matter in multiple sclerosis. Brain Pathol *12*, 154-169.

Podgorski, M.R., Goulding, N.J., Hall, N.D., Flower, R.J., and Maddison, P.J. (1992). Autoantibodies to lipocortin-1 are associated with impaired glucocorticoid responsiveness in rheumatoid arthritis. The Journal of rheumatology *19*, 1668-1671.

Pott Godoy, M.C., Tarelli, R., Ferrari, C.C., Sarchi, M.I., and Pitossi, F.J. (2008). Central and systemic IL-1 exacerbates neurodegeneration and motor symptoms in a model of Parkinson's disease. Brain : a journal of neurology *131*, 1880-1894.

Prasain, N., and Stevens, T. (2009). The actin cytoskeleton in endothelial cell phenotypes. Microvasc Res *77*, 53-63.

Probst-Cousin, S., Kowolik, D., Kuchelmeister, K., Kayser, C., Neundorfer, B., and Heuss, D. (2002). Expression of annexin-1 in multiple sclerosis plaques. Neuropathology and applied neurobiology *28*, 292-300.

Proia, P., Schiera, G., Salemi, G., Ragonese, P., Savettieri, G., and Di Liegro, I. (2009). Neuronal and BBB damage induced by sera from patients with secondary progressive multiple sclerosis. International journal of molecular medicine *24*, 743-747.

Prossnitz, E.R., Arterburn, J.B., and Sklar, L.A. (2007). GPR30: A G protein-coupled receptor for estrogen. Molecular and cellular endocrinology *265-266*, 138-142.

Puntener, U., Booth, S.G., Perry, V.H., and Teeling, J.L. (2012). Long-term impact of systemic bacterial infection on the cerebral vasculature and microglia. Journal of neuroinflammation *9*, 146.

Qin, L., Wu, X., Block, M.L., Liu, Y., Breese, G.R., Hong, J.S., Knapp, D.J., and Crews, F.T. (2007). Systemic LPS causes chronic neuroinflammation and progressive neurodegeneration. Glia *55*, 453-462.

Rakesh, S. (2007). Nitric oxide in neurodegeneration. Annals of Neurosciences *14*.

Ransohoff, R.M., and Brown, M.A. (2012). Innate immunity in the central nervous system. The Journal of clinical investigation *122*, 1164-1171.

Ransohoff, R.M., and Perry, V.H. (2009). Microglial physiology: unique stimuli, specialized responses. Annual review of immunology *27*, 119-145.

Reale, M., Iarlori, C., Thomas, A., Gambi, D., Perfetti, B., Di Nicola, M., and Onofrj, M. (2009). Peripheral cytokines profile in Parkinson's disease. Brain, behavior, and immunity *23*, 55-63.

Relton, J.K., Strijbos, P.J., O'Shaughnessy, C.T., Carey, F., Forder, R.A., Tilders, F.J., and Rothwell, N.J. (1991). Lipocortin-1 is an endogenous inhibitor of ischemic damage in the rat brain. The Journal of experimental medicine *174*, 305-310.

Rescher, U., Danielczyk, A., Markoff, A., and Gerke, V. (2002). Functional activation of the formyl peptide receptor by a new endogenous ligand in human lung A549 cells. J Immunol *169*, 1500-1504.

Rescher, U., and Gerke, V. (2004). Annexins--unique membrane binding proteins with diverse functions. Journal of cell science *117*, 2631-2639.

Ridley, A.J. (1999). Rho family proteins and regulation of the actin cytoskeleton. Progress in molecular and subcellular biology *22*, 1-22.

Rivest, S. (2009). Regulation of innate immune responses in the brain. Nature reviews Immunology *9*, 429-439.

Romero, I.A., Radewicz, K., Jubin, E., Michel, C.C., Greenwood, J., Couraud, P.O., and Adamson, P. (2003). Changes in cytoskeletal and tight junctional proteins correlate with decreased permeability induced by dexamethasone in cultured rat brain endothelial cells. Neuroscience letters *344*, 112-116.

Rosengarth, A., and Luecke, H. (2003). A calcium-driven conformational switch of the N-terminal and core domains of annexin A1. Journal of molecular biology *326*, 1317-1325.

Rothwell, N.J., and Relton, J.K. (1993). Involvement of interleukin-1 and lipocortin-1 in ischaemic brain damage. Cerebrovascular and brain metabolism reviews *5*, 178-198.

Roviezzo, F., Getting, S.J., Paul-Clark, M.J., Yona, S., Gavins, F.N., Perretti, M., Hannon, R., Croxtall, J.D., Buckingham, J.C., and Flower, R.J. (2002). The annexin-1 knockout mouse: what it tells us about the inflammatory response. Journal of physiology and pharmacology : an official journal of the Polish Physiological Society *53*, 541-553.

Saijo, K., Winner, B., Carson, C.T., Collier, J.G., Boyer, L., Rosenfeld, M.G., Gage, F.H., and Glass, C.K. (2009). A Nurr1/CoREST pathway in microglia and astrocytes protects dopaminergic neurons from inflammation-induced death. Cell *137*, 47-59.

Sakakibara, A., Furuse, M., Saitou, M., Ando-Akatsuka, Y., and Tsukita, S. (1997). Possible involvement of phosphorylation of occludin in tight junction formation. The Journal of cell biology *137*, 1393-1401.

Sambrook, J.F., E F; Maniatis,Tom (1989). Molecular cloning : a laboratory manual.

Sandoval, K.E., and Witt, K.A. (2011). Age and 17beta-estradiol effects on blood-brain barrier tight junction and estrogen receptor proteins in ovariectomized rats. Microvasc Res *81*, 198-205.

Sato, T., Haimovici, R., Kao, R., Li, A.F., and Roy, S. (2002). Downregulation of connexin 43 expression by high glucose reduces gap junction activity in microvascular endothelial cells. Diabetes *51*, 1565-1571.

Sawada, M., Sawada, H., and Nagatsu, T. (2008). Effects of aging on neuroprotective and neurotoxic properties of microglia in neurodegenerative diseases. Neuro-degenerative diseases *5*, 254-256.

Schapira, A.H., and Jenner, P. (2011). Etiology and pathogenesis of Parkinson's disease. Movement disorders : official journal of the Movement Disorder Society *26*, 1049-1055.

Schiffenbauer, J., Johnson, H.M., Butfiloski, E.J., Wegrzyn, L., and Soos, J.M. (1993). Staphylococcal enterotoxins can reactivate experimental allergic encephalomyelitis. Proc Natl Acad Sci U S A *90*, 8543-8546.

Schlaepfer, D.D., and Haigler, H.T. (1987). Characterization of Ca2+-dependent phospholipid binding and phosphorylation of lipocortin I. J Biol Chem *262*, 6931-6937.

Schwarting, R.K., and Huston, J.P. (1996). The unilateral 6-hydroxydopamine lesion model in behavioral brain research. Analysis of functional deficits, recovery and treatments. Progress in neurobiology *50*, 275-331.

Seebach, J., Donnert, G., Kronstein, R., Werth, S., Wojciak-Stothard, B., Falzarano, D., Mrowietz, C., Hell, S.W., and Schnittler, H.J. (2007). Regulation of endothelial barrier function during flow-induced conversion to an arterial phenotype. Cardiovascular research *75*, 596-607.

Serhan, C.N. (2007). Resolution phase of inflammation: novel endogenous anti-inflammatory and proresolving lipid mediators and pathways. Annual review of immunology *25*, 101-137.

Serhan, C.N., Brain, S.D., Buckley, C.D., Gilroy, D.W., Haslett, C., O'Neill, L.A., Perretti, M., Rossi, A.G., and Wallace, J.L. (2007). Resolution of inflammation: state of the art, definitions and terms. FASEB J *21*, 325-332.

Serrats, J., Schiltz, J.C., Garcia-Bueno, B., van Rooijen, N., Reyes, T.M., and Sawchenko, P.E. (2010). Dual roles for perivascular macrophages in immune-to-brain signaling. Neuron *65*, 94-106.

Silwedel, C., and Forster, C. (2006). Differential susceptibility of cerebral and cerebellar murine brain microvascular endothelial cells to loss of barrier properties in response to inflammatory stimuli. Journal of neuroimmunology *179*, 37-45.

Simka, M. (2009). Blood brain barrier compromise with endothelial inflammation may lead to autoimmune loss of myelin during multiple sclerosis. Current neurovascular research *6*, 132-139.

Simoes, R.L., and Fierro, I.M. (2005). Involvement of the Rho-kinase/myosin light chain kinase pathway on human monocyte chemotaxis induced by ATL-1, an aspirin-triggered lipoxin A4 synthetic analog. J Immunol *175*, 1843-1850.

Simola, N., Morelli, M., and Carta, A.R. (2007). The 6-hydroxydopamine model of Parkinson's disease. Neurotoxicity research *11*, 151-167.

Simpson, J.E., Wharton, S.B., Cooper, J., Gelsthorpe, C., Baxter, L., Forster, G., Shaw, P.J., Savva, G., Matthews, F.E., Brayne, C*., et al.* (2010). Alterations of the blood-brain barrier in cerebral white matter lesions in the ageing brain. Neuroscience letters *486*, 246-251.

Singh, A.K., and Jiang, Y. (2004). How does peripheral lipopolysaccharide induce gene expression in the brain of rats? Toxicology *201*, 197-207.

Skrahina, T., Piljic, A., and Schultz, C. (2008). Heterogeneity and timing of translocation and membrane-mediated assembly of different annexins. Exp Cell Res *314*, 1039-1047.

Smith, S.F., Tetley, T.D., Datta, A.K., Smith, T., Guz, A., and Flower, R.J. (1995). Lipocortin-1 distribution in bronchoalveolar lavage from healthy human lung: effect of prednisolone. J Appl Physiol *79*, 121-128.

Sohrabji, F., and Bake, S. (2006). Age-related changes in neuroprotection: is estrogen pro-inflammatory for the reproductive senescent brain? Endocrine *29*, 191-197.

Solito, E., Christian, H.C., Festa, M., Mulla, A., Tierney, T., Flower, R.J., and Buckingham, J.C. (2006). Post-translational modification plays an essential role in the translocation of annexin A1 from the cytoplasm to the cell surface. FASEB J *20*, 1498-1500.

Solito, E., de Coupade, C., Canaider, S., Goulding, N.J., and Perretti, M. (2001). Transfection of annexin 1 in monocytic cells produces a high degree of spontaneous and stimulated apoptosis associated with caspase-3 activation. Br J Pharmacol *133*, 217-228.

Solito, E., de Coupade, C., Parente, L., Flower, R.J., and Russo-Marie, F. (1998a). Human annexin 1 is highly expressed during the differentiation of the epithelial cell line A 549: involvement of nuclear factor interleukin 6 in phorbol ester induction of annexin 1. Cell Growth Differ *9*, 327-336.

Solito, E., Froud, K., Christian, H., Morris, J., and Buckingham, J. (2003a). Opposite effects of dexamethasone and oestardiol on annexin 1 expression. Endocrine Abstracts *Endocrine Abstracts*, 65.

Solito, E., McArthur, S., Christian, H., Gavins, F., Buckingham, J.C., and Gillies, G.E. (2008). Annexin A1 in the brain--undiscovered roles? Trends Pharmacol Sci *29*, 135-142.

Solito, E., Mulla, A., Morris, J.F., Christian, H.C., Flower, R.J., and Buckingham, J.C. (2003b). Dexamethasone induces rapid serine-phosphorylation and membrane translocation of annexin 1 in a human folliculostellate cell line via a novel nongenomic mechanism involving the glucocorticoid receptor, protein kinase C, phosphatidylinositol 3-kinase, and mitogen-activated protein kinase. Endocrinology *144*, 1164-1174.

Solito, E., Nuti, S., and Parente, L. (1994). Dexamethasone-induced translocation of lipocortin (annexin) 1 to the cell membrane of U-937 cells. Br J Pharmacol *112*, 347-348.

Solito, E., Raguenes-Nicol, C., de Coupade, C., Bisagni-Faure, A., and Russo-Marie, F. (1998b). U937 cells deprived of endogenous annexin 1 demonstrate an increased PLA2 activity. Br J Pharmacol *124*, 1675-1683.

Solito, E., Romero, I.A., Marullo, S., Russo-Marie, F., and Weksler, B.B. (2000). Annexin 1 binds to U937 monocytic cells and inhibits their adhesion to microvascular endothelium: involvement of the alpha 4 beta 1 integrin. J Immunol *165*, 1573-1581.

Sospedra, M., and Martin, R. (2005). Antigen-Specific Therapies in Multiple Sclerosis. International reviews of immunology *24*, 393-413.

Steiner, O., Coisne, C., Engelhardt, B., and Lyck, R. (2011). Comparison of immortalized bEnd5 and primary mouse brain microvascular endothelial cells as in vitro blood-brain barrier models for the study of T cell extravasation. Journal of cerebral blood flow and metabolism : official journal of the International Society of Cerebral Blood Flow and Metabolism *31*, 315-327.

Stevens, T.R., Smith, S.F., and Rampton, D.S. (1993). Antibodies to human recombinant lipocortin-I in inflammatory bowel disease. Clin Sci (Lond) *84*, 381-386.

Stevenson, B.R., and Keon, B.H. (1998). The tight junction: morphology to molecules. Annual review of cell and developmental biology *14*, 89-109.

Stolp, H.B., and Dziegielewska, K.M. (2009). Review: Role of developmental inflammation and blood-brain barrier dysfunction in neurodevelopmental and neurodegenerative diseases. Neuropathology and applied neurobiology *35*, 132-146.

Strazielle, N., and Ghersi-Egea, J.F. (2005). Factors affecting delivery of antiviral drugs to the brain. Reviews in medical virology *15*, 105-133.

Strijbos, P.J., Horan, M.A., Carey, F., and Rothwell, N.J. (1993). Impaired febrile responses of aging mice are mediated by endogenous lipocortin-1 (annexin-1). The American journal of physiology *265*, E289-297.

Strijbos, P.J., Tilders, F.J., Carey, F., Forder, R., and Rothwell, N.J. (1991). Localization of immunoreactive lipocortin-1 in the brain and pituitary gland of the rat. Effects of adrenalectomy, dexamethasone and colchicine treatment. Brain research *553*, 249-260.

Sumanasekera, W.K., Sumanasekera, G.U., Mattingly, K.A., Dougherty, S.M., Keynton, R.S., and Klinge, C.M. (2007). Estradiol and dihydrotestosterone regulate endothelial cell barrier function after hypergravity-induced alterations in MAPK activity. American journal of physiology Cell physiology *293*, C566-573.

Taddei, A., Giampietro, C., Conti, A., Orsenigo, F., Breviario, F., Pirazzoli, V., Potente, M., Daly, C., Dimmeler, S., and Dejana, E. (2008). Endothelial adherens junctions control tight junctions by VE-cadherin-mediated upregulation of claudin-5. Nature cell biology *10*, 923-934.

Tansey, M.G., McCoy, M.K., and Frank-Cannon, T.C. (2007). Neuroinflammatory mechanisms in Parkinson's disease: potential environmental triggers, pathways, and targets for early therapeutic intervention. Experimental neurology *208*, 1-25.

Teunissen, C.E., Koel-Simmelink, M.J., Pham, T.V., Knol, J.C., Khalil, M., Trentini, A., Killestein, J., Nielsen, J., Vrenken, H., Popescu, V.*, et al.* (2011). Identification of biomarkers for diagnosis and progression of MS by MALDI-TOF mass spectrometry. Mult Scler *17*, 838-850.

Thomas, W.E. (1999). Brain macrophages: on the role of pericytes and perivascular cells. Brain research Brain research reviews *31*, 42-57.

Thymiakou, E., and Episkopou, V. (2011). Detection of signaling effector-complexes downstream of bmp4 using PLA, a proximity ligation assay. Journal of visualized experiments : JoVE.

Toornvliet, R., van Berckel, B.N., Luurtsema, G., Lubberink, M.*, et al.* (2006). Effect of Age on Functional P-Glycoprotein in the Blood-Brain Barrier Measured by Use of (R)-[(11)C]Verapamil and Positron Emission Tomography. Clinical pharmacology and therapeutics *79*, 540-548.

Tsukita, S., Furuse, M., and Itoh, M. (2001). Multifunctional strands in tight junctions. Nature reviews Molecular cell biology *2*, 285-293.

Tubridy, N., Behan, P.O., Capildeo, R., Chaudhuri, A., Forbes, R., Hawkins, C.P., Hughes, R.A., Palace, J., Sharrack, B., Swingler, R.*, et al.* (1999). The effect of anti-alpha4 integrin antibody on brain lesion activity in MS. The UK Antegren Study Group. Neurology *53*, 466-472.

van Engeland, M., Nieland, L.J., Ramaekers, F.C., Schutte, B., and Reutelingsperger, C.P. (1998). Annexin V-affinity assay: a review on an apoptosis detection system based on phosphatidylserine exposure. Cytometry *31*, 1-9.

van Nieuw Amerongen, G.P., Beckers, C.M., Achekar, I.D., Zeeman, S., Musters, R.J., and van Hinsbergh, V.W. (2007). Involvement of Rho kinase in endothelial barrier maintenance. Arterioscler Thromb Vasc Biol *27*, 2332-2339.

Vastag, B. (2010). Biotechnology: Crossing the barrier. Nature *466*, 916-918.

Vegeto, E., Benedusi, V., and Maggi, A. (2008). Estrogen anti-inflammatory activity in brain: a therapeutic opportunity for menopause and neurodegenerative diseases. Frontiers in neuroendocrinology *29*, 507-519.

Verma, S., Nakaoke, R., Dohgu, S., and Banks, W.A. (2006). Release of cytokines by brain endothelial cells: A polarized response to lipopolysaccharide. Brain, behavior, and immunity *20*, 449-455.

Vigna, E., and Naldini, L. (2000). Lentiviral vectors: excellent tools for experimental gene transfer and promising candidates for gene therapy. The journal of gene medicine *2*, 308-316.

von Bernhardi, R., Tichauer, J.E., and Eugenin, J. (2010). Aging-dependent changes of microglial cells and their relevance for neurodegenerative disorders. Journal of neurochemistry *112*, 1099-1114.

Vong, L., D'Acquisto, F., Pederzoli-Ribeil, M., Lavagno, L., Flower, R.J., Witko-Sarsat, V., and Perretti, M. (2007). Annexin 1 cleavage in activated neutrophils: a pivotal role for proteinase 3. J Biol Chem *282*, 29998-30004.

Wade, C.B., and Dorsa, D.M. (2003). Estrogen activation of cyclic adenosine 5'-monophosphate response element-mediated transcription requires the extracellularly regulated kinase/mitogen-activated protein kinase pathway. Endocrinology *144*, 832-838.

Walther, A., Riehemann, K., and Gerke, V. (2000). A novel ligand of the formyl peptide receptor: annexin I regulates neutrophil extravasation by interacting with the FPR. Molecular cell *5*, 831-840.

Wee Yong, V. (2010). Inflammation in neurological disorders: a help or a hindrance? The Neuroscientist : a review journal bringing neurobiology, neurology and psychiatry *16*, 408-420.

Weksler, B.B., Subileau, E.A., Perriere, N., Charneau, P., Holloway, K., Leveque, M., Tricoire-Leignel, H., Nicotra, A., Bourdoulous, S., Turowski, P.*, et al.* (2005). Blood-brain barrier-specific properties of a human adult brain endothelial cell line. FASEB J *19*, 1872-1874.

Weller, R.O., Djuanda, E., Yow, H.Y., and Carare, R.O. (2009). Lymphatic Drainage of the Brain and the Pathophysiology of Neurological Disease. Acta neuropathologica *117*, 1-14.

Whalen, M.J., Carlos, T.M., Kochanek, P.M., and Heineman, S. (1998). Blood-brain barrier permeability, neutrophil accumulation and vascular adhesion molecule expression after controlled cortical impact in rats: a preliminary study. Acta Neurochir Suppl *71*, 212-214.

Whitton, P.S. (2007). Inflammation as a causative factor in the aetiology of Parkinson's disease. Br J Pharmacol *150*, 963-976.

Wilhelm, I., Fazakas, C., and Krizbai, I.A. (2011). In vitro models of the blood-brain barrier. Acta neurobiologiae experimentalis *71*, 113-128.

Williams, L.A., Martin-Padura, I., Dejana, E., Hogg, N., and Simmons, D.L. (1999). Identification and characterisation of human Junctional Adhesion Molecule (JAM). Molecular immunology *36*, 1175-1188.

Williams, S.L., Milne, I.R., Bagley, C.J., Gamble, J.R., Vadas, M.A., Pitson, S.M., and Khew-Goodall, Y. (2010). A proinflammatory role for proteolytically cleaved annexin A1 in neutrophil transendothelial migration. J Immunol *185*, 3057-3063.

Wilson, A.C., Clemente, L., Liu, T., Bowen, R.L., Meethal, S.V., and Atwood, C.S. (2008). Reproductive hormones regulate the selective permeability of the blood-brain barrier. Biochimica et biophysica acta *1782*, 401-407.

Wittchen, E.S., Haskins, J., and Stevenson, B.R. (1999). Protein interactions at the tight junction. Actin has multiple binding partners, and ZO-1 forms independent complexes with ZO-2 and ZO-3. J Biol Chem *274*, 35179-35185.

Wojciak-Stothard, B., Entwistle, A., Garg, R., and Ridley, A.J. (1998). Regulation of TNF-alpha-induced reorganization of the actin cytoskeleton and cell-cell junctions by Rho, Rac, and Cdc42 in human endothelial cells. J Cell Physiol *176*, 150-165.

Wojciak-Stothard, B., Potempa, S., Eichholtz, T., and Ridley, A.J. (2001). Rho and Rac but not Cdc42 regulate endothelial cell permeability. Journal of cell science *114*, 1343-1355.

Wojciak-Stothard, B., and Ridley, A.J. (2002). Rho GTPases and the regulation of endothelial permeability. Vascular pharmacology *39*, 187-199.

Wojciak-Stothard, B., and Ridley, A.J. (2003). Shear stress-induced endothelial cell polarization is mediated by Rho and Rac but not Cdc42 or PI 3-kinases. The Journal of cell biology *161*, 429-439.

Wojciak-Stothard, B., Williams, L., and Ridley, A.J. (1999). Monocyte adhesion and spreading on human endothelial cells is dependent on Rho-regulated receptor clustering. The Journal of cell biology *145*, 1293-1307.

Wolburg, H., and Lippoldt, A. (2002). Tight junctions of the blood-brain barrier: development, composition and regulation. Vascular pharmacology *38*, 323-337.

Wong, M.L., Rettori, V., al-Shekhlee, A., Bongiorno, P.B., Canteros, G., McCann, S.M., Gold, P.W., and Licinio, J. (1996). Inducible nitric oxide synthase gene expression in the brain during systemic inflammation. Nat Med *2*, 581-584.

Wong, R.K., Baldwin, A.L., and Heimark, R.L. (1999). Cadherin-5 redistribution at sites of TNF-alpha and IFN-gamma-induced permeability in mesenteric venules. The American journal of physiology *276*, H736-748.

Wong, V. (1997). Phosphorylation of occludin correlates with occludin localization and function at the tight junction. The American journal of physiology *273*, C1859-1867.

Woods, M.D., Kiss, J.Z., Smith, T., Buckingham, J.C., Flower, R., and Antoni, F.A. (1990). Localization of lipocortin-1 in rat hypothalamus and pituitary gland. Biochem Soc Trans *18*, 1236-1237.

Wu, C.C., Croxtall, J.D., Perretti, M., Bryant, C.E., Thiemermann, C., Flower, R.J., and Vane, J.R. (1995). Lipocortin 1 mediates the inhibition by dexamethasone of the induction by endotoxin of nitric oxide synthase in the rat. Proc Natl Acad Sci U S A *92*, 3473-3477.

Wu, Y., and Zhou, B.P. (2010). TNF-alpha/NF-kappaB/Snail pathway in cancer cell migration and invasion. British journal of cancer *102*, 639-644.

Xiao, F., Arnold, T.C., Zhang, S., Brown, C., Alexander, J.S., Carden, D.L., and Conrad, S.A. (2004). Cerebral cortical aquaporin-4 expression in brain edema following cardiac arrest in rats. Academic emergency medicine : official journal of the Society for Academic Emergency Medicine *11*, 1001-1007.

Yan, E.B., Hellewell, S.C., Bellander, B.M., Agyapomaa, D.A., and Morganti-Kossmann, M.C. (2011). Post-traumatic hypoxia exacerbates neurological deficit, neuroinflammation and cerebral metabolism in rats with diffuse traumatic brain injury. Journal of neuroinflammation *8*, 147.

Yang, S.H., Liu, R., Perez, E.J., Wang, X., and Simpkins, J.W. (2005). Estrogens as protectants of the neurovascular unit against ischemic stroke. Current drug targets CNS and neurological disorders *4*, 169-177.

Yang, Y.X., Wood, N.W., and Latchman, D.S. (2009). Molecular basis of Parkinson's disease. Neuroreport *20*, 150-156.

Yazid, S., Leoni, G., Getting, S.J., Cooper, D., Solito, E., Perretti, M., and Flower, R.J. (2010). Antiallergic cromones inhibit neutrophil recruitment onto vascular endothelium via annexin-A1 mobilization. Arterioscler Thromb Vasc Biol *30*, 1718-1724.

Yazid, S., Solito, E., Christian, H., McArthur, S., Goulding, N., and Flower, R. (2009). Cromoglycate drugs suppress eicosanoid generation in U937 cells by promoting the release of Anx-A1. Biochem Pharmacol *77*, 1814-1826.

Ye, L., Martin, T.A., Parr, C., Harrison, G.M., Mansel, R.E., and Jiang, W.G. (2003). Biphasic effects of 17-beta-estradiol on expression of occludin and transendothelial resistance and paracellular permeability in human vascular endothelial cells. J Cell Physiol *196*, 362-369.

Yong, V.W., and Marks, S. (2010). The interplay between the immune and central nervous systems in neuronal injury. Neurology *74 Suppl 1*, S9-S16.

Young, K.A., Hirst, W.D., Solito, E., and Wilkin, G.P. (1999). De novo expression of lipocortin-1 in reactive microglia and astrocytes in kainic acid lesioned rat cerebellum. Glia *26*, 333-343.

Zamboni, P., Menegatti, E., Bartolomei, I., Galeotti, R.*, et al.* (2007). Intracranial Venous Haemodynamics in Multiple Sclerosis. Current neurovascular research *4*, 252-258.

Zeevi, N., Pachter, J., McCullough, L.D., Wolfson, L., and Kuchel, G.A. (2010). The blood-brain barrier: geriatric relevance of a critical brain-body interface. Journal of the American Geriatrics Society *58*, 1749-1757.

Zehendner, C.M., Librizzi, L., de Curtis, M., Kuhlmann, C.R., and Luhmann, H.J. (2011). Caspase-3 contributes to ZO-1 and Cl-5 tight-junction disruption in rapid anoxic neurovascular unit damage. PloS one *6*, e16760.

Zhang, S., Wang, X.J., Tian, L.P., Pan, J., Lu, G.Q., Zhang, Y.J., Ding, J.Q., and Chen, S.D. (2011). CD200-CD200R dysfunction exacerbates microglial activation and dopaminergic neurodegeneration in a rat model of Parkinson's disease. Journal of neuroinflammation *8*, 154.

Zhou, Z., Gengaro, P., Wang, W., Wang, X.Q., Li, C., Faubel, S., Rivard, C., and Schrier, R.W. (2008). Role of NF-kappaB and PI 3-kinase/Akt in TNF-alpha-induced cytotoxicity in microvascular endothelial cells. American journal of physiology Renal physiology *295*, F932-941.

Zlokovic, B.V. (2005). Neurovascular mechanisms of Alzheimer's neurodegeneration. Trends in neurosciences *28*, 202-208.

Chapter 10 - Appendix

10.1 Composition of solutions

Where not stated within brackets, reagents have been bought from Sigma-Aldrich, UK.

10.1.1 Solutions for general usage

Phosphate buffered saline PBS (0.01M)	**Final concentration**
NaCl	0.138M
KCl	0.0027M
Distilled H_2O	100% (v/v)
pH 7.4	

Saline solution	**Final concentration**
NaCl	0.9% (w/v)
Distilled H_2O	100% (v/v)
pH 7.4	

Tris buffered saline (TBS) 1X	**Final concentration**
Tris.HCl	25 mM
NaCl	150 mM
KCl	2 mM
pH 7.4	

10.1.2 Solutions for *in-vivo* usage

Sucrose solution for cryo-preservation	**Final concentration**
Sucrose	30% (w/v)
PBS 0.01 M	100% (v/v)
pH 7.4	

Evan's Blue solution	**Final concentration**
Evan's Blue	2% (w/v)
PBS 0.01 M	100% (v/v)
pH 7.4	

6-Hydroxydopamine (6-OHDA) lesioning solution	**Final concentration**
6-OHDA	2 mg/ml
NaCl	0.9% (w/v)
Ascorbic acid	0.1% (w/v)
Saline	100% (v/v)
pH 7.4	

10.1.3 Cell culture

Dulbecco' modified eagle medium (DMEM; Lonza, CH)	**500 ml**	**Final concentration**
Heat inactivated fetal calf serum (FCS; Lonza, CH)		10%
Gentamycin (Invitrogen, UK)		50 µg/ml
Non-essential amminoacids (NEAA 100X; Invitrogen, UK)		100 µM

Endothelial cell growth medium (EGM-2 MV; Lonza, CH)	**500 ml**	**Final concentration**
Heath inactivated fetal calf serum (FCS; Lonza, CH)		2.5%
VEGF		half provided vial
IGF-1		half provided vial
EGF		half provided vial
Basic FGF		half provided vial
Hydrocortisone		whole provided vial
Ascorbic acid		whole provided vial
Gentamycin		whole provided vial

Dulbecco's phosphate buffered saline w/o Ca^{2+}/Mg^{2+} (DPBS w/o Ca^{2+}/Mg^{2+}; Lonza, CH)	**500 ml**	**Final concentration**
KCl		200 mg/ml
KH_2PO_4		200 mg/ml
NaCl		0.8% (w/v)
$MgCl_2 \cdot 6H_2O$		100 mg/l
CaCl		100 mg/ml
NaH_2PO_4		1.15 g/l

Henk's balanced salt solution w/o Ca^{2+}/Mg^{2+} 500 ml	**Final concentration**
(HBSS w/o Ca^{2+}/Mg^{2+}; Lonza, CH)	
KCl	400 mg/l
KH_2PO_4	60 mg/l
NaCl	8 g/l
$NaHCO_3$	350 mg/ml
$NaH_2PO_4 \cdot 7\ H_2O$	90 mg/l

Coating solution for routine passaging of hCMEC/D3	**Final concentration**
Thin rat tail collagen type I (BD Biosciences, UK)	150 µg/ml
Double distilled H_2O or DPBS without Ca^{2+}/Mg^{2+}	100% (v/v)
pH 7.4	

Trypsin solution	**Final concentration**
Trypsin (Lonza; CH)	0.25% (w/v)
EDTA	0.38% (w/v)

Freezing medium	**Final concentration**
Dimethylsulfoxide (DMSO)	10% (v/v)
FCS (Lonza, CH)	90% (v/v)

Stable integration selecting solution	**Final concentration**
G418® (Invitrogen; UK)	200 – 400 µg/ml
Cell growth medium	100% (v/v)

Fibronectin for transwell coating	**Final concentration**
Fibronectin from bovine plasma in 0.5 M NaCl, 0.05 M Tris, pH 7.5	10 µg/ml
DPBS without Ca^{2+}/Mg^{2+}	100% (v/v)
pH 7.4	

Collagen for Transwell coating	**Final concentration**
Collagen from calf skin in 0.1 M acetic acid	50 µg/ml
DPBS without Ca^{2+}/Mg^{2+}	100% (v/v)
pH 7.4	

17 β-estradiol stock solution	**Final concentration**
17 β-estradiol	100 µM
Ethanol	100% (v/v)

Propylpryazole-triol (PPT) stock solution	**Final concentration**
PPT (Tocris Bioscience, UK)	100 mM
Ethanol	100% (v/v)

Diarylpropionitrile (DPN) stock solution	**Final concentration**
DPN (Tocris Bioscience, UK)	100 mM
Ethanol	100% (v/v)

G-1 stock solution	**Final concentration**
G-1 (Tocris Bioscience, UK)	100 mM
Ethanol	100% (v/v)

Phenyl-trifluoromethyl-pyrazolo-phenol (PHTPP) stock solution	**Final concentration**
PHTPP (Tocris Bioscience, UK)	100 mM
Ethanol	100% (v/v)

G-15 stock solution	**Final concentration**
G-15 (Tocris Bioscience, UK)	100 mM
Ethanol	100% (v/v)

TNF-α stock solution	**Final concentration**
TNF-α (R&D Systems, UK)	100 µg/ml
BSA	0.1% (w/v)
DPBS with Ca^{2+}/Mg^{2+}	1X

IFN-γ stock solution	**Final concentration**
IFN-γ (R&D Systems, UK)	100 µg/ml
BSA	0.1% (w/v)
DPBS with Ca^{2+}/Mg^{2+}	1X

Lipopolisaccharide (LPS) stock solution	**Final concentration**
LPS (Clone 0111:B4; Sigma, UK)	1 mg/ml
NaCl	0.9% (w/v)
Saline	100% (v/v)

Griess reagent	**Final concentration**
Sulfanilamide	1% (w/v)
Naphthylethylenediamine dihydrochloride	0.1% (w/v)
Phosphoric acid solution	5% (v/v)

10.1.4 Solutions for *ex-vivo* usage

Trichloroacetic acid (TCA) solution	**Final concentration**
Trichloroacetic acid	60% (w/v)
Distilled H_2O	100% (v/v)

Proteinase K stock solution	**Final concentration**
Proteinase K	10 mg/ml
Distilled H_2O	100% (v/v)

Lysis buffer for genotyping	**Final concentration**
Tris.HCl	250 mM
EDTA	25 mM
NaCl	500 mM
SDS	2.5% (w/v)

10.1.5 Primary murine cerebrovascular endothelial cells isolation

Wash buffer	**100 ml**	**Final concentration**
HEPES buffer		10 mM
BSA		0.1% (w/v)
HBSS without Ca^{2+}/Mg^{2+}		1X
pH 7.4		

BSA stock solution	**Final concentration**
BSA	30% (w/v)
HBSS without Ca^{2+}/Mg^{2+}	1X

Density centrifugation solution	**Final concentration**
BSA	25% (w/v)
Wash buffer	

Enzyme cocktail	**10 ml/prep**	**Final concentration**
Collagenase/Dispase (Roche, UK)		2 mg/ml
DNase I		20 IU/ml
Tosylysine Chloromethyl Ketone Hydrochloride (TLCK)		0.147 µg/ml

Rat tail type I collagen	**Final concentration**
Filter sterile rat tail type I collagen (home-made)	0.33 mg/ml
Distilled H_2O	100% (v/v)

Cell growth medium	Final concentration
FBS (Lonza, CH)	20% (v/v)
Heparin ($C_{initial}$ = 50 mM)	80 µg/ml
Gentamicin	50 µg/ml
Selenium, Insulin, Transferrin (SIT) supplement	1X
Endothelium supplement ($C_{initial}$ = 7.5 mg/ml)	75 µg/ml
Vitamin C ($C_{initial}$ = 170 mM)	75 µM
Puromycin ($C_{initial}$ = 1 mg/ml)*	4 µg/ml
DMEM (low glucose, 1000 mg/l; Invitrogen, UK)	
*for the first three days only	

10.1.6 Protein extraction for cells and tissue samples

RIPA extraction buffer	Final concentration
Tris.HCl pH 7.4	50 mM
NaCl	150 mM
EDTA	1mM
Sodium deoxycholate	1% (w/v)
Triton X-100	1% (w/v)
SDS	0.1% (w/v)
Protease/phosphatase inhibitors cocktail	

Soluble proteins extraction buffer	Final concentration
HEPES	25 mM
NaCl	150 mM
EDTA	4 mM
EGTA	10 mM
Triton X-100	1% (v/v)
pH 7.5	
Protease/phosphatase inhibitors cocktail	

Insoluble proteins extraction buffer	Final concentration
HEPES	25 mM
NaCl	150 mM
EDTA	4 mM
EGTA	10 mM
Triton X-100	1% (v/v)
SDS	1% (w/v)
pH 7.5	
Protease/phosphatase inhibitors cocktail	

Soluble β-actin extraction buffer	**Final concentration**
DPBS with Ca^{2+}/Mg^{2+}	1X
Triton X-100	1% (v/v)
Unlabelled phalloidin	1 µg/ml
Protease/phosphatase inhibitors cocktail	

Insoluble β-actin extraction buffer	**Final concentration**
DPBS with Ca^{2+}/Mg^{2+}	1X
Triton X-100	1% (v/v)
SDS	2% (w/v)
Protease/phosphatase inhibitors cocktail	

Protein extraction buffer for brain cytokines	**Final concentration**
NaCl	150 mM
Tris.HCl pH 7.4	25 mM
EDTA	1mM
Protease/phosphatase inhibitors cocktail	

Protease and phosphatase inhibitors mix	**Final concentration**
PMSF	1mM
Aprotinin	10 µg/ml
NaF	25 mM
Na_3VO_3	1mM

10.1.7 Co-immunoprecipitation

RIPA buffer without SDS	**Final concentration**
Tris.HCl	50 mM
EDTA	10 mM
NaCl	150 mM
NP-40 (Nonidet P-40)	1% (v/v)
Sodium deoxycholate	1% (w/v)

Low salt buffer	**Final concentration**
Tris.HCl	10 mM
NaCl	150 mM
EDTA	2 mM
NP-40	0.2% (v/v)
pH 7.4	

High salt buffer	Final concentration
Tris.HCl	10 mM
NaCl	500 mM
EDTA	2 mM
NP-40	0.2% (v/v)
pH 7.4	

Beads resuspension buffer	Final concentration
Tris.HCl	10 mM
pH 7.4	

10.1.8 SDS-PAGE and Immunoblotting

Resolving acrylamide gel	Final concentration
40% Acrylamide/Bis-Acrylamide mixture (37.5:1 ratio) (Biorad, UK)	8%-15%
Tris.HCl pH 8.8	0.375M
20% (w/v) sodium dodecyl sulphate solution	0.1% (w/v)
Tetramethylethylenediamine (TEMED)	1:1000
Ammonium persulfate (APS)	0.05% (w/v)
Distilled H_2O	

Stacking acrylamide gel	Final concentration
40% Acrylamide/Bis-Acrylamide mixture (37.5:1 ratio)	4%
Tris.HCl pH 6.8	0.126M
20% (w/v) sodium dodecyl sulfate solution	0.1% (w/v)
Tetramethylethylenediamine (TEMED)	1:1000
Ammonium persulfate (APS)	0.05% (w/v)
Distilled H_2O	

Loading buffer 3X	Final concentration
Tris.HCl pH 6.8	0.2M
Glycerol	30% (v/v)
β-mercaptoethanol	15% (w/v)
SDS	6% (w/v)
Bromophenol blue	few grains

Running buffer 1X	**Final concentration**
Tris.HCl	25 mM
Glycine	192 mM
SDS	0.1% (w/v)
pH 8.3	

Transfer buffer 1X	**Final concentration**
Tris.HCl	25 mM
Glycine	192 mM
Methanol	10% (v/v)

Blocking solution	**Final concentration**
BSA	3% (w/v)
TBS	1X
Tween-20	0.05% (v/v)

TBS-T	**Final concentration**
TBS	1X
Tween-20	0.05% (v/v)

10.1.9 DNA transfection, amplification and DNA gel electrophoresis

Tris acetate EDTA (TAE) buffer	**Final concentration**
Tris-Acetate (50X; Invitrogen, UK)	40 mM
EDTA	1 mM

Agarose gel for DNA analysis	**Final concentration**
Agarose (Invitrogen, UK)	0.8-2%
TAE buffer	1X
Ethidium Bromide	0.8 ng/µl

Gel loading buffer 10X	**Final concentration**
Glycerol	30% (v/v)
Bromophenol blue	0.25% (w/v)
Distilled H_2O	100% (v/v)

Ampicillin stock solution	**Final concentration**
Ampicillin	1 mg/ml
Distilled H_2O	100% (v/v)
Filter sterilised	

Luria Bertani (LB) broth	**Final concentration**
Bacto tryptone (Invitrogen, UK)	1% (w/v)
Bacto-yeast extract (Invitrogen, UK)	0.5% (w/v)
NaCl	1%

LB Bacto-agar	**Final concentration**
(All reagents from Invitrogen, UK)	
Bacto tryptone	1%
Bacto-yeast extract	0.5%
NaCl	1%
Agar	1.5%

Non-selective SOC medium	**Final concentration**
(All reagents from Invitrogen, UK)	
Bacto-tryptone	2% (w/v)
Yeast extracts	0.5% (w/v)
NaCl	8.6 mM
KCl	2.5 mM
$MgSO_4$	20 mM
Glucose	20 mM
pH 7.0	

$CaCl_2$ solution for HEK293FT transfection	**Final concentration**
$CaCl_2$	2M
Distilled H_2O	100% (v/v)

2X Hank's Balanced Salts (HBS) solution	**Final concentration**
HEPES	50 mM
NaCl	281 mM
Na_2HPO_4	1.5 mM
pH 7.08-7.1	
Filter sterilized	

Sodium butyrate stock solution	**Final concentration**
Sodium butyrate	1 M
PBS	0.01 M
Freshly prepared before use	

Tris-EDTA (TE) buffer	**Final concentration**
Tris.HCl pH 8	10 mM
EDTA	1 mM

10.1.10 Enzyme-linked immunosorbent assay (ELISA)

Bicarbonate buffer	**Final concentration**
$NaHCO_3$	25 mM
Na_2CO_3	25 mM
Distilled H_2O	100% (v/v)
pH 9.6	

Blocking buffer	**Final concentration**
BSA	1% (w/v)
DPBS without Ca^{2+}/Mg^{2+}	1X
Distilled H_2O	100% (v/v)

Assay diluent	**Final concentration**
PBS	0.01 M
Tween-20	0.05% (v/v)

Wash buffer	**Final concentration**
NaCl	0.9% (w/v)
Tween-20	0.05% (v/v)
Distilled H_2O	100% (v/v)

Wash buffer (auto-antibody protocol)	**Final concentration**
PBS	0.01 M
Tween-20	0.05% (v/v)
Distilled H_2O	100% (v/v)

Stop reaction	**Final concentration**
H_2SO_4	2M
Distilled H_2O	100% (v/v)

Antibody buffer (auto-antibody protocol)	**Final concentration**
EDTA	1 mM
Tween-20	0.05% (v/v)
FCS	1% (v/v)
PBS	0.01M
pH 7.5	

10.1.11 Histochemistry and immunophenotyping on cells and tissue

Anti-freeze solution	**Final concentration**
$NaH_2PO_4 \cdot H_2O$	11.53 mM
Na_2HPO_4	38.5 mM
NaCl	150 mM
Polyvinylpyrrolidone	1% (w/v)
Sodium Azide	0.02% (w/v)
Ethanediol	50% (v/v)

Sudan Black	**Final concentration**
Sudan Black	0.5% (w/v)
Ethanol	70% (v/v)
Distilled H_2O	30% (v/v)

Permeabilization buffer	**Final concentration**
TBS	1X
Triton X-100	0.2-0.5% (v/v)

Blocking solution	**Final concentration**
Normal goat serum (NGS)	10% (v/v)
BSA	1% (w/v)
TBS	1X
Triton X-100	0.1% (v/v)

Blocking solution (for human tissue)	**Final concentration**
BSA	10% (w/v)
TBS	1X
Triton X-100	0.5% (v/v)

Peroxidase inhibiting buffer (for human tissue)	**Final concentration**
H_2O_2	0.3% (v/v)
PBS	0.01 M

Washing solution (for human tissue)	**Final concentration**
TBS	1X
Triton X-100	0.05% (v/v)

Developing solution (for human tissue)	**Final concentration**
Diaminobenzidine	0.025% (v/v)
H_2O_2	0.01% (v/v)
TBS	1X

Antibody buffer	**Final concentration**
TBS	1X
NGS	1% (v/v)
BSA	0.1% (w/v)
Triton X-100	0.1% (v/v)

Paraformaldehyde (PFA) for tissue and cell fixation	**Final concentration**
PFA (VWR International, UK)	4% (w/v)
PBS pH 7.4; filtered	0.01 M

Mowiol	**Final concentration**
Mowiol (Calbiochem; UK)	10% (w/v)
Glycerol	25% (v/v)
Distilled H_2O	25% (v/v)
Sodium Azide	0.02% (w/v)
Tris.HCl pH 8.5	50% (v/v)

Eosin Y counterstain	**Final concentration**
Eosin Y	0.1% (w/v)
Ethanol	80% (v/v)
Glacial acetic acid	0.44% (v/v)
Distilled H_2O	20% (v/v)

Staining solution for β-galactosidase activity	**Final concentration**
$K_4Fe(CN)6{\cdot}3H_2O$	30 mM
$K_3Fe(CN)_6$	30 mM
$MgCl_2$	2 mM
Na-deoxycholate	0.01% (w/v)
Triton X-100	0.02% (v/v)
X-gal	2 mg/ml
PBS	0.01M

Rinse buffer for β-galactosidase activity	**Final concentration**
$NaH_2PO_4.2H_2O$	100mM
$Na_2HPO_4.12H_2O$	100mM
Triton X-100	0.1% (v/v)
Distilled H_2O	100% (v/v)

Harris Hematoxylin solution	**Final concentration**
Alcoholic hematoxylin solution	0.5% (v/v)
HgO	0.25% (w/v)
$KAl(SO_4)_2$	10% (w/v)
Glacial acetic acid	2% (v/v)
Distilled H_2O	100% (v/v)

10.1.12 Flow cytometry

Blocking solution	**Final concentration**
DPBS with Ca^{2+}/Mg^{2+}	1X
BSA	3% (w/v)
with or without saponin 10% (w/v)	0.025-0.1% (w/v)

Wash buffer	**Final concentration**
NGS	1% (v/v)
BSA	0.1% (w/v)
DPBS with Ca^{2+}/Mg^{2+}	1X
with or without saponin 10% (w/v)	0.025-0.1% (w/v)

Antibody buffer	**Final concentration**
DPBS with Ca^{2+}/Mg^{2+}	1X
BSA	0.1% (w/v)
with or without saponin 10% (w/v)	0.025-0.1% (w/v)

10.2 Antibodies

Antibodies used throughout the project are listed here, along with their source, the final concentration/dilution factor used and which application they have been optimised for.

10.2.1 Primary antibodies

Antibody	Species	Company	Cat. Number	Dilution Factor/Final concentration	Application
Anti-ANXA1	Ms	Not commercial	Solito *et al.* , 2000	50 ng/ml	FC; E
Anti-ANXA1	Rb	Life Technologies	71-3400	1:1000	IF; FC; E
Anti-ANXA1	Rb	Not commercial	Solito *et al.* , 1998a	1:1000	IF; WB; FC
Anti-Akt	Rb	Cell signaling	4685	1:1000	WB
Anti-Cd11b	Rt	Abcam	ab6332	1:300	IF
Anti-CD31	Rb	Novus Biologicals	NB100-92205	1:100	IF
Anti-Cdc42	Ms	Cell Biolabs	240201	1:200	WB
Anti-claudin 5	Ms	Life Technologies	35-2500	1:100	IF; WB
Anti-claudin 5	Rb	Santa Cruz Biotech	sc-28670	1:50; 1:500	IF; WB
Anti-COX2	Rb	Cayman Chemical	160106	1:500	WB
Anti-ERα	Ms	Santa Cruz Biotech	sc-130072	1:1000	FC
Anti-ERβ	Ms	Santa Cruz Biotech	sc-133554	1:150	FC
Anti-FPR1	Ms	R&D systems	MAB3744	1:100	IF; FC
Anti-FPR2	Ms	R&D systems	MAB3749	1:100	IF; FC
Anti-GAPDH	Rb	Abcam	ab9483	1:5000	WB
Anti-GPR30	Ms	R&D systems	AF5534	1:500	FC
Anti-Histone H3	Rb	Cell signaling	9717	1:1000	WB
Anti-Iba1	Rb	Wako	019-19741	1:2000	IF
Anti-iNOS	Rb	Sigma-Aldrich	N7782	1:500	WB
Anti-IκB	Rb	Cell signaling	4812	1:1000	WB
Anti-Laminin	Rb	Sigma-Aldrich	L9393	1:500	IF
Anti-MDR1	Rb	Santa Cruz Biotech	sc-1517R	1:100	WB
Anti-occludin	Ms	Life Technologies	33-1500	1:100	IF; WB
Anti-p38 MAPK	Rb	Cell signaling	9212	1:1000	WB

Anti-p44/42 MAPK (ERK1/2)	Rb	Cell signaling	4695	1:1000	WB
Anti-p65	Rb	Cell signaling	4764	1:1000	WB
Anti-PDGFR (CD140b)	Rat	eBioscience	14-1402-82	1:250	IF
Anti-Perlecan	Rb	Sigma-Aldrich	HPA018892	1:3000	IF
Anti-phospho Akt	Rb	Cell signaling	4056	1:1000	WB
Anti-phospho IκB	Ms	Cell signaling	9246	1:1000	WB
Anti-phospho p38 MAPK	Rb	Cell signaling	9215	1:200	WB
Anti-phospho p44/42 MAPK (ERK1/2)	Rb	Cell signaling	8544	1:1000	WB
Anti-phospho SAPK/JNK	Rb	Cell signaling	4668	1:1000	WB
Anti-Phospho Ser ANXA1	Rb	Not commercial	Solito *et al.* , 2003b	1:500	WB
Anti-Phospho Tyr ANXA1	Rb	Not commercial	Solito *et al.* , 2003b	1:500	WB
Anti-Rac1	Ms	Cell Biolabs	240106	1:200	WB
Anti-RhoA	Ms	Santa Cruz Biotech	sc-179	1:250	WB
Anti-SAPK/JNK	Rb	Cell signaling	9258	1:1000	WB
Anti-Tyrosine Hydroxylase (TH)	Ms	Millipore	MAB318	1:4000	IF
Anti-VE Cadherin	Rb	Santa Cruz Biotech	sc-28644	1:80; 1:250	IF; WB
Anti-ZO1	Rb	Life Technologies	40-2200	1:80; 1:100	IF; WB
Anti-β actin	Rb	Abcam	ab6276	1:5000	WB
Anti-β Galactosidase	Rb	MP Biomedicals	55976	1:100	IF

Table 10.1 Primary antibodies used throughout the study. Detailed information about primary antibodies is here reported. Abbreviations: Dk=donkey; Gt=goat; Ms=mouse; Rb=rabbit; Rt=rat. IF=immunofluorescence; FC=flow cytometry; WB=western blotting; E=ELISA.

10.2.2 Secondary antibodies and fluorescently conjugated phalloidins

Antibody	Species	Company	Cat. Number	Dilution Factor/Final concentration	Application
AF488-Phalloidin	N.A.	Life Technologies	A-12379	1:40	IF
Rhodamine-Phalloidin	N.A.	Life Technologies	R-415	1:40	IF
Anti-mouse IgG AF488 conj.	Gt	Life Technologies	A-11029	1:500	IF; FC
Anti-mouse IgG AF594 conj.	Gt	Life Technologies	A-11005	1:500	IF; FC
Anti-mouse IgG HRP conjugated	Gt	Sigma-Aldrich	A-5906	1:15000	WB
Anti-rabbit IgG AF488 conj.	Gt	Life Technologies	A-11034	1:500	IF; FC
Anti-rabbit IgG AF594 conj.	Gt	Life Technologies	A-11012	1:500	IF; FC
Anti-rabbit IgG AP conjugated	Gt	Sigma-Aldrich	A-8025	1:10000	IF
Anti-rabbit IgG HRP conjugated	Gt	AbD Serotec	STAR54	1:10000	WB
Anti-rat IgG FITC conj.	Dk	Beckman - Coulter	732978	1:500	IF; FC
Anti-rat IgG FITC conj.	Dk	Beckman - Coulter	732978	1:500	IF; FC
Anti-rat IgG FITC conj.	Dk	Beckman - Coulter	732978	1:500	IF; FC

Table 10.2 Secondary antibodies and fluorescently conjugated phalloidin used throughout the study. Detailed information about secondary antibodies is here reported. Abbreviations: Dk=donkey; Gt=goat; Ms=mouse; Rb=rabbit; Rt=rat. IF=immunofluorescence; FC=flow cytometry; WB=western blotting; E=ELISA.

10.3 Primers sequences

Primer name	Sequence (5' - 3')	Annealing temperature
ANXA1 exon 3 F	gccttgcacaaagctatcatgg	55°C
ANXA1 exon 4 R	gcattggtcctcttggttaagaatg	55°C
ANXA1 F	gcggcggatccatggcaatggtatcagaattcctc	58°C
ANXA1 R	gcgaggatggattgaaggtaggataggggctca	58°C
GAPDH F	aaggtgaaggtcggagtcaacg	58°C
GAPDH R	ggcagagatgatgacccttttggc	58°C
Human CD14 F	cccctgcgtgtgct	60°C
Human CD14 R	caggattgtcagacagg	60°C
Human MD2 F	ctgcaactcatccgatgcaag	56°C
Human MD2 R	cagtctctcctttcagagctctgc	56°C
Human TLR2 F	ggcttctctgtcttgtgacc	56°C
Human TLR2 R	gggcttgaaccaggaagacg	56°C
Human TLR4 F	tgtattcaaggtctggctgg	50°C
Human TLR4 R	gcaacctttgaaactcaagcc	50°C
LacZ F	tactgtcgtcgtcccctcaaactg	55°C
LacZ R	gttgcaccacagatgaaacgc	55°C

Table 10.3 List of primers used throughout the study. General information about primers used in this study is reported here.

10.4 Lentiviral particles production

10.4.1 Plasmid maps

A

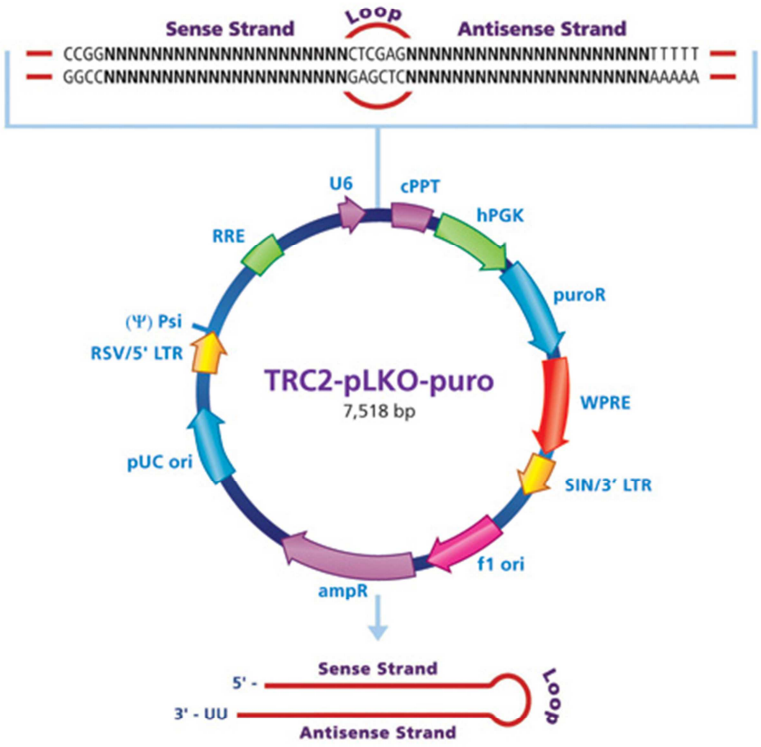

B

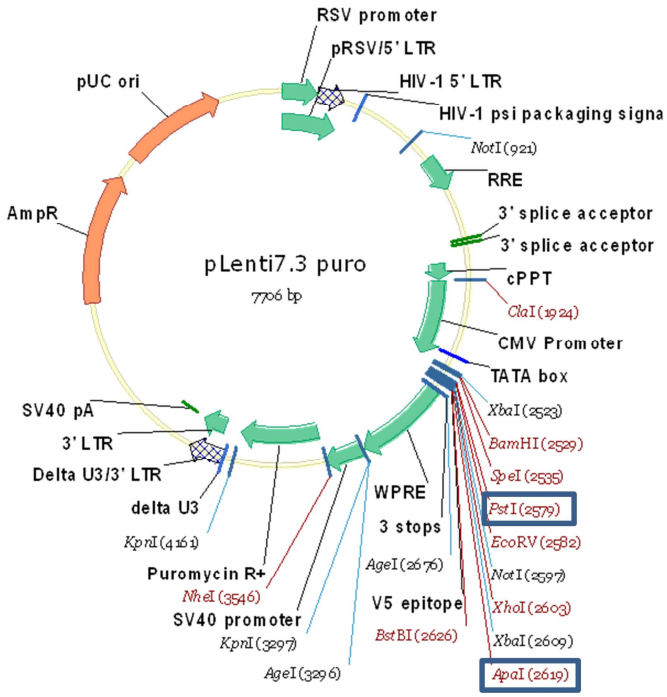

Figure 10.1 Maps of the plasmids that are used for production of lentiviral particles. A| The TRC2-pLKO-puro vectors are used for transient or stable transfection of shRNA sequences as well as production of lentiviral particles. Usually length is around 7500 bp and it contains various elements. The Woodchuck Hepatitis Post-Transcriptional Regulatory Element (WPRE) allows for enhanced expression of the transgene delivered by lentiviruses. A strong ubiquitous promoter (hPGK) guarantees strong expression of a puromycin selectable marker (puroR) allowing for positively selection of only those that stably acquired the viral genome into their genomic sequence. Self-inactivating replication incompetent viral particles can be produced in packaging cells (HEK293T) by co-transfection with compatible packaging plasmids (see General methods for the details). **B|** Modified pLENTI 7.3 vector used for cloning the human cDNA of ANXA1 in order to produce viral particles for ANXA1 over-expression. It contains several components: two Inverted terminal repeats (ITRs), the cytomegalovirus promoter (CMV), a multiple cloning site (MCS) where to insert the desired sequence to be over-expressed, the WPRE and the central Polypurine Tract (cPPT) sequence from the HIV-1 integrase gene, which promotes at least 4-fold increase in protein expression compared to vectors lacking this element. Restriction enzymes used for the cloning strategy (*Pst*I and *Apa*I) are indicated in blue squares.

10.4.2 Lentiviral particles production

10.4.2.1 Molecular cloning

In order to produce lentiviral particles bearing short hairpin RNA (shRNA) sequences directed against human Annexin A1 (NCBI accession number NM_000700) transcriptional products (messenger RNA, mRNA), we obtained a kind gift from Dr. M. de Graauw (Leiden University, NL) consisting on 5 plasmids (commercially available from Sigma-Aldrich, UK), each of those consisting on modified lentiviral genomic sequences containing validated shRNA directed against human Annexin A1 (TRC2.0 Mission® shRNA vectors; Sigma-Aldrich, UK). Due to their long catalogue number, these plasmids were identified by abbreviated numbers: 1257, 1258, 1259, 1260 and 1261; Figure 10.1, Panel A, shows the general features of this type of vectors. Since they did not need any molecular modification, they were simply amplified by transformation and *MaxiPrep* procedure.

In order to produce lentiviral particles containing the coding sequence (cDNA) for ANXA1, molecular cloning had to be performed on a plasmid encoding for the viral genome. This plasmid was originally modified by Dr. E. Pazarentzos and is based on the vector pLENTI 7.3, which is a standard plasmid to produce high titres of recombinant lentiviral particles (from Invitrogen, UK). Briefly, as shown in Figure 10.1, Panel B, the vector contains two ITR sequences, among which the cytomegalovirus (CMV) promoter is present and the transgene should be placed within the multiple cloning site (MCS). The cloning strategy adopted was the following: human coding sequence for ANXA1 was obtained by co-digestion of 1 µg of the plasmid pRCMV-ANXA1 (Solito *et al.*, 1998) with 10 international units (IU) of the restriction enzyme *Apa*I (Fermentas, Thermo Scientific, UK) and 10 IU of *Pst*I (Fermentas, Thermo Scientific, UK) following manufacturer instructions. The modified vector pLENTI 7.3 was linearized following the same cloning strategy. Digestion products were purified QIAQuick Gel extraction purification kit (Qiagen, UK) and ligation was performed overnight at 16°C, using T4 DNA ligase (Invitrogen, UK) and a molecular ratio backbone:insert of 1:3 (sticky-sticky ends ligation, as suggested by several molecular biology manuals (Sambrook, 1989) and by the enzyme datasheet); a negative control (absence of the insert) has been included to help interpretation of the results. Finally, 10 µl of the ligation were used to transform heat-competent bacteria DH5α (Invitrogen, UK) through heat-shock protocol,

which briefly involves: incubation of 100 µl of bacteria suspension and DNA on ice for 30 minutes to allow the latter to stick to the bacterial wall surface; 45 sec heat shock at 42°C; 1 hour recovery at 37°C with vigorous shaking in presence of non-selective SOC-medium (Invitrogen, UK). 100/200 µl of suspension were pleated on LB-agar plates containing the selective antibiotic for those plasmids (Ampicillin; Sigma-Aldrich) and incubated at 37°C overnight. Resistant colonies were picked-up and grown overnight at 37°C in selective LB broth. Plasmid DNA was checked for identity by sequencing (ANXA1 F and ANXA1 R: Section 10.3) through gene sequencing core facilities at Hammersmith Campus (Imperial College London, UK) and by restriction reactions using *Apa*I, *Pst*I and *Kpn*I (Fermentas, Thermo Scientific, UK).

10.4.2.2 Lentiviral particles production

Virulent media was produced in HEK293FT cells (Invitrogen, UK), routinely cultured in Dulbecco Modified Eagle medium (DMEM; Lonza, CH) supplemented with 1X non-essential amino acids (Lonza, CH) and 10% FCS. Plasmids encoding Vesicular Stomatitis Virus Glycoprotein (pVSV-G; encoding for the G-protein of the viral envelope), group antigen and reverse transcriptase (pGag.Pol) and mRNA export helper protein (pRev; containing the minimal set of lentiviral genes required to generate the virion structural proteins and packaging functions) were used for transfection. Two hours prior to transfection, the medium was replaced with fresh DMEM 10% FCS. 5.4 µg of the pVSV-G, 3.8 µg of the pRev, 7.8 µg of the pGag.Pol, 9 µg of the pAdVantage and 20 µg of the lentiviral transgene plasmid were mixed. $CaCl_2$ solution was added (final concentration 250 mM; final volume 500 µl), mixed thoroughly and incubated for 5 minutes. Meanwhile, 500 µl of 2X HBS solution was prepared in a 15 ml conical tube. After 5 minutes incubation, the DNA/$CaCl_2$ mixture was added drop by drop into 15 ml conical tube while vigorously shaking the tube on a vortex machine. The mix was immediately added to the dish drop by drop. After 16 hours transfection, medium was aspirated and replaced with fresh warm medium containing sodium butyrate (1 mM) as enhancing transcriptional agent. After 3 days post transfection, the supernatant was harvested and centrifuged (500x*g*, 10 minutes, RT) to remove cells and large debris, then passed through a 0.45 µm sterile filter (Millipore, UK).

10.5 Characterisation of hCMEC/D3 cells with modified ANXA1 expression

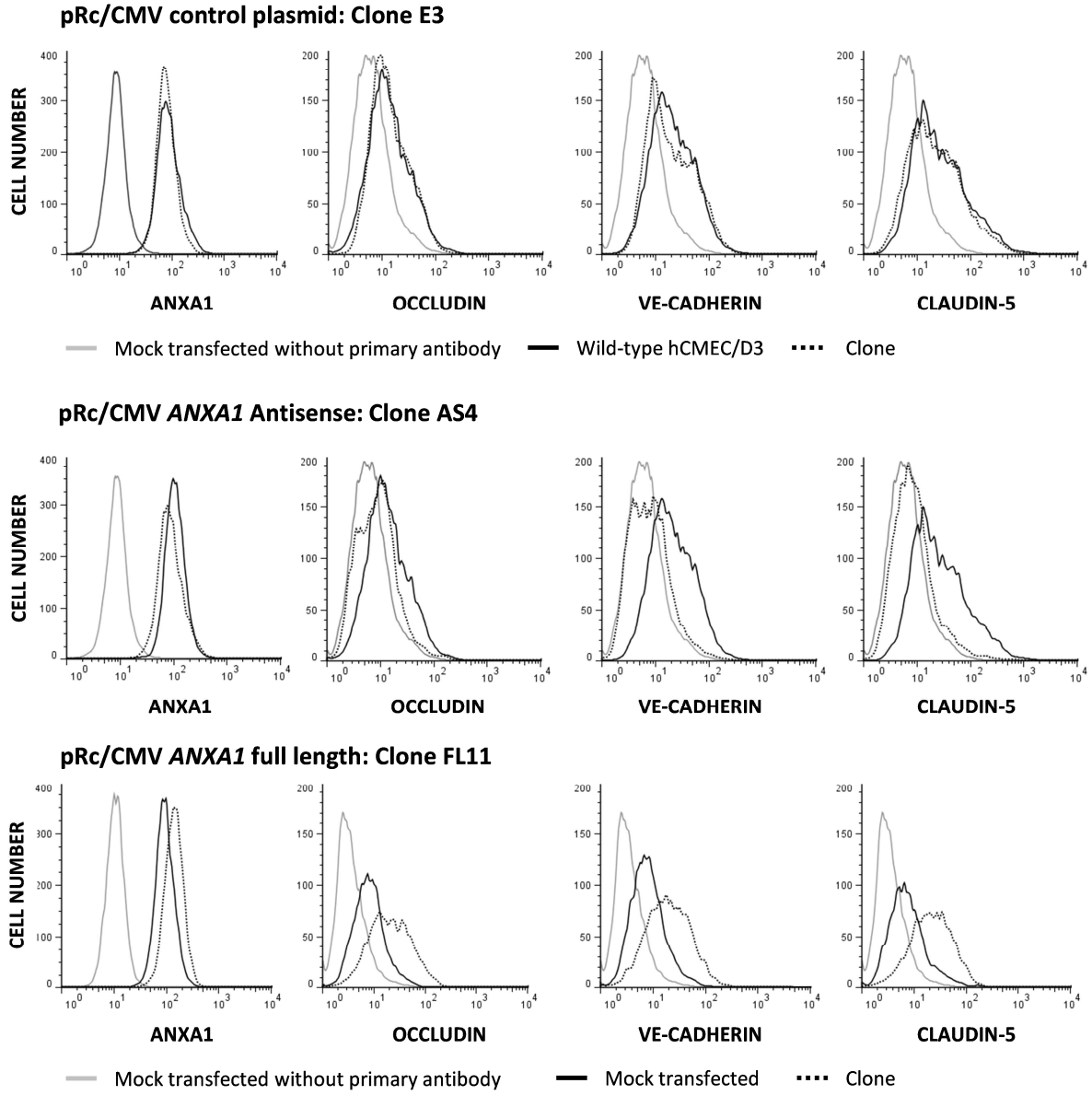

Figure 10.2 Immunophenotyping of stable hCMEC/D3 clones. Flow cytometric analysis of ANXA1 and tight- (occludin, claudin-5) and adherens- (VE-cadherin) junctions expression in stably transfected hCMEC/D3 cells that have been chosen to conduct the majority of the functional studies described in the thesis. These clones were chosen as the best ones since they showed the best ANXA1 expression modification. At least 10000 events were analysed per profile, and histograms represent one of at least *n*=3 independent experiments.

10.6 Assessment of endocytosis on hCMEC/D3 monolayers

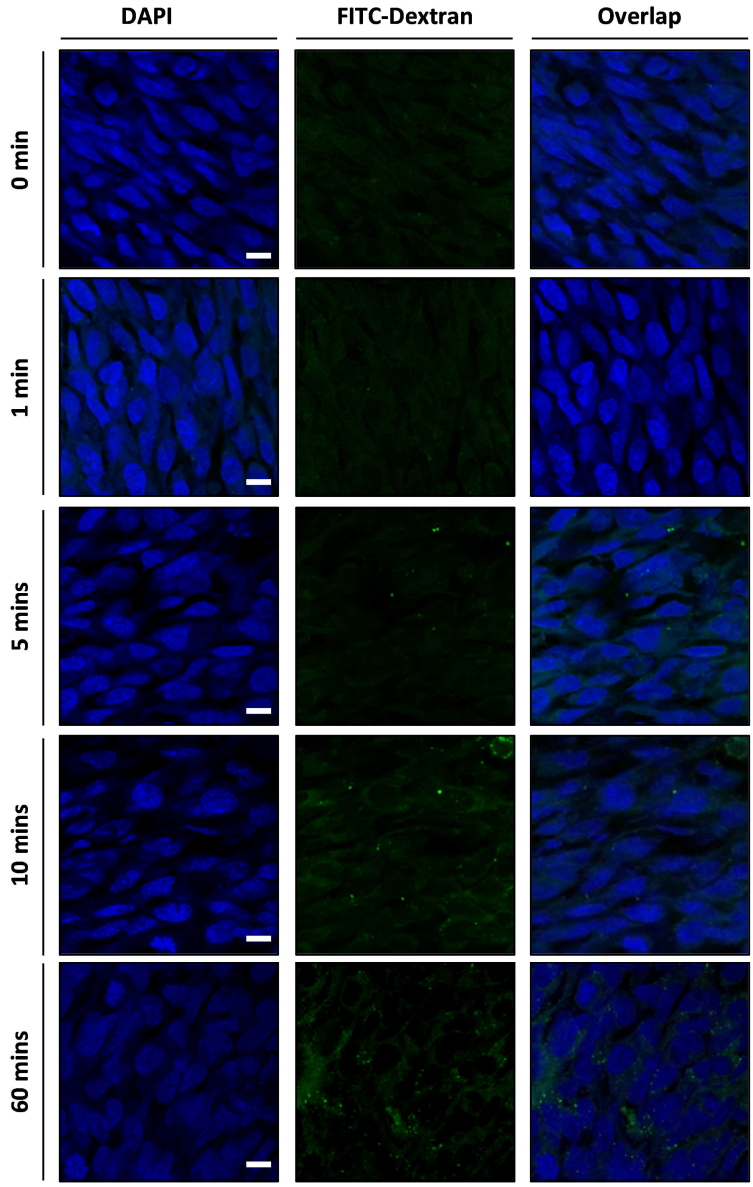

Figure 10.3 Evaluation of hCMEC/D3 endocytosis of 70 kDa FITC-dextran. Representative confocal microscopic analysis on confluent monolayers of hCMEC/D3 cells incubated for various time points with a 3 mg/ml solution of 70kDa FITC-Dextran. *Z*-stack profiles were recorded with a confocal microscope and analyzed for presence of endocytotic cytoplasmic vesicles. No evident sign of significant endocytosis was detected at any time point, indicating that the movement of fluorescent molecules from apical to baso-lateral regions is occurring mainly through the paracellular pathway. Pictures are representative of *n*=3 samples/time point; scale bar is 5 µm.

10.7 Demographic data from human *post-mortem* brains and plasma samples

Disease	Number of cases	Mean age (range), years	Disease duration (years)	Gender ratio (M:F)	*Post-mortem* delay (hours)
Multiple Sclerosis	11	63.2 (43-81)	30 (14-50)	4:7	9-27
Parkinson's disease	7	73.7 (62-87)	13 (5-27)	5:2	7-26
Non-neurologic controls	6	83.6 (81-88)	n/a	3:3	7-47

Table 10.4 Human tissue demographic data. General information about age and disease of the *post-mortem* brain tissue analysed in the study.

Patient	Age	Gender	MS type	Treatment
BUH00115	49	M	R/R	NONE
BUH00116	45	F	R/R	NONE
BUH00117	49	M	R/R	COPAXONE
BUH00118	64	F	PP	AVONEX
BUH00119	65	F	R/R	NONE
BUH00121	44	F	R/R	REBIF
BUH00122	51	F	R/R	REBIF
BUH00123	60	F	SP	REBIF

Table 10.5 Human plasma demographic data. Information about the patients, who donated blood samples for further plasma isolation. R/R: relapsing remitting; SP: secondary progressive; PP: primary progressive. Treatments: REBIF & AVONEX are interferon-β, COPAXONE is glatiramer acetate. All patients are of Caucasian ethnic origin; control plasma samples used for the study are from 9 disease-free, age- and sex-matched donors.

10.8 Surgical rodent ovariectomy

Briefly, 3 months old female C57BL/6 mice (Charles River, UK) were deeply anaesthetised with a mixture of hypnorm/hypnovel (1:1:2; respectively, hypnorm:hypnovel:water) and sham operated or ovariectomised according to standard procedures. Briefly, dorsal midline incisions inferior to palpated rib cage and each kidney were performed to expose the ovaries, which were then removed. Micro-osmotic pumps (Alzet model 2002; 0.5 ± 0.1µl/hr rate of release for 2 weeks; DURECT Co., USA) filled with either vehicle (23 mg/ml 2-Hydroxypropyl-β-cyclodextrin solution) or β-cyclodextrin-encapsulated 17β-estradiol (4.2 µg/ml sterile water solution) were implanted subcutaneously in the ovariectomized (OVX) animals. Minipumps guaranteed the release of 2 µg/kg/day of 17β-estradiol per animal for 14 days; this dose was chosen to ensure a response to estradiol close to physiological levels (Andersson *et al.*, 2005). After 2 weeks from surgery and implantation, each group (OVX+vehicle; OVX+estradiol; sham operated) was divided in two sub-groups (*n*=5): one group was treated with 3 mg/kg LPS *i.p.* while the second one with 100 µl 0.9% NaCl solution. 3 hours later, all the animals underwent intravenous administration of Evans Blue and extravasation was assessed as described in the General methods.

10.9 Experimental plan for Chapter 6

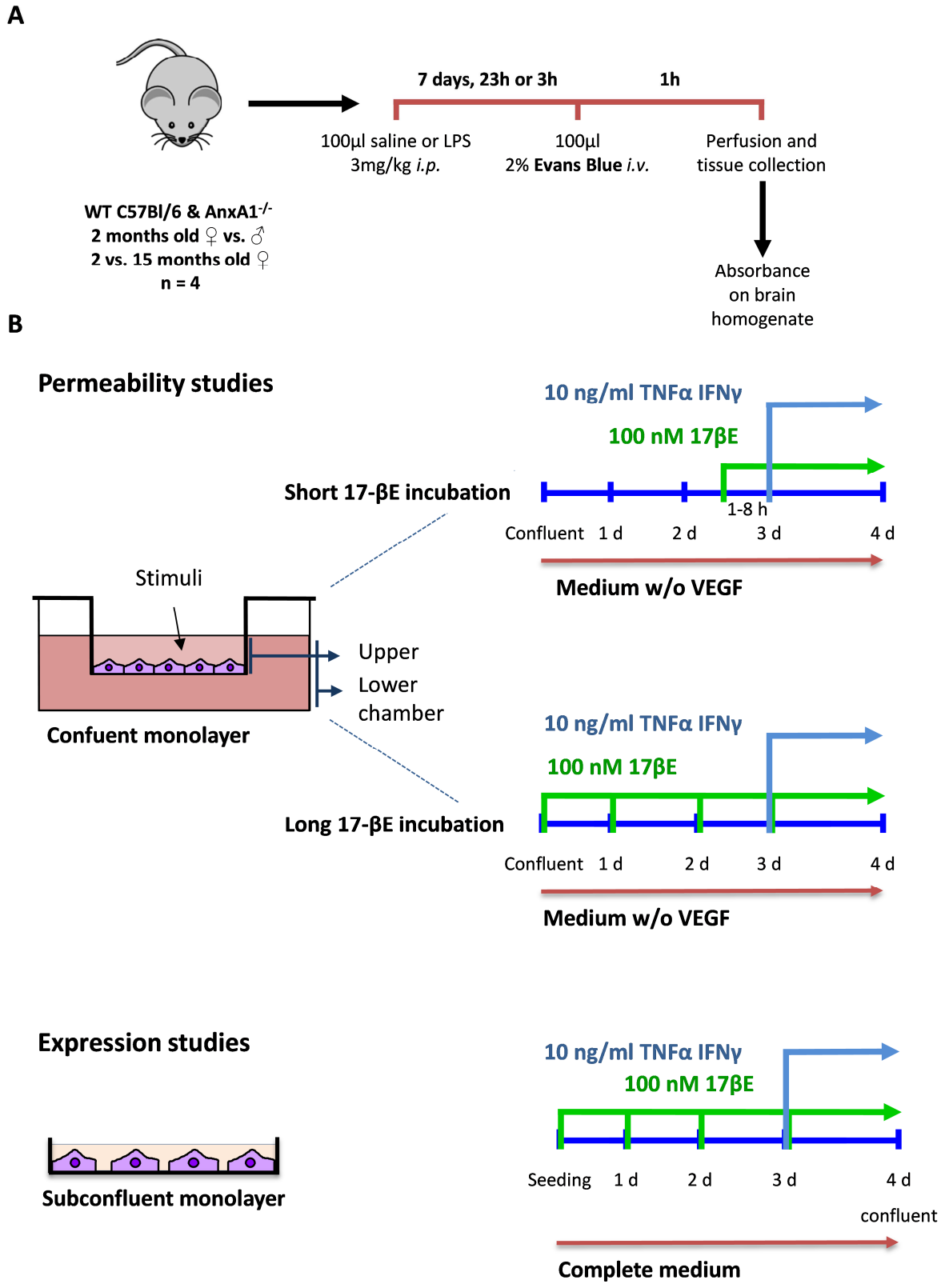

Figure 10.4 Experimental time plan for *in vivo* and *in vitro* experiments. *In vivo* and *in vitro* stimulation time points for the experiments described in Chapter 6. 17-βE is 17β-estradiol.

10.10 TNF-α cell signalling pathways are not modulated by β-estradiol

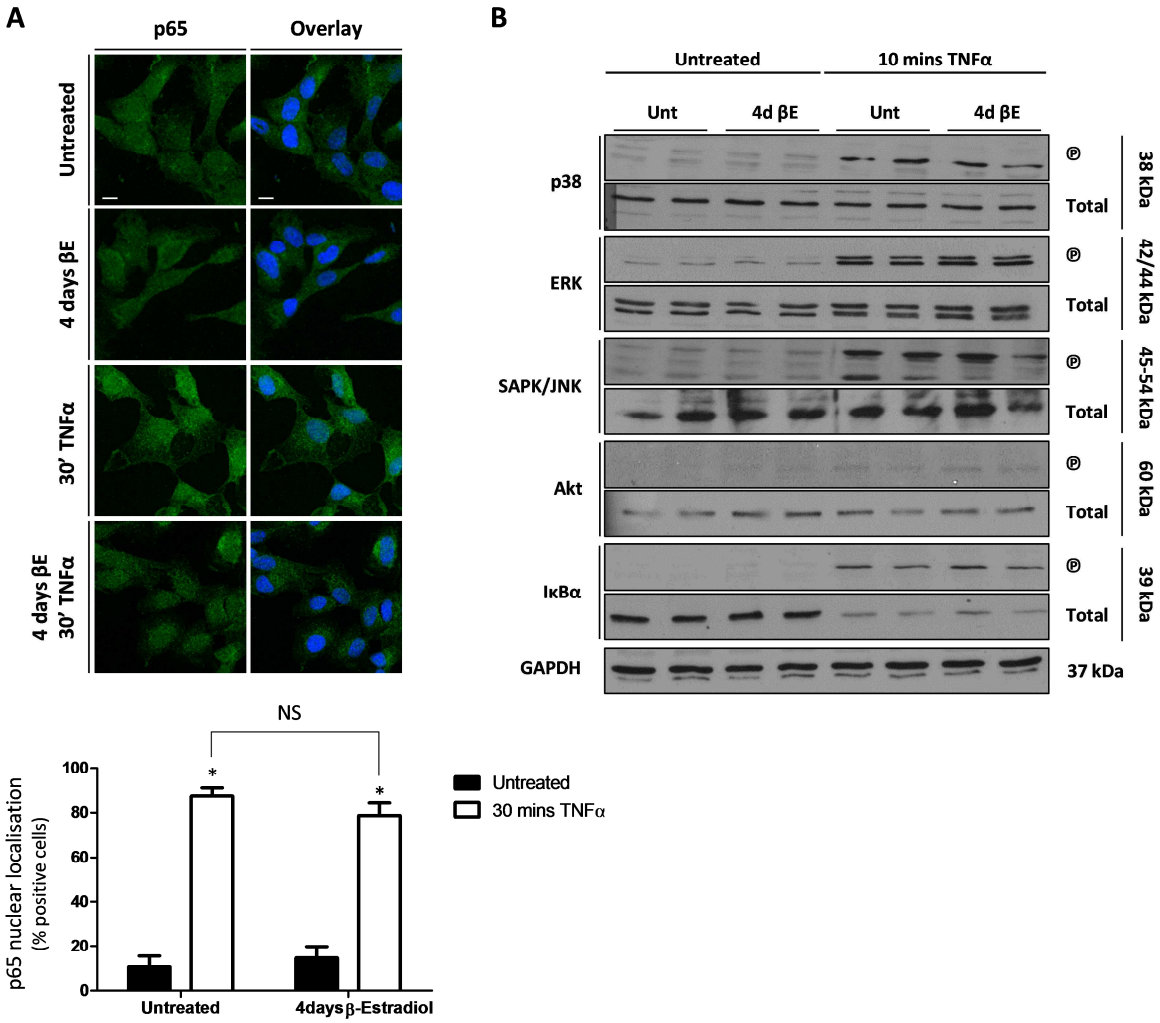

Figure 10.5 TNF-α activates numerous cell signalling pathways which are not modulated by pre-exposure with β-estradiol. A| Sub-confluent cells grown on labtek devices were (or not) pre-exposed to estradiol and then stimulated (or not) with TNF-α for 30 minutes. Immediately washed and fixed for 10 minutes, cells were permeabilized and stained for p65 (one subunit of the most common forms of NF-κB). Semi quantitative analysis of nuclear p65 was conducted as described (Maggi *et al.*, 2004) by counting 50 cells/coverslip and expressing the results as percentage of total counted cells. Data are presented as mean ± SEM. The experiments were performed in duplicate and cells were counted in a blind manner. Two-ways ANOVA was performed; * indicates $p<0.05$ *vs.* untreated and 4 days 17 β-estradiol treated. Similar results (*i.e.* no effects of the steroid on the inflammatory response) were obtained after a longer incubation with the cytokine (24 hours). **B|** Representative Immuno-blots show the main signalling pathways activated by TNF-α (10 minutes incubation) and absence of estradiol-dependent influence. Typical examples are reported.

10.11 hCMEC/D3 respond to LPS less well than pro-inflammatory cytokines

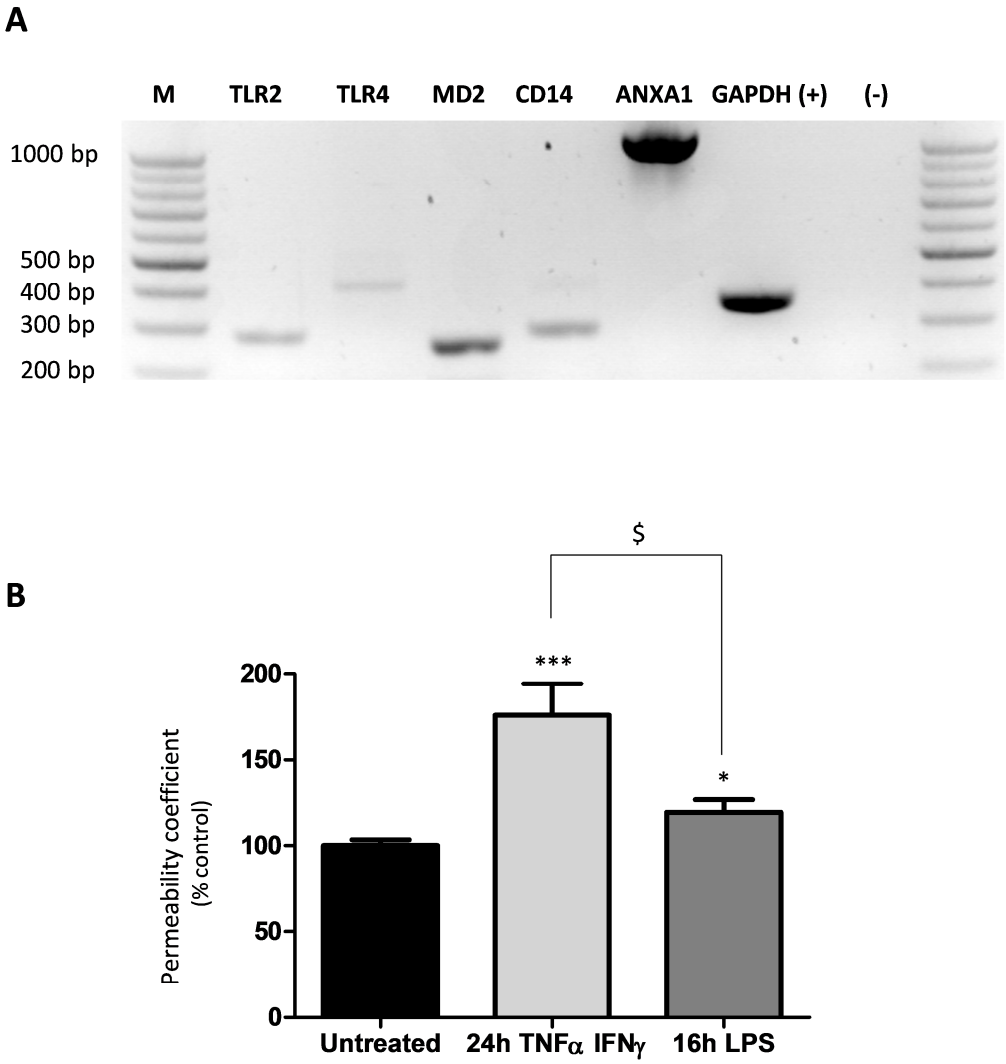

Figure 10.6 hCMEC/D3 cell line responds to LPS. A| RT-PCR was performed to assess the actual expression of TLR2, TLR4, MD2 and CD14 by unstimulated hCMEC/D3 cells; this suggested their ability to detect, and possibly respond, to exogenous inflammogens like LPS. 10 µl of PCR reaction volume were loaded, while 5 µl were loaded for the highly expressed ANXA1 and GAPDH and negative control (that is, a PCR reaction run with GAPDH primers and nuclease-free water as template). Length of the expected bands: TLR2: 292 bp; TLR4: 438 bp; MD-2: 293 bp; CD14: 236 bp; ANXA1: 1100 bp; GAPDH: 350 bp. 100 bp marker was also run in parallel (lane M). **B|** Validation of hCMEC/D3 cells as a model to assess the effect of pro-inflammatory stimuli on endothelial paracellular permeability was accomplished by comparing the effects of 24 hours incubation with 10 ng/ml TNFα and 10 ng/ml IFNγ [as reported by others (Haarmann *et al.*, 2010; Lopez-Ramirez *et al.*, 2012)] with that caused by overnight incubation with LPS [10 ng/ml; (Descamps *et al.*, 2003)]. 70 kDa-FITC-conjugated dextran was used. Results indicate 3 independent experiments, each of them performed in duplicate, and are presented as mean ± SEM. Student *t*-test was performed; *** indicates $p < 0.001$ *vs.* untreated, * $p < 0.05$ while $ indicates $p < 0.05$ *vs.* TNFα-IFNγ treated samples.

10.12 Experimental plan for Chapter 7

A Impact of peripheral inflammation

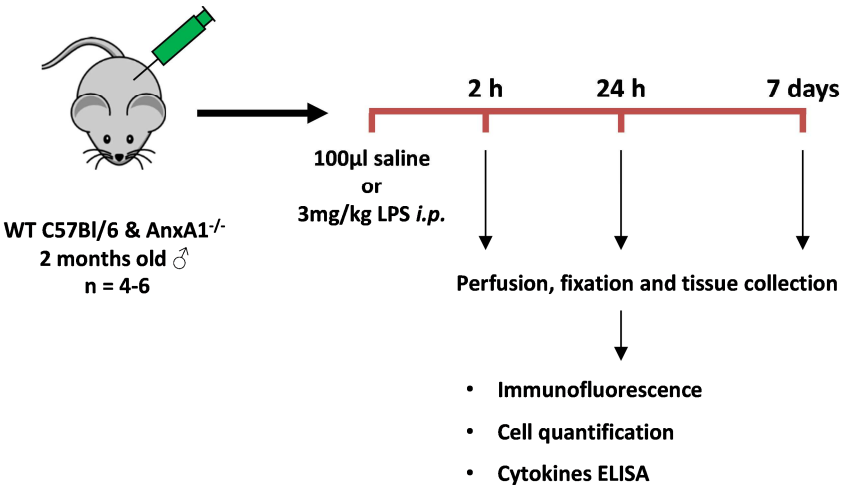

B Impact of neurodegeneration

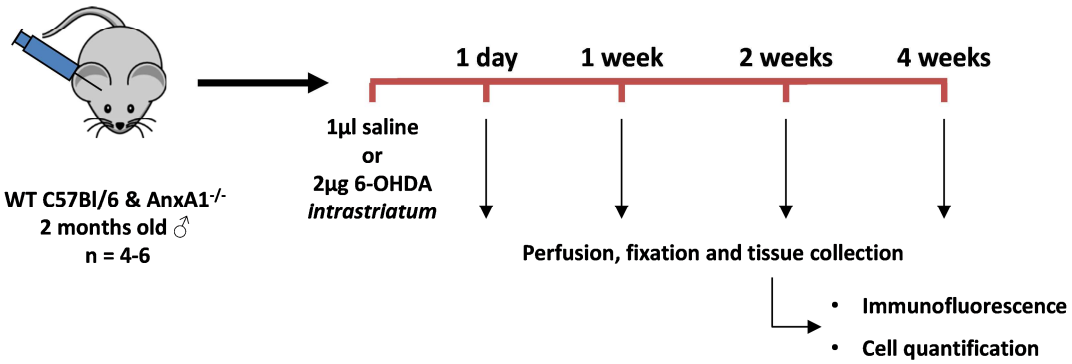

C Synergy between neurodegeneration and peripheral inflammation

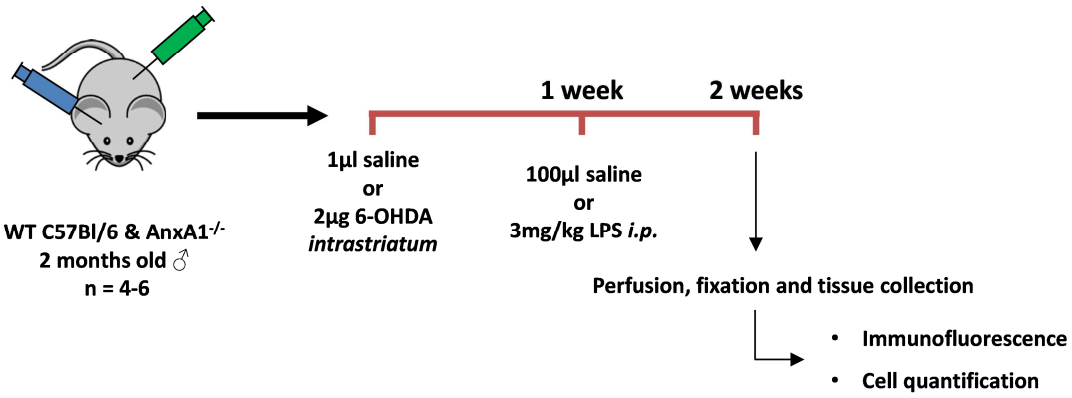

Figure 10.7 Experimental time plan for *in vivo* experiments. *In vivo* stimulation time points for the experiments described in Chapter 7. 6-OHDA is 6-hydroxydopaamine.

10.13 Schematic representation of substantia nigra pars compacta and ventral tegmental area throughout the midbrain

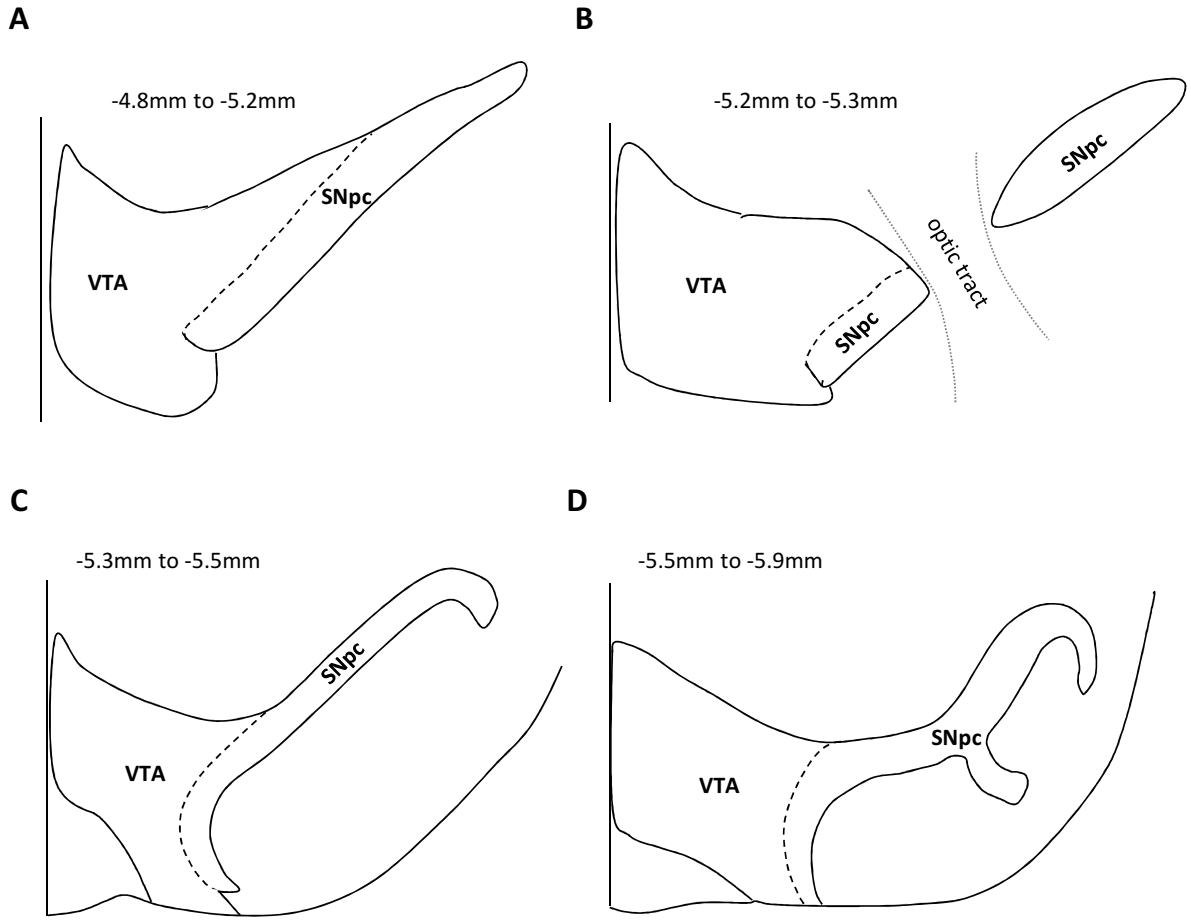

Figure 10.8 Definition of area boundaries for the substantia nigra pars compacta and the ventral tegmental area. Figures represent schematic examples of unilateral mesencephalic region, focusing on the shape and distribution of the SNpc and VTA from the initial rostral part (A) until the final caudal part (D). Coordinates are meant from the bregma. Based on Ikemoto, 2007 and modified with permission of Dr Simon McArthur.

10.14 Annexin A1 role in central regulation of apoptotic cells phagocytosis

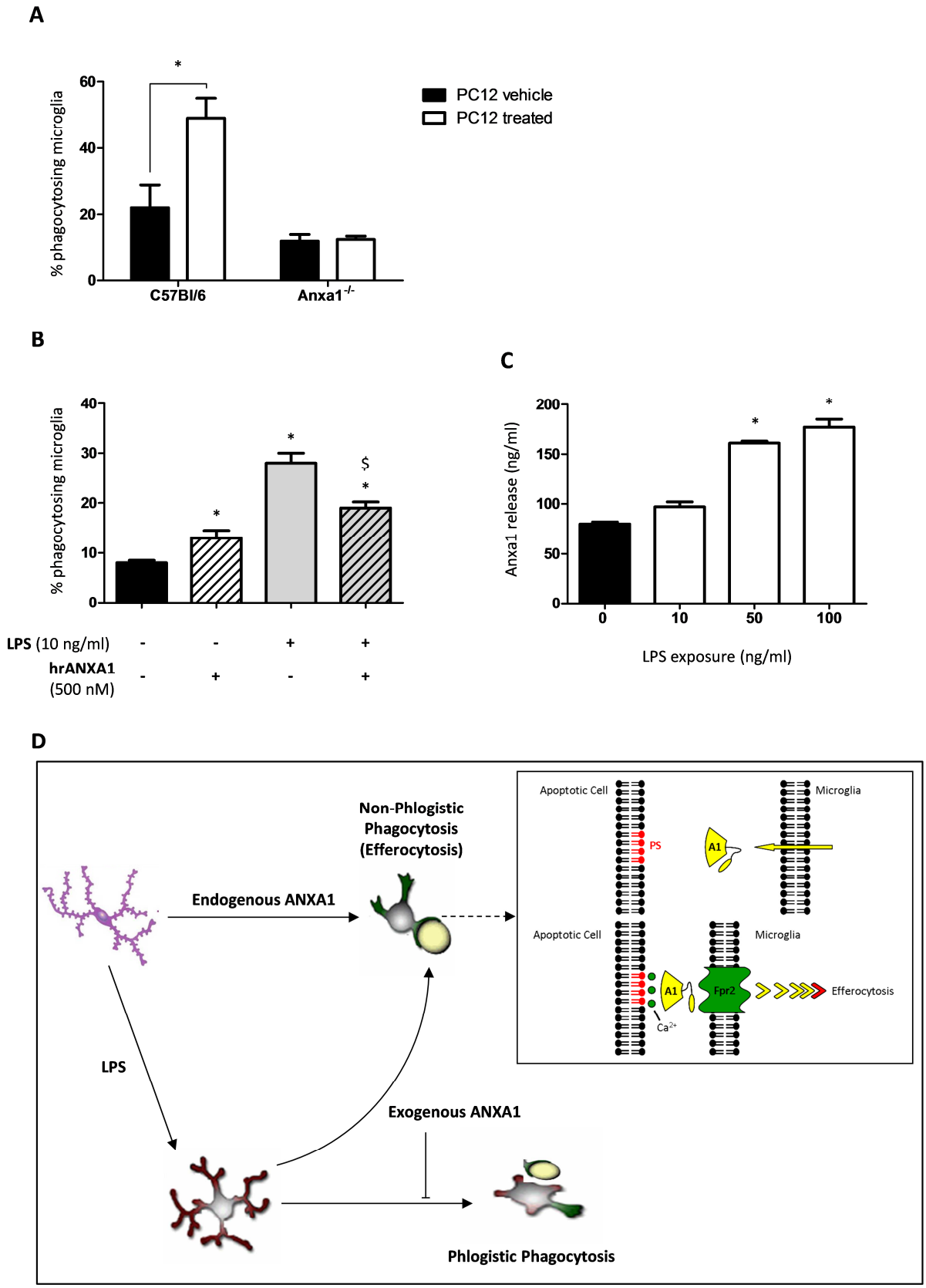

Figure 10.9 Most relevant results concerning the role of Annexin A1 in regulating phlogistic and non-phlogistic phagocytosis of apoptotic cells. This figure reports the most significant results presented in McArthur *et al.*, 2010 and correlated to the scopes of Chapter 7. **A|** Microglia cells isolated from Anxa1 null mice show impaired phagocytosis of apoptotic PC12 cell line (rat pheochromocytoma cell line from adrenal medulla; used as a model of apoptotic cells since they selectively die if treated overnight with 6-OHDA toxin). Data are presented as percentage of microglia cells with PC12 incorporated (phagocytized) and are indicated as mean ± SEM, n = 3). Two-way ANOVA and Bonferroni *post-hoc* test were performed. * indicates p<0.05. **B|** BV2 murine cell line was chosen as a model of microglia cells (Blasi *et al.*, 1990). These cells express typical microglial cell surface markers and exhibit the characteristic effector functions of native microglia, therefore representing a good model for investigating microglial regulation. 500 nM human recombinant ANXA1 was administered to LPS-activated (10 ng/ml; overnight incubation) BV2 cells co-incubated with non-apoptotic PC12. The inflammogen was shown to cause indiscriminate phagocytosis of alive/non-target cells, but this effect could be reverted by incubation with the anti-inflammatory molecule. Data are mean ± SEM, n=3 experiments. Two-way ANOVA and Bonferroni *post-hoc* test were performed. * indicates $p < 0.05$ versus untreated BV2 cells, while $ indicates p<0.05 versus LPS-treated BV2 cells. **C|** Dose-response analysis of BV2 Anxa1 medium release under LPS stimulation (overnight incubation). One-way ANOVA and Bonferroni *post-hoc* test were performed. * indicates p<0.05 *vs.* vehicle treated (0 ng/ml LPS) group. **D|** Schematic representation of the proposed ANXA1 role in controlling microglial phagocytosis. Microglia cells constitutively produce and release ANXA1, which enables non-phlogistic phagocytosis through binding to PS externalized on the apoptotic neurone surface. The phospholipid binding induces a conformational change in the ANXA1 molecule, allowing presentation of the N-terminal domain to the receptor Fpr2 on microglia surface, triggering the engulfment of the cell body. In inflammatory conditions, modelled by LPS stimulation *in vitro*, microglia is activated and aberrantly phagocytises non-apoptotic cells, an effect which cannot be reversed by endogenous levels of ANXA1. The addition of exogenous recombinant ANXA1, however, reverses the activation of the microglia and promotes their non-inflammatory phagocytic phenotype.

Publications and other contributions

Publications

- **Cristante E**, McArthur S, Romero IA, Wylezinska-Arridge M, Lopez-Tremoleda J, Couraud PO, Christian H, Weksler BB, Malaspina A & Solito E. Feature Article: Identification of an Essential Endogenous Regulator of Blood-Brain Barrier Integrity, and Its Pathological and Therapeutic Implications. Proc Natl Acad Sci U S A 110, 832-841

- **Cristante E**, McArthur S, Solito E. A role for Annexin A1 in mediating the effects of estrogen on the blood brain barrier in normal and inflammatory conditions. 2013 (Arterioscler Thromb Vasc Biol; submitted)

- **Cristante E** and Solito E. The impact of blood brain barrier malfunction: impact of the peripheral inflammation into the brain. Review 2013 (in preparation)

- **Cristante E**, McArthur S, Gillies GE and Solito E. Annexin A1 role in the peripheral Inflammation impact on an animal model of nigrostriatal dopaminergic neurodegeneration. 2013 (in preparation)

- McArthur S, **Cristante E**, Paterno M, Christian H, Roncaroli F, Gillies GE, and Solito E. Annexin A1: a central player in the anti-inflammatory and neuro- protective role of microglia. J Immunol. 2010 Nov 15;185(10):6317-28

Meetings attendance

- London Vascular Biology forum. December 2011, London. Abstract selected for poster presentation.
  "**Sex dimorphism in inflammation: a role for Annexin A1 in mediating the effects of estrogen on the blood brain barrier**"

- 1st Early career symposium on blood brain barriers. November 2011, Milton Keynes (UK). Abstract selected for oral communication.
  "**Sex dimorphism in inflammation: a role for Annexin A1 in mediating the effects of estrogen on the blood brain barrier**"

- 14th Symposium on signal transduction in the blood brain barriers. September 2011, Istanbul. Abstract selected for oral communication.
  "**Sex dimorphism in inflammation: a role for Annexin A1 in mediating the effects of estrogen on the blood brain barrier**"

- 6th International Conference on Annexins. August 2011, Barcelona. Abstract selected for oral communication.
  "**Characterisation of formyl peptide receptor 1 (FPR1) and FPRL-1 interactions: team-working is better than individualism**"

- Neuroscience 2010. November 2010, San Diego. Abstract selected for poster presentation.
  "**Role of Annexin A1 at the blood brain barrier level in mediating the brain response to inflammation**"

- WorldPharma 2010. July 2010, Copenhagen. Abstract selected for oral communication.
  "**Role of Annexin A1 at the blood brain barrier level in mediating the brain response to inflammation**"

- London Vascular Biology forum. December 2009, London. Abstract selected for poster presentation.
  "**A role for Annexin A1 in mediating the effects of estrogen on the blood brain barrier in normal and inflammatory conditions**"

- 5th International Conference on Annexins. September 2009, Bordeaux. Abstracted selected for poster presentation.
  "**The impact of peripheral inflammation in the brain: a new role for the systemic anti-inflammatory molecule Annexin A1**"

Awards

- Best oral communication prize, 14th Symposium on signal transduction in the blood brain barriers (Sept 2011)

- Travel grant from “British Society for Neuroendocrinology” to participate to the 14th Symposium on Signal transduction in the blood brain barriers (Sept 2011)

- Travel grant from “Guarantors of Brain” to participate to Neuroscience 2010 (July 2010)

- Travel grant from “British Pharmacological Society” to participate to WorldPharma 2010 (July 2010)